1-1-1989

Model copolymerization reactions :: investigations of alkyl radical-alkene addition reactions/

Douglas Adam Cywar
University of Massachusetts Amherst

MODEL COPOLYMERIZATION REACTIONS: INVESTIGATIONS OF ALKYL RADICAL-ALKENE ADDITION REACTIONS

A Dissertation Presented

by

DOUGLAS ADAM CYWAR

Submitted to the Graduate School of the

University of Massachusetts in partial fulfillment

of the requirements for the degree of

DOCTOR OF PHILOSOPHY

February, 1989

Department of Polymer Science and Engineering

MODEL COPOLYMERIZATION REACTIONS: INVESTIGATIONS OF ALKYL RADICAL-ALKENE ADDITION REACTIONS

A Dissertation Presented

by

DOUGLAS ADAM CYWAR

Approved as to style and content by:

David A. Tirrell, Chairman of Committee

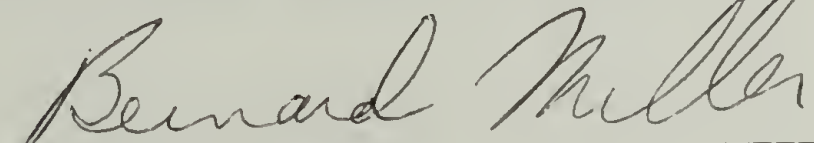

Bernard Miller, Member

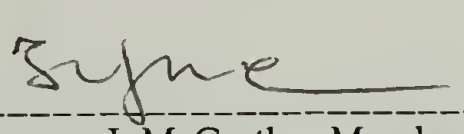

Thomas J. McCarthy, Member

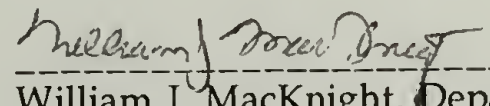

William J. MacKnight, Department Head
Department of Polymer Science and Engineering

For my wife, Paulette, and children, Erica and Adam.

ACKNOWLEDGEMENTS

My sincere thanks go to Professor David Tirrell for guiding my research and setting a scholarly example from which I have learned much, and for allowing me considerable freedom in my schedule so that I could care for my daughter during the day. The valuable time and suggestions contributed to my education by Professors B. Miller and T. McCarthy are appreciated.

I am indebted to Douglas Wicks for his valuable technical assistance in many areas. No matter how busy, Doug always took time out to help me. I would also like to thank Glenn Prementine and Sharon Jones for teaching me many of the techniques necessary for organic synthesis.

ABSTRACT

MODEL COPOLYMERIZATION REACTIONS: INVESTIGATIONS OF ALKYL RADICAL-ALKENE ADDITION REACTIONS

FEBRUARY 1989

DOUGLAS ADAM CYWAR, B.S., UNIVERSITY OF FLORIDA

Ph.D., UNIVERSITY OF MASSACHUSETTS

Directed by: Professor David A. Tirrell

The relative rates of addition of styrene and acrylonitrile (k_S/k_A) to the 1-phenylethyl (**2a**), 1-(1,3-diphenyl)propyl (**2b**), and 4-(4-phenyl)butyronitrile (**2c**) radicals were measured. Each radical was generated by photolysis at 33 °C of the respective ^{13}C enriched azo compound - 1,1'-azobis(1-phenyl[1-^{13}C]ethane) (**1a**), 1,1'-azobis(1,3-[1-^{13}C]diphenylpropane) (**1b**), or 4,4'-azobis(4-phenyl[4-^{13}C]butyronitrile) (**1c**) - in benzene solution containing styrene and acrylonitrile. The syntheses of **1a** from [1-^{13}C]acetic acid (15% yield) and **1b** and **1c** both from $Ba^{13}CO_3$ (10% and 1.2% yield) are described. Determination of the relative concentrations of the enriched end groups in the resultant copolymers by ^{13}C NMR analysis afforded the rate constant ratios, and the results are as follows: $k_S/k_A = 0.20 \pm 0.02$ for **2a**, 0.21 ± 0.01 for **2b**, and 0.52 ± 0.03 for **2c**. The 2.5-fold increase in k_S/k_A observed for **2c** as compared to **2a** or **2b** indicates that a cyano group in a position gamma to an a-phenylalkyl radical can bring about an appreciable decrease in the relative rate of acrylonitrile addition. These results are consistent with the penultimate model treatment of the styrene-acrylonitrile copolymerization by Hill, O'Donnell, and O'Sullivan, and offer clear evidence for the existence of a penultimate unit effect. In an associated investigation, the rate constant ratio for addition of methyl methacrylate and acrylonitrile (k_{MMA}/k_A) to **2a** was determined to be 0.44 ± 0.03. Further analysis of data from this determination provided $k_{MMA}/k_A = 2.4 \pm 0.4$ for the 2-(4-phenyl)pentanenitrile radical.

Also described within are determinations of the relative rates of addition of acrylonitrile, styrene, and methyl acrylate to the 5-phenyl-1-pentyl and 5-cyano-1-pentyl radicals, which were generated by $NaBH_4$ reduction of alkylmercuric bromides. For each of the competitions investigated, it was found that there was no significant difference between the selectivities of these radicals.

TABLE OF CONTENTS

LIST OF TABLES

LIST OF FIGURES

Page

Figure

Page

Figure

Page

Figure

Page

Figure

LIST OF SCHEMES

CHAPTER I

INTRODUCTION

Addition reactions of alkyl radicals with alkenes present a natural dichotomy of "small" radicals, such as methyl or cyclohexyl, vs. macromolecular, "growing polymer", radicals (1). Much of what is known about alkyl radical-alkene addition has been learned from studies of radical copolymerization, as there has been a great deal of work in this area. Information gathered from such a study is often stated in the context of a kinetic model supposed for the copolymerization process, however, and the usefulness of the information will thus depend on the nature of assumptions made in the formulation of the model.

Nearly all kinetic models of copolymerization assume that macroradical reactivity is determined only by the local chain-end structure (ie., that about the radical center), rather than by the structure (or size) of the macroradical as a whole. This provides common ground for studies of small and macro- radical alkene addition reactions, as similar reactivities should be observed for a macroradical and a small radical with a structure analogous to the chain-end. Obviously, the validity of this assumption will depend on how one specifies "local chain-end structure." Different models of copolymerization make different assumptions concerning the effects of remote substituents on radical reactivity, corresponding to the different levels of complexity of the models in defining chain-end structure.

Investigations reported within seek to determine the extent to which the chemoselectivity of small alkyl radicals can be affected by the nature of substituents in positions remote to the radical centers; eg, by the nature of γ and ε-substituents. The systems chosen for study are analogues of radical copolymerizations, most notably for styrene-acrylonitrile (SAN) copolymerization. These investigations were undertaken to gather fundamental information concerning small alkyl radical-alkene addition reactions, and it was hoped, as follows from the preceding discussion, that these studies might unambiguously indicate the validity of some common assumptions made in radical copolymerization studies.

Outlined in subsequent sections of this chapter are some important kinetic models used to treat radical copolymerization, and some methodologies by which the propriety of a given model can be assessed. For fuller treatment of topics discussed, the reader is referred to reviews of copolymerization by Tirrell (2) and by Hill, O'Donnell, and O'Sullivan (3).

A. Kinetic models of copolymerization

1. The terminal model

The first useful model of the copolymerization process was independently arrived at in 1944 by Mayo and Lewis (4), by Alfrey and Goldfinger (5), and by Wall (6). This model assumes that only the identity of the terminal monomeric unit (ie., identity of the last monomer to have added) of a growing chain need be specified to characterize its reactivity. Therefore only four propagation rate constants are necessary to describe the addition reactions of the two kinetically distinguishable radicals (Scheme 1.1, p. 3). Accordingly, the rates of monomer disappearance are given by equations 1 and 2, where $[M_1]$ and $[M_2]$ are monomer feed

$$\frac{-d[M_1]}{dt} = k_{11}[M_1][M_1^{\cdot}] + k_{21}[M_1][M_2^{\cdot}] \qquad (1)$$

$$\frac{-d[M_2]}{dt} = k_{12}[M_2][M_1^{\cdot}] + k_{22}[M_2][M_2^{\cdot}] \qquad (2)$$

concentrations, and $[M_1\cdot]$ and $[M_2\cdot]$ are the concentrations of growing chains with terminal residues derived from M_1 and M_2, respectively. Dividing equation 1 by equation 2 gives

$$\frac{d[M_1]}{d[M_2]} = \frac{k_{11}[M_1][M_1^{\cdot}] + k_{21}[M_1][M_2^{\cdot}]}{k_{12}[M_2][M_1^{\cdot}] + k_{22}[M_2][M_2^{\cdot}]} \qquad (3)$$

as the instantaneous molar ratio of M_1 and M_2 in the copolymer. An assumption of steady state concentrations for $M_1\cdot$ and $M_2\cdot$ is now made, which means that the rates of intraconversion of the two types of chains must be equal (equation 4). Substitution of equation 4 into equation 3

$$k_{12}[M_2][M_1^{\cdot}] = k_{21}[M_1][M_2^{\cdot}] \qquad (4)$$

allows the elimination of the radical concentrations, and equation 5 is thus obtained,

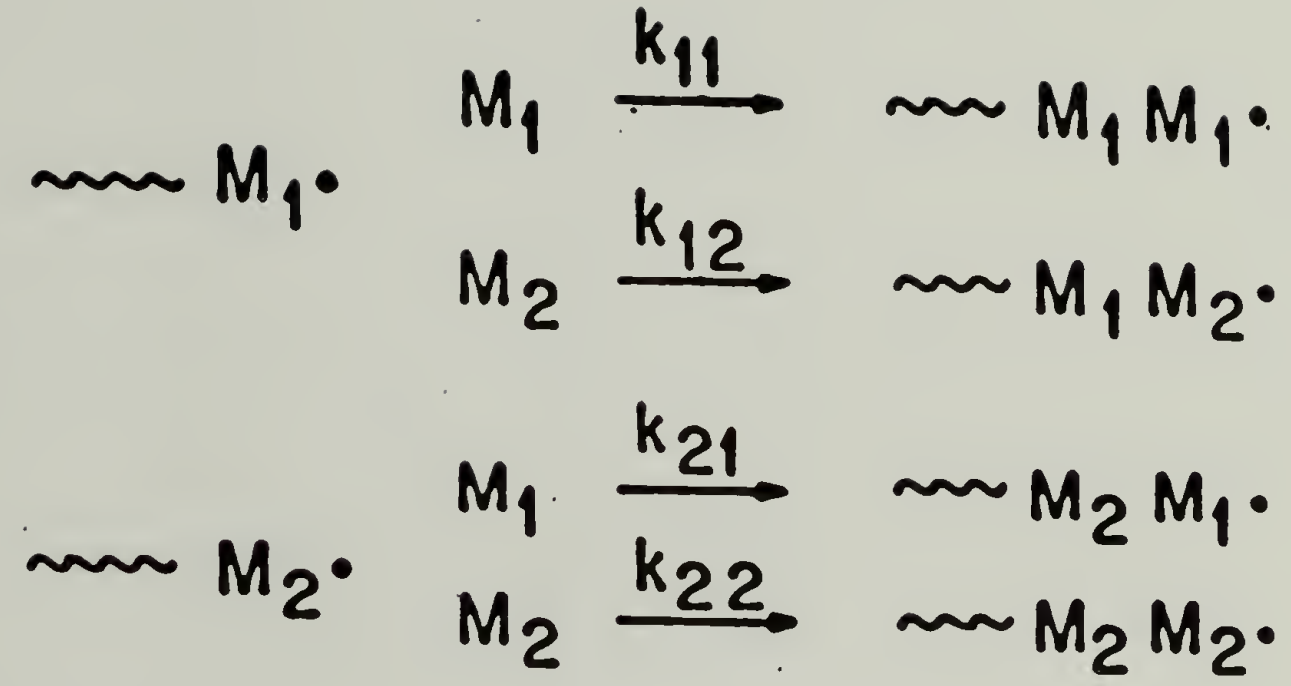

Scheme 1.1. The terminal model of copolymerization.

$$\frac{d[M_1]}{d[M_2]} = \frac{r_1 \frac{[M_1]}{[M_2]} + 1}{r_2 \frac{[M_2]}{[M_1]} + 1} \qquad (5)$$

where $r_1 = k_{11}/k_{12}$ and $r_2 = k_{22}/k_{21}$. This equation can be rearranged (multiply by $[M_1]/[M_1]$) to yield the more familiar form of equation 6:

$$\frac{d[M_1]}{d[M_2]} = \frac{[M_1]}{[M_2]} \cdot \frac{r_1[M_1] + [M_2]}{[M_1] + r_2[M_2]} \qquad (6)$$

Equation 6 (often termed the Mayo-Lewis equation) expresses the composition of the copolymer as a function of the monomer feed ratio $[M_1]/[M_2]$ and the parameters r_1 and r_2, which are termed "reactivity ratios." The reactivity ratios are simply the relative rates of addition of the monomers to each type of chain end. The monomer feed ratio $[M_1]/[M_2]$ is generally a function of time in a copolymerization. Therefore, if an initial feed ratio is inserted into equation 6, this equation will only give the correct copolymer composition (in general) for a low conversion polymerization, wherein the feed ratio has not drifted too far from its initial value.

The values of the reactivity ratios can be indicative of the sequence distribution of the monomeric units in the copolymer. If $r_1 = r_2 = 1$, a random distribution is expected because neither type of chain has a preference for the addition of one type of monomer over the other. If $r_1 = r_2 = 0$, then a strictly alternating sequence of the monomers is expected because each chain adds exclusively the monomer other than that which comprises its terminal unit. If $r_1 > 1$ and $r_2 > 1$, then long sequences of each monomer uninterrupted by the other are expected because each chain prefers to add the same monomer that comprises its terminal unit.

For many years the standard method of determining r_1 and r_2 from copolymerization data was based on a method which can lead to erroneous results; several authors have discussed this topic (7-10), and the method of Tidwell and Mortimer (7, 8) is now generally accepted as the best way to go about this. There has been a recent extensive listing of reactivity ratios (11).

2. The penultimate model

This model (12) is simply an extension of the terminal model for the case where the reactivity of a chain is assumed to be influenced by the monomeric unit that precedes the terminal unit (the penultimate unit) as well as by the terminal unit. For the polymerization of monosubstituted olefins, this means that chain reactivity is sensitive to the nature of substituents in a position γ as well as α to the radical center. There are thus four kinetically distinct radicals each competing for comonomer, and eight propagation rate equations are required (Scheme 1.2, p. 6). A derivation analogous to that for the terminal model gives equation 7,

$$\frac{d[M_1]}{d[M_2]} = \frac{1 + \dfrac{r_1'X(r_1X + 1)}{r_1'X + 1}}{1 + \dfrac{r_2'(r_2 + X)}{X(r_2' + X)}} \qquad (7)$$

where $X = [M_1]/[M_2]$ and the reactivity ratios are defined as: $r_1 = k_{111}/k_{112}$, $r_1' = k_{211}/k_{212}$, $r_2 = k_{222}/k_{221}$, and $r_2' = k_{122}/k_{121}$. For the case of $r_1 = r_1'$, $r_2 = r_2'$, that is, the case where the identities of the penultimate units are insignificant in regard to the relative rates of addition of monomer, equation 7 reduces to equation 6 as it should. It may also be useful to define the ratios $s_1 = k_{211}/k_{111}$ and $s_2 = k_{122}/k_{222}$. The values s_1 and s_2 have no effect in regard to the composition predictions of the penultimate model; however, they do affect the propagation rate predictions (13).

The author is aware of several systems for which penultimate effects are suspected, usually on the basis of composition data which cannot be fit well by equation 6. These copolymerizations are those of styrene and acrylonitrile (14), styrene and fumaronitrile (15), styrene and maleic anhydride (16), styrene and benzylidenemalonitrile (17), p-chlorostyrene and methyl acrylate (18), tetrachlorocyclopropene and vinyl acetate (19), methyl acrylate and butadiene (20), and styrene and 2,3,4-trimethyl-3-pentyl methacrylate (21). Penultimate effects are generally ascribed to electrostatic repulsions or steric interactions between penultimate unit substituents and incoming monomers. The last system listed above is interesting in this regard, as the preparation of the bulky acrylic monomer and subsequent investigation of its copolymerization behavior with styrene (21) was specifically undertaken in a "search for a steric penultimate effect." It was found that when styrene is the penultimate

$$\sim M_1M_1\bullet + M_1 \xrightarrow{k_{111}} \sim M_1M_1\bullet$$

$$\sim M_1M_1\bullet + M_2 \xrightarrow{k_{112}} \sim M_1M_2\bullet$$

$$\sim M_1M_2\bullet + M_2 \xrightarrow{k_{122}} \sim M_2M_2\bullet$$

$$\sim M_1M_2\bullet + M_1 \xrightarrow{k_{121}} \sim M_2M_1\bullet$$

$$\sim M_2M_1\bullet + M_1 \xrightarrow{k_{211}} \sim M_1M_1\bullet$$

$$\sim M_2M_1\bullet + M_2 \xrightarrow{k_{212}} \sim M_1M_2\bullet$$

$$\sim M_2M_2\bullet + M_2 \xrightarrow{k_{222}} \sim M_2M_2\bullet$$

$$\sim M_2M_2\bullet + M_1 \xrightarrow{k_{221}} \sim M_2M_1\bullet$$

Scheme 1.2. The penultimate model of copolymerization.

monomer, both styryl and 2,3,4-trimethyl-3-pentyl methacryl radicals have an equal preference (factor of 1.7) to add the opposite monomer. However, when the penultimate unit bears the bulky ester group, markedly different behavior is observed. 2,3,4-Trimethyl-3-pentyl methacryl radicals now have a much greater preference for styrene (factor of 4.4) than in the previous case, and the preference of the styryl radicals is reversed- now adding styrene 1.3 times faster than the acrylic monomer. These results support the notion of a penultimate effect that arises from steric interactions, as the presence of the large ester group in the penultimate unit resulted in a depression of the relative rate of addition of the bulky acrylic monomer regardless of the nature of the terminal unit.

3. Other models

The terminal and penultimate models both assume that the propagation steps represented in Schemes 1.1 and 1.2 are essentially irreversible. However for some systems, such as SO_2-olefin (22-27) and methyl methacrylate-acrylonitrile copolymerization (28), under certain conditions (eg., high temperature) this may not be true, and models which describe copolymerization with depropagation have been developed (29, 30). These models have in common with the penultimate model the fact that the last two monomeric units of a growing chain must be considered in developing an expression for composition.

Another kinetic model of copolymerization invoked for some systems grows out of consideration of the possible chemical association of comonomer to form a new species capable of radical addition. For example, there are many olefinic comonomer pairs that form 1:1 charge transfer (CT) complexes, often highly colored. It was pointed out in 1946 (31) that 1:1 copolymers are often produced over a wide range of feed compositions for copolymerization of maleic anhydride with various vinyl aromatic compounds, systems for which such colored complexes are readily observed, although it was not suggested that the complexes actually add to the radicals. Several years later, however, other workers (22-26) suggested that the highly alternating copolymers obtained from SO_2-olefin copolymerizations did in fact arise from concerted addition of 1:1 SO_2-olefin complex, evidence for which was obtained from optical spectroscopy. There are now many who accept the notion of concerted addition of CT complexes to free radicals, although this is still an uncertain and hotly debated topic (16, 21, 32-39). The "terminal complex participation" model of copolymerization has been developed by Seiner and Litt (40-43), wherein chain growth occurs via competitive additions of free and complexed

comonomer. The eight propagation steps that are considered in this model are illustrated in Scheme 1.3 (p. 9); the reader is referred to the publications for composition equations, as they are quite lengthy. It is noted here that the copolymerization of styrene and maleic anhydride has been studied extensively (16, 44-48) in regard to the idea of chain growth via CT complex addition.

There are other ways in which one can consider the role of a CT complex in radical copolymerization. For example, the complex may dissociate upon attack by the radical, leading to the addition of only one of the monomers. The role of the complex is then only to change the monomer reactivity. A general kinetic treatment for this situation has been formulated (49).

Two other alternate copolymerization models will now be mentioned. One attempts to account for preferential solvation of the growing chain (50, 51). The importance of solvent and conversion are considered, as these can change the polarity of the system and the local concentration of monomer about the radical centers. The other is termed the "hot radical theory", and is based on the fact that in the moment of its formation, the reaction product contains the heat of an exothermic elementary reaction in the form of excitation of internal (mainly vibrational) degrees of freedom (52). This theory then assumes that such vibrationally excited radicals are capable of reaction prior to complete deactivation, and that they may have a reactivity different from that of the vibrationally deactivated species.

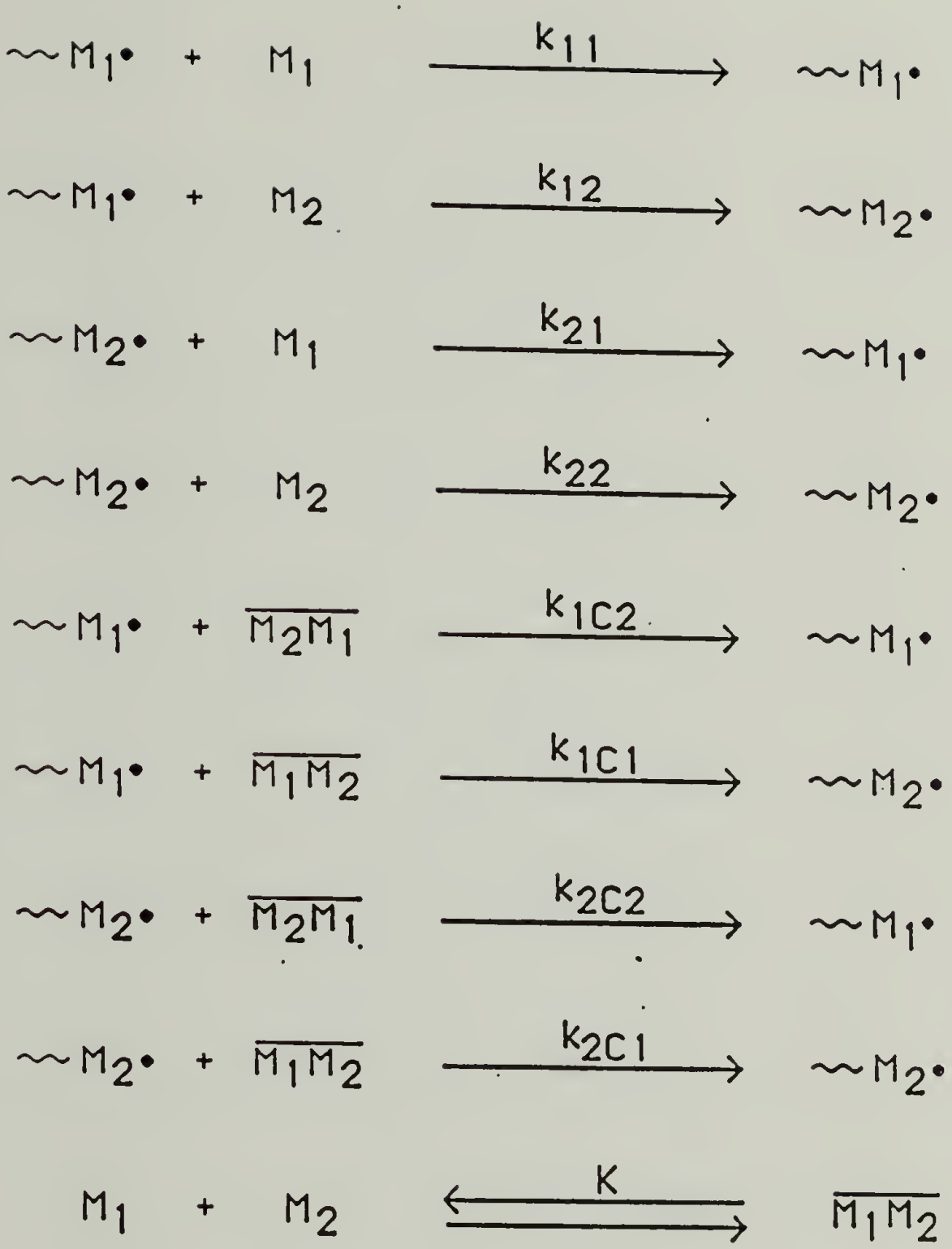

Scheme 1.3. The terminal complex-participation model.

B. Evaluation of copolymerization models

1. Composition and sequence

The simplest and most frequently used test of a copolymerization model is its ability to predict copolymer composition. The terminal model can adequately describe the composition data for the vast majority of radical copolymerizations investigated to date. However, this does not necessarily mean that the underlying assumptions of this model are generally correct, because composition predictions are not a very sensitive test of copolymerization mechanism. It was pointed out as early as 1946 that deviations from the predictions of the terminal model should be detected most readily in measurements of *sequence*, rather than *composition* (12). Because sequence measurements even now are not routinely accessible, stringent tests of the terminal model have been applied only in a relatively small number of copolymerization systems.

One system that has been tested in this regard is the copolymerization of styrene (S) and acrylonitrile (A). In 1982 Hill, O'Donnell, and O'Sullivan published a thorough analysis of this system (53). As can be seen from Figure 1.1 (p. 11), the terminal, penultimate, and complex participation models are all able to fit the experimentally observed composition data reasonably well. Each of these models can also make definite predictions concerning comonomer sequence lengths; for each model, one can express the probability for formation of any particular sequence as a function of the feed ratio and reactivity ratios (in addition to an equilibrium constant for CT complex formation in the case of the complex model). From ^{13}C NMR measurements, Hill et al. determined the number fraction of several sequences, such as an ASA sequence, and with the aid of a computer then compared the "best-fit" predictions of each model to the experimental data. Their results are reproduced in Fig. 1.2 (p. 12) for the ASA sequence, and it can be seen that the penultimate model can provide the best fit. Primarily on the basis of the sequence data fits, Hill et al. concluded that the penultimate model offers the best description of this copolymerization. The best-fit penultimate reactivity ratios which were thus used to predict composition and sequence are as follows: $r_{SS} = 0.229$, $r_{AS} = 0.634$, $r_{AA} = 0.039$, and $r_{SA} = 0.091$. (For r_{ij}, i refers to the identity of the penultimate unit and j refers to the terminal unit). From these values, it appears that regardless of the identity of the terminal unit, the relative affinity of the macroradical for acrylonitrile is depressed approximately 2.5-fold by a cyano group γ to the radical center.

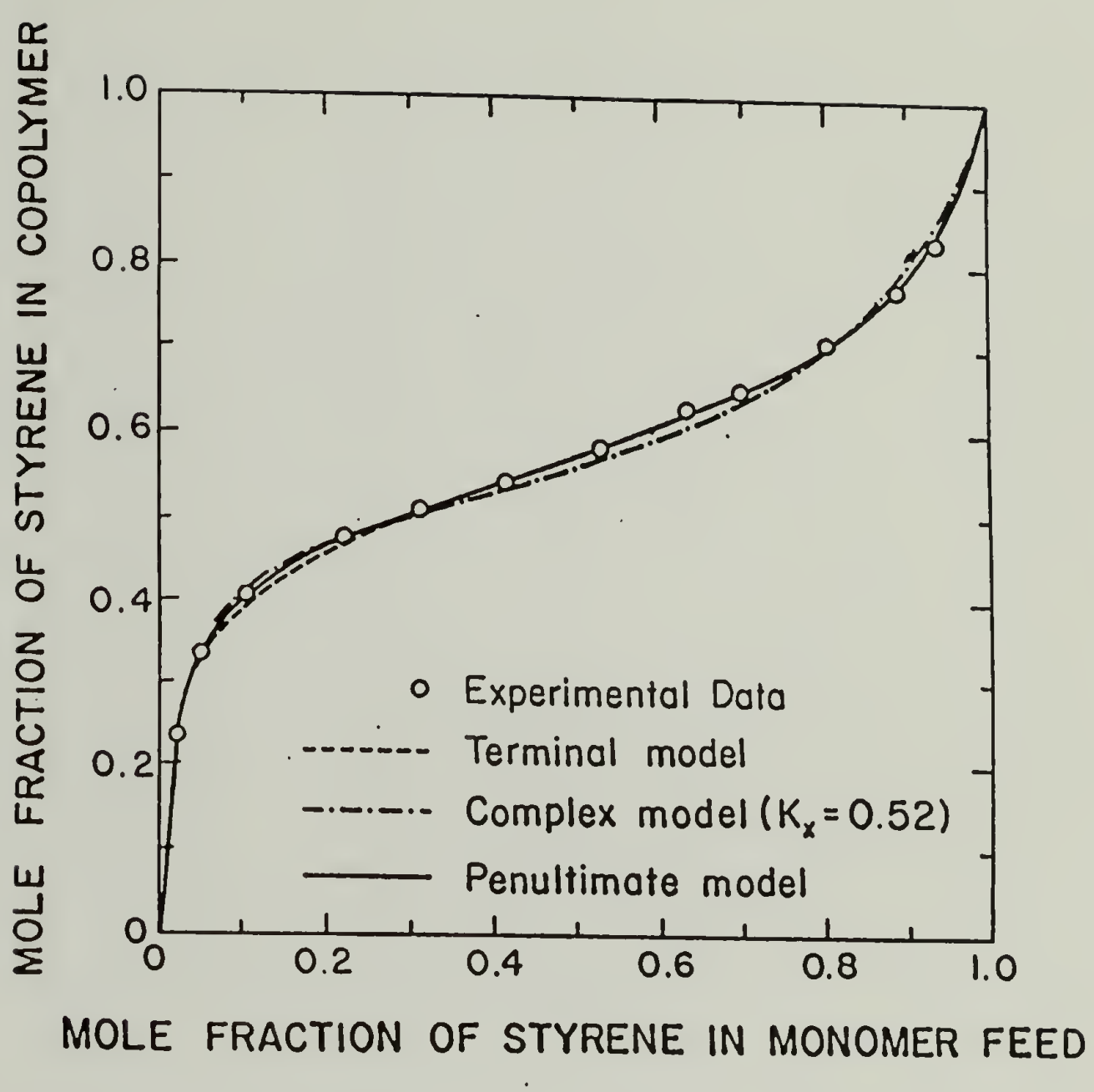

Figure 1.1. Copolymer composition curve for the copolymerization of styrene and acrylonitrile in bulk at 60 °C (53).

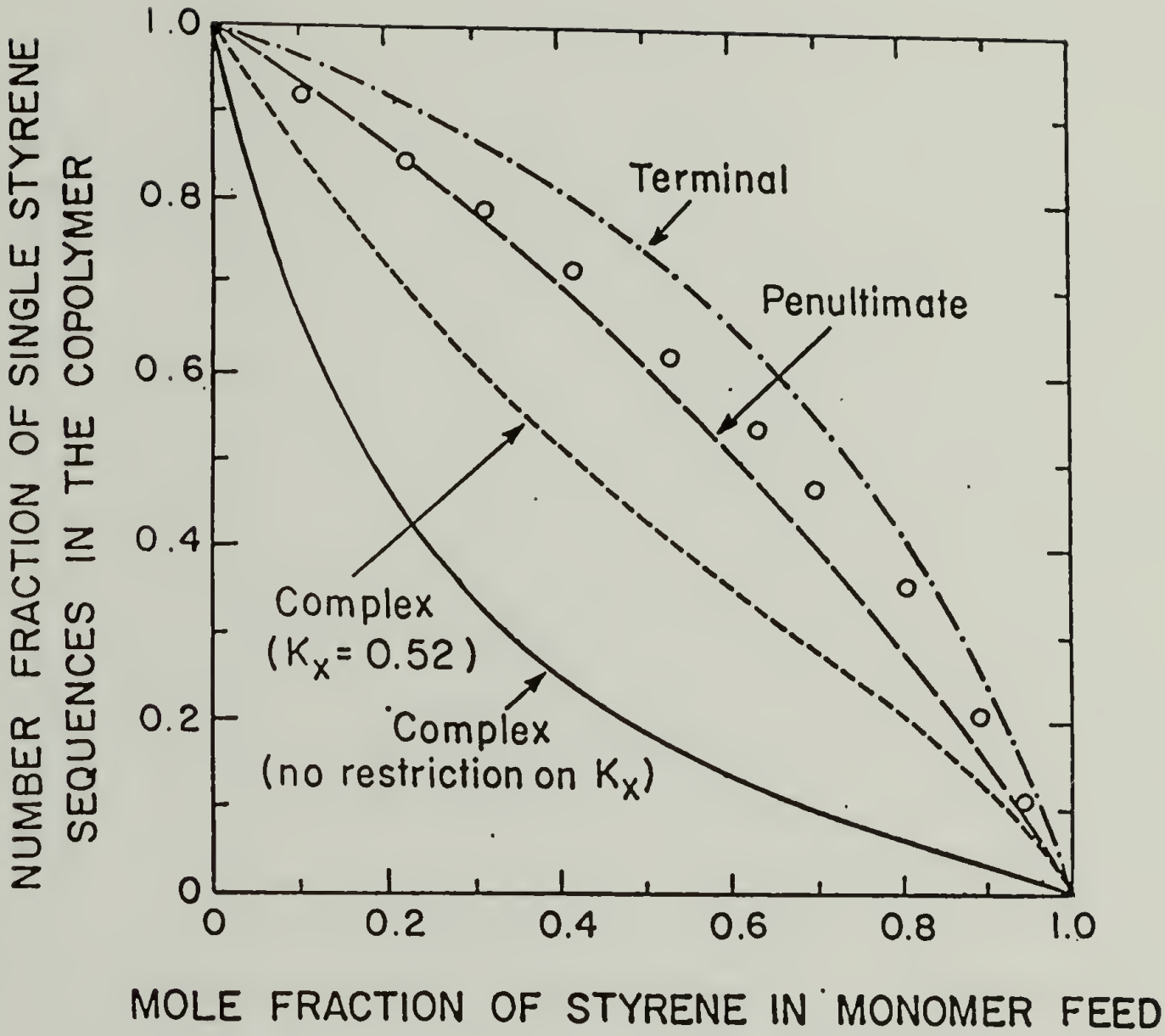

Figure 1.2. Number fraction of single styrene sequences in copolymers of styrene and acrylonitrile, as a function of the mole fraction of styrene in the monomer feed mixture (53).

2. Rate of polymerization

Another test of a copolymerization model is its ability to predict overall rate of copolymerization. Fairly recently, Fukuda and coworkers have used the rotating-sector technique to individually measure the propagation and termination rate constants for the copolymerization of styrene and methyl methacrylate (13). Shown in Fig. 1.3 (p. 14) are the observed propagation rate constants as a function of the mole fraction of styrene in the feed, plotted along with the predictions of the terminal and penultimate models. It is clear that the terminal model incorrectly predicts the propagation rate constant, although the penultimate model can fit the data very well.

This result is in spite of the fact that the composition data for this copolymerization system conforms to the terminal model within experimental error. In terms of penultimate model reactivity ratios (where styrene = 1 and methyl methacrylate = 2), $r_1 = r_1'$ and $r_2 = r_2'$ but s_1 and s_2 are different from unity (the value of s_i demanded by the terminal model). The values used for the s_i parameters to obtain the fit shown in Fig. 1.3 are as follows: $s_1 = 0.30$ and $s_2 = 0.53$. From the value of s_1, one interprets that an SS terminated macroradical adds styrene about 3 times as fast as does the MS terminated chain; from s_2, one interprets that an MM terminated macroradical adds methyl methacrylate about twice as fast as does the SM terminated chain. It will be recalled that the values of the s_i parameters do not affect the penultimate model composition predictions.

The measurements made by Fukuda et al. for this system were very difficult. The work (13) was published in 1985, and it was the first report of a truly complete set of kinetic data on a copolymerization system. In this publication, the authors state: "Of the great number of reactivity ratio values reported in the literature, relatively few seem to have been established with adequate justification of the assumed terminal model. Accordingly, one should not hasten to conclude that the failure of the Mayo-Lewis equation [equation 6] is particularly exceptional."

3. Model reactions

All of the copolymerization models discussed in this chapter assume that the reactivity of a radical is determined by only the local chain-end structure. This is a necessary simplification if one is to quantitatively describe a copolymerization, as an enormous number of chemically distinct radicals exist at any time during the reaction. The analysis of a copolymerization in

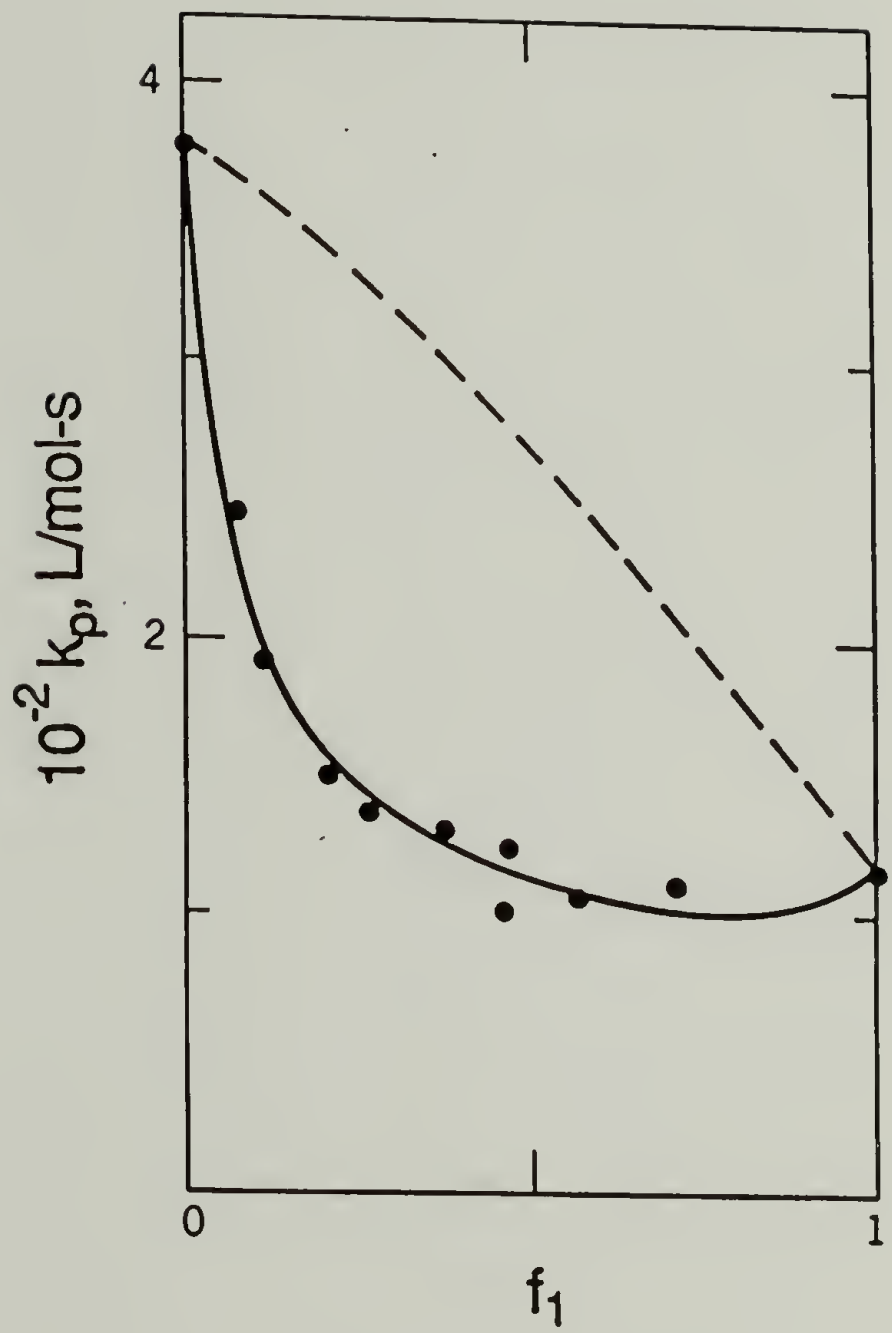

Figure 1.3. Propagation rate constant for radical copolymerization of styrene and methyl methacrylate, as a function of the mole fraction of styrene in the monomer feed f_1. The solid circles represent experimental data; the dotted line is that calculated according to the terminal model; the solid line is that calculated according to the penultimate model (13).

terms of one of these models therefore inevitably leads to conclusions about chain-end reactivity. If the model is physically meaningful, then these conclusions should not be in conflict with what is known about the behavior of simple (small) radicals of analogous structure to the chain-ends. The evaluation of copolymerization models from this viewpoint is thus understood to refer to a "model reaction" approach.

This approach is embodied in the comparison of terminal model reactivity ratios to the relative rates of addition of olefins to simple alkyl radicals. For example, Giese and Meixner (54) measured relative rates of addition of cyclohexyl radical to styrene and various alkenes, and determined that the relationship of equation 8 adequately correlated these rates with

$$- \log r = 0.58 \log k - 0.16 \qquad (8)$$

reactivity ratios for radical copolymerization of the alkenes with styrene ($r = k_{11}/k_{12}$ for M_1 = styrene and M_2 = alkene; k = rate of alkene addition to cyclohexyl/rate of styrene addition to cyclohexyl). A linear free energy relationship such as this would not be expected if strong penultimate or higher order effects were the rule in the radical copolymerizations.

In most previous studies that have dealt with (absolute) rate equations of copolymerization, the propriety of the terminal model has been assumed with regard to the propagation step, and the primary concern has been with the mechanism of the termination step. Walling derived an equation for overall copolymerization rate assuming "chemically controlled" termination, ie., assuming that termination reactions by coupling of macroradicals are kinetically distinguishable on the basis of the identity of terminal monomeric units (55). This equation, which is based on a terminal model description of propagation, contains a "cross-termination factor" ϕ (eqn. 9, where k_{tij} are the rates of coupling between radicals bearing

$$\phi = \frac{k_{t12}}{(k_{t11} \cdot k_{t22})^{1/2}} \qquad (9)$$

terminal i and j residues) which can be evaluated from overall rates of (homo- and co-) polymerization and initiation. For many systems, values of ϕ much greater than unity have been obtained (13). One might immediately wonder if such a preference for cross termination is consistent with what is known about the coupling of low molecular weight radicals. Along

these lines, Ito (56) investigated the coupling of 1-phenylethyl and 2-methylpropionitrile radicals, which may be regarded as models for the chain-ends in a copolymerization of styrene and methacrylonitrile, and observed ϕ values close to unity. This observation is clearly in conflict with a ϕ value of 6 obtained by Ito from a kinetic analysis of the styrene-methacrylonitrile copolymerization, and this investigation is a good example of the use of model reactions. It now appears from the work of Fukuda and coworkers (13) that conflicts of this nature may be due to the inappropriate use of the terminal model to describe the propagation step in copolymerization, and the reader is referred to their publication for discussion of this topic.

Previous investigations from this laboratory have used the model reaction approach to assess the use of the penultimate and complex participation models. Jones and Prementine (57) determined relative rates of addition of acrylonitrile and styrene to a series of n-alkyl radicals bearing different γ-substituents in an effort to test the physical plausibility of the penultimate model, which postulates (for polymerization of monosubstituted olefins) that substituents γ to a radical center can significantly alter chemoselectivity. The results are summarized in Figure 1.4 (p. 17), and show the relative rate of acrylonitrile addition to be reduced 3.5-fold by the introduction of a γ-cyano group as compared to a γ phenyl, methyl, or propyl group. This finding is in remarkable agreement with the substituent effect postulated by Hill et al. from their penultimate model treatment of the SAN copolymerization (vide supra) (53), wherein the relativity affinity of a growing macroradical for acrylonitrile is depressed approximately 2.5-fold by a γ-cyano group (ie., a penultimate acrylonitrile unit) regardless of the nature of the terminal unit. This investigation (of Jones et al.) was, to quote the authors, "the first direct determination of the magnitude of the substituent effects which must be operative if the penultimate model is to be a physically meaningful description of radical copolymerizations of monosubstituted olefins."

Butler and coworkers have presented evidence for participation of a comonomer charge transfer complex in the radical copolymerization of N-phenylmaleimide (NPM) and chloroethyl vinyl ether (CEVE) based on observed changes in copolymer stereochemistry with variation in reaction conditions (36). In independent investigations, Jones (37, 38) and Prementine (39) studied addition reactions of the n-butyl (37, 38) and benzyl (39) radicals in NPM-CEVE solutions which contained relatively high concentrations of the NPM-CEVE complex. Both investigations were essentially trapping experiments, and in both it was found

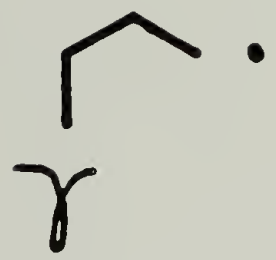

γ	K_A / K_S
$-CH_3$	24.5 ± 1.1
$-CH_2CH_2CH_3$	26.3 ± 2.4
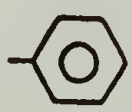	22.6 ± 2.0
$-CN$	6.8 ± 0.6

Figure 1.4. Relative rates of addition of acrylonitrile and styrene (k_A/k_S) to alkyl radicals (57).

that greater than 90% of consumed monomer could be accounted for in terms of products which resulted from the addition of single molecules of monomer to the radicals. Such results are inconsistent with the notion of concerted addition of complex, and cast some doubt on the conclusions of Butler at al., although in this regard it is possible that important differences exist between macroradicals in the NPM-CEVE copolymerization and the n-butyl and benzyl radicals. Similarly, it was found using trapping experiments that reaction of n-butyl radical in the presence of appreciable amounts of the charge transfer complex of styrene and acrylonitrile resulted in no significant amount of products which would have resulted from concerted addition of complex (37).

Prementine has determined the relative rates of addition of styrene and acrylonitrile (k_A/k_S) to the 2-propionitrile (58) and 2-(4-phenyl)butyronitrile (39) radicals, which have structures analogous to A and SA terminated macroradicals in the SAN copolymerization. The following were obtained: $k_A/k_S = 0.12 \pm 0.03$ for 2-propionitrile, and $k_A/k_S = 0.15 \pm 0.03$ for 2-(4-phenyl)butyronitrile. These results are consistent with the penultimate model treatment of the SAN copolymerization by Hill et al. (53), and show that k_A/k_S for an α-cyanoalkyl radical is relatively insensitive to the introduction of a γ-phenyl group. This was similar to what had been observed previously for primary radicals (57) (see Figure 1.4, p. 17).

C. Alkyl radical-alkene addition reactions

The addition of alkyl radicals to alkenes has been studied extensively (59-64). Rate constant data for the liquid phase addition reactions of carbon-centered free radicals - both "small" and polymeric - have been compiled (1). That compilation offers mainly relative rates of addition of various alkenes to alkyl, aryl, vinyl, and acyl radicals, although some absolute rate data may be found. Included is a selection of more carefully determined propagation rate constants for homopolymerization, although relative rate constants from copolymerization studies (ie., reactivity ratios) have been omitted (these are compiled in refs. 11 and 65). Recently, absolute rate constants for the liquid phase reactions of t-butyl radical with 24 substituted ethenes of widely varying structure have been measured (64). For rate data pertaining to radical addition reactions in the gas phase, the reader is referred to a compilation by Kerr and Parsonage (66).

In 1983 Giese published an elegant review (63) of the formation of CC bonds by addition of free radicals to alkenes, presenting an analysis of rate and orientation of addition in terms of polar and steric effects, and showing that variations in reactivity and selectivity can be rationalized using frontier molecular orbital theory. Some important generalizations and conclusions from this work will be reiterated here; as a fairly complete (yet concise) bibliography was compiled by Giese, only some selected works will be referenced in the following. In regard to nomenclature, the β position of an alkene refers to the olefinic carbon which is not attacked by the radical in an addition reaction.

There is ample evidence that alkyl radicals are of a nucleophilic character. Measurement of absolute and relative rates of alkene addition (64, 67-71) demonstrate that olefins with electron-poor π systems (eg., acrylic monomers) add more rapidly than those with electron rich systems (eg., butadiene and styrene). In a study of the effect of β alkene substituents, Giese correlated relative rate data with Hammett σ-parameters for several systems, and obtained positive ρ values in all cases (63). The plots showed only relatively small deviations from linearity for the cases of radical-stabilizing and space filling groups, which led Giese to conclude that alkene β-substituents exert mainly polar effects on the rate of addition of free radicals.

Studies by Giese on the addition of 1,2-disubstituted alkenes to cyclohexyl radical led to the conclusion that α-substituents (groups attached to the olefinic carbon that is attacked)

exert both polar and steric effects on the rate of addition. The steric effects of α-substituents, and absence of β steric effects, can be rationalized in terms of a transition state that places the attacking radical near to α but far from β substituents.

The preferred attack of radicals at the lower alkylated carbon atom of alkenes is sometimes explained in terms of the differences in stability of the newly formed radical centers. Based on the results of several studies, Giese concluded that this is not a convincing argument, and concurred with Walling (59), Ruchardt (61), and Tedder et al. (60, 62) in pointing out the dominant influence of steric parameters on the regioselectivity of free radical addition.

The gradation in selectivity and reactivity of primary, secondary, and tertiary alkyl radicals is interesting. Tertiary radicals are found to be more reactive and more selective than secondary and primary radicals (68, 72-74). In general, substituents at the radical center exert both polar and steric effects on the rate of alkene addition, and the effects of radical-stabilizing substituents are relatively small unless the substituents can exert a strong stabilizing influence (eg., a phenyl group, leading to a reduced rate of addition) (63). Giese has offered an explanation (63) for this behavior based on frontier molecular orbital theory (FMO) (75), in accord with the existence of an early transition state for the exothermic addition reactions of nucleophilic alkyl radicals and alkenes. Interactions between the singly occupied orbital (SOMO) of the radical and the lowest unoccupied orbital (LUMO) of the alkene are considered. The introduction of electron donating groups on the radical is seen to lower the difference in energy between the SOMO and LUMO, and the rate of reaction increases owing to better frontier orbital interaction. Corresponding increases in selectivity are thus understood in terms of *relative* SOMO-LUMO energy differences. For reaction with given alkenes of differing LUMO energies, the relative energy differences - and hence relative reaction rates - will be greater the more closely matched the absolute energies of the SOMO and LUMO's become. Put another way, the effect of alkene substituent variation increases with increase of the reactivity of the alkenes.

Most of the conclusions made by Giese in his review were based on studies of the relative rates of addition of alkenes. Munger and Fischer (64) have recently determined absolute rates of addition, and temperature dependencies thereof, of a wide variety of olefins to the t-butyl radical. These authors agreed with Giese's conclusions, and were able to put many of them on a more quantitative basis through various correlations of rate, activation energy, alkene electron affinity, and radical ionization potential. An important result of this work was the linear

dependence of activation energy on substrate electron affinity that was demonstrated for the addition of t-butyl radicals to mono- and 1,1-disubstituted olefins, a correlation that Munger and Fischer expected on the basis of FMO theory.

Two methods for the measurement of the relative rates of addition of alkenes to alkyl radicals are now discussed; these methods were used in investigations reported within.

1. Reduction of alkylmercuric halides

Giese has described (71, 76) the method pictured schematically in Scheme 1.4 (p. 22) for the determination of relative rate constants; this will be hereafter referred to as the "mercury method." The radicals are generated in the presence of a large excess of olefin by reaction of an alkylmercuric halide (or acetate) with $NaBH_4$. A radical thus produced adds a molecule of olefin to make an adduct radical, which subsequently abstracts a hydrogen atom from organomercuric hydride present as an intermediate in the chain reaction. This sequence of events happens because of the very different selectivity that the first formed alkyl radical has for olefin and hydrogen donor as compared to the adduct radical (71). Accordingly, the two types of radicals should be of different structure; typically, the first formed radical is a simple hydrocarbon while the adduct radical has α-substituents derived from common monomers (eg., phenyl, carboxyalkyl, cyano). The molar ratio of the final adducts in the reaction mixture is usually determined by gas or liquid chromatography, allowing calculation of the rate constant ratio.

The accepted mechanism of the reaction is shown in Scheme 1.5 (p. 23). The mechanism of the formation of the alkyl radical that initiates the chain reaction is unknown.

A free-radical mechanism was first implicated for the reduction of RHgX to RH when Pasto and Gontarz (77) observed loss of stereochemistry in the $NaBD_4$ reductions of erythro- and threo-3-hydroxy-2-butylmercuric acetate. Gray and Jackson (78) studied the $NaBH_4$ reductions of the substituted norbornenyl and nortricyclyl compounds shown in Scheme 1.6 (p. 24), obtaining the same products and distribution thereof for each. This led Gray and Jackson to suggest the equilibrium between the radical species shown also in Scheme 1.6. Whitesides and San Filippo (79) investigated the tri-n-butyltin hydride (Bu_3SnH) reduction of the analogous alkyl chlorides (ie., Cl in place of HgCl) and obtained a nearly identical result; the reduction of alkyl chlorides with Bu_3SnH is known to proceed by a free radical mechanism (80).

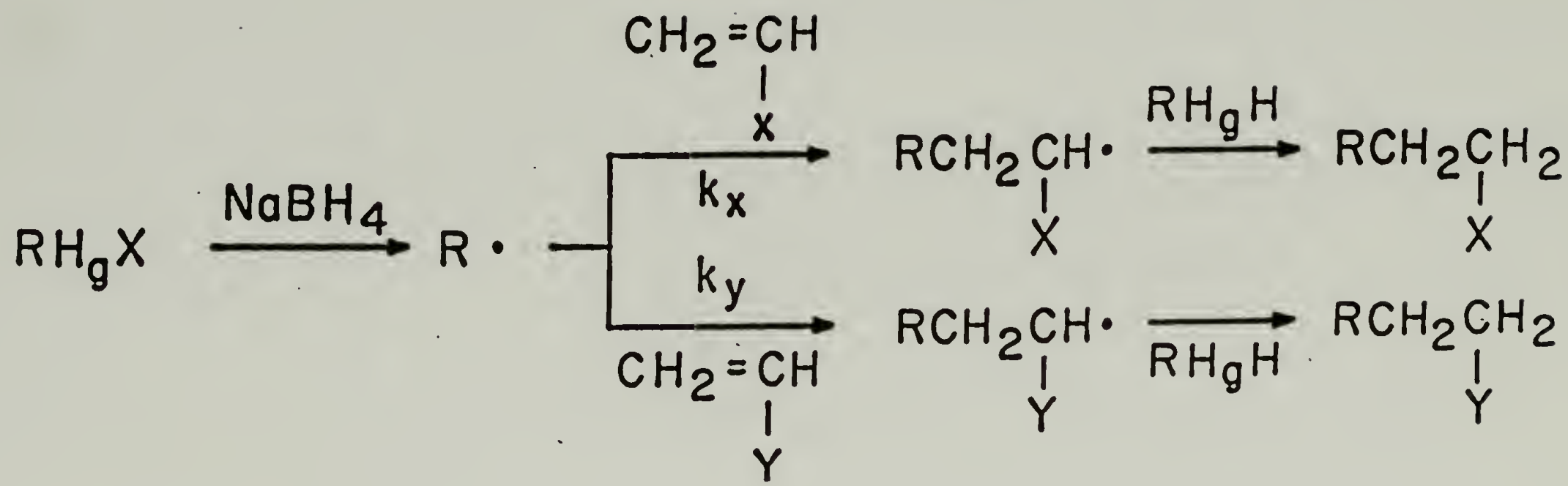

Scheme 1.4. The "mercury method" for the determination of relative rates of addition of monomers to alkyl radicals.

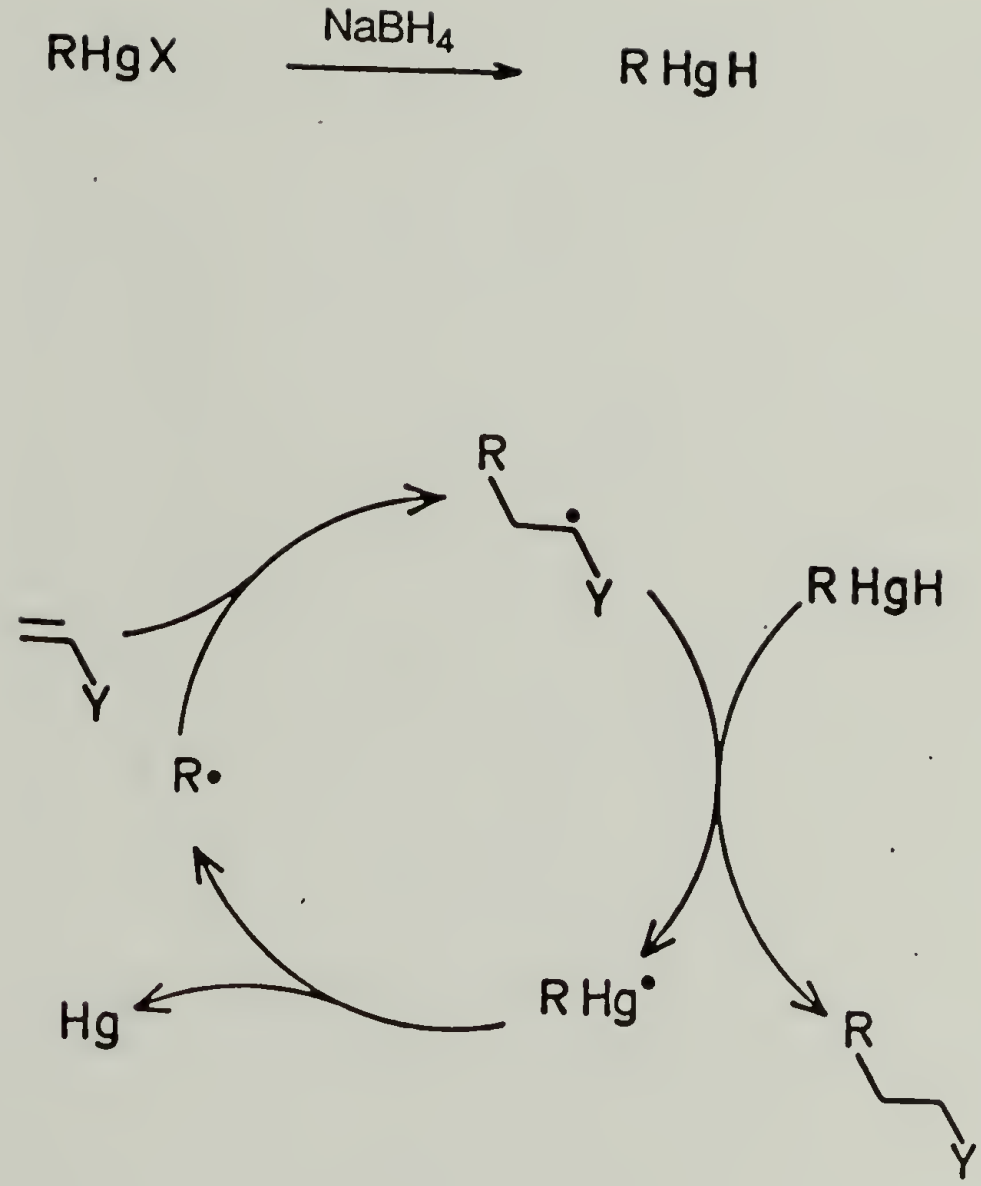

Scheme 1.5. The mechanism of mercury method reactions.

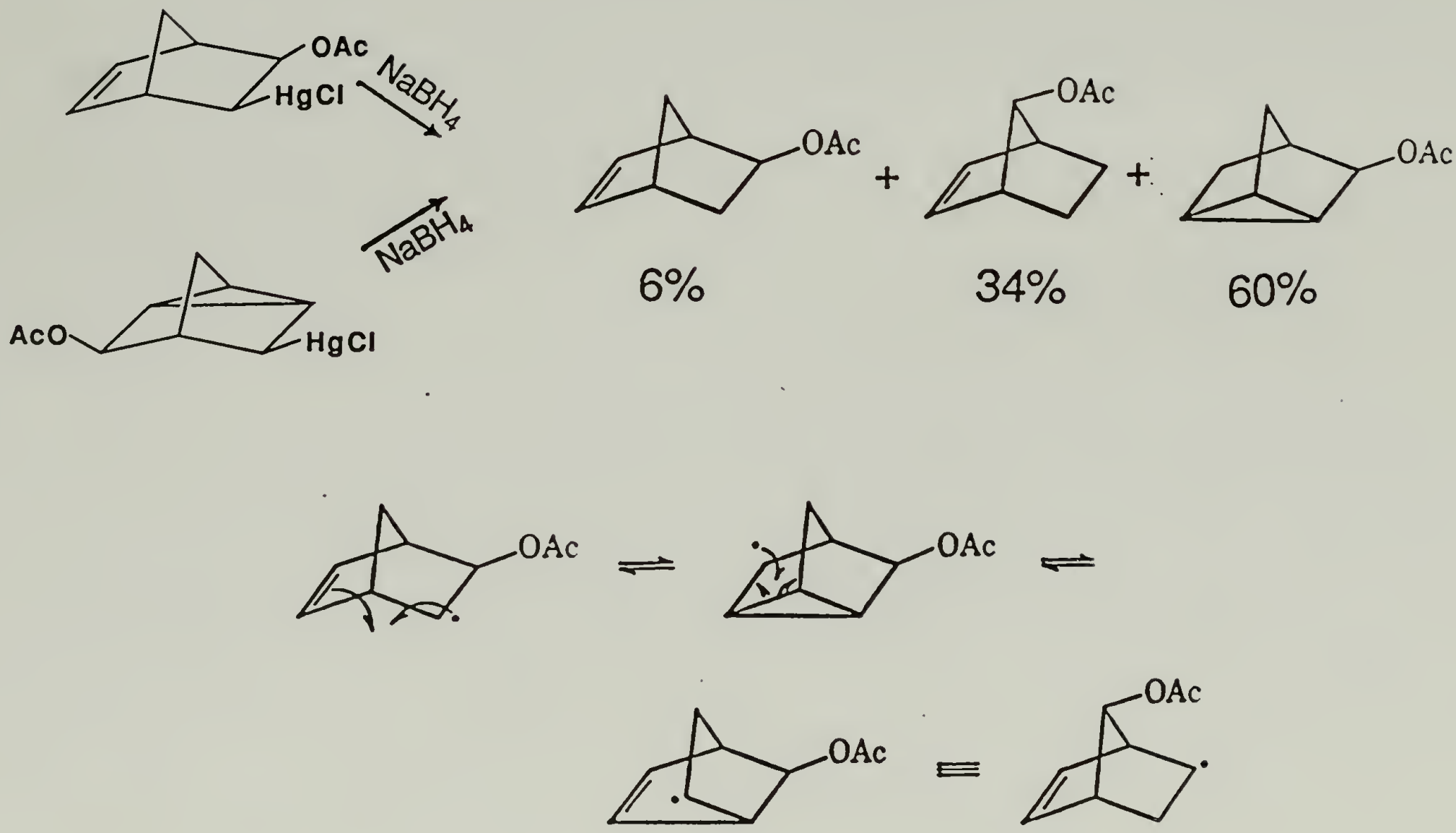

Scheme 1.6. Reduction of substituted norbornenyl and nortricyclyl compounds (78).

Whitesides and San Filippo (79) also studied many other substrates in confirming a free radical mechanism. They investigated the possibility of carbocationic intermediates, using substrates (eg., neophylmercuric bromide) that would give rearranged products characteristic of such an intermediate if present. No such products were found. Also, the reduction of endo- and exo-2-norbornylmercuric bromides with $NaBD_4$ were found to give identical product distributions of endo- and exo-norbornane-d, irrespective of the stereochemistry of the starting material. The high amount of deuterium incorporation in the products, even for reaction in tetrahydrofuran-water, excluded the possibility of an anionic intermediate. The product distributions for the norbornyl reactions were found to be identical whether $NaBH_4$ or a number of other hydrides (or deuterides), such as Bu_3SnH and diethylaluminum hydride, were used. Based primarily on this, Whitesides proposed that the in-situ produced RHgH was delivering the hydrogen atom to the radical Although an alkylmercuric hydride has never been isolated, there now exists some good kinetic evidence (81-83) for the existence of such a species and its role in the reaction as hydrogen donor. Some final evidence mentioned here is the observation of the products expected of a non-caged, free radical chain mechanism when alkylmercuric halides are reduced in the presence of radical traps such as molecular oxygen (84) or nitroxides (79).

2. Carbon-13 enriched free radical initiators

Bevington and coworkers have reported the use of ^{13}C enriched azobis(isobutyronitrile) (AIBN) in a series of investigations of the reactivity of the 2-methyl-2-propionitrile radical (85). They describe a simple but quite useful method for the determination of relative rate constants, wherein the radical to be studied is generated by thermolysis or photolysis of a ^{13}C enriched azo compound in the presence of known amounts of two monomers. The ^{13}C enriched primary radical thus produced adds one or the other of the monomers, and the reaction proceeds to give copolymer which then contains two ^{13}C enriched end groups of chemically distinct structure according to the identity of the monomeric units adjacent to the initiator fragment. The copolymer is isolated from low molecular weight impurities, such as those produced from combination and disproportionation of the primary radicals, and ^{13}C NMR spectra are recorded under conditions suitable for quantitative signal integration. Intense signals arising from the enriched carbons in the end groups are seen, assuming that the polymer is not of exceedingly high molecular weight. If the site of enrichment of the initiator has been properly chosen, and

a sufficiently powerful NMR spectrometer is used, different chemical shifts for signals from the different end groups will be observed. Integration of the signals then gives the relative amounts of the end groups and allows a simple calculation of the rate constant ratio for addition, assuming that the conversion of the copolymerization was held to values low enough to have kept the monomer feed ratio relatively constant during the reaction.

This method assumes the unimportance of primary radical chain-termination reactions, as well as chain-transfer reactions involving the initiator and leading to the incorporation of ^{13}C enriched sites in the polymer. For copolymerization of monosubstituted olefins, there is also the assumption that the initiating radical adds the monomers in a "head-to-tail" fashion. However, the presence of a significant amount of chain structures resulting from these processes may be obvious, as the chemical shifts of signals arising from the initiator fragments may be quite different from those expected on the basis of simple head-to-tail addition. For example, in this way Bevington et al. (86) observed a significant amount of endgroups resulting from head-to-head addition of the 2-methyl-2-propionitrile radical to vinyl acetate or vinyl formate, but no such evidence for head addition was found in the case of styrene or methyl methacrylate. The result concerning styrene is consistent with that obtained by Moad (87) in a similar study.

The photolysis of azoalkanes has been used as a convenient source of alkyl radicals in many studies of their rates and reactions. Radicals produced by irradiation of azoalkanes at 366 nm behave as thermally equilibrated free radicals (88), which is of great importance if one wishes to use them as models for growing copolymer chains. Use of higher energy radiation (λ = 200 nm) can result in the formation of vibrationally excited radicals (89).

The behavior of azo compounds in response to irradiation is an interesting subject. While diaryl azo compounds generally undergo only trans-cis isomerization, decomposition usually results for dialkyl or alkyl-aryl ("mixed") azo compounds, in addition to isomerization (90). The mechanism of decomposition of several mixed azo compounds, as depicted in Scheme 1.7 (p. 27), has been well established through stereochemical, CIDNP, and kinetic investigations (91). Photolysis results in a thermally unstable cis-isomer, and dissociation of the alkyl C-N bond occurs to give a phenyldiazenyl radical, followed by a rapid loss of N_2.

The exact mechanism of the photodecomposition of dialkyl azo compounds is still uncertain, although it appears that it may depend on the particular compound and conditions under investigation (90). A concerted mechanism for loss of N_2 in which C-N bonds are broken

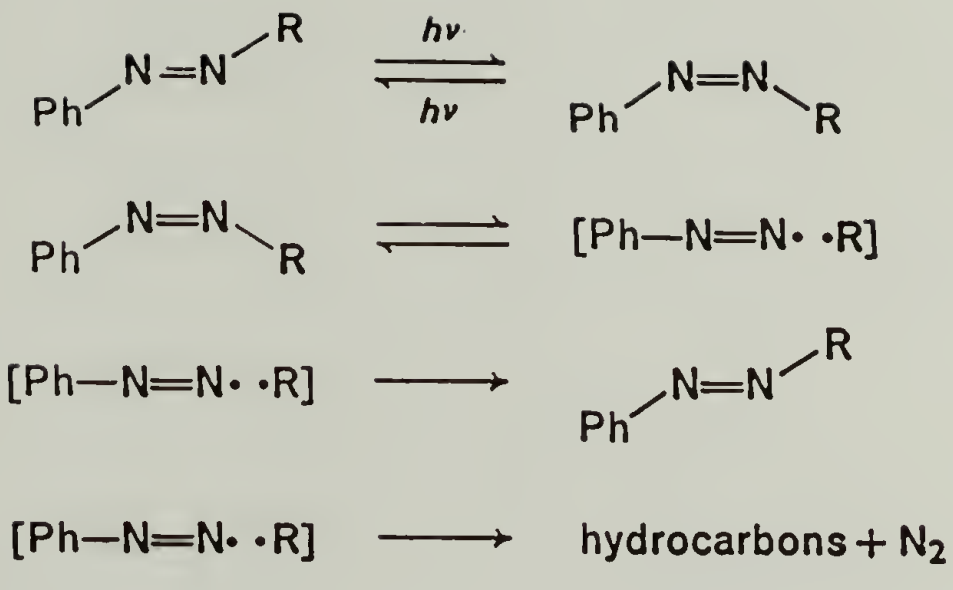

Scheme 1.7. Mechanism of decomposition of mixed azo compounds (90).

simultaneously cannot be ruled out, as alkyldiazenyl radicals have in general proved to be elusive species. However, good evidence exists for such a radical in at least one case. In a CIDNP study of 1-norbornyl-azo-2-(2-phenyl)propane (ie., the azoalkane which decomposes to give norbornyl and cumyl radicals), Green et al. (91) have shown the cis thermal mechanism of Scheme 1.7 to be operative, wherein the 1-norbornyldiazenyl radical is produced. A number of investigations (91-93) of the photodecomposition of AIBN have produced conflicting results. In a 1975 review (90) of the situation in regard to azoalkane photolysis, Drewer made the interesting remark that perhaps a two-step loss of N_2 is characteristic of the cis thermal mechanism while the concerted loss occurs with true photodissociation.

D. General description of experiments

Most of the investigations described within were prompted from the results of earlier investigations from the author's laboratory (directed by D.A. Tirrell), work which has already been discussed. The results from the γ-substituent effect experiments (Fig. 1.4, p. 17) provided the motivation for the experiments outlined in Scheme 1.8 (p. 30), which make use of Giese's mercury method. Gas chromatography is used to determine the relative amounts of the adducts produced in the reactions. These experiments sought to determine if different selectivities would be observed for a primary alkyl radical bearing ε-phenyl and ε-cyano substituents, as was observed for the analogous γ substituted radicals. The experiments might show whether an "antepenultimate effect" is physically plausible for copolymerization of monosubstituted olefins, for an effect on chain reactivity by the nature of the third-to-last monomeric unit (ie., the antepenultimate unit) would correspond to an ε-substituent effect.

The γ-substituent effect experiments of Jones and Prementine (57) provided evidence for the existence of a penultimate unit effect in SAN copolymerization. However, one can hardly expect primary alkyl radicals to be realistic models of SAN macroradicals. The former do not bear the α-phenyl and α-cyano substituents present in the macroradicals, and these substituents would be expected to be major influences in regard to selectivity. This provided motivation for the experiments outlined in Scheme 1.9 (p. 31), using ^{13}C enriched azo initiators to generate the radicals 2a, 2b, and 2c, which all bear α-phenyl groups. The relative rates of addition of styrene and acrylonitrile (k_S/k_A) are determined via ^{13}C NMR endgroup analysis of the copolymers, according to the method described in the preceding section. The k_S/k_A values obtained for 2b and 2c should be directly comparable to the best-fit penultimate model reactivity ratios of Hill et al. (53) for SS and AS terminated chains. Comparison of k_S/k_A for 2b and 2c with that obtained for 2a should help ascertain if any observed differences in selectivity can be attributed to the presence of one - or both - of the γ-substituents.

The relative rates of addition of methyl methacrylate and acrylonitrile to 2a are also determined by the ^{13}C NMR method, and these experiments are outlined in Scheme 1.10 (p. 32). There was no particular motivation for this work, other than to simply gather fundamental information.

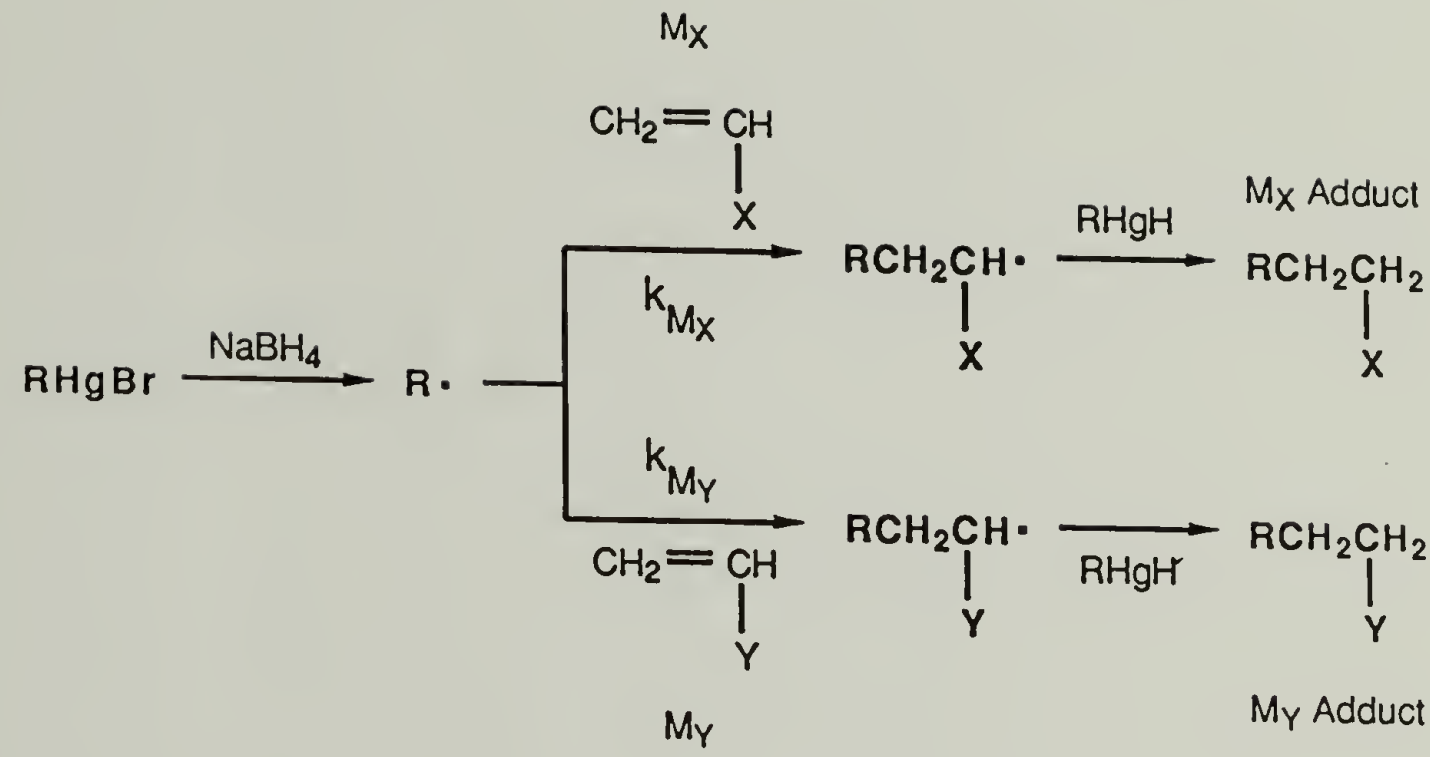

X , Y = C_6H_5 , CN , CO_2CH_3

M_X , M_Y = styrene (S) , acrylonitrile (A) , methyl acrylate (MA)

R = 5-phenylpentyl, 5-cyanopentyl

Scheme 1.8. Mercury method experiments.

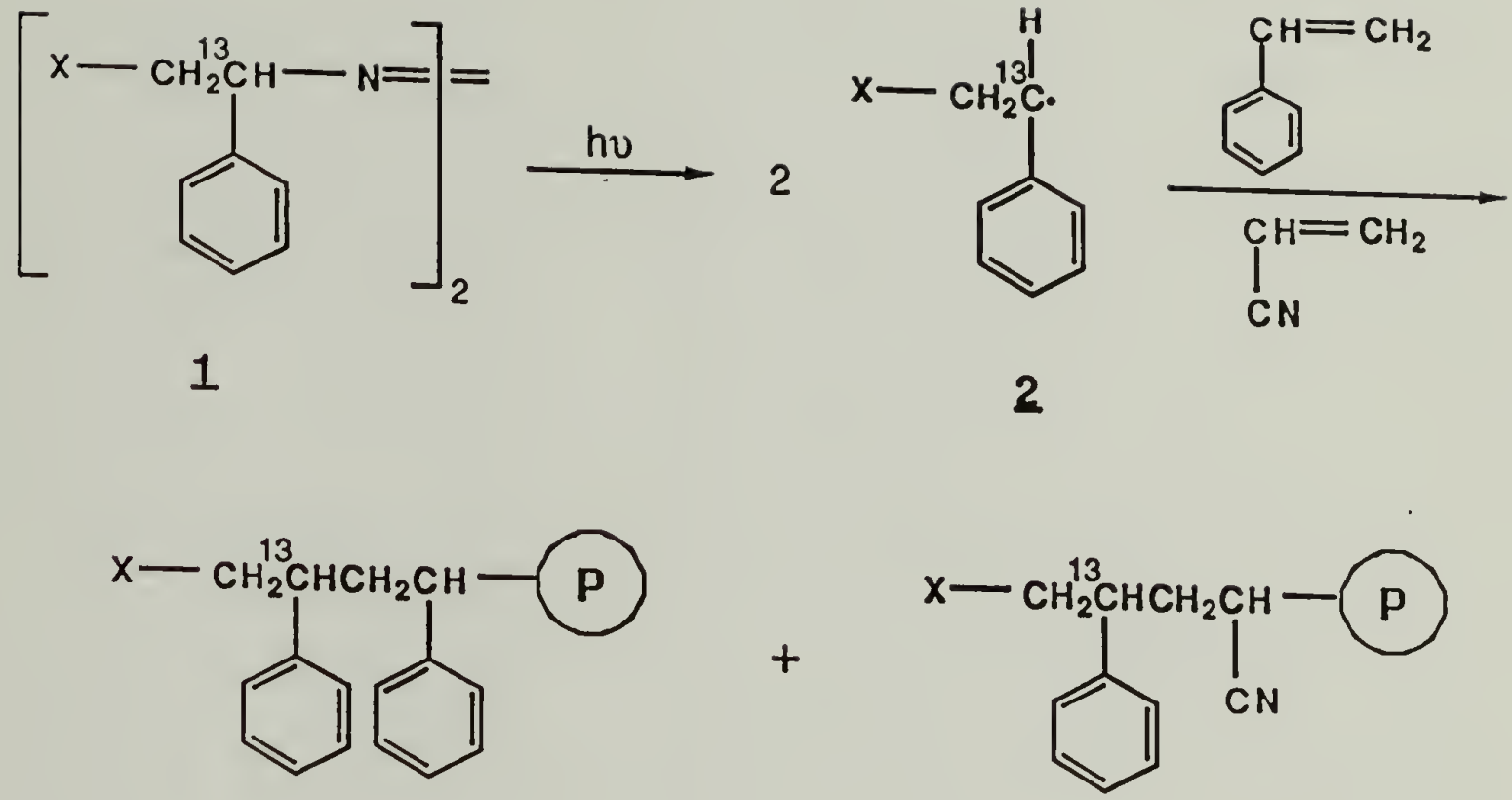

(P) = copolymer chain

a : X = H

b : X = CH_2–C$_6$H$_5$

c : X = CH_2CN

Scheme 1.9. Use of ^{13}C-enriched azoalkanes **1a-c** as polymerization initiators to produce SAN copolymers containing enriched end-groups **3a-c** and **4a-c**.

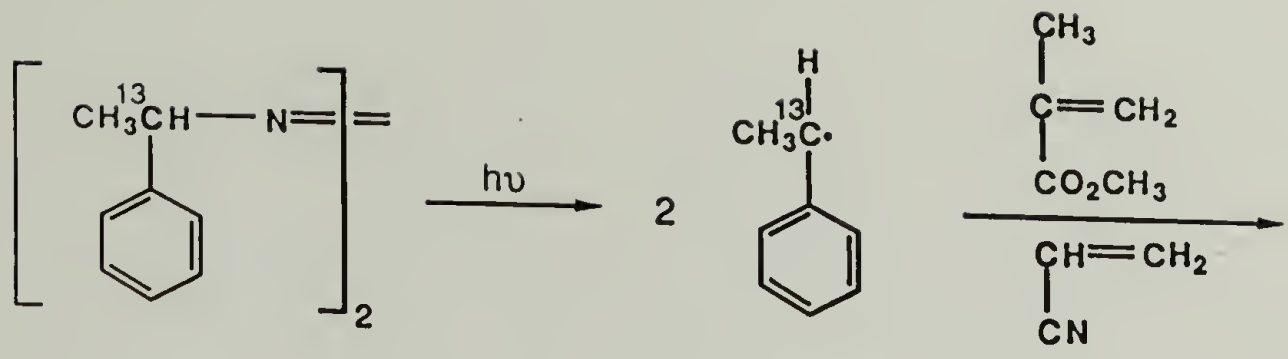

1a

2a

5

6

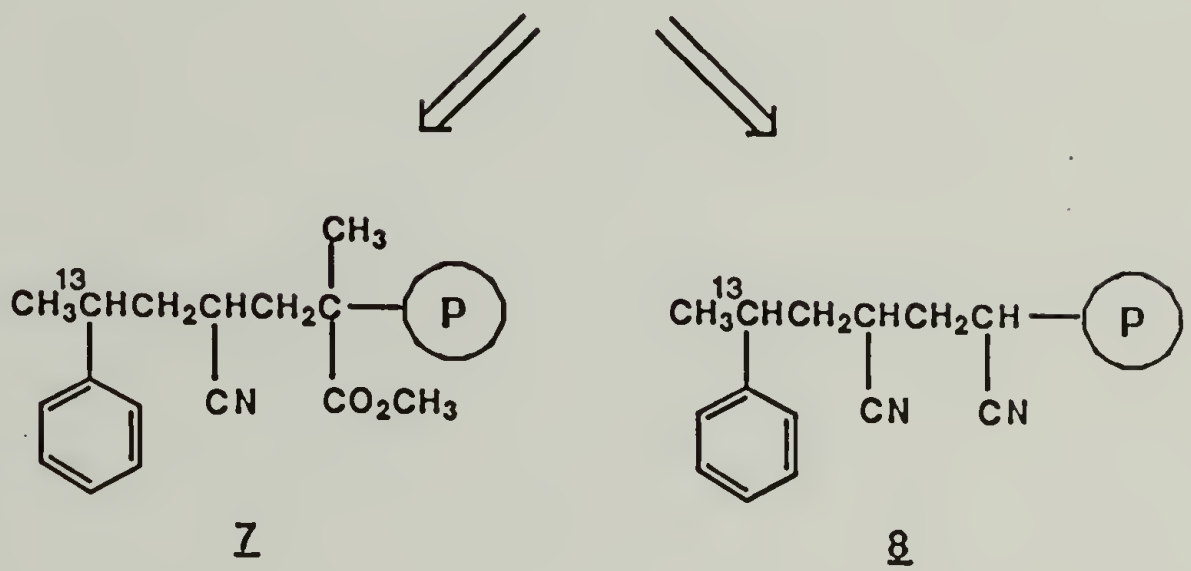

7

8

P = copolymer chain

Scheme 1.10. Use of 1,1'-azobis(1-phenyl[1-^{13}C]ethane) (**1a**) as polymerization initiator to produce AMMA copolymers containing enriched end-groups 5-8.

CHAPTER II

EXPERIMENTAL

A. Materials

All solvents and reagents used in this work are listed below. They were used as received from the specified sources unless otherwise stated. Purification procedures that begin with the phrase "for dry" are only meant to apply to preparations which call for the "dry" material. Distillation temperatures are uncorrected. The format used is as follows:

Name (name abbreviation, and/or psuedonym), grade and/or minimum purity, source abbreviation, purification procedure

Acetic acid, glacial, **F**

[1-^{13}C]Acetic acid, 99 atom % ^{13}C, **S**

Acetone-d_6, 99 atom % D, **A**

Acetophenone, 99%, **A**

Acrylonitrile, 99%, **A**, freshly distilled from CaH_2 under N_2 - b.p. 77 °C

Aluminum chloride, anhydrous 99%, **A**

Barium ^{13}C-carbonate, 99 atom % ^{13}C, **A**

Benzene, spectrophotometric 99%, **A**, for dry - distilled from $LiAlH_4$ under N_2 - b.p. 80 °C

Benzoyl chloride, 99%, **A**

Borane-methyl sulfide complex, 10.0-10.2 M BH_3, **A**

Borane-tetrahydrofuran complex, 1 M BH_3 in THF, **A**

Bromobenzene, 99%, **A**

Bromobenzene-d_5, 99 atom % D, **A**

8-Bromooctanoic acid, 98%, **A**

5-Bromo-1-pentene, 97%, **A**

(2-Bromoethyl)benzene, 98%, **A**, distilled - b.p. 60 °C/1 mm Hg

1-Bromo-3-phenylpropane, 95%, **A**, distilled - b.p. 60 °C/1 mm Hg

Cadmium chloride, anhydrous 99%, **A**

Calcium chloride, anhydrous, **F**

Calcium hydride, 95%, **A**

Chloroform, HPLC grade 99.9%, **A**, for dry - distilled from CaH_2 under N_2 - b.p. 61 °C

Chloroform-d, 99.6 atom % D, **A**

Cyclohexane, 99%, **A**

Cyclohexene, 99%, **A**

Deuterium oxide, 99.8 atom % D, **A**

Dichloromethane (methylene chloride), spectrophotometric grade 99%, **A**

Dichloromethane-d_2, 99.6 atom % D, **A**

Diglyme (1,2-dimethoxyethane, ethylene glycol dimethyl ether), 99%, **A**

Diglyme-d_{14}, 99 atom % D, **S**

N,N-Dimethylformamide (DMF), HPLC grade 99.9%, **A**

N,N-Dimethylformamide-d_7 (DMF-d_7), 99 atom % D, **A**

Dimethyl sulfoxide (methyl sulfoxide, DMSO), HPLC grade 99.9%, **A**

Dimethyl sulfoxide-d_6(DMSO-d_6), 99 atom % D, **A**

95% Ethanol (ethyl alcohol), practical grade, **F**

Ethanol (ethyl alcohol), absolute, **F**, for dry - distilled from sodium under N_2 - b.p. 78 °C

Ether (diethyl ether), practical grade, **F**

Ether (diethyl ether), anhydrous, **M**

Ethylene oxide, 98%, **F**

Ethyl formate, 97%, **A**, distilled under N_2 - b.p. 52 °C

Ethyl 3-phenyl-3-ketopropionate (ethyl benzoyl acetate), 97%, **A**, distilled - b.p. 90 °C/1 torr

Hexane, HPLC grade 95%, **A**

Hydrazine, anhydrous, **A**

Hydrazine hydrate, hydrazine content 64 % (w/w), **A**

Hydrochloric acid, 38% HCl, **F**

Iodine, reagent grade, **F**

Isopropanol, practical grade, **F**

Lithium aluminum hydride, 95%, **A**

Magnesium, 99%, **F**

Magnesium sulfate, anhydrous, **M**

Mercuric acetate, 98%, **Af**

Mercuric bromide, 98%, **A**

Mercuric oxide, yellow 99%, **A**

Methanol (methyl alcohol), spectrophotometric grade 99.9%, **A**

Methyl acrylate, 99%, **A**, freshly distilled from CaH_2 under N_2 - b.p. 80 °C

Methyl methacrylate, 99%, **A**, freshly distilled from CaH_2 under N_2 - b.p. 100 °C

N-Methyl-N-nitroso-p-toluenesulfonamide (Diazald), 99%, **A**

Nonanedinitrile (azelanitrile), 95%, **A**, distilled - b.p. 130 °C/1 mm Hg

5-Phenyl-1-pentanol, 99%, **A**

Phosphorous tribromide, 99%, **A**

Phthalic anhydride, 99%, **A**

Platinum oxide monohydrate, 99.99%, **A**

Potassium bromide, IR grade 99%, **A**

Pyridine, anhydrous 99%, **A**

Silica gel, Kieselgel 60 230-400 mesh, **Me**

Sodium, lump in oil 99%, **A**

Sodium bicarbonate, 98%, **F**

Sodium borohydride, 99%, **A**

Sodium bromide, 99%, **F**

Sodium carbonate, 99%, **F**

Sodium chloride, 99%, **F**

Sodium cyanide, 98%, **F**

Sodium hydroxide, 97%, **F**

Styrene, 99%, **A**, freshly distilled from CaH_2 under N_2 - b.p. 40 °C/15 mm Hg

Sulfuric acid, 95%, **F**

Sulfuryl chloride, 97%, **A**, distilled under N_2 - b.p. 68 °C

Tetrahydrofuran (THF), HPLC grade 99.9%, **A**

Tetramethylsilane (TMS), NMR grade 99.9%, **A**

Thionyl chloride, 99%, **A**

Toluene, anhydrous 99%, **A**

p-Toluenesulfonyl chloride (TsCl), 98%, **A**, recrystallized from hexane - m.p. 92 °C

Triethylamine, 99%, **A**, distilled from CaH_2 under N_2 - b.p. 89 °C

Sources

A - Aldrich Chemical Company

F - Fisher Scientific

M - Mallinkrodt

Me - E. Merck

S - Stohler/KOR Stable Isotopes

B. Methods

The experimental procedures used to prepare polymers and compounds of low molecular weight are included in this section. With regard to data given in procedures for azo compounds and precursors thereof, in all cases the melting or boiling point of a natural-abundance compound was identical to that of the corresponding ^{13}C enriched compound. Spectral data given at the end of procedures do not include solvent signals (where applicable) or, in some cases, signals believed to arise from impurities. No signals attributed to impurities were observed in the spectra of the azo compounds **1a, 1b,** and **1c,** however, with the exception of those from small amounts of water. Frequencies of IR absorption are correct to within $\pm$ 10 cm^{-1} and wavelengths of UV absorption are correct to within $\pm$ 1 nm. ^{1}H NMR chemical shifts are correct to within $\pm$ 0.03 ppm for spectra recorded at 200 and 300 MHz and to within $\pm$ 0.1 ppm for spectra recorded at 60, 80, and 90 MHz. ^{13}C NMR chemical shifts are correct to within $\pm$ 0.03 ppm. ^{1}H NMR, ^{13}C NMR, and IR spectra of azo compounds and their precursors are found in Appendix A (p. 142). The order of these spectra in Appendix A is the same order in which the corresponding data occur in the procedures.

A Rayonet Model RMR 400 photochemical reactor fitted with four 350-nm lamps was used for the preparation of homo- and copolymers. For polymerizations at 33 °C, the temperature was maintained by blowing a stream of air through the reactor (to partially dissipate the heat generated by the lamps) at a rate such that an equilibrium temperature of 33 $\pm$ 1 °C was obtained. For polymerizations at temperatures other than 33 °C, a hot or cold water bath contained in a glass beaker was used. It was necessary to adjust the temperature of such a bath about every 5 minutes in order to maintain a given temperature within $\pm$ 2 °C. Conversions were calculated for the polymerizations in each case from the total weight of monomer and the weight of dried polymer obtained upon the first precipitation.

Abbreviations used in the procedures given below include "h" for hour(s), "min" for minute(s), "ml" for milliliter(s), "l" for liter(s), "g" for gram(s), "mg" for milligram(s), "mmol" for millimole(s), "mp" for melting point, "bp" for boiling point, "DMF" for N,N-dimethylformamide, and "DMSO" for dimethyl sulfoxide.

1. **Preparation of alkylmercuric bromides and precursors thereof**

(a) 1-Bromo-5-phenylpentane. 5-Phenyl-1-pentanol (25 g, 152 mmol) contained in a round-bottom flask was cooled to -5 °C. Phosphorous tribromide (7.2ml, 76 mmol) was added dropwise with stirring over a period of 2.5 h. The solution was then allowed to warm to room temperature and stirring was continued overnight. At the end of this time the solution was poured slowly into 50 ml ice-water and the organic layer was separated. The crude product thus obtained was successively washed with 3 x 10 ml ice-cold concentrated H_2SO_4 , 3 x 10 ml saturated aqueous $NaHCO_3$, and 2 x 10 ml H_2O. After drying over $CaCl_2$ overnight the crude product was subsequently distilled (bp 99-101.5 °C/ 1.5 mm Hg) to yield 20.9 g (61%) of 1-bromo-5-phenylpentane as a clear, colorless liquid. ^1H NMR (60 MHz, $CDCl_3$) δ: 1.6 (m, 6H), 2.6 (t, 2H), 3.4 (t, 2H), 7.2 (br s, 5H).

(b) 5-Phenyl-1-pentylmagnesium bromide and 3-phenyl-1-propylmagnesium bromide. To 3 g (123 mmol) Mg in 25 ml anhydrous ether was added 1 ml of the required alkyl bromide (either 1-bromo-5-phenylpentane or 1-bromo-3-phenylpropane) and a few crystals of iodine. After 15 min the reaction had initiated and the remaining alkyl bromide (120 mmol total were added, including that used to initiate the reaction) in 50 ml of anhydrous ether was added dropwise over a period of 20 min. After the addition was complete, the reaction was refluxed under N_2 for 1 h and then allowed to stand at room temperature under N_2 overnight. At the end of this time the unreacted Mg had settled to the bottom. The clear solution was then transferred under N_2 via a double-tipped needle into a septum-capped round-bottom flask which had been previously flushed with N_2. In this way, 65 ml of an approximately 1.6 M solution of either 5-phenyl-1-pentylmagnesium bromide or 3-phenyl-1-propylmagnesium bromide was obtained.

(c) 5-Phenyl-1-pentylmercuric bromide. To 65 ml of a 1.6 M solution (104 mmol) of 5-phenyl-1-pentylmagnesium bromide in ether was added 43 g (120 mmol) $HgBr_2$ over a period of 45 min. The reaction was done in a 250-ml 3-neck round-bottom flask under N_2 with stirring. After the addition was complete, the reaction was refluxed for 1.5 h, cooled to room temperature, and 20 ml water was added very slowly. The ether layer was then separated, washed three times with 15 ml portions of 2 N HCl, and dried over $MgSO_4$. The ether was subsequently removed on a rotary evaporator and the resulting solid was recrystallized twice from cyclohexane. After drying in vacuo, 28.9 g (65%) 5-phenyl-1-pentylmercuric bromide was obtained as a white, crystalline solid; mp 52-53 °C. Anal. calcd. for $C_{11}H_{15}HgBr$: C, 30.95%; H

3.54%. Found: C, 30.69%; H, 3.49%. ^{1}H NMR (300 MHz, $CDCl_3$) δ: 1.42 (m, 2H), 1.64 (m, 2H), 1.77 (m, 2H), 2.04 (t, 2H), 2.59 (t, 2H), 7.22 (m, 5H). IR (melt) cm^{-1}: 3030, 2930, 2860, 1600, 1500, 1460, 1180, 1140, 750, 700.

(d) 5-Hexenenitrile. 5-Bromo-1-pentene (31.75 g, 213 mmol) was added dropwise over 20 min to a stirred suspension of 11.66 g (238 mmol) NaCN in 135 ml DMSO at 60 °C. The temperature was maintained at 60 °C throughout the addition. After the addition was complete, the solution was stirred at 60 °C for an additional 2 h and then taken briefly to 90 °C before cooling to room temperature. The reaction mixture was diluted with H_2O to a volume of 500 ml and extracted with three 100 ml portions of ether. The combined ether extracts were washed successively with 75 ml 2 N HCl, 100 ml saturated aqueous $NaHCO_3$, and 100 ml H_2O. After drying over $MgSO_4$ and removal of the ether, the crude product was obtained as a yellow liquid and distilled (bp 165-166 °C) to afford 14.1 g (70%) of 5-hexenenitrile as a clear, colorless liquid. ^{1}H NMR (200 MHz, $CDCl_3$) δ: 1.76 (m, 2H), 2.22 (m,2H), 2.34 (t, 2H), 5.10 (m, 2H), 5.75 (m, 1H). IR (neat) cm^{-1}: 3090, 2940, 2250, 1640, 1430, 990, 920.

(e) 5-Cyano-1-pentylmercuric bromide. To 41.1 ml 1 M BH_3 in THF at 0 °C was added dropwise 6.75 g (82 mmol) cyclohexene in 40 ml THF. The mixture was stirred for 75 min at 0 °C and allowed to warm to room temperature, after which 3.90 g (41 mmol) of 5-hexenenitrile in 40 ml THF was added all at once. After stirring the mixture at room temperature overnight, 13.1 g (41 mmol) of mercuric acetate was added. The reaction was stirred for 15 min and then poured into 100 ml of ice-water. To this mixture was added 49 ml of an aqueous 1 M solution (49 mmol) of NaBr with stirring. The precipitate which resulted was filtered and washed with several 50 ml portions of H_2O. This crude product was purified by successive recrystallizations from DMF, absolute ethanol, and cyclohexane. Finally obtained as a white, crystalline solid was 5.87 g (38%) of 5-cyano-1-pentylmercuric bromide; mp 102-104 °C. Anal. calcd. for $C_6H_{10}NHgBr$: C, 19.13%; H, 2.67%; N, 3.72%. Found: C, 19.31%; H, 2.64%; N, 3.54%. ^{1}H NMR (300 MHz, $CDCl_3$) δ: 1.56 (m, 2H), 1.72 (m, 2H), 1.85 (m, 2H), 2.11 (t, 2H), 2.37 (t, 2H). IR (melt) cm^{-1}: 2930, 2860, 2250, 1460, 1430, 1140, 890, 810, 680.

2. Preparation of adducts and precursors thereof

(a) 1,7-Diphenyl-4-heptanol. A solution of 4.1 ml (50 mmol) ethyl formate in 25 ml anhydrous ether was added dropwise over a period of 45 min to 63 ml of a 1.6 M solution (100 mmol) of 3-phenyl-1-propylmagnesium bromide in ether (prepared as described previously).

The reaction was done under a N_2 atmosphere and was magnetically stirred during the addition. After the addition was complete, the reaction was refluxed for 0.5 h. At the end of this time the solution was cooled to room temperature, 70 ml 2 N aqueous HCl was added, and the product was extracted with 3 x 50 ml ether. The combined ether extracts were dried over $MgSO_4$ and the ether subsequently removed to leave an oily residue, which was vacuum distilled (bp 185 °C/2 mm Hg) to yield 6.52 g (50%) 1,7-diphenyl-4-heptanol as a clear, colorless liquid. ^1H NMR (90 MHz, $CDCl_3$) δ: 1.5 (m, 8H), 2.4 (s, 1H, exchanged with D_2O), 3.5 (quintet, 1H), 7.2 (br s, 10H).

(b) 1,7-Diphenylheptane. 1,7-Diphenyl-4-heptanol (6.52 g, 25 mmol) was dissolved in 50 ml dry pyridine and cooled to 0 °C. Para-toluenesulfonyl chloride (4.76 g, 25 mmol) was added in small portions and the flask was placed in the refrigerator (0 °C). After 4 days the reaction mixure was poured into 300 g ice-water and the tosyl ester was extracted into 3 x 100 ml ether. The combined ether extracts were washed three times with cold 75 ml portions of aqueous 6 N HCl to remove pyridine and then dried over Na_2CO_3. Subsequent removal of the ether yielded 5.75 g (55%) of the crude tosylate as an oil. The tosylate was then dissolved in 80 ml anhydrous ether and this solution was added dropwise to a solution of 2.0 g (5.3 mmol) $LiAlH_4$ in 175 ml anhydrous ether. This addition was performed under a N_2 atmosphere with stirring; the rate of addition was such that a gentle reflux was maintained. After the addition was complete, refluxing was continued for 5.5 h. The solution was then cooled to room temperature and slow, dropwise additions of 2 ml H_2O, 2 ml aqueous 15% (w/w) NaOH, and 6 ml H_2O were made in succession. The inorganic salts were removed by filtration, washed with 100 ml ether, and discarded. The ether wash was combined with the filtrate and the solution was dried over $MgSO_4$. The ether was subsequently removed and the oil which remained was vacuum distilled to yield 1.38 g (40% from the tosylate or 22% overall from 1,7-diphenyl-4-heptanol) of 1,7-diphenylheptane as a clear, colorless liquid. ^1H NMR (200 MHz, $CDCl_3$) δ: 1.33 (br s, 6H), 1.59 (m, 4H), 2.58 (t, 4H), 7.19 (m, 10H).

(c) Methyl 8-cyanooctanoate. A solution of 2.10 g (9.46 mmol) 8-bromooctanoic acid in 200 ml anhydrous ether was placed in a 500-ml beaker and cooled to 0 °C. To this solution was slowly added, with stirring, a 0.40 M solution of diazomethane in ether (95) until nitrogen evolution had ceased and the solution remained yellow in color. This required approximately 30 ml of the diazomethane solution. [Caution: All operations involving diazomethane solutions should be conducted in glassware that is free of scratches, chips, or any rough surfaces

so that the possibility of an explosion is minimized.] The beaker was then left in a fume hood overnight to allow the ether and excess diazomethane to evaporate. The crude ester that remained was then added dropwise to a stirred suspension of 0.510 g (10.4 mmol) NaCN in 10 ml DMSO at 60 °C. After the addition was complete, the solution was stirred at 60 °C for an additional 1 h and then taken briefly to 90 °C before cooling to room temperature. The reaction mixture was poured into 150 ml ice-water and extracted into 100 ml ether. The ether extract was washed successively with 20 ml 6 N HCl, 20 ml 10% (w/w) NaOH, and 6 x 20 ml H_2O before drying over $MgSO_4$. The ether was subsequently removed and the residue distilled (bp 140 °C/1 mm Hg) to yield 1.09 g (63% from 8-bromooctanoic acid) methyl 8-cyanooctanoate as a clear, colorless liquid. ^1H NMR (300 MHz, $CDCl_3$) δ: 1.34 and 1.45 (both br s, 6H combined), 1.64 (m, 4H), 2.31 (m, 4H), 3.66 (s, 3H). IR (neat) cm^{-1}: 2940, 2870, 2250, 1740,1460, 1370-1140 broad, 1100, 1020, 730.

(d) 7-Phenyl-1-heptanol. A round-bottom flask was fitted with a N_2 inlet and outlet and charged with 62.5 ml of a 1.6 M solution (100 mmol) of 5-phenyl-1-pentylmagnesium bromide (prepared as described previously). After cooling the solution to -5 °C, 4.84 g (110 mmol) of ice-cold ethylene oxide was slowly added, with stirring, via a double-tipped needle. Upon gradually warming to room temperature over a period of 15 min, gentle boiling of the solution was observed. After the boiling had stopped, the solution was refluxed for 45 min. At the end of this time the solution was cooled to room temperature, 70 ml 2 N aqueous HCl was added, and the product was extracted with 3 x 50 ml ether. The combined ether extracts were dried over $MgSO_4$ and the ether subsequently removed to leave an oily residue, which was vacuum distilled (bp 115-117 °C/1 mm Hg) to yield 11.14 g (58%) 7-phenyl-1-heptanol as a clear, colorless liquid. ^1H NMR (300 MHz, $CDCl_3$) δ: 1.31 (br s, 6H), 1.53 (m, 4H), 2.57 (t, 2H), 2.99 (s, 1H, exchanged with D_2O), 3.53 (t, 2H), 7.20 (m, 5H).

(e) 1-Bromo-7-phenylheptane. To 20 g (104 mmol) of 7-phenyl-1-heptanol at -5 °C was added dropwise, with stirring, 5.0 ml (53 mmol) phosphorous tribromide. The addition took 2.5 h, after which the solution was warmed to room temperature and stirred overnight. The solution was then poured into 150 ml ice-water and the organic layer separated. The crude product thus obtained was successively washed with 3 x 10 ml ice-cold concentrated H_2SO_4, 3 x 10 ml saturated aqueous $NaHCO_3$, and 2 x 10 ml H_2O. After drying over $CaCl_2$, 18.1 g (68%) of crude 1-bromo-7-phenylheptane was obtained as a clear yellow liquid and used in the next step without further purification.

(f) 8-Phenyloctanenitrile. 1-Bromo-7-phenylheptane (18.1 g, 71 mmol) was added dropwise with stirring to a suspension of 3.90 g (79.1 mmol) NaCN in 45ml DMSO heated to 60 °C. The temperature was maintained at 60 °C throughout the addition. After the addition was complete, the solution was stirred for an additional 2 h and then taken briefly to 90 °C before cooling to room temperature. The crude reaction mixture was diluted to a volume of 500 ml with H_2O and extracted three times with 100 ml portions of ether. The combined ether extracts were washed successively with 50 ml aqueous 2 N HCl, 50 ml saturated aqueous $NaHCO_3$, and 50 ml H_2O. After drying over $MgSO_4$ and removal of the ether, the remaining yellow oil was distilled (bp 114-117 °C/1 mm Hg) to yield 7.05 g (49%) 8-phenyloctanenitrile as a clear, colorless liquid. ^1H NMR (200 MHz, $CDCl_3$) δ: 1.3 (m, 6H), 1.6 (m, 4H), 2.29 (t, 2H), 2.60 (t,2H), 7.20 (m, 5H). IR (neat) cm^{-1}: 3030, 2930, 2860, 1600, 1500, 1460, 1430, 740, 700.

(g) 8-Phenyloctanoic acid. A mixture of 7.05 g (35.1 mmol) 8-phenyloctanenitrile and 20 ml concentrated HCl was heated with stirring at 90 °C for 4 h. After cooling, the organic layer was extracted into 50 ml ether and dried over $MgSO_4$. The ether was subsequently removed and the residual liquid was vacuum distilled (bp 165 °C/0.5 mm Hg) to give 6.17 g (80%) 8-phenyloctanoic acid as a clear, colorless liquid. ^1H NMR (200 MHz, $CDCl_3$) δ: 1.33 (br s, 6H), 1.61 (br s, 4H), 2.33 (t, 2H), 2.59 (t, 2H), 7.20 (m, 5H).

(h) Methyl-8-phenyloctanoate. A solution of 6.17 g (28.0 mmol) 8-phenyloctanoic acid in 500 ml anhydrous ether was placed in a 1-l beaker and cooled to 0 °C. To this solution was slowly added, with stirring, a 0.40 M solution of diazomethane in ether (95) until nitrogen evolution had ceased and the solution remained yellow in color. This required approximately 75 ml of the diazomethane solution. [Caution: All operations involving diazomethane solutions should be conducted in glassware that is free of scratches,chips, or any rough surfaces so that the possibility of an explosion is minimized.] The beaker was then left in a fume hood overnight to allow the ether and excess diazomethane to evaporate. The residual liquid was then vacuum distilled (bp 120 °C/0.10 torr) and further purified by column chromatography on a 5 x 18 cm column of Kieselgel 60 (230-400 mesh) silica gel with elution by 9:1 ether/hexane. There was finally obtained 3.93 g (60%) methyl 8-phenyloctanoate as a clear, colorless liquid. ^1H NMR (300 MHz, $CDCl_3$) δ: 1.34 (br s, 6H), 1.63 (br s, 4H), 2.31 (t, 2H), 2.61 (t, 2H), 3.69 (s, 3H), 7.20 (m, 5H). IR (neat) cm^{-1}: 3030, 2930, 2860, 1740, 1600, 1460, 1440, 1100-1300 broad, 750, 700.

3. Preparation of azo compounds and precursors thereof

(a) [1-^{13}C]Acetyl chloride. To a 10-ml round-bottom flask was added 1.00 g (16.4 mmol) of 99 atom % [1-^{13}C]acetic acid. A stream of dry N_2 was directed into the open flask. The flask was cooled to 0 °C, and 2.20 g (18.8 mmol) of thionyl chloride was added dropwise, with stirring, over a period of 15 min. After the addition, the reaction was stirred at 25 °C for 30 min, the flask was fitted with a condenser, and the reaction mixture was refluxed under N_2 for 1 h. After the mixture cooled to room temperature, the reflux condenser was replaced with a still head. Distillation (50-52 °C) under N_2 yielded 1.0 g (77%) of [1-^{13}C]acetyl chloride. ^{1}H NMR (200 MHz, $CDCl_3$) δ: 2.67 (d). IR (neat) cm^{-1}: 1770, 1680, 1420, 1370, 1280, 1090, 1020, 950.

(b) [1-^{13}C]Acetophenone. To a 25-ml round-bottom flask was added 1.0 g (12.7 mmol) of [1-^{13}C]acetyl chloride and 7 ml of dry benzene. After the flask was cooled to -5 °C, 1.98 g (14.8 mmol) of anhydrous $AlCl_3$ was added in small portions over 40 min with stirring. After the addition, the reaction was stirred at 25 °C for 4 h. Throughout the addition and subsequent reaction dry N_2 was bubbled through the mixture, which was contained in an open flask. Benzene was added periodically to make up for losses due to evaporation. The reaction mixture was then poured into 30 ml of aqueous 1 N HCl and extracted with three 30 ml portions of ether. The combined ether extracts were washed with 20 ml aqueous 10% (w/w) NaOH and then with 20 ml H_2O. After drying over $MgSO_4$ and removal of the ether, 1.35 g of crude yellow [1-^{13}C]acetophenone (77% pure, 67% yield) was obtained. ^{1}H NMR (200 MHz, $CDCl_3$) δ: 2.60 (d, 3H), 7.51 (m, 3H), 7.96 (m, 2H). IR (neat) cm^{-1}: 3070, 3030, 1640, 1600, 1450, 1370, 1250, 950, 760, 690.

(c) [1-^{13}C]Acetophenone azine and acetophenone azine. The crude [1-^{13}C]acetophenone from above (1.35 g, 8.66 mmol, 77% pure) was dissolved in 2.5 ml of absolute ethanol to which 10 mg of acetic acid had been added. Hydrazine hydrate (0.208 g, 4.16 mmol of hydrazine) was then added dropwise, with stirring, to the solution contained in an open 10-ml round-bottom flask. The reaction was stirred at 60 °C for 2 h, during which time the volume of the solution became full with crystals that separated. The precipitated yellow crystals were collected by filtration, washed with 10 ml of cold methanol, and dried in vacuo to give 0.95 g (93%) [1-^{13}C]acetophenone azine; mp 122-123 °C. ^{1}H NMR (200 MHz, $CDCl_3$) δ: 2.31 (d, 3H), 7.40 (m, 3H), 7.90 (m, 2H). IR (KBr) cm^{-1}: 3060, 1550, 1500, 1450, 1370, 1270, 1180, 1030, 760, 690. The natural-abundance compound, acetophenone azine, was prepared from acetophenone in the

same manner; spectral data follow. ^{1}H NMR (200 MHz, $CDCl_3$) δ: 2.32 (s, 3H), 7.41 (m, 3H), 7.91 (m, 2H). IR (KBr) cm^{-1}: 3060, 1600, 1560, 1450, 1370, 1290, 1080, 1020, 760, 690.

(d) **N,N'-Bis(1-phenyl[1-^{13}C]ethyl)hydrazine and N,N'-bis(1-phenylethyl)hydrazine.** [1-^{13}C]Acetophenone azine (0.95g, 3.99 mmol) was suspended in 30 ml of acetic acid in a 250-ml bottle, and 110 mg of $PtO_2 \cdot H_2O$ was added. Hydrogenation was then accomplished by using a Paar Model 3911 low-pressure hydrogenation apparatus, the theoretical amount of hydrogen being absorbed in about 10 min at 25 °C and an initial pressure of 34 psi. After filtration of the catalyst and removal of the acetic acid under vacuum, the oily residue was dissolved in 30 ml of ether and stirred for 2 h with 20 ml of 10% (w/w) aqueous NaOH to remove any remaining acid. After separation of the organic layer and removal of the ether, 0.93 g (98%) of the crude N,N'-bis(1-phenyl[1-^{13}C]ethyl)hydrazine was obtained. ^{1}H NMR (200 MHz, CD_2Cl_2) δ: 1.24 (m, 6H), 2.87 (br, 2H, exchanged with D_2O), 3.59 (m, 1H), 4.28 (m, 1H), 7.29 (m, 10H). IR (neat) cm^{-1}: 3100-3400 broad, 3070, 3030, 2970, 2930, 1610, 1500, 1460,1380,1080, 760, 700. The natural-abundance compound, N,N'-bis(1-phenylethyl)hydrazine, was prepared from acetophenone azine in the same manner; spectral data follow. ^{1}H NMR (200 MHz, $CDCl_3$) δ: 1.25 (m, 6H), 3.30 (br s, 2H, exchanged with D_2O), 3.96 (m, 2H), 7.30 (m, 5H). IR (neat) cm^{-1}: 3100-3400 broad, 3070, 3030, 2970, 2930, 1610, 1490, 1450, 1370, 1280, 1030, 760, 700.

(e) **1,1'-Azobis(1-phenyl[1-^{13}C]ethane) (1a) and 1,1'-azobis(1-phenylethane).** The crude N,N'-bis(1-phenyl[1-^{13}C]ethyl)hydrazine (0.93 g, 3.88 mmol) was added to 15 ml of H_2O in a 50-ml round-bottom flask, and 0.90 g (4.2 mmol) of yellow HgO was then added in portions over 10 min. After stoppering the flask and shaking for 20 min, 0.22 g (1.0 mmol) of additional HgO was added and shaking continued for 90 min. A 20 ml portion of ether was then added to the mixture, and the HgO removed by filtration. The filtrate was extracted with three 10 ml portions of ether and the combined extracts dried over $MgSO_4$. After removal of the ether in vacuo, a yellow solid residue of crude azo compound was obtained. Recrystallization twice from methanol (45 to -28 °C) gave 0.287 g (31%) of 1,1'-azobis(1-phenyl[1-^{13}C]ethane) in the form of white crystals; mp 71-72 °C. Anal. calcd. for $^{13}C_2C_{14}H_{18}N_2$: C, 80.79%; H, 7.55%; N, 11.66%. Found: C, 80.32%; H, 7.53%; N, 11.82%. ^{1}H NMR (200 MHz, $CDCl_3$) δ: 1.52 (m, 6H), 4.28 (quartet, 1H), 4.96 (quartet, 1H), 7.34 (m, 10H). IR (KBr) cm^{-1}: 3030, 2980, 2910, 1610, 1500, 1460, 1280, 1080, 770, 700. ^{13}C NMR (75 MHz, acetone-d_6) δ: 77.20. UV (0.032 M benzene solution): ε_{max}(359 nm) = 48 M^{-1} cm^{-1}. The natural-abundance compound, 1,1'-azobis(1-phenylethane), was prepared from N,N'-bis(1-phenylethyl)hydrazine in the same manner;

spectral data follow. ^{1}H NMR (200 MHz, $CDCl_3$) δ: 1.52 (d, 6H), 4.62 (quartet, 2H), 7.34 (m, 10H). IR (KBr) cm^{-1}: 3030, 2980, 2930, 1500, 1460, 1280, 1080, 1010, 770, 700. ^{13}C NMR (75 MHz, acetone-d_6) δ: 20.76, 77.18, 128.10, 128.14, 129.32, 142.52. UV (0.028 M benzene solution): ε_{max}(359 nm) = 48 M^{-1} cm^{-1}.

(f) [1-^{13}C]Benzoic acid. A modification of the procedure of Dauben, Reid, and Yankwich (96) was used. The apparatus depicted in Figure 2.1 (p. 46) was assembled using a 3-neck 1000-ml round-bottom flask (29/42 center joint and 24/40 side joints), a 1000-ml single-neck round-bottom flask (24/40 joint), a 250-ml addition funnel (24/40 joints), a Nuova II hot plate/ magnetic stirrer (1000 r.p.m. maximum; Fisher Scientific Co.), and a 2.5" x 0.75" egg-shaped stir bar (Aldrich Chemical Co.). With regard to Figure 2.1, "A" represents a glass stopcock (25/52 plug, 8 mm bore) as do B,C,D, and E (these have 17/40 plugs with 3 mm bores). The ball joints below B, D, and E were connected to those stopcocks at their male sides and all were 28/12. A column of Drierite separated D from the addition funnel, and the manometer was of the simple straight tube type. Ground glass plugs were placed in F and G, and the system was checked for leaks.

A phenylmagnesium bromide solution was prepared by placing 9.10 g magnesium (0.374 mole) in a 3-neck 1-l round-bottom flask fitted with a N_2 inlet, condenser, and 500-ml addition funnel. After flushing with N_2, a solution of 3.0 ml bromobenzene (4.5 g, 0.029 mole) in 30 ml anhydrous ether was added. After about 15 min, the reaction had initiated and about 50 ml additional anhydrous ether was added so that the initial reaction would not become too vigorous. After 10 min, dropwise addition of a solution of 34.3 ml bromobenzene (51.2 g, 0.326 mole) in 420 ml anhydrous ether was begun. The reaction mixture was stirred vigorously throughout the addition, which required about 2 h to complete. The heat of reaction was sufficient to cause the ether to reflux gently during this time. After the addition was complete, the reaction mixture was left to stand overnight under N_2, and this allowed unreacted Mg to settle. The clear orange solution was then transferred under N_2 via a double-tipped needle into a septum-capped 1-l round-bottom flask which had been previously flushed with N_2. A 20 ml aliquot was removed for titration (97) to determine the phenylmagnesium bromide concentration, which was about 0.68 M.

The ground glass plug in F was then replaced with a rubber septum, 50.0 g $Ba^{13}CO_3$ (0.252 mole; 99 atom %) were placed in the single neck 1-l round-bottom flask, and 250 ml concentrated H_2SO_4 were placed in the addition funnel. A volume of Grignard solution that contained 0.280

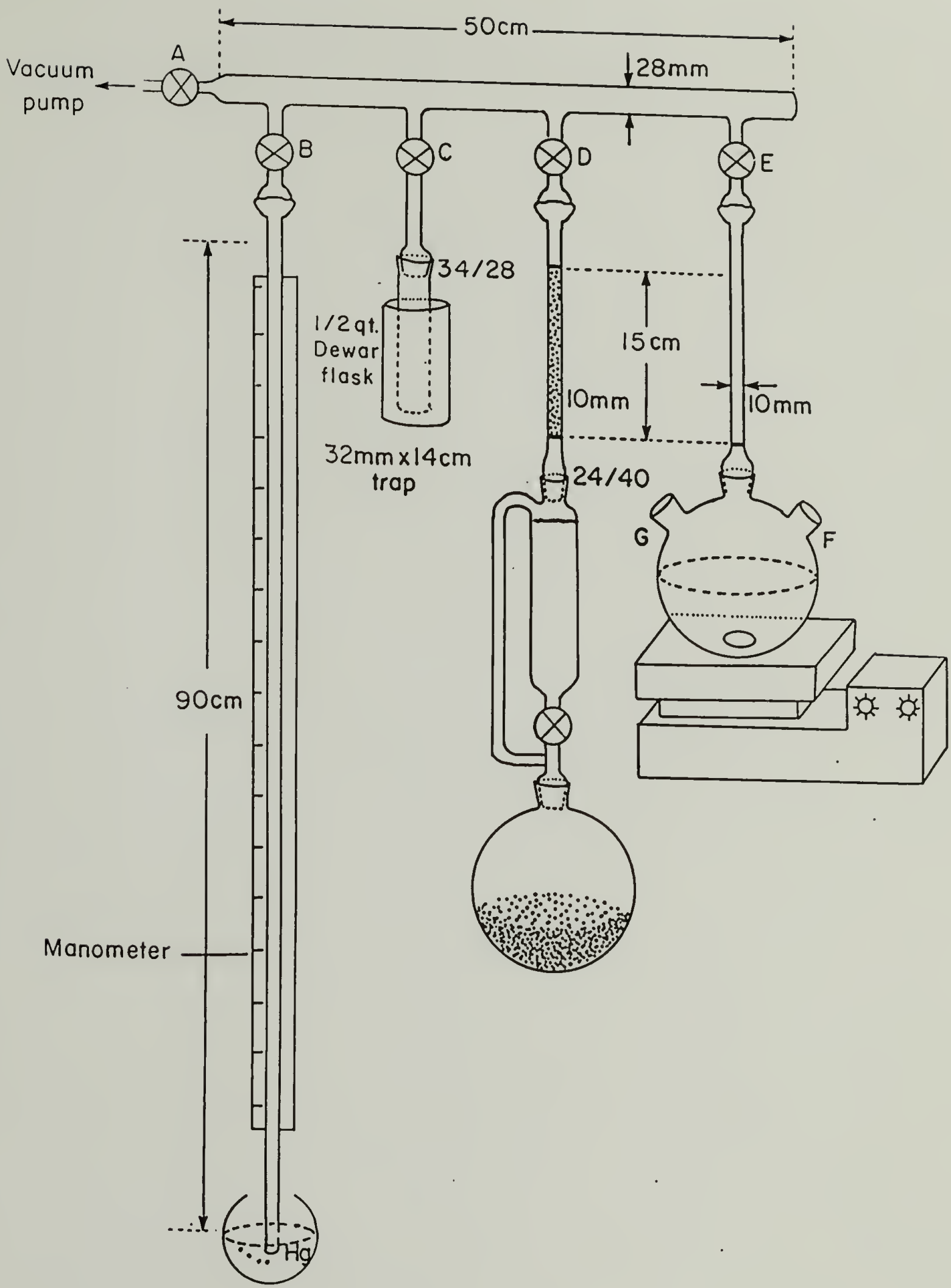

Figure 2.1. Carbonation apparatus.

mole phenylmagnesium bromide (about 412 ml) was transferred under N_2 through F into the 3-neck 1-l round-bottom flask via a double-tipped needle. The rubber septum in F was then replaced with a ground glass plug and stopcock E was closed. With stopcocks A.B,C, and D open, and the 1/2 quart Dewar flask empty, the system was evacuated to a pressure of about 0.25 mm Hg. Stopcock A was then closed and the Dewar flask filled with liquid N_2. Dropwise addition of the H_2SO_4 to the $Ba^{13}CO_3$ was then begun; this was done very slowly initially, but more rapidly later. The $^{13}CO_2$ produced was condensed into the liquid N_2 trap almost as quickly as it was produced. After the addition was complete (20 min), the H_2SO_4 mixture was heated using a heat gun to drive out any remaining $^{13}CO_2$. Stopcocks C and D were then closed and the Drierite column, addition funnel, and single-neck 1-l round-bottom flask were removed. At this time the Grignard solution was cooled to -25 °C in a dry ice-isopropanol mixture and the stirrer was turned on full power. Stopcock E was opened, and stopcock A was opened only momentarily to bring the system to apressure of about 170 mm Hg. Stopcock C was then opened immediately and the Dewar flask removed. The production of the gaseous $^{13}CO_2$ was controlled by warming the trap with a heat gun or by cooling with a liquid N_2 bath. The $^{13}CO_2$ was produced as rapidly as possible without exceeding a pressure of 500 mm Hg, and after about 15 min the Grignard solution had absorbed a sufficient amount so that no solid $^{13}CO_2$ remained. The dry ice-isopropanol bath was maintained at -25 to -20 °C during this time. After 5 additional min, the pressure remained constant at about 200 mm Hg. The dry ice-isopropanol bath and magnetic stirrer were then removed and the reaction flask immersed in a liquid N_2 bath so as to draw in any remaining $^{13}CO_2$. After the reaction mixture was completely frozen, stopcock E was closed. The mixture was then warmed to 0 °C and held at this temperature for 15 min. During this time the flask was manually agitated by rotating about the ball joint between E and the flask, as the magnetic stir bar had become immobilized in a voluminous precipitate. The flask was then opened to the air and 150 ml aqueous 2 N HCl was added. The mixture was transferred to a 1-l separatory funnel and the organic layer was separated. After washing with 50 ml aqueous 2 N HCl and 2 x 50 ml H_2O, the solution was dried over $MgSO_4$. The ether was removed and the crude benzoic acid recrystallized from 100 ml benzene, concentrating the mother liquor to half-volume twice, to give 23.0 g product. The final mother liquor was evaporated to dryness, the residue sublimed at 95 °C/0.5 mm Hg, and the material thus obtained recrystallized from 15 ml benzene to give an additional 2.8 g product. The total yield of [1-^{13}C]benzoic acid was 25.8 g (84%); mp 122-123 °C. Anal. calcd. for $^{13}C_1C_6H_7O_2$: C,

69.10%; H, 4.91%. Found: C, 68.80%; H, 4.93%. ^{1}H NMR (200 MHz, $CDCl_3$) δ: 7.48 (m, 2H), 7.63 (m, 1H), 8.14 (m, 2H). IR (KBr pellet) cm^{-1}: 3400-2200 broad, 1650, 1460, 1420, 1330, 1280, 1190, 930, 810, 700.

(g) [1-^{13}C]Benzoyl chloride. A 500-ml round-bottom flask was fitted with a condenser and N_2 inlet and outlet. To this flask was added 51.59 g (0.419 mole) [1-^{13}C]benzoic acid, 39 ml (0.535 mole) $SOCl_2$, and 97 ml CH_2Cl_2. The mixture was refluxed with stirring under a slow N_2 flush for 4 h, and then allowed to stir overnight at 35 °C, also under a slow N_2 flush. The condenser was replaced with a still head and the CH_2Cl_2 and excess $SOCl_2$ were distilled off. The remaining liquid was vacuum distilled (bp 50 °C/2 mm Hg) to yield 54.49 g (92%) [1-^{13}C]benzoyl chloride. ^{1}H NMR (200 MHz, $CDCl_3$) δ: 7.51 (m, 2H), 7.69 (m, 1H), 8.12 (m, 2H). IR (neat) cm^{-1}: 3060, 1720, 1590, 1450, 1320, 1200, 1180, 850, 770, 660.

(h) 1,3-Diphenyl-1-[1-^{13}C]propanone. A Grignard solution was prepared in the manner described previously for phenylmagnesium bromide (see preparation of [1-^{13}C]benzoic acid) from 2.50 g (103 mmol) Mg, 19.10 g (103 mmol) (2-bromoethyl)benzene, and 125 ml anhydrous ether. The Grignard solution was decanted into a 250-ml 3-neck round-bottom flask fitted with an addition funnel, mechanical stirrer, reflux condenser, and N_2 inlet and outlet. After cooling to 0 °C in an ice-water bath, 9.44 g (51.5 mmol) anhydrous $CdCl_2$ was added with stirring over 5 min. The reaction mixture was stirred for an additional 10 min at 0 °C, allowed to warm to room temperature, and then refluxed for 10 min. The condenser was then replaced with a still head and the ether distilled off until a nearly dry residue remained. [Caution: evaporation to dryness of ether solutions which contain peroxides may result in an explosion]. At this time 80 ml dry benzene was added, distilled off until a nearly dry residue remained, and a final addition of 110 ml dry benzene was made. The reaction mixture was cooled to room temperature and 7.10 g (50.2 mmol) [1-13C]benzoyl chloride was added dropwise over 2 min with vigorous stirring. The reaction was then refluxed for 1.5 h. After cooling to room temperature, the reaction mixture was opened to the air and 80 ml of ice-water was added. After adding enough aqueous 1 N H_2SO_4 to dissolve a white precipitate, the phases were separated. The aqueous phase was extracted with 30 ml benzene and the extract added to the organic phase. The organic phase was then washed with 30 ml each of H_2O, aqueous 5% (w/w) NaOH, and H_2O twice more. After drying over $MgSO_4$, the solvent was removed in vacuo and the residue recrystallized from 95% ethanol to yield 5.23 g (49%) of 1,3-diphenyl-1-[1-^{13}C]propanone as white plates; mp 67-68 °C. ^{1}H NMR (200 MHz, $CDCl_3$) δ: 3.08 (m, 2H), 3.30 (m, 2H), 7.27 (m,

5H), 7.49 (m, 3H), 7.96 (m, 2H). IR (KBr) cm^{-1}: 3030, 2930, 1640, 1450, 1370, 1290, 970, 750, 690. The natural-abundance compound, 1,3-diphenyl-1-propanone, was prepared from benzoyl chloride in the same manner; spectral data follow. ^1H NMR (200 MHz, $CDCl_3$) δ: 3.07 (m, 2H), 3.30 (m, 2H), 7.27 (m, 5H), 7.49 (m, 3H), 7.96 (m, 2H). IR (KBr) cm^{-1}: 3030, 2930, 1680, 1370, 1300, 1210, 980, 740, 690.

(i) 1,3-Diphenyl-1-[1-^{13}C]propanone azine and 1,3-diphenyl-1-propanone azine. A solution of 4.93 g (23.4 mmol) 1,3-diphenyl-1-[1-^{13}C]propanone, 0.374 g (11.7 mmol) anhydrous hydrazine, and one drop acetic acid in 31 ml absolute ethanol was refluxed under N_2 for 2.5 h. The solution was then allowed to stand at room temperature for 2 days. The solid that had precipitated was then filtered, washed with 20 ml ice-cold anhydrous ethanol, and dried under vacuum to give 3.22 g (66%) of 1,3-diphenyl-1-[1-^{13}C]propanone azine as yellow prisms; mp 114-115 °C. Anal. calcd. for $^{13}C_2C_{28}H_{28}N_2$: C, 86.56%; H, 6.74%; N, 6.69%. Found: C, 86.43%; H, 6.71%; N, 6.58%. ^1H NMR (200 MHz, $CDCl_3$) δ: 2.82 (m, 2H), 3.18 (m, 2H), 7.20 (m, 5H), 7.45 (m, 3H), 7.93 (m, 2H). IR (KBr) cm^{-1}: 3020, 2930, 1550, 1500, 1450, 1280, 1180, 1030, 750, 690. The natural-abundance compound, 1,3-diphenyl-1-propanone azine, was prepared from 1,3-diphenyl-1-propanone in the same manner; spectral data follow. ^1H NMR (200 MHz, $CDCl_3$) δ: ^1H NMR (200 MHz, $CDCl_3$) δ: 2.82 (m, 2H), 3.18 (m, 2H), 7.20 (m, 5H), 7.45 (m, 3H), 7.93 (m, 2H). IR (KBr) cm^{-1}: 3030, 2950, 1600, 1570, 1500, 1450, 1290, 1180, 1030, 750, 690.

(j) N,N'-Bis(1,3-diphenyl[1-^{13}C]propyl)hydrazine and N,N'-bis(1,3-diphenylpropyl)hydrazine. A 100-ml 3-neck round bottom flask fitted with a reflux condenser, addition funnel, and N_2 inlet and outlet was charged with a solution of 3.13g (7.45 mmol) 1,3-diphenyl-1-[1-^{13}C]propanone azine in 27 ml dry toluene. After the system was flushed with N_2, the solution was heated to reflux and 1.65 ml of 10 M $BH_3 \cdot Me_2S$ (16.5 mmol BH_3) was added dropwise over 10 min. The reaction was refluxed for an additional 6 h, cooled to room temperature, and 5.0 ml methanol was added dropwise over 30 min with stirring (vigorous foaming). After stirring overnight at room temperature, the solution was cooled to 0 °C in an ice-water bath and anhydrous HCl was bubbled through the solution for 5 min (vigorous foaming). After stirring overnight at room temperature, the solvent was removed in vacuo to leave 4.9 g of a colorless oil. This was dissolved in 30 ml CH_2Cl_2, and the solution transferred to a separatory funnel and washed with 30 ml aqueous 10% (w/w) NaOH. After ensuring that the pH of the aqueous phase was >10, the phases were separated. The aqueous phase was extracted with 30 ml CH_2Cl_2 and the extract added to the organic phase. The organic phase

was then washed with 30 ml H_2O and 30 ml saturated aqueous NaCl. After drying the organic phase over $MgSO_4$, the solvent was removed in vacuo to yield 3.14 g (100%) of crude N,N'-bis(1,3-diphenyl[1-^{13}C]propyl)hydrazine as a colorless oil. This was used in the next step without further purification. ^{1}H NMR (200 MHz, $CDCl_3$) δ: 1.7-2.8 (m, 10H, 8H after D_2O exchange), 3.45 (m, 1H), 4.12 (m, 1H), 7.24 (m, 20H). IR (neat) cm^{-1}: 3100-3400 broad, 3070, 3030, 2930, 2860, 1610, 1500, 1460, 750, 700. The natural-abundance compound, N,N'-bis(1,3-diphenylpropyl)hydrazine, was prepared from 1,3-diphenyl-1-propanone azine in the same manner; spectral data follow. ^{1}H NMR (80 MHz, $CDCl_3$) δ: 1.9 (m, 4H), 2.3-3.2 (m, 6H, 4H after D_2O exchange), 3.7 (m, 2H), 7.1 (m, 20H). IR (neat) cm^{-1}: 3100-3400 broad, 3070, 3030, 2930, 2860, 1610, 1500, 1460, 750, 700.

(k) 1,1'-Azobis(1,3-[1-^{13}C]diphenylpropane) (1b) and 1,1'-azobis(1,3-diphenylpropane). In a 100-ml round-bottom flask was mixed 3.14 g (7.45 mmol) N,N'-bis(1,3-diphenyl[1-^{13}C]propyl)hydrazine and 20 ml H_2O. After the addition of 2.20 g (10.2 mmol) yellow HgO the flask was stoppered and shaken for 1.5 h. At the end of this time 30 ml CH_2Cl_2 was added and the mixture filtered through a Celite pad. The organic phase was separated and dried for 30 min over $MgSO_4$. The solvent was subsequently removed in vacuo and the crude residue left in an open flask in the dark for 3 days. The solid thus obtained was recrystallized twice from 25 ml 5:1 methanol/benzene and dried under vacuum to give 1.30 g (42%) of 1,1'-azobis(1,3-[1-^{13}C]diphenylpropane) as white needles; mp 78-100. Anal. calcd. for $^{13}C_2C_{28}H_{30}N_2$: C, 86.15%; H, 7.19%; N, 6.66%. Found: C, 86.34%; H, 7.15%; N, 6.48%. ^{1}H NMR (200 MHz, $CDCl_3$) δ: 2.43 (m, 8H), 4.18 (m, 1H), 4.86 (m, 1H), 7.20 (m, 20H). IR (KBr) cm^{-1}: 3070, 3030, 2950, 2890, 1600, 1500, 1460, 1030, 750, 700. ^{13}C NMR (75 MHz, $CDCl_3$) δ: 81.66, 81.74. UV (0.033 M benzene solution): ε_{max}(362 nm) = 48 M^{-1} cm^{-1}. The natural-abundance compound, 1,1'-azobis(1,3-diphenylpropane), was prepared from N,N'-bis(1,3-diphenylpropyl)hydrazine in the same manner; spectral data follow. ^{1}H NMR (200 MHz, $CDCl_3$) δ: 2.43 (m, 8H), 4.53 (m, 2H), 7.20 (m, 20H). IR (KBr) cm^{-1}: 3080, 3030, 2940, 2890, 1600, 1500, 1460, 1030, 750, 700. ^{13}C NMR (75 MHz, $CDCl_3$) δ: 31.97, 32.24, 36.22, 36.72, 81.66, 81.75, 125.80, 125.92, 127.48, 127.61, 127.88, 127.92, 128.26, 128.38, 128.56, 128.66, 139.76, 140.05, 141.38, 141.51. UV (0.032 M benzene solution): ε_{max}(362 nm) = 48 M^{-1} cm^{-1}.

(l) Ethyl 3-phenyl-3-keto[3-^{13}C]propionate. The procedure of Straley and Adams (98) for the preparation of the compound naturally abundant in ^{13}C was used. From 54.29 g (0.384 mole) [1-^{13}C]benzoyl chloride (prepared as described previously), 48.30 g (65%) of ethyl

3-phenyl-3-keto[3-^{13}C]propionate was obtained as a faintly yellow liquid; bp 90-95 °C/1 mm Hg. ^{1}H NMR (200 MHz, $CDCl_3$) δ: 1.25 (t, 3H), 3.99 (d, 2H), 4.21 (quartet, 2H), 7.66 (m, 5H). IR (neat) cm^{-1}: 3000, 1740, 1640, 1600, 1320, 1260, 1200, 1150, 1040, 760, 700.

(m) Ethyl 3-phenyl-3-methoxylimino[3-^{13}C]propionate and ethyl 3-phenyl-3-methoxyliminopropionate. The procedure of Secor and Sanders (99) for the preparation of the compound naturally abundant in ^{13}C was used. From 48.10 g (0.249 mole) ethyl 3-phenyl-3-keto[3-^{13}C]propionate, 46.48 g (84%) of ethyl 3-phenyl-3-methoxylimino[3-^{13}C]propionate was obtained as a clear, colorless liquid; bp 110-115 °C/1 mm Hg. ^{1}H NMR (200 MHz, $CDCl_3$) δ: 1.21 (t, 3H), 3.75 (d, 2H), 4.01 (s, 3H), 4.15 (quartet, 2H), 7.37 (m, 3H), 7.63 (m, 2H). IR (neat) cm^{-1}: 2980, 2930, 1730, 1330, 1270, 1250, 1040, 900, 770, 700. The natural-abundance compound, ethyl 3-phenyl-3-methoxyliminopropionate, was prepared from ethyl 3-phenyl-3-ketopropionate (ethyl benzoyl acetate) in the same manner; spectral data follow. ^{1}H NMR (200 MHz, $CDCl_3$) δ: 1.20 (t, 3H), 3.74 (s, 2H), 4.00 (s, 3H), 4.14 (quartet, 2H), 7.36 (m, 3H), 7.62 (m, 2H). IR (neat) cm^{-1}: 2980, 2940, 1740, 1450, 1260, 1170, 1050, 910, 770, 700.

(n) 3-Amino-3-phenyl-1-[3-^{13}C]propanol and 3-amino-3-phenyl-1-propanol. The procedure of Secor and Sanders (98) for the preparation of the compound naturally abundant in ^{13}C was used. From 46.28 g (0.209 mole) ethyl 3-phenyl-3-methoxylimino[3-^{13}C]propionate, 20.38 g (65%) of 3-amino-3-phenyl-1-[3-^{13}C]propanol was obtained as white needles; mp 71-72 °C. ^{1}H NMR (200 MHz, $CDCl_3$) δ: 1.88 (m, 2H), 2.63 (br, 2H, exchanged with D_2O), 3.79 (m, 2.5H), 4.45 (t, 0.5H), 7.30 (m, 5H). IR (KBr) cm^{-1}: 3350, 3280, 3140, 2850, 1600, 1440, 1050, 970, 760, 700. The natural-abundance compound, 3-amino-3-phenyl-1-propanol, was prepared from ethyl 3-phenyl-3-methoxyliminopropionate in the same manner; spectral data follow. ^{1}H NMR (200 MHz, $CDCl_3$) δ: 1.89 (m, 2H), 2.66 (br s, 3H, exchanged with D_2O), 3.80 (m, 2H), 4.12 (t, 1H), 7.30 (m, 5H). IR (KBr) cm^{-1}: 3350, 3280, 3140, 2850, 1600, 1440, 1050, 960, 770, 700.

(o) 3-Phenyl-3-phthalimido-1-[3-^{13}C]propanol and 3-phenyl-3-phthalimido-1-propanol. A finely ground, intimate mixture of 20.23 g (0.134 mole) 3-amino-3-phenyl-1-[3-^{13}C]propanol and 19.84 g (0.134 mole) phthalic anhydride was heated at 170 °C under N_2 with magnetic stirring in a 500-ml round-bottom flask for 1.5 h. After cooling, the solid was dissolved in 250 ml CH_2Cl_2 and the solution dried over $MgSO_4$. The CH_2Cl_2 was subsequently removed and the residue crystallized upon standing overnight; no further purification was necessary. The yield of 3-phenyl-3-phthalimido-1-[3-^{13}C]propanol was 35.90 g (95%); mp 95-100 °C. ^{1}H NMR (200 MHz, $CDCl_3$) δ: 1.64 (br s, 1H, exchanged with D_2O), 2.54 (m, 1H), 2.82 (m, 1H), 3.71 (m, 2H),

5.27 (m, 0.5H), 5.96 (m, 0.5H), 7.30 (m, 3H), 7.54 (m, 2H), 7.68 (m, 2H), 7.79 (m, 2H). IR (KBr) cm^{-1}: 3420, 2930, 2870, 1770, 1700, 1390, 1350, 1080, 1040, 710. The natural-abundance compound, 3-phenyl-3-phthalimido-1-propanol, was prepared from 3-amino-3-phenyl-1-propanol in the same manner; spectral data follow. ^1H NMR (200 MHz, $CDCl_3$) δ: 1.99 (br s, 1H, exchanged with D_2O), 2.52 (m, 1H), 2.81 (m, 1H), 3.68 (m, 2H), 5.59 (m, 1H), 7.30 (m, 3H), 7.54 (m, 2H), 7.67 (m, 2H), 7.79 (m, 2H). IR (KBr) cm^{-1}: 3530, 3450 (s), 2940, 1770, 1700, 1390, 1360, 1090, 1060, 710.

(p) 3-Phenyl-3-phthalimido-1-[3-^{13}C]propyl 4-methylphenylsulfonate and 3-phenyl-3-phthalimido-1-propyl 4-methylphenylsulfonate. In a 2-l round-bottom flask was placed 35.50 g (0.126 mole) 3-phenyl-3-phthalimido-1-[3-^{13}C]propanol and 1 l anhydrous pyridine. After the solid had dissolved, the solution was cooled to 0 °C and 28.10 g (0.147 mole) p-toluenesulfonyl chloride was added in several portions over 2 min. The flask was then capped with a rubber septum, flushed with N_2, and left at 0 °C for 48 h. The solution was then poured into 1.5 l ice-water and extracted with 3 x 200 ml $CHCl_3$. The combined $CHCl_3$ extracts were then washed with ice-cold 200 ml portions of aqueous 3 N HCl until a wash remained acidic. It was necessary to cool the $CHCl_3$ solution several times to keep it below 35 °C. The $CHCl_3$ solution was then washed with 2 x 100 ml saturated aqueous $NaHCO_3$ and 100 ml saturated aqueous NaCl. After drying over $MgSO_4$, the $CHCl_3$ was removed in vacuo to leave 51.44 g (90%) of 3-phenyl-3-phthalimido-1-[3-^{13}C]propyl 4-methylphenylsulfonate as a light green oil. This crude product was used directly in the next step. ^1H NMR (200 MHz, $CDCl_3$) δ: 2.36 (s, 3H), 2.68 (m, 1H), 2.98 (m, 1H), 4.07 (m, 2H), 5.08 (m, 0.5 H), 5.78 (m, 0.5 H), 7.48 (m, 13H). IR (neat) cm^{-1}: 3050, 2980, 1770, 1700, 1600, 1460, 1360, 1180, 1100, 920, 730. The natural-abundance compound, 3-phenyl-3-phthalimido-1-propyl 4-methylphenylsulfonate, was prepared from 3-phenyl-3-phthalimido-1-propanol in the same manner; spectral data follow. ^1H NMR (200 MHz, $CDCl_3$) δ: 2.37 (s, 3H), 2.69 (m, 1H), 2.97 (m, 1H), 4.06 (m, 2H), 5.44 (m, 5H), 7.51 (m, 13H). IR (neat) cm^{-1}: 3040, 2940, 1770, 1700, 1590, 1350, 1180, 1090, 990, 920, 750.

(q) 4-Phenyl-4-phthalimido[4-^{13}C]butyronitrile and 4-phenyl-4-phthalimidobutyronitrile. In a 250-ml round-bottom flask was placed 51.04 g (0.113 mole) 3-phenyl-3-phthalimido-1-[3-^{13}C]propyl 4-methylphenylsulfonate and 45 ml DMSO. After the oil had dissolved, the solution was heated to 40 °C and a suspension of 6.52 g (0.133 mole) NaCN in 30 ml DMSO was added all at once. The mixture was maintained at 40 °C with stirring for 1 h, then heated to 60 °C for 0.5 h, and finally allowed to cool to room temperature. The mixture was then poured into 700 ml H_2O and extracted with 6 x 100 ml $CHCl_3$. The

combined $CHCl_3$ extracts were washed with 100 ml aqueous 1 N HCl, 3 x 100 ml H_2O, and 100 ml saturated aqueous NaCl. After drying over $MgSO_4$, the $CHCl_3$ was subsequently removed to leave 21.64 g (65%) of 4-phenyl-4-phthalimido[4-^{13}C]butyronitrile as a white solid; mp 125-127 °C. [Occasionally when performing this reaction with natural abundance starting material, a thick brown liquid rather than solid material was obtained at this point. In this case trituration with ether was found to be effective. It is noted that this difficulty is least likely to occur when the starting material is free of pyridine and the DMSO and NaCN are dry.] ^{1}H NMR (200 MHz, $CDCl_3$) δ: 2.41 (m, 2H), 2.75 (m, 1H), 2.97 (m, 1H), 5.07 (m, 0.5H), 5.76 (m, 0.5H), 7.34 (m, 3H), 7.55 (m, 2H), 7.71 (m, 2H), 7.82 (m, 2H). IR (KBr) cm^{-1}: 3060, 2940, 2250, 1770, 1700, 1390, 1350, 1110, 1090, 710. The natural-abundance compound, 4-phenyl-4-phthalimidobutyronitrile, was prepared from 3-phenyl-3-phthalimido-1-propyl 4-methylphenylsulfonate in the same manner; spectral data follow. ^{1}H NMR (200 MHz, $CDCl_3$) δ: 2.40 (m, 2H), 2.74 (m, 1H), 2.96 (m, 1H), 5.42 (m, 1H), 7.34 (m, 3H), 7.54 (m, 2H), 7.70 (m, 2H), 7.82 (m, 2H). IR (KBr) cm^{-1}: 3070, 2940, 2250, 1770, 1700, 1390, 1360, 1110, 1090, 710.

(r) **4-Amino-4-phenyl[4-^{13}C]butyronitrile and 4-amino-4-phenylbutyronitrile.** In a 1-l Erlenmeyer flask were placed 21.44 g (73.9 mmol) 4-phenyl-4-phthalimido[4-^{13}C]butyronitrile, 625 ml 95% ethanol, and 7.98 g hydrazine hydrate (160 mmol hydrazine). The mixture was heated at 60 °C for 2 h with stirring and then 350 ml aqueous 1 N HCl was added. Heating at 60 °C with stirring was continued for an additional 2 h. The mixture was then cooled to 0 °C and filtered. The filtrate was transferred to a 2-l round-bottom flask and placed on a rotary evaporator to remove the ethanol. Solid NaOH was then added to the aqueous mixture which remained until the pH was greater than 10. The temperature of the mixture was kept below 40 °C during this addition by means of an ice bath. The mixture was then extracted with 4 x 125 ml $CHCl_3$ and the combined extracts were dried over $MgSO_4$. The $CHCl_3$ was subsequently removed and the liquid that remained was dissolved in 1.0 l anhydrous ether. Dry HCl was bubbled through this solution until no further solid was observed to precipitate. The mixture was then filtered and the solid thus obtained dried in vacuo to yield 13.61 g (94%) 4-amino-4-phenyl[4-^{13}C]butyronitrile hydrochloride; mp 178-184 °C. The hydrochloride salt was then converted to the base by placing 13.46 g (68.5 mmol) of the HCl salt in a 125 ml separatory funnel and adding 50 ml aqueous 15% (w/w) NaOH. The free amine separated as the top layer, and was extracted into 7 x 15 ml $CHCl_3$. To the combined $CHCl_3$ extracts was added 100 ml benzene. This solution was dried over $MgSO_4$, the solvent

subsequently removed, and the liquid product that remained was left on a vacuum line overnight before use in the next step. The final yield of 4-amino-4-phenyl[4-^{13}C]butyronitrile as a clear yellow liquid was 10.93 g (94% based on 4-phenyl-4-phthalimido[4-^{13}C]butyronitrile; HCl salt removed for analysis is accounted for in calculating this yield). ^{1}H NMR (200 MHz, $CDCl_3$) δ: 1.49 (br s, 2H, exchanged with D_2O), 1.98 (m, 2H), 2.34 (m, 2H), 3.68 (t, 0.5H), 4.36 (t, 0.5H), 7.31 (m, 5H). IR (neat) cm^{-1}: 3380, 3310, 3030, 2930, 2250, 1600, 1460, 890, 770, 710. The natural-abundance compound, 4-amino-4-phenylbutyronitrile, was prepared from 4-phenyl-4-phthalimidobutyronitrile in the same manner; spectral data follow. ^{1}H NMR (200 MHz, $CDCl_3$) δ: 1.50 (br s, 2H, exchanged with D_2O), 1.98 (m, 2H), 2.34 (m, 2H), 4.03 (t, 1H), 7.32 (m, 5H). IR (neat) cm^{-1}: 3380, 3320, 3030, 2930, 2250, 1600, 1460, 890, 770, 710.

(s) N,N'-Bis(1-phenyl[1-^{13}C]-3-cyanopropyl)sulfonamide and N,N'-bis(1-phenyl-3-cyanopropyl)sulfonamide. A 250-ml 3-neck round-bottom flask was fitted with a 25-ml addition funnel, a N_2 inlet, and a N_2 outlet. A solution of 10.79 g (67.4 mmol) 4-amino-4-phenyl[4-^{13}C]butyronitrile and 6.82 g (67.4 mmol) dry triethylamine in 38 ml dry, ethanol-free $CHCl_3$ was placed in the flask. The solution was cooled to -30 °C by means of a dry ice-isopropanol bath and a solution of 4.55 g (33.7 mmol) freshly distilled sulfuryl chloride in 14 ml dry, ethanol-free $CHCl_3$ was added dropwise over 45 min. During this addition a fast N_2 flush was maintained and the solution magnetically stirred as vigorously as possible using an egg-shaped stir bar. After the addition was complete, the reaction mixture was stirred for an additional 1 h at -30 °C and then stirred at room temperature overnight. At this point the reaction mixture was transferred to a separatory funnel, with the aid of 30 ml additional $CHCl_3$, and washed with 2 x 20 ml H_2O. After drying over $MgSO_4$, the $CHCl_3$ solution was concentrated to a volume of 20 ml and the sulfonamide was isolated by column chromatography on a 5 x 18 cm column of Kieselgel 60 (230-400 mesh) silica gel with elution by 9:1 ether/hexane. Thus obtained was 7.28 g (56%) of N,N'-bis(1-phenyl[1-^{13}C]-3-cyanopropyl)sulfonamide as a white solid; mp 130-132 °C. ^{1}H NMR (200 MHz, $CDCl_3$) δ: 2.05 (m, 8H), 3.92 (m, 1H), 4.61 (m, 1H), 4.94 (m, 2H, exchanged with D_2O), 7.19 (m, 10H). IR (KBr) cm^{-1}: 3250, 2250, 1450, 1330, 1160, 1070, 1010, 950, 770, 710. The natural-abundance compound, N,N'-bis(1-phenyl-3-cyanopropyl)sulfonamide, was prepared from 4-amino-4-phenylbutyronitrile in the same manner; spectral data follow. ^{1}H NMR (200 MHz, $CDCl_3$) δ: 1.82 (m, 4H), 2.13 (m, 4H), 4.24 (m, 2H), 5.20 (br , 2H, exchanged with D_2O), 7.19 (m, 10H). IR (KBr) cm^{-1}: 3250, 2260, 1450, 1340, 1160, 1100, 1080, 950, 770, 710.

(t) 4,4'-Azobis(4-phenyl[4-^{13}C]butyronitrile) (1c) and 4,4'-azobis(4-phenylbutyronitrile). A mixture of 0.88 g (2.30 mmol) finely ground N,N'-bis(1-phenyl[1-^{13}C]-3-cyanopropyl)sulfonamide, 0.18 g (4.50 mmol) NaOH, 7.0 ml Clorox (4.94 mmol NaOCl), and 7.0 ml H_2O was stirred for 72 h in an open 30-ml beaker. At the end of this time, the precipitated crude azo compound was filtered from the mixture and recrystallized twice from methanol (55 to 20 °C). The yield of 4,4'-azobis(4-phenyl[4-^{13}C]butyronitrile) as white needles was 0.110 g (15%); mp 124-125 °C. Anal. calcd. for $^{13}C_2C_{18}H_{20}N_4$: C, 76.07%; H, 6.33%; N, 17.60%. Found: C, 75.81%; H, 6.32%; N, 17.57%. ^{1}H NMR (200 MHz, $CDCl_3$) δ: 2.08 (m, 4H), 2.34 (m, 4H), 4.26 (t, 1H), 4.95 (t, 1H), 7.40 (m, 10H). IR (KBr) cm^{-1}: 3030, 2940, 2900, 2260, 1500, 1450, 1430, 1310, 1040, 770, 710. ^{13}C NMR (75 MHz, acetone-d_6) δ: 81.14. UV (0.027 M benzene solution): ε_{max}(363 nm) = 43 M^{-1} cm^{-1}. The natural-abundance compound, 4,4'-azobis(4-phenylbutyronitrile), was prepared from N,N'-bis(1-phenyl-3-cyanopropyl)sulfonamide in the same manner; spectral data follow. ^{1}H NMR (200 MHz, $CDCl_3$) δ: 2.08 (m, 4H), 2.35 (m, 4H), 4.61 (t, 2H), 7.39 (m, 10H). IR (KBr) cm^{-1}: 3040, 2950, 2910, 2260, 1500, 1450, 1430, 1310, 1050, 770, 710. ^{13}C NMR (75 MHz, acetone-d_6) δ: 14.19, 31.13, 81.13, 119.74, 128.61, 128.88, 129.68, 139.73. UV (0.026 M benzene solution): ε_{max}(363 nm) = 43 M^{-1} cm^{-1}.

4. Mercury method reactions

All monomers were deoxygenated with N_2 prior to use. The general procedure was as follows: To a 2-ml glass ampule was added 1.0 ml DMF and either 40 mg (0.094 mmol) of 5-phenyl-1-pentylmercuric bromide or 25 mg (0.066 mmol) of 5-cyano-1-pentylmercuric bromide. After capping with a septum and deoxygenating with N_2, precisely known quantities (3-6 mmol) of styrene and acrylonitrile, styrene and methyl acrylate, or acrylonitrile and methyl acrylate were introduced via syringe. The solution was cooled to 0 °C in an ice bath and 100 μl of a 1 M solution of $NaBH_4$ in DMF was added all at once. The reaction mixture was kept at 0 °C for 60 min before analysis by gas chromatography; elemental Hg produced in the reaction had settled to the bottom of the ampule by this time. Listed in Table 2.1 (p. 56) and Table 2.2 (p. 57) are the molar ratio of total alkene (monomer) to alkylmercuric bromide ([M]/[P]) and the molar alkene ratio ([M_x]/[M_y]) for each of these experiments.

Table 2.1. Mercury Method Data for the 5-Phenyl-1-pentyl Radical.[a]

competition[b] M_X / M_Y	[M] / [P][c]	$[M_X]$ / $[M_Y]$	$[M_X$ Adduct] / [M_Y Adduct]
A/S	40	0.302	4.16
		0.212	2.63
	55	0.0955	0.892
		0.191	3.04
		0.142	2.04
		0.0927	1.23
		0.102	1.50
		0.153	2.42
		0.110	1.83
		0.150	2.72
	75	0.207	4.09
		0.103	1.73
		0.154	2.85
MA/S	55	0.203	4.09
		0.300	1.24
		0.504	2.28
A/MA	55	0.699	3.26
		0.260	0.856
		0.466	1.54
		0.662	2.17

[a] Conditions: DMF solution, 0.085 M 5-phenyl-1-pentylmercuric bromide, 0.091 M $NaBH_4$, 60 min at 0 °C.

[b] M_X = acrylonitrile (A) or methyl acrylate (MA); M_Y = styrene (S) or methyl acrylate (MA).

[c] The [M]/[P] parameter is the ratio of the total alkene (monomer) concentration to the radical precursor (5-phenyl-1-pentylmercuric bromide) concentration.

Table 2.2. Mercury Method Data for the 5-Cyano-1-pentyl Radical.[a]

competition[b] M_X / M_Y	[M] / [P][c]	$[M_X]$ / $[M_Y]$	$[M_X$ Adduct] / $[M_Y$ Adduct]
A/S	45	0.206	3.26
		0.126	2.11
		0.100	1.55
		0.086	1.30
		0.0955	1.19
	55	0.158	2.19
		0.214	3.33
		0.160	2.44
		0.108	1.74
		0.0967	1.26
MA/S	40	0.204	3.14
		0.252	0.997
		0.445	1.74
	55	0.652	2.35
		0.254	0.956
		0.455	1.99
		0.655	3.05
	75	0.252	0.947
		0.449	1.82
		0.653	2.45
		0.250	0.835
		0.455	1.87
A/MA	40	0.649	2.88
		0.247	0.723
		0.454	1.21
	55	0.675	2.05
		0.237	0.706
		0.328	1.00
		0.674	2.02
		0.248	0.772
		0.451	1.33
	75	0.671	1.94
		0.242	0.759
		0.453	1.37
		0.678	2.09

[a] Conditions: DMF solution, 0.060 M 5-cyano-1-pentylmercuric bromide, 0.091 M $NaBH_4$, 60 min at 0 °C.

[b] M_X = acrylonitrile (A) or methyl acrylate (MA); M_Y = styrene (S) or methyl acrylate (MA).

[c] The [M]/[P] parameter is the ratio of the total alkene (monomer) concentration to the radical precursor (5-cyano-1-pentylmercuric bromide) concentration.

5. Homopolymers

(a) **Polystyrene (PS).** Polystyrene samples derived from 1,1'-azobis(1-phenyl[1-^{13}C]ethane) (**1a**) and natural abundance **1a** were prepared using the following procedure: To 0.9 g of styrene in a glass tube was added 14.5 mg of the azo compound. The tube was capped with a septum and the solution deoxygenated with N_2. The tube was then irradiated for 1.5 h at 33 °C. After irradiation the solution was added dropwise to 150 ml of rapidly stirred methanol to precipitate about 60 mg (7%) of polymer, which was filtered, redissolved in $CHCl_3$, reprecipitated into methanol, and filtered before drying to constant weight under vacuum. PS samples derived from **1a** at polymerization temperatures other than 33 °C were prepared in the same way except for the use of a water bath as described at the start of this chapter.

PS samples derived from 1, 1'-azobis(1,3-[1-^{13}C]diphenylpropane) (**1b**) and natural-abundance **1b** were prepared at 33 °C in the same manner as just described except for the use of 3.2 g of benzene as a diluent, 40 mg azo compound, and an irradiation time of 6 h. PS samples derived from 4,4'-azobis(4-phenyl[4-^{13}C]butyronitrile) (**1c**) and natural-abundance **1c** were also prepared according to the same general procedure except for the use of 2.6 g of benzene as a diluent, 25 mg azo compound, and an irradiation time of 12 h.

(b) **Poly(acrylonitrile) (PAN).** Poly(acrylonitrile) samples derived from 1,1'-azobis(1-phenyl[1-^{13}C]ethane) (**1a**) and natural abundance **1a** were prepared using the following procedure: To 1.0 g of acrylonitrile in a glass tube were added 2.6 g of benzene and 14.5 mg of the azo compound. The tube was capped with a septum and the solution deoxygenated with N_2. The tube was then irradiated for 3.0 h at 33 °C. Because PAN precipitated from benzene, it was necessary to dissolve the polymer in about 25 ml DMSO before precipitation into 500 ml of rapidly stirred methanol. After filtering and allowing the polymer to dry in the air for 2 h, the polymer was redissolved in about 10 ml DMF and reprecipitated into 500 ml methanol before drying to constant weight under vacuum. Roughly 300 mg polymer was obtained. PAN samples derived from **1a** at polymerization temperatures other than 33 °C were prepared in the same way except for the use of a water bath.

PAN samples derived from 1, 1'-azobis(1,3-[1-^{13}C]diphenylpropane) (**1b**) and natural-abundance **1b** were prepared at 33 °C in the same manner as just described except for the use of 3.2 g benzene, 40 mg azo compound, and an irradiation time of 1 h. PAN samples derived from 4,4'-azobis(4-phenyl[4-^{13}C]butyronitrile) (**1c**) and natural-abundance **1c** were also prepared

according to the same general procedure except for the use of 0.7 g acrylonitrile, 2.6 g benzene, 15 mg azo compound, and an irradiation time of 4 h.

(c) Poly(methyl methacrylate) (PMMA). Poly(methyl methacrylate) samples were prepared using the following procedure: To 0.9 g of methyl methacrylate in a glass tube were added 2.6 g of benzene and either 15 mg of 1,1'-azobis(1-phenyl[1-^{13}C]ethane) (**1a**) or 15 mg of natural-abundance **1a**. The tube was capped with a septum and the solution deoxygenated with N_2. The tube was then irradiated for 4 h at 33 °C. After irradiation the solution was added dropwise to 150 ml of rapidly stirred methanol to precipitate about 160 mg (18%) of polymer, which was filtered, redissolved in $CHCl_3$, reprecipitated into methanol, and filtered before drying to constant weight under vacuum.

6. Copolymers

(a) Styrene-acrylonitrile (SAN) copolymers derived from 1,1'-azobis(1-phenyl[1-^{13}C]ethane) (1a) and natural-abundance 1a. To 14.5 mg of **1a** dissolved in 2.62 g of benzene in a septum-capped, N_2 flushed glass tube were added by syringe a total of 0.95 g (9-11 mmol) of N_2-sparged monomer (styrene and acrylonitrile). The tube was irradiated for 3 h at 33 °C. The solution was then added dropwise to 150 ml of rapidly stirred methanol to precipitate about 95 mg (10%) of polymer, which was filtered, redissolved in $CHCl_3$, reprecipitated into methanol, and filtered before drying to constant weight under vacuum. The polymerization data for the eight enriched copolymers used in the **3a/4a** end group analysis are listed in Table 2.3 (p. 60). For each copolymer in Table 2.3 there was prepared an unenriched copolymer at the same, or nearly the same, monomer feed ratio. These copolymers containing ^{13}C in naturally abundant amounts were prepared exactly as above, except for the use of unenriched **1a**. The polymerization data for these copolymers are found in Table B-1 (p. 198) in Appendix B.

(b) Styrene-acrylonitrile (SAN) copolymers derived from 1, 1'-azobis(1,3-[1-^{13}C]diphenylpropane) (1b) and natural-abundance 1b. To 80 mg of **1b** dissolved in 5.0 g of benzene in a septum-capped, N_2 flushed glass tube were added by syringe a total of 2.1 g (21-24 mmol) of N_2-sparged monomer (styrene and acrylonitrile). The tube was irradiated for 140-220 min at 33 °C. The solution was then added dropwise to 350 ml of rapidly stirred methanol to precipitate about 170 mg (8%) of polymer, which was filtered, redissolved in $CHCl_3$, reprecipitated into methanol, and filtered before drying to constant weight under vacuum. Polymerization data for nine enriched copolymers derived from **1b** are listed in Table 2.4

Table 2.3. Polymerization Data for ^{13}C Enriched SAN Copolymers Derived from **1a**.[a]

copolymer	styrene, mmol	acrylonitrile, mmol	styrene / acrylonitrile ([S]/[A])	polymer, mg	convn, %	[3a]/[4a]
1	7.827	2.554	3.06	101	10.6	0.707
2	7.884	2.350	3.35	97	10.3	0.736
3	8.048	2.177	3.70	95	10.1	0.971
4	8.230	1.692	4.86	90	9.5	0.971
5	8.381	1.513	5.54	87	9.1	1.13
6	8.428	1.314	6.41	87	9.2	1.29
7	8.580	1.187	7.23	83	8.7	1.51
8	8.594	0.9404	9.14	82	8.7	1.90

[a] Conditions: 14.5 mg of **1a**; 2.62 g of benzene; 33 °C; 3 h irradiation with 350 nm light.

Table 2.4. Polymerization Data for ^{13}C Enriched SAN Copolymers Derived from **1b**.[a]

copolymer	styrene, mmol	acrylonitrile, mmol	styrene / acrylonitrile ([S]/[A])	polymer, mg	convn, %	time[b], min	[3b]/[4b]
9	15.84	7.821	2.02	152	7.4	148	0.391
10	17.30	5.090	3.40	236	11.4	215	0.763
11	17.55	4.387	4.00	137	6.6	186	0.855
12	17.95	3.707	4.84	162	7.8	186	1.04
13	18.24	3.215	5.67	167	8.1	203	1.20
14	18.40	2.863	6.43	165	8.0	203	1.34
15	18.55	2.557	7.26	164	7.9	216	1.45
16	18.69	2.341	7.98	151	7.3	216	1.69
17[c]	6.37	7.71	0.83	111	10.3	146	—

[a] Conditions: 80 mg of **1b**; 5.0 g of benzene; 33 °C.
[b] This is the time of irradiation with 350 nm light.
[c].Copolymer 17 was prepared with 40 mg of **1b**; 2.6 g benzene.

(p. 61); eight of these, numbered 9-16 in Table 2.4, were used in the **3b/4b** end group analysis. For each of these eight copolymers, there was prepared an unenriched copolymer at the same, or nearly the same, monomer feed ratio. These copolymers containing ^{13}C in naturally abundant amounts were prepared exactly as above, except for the use of unenriched **1b**. The polymerization data for these copolymers are found in Table B-2 (p. 199) in Appendix B.

(c) Styrene-acrylonitrile (SAN) copolymers derived from 4,4'-azobis(4-phenyl[4-^{13}C]butyronitrile) (1c) and natural-abundance 1c. To 25 mg of **1c** dissolved in 2.62 g of benzene in a septum-capped, N_2 flushed glass tube were added by syringe a total of 0.96 g (9-13 mmol) of N_2-sparged monomer (styrene and acrylonitrile). The tube was irradiated for 130-210 min at 33 °C. The solution was then added dropwise to 200 ml of rapidly stirred methanol to precipitate about 85 mg (9%) of polymer, which was filtered, redissolved in $CHCl_3$, reprecipitated into methanol, and filtered before drying to constant weight under vacuum. Polymerization data for ten enriched copolymers derived from **1c** are listed in Table 2.5 (p. 63); eight of these, numbered 18-25 in Table 2.5, were used in the **3c/4c** end group analysis. For each of these eight copolymers, there was prepared an unenriched copolymer at the same, or nearly the same, monomer feed ratio. These copolymers containing ^{13}C in naturally abundant amounts were prepared exactly as above, except for the use of unenriched **1c**. The polymerization data for these copolymers are found in Table B-3 (p. 200) in Appendix B.

(d) Acrylonitrile-methyl methacrylate (AMMA) copolymers. To 15 mg of 1,1'-azobis(1-phenyl[1-^{13}C]ethane) **(1a)** dissolved in 2.62 g of benzene in a septum-capped, N_2 flushed glass tube were added by syringe a total of 0.97 g (10-13 mmol) of N_2-sparged monomer (acrylonitrile and methyl methacrylate). The tube was irradiated for 54 min at 33 °C. The solution was then added dropwise to 150 ml of rapidly stirred methanol to precipitate about 115 mg (12%) of polymer, which was filtered, redissolved in $CHCl_3$, reprecipitated into methanol, and filtered before drying to constant weight under vacuum. Polymerization data for nine enriched copolymers and one unenriched copolymer derived from **1a** are listed in Table 2.6 (p. 64); eight of these, numbered 28-35 in Table 2.6, were used in the **5/6** end group analysis.

Table 2.5. Polymerization Data for ^{13}C Enriched SAN Copolymers Derived from **1c**.[a]

copolymer	styrene, mmol	acrylonitrile, mmol	styrene / acrylonitrile ([S]/[A])	polymer, mg	convn, %	time[b], min	[3c]/[4c]
18	7.805	2.835	2.75	72	7.5	190	1.40
19	7.561	3.141	2.41	79	8.3	190	1.32
20	7.464	3.492	2.14	78	8.1	180	1.08
21	7.391	3.952	1.87	86	8.8	180	0.870
22	6.954	4.269	1.63	89	9.4	180	0.813
23	6.646	4.800	1.38	82	8.7	162	0.661
24	6.610	5.818	1.14	90	9.0	144	0.576
25	5.836	6.694	0.872	91	9.4	137	0.444
26[c]	6.431	5.735	1.12	98	10.1	165	—
27[d]	7.084	4.352	1.63	84	8.7	202	0.789

[a] Conditions: 25 mg of **1c**; 2.62 g of benzene; 33 °C.
[b] This is the time of irradiation with 350 nm light.
[c] Copolymer 26 was used only for NOE measurements.
[d] Copolymer 27 is derived from a lower melting sample of **1c**. The [**3c**]/[**4c**] ratio of this copolymer was not used for the rate constant ratio determination and is included for purpose of comparison only.

Table 2.6. Polymerization Data for ^{13}C-Enriched AMMA Copolymers.[a]

copolymer	methyl methacrylate, mmol	acrylonitrile, mmol	methyl methacrylate / acrylonitrile ([MMA] / [A])	polymer, mg	convn, %	[5]/[6]	[7]/[8]
28	8.905	1.346	6.62	90	9.3	2.74	—
29	8.914	1.536	5.80	106	10.9	2.64	—
30	8.751	1.740	5.03	110	11.4	2.20	—
31	8.517	2.060	4.13	115	12.0	1.90	—
32	8.346	2.444	3.42	121	12.5	1.25	—
33	8.169	3.068	2.66	124	12.6	1.14	6.78
34	7.348	4.259	1.72	120	12.5	0.683	3.72
35	6.286	6.295	0.999	108	11.2	0.431	3.00
36[b]	8.797	1.672	5.26	217	22.4	—	—
37[c]	8.686	1.653	5.25	230	24.0	—	—

[a] Conditions: 15 mg of **1a**; 2.62 g of benzene; 33 °C; 54 min irradiation with 350 nm light.
[b] The irradiation time for copolymer 36 was 3 h. Because of the high conversion, this copolymer was used only for NOE and T_1 measurements.
[c] Copolymer 37 was prepared from natural-abundance **1a** and the irradiation time was 3 h; other conditions were the same.

C. Measurements

1. Routine measurements

Proton nuclear magnetic resonance (^{1}H NMR) spectra were recorded at 300 MHz on a Varian XL-300 spectrometer, at 200 MHz on a Varian XL-200 spectrometer, at 90 MHz on a Perkin-Elmer R-32 spectrometer, at 80 MHz on a Varian CFT-20 spectrometer, and at 60 MHz on a Varian T-60. Carbon-13 nuclear magnetic resonance (^{13}C NMR) spectra of azo compounds were recorded with broad-band decoupling at either 75 MHz on a Varian XL-300 spectrometer or at 50 MHz on a Varian XL-200 spectrometer. Chemical shifts for all NMR spectra of low molecular weight compounds are reported as parts-per-million downfield from tetramethylsilane.

Infrared (IR) spectra were obtained on a Perkin-Elmer Model 1320 spectrometer. Solid samples were analyzed as KBr pellets; liquids were analyzed neat between sodium chloride plates. The spectra were calibrated using the 1601 cm^{-1} polystyrene absorbance as reference.

Ultraviolet (UV) spectra were obtained on a Beckman DU-7 spectrophotometer using cells with 1 cm path length.

Gel permeation chromatography was done using an apparatus consisting of a Waters Model 501 solvent delivery system, a Rheodyne sample injector (100 µl loop), four micro-styrogel columns (10 nm, 50 nm, 10^3 nm, and 10^4 nm; 8 in. × 0.25 in.), a Waters Model R401 Differential Refractometer detector, and a Hewlett-Packard Model 3380A integrator. The apparatus was calibrated using polystyrene samples of known molecular weight and narrow molecular weight distribution. Molecular weights are reported as polystyrene molecular weights of identical elution volume.

Melting points were obtained on a Fisher-Johns apparatus and are uncorrected. Elemental analyses were performed by the University of Massachusetts Microanalytical Laboratory. Combined gas chromatography/mass spectrometry (GC/MS) measurements were performed by the University of Massachusetts Agricultural Experiment Station GC/MS Facility.

2. Gas chromatographic analyses of mercury method reactions

The molar ratio of adducts present in each reaction mixture was determined by gas chromatography (GC) using a Varian Series 1400 Gas Chromatograph equipped with a flame ionization detector and a Hewlett-Packard 3380A integrator. The helium carrier gas flow rate

was 25 ml/min, and the hydrogen and air flow rates to the detector were 30 and 300 ml/min respectively. A 9' x 0.25" stainless steel column packed with 3% SE-30 on 80/100 Supelcoport was used for all of the analyses with the exception of the 5-cyano-1-pentylmercuric bromide/acrylonitrile/methyl acrylate system; for these analyses a 10' x 0.25" glass column packed with 10% SP-1000 on 80/100 Supelcoport was used. The injector and detector temperatures were both 250 °C for all of the analyses. The isothermal column temperature was 200 °C for analyses of reaction mixtures that contained 5-phenyl-1-pentylmercuric bromide as the radical precursor; for reaction mixtures that contained 5-cyano-1-pentylmercuric bromide as the radical precursor, the isothermal column temperature was 175 °C. A 3 µl aliquot was withdrawn by syringe from each reaction mixture for injection into the gas chromatograph.

Adduct peaks were identified by comparison of their retention times and mass spectra with those of authentic samples of at least 95% purity. Compiled in Appendix C (p. 201) are mass spectra of authentic samples and mass spectra of adducts as produced in the reaction mixtures. These spectra were recorded using combined gas chromatography/mass spectrometry.

Prior to the analyses of reaction mixtures, the relative detector response factor (R.F.) for the system under consideration was determined. This was simply a detector calibration. With respect to a chromatogram of a reaction mixture from a particular $RHgBr/M_x/M_y$ system (symbols and abbreviations as in Scheme 1.8, p. 30), the product of the R.F. and the adduct peak area ratio gave the respective molar ratio of the adducts present in the mixture: (R.F.)(Area of M_x Adduct Peak/Area of M_y Adduct Peak) = ([M_x Adduct]/[M_y Adduct]). The R.F. was determined from the slope of a plot of molar adduct ratio ([M_x Adduct]/[M_y Adduct]) versus peak area ratio (Area of M_x Adduct Peak/Area of M_y Adduct Peak) for three DMF solutions of known adduct composition. These "standard" solutions were prepared from the authentic samples and had molar adduct ratios of typically 0.5, 1.0, and 2.0; the total adduct concentration in each was about 5% (w/w). In all cases, the plots which were used to determine the various R.F. values gave linear least-squares-fit lines that passed through the origin and had correlation coefficients greater than 0.99. Compiled in Table 2.1 (p. 56) are the molar adduct ratios found in reaction mixtures which contained 5-phenyl-1-pentylmercuric bromide as the radical precursor; Table 2.2 (p. 57) lists the data for the 5-cyano-1-pentylmercuric bromide systems.

3. ^{13}C NMR analyses of polymers

Chemical shifts recorded for $CDCl_3$ solutions were measured with reference to the center peak of the $CDCl_3$ triplet that occurs at 77.00 ppm. [All solvent shifts quoted here are relative to tetramethylsilane (TMS)]. Spectra obtained for dimethyl sulfoxide-d_6 (DMSO-d_6) solutions were referenced using the center line of the DMSO-d_6 multiplet at 39.50 ppm; those obtained for N,N-dimethylformamide-d_7 (DMF-d_7) solutions were referenced using the center line of the DMF-d_7 multiplet at 35.20 ppm. For polymer solutions prepared with "deuterated diglyme" (the phrase hereafter used), a 3:2 mixture of diglyme and diglyme-d_{14} was used. Spectra recorded at 140 °C for these solutions were referenced using a natural-abundance diglyme signal that occurs at 70.88 ppm relative to TMS *at room temperature* (see Fig. D-1, p. 210). Solutions of polymer in "deuterated bromobenzene" (the phrase hereafter used) were prepared with a 3:2 mixture of bromobenzene and bromobenzene-d_5. Spectra recorded at 136 °C for these solutions were referenced using a bromobenzene-d_5 signal that occurs at 130.89 ppm relative to TMS *at room temperature* (see Fig. D-2, p. 211).

(a) Homopolymers. All ^{13}C NMR spectra of homopolymers, with the exception of those of polystyrenes derived from 1,1'-azobis(1-phenyl[1-^{13}C]ethane) (**1a**) at different polymerization temperatures (Fig. D-12, p. 221), were obtained at 75 MHz on a Varian XL-300 NMR spectrometer using 2% (w/w) solutions. A standard single pulse sequence, broad-band ^1H decoupling, an 80° pulse width, a 1.9 s delay between pulses, and an acquisition time of 0.90 s were used. The spectra of PS samples derived from **1a** at different polymerization temperatures were obtained at 50 MHz on a Varian XL-200 NMR spectrometer using 2% (w/w) solutions. A standard single pulse sequence, broad-band ^1H decoupling, an 80° pulse width, a 1.5 s delay between pulses, and an acquisition time of 0.75 s were used.

(b) Copolymers. All ^{13}C NMR spectra of copolymers were obtained at 75 MHz on a Varian XL-300 NMR spectrometer using 2% (w/w) solutions. All were recorded using a standard single pulse sequence with the exception of those from inversion-recovery experiments.

Inversion-recovery experiments were performed on ^{13}C enriched copolymers to determine spin-lattice relaxation times (T_1 values) of signals from the end groups. For these experiments a two pulse sequence was used that consisted of a 180° pulse, a variable delay time, a 90° pulse immediately followed by acquisition, and a final delay time before the next 180° pulse. The total time following the 90° pulse and before the next 180° pulse was greater than 5 times T_1. The delay following the 180° pulse, termed the "relaxation delay time", was varied over a

range from about 0.1 to 10 times the expected T_1 so as to create an array of seven or eight experiments. From the array of spectra thus obtained, the XL-300 computer calculated "best-fit" T_1 values following identification of the signals of interest. Error values based on the goodness of the fit were given with the T_1 values. For further details concerning the nature of the inversion-recovery experiments, the reader is referred to the XL-300 instrument manual (100).

The 90° pulse width of the XL-300 for ^{13}C was determined from experiments, performed on a dioxane sample, in which the pulse width was systematically varied in order to determine the value (typically 16.5 μs) for which maximum signal intensity was attained (100).

Copolymer spectra recorded with the nuclear Overhauser effect (NOE) were obtained with broad-band ^1H decoupling; those recorded with suppression of (without) the NOE were obtained using a gated ^1H decoupling sequence in which the decoupler was only on during acquisition. A delay between pulses of sufficient duration ($>5 \times T_1$) to allow the NOE to fade was used in conjunction with the gated decoupling sequence. For the purpose of comparing end group peak area ratios obtained from spectra of an enriched copolymer recorded with and without the NOE, spectra were obtained in each case using acquisition parameters that were identical except for those relating to the decoupler sequence.

Spectra of ^{13}C enriched copolymers were recorded under conditions appropriate for quantitative signal integration. Pulse delays of at least 5 times the longest end group T_1 were used in each case to ensure complete (>99%) relaxation of the nuclei. For spectra recorded with the NOE, it was determined that there was no significant difference between end group peak area ratios for spectra recorded with and without the NOE. These measurements of T_1 and peak area ratio were made on one copolymer for each class of endgroups. Table 2.7 (p. 69) summarizes the results of these measurements and Table 2.8 (p. 70) gives the conditions and acquisition parameters used to obtain copolymer spectra. Contained in Appendix D are the stacked spectra from inversion-recovery experiments (Figs. D-3 through D-7, pp. 212-216); also in Appendix D are the stacked spectra of copolymers that were recorded with and without the NOE (Figs. D-8 through D-11, pp. 217-220).

The end group signals of enriched styrene-acrylonitrile (SAN) copolymers derived from **1a**, **1b**, or **1c** were assigned by comparison of copolymer spectra with spectra of polystyrene and poly(acrylonitrile) samples prepared with the same initiator, and from variations in signal intensity with changes in monomer feed composition. Peak areas were apportioned between end

Table 2.7. Spin-Lattice Relaxation Time (T_1) and Nuclear Overhauser Effect (NOE) Measurements for ^{13}C Enriched Copolymers.[a]

copolymer[b]	endgroups	T_1 range[c], s	peak area ratio[d] with the NOE	peak area ratio[d] without the NOE	difference in peak area ratio with and without the NOE, %
1	**3a + 4a**	0.42 - 0.64	—	—	—
10	**3b + 4b**	1.23 - 1.76	0.763	0.754	1.2
22	**3c + 4c**	0.87 - 1.63	—	—	—
26	**3c + 4c**	—	0.481	0.480	0.2
36	**5 + 6**	0.40 - 0.60	1.88	1.94	3.2
35	**7 + 8**	0.35 - 0.58	3.00	2.87	4.3

[a] Conditions: $CDCl_3$ solution at 20 °C for copolymers 1, 35, and 36; deuterated diglyme solution at 140 °C for copolymer 10; and deuterated bromobenzene solution at 136 °C for copolymers 22 and 26.

[b] Polymerization data for copolymer 1 are found in Table 2.3; for copolymer 10 in Table 2.4; for copolymers 22 and 26 in Table 2.5; for copolymers 35 and 36 in Table 2.6.

[c] This is the lowest T_1 value (minus the ± error) to the highest T_1 value (plus the ± error) measured for all signals from the endgroups

[d] This is **3b/4b** for endgroups **3b + 4b**, **3c/4c** for endgroups **3c + 4c**, etc.

Table 2.8. Conditions and Acquisition Parameters for ^{13}C NMR Analyses of ^{13}C Enriched Copolymers.[a]

copolymers[b]	endgroups	solvent	temperature, °C	acquisition time, s	pulse delay[c], s
1-8	**3a + 4a**	$CDCl_3$	20	0.970	3.75
9-17	**3b + 4b**	deuterated diglyme[d]	140	0.905	8.80
18-27	**3c + 4c**	deuterated bromobenzene[e]	136	0.905	8.16
28-36	**5+6 and 7+8**	$CDCl_3$	20	0.834	3.00

[a] A 90° pulse was used for all. Conditions and acquisition parameters for analyses of natural-abundance copolymers were identical to those for the corresponding enriched copolymers.
[b] Polymerization data for copolymers 1-8 are found in Table 2.3; for copolymers 9-17 in Table 2.4; for copolymers 18-27 in Table 2.5; for copolymers 28-36 in Table 2.6.
[c] This refers to the total time between pulses rather than the time between the end of an acquisition and the next pulse.
[d] A 3:2 mixture of diglyme (1,2-dimethoxyethane) and diglyme-d_{14}.
[e] A 3:2 mixture of bromobenzene and bromobenzene-d_5.

groups 3a and 4a, 3b and 4b, or 3c and 4c in each spectrum by drawing vertical lines from the local spectral minima occurring between signals of differing assignment to the base line of the normalized spectrum of the corresponding unenriched copolymer. Peak areas were determined by a cut-and-weigh method.

The end group signals of enriched acrylonitrile-methyl methacrylate (AMMA) copolymers were assigned with considerations analogous to those described above for the SAN copolymers. Peak areas were determined by electronic integration. Peak areas were apportioned between end groups 5 and 6 or 7 and 8 in each spectrum displayed on the XL-300 computer screen by positioning vertical cursors at the local spectral minima which occur between signals of differing assignment. This procedure is directly analogous to "drawing vertical lines" in the cut-and-weigh method described above for the SAN copolymers.

CHAPTER III

RESULTS AND DISCUSSION

A. Relative rates of addition of alkenes to ε-substituted n-alkyl radicals

The rate constant ratios for addition of acrylonitrile and styrene, methyl acrylate and styrene, and acrylonitrile and methyl acrylate to the 5-phenyl-1-pentyl and 5-cyano-1-pentyl radicals were determined. The radicals were generated by reduction of 5-phenyl-1-pentylmercuric bromide or 5-cyano-1-pentylmercuric bromide with $NaBH_4$ in the presence of known amounts of alkene, according to Scheme 1.8 (p. 30). The syntheses of the alkylmercuric bromides are outlined in Scheme 3.1 (p. 74). The "mercury method reactions" represented in Scheme 1.8 were done in deoxygenated N,N-dimethylformamide at 0 °C, and the molar ratio of adducts present in each reaction mixture was determined by gas chromatography (see Chapter II, p. 65). A large excess of total alkene (> 40 times that stoichiometrically required) was used in each reaction to ensure that the relative amounts of the two alkenes did not change as the reaction proceeded.

Authentic samples of the adducts (1,7-diphenylheptane, methyl 8-cyanooctanoate, 8-phenyloctanenitrile, methyl 8-phenyloctanoate, and nonanedinitrile) were necessary for the calibration of the detector in the gas chromatograph. Nonanedinitrile was purchased and the other adducts were synthesized as outlined in Schemes 3.2 (p. 75) and 3.3 (p. 76). Mass spectra of these authentic samples and mass spectra of adducts produced in the mercury method reaction mixtures were obtained using combined gas chromatography/mass spectrometry. Comparison of the fragmentation patterns confirmed that the adducts produced in the reactions had structures identical to those of the corresponding authentic samples (see Appendix C).

As outlined in Scheme 1.8 (p. 30), three competitions (styrene/acrylonitrile, methyl acrylate/styrene, and acrylonitrile/methyl acrylate) for both the 5-phenyl-1-pentyl radical and 5-cyano-1-pentyl radical were investigated. Presented in Figures 3.1 to 3.6 (pp. 77-79) are plots, prepared from data in Tables 2.1 and 2.2 (pp. 56-57), of molar adduct ratio versus molar alkene ratio for each of the systems studied. Each plot is linear, as expected, and the linear least-squares-fit line for each passes very near the origin. The slope of the line obtained in each case is the ratio of the rates of addition (or the "relative rate of addition") of the

respective alkenes to the radical. Presented in Table 3.1 (p. 80) are the relative rates of addition of acrylonitrile and styrene (k_A/k_S), of methyl acrylate and styrene (k_{MA}/k_S), and of acrylonitrile and methyl acrylate (k_A/k_{MA}) to the 5-phenyl-1-pentyl and 5-cyano-1-pentyl radicals as given by the slopes of the best-fit lines.

As can be seen from Table 3.1 (p. 80), there were no significant differences between the selectivities of the 5-phenyl-1-pentyl and 5-cyano-1-pentyl radicals for any of the three competitions investigated. Both radicals show a large preference for acrylonitrile over styrene ($k_A/k_S = 15.8$), although not to the extent observed for 1-hexyl radical ($k_A/k_S = 26.2$) by Jones and coworkers (54) or for cyclohexyl radical ($k_A/k_S = 24$) by Giese (72). From these observations it appears that the rate constant ratio can be sensitive to the nature of the ε-substituent; replacement of a methyl group in the epsilon position with either a phenyl or cyano group reduces the preference for acrylonitrile over styrene by a factor of about 1.7. This is a different pattern of behavior than that observed by Jones et al. for simple alkyl radicals bearing different γ-substituents (see Fig. 1.4, p. 17). They found k_A/k_S for 1-butyl and 3-phenyl-1-propyl radicals to be very similar to each other and to that for cyclohexyl radical, although for 3-cyano-1-propyl radical, a 3.5-fold reduction in this ratio was observed.

It is interesting that no difference in k_A/k_S was found for 5-phenyl-1-pentyl and 5-cyano-1-pentyl in light of the fact that such a large difference exists for 3-phenyl-1-propyl and 3-cyano-1-propyl. If the difference in k_A/k_S for 3-phenyl-1-propyl and 3-cyano-1-propyl was due to a "through-space" interaction that exists between the unpaired electron and the γ-substituent, one might expect a difference in k_A/k_S of a similar or even greater magnitude for the ε-substituted radicals, because conformations which place the ε-substituent in close proximity to the unpaired electron should be easily attained. One can imagine, for example, the chair-like conformation for 5-phenyl-1-pentyl radical depicted in Fig. 3.7 (p. 81).

If primary alkyl radicals can be taken as models for styrene-acrylonitrile (SAN) macroradicals, the results presented here for ε-substituted radicals would argue that the identity of the third-to-last (or antepenultimate) unit of a SAN macroradical does not affect its selectivity. The penultimate model would therefore be sufficient to describe SAN copolymerization, inasmuch as this model can account for γ-substituent effects which are suggested by the work of Jones et al. (57).

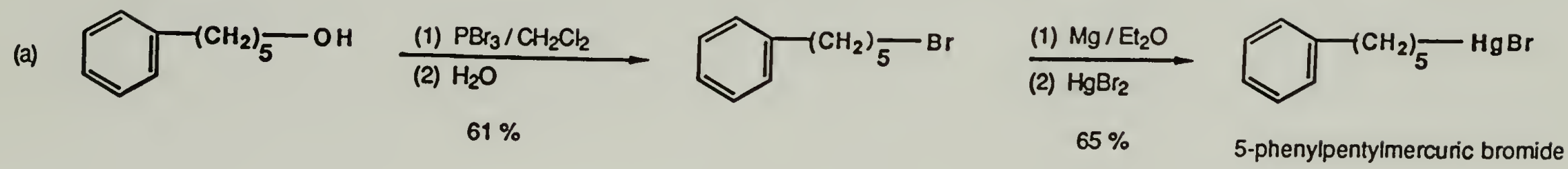

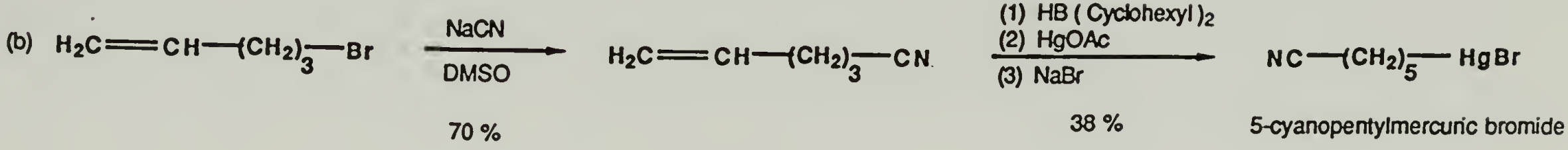

Scheme 3.1. Synthesis of (a) 5-phenyl-1-pentylmercuric bromide, and (b) 5-cyano-1-pentylmercuric bromide.

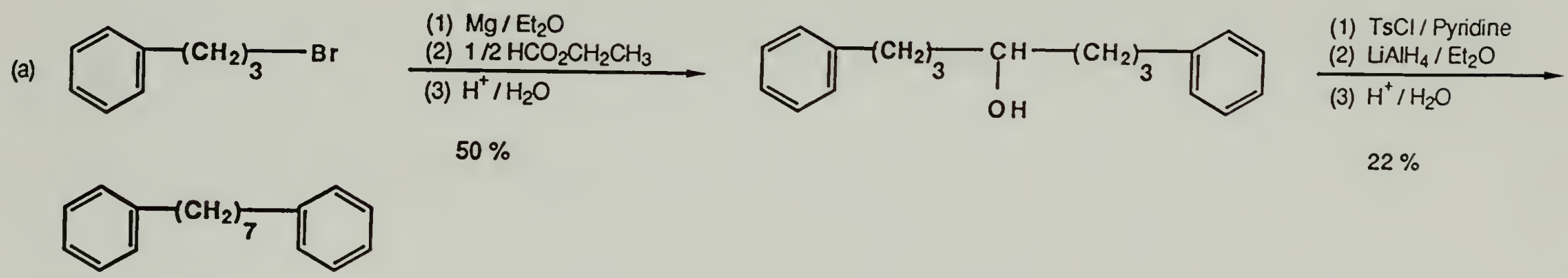

Scheme 3.2. Synthesis of (a) 1,7-diphenylheptane, and (b) methyl 8-cyanooctanoate.

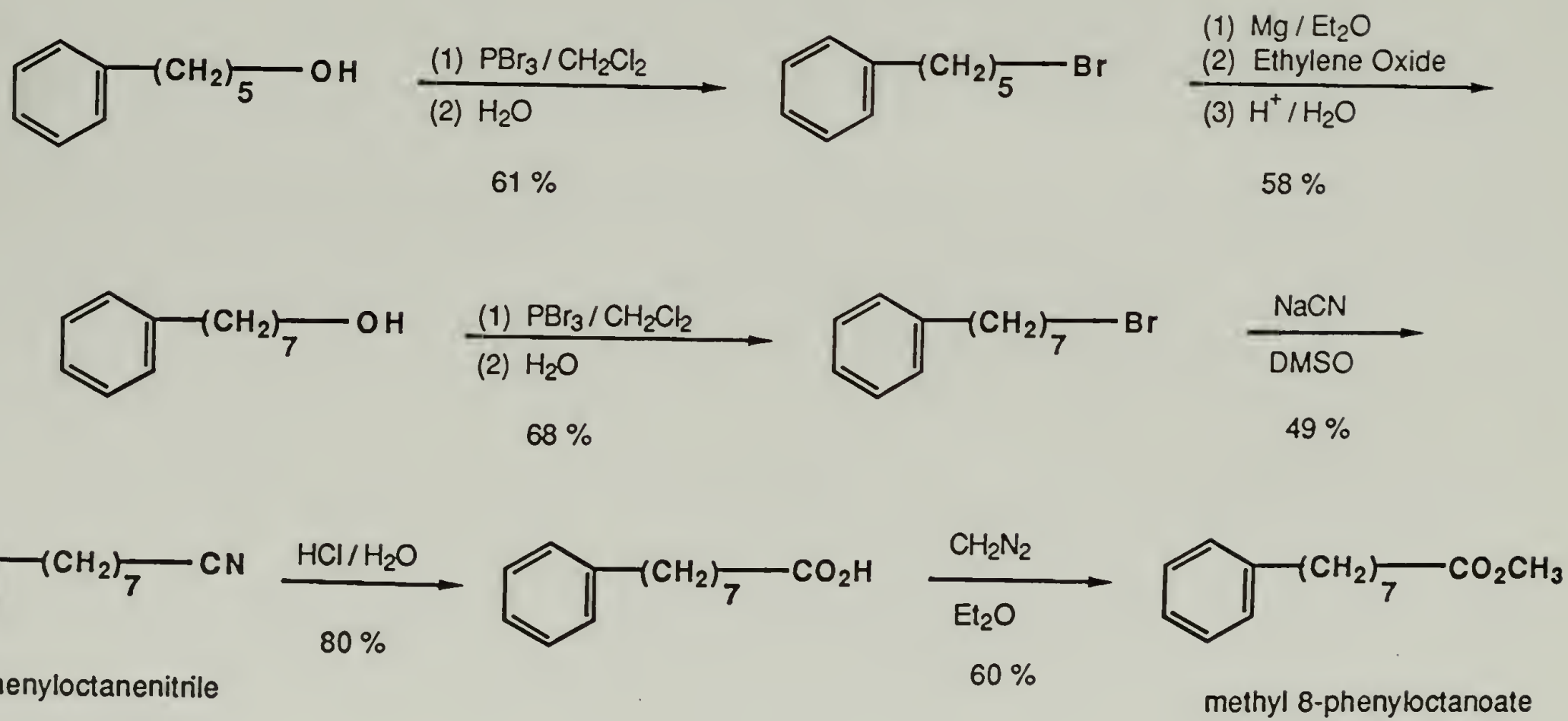

Scheme 3.3. Synthesis of 8-phenyloctanenitrile and methyl 8-phenyloctanoate.

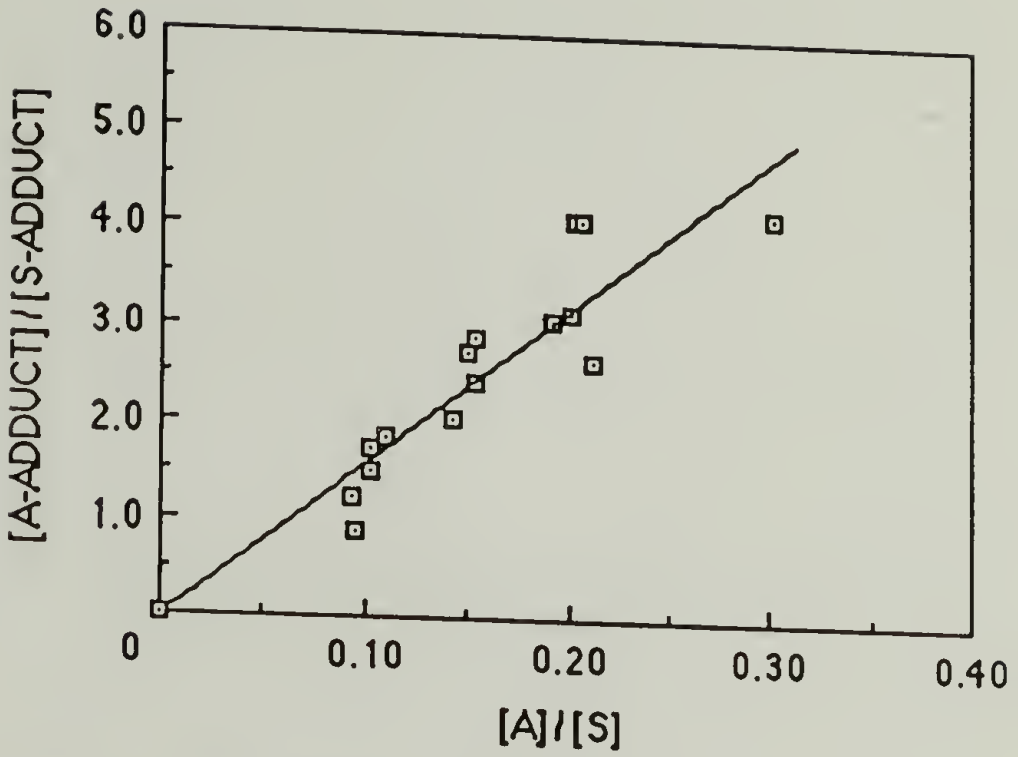

Figure 3.1. Plot of adduct ratio vs. alkene ratio for the competitive addition of acrylonitrile (A) and styrene (S) to the 5-phenyl-1-pentyl radical.

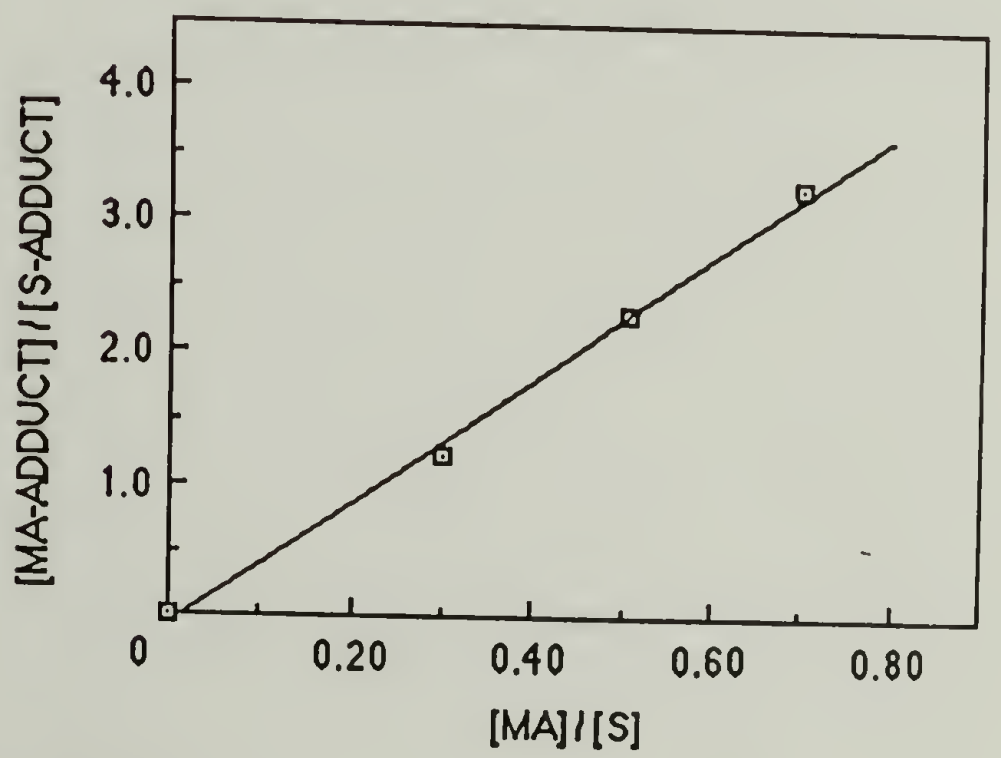

Figure 3.2. Plot of adduct ratio vs. alkene ratio for the competitive addition of methyl acrylate (MA) and styrene (S) to the 5-phenyl-1-pentyl radical.

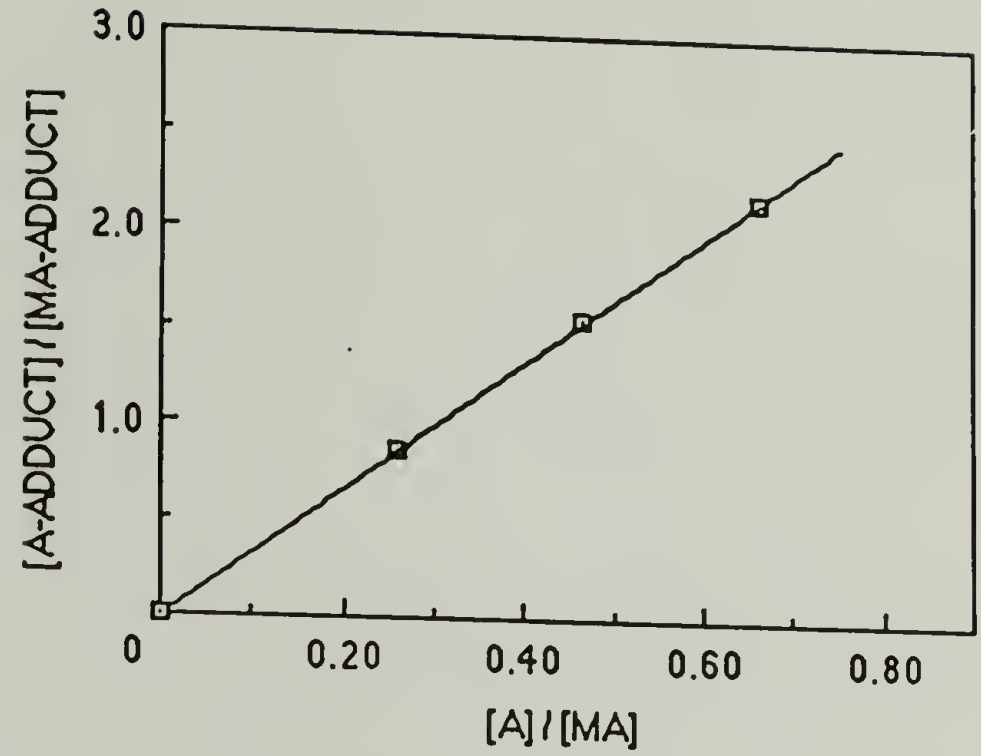

Figure 3.3. Plot of adduct ratio vs. alkene ratio for the competitive addition of acrylonitrile (A) and methyl acrylate (MA) to the 5-phenyl-1-pentyl radical.

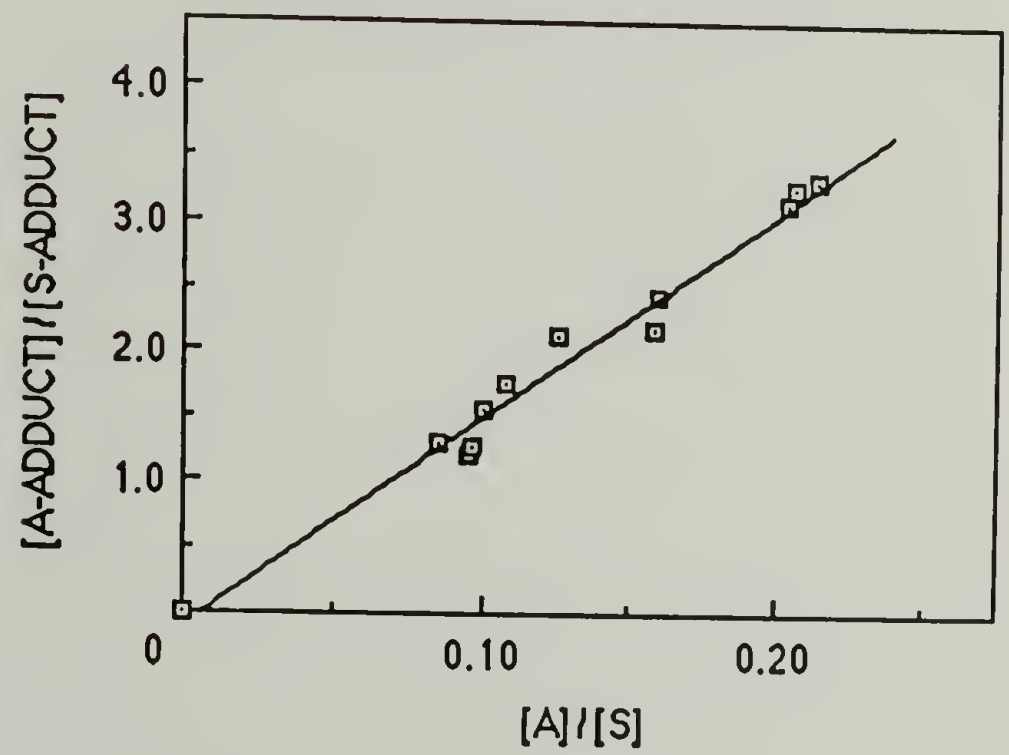

Figure 3.4. Plot of adduct ratio vs. alkene ratio for the competitive addition of acrylonitrile (A) and styrene (S) to the 5-cyano-1-pentyl radical.

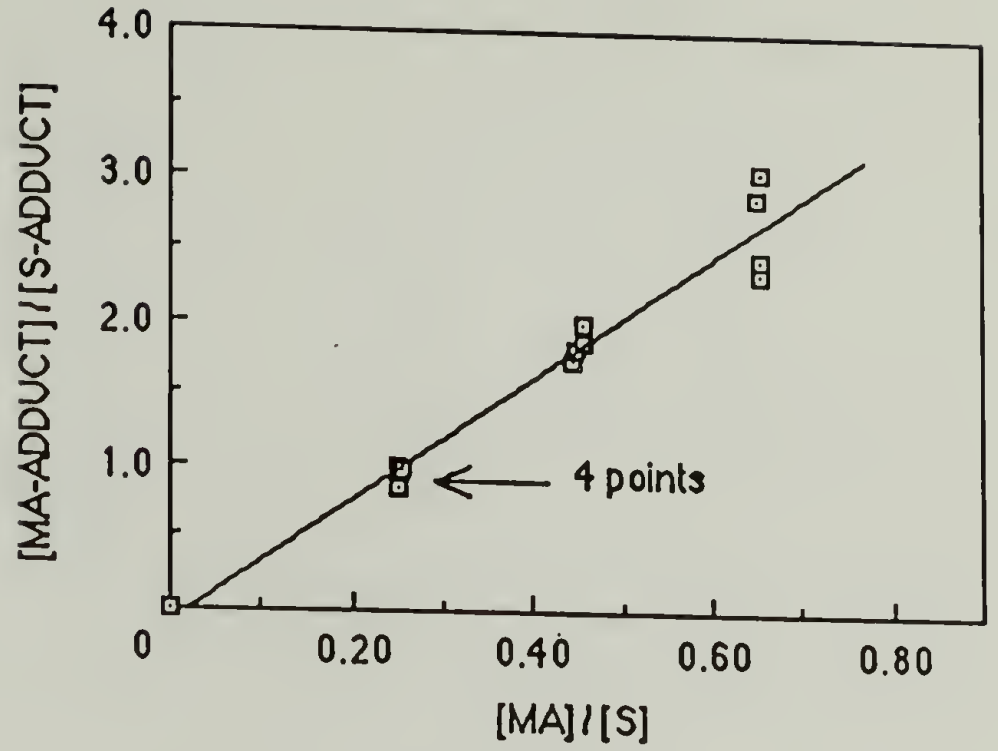

Figure 3.5. Plot of adduct ratio vs. alkene ratio for the competitive addition of methyl acrylate (MA) and styrene (S) to the 5-cyano-1-pentyl radical.

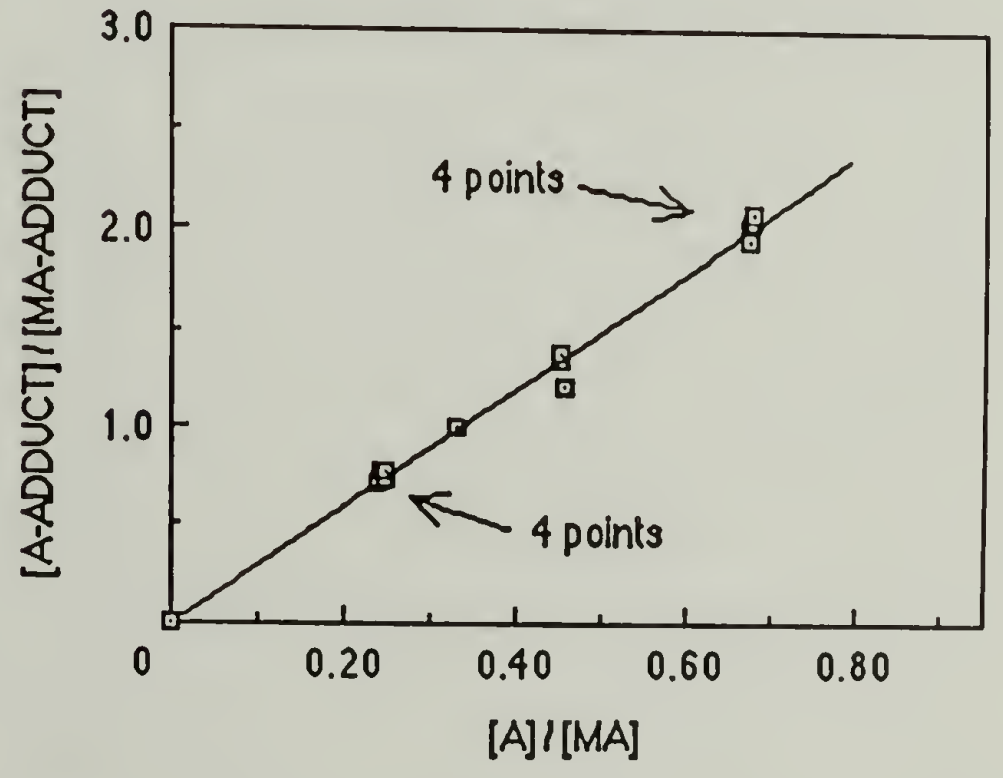

Figure 3.6. Plot of adduct ratio vs. alkene ratio for the competitive addition of acrylonitrile (A) and methyl acrylate (MA) to the 5-cyano-1-pentyl radical.

Table 3.1. Mercury Method Results: Relative Rates of Addition of Alkenes to Alkyl Radicals.

radical	competition[a] M_X/M_Y	k_{M_X} / k_{M_Y}
5-phenyl-1-pentyl	A/S	15.8 ± 2.9[b]
	MA/S	4.68 ± 0.27
	A/MA	3.28 ± 0.01
5-cyano-1-pentyl	A/S	15.8 ± 1.3
	MA/S	4.25 ± 0.38
	A/MA	2.98 ± 0.12

[a] M_X = acrylonitrile (A) or methyl acrylate (MA); M_Y = styrene (S) or methyl acrylate (MA).

[b] Rate constant ratios are reported as the slope of the linear least squares fit line ± the standard deviation of the slopes of the origin-to-point lines.

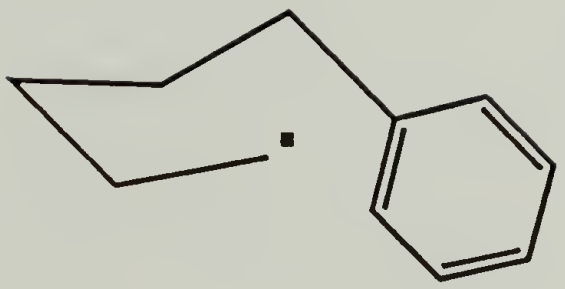

Figure 3.7. Possible conformation of 5-phenyl-1-pentyl radical.

B. Relative rates of addition of alkenes to 1-(1-phenyl)alkyl radicals

1. Preparation of azo compounds

Two widely used routes for the preparation of symmetrical aliphatic azo compounds are illustrated in Scheme 3.4 (p. 97) (101). The older method involves reduction of a ketazine (RC=N-N=CR) to the N,N'-dialkylhydrazine, usually accomplished by catalytic hydrogenation, followed by an oxidation step, for which mercuric oxide is typically used. The other method requires an N,N'-dialkylsulfonamide, generally prepared from the amine and sulfuryl chloride, and the desired azoalkane is produced upon reaction with base and hypochlorite. A wide variety of reagents and specific procedures have been used; the reader is referred to a review by Timberlake and Stowell (101) in this regard, as well as for a discussion of several other routes to azoalkanes.

The compounds 1,1'-azobis(1-phenyl[1-^{13}C]ethane) (**1a**) and 1,1'-azobis(1,3-[1-^{13}C]diphenylpropane) (**1b**) were prepared from the ketazines, as the required ketone precursors could be prepared easily and economically from available ^{13}C enriched starting materials. The same route could not be employed for the preparation of 4,4'-azobis(4-phenyl[4-^{13}C]butyronitrile) (**1c**), however, because of the sensitivity of a cyano group to reduction. This compound was prepared by oxidation of the corresponding sulfonamide, thereby avoiding a harsh reduction step.

The synthesis of 1,1'-azobis(1-phenylethane) has been reported (102-110), and in all but one case (108) the starting material has been acetophenone azine. Preparation from the azine generally involves crystallization of the crude product (an oil) from methanol, and the pure *meso* form is thus obtained as a white, crystalline solid (109). Greene et al. (110) prepared optically pure *SS*-(-)-1,1'-azobis(1-phenylethane) from the optically pure amine, and found it to be a pale yellow liquid. *Meso*-1,1'-azobis(1-phenylethane) was first shown to be an effective polymerization initiator by Cohen (103) in 1950. A ^{13}C enriched form of this compound, 1,1'-azobis(1-phenyl[1-^{13}C]ethane) (**1a**), was prepared here in 15% overall yield starting from [1-^{13}C]acetic acid (99 atom %), as outlined in Scheme 3.5 (p. 98). The experimental procedures used are essentially the same as those used by others (109), so it is assumed that it is the pure *meso* form of **1a** that was isolated. Natural-abundance 1a was also prepared, starting from acetophenone . The proton-decoupled ^{13}C NMR spectrum of 1a showed

an intense signal at 77.2 ppm - the same chemical shift as was observed for the methine carbon in the spectrum of natural-abundance **1a** (Fig. 3.8, p. 99).

1,1'-Azobis(1,3-[1-^{13}C]diphenylpropane) (**1b**) was prepared in 10% overall yield starting from $Ba^{13}CO_3$ (99 atom %), as outlined in Scheme 3.6 (p. 100). Natural-abundance 1b was prepared in the same way starting from benzoyl chloride, and this is believed to be the first report of this azo compound. The synthesis of **1b** as described in Ch. II (p. 50) calls for two recrystallizations of the crude product from methanol-benzene and gives a final product that is a mixture of the *dl* and *meso* forms. (The *dl* designation refers to a mixture of the *RR* and *SS* forms). This conclusion is based on the following observations made for samples of natural-abundance 1b: First, a sample purified by two recrystallizations has a broad melting range of 78-100 °C, while a sample recrystallized six times has a sharp melting point at 109 °C. Identical elemental analyses, IR spectra, and UV spectra are obtained for these two samples, and all are consistent with the expected structure. Second, the proton-decoupled ^{13}C NMR spectrum of the lower melting sample has twice as many signals as that of the higher melting (cf. Figs. 3.9 and 3.10, pp. 101-102); within 0.5 ppm of every signal that appears in the spectrum of the higher melting sample there occurs an additional signal in the spectrum of the lower melting sample. This observation is not due to the different signal frequencies at which the spectra of Figs. 3.9 and 3.10 were recorded - it was ascertained that a spectrum similar to that recorded at 50 MHz (Fig. 3.10) was also obtained at 75 MHz. Third, the ^{1}H NMR of the lower melting sample is more complex than that of the higher melting (Fig. 3.11, p. 103), although the spectra are very similar overall and the relative areas of the methylene, methine, and aromatic signals in each spectrum are as expected. Finally, samples of crude azo compound which are recrystallized between two and six times have melting and spectral characteristics which are intermediate to those described above. A reasonable explanation for these observations is that of the two samples, both chemically pure, the lower melting is a *dl* and *meso* mixture, and the higher melting is pure *meso* or pure *dl*. The sample of (^{13}C enriched) 1b used to prepare SAN copolymers was purified by just two recrystallizations, and was thus a *dl* and *meso* mixture. In its proton-decoupled ^{13}C NMR spectrum (Fig. 3.12, p. 104) there are two intense signals at 81.66 and 81.74 ppm - the same chemical shifts as are observed for the methine carbons of natural-abundance **1b** (cf. Fig. 3.9).

4,4'-Azobis(4-phenyl[4-^{13}C]butyronitrile) (**1c**) was prepared in 1.2% overall yield starting from $Ba^{13}CO_3$ (99 atom %) as outlined in Scheme 3.7 (p. 105). Natural-abundance 1c was

prepared in the same way starting from ethyl 3-phenyl-3-ketopropionate (ethyl benzoyl acetate), and this is believed to be the first report of this azo compound. The synthesis of **1c** as described in Ch. II (p. 55) calls for two recrystallizations of the crude product from methanol and gives a final product that is either the pure *meso* or pure *dl* form. This conclusion is based on the following observations made for samples of ^{13}C enriched **1c**: First, a sample that was purified by only one recrystallization has a mp that is broad and low (68-80 °C) compared to that of a sample purified by two recrystallizations (124-125 °C). This observation in itself cannot support the claim made above, however, because the lower melting material contains an impurity of unknown composition. Nevertheless, identical IR and UV spectra are obtained for the two samples, and the elemental analysis of the higher melting material is consistent with the formula of **1c**. Second, the proton-decoupled ^{13}C NMR spectrum of the higher melting sample has a single intense signal in the region expected for the methine carbon, while the spectrum of the lower melting sample has two intense signals in this region, as well as another signal in a different area that arises from a ^{13}C enriched impurity (Fig. 3.13, p. 106). Finally, two overlapping triplets are observed for each signal from the methine protons in the ^{1}H NMR spectrum of the of the lower melting sample, while a single triplet is seen for each for the higher melting (Fig. 3.14, p. 107). Based on these observations, and by comparison to characteristics described previously for **1b**, it seems reasonable that the higher melting material is the pure *meso* or *dl* form of **1c**. This was the sample of **1c** used to prepare SAN copolymers. Its proton-decoupled ^{13}C NMR spectrum ("b" in Fig. 3.13, p. 106) shows an intense signal at 81.13 ppm - the same chemical shift as is observed for the methine carbon of natural-abundance **1c** (Fig. 3.15, p. 108).

2. Rate constant ratio determinations for styrene and acrylonitrile additions

The rate constant ratios for addition of styrene and acrylonitrile to the 1-phenyl[1-^{13}C]ethyl (**2a**), 1-(1,3-diphenyl)[1-^{13}C]propyl (**2b**), and 4-(4-phenyl)[4-^{13}C]butyronitrile (**2c**) radicals were determined. The assumption will be made that there is no difference between the ^{13}C enriched and natural-abundance forms of **2a**, **2b**, or **2c** with regard to their respective preferences for addition of styrene and acrylonitrile; accordingly, the results and abbreviations for the ^{13}C enriched radicals will be generalized to include the natural-abundance radicals, although it is clear that the k_A/k_S determinations were made for only the enriched radicals. The radicals were generated by photolysis of 1,1'-azobis(1-phenyl[1-^{13}C]ethane) (**1a**), 1, 1'-

azobis(1,3-diphenyl[1-^{13}C]propane) (1b), and 4,4'-azobis(4-phenyl[4-^{13}C]butyronitrile) (1c) in the presence of known amounts of styrene and acrylonitrile, according to Scheme 1.9 (p. 31), and styrene-acrylonitrile (SAN) copolymers containing ^{13}C enriched end groups (3 and 4) were produced. These experiments were performed at 33 °C in benzene solution under steady-state irradiation, and all copolymers remained soluble throughout the reaction. To minimize drift in monomer feed composition, the conversion of each copolymerization was limited to 7-11% (cf. Tables 2.3, 2.4, and 2.5, pp. 60, 61, and 63). The molecular weights of the enriched copolymers (Table 3.2, p. 109) were estimated by comparison of gel permeation chromatograms with those of polystyrene samples having known molecular weights and narrow distributions thereof ($M_w/M_n < 1.1$).

Presented in Fig. 3.16 (p. 110) are ^{13}C NMR spectra of polystyrenes prepared by using enriched and unenriched 1a. Two new signals appear at 36.78 and 37.39 ppm in the spectrum of the enriched polymer and are assigned to the two alternative stereochemical configurations of end group 3a. Similarly, Figs 3.17 and 3.18 (pp. 111-112) show polystyrenes derived from 1b and 1c. Two new signals appear at 42.54 and 43.08 ppm in the spectrum of the enriched polystyrene from 1b, and these are assigned to 3b. For the polystyrene from 1c, two new signals are seen at 42.17 and 42.48 ppm, these being only partially resolved, and these are assigned to 3c. In each case, the chemical shifts of the signals assigned to end groups 3 are within 2 ppm of those calculated using a method described by Silverstein et al. (111). The integral areas of the two signals observed for each of the end groups 3 are equal, and this would imply that the stereochemistry in each is the result of random placement of styrene monomer. New signals also occur in the region of 48-50 ppm for spectra of enriched polystyrenes from 1b and 1c, although these are quite small; in each case the total integral area of the signals is less than 7% that of the corresponding end group signals assigned above. The origin of these signals at 48-50 ppm is unknown, but they almost certainly arise from ^{13}C enriched initiator fragments that are incorporated in the polymer. Spectra which were taken after several reprecipitations of the polystyrenes showed that the relative intensities of the signals did not change, so it is unlikely the signals arise from occluded low molecular weight impurities.

Expanded plots of polystyrene (PS) spectra in the regions of the end group signals are presented in Figs. 3.19, 3.20, and 3.21 (pp. 113-115). Of these, only the spectra of polystyrenes derived from 1a (Fig. 3.19) are actually portions of the full spectra just discussed, which were all recorded at 20 °C using $CDCl_3$ solutions. The partial spectra of polystyrenes derived from 1b

(Fig. 3.20) and 1c (Fig. 3.21) were recorded using other solvents and temperatures to facilitate comparison to SAN copolymer spectra (vide infra). Spectra of polystyrenes derived from 1b were obtained at 140 °C using deuterated diglyme solutions, and the signals assigned to 3b occur under these conditons at 43.54 and 43.77 ppm. Considerable fine structure is evident in the 3b signals, and it appears that the two principal signals are composed of a total of at least six individual lines. For polystyrenes derived from 1c, spectra were obtained using deuterated bromobenzene solutions at 136 °C. Under these conditions the two signals assigned to 3c, which were partially resolved in $CDCl_3$ solution, now overlap to an even greater extent and essentially one signal centered at 42.58 ppm is obtained.

^{13}C NMR spectra of polyacrylonitriles prepared by using enriched and natural-abundance 1a, 1b, and 1c are shown in Figs. 3.22, 3.23, and 3.24 (pp. 116-118). In each case new signals arise in the spectrum of the enriched polymer, and these are assigned to 4a, 4b, or 4c, as the case may be. The natural-abundance signals were assigned according to Pichot and Pham (112). The spectral region obscured by dimethyl sulfoxide-d_6 (DMSO-d_6) was observed for each polyacrylonitrile (PAN) in N,N-dimethylformamide-d_7 (DMF-d_7), and no signals were seen. Expanded plots of spectra obtained using the DMF-d_7 solutions are presented in Figs. 3.25, 3.26, and 3.27 (pp. 119-121). Three distinct signals are seen at 37.92, 38.05, and 38.75 ppm for end group 4a; four signals are seen at 43.56, 43.78, 44.13, and 44.21 ppm for 4b; and four signals are seen at 42.94, 43.16, 43.60, and 43.72 ppm for 4c. The chemical shifts of the end group signals all occur within 2 ppm of the calculated shifts.

One cannot help but notice the similarity of the signals from end groups 4a-c to each other. It is believed that in each case there are two "parent" signals, and these correspond to the two alternative stereochemical configurations possible for end group 4 if it is envisioned to be composed of the initiator fragment and one acrylonitrile unit as pictured in Scheme 1.9 (p. 31). Splitting of each of these signals would then correspond to further configurations which are possible as the placement of further acrylonitrile units are taken into consideration. For example, one would expect four signals - or a "doublet of doublets" - on this basis if end group 4 includes the initiator fragment and two adjacent acrylonitrile units. These signals should be of equal intensity if the placement of the acrylonitrile units were at random. This is precisely what is seen for 4b and 4c. For endgroup 4a, however, only three distinct signals are observed. It is conjectured that for the configuration of 4a associated with the signal that is farthest downfield (at 38.75 ppm) there is little difference, as far as the magnetic environment of the

enriched carbon is concerned, between the two alternative ways in which the second acrylonitrile unit (the unit farther from the initiator fragment) can be placed with respect to the first. This is consistent with the fact that the integral area of the peak at 38.75 ppm is equal to twice the area of either of the other two signals that occur at 37.92 and 38.05 ppm.

As mentioned above, the fact that 1:1 area ratios are observed for the signals comprising end groups 3 or 4 implies that the stereochemistry in each case is the result of random placement of monomer. However, it may be that there are radical-monomer interactions capable of influencing the stereochemistry of the end groups, and that at the polymerization temperature of 33 °C, these interactions are of magnitudes such that equal proportions of the different possible configurations just happen to be produced. Since the magnitudes of these interactions would probably be dependent on the temperature, the relative areas of the end group signals might be temperature dependent. This possibility was investigated for end groups 3a and 4a by performing the polymerizations of styrene and acrylonitrile at different temperatures, using **1a** as initiator. Over the temperature range 0-52 °C, the areas of the signals from 3a were found to remain in a 1:1 ratio. Over the range 0-60 °C, the areas of the signals from 4a remained in the 1:1:2 ratio described above . (The spectra obtained from these experiments are given in Appendix D, Figs. D-12 and D-13, pp. 221, 223). It should be kept in mind that the stereochemistry of an endgroup is not fixed until two monomer molecules have added to the primary radical (113) formed upon initiator decomposition, defining an end group as being composed of the initiator residue and one monomer unit as pictured in Scheme 1.9 (p. 31). Accordingly, interactions that would influence end group stereochemistry would be those between an incoming monomer and the radical that is formed upon the addition of one molecule of monomer to the primary radical. These interactions would most likely take the form of repulsions or attractions between specific groups. The radical formed upon addition of styrene to 2a is the 1-(1,3-diphenyl)butyl radical, and that formed upon addition of acrylonitrile to 2a is the 2-(4-phenyl)pentanenitrile radical. Therefore, it is inferred that there exist no such interactions of any significance, over the temperature ranges studied, for the case of 1-(1,3-diphenyl)butyl radical adding styrene or for the case of 2-(4-phenyl)pentanenitrile adding acrylonitrile.

Spectra of SAN copolymers prepared with enriched and natural-abundance 1a, 1b, and 1c are shown in Figs. 3.28, 3.29, and 3.30 (pp. 122-124). In each case, intense signals not present in the spectrum of the natural-abundance copolymer are seen in the spectrum of the ^{13}C enriched

sample, and these are assigned to the end groups in accordance with the initiator 1 that was used. These spectra were recorded using $CDCl_3$ solutions. The signals assigned to 3a + 4a appear in the region of 36.7-38.0 ppm; those assigned to **3b + 4b** are seen at 42.1-43.8 ppm, and those for 3c + 4c are at 41.5-43.3 ppm. In all cases, only small overlaps of these signals with natural-abundance signals are seen. Only for the copolymers derived from **1a** was the use of $CDCl_3$ as a solvent found to be satisfactory with regard to the resolution of end group signals into their **3** and **4** components. Other solvents at elevated temperatures were necessary for the copolymers derived from **1b** and **1c**.

Copolymer spectra recorded using solvents and temperatures necessary to resolve the end group signals, and expanded in the regions of interest, are presented in Figs. 3.31, 3.32, and 3.33 (pp. 125, 127, 129). Each figure includes spectra of copolymers prepared with the same ^{13}C enriched initiator **1** at two different monomer feed compositions. A natural-abundance copolymer was prepared for every enriched copolymer to ensure correct base-line assignment in the spectral regions corresponding to the end groups **3** and **4**. In each case, the natural-abundance copolymer spectrum is normalized with respect to that of the enriched sample on the basis of neighboring (natural-abundance) signal intensities. These spectra were recorded under conditions suitable for quantitative signal integration (see Ch. II, p. 67). Pulse delays of at least 5 times the longest end group T_1 were used. Spectra of copolymers derived from **1a** (Fig. 3.31) were recorded with suppression of the nuclear Overhauser effect (NOE); those of copolymers derived from **1b** (Fig. 3.32) and **1c** (Fig. 3.33) were recorded without NOE suppression after it was determined that the **3b/4b** and **3c/4c** peak area ratios were unaffected by the NOE. For each initiator **1**, copolymers were prepared at eight different monomer feed compositions; spectra not shown here are given in Appendix D (Figs. D-14 through D-31, pp. 224-241).

The end group signals were assigned by comparison of copolymer spectra with spectra of PS and PAN samples, and from variations in signal intensity with changes in monomer feed composition. The signal(s) assigned to endgroup **3a** appear at 36.75 and 37.42 ppm, those from **3b** appear at 43.54 and 43.77 ppm, and that from **3c** appears at 42.58 ppm. These chemical shifts are identical to those from polystyrene spectra recorded under the same conditions (vide supra), although one can see from comparison of copolymer and PS spectra that the fine structures of the signals tend to be a little different . As for end groups **4**, signals assigned to **4a** appear at 37.12 and 38.00 ppm, those from **4b** appear at 43.34, 43.60, and 44.30 ppm, and those from 4c appear at

42.13, 42.38, and 43.10 ppm. In each case, the signal that is farthest downfield has significant fine structure, and is composed of two or three peaks that change in relative intensity with copolymer composition. The chemical shifts and general appearances of the end group signals are different from (although similar to) those observed for PAN samples in DMF-d_7. This is expected, however, because of the different solvents and temperatures used to obtain PAN and copolymer spectra. To aid in the assignments of the signals for **4b**, a copolymer was prepared at a feed composition that was high enough in acrylonitrile ([S]/[A] = 0.83) so that signals from **3b** would be negligible compared to those of **4b**. This copolymer is soluble in diglyme at 140 °C (unlike PAN), and its spectrum is given in Fig. 3.34 (p. 130). As can be seen from Figs. 3.31, 3.32, and 3.33, variations in end group signal intensity with changes in monomer feed composition are as expected in all cases.

The 3/4 peak area ratios obtained by integration of end group signals are given in Tables 2.3, 2.4, and 2.5 (pp. 60, 61, 63), corresponding to copolymers prepared with **1a**, **1b**, and **1c**. Relevant polymerization data are also found in these tables. Eight enriched copolymers were prepared from each initiator **1**; in each case, the range of monomer feed composition was sufficient to impart a significant range (typically about 0.4-1.6) to the respective 3/4 peak area ratio. Figures 3.35, 3.36, and 3.37 (pp. 131-132) present plots of relative end group concentration (ie., 3/4 peak area ratio) as a function of monomer feed composition ([S]/[A]). Each plot is linear, as expected, and the linear least-squares-fit line for each passes very near the origin. The slope of the line obtained in each case is the ratio of the rates of addition (or the "relative rate of addition") of styrene and acrylonitrile (k_S/k_A) to the radical **2**. From Fig. 3.35, k_S/k_A = 0.20 ± 0.02 for the 1-phenylethyl radical (**2a**); from Fig. 3.36, k_S/k_A = 0.21 ± 0.01 for the 1-(1,3-diphenyl)propyl radical (**2b**); and from Fig. 3.37, k_S/k_A = 0.52 ± 0.03 for the 4-(4-phenyl)butyronitrile radical (**2c**). The quoted error in each case is the standard deviation of the origin-to-point slopes. The relative standard deviation of a 3/4 determination was about 3%, as estimated by repeated analyses undertaken for several samples. Systematic error in [S]/[A] due to conversion effects, a subject discussed below, overshadows any random error in this parameter.

The errors given above for k_S/k_A values do not take into account drifts in monomer feed composition which may have occurred during the polymerizations. Although the conversions were low (< 11%), without specific examination it is difficult to be sure of anything. Therefore an attempt was made to estimate errors in the k_S/k_A values which may have resulted from the

finite conversions. All that was desired was a general idea of the magnitudes involved, rather than a rigorous analysis designed to account quantitatively for conversion effects. For any of the copolymerizations, the final feed composition can be calculated with knowledge of the conversion and the final overall copolymer composition, and an average feed composition can then be obtained. Such average values were calculated for three of the eight copolymerizations performed for each k_S/k_A determination. The initial feed compositions of these copolymerizations were representative of the entire range investigated in each case, and conversions were typical. Copolymer compositions were determined by nitrogen analysis. New 3-point plots were drawn using the averaged feed compositions, and the slopes of the best-fit lines gave the following : $k_S/k_A = 0.19$ for **2a**, $k_S/k_A = 0.20$ for **2b**, and $k_S/k_A = 0.49$ for 2c. Each value is slightly lower than that given previously, but still within the quoted error range. It is evident that conversion effects are insignificant. It is of interest to note here that the copolymer compositions determined for this analysis are quite close to those of Hill et al. (53) for bulk SAN copolymerization; for example, Hill et al. obtained a styrene mole fraction of 0.77 for a copolymer prepared with a feed composition [S]/[A] = 7.98, while a value of 0.78 was obtained in this work for a copolymer prepared at this same feed composition.

Some alternate methods of data analysis will now be discussed. The relative endgroup concentrations plotted in Figs. 3.35, 3.36, and 3.37 - the plots from which the k_S/k_A values were determined - were measured for each enriched copolymer by integration of the end group signals after a baseline had been assigned using the normalized spectrum of the natural-abundance copolymer prepared at the same feed ratio. This procedure was undertaken to minimize the effects of coincidence of natural-abundance and enriched signals. However, for the copolymers prepared from **1a** and **1b**, the natural-abundance signals in the region of the end groups are small and quite broad compared to those of the end groups. Accordingly, it was expected for these copolymers that the baseline assignment procedure just mentioned might have been unnecessary. Indeed, identical results were obtained when an alternate method of analysis was employed in which the baselines were assigned in each spectrum by simply drawing a horizontal line at the level of the deepest local minimum that occurred between the end group signals. On the other hand, for copolymers derived from **1c** at low [S]/[A] ratios (less than about 1.9; see Fig. 3.33, p. 129, and Figs. D-26 to D-31, pp. 236-241), there is a significant amount of overlap of natural-abundance and enriched signals in the region of 42.0-42.5 ppm. This affects the intensities of signals assigned to **4c** in this region (ie., the **4c** signals upfield to the 3c

multiplet), although the 4c multiplet that occurs further downfield at 43.10 ppm is relatively unaffected. This multiplet corresponds to the two partially resolved 4c signals at 43.60 and 43.72 ppm in the spectrum of PAN prepared from **1c** (Fig. 3.27, p. 121), and in this spectrum the sum of the integral areas of these signals is equal to the sum of the areas of the other 4c signals further upfield at 42.94 and 43.16 ppm. Should this relationship hold true for the corresponding signals in the copolymers, a valid alternate method of data analysis would then be to take the total integral area for 4c in the copolymer spectra as twice the area of the downfield 4c multiplet at 43.10 ppm, thus disregarding the 4c signals appearing further upfield that are overlapped by natural-abundance signals. Applying this alternate method gave a plot of [3c]/[4c] vs. [S]/[A] that was linear (correlation coefficient = 0.97) and passed near to the origin, and $k_S/k_A = 0.58 \pm 0.06$ was obtained from the slope. This value for 2c agrees within experimental error with that obtained by the normal analysis ($k_S/k_A = 0.52 \pm 0.03$), a result which serves to increase confidence that the interference of natural-abundance signals with the 4c signals occurring upfield to the 3c multiplet did not have a great effect upon the rate constant ratio determination for 2c.

A final alternate method of analysis concerns the determination of k_S/k_A for 2b. Inspection of spectra for enriched copolymers derived from **1b** reveals that in each case there is a well resolved 4b multiplet at 44.30 ppm, while the other signals occurring downfield and assigned to 4b and 3b are not well resolved from each other (see Fig. 3.32, p. 127, and Figs. D-20 to D-25, pp. 230-235). The well resolved multiplet at 44.30 ppm corresponds to the two partially resolved 4b signals at 44.13 and 44.21 ppm in the spectrum of PAN prepared from **1b** (Fig. 3.26, p. 120), and in this spectrum the sum of the integral areas of these signals is equal to the sum of the areas of the other 4b signals further upfield at 43.56 and 43.78 ppm. Should this relationship be true for the corresponding signals in the copolymers, a valid alternate method of data analysis would then be to take the total integral area for 4b in the copolymer spectra as twice the area of the downfield 4b multiplet at 43.30 ppm, and thus the area for 3b is given by subtracting the area of the 4b multiplet at 43.30 ppm from the summed integral areas of the upfield 3b and 4b signals at 43.2-44.0 ppm. Application of this alternate method resulted in a plot of [3b]/[4b] vs. [S]/[A] that was linear (correlation coefficient = 0.99) and passed near to the origin; $k_S/k_A = 0.21$ was obtained from the slope. This is an identical result as obtained by the normal analysis, and gives one confidence that the somewhat poor resolution of 3b and 4b

signals in the range of 43.2-44.0 ppm did not have a great effect upon the k_S/k_A determination for 2b.

The results obtained for the addition of styrene and acrylonitrile to the 1-(1-phenyl)alkyl radicals 2 can best be interpreted in the context of the previous investigation (57) from this laboratory of acrylonitrile-styrene addition to n-alkyl radicals, and in the context of the penultimate model analysis of SAN copolymerization by Hill, O'Donnell, and O'Sullivan (53). Figure 3.38 (p. 133) presents k_A/k_S values for comparison; these are reciprocals of the values obtained for 2a-c in this work, while the values for the macroradicals from the work of Hill et al. are reciprocals of the best-fit penultimate reactivity ratios. A number of related observations are now made. First, the 2.5-fold decrease in k_A/k_S for 2c as compared to the nearly identical values for 2a and 2b is most striking, and clearly shows that a cyano substituent in a position gamma to a 1-(1-phenyl)alkyl radical can have a relatively large effect on the radical's preference for addition of acrylonitrile. Second, this 2.5-fold decrease in k_A/k_S for 2c is consistent with a similar 3.5-fold decrease observed in previous work for 4-butyronitrile radical as compared to 3-phenylpropyl, hexyl, and butyl. Third, the 2.5-fold decrease in k_A/k_S for 2c as compared to 2b agrees very well with the 2.7-fold decrease postulated by Hill et al. for a macroradical with an SS end as compared to an AS end. Fourth, the actual magnitudes of k_A/k_S for 2b and 2c agree very well with those of the SS and AS terminated macroradicals, respectively; in each case, the values for the small radicals are higher than those for the corresponding macroradicals by the same factor of about 1.2.

The foregoing observations provide strong evidence for the existence of penultimate effects in SAN copolymerization. Indeed, it would be unusual if SS and AS terminated macroradicals did not exhibit the selectivity differences observed for small radicals 2b and 2c, which have structures essentially identical to the propagating ends of the macroradicals. The most likely explanation for the reduction in the relative rate of acrylonitrile addition to an alkyl radical bearing a γ-cyano group is the development in the transition state of dipolar repulsion between cyano groups on the monomer and radical. When the results of the separate investigations summarized in Fig. 3.38 are taken together, one is compelled to conclude that the penultimate model is a physically meaningful description of SAN copolymerization. In a broader context, it is felt that the measurements of k_S/k_A that were made for 2a, 2b, and 2c constituted the first truly rigorous test of the physically plausibility of the penultimate model of copolymerization.

3. Rate constant ratio determinations for methyl methacrylate and acrylonitrile additions

The procedure used to obtain the rate constant ratio for addition of methyl methacrylate and acrylonitrile (k_{MMA}/k_A) to 1-phenylethyl radical (**2a**) is entirely analogous to that described in the previous section for the measurement of k_S/k_A for **2a**. Acrylonitrile-methyl methacrylate (AMMA) copolymers were prepared with 1,1'-azobis(1-phenyl[1-^{13}C]ethane) (**1a**) in benzene solution at 33 °C, according to Scheme 1.10 (p. 32), and determination of the relative ^{13}C enriched end group concentrations (**5/6**) by ^{13}C NMR affords the value of k_{MMA}/k_A. It is also possible to determine k_{MMA}/k_A for the 2-(4-phenyl)pentanenitrile radical from the same data, owing to the unexpected resolution of signals from end group 6. It is noted here that all of the AMMA copolymers remained soluble throughout the polymerization reactions. As before, molecular weights were estimated by gel permeation chromatography (GPC) using polystyrene standards, and were found to be 44,000 ± 4,000 for all of the enriched AMMA copolymers.

Shown in Figure 3.39 (p. 134) are ^{13}C NMR spectra of poly(methyl methacrylate) (PMMA) samples prepared by using enriched and unenriched **1a**. New signals appear at 35.74, 35.93, 36.20, and 36.72 ppm in the spectrum of the enriched polymer and are assigned to end group **5**. Figure 3.40 (p. 135) is an expansion of the spectrum of the enriched polymer in the end group region.

Figure 3.41 (p. 136) presents spectra of AMMA copolymers prepared with enriched and unenriched **1a** at the same monomer feed composition. Intense signals not observed for the natural-abundance copolymer are seen in the spectrum of the enriched copolymer in the region of 35-39 ppm, and these are assigned to end groups **5** + **6**. In this spectral region there occur no natural-abundance signals for the entire range of feed compositions investigated.

Figure 3.42 (p. 137) shows partial spectra of enriched AMMA copolymers prepared at two different monomer feed compositions; spectra of copolymers prepared at six other feed compositions are presented in Appendix D (Figs. D-32 through D-34, pp. 242-244). These spectra were recorded under conditions suitable for quantitative signal integration (see Ch. II, p. 67) using $CDCl_3$ solutions. The signals observed in the spectrum of enriched PMMA (Fig. 3.40) and assigned to end group **5** again appear at 35.74, 35.93, 36.20, and 36.72 ppm. In addition, several small signals at 35.85, 36.40, and 36.57 ppm are observed. These small signals are also assigned to end group **5** based on their change in intensity with monomer feed composition. The chemical shifts quoted for **5** are from the bottom spectrum in Fig. 3.42, which corresponds to a

copolymer prepared at a feed composition relatively high in methyl methacrylate ([MMA]/[A] = 6.62). It is evident from the top spectrum in Fig. 3.42, for a copolymer prepared with a feed much lower in methyl methacrylate ([MMA]/[A] = 0.999), that the intensities of the signals from 5 vary significantly with respect to each other as a function of the feed composition. Although stereochemical effects might contribute, this observation is probably due to a compositional change in the end group with respect to monomeric units further removed from the initiator residue than the first. The signals assigned to 6, which is the end group obtained upon addition of acrylonitrile to the primary radical **2a**, show an even greater sensitivity to end group composition. Distinctly different signals are seen for 6 according to whether the second monomer to have added to **2a** (after acrylonitrile) was methyl methacrylate or acrylonitrile, and end groups 7 and 8 are defined on this basis according to Scheme 1.10 (p. 32). (Note that 7 and 8 are both 6, by definition.) The relative amounts of end groups 7 and 8 (ie., 7/8) will be a measure of k_{MMA}/k_A for the 2-(4-phenyl)pentanenitrile radical, which is the radical obtained upon addition of acrylonitrile to the primary radical 2a. The signal assignments for 6 as opposed to 5, as well as for 7 as opposed to 8, were made according to variations in the respective relative signal intensities with changes in feed composition, and by comparison to the spectrum of PAN prepared with **1a** (Fig. 3.25, p. 119). Signals assigned to 8 only appear for copolymers prepared with feeds rich in acrylonitrile ([MMA]/[A] < 3.0), as it should be. The chemical shifts of the signals from end group 8 should be identical to those for **4a** in the PAN spectrum, assuming spectra are recorded under identical conditions, because 8 and **4a** only differ in structure at sites far removed from the site of ^{13}C enrichment. Presented in Fig. 3.43 (p. 138) is a spectrum of the copolymer prepared with [MMA]/[A] = 0.999 and recorded using the same solvent (DMF-d_7) as was used for the PAN spectrum (Fig. 3.25, p. 119). End groups 7 and 8 have a similar overall appearance as compared to that in $CDCl_3$ (Fig. 3.42), and the chemical shifts observed for 8 in this spectrum are identical to those for **4a** in the PAN spectrum. The chemical shifts of the signals assigned to end groups 7 and 8 (and thus 6) in $CDCl_3$ are now listed: (7) 37.05 and 37.82 ppm; (8) 37.92, 38.05, and 38.75 ppm.

The 5/6 and 7/8 peak area ratios obtained by integration of end group signals are given in Table 2.6 (p. 64), where polymerization data for AMMA copolymers are also found. Figures 3.44 and 3.45 (p. 139) present plots of relative end group concentration (ie., 5/6 or 7/8 peak area ratio) as a function of monomer feed composition ([MMA]/[A]). Each plot is linear, as expected,

and the linear least-squares-fit line for each passes very near the origin. The slopes of the lines are the relative rates of addition of methyl methacrylate and acrylonitrile (k_{MMA}/k_A) to the radicals. From Fig. 3.44, $k_{MMA}/k_A = 0.44 \pm 0.03$ for 1-phenylethyl (2a); and from Fig. 3.45, $k_{MMA}/k_A = 2.4 \pm 0.4$ for 2-(4-phenyl)pentanenitrile. The quoted error in each case is the standard deviation of the origin-to-point slopes. The relative standard deviation of a 5/6 or a 7/8 determination was about 3%, as estimated by repeated analyses undertaken for a few samples. The effects of finite conversion were estimated using a procedure analogous to that described previously for the SAN copolymers, and were found to be insignificant.

The parameter k_{MMA}/k_A for **2a** should be comparable to the product of k_S/k_A for 2a and the reciprocal of the terminal model reactivity ratio r_1 for styrene-methyl methacrylate free radical copolymerization. (The parameter r_1 is k_S/k_{MMA} for a macroradical bearing a terminal styrene unit.) Of course, agreement between the two can be expected only if the selectivities of 1-phenylethyl radical and the styryl terminated macroradical are similar. Recently Fukuda and coworkers have determined r_1 to be 0.52 ± 0.01 in their careful analysis of styrene-methyl methacrylate copolymerization (13); this value agrees quite well with the arithmetic mean of 0.51 calculated from 48 values listed in the Polymer Handbook (65) for measurements in the range of 25-132 °C. Using $r_1 = 0.52 \pm 0.01$, and $k_S/k_A = 0.20 \pm 0.02$ as previously determined, a value of 0.38 ± 0.04 for the product $(1/r_1)(k_S/k_A)$ is obtained. This agrees within experimental error with the value of 0.44 ± 0.03 for k_{MMA}/k_A as determined here for 2a. It thus appears that 1-phenylethyl radical is a reasonable model of a styryl terminated chain in a copolymerization of styrene and methyl methacrylate, at least in regard to chemoselectivity.

The parameter k_{MMA}/k_A for 2-(4-phenyl)pentanenitrile should be comparable to the reciprocal of the terminal model reactivity ratio r_2 for methyl methacrylate-acrylonitrile free radical copolymerization. (The parameter r_2 is k_A/k_{MMA} for a macroradical bearing a terminal acrylonitrile unit.) The radicals under consideration are both secondary alkyl, and both bear alpha cyano groups, so there should be some agreement. One may expect differences because the substituents gamma to the radical center in each case are quite different, and it is uncertain as to what extent k_{MMA}/k_A for a 2-alkanenitrile radical is affected by a γ-phenyl, γ-methyl-γ'-carbomethoxy, or γ-cyano group. Nevertheless, the k_{MMA}/k_A value of 2.4 ± 0.4 determined for 2-(4-phenyl)pentanenitrile agrees within experimental error to the reciprocal of a published r_2 value of 0.46 ± 0.08 ($1/0.46 = 2.2$) (28). This reactivity ratio was determined

using ^{1}H NMR for copolymerization in dimethyl sulfoxide at 50-180 °C, and both composition and sequence data were fit. However, values of r_2 determined by four other groups (114-117) at 1 atm (pressure dependent reactivity ratios are observed for this system (117)) range from 0.10 to 0.16, and these obviously are not consistent with our k_{MMA}/k_A value. The reason for the large difference in published r_2 values is unknown, as all of the investigations appear proper. Discrepancies of this sort are not uncommon, however, and the reader is referred to an excellent discussion in this regard by Tidwell and Mortimer (8).

With regard to the general method used, the determination of k_{MMA}/k_A for 2-(4-phenyl)pentanenitrile shows that a rate constant ratio can be determined for a radical different from that obtained upon initiator decomposition if sufficient resolution of the ^{13}C NMR signals from the end groups can be attained. This is an important illustration, as NMR spectrometers of the future will certainly be more powerful than those used today.

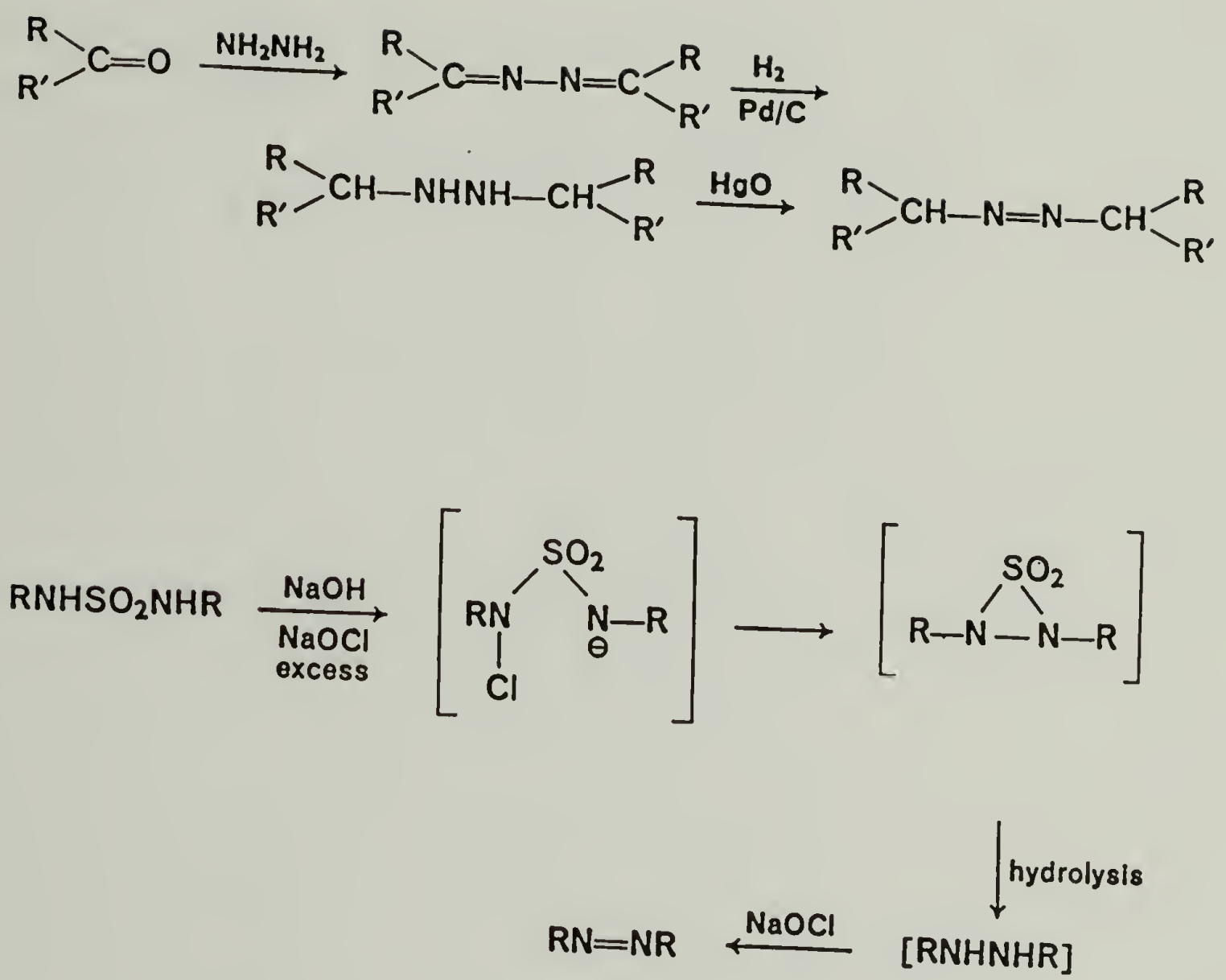

Scheme 3.4. Two widely used routes to azoalkanes (90).

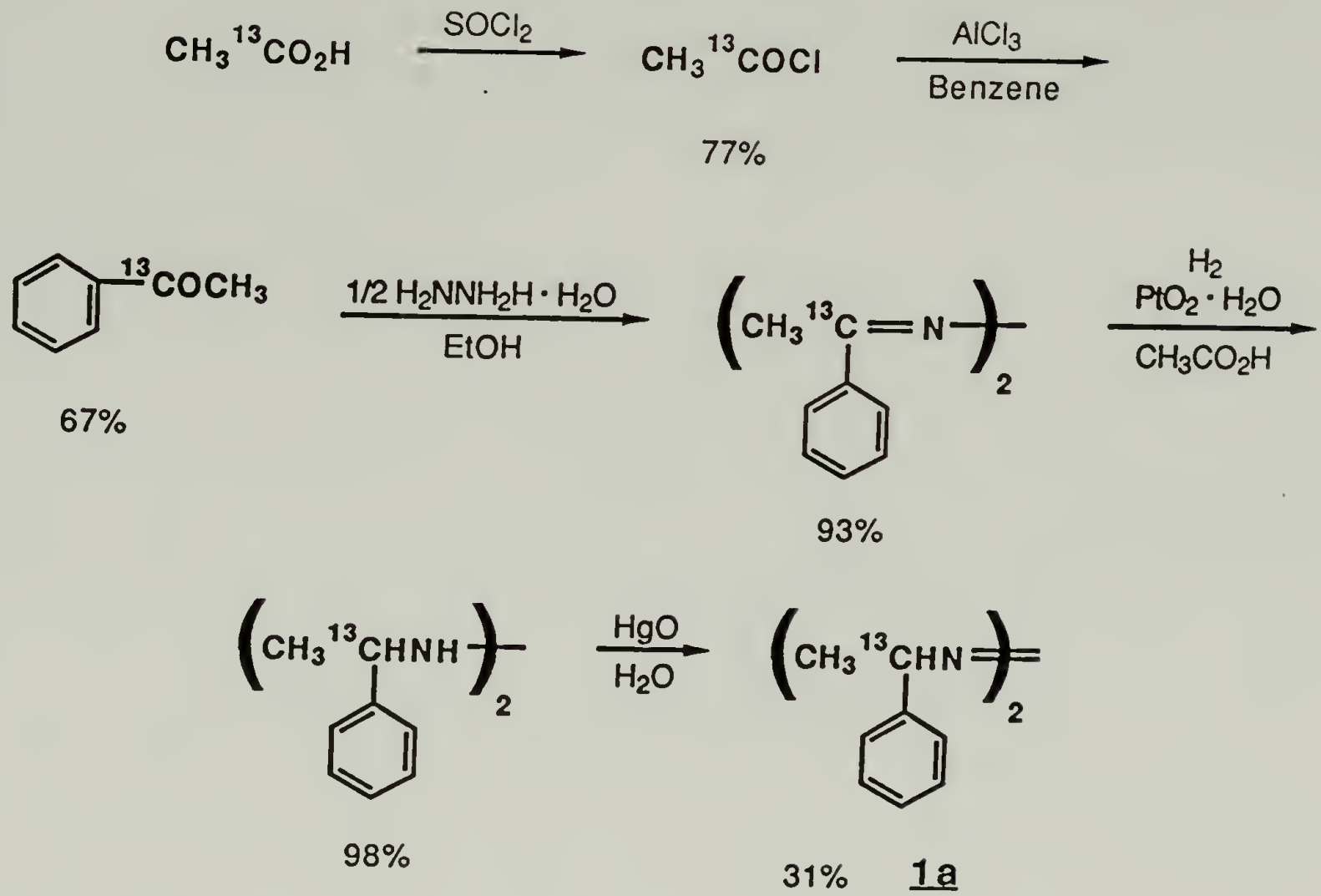

Scheme 3.5. Synthesis of 1,1'-azobis(1-phenyl[1-^{13}C]ethane) (**1a**).

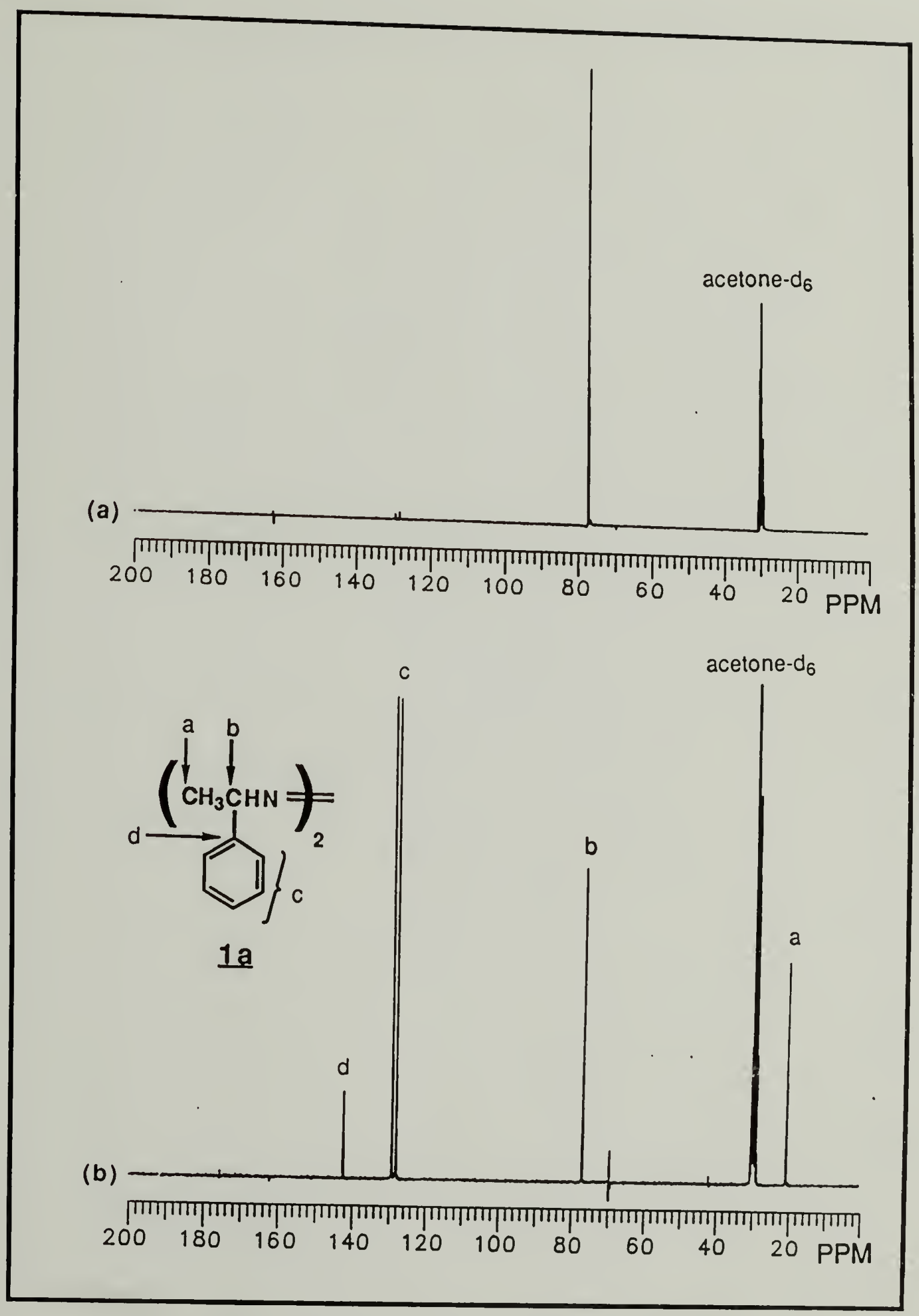

Figure 3.8. 75 MHz ^{13}C NMR spectra of (a) enriched and (b) natural-abundance 1,1'-azobis(1-phenyl[1-^{13}C]ethane) (**1a**) in acetone-d_6.

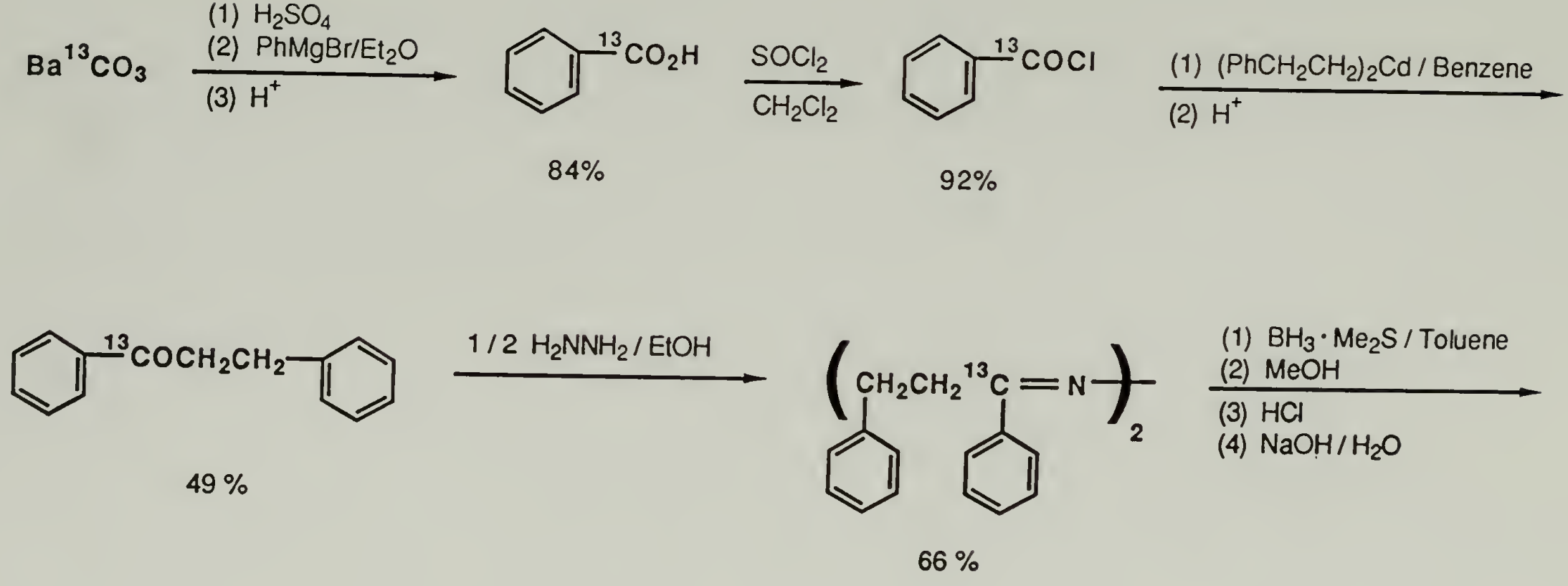

Scheme 3.6. Synthesis of 1,1'-azobis(1,3-diphenyl[1-^{13}C]propane) (**1b**).

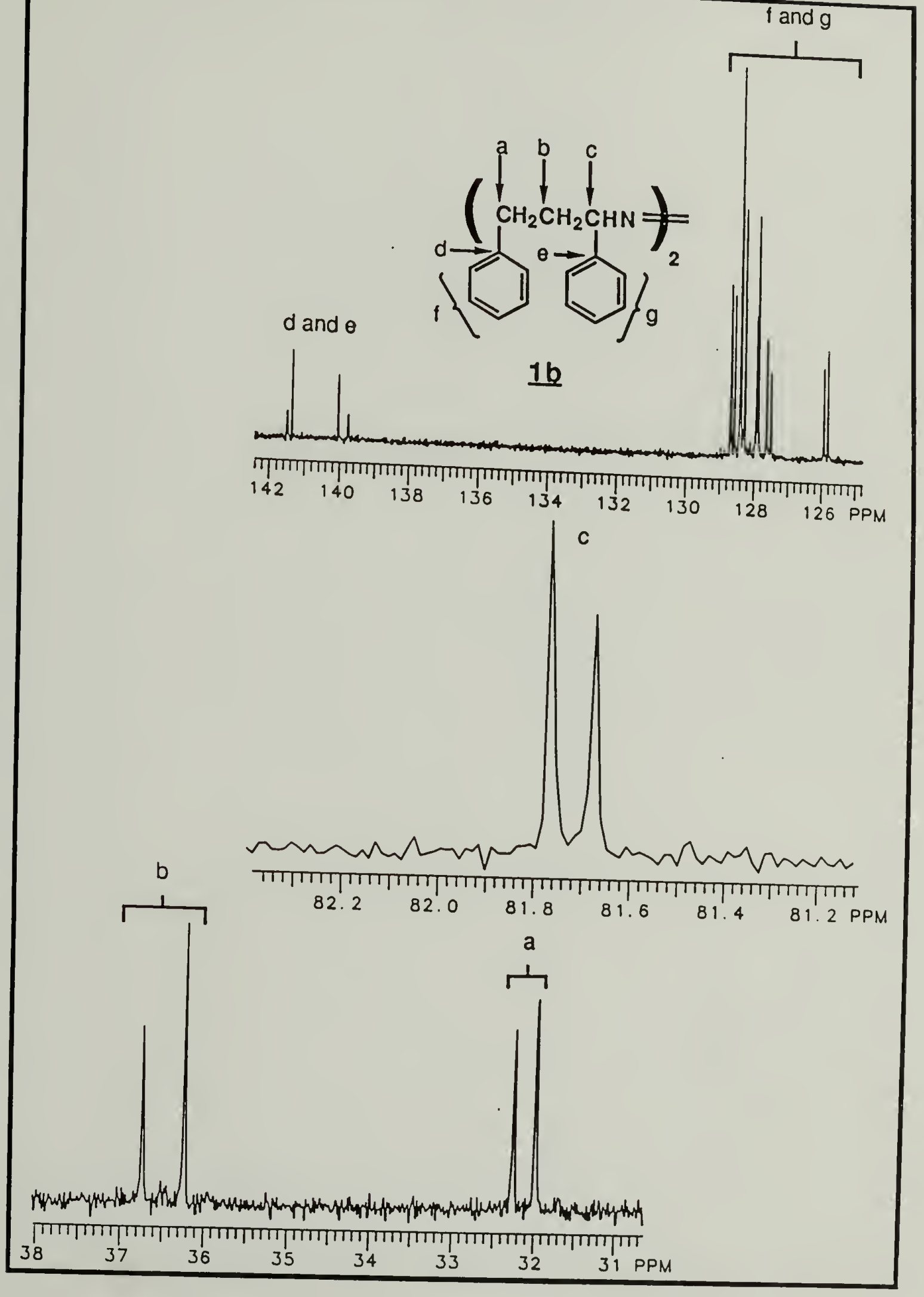

Figure 3.9. 75 MHz ^{13}C NMR spectrum of a low-melting sample of natural-abundance 1,1'-azobis(1,3-diphenylpropane) (**1b**) in $CDCl_3$. Spectral regions not shown contain no sample signals.

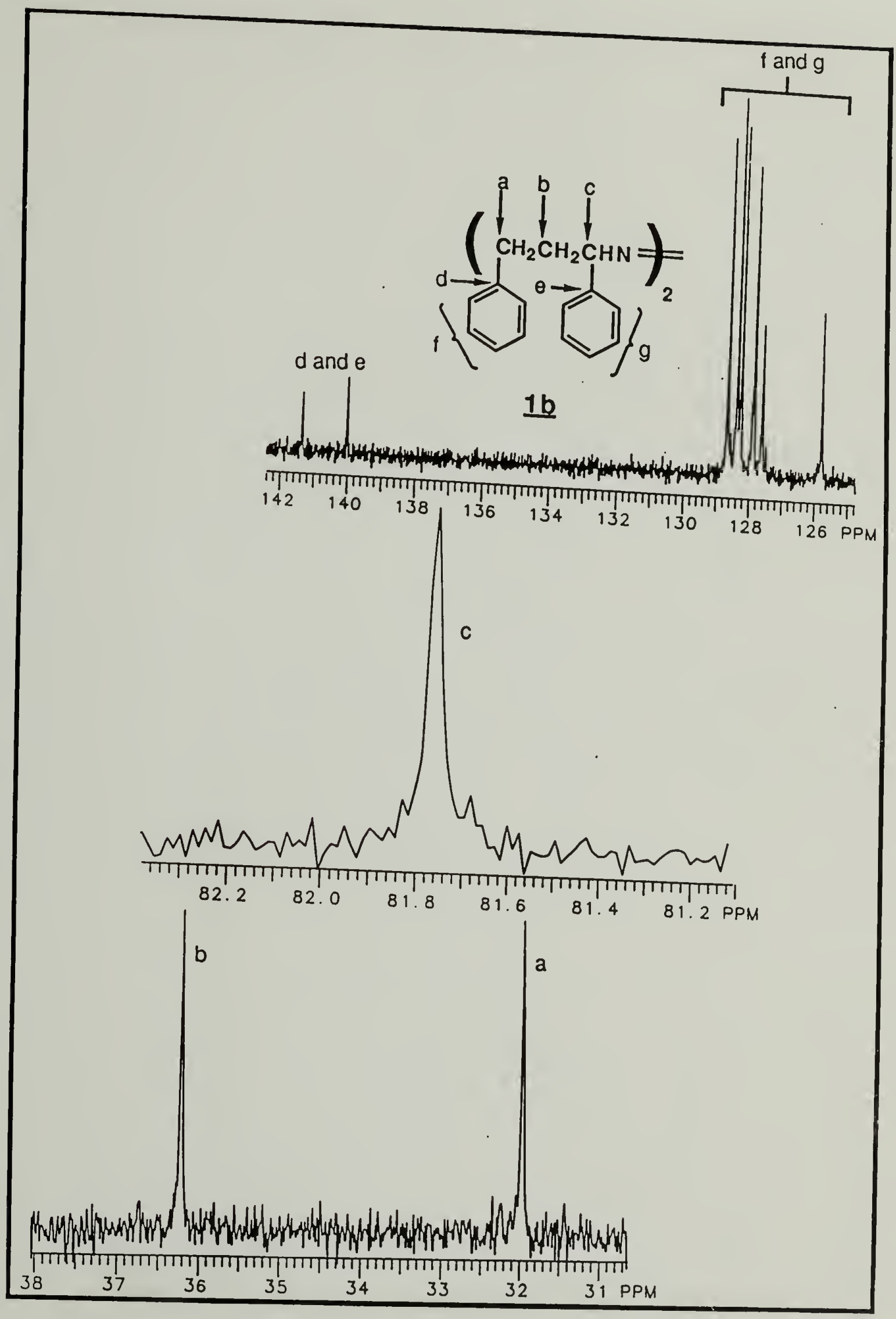

Figure 3.10. 50 MHz ^{13}C NMR spectrum of a high-melting sample of natural-abundance 1,1'-azobis(1,3-diphenylpropane) (**1b**) in $CDCl_3$. Spectral regions not shown contain no sample signals.

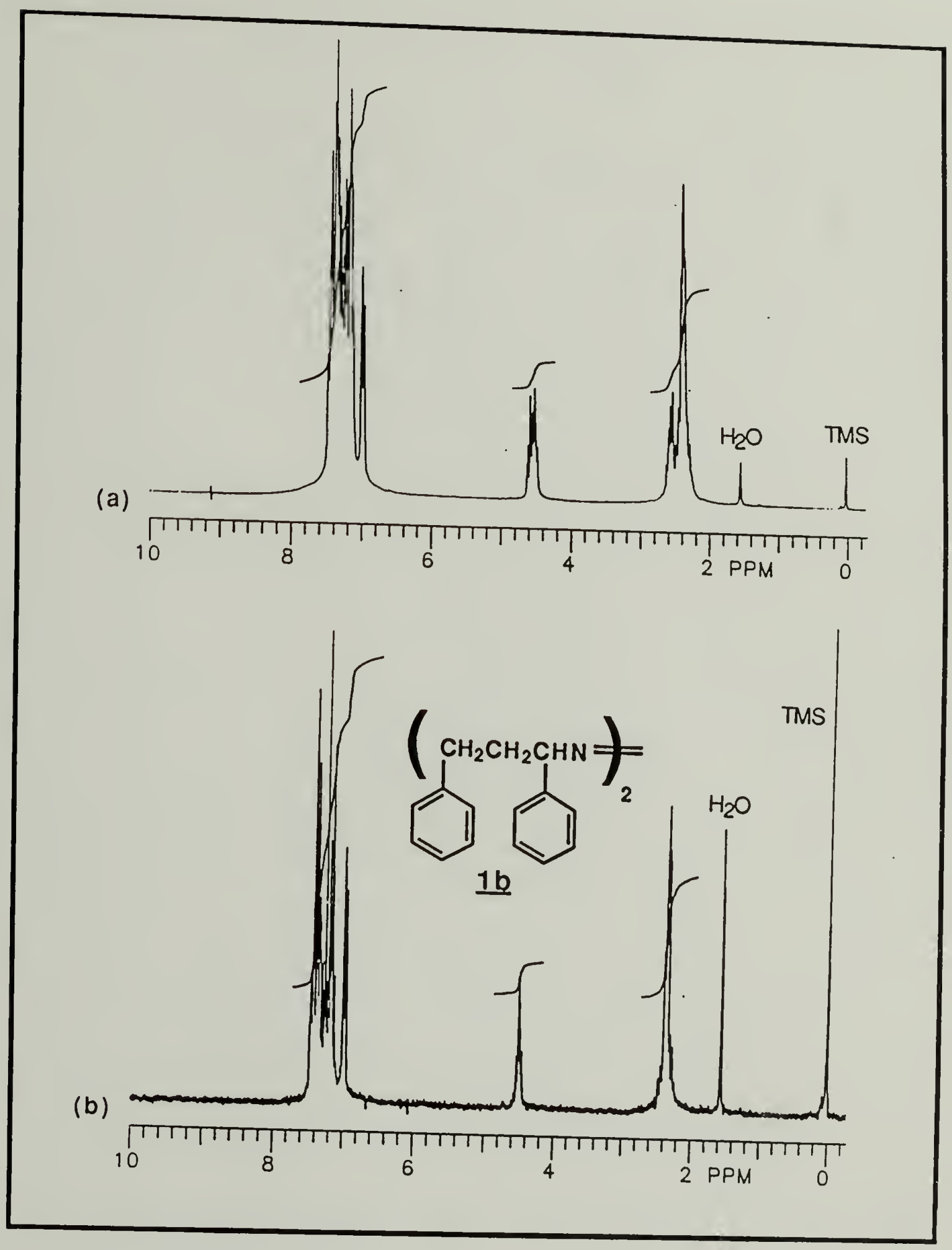

Figure 3.11. 200 MHz ^{1}H NMR spectra of (a) low-melting and (b) high-melting samples of natural-abundance 1,1'-azobis(1,3-diphenylpropane) (**1b**) in $CDCl_3$.

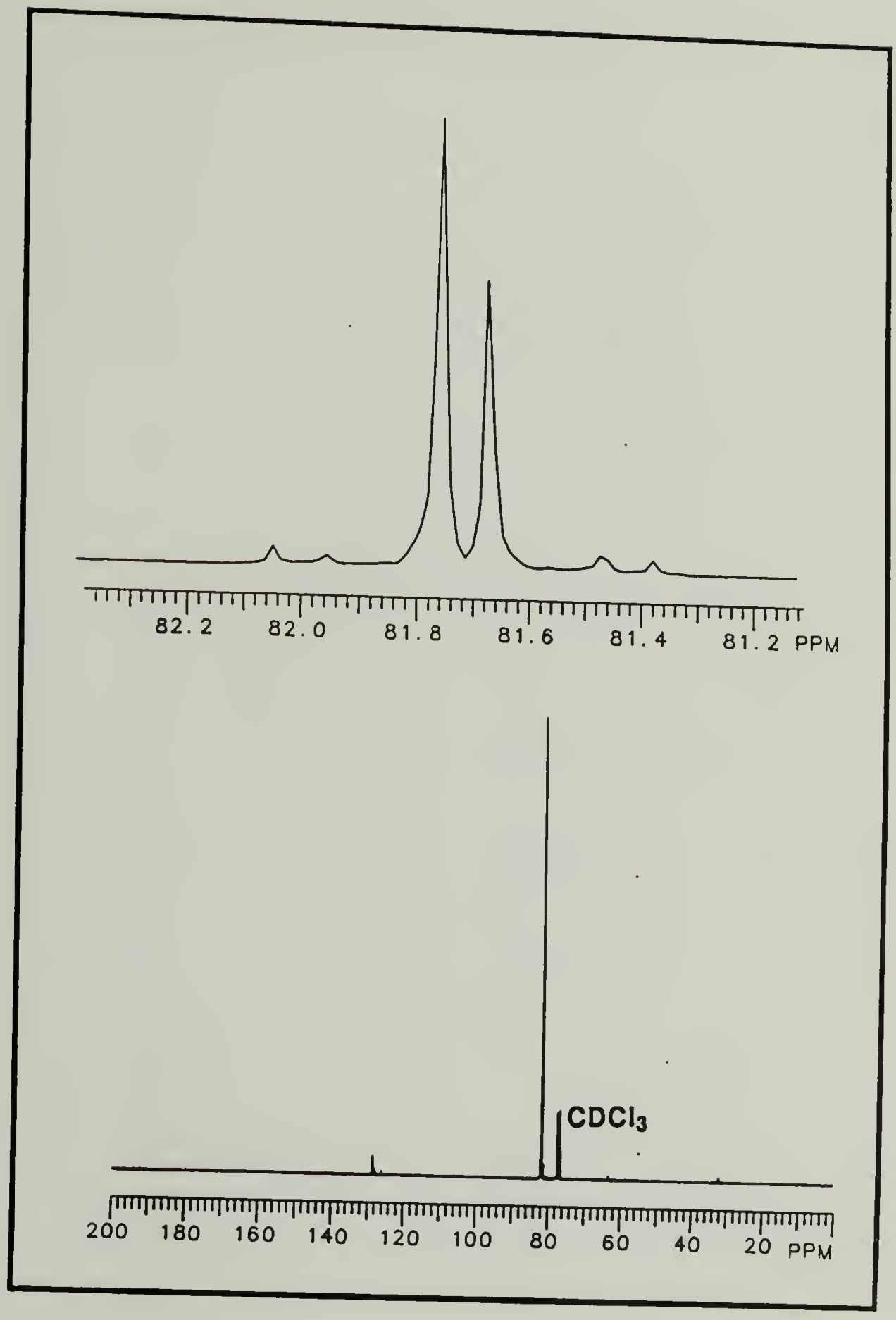

Figure 3.12. 75 MHz ^{13}C NMR spectrum of 1,1'-azobis(1,3-[1-^{13}C]diphenylpropane) **(1b)** in $CDCl_3$ (compare to Fig. 3.9).

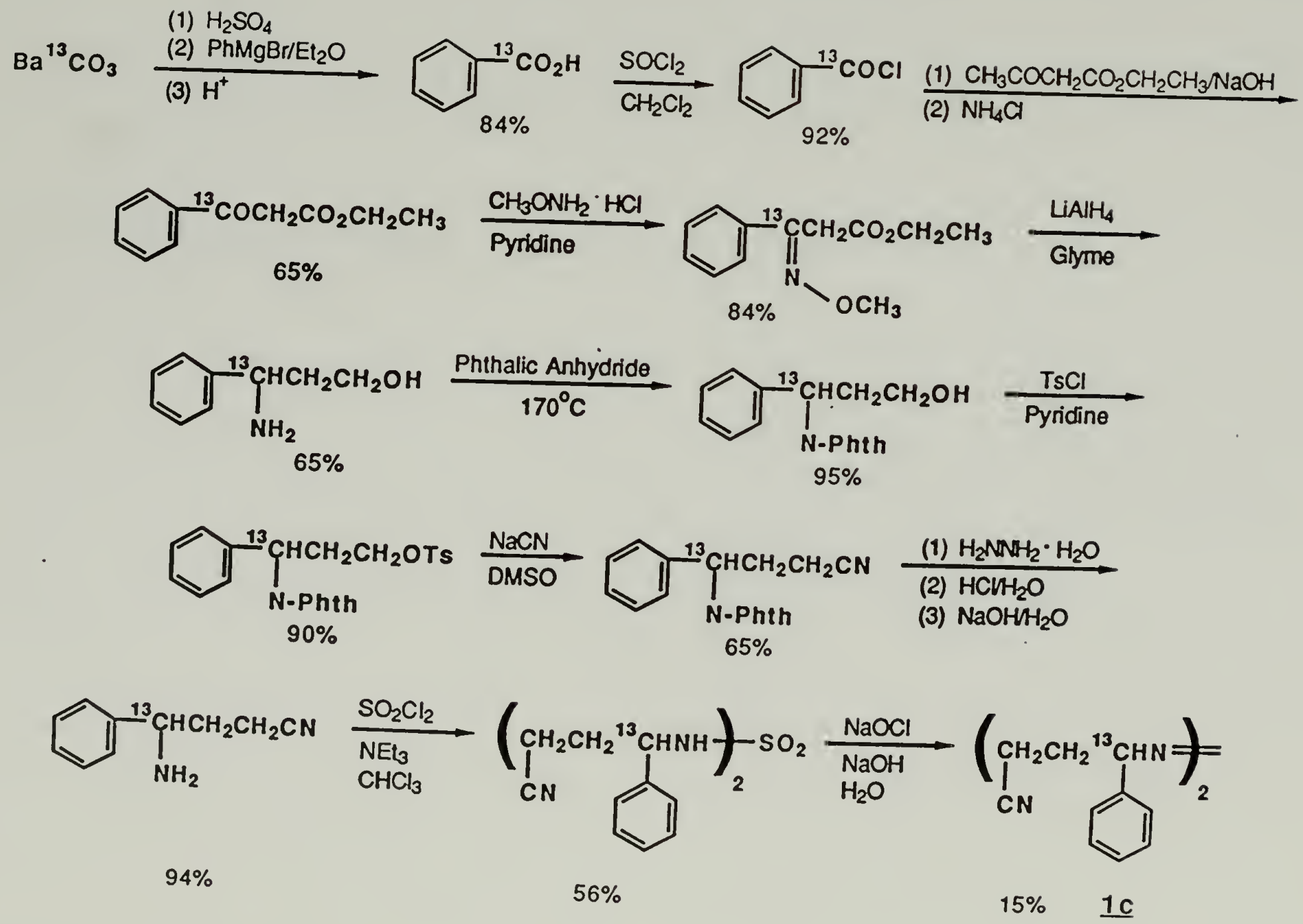

Scheme 3.7. Synthesis of 4,4'-azobis(4-phenyl[4-^{13}C]butyronitrile) (1c).

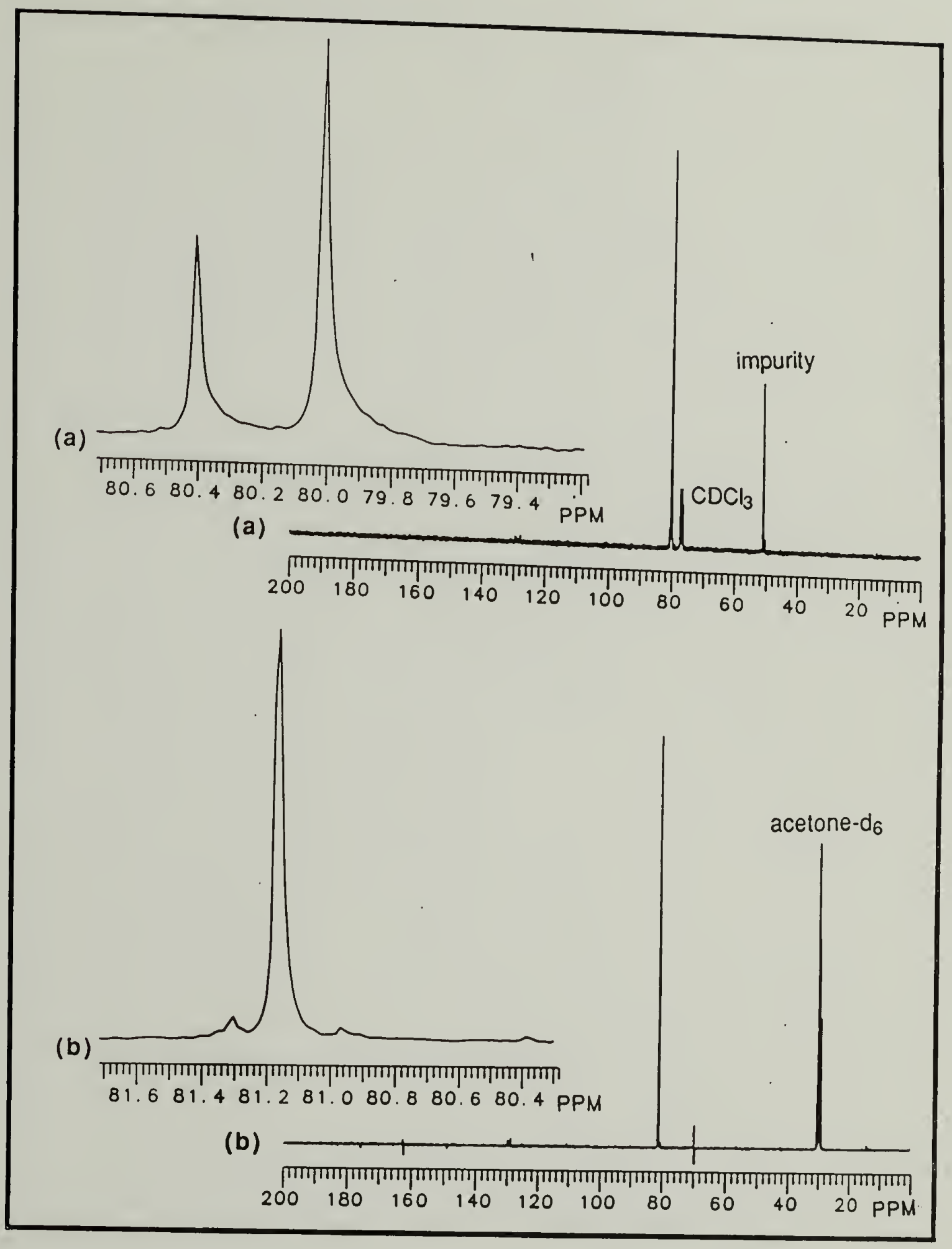

Figure 3.13. 75 MHz ^{13}C NMR spectra of (a) low melting and (b) high melting samples of 4,4'-azobis(4-phenyl[4-^{13}C]butyronitrile) (1c).

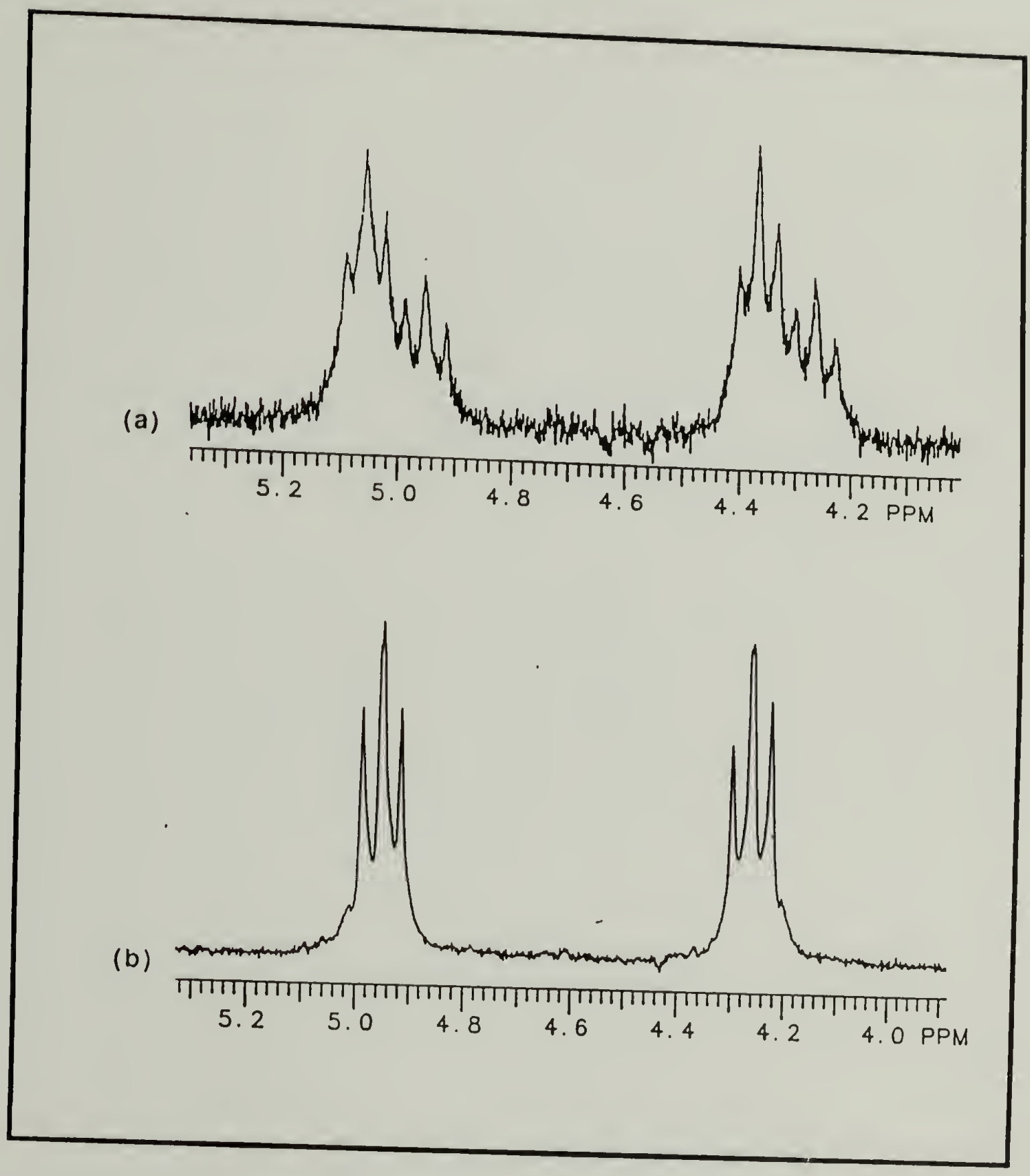

Figure 3.14. 200 MHz ^{1}H NMR spectra of methine protons of (a) low-melting and (b) high-melting samples of 4,4'-azobis(4-phenyl[4-^{13}C]butyronitrile) (1c) in $CDCl_3$.

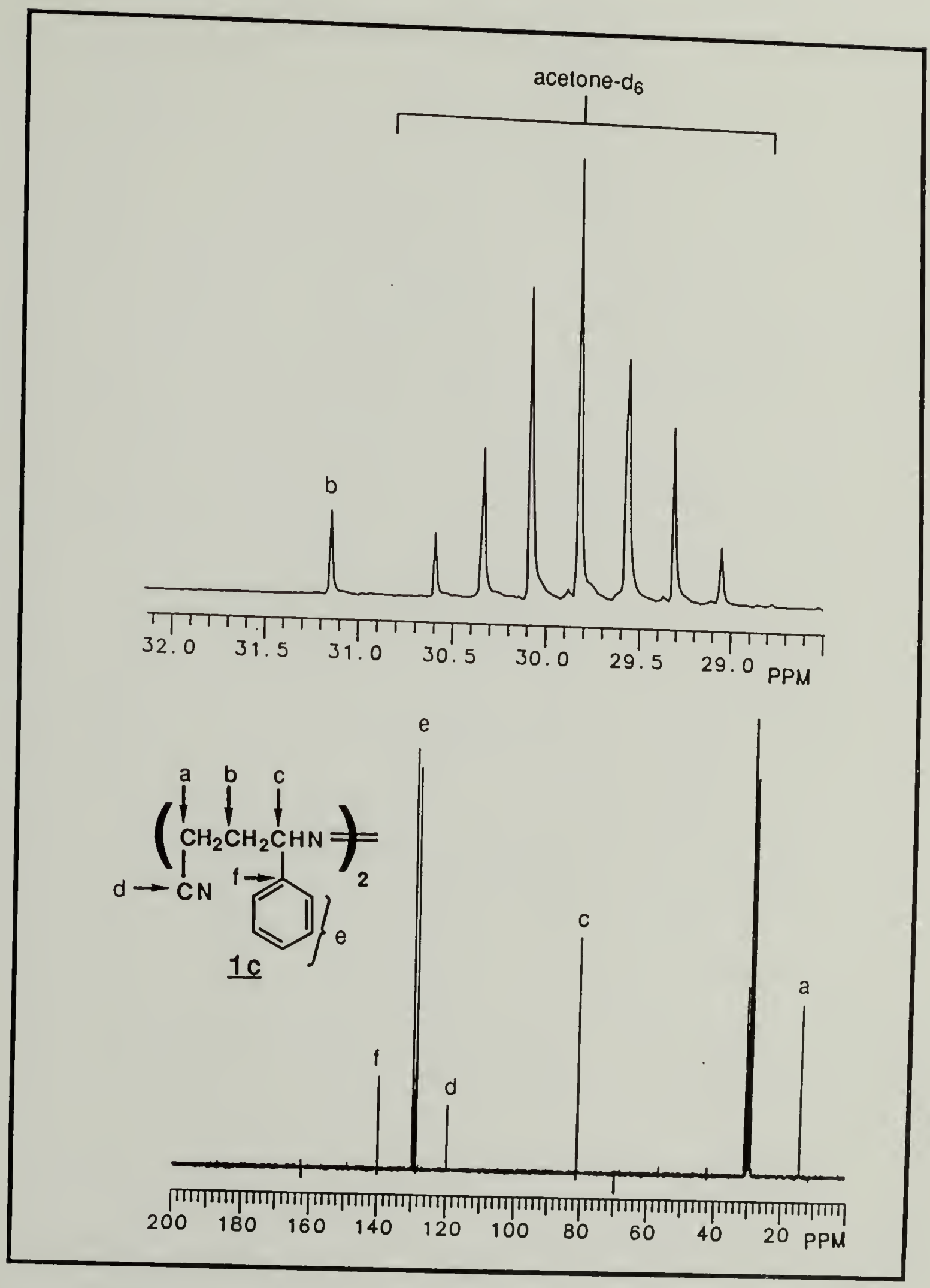

Figure 3.15. 75 MHz ^{13}C NMR spectrum of (natural-abundance) 4,4'-azobis(4-phenylbutyronitrile) (1c) in acetone-d_6 (compare to "b" in Fig. 3.13).

Table 3.2. Molecular Weights of Enriched SAN Copolymers.[a]

copolymer[b]	$M_p \times 10^{-3}$ [c]
1	19
2	19
3	18
4	14
5	16
6	16
7	14
8	11
9	29
10	26
11	29
12	24
13	22
14	19
15	19
16	19
18	29
19	26
20	29
21	36
22	29
23	32
24	44
25	44

[a] Molecular weights are reported as polystyrene molecular weights of elution volume equal to that of the peak in the observed elution profile.

[b] Copolymers 1-8 are derived from **1a**, copolymers 9-16 are derived from **1b**, and copolymers 18-25 are derived from **1c**; polymerization data are given in Tables 2.3, 2.4, and 2.5.

[c] The errors in the M_p values are estimated to be ± 15%.

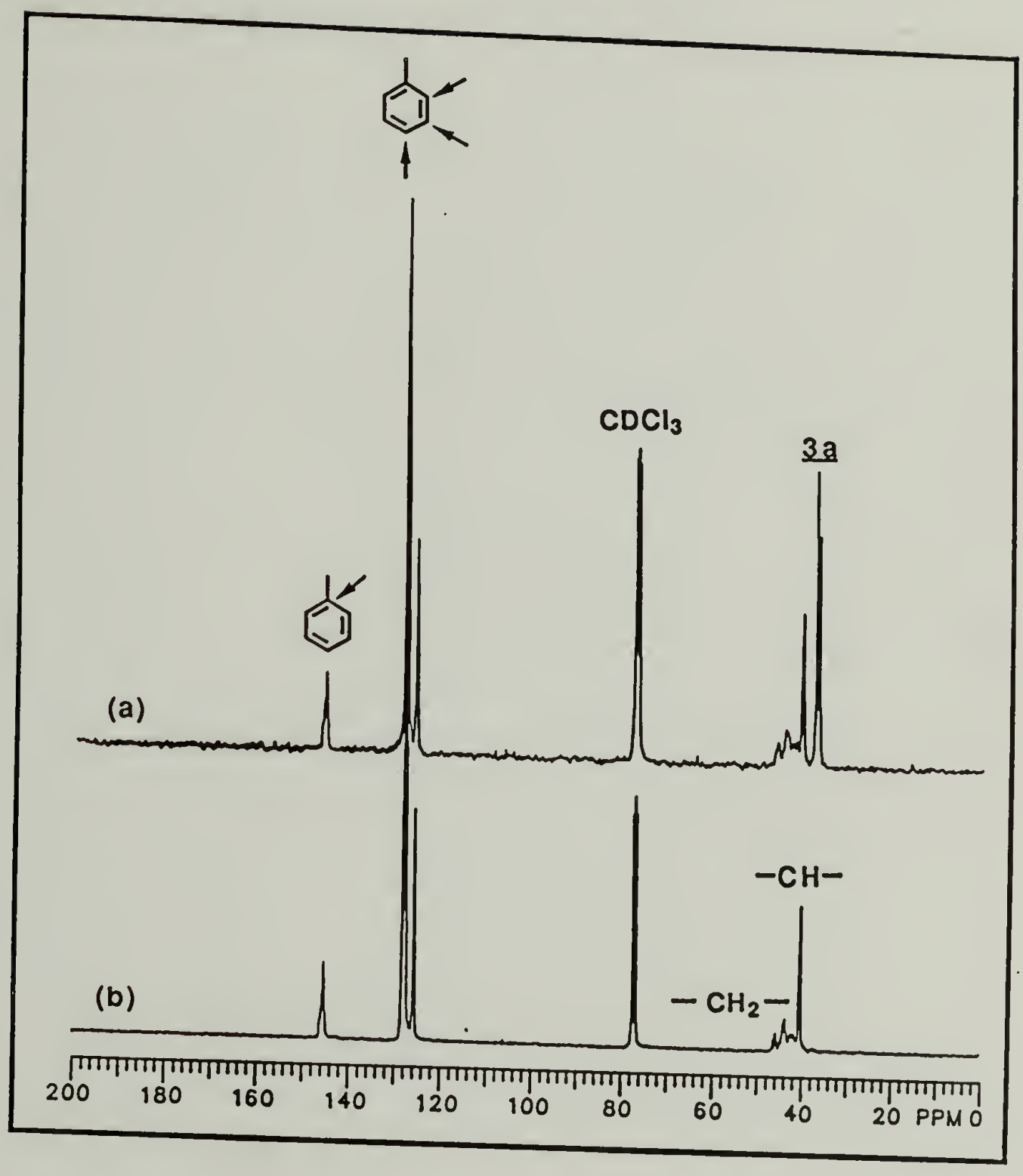

Figure 3.16. 75 MHz ^{13}C NMR spectra of (a) enriched and (b) natural-abundance polystyrene, derived from **1a**, in $CDCl_3$.

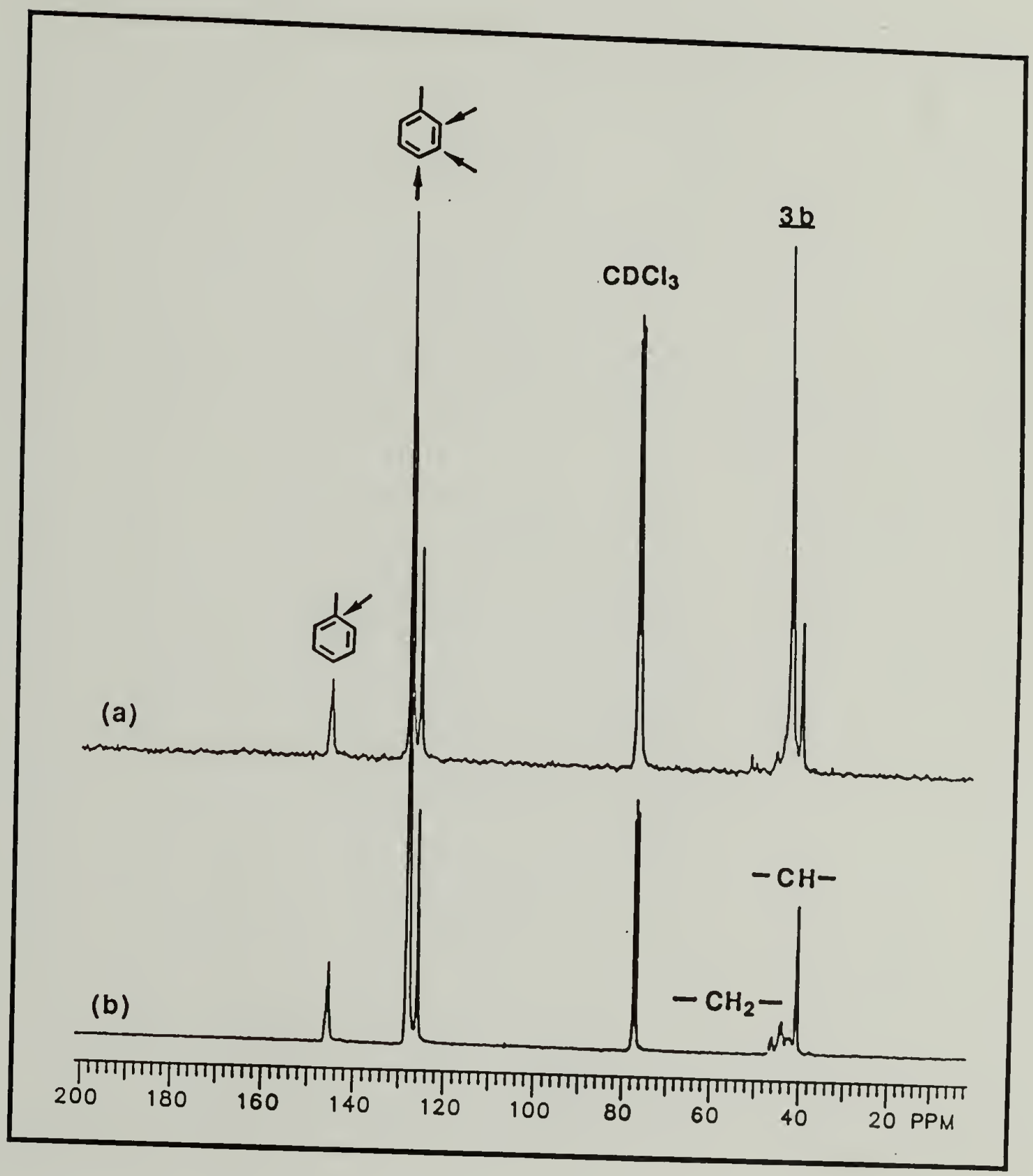

Figure 3.17. 75 MHz ^{13}C NMR spectra of (a) enriched and (b) natural-abundance polystyrene, derived from **1b**, in $CDCl_3$.

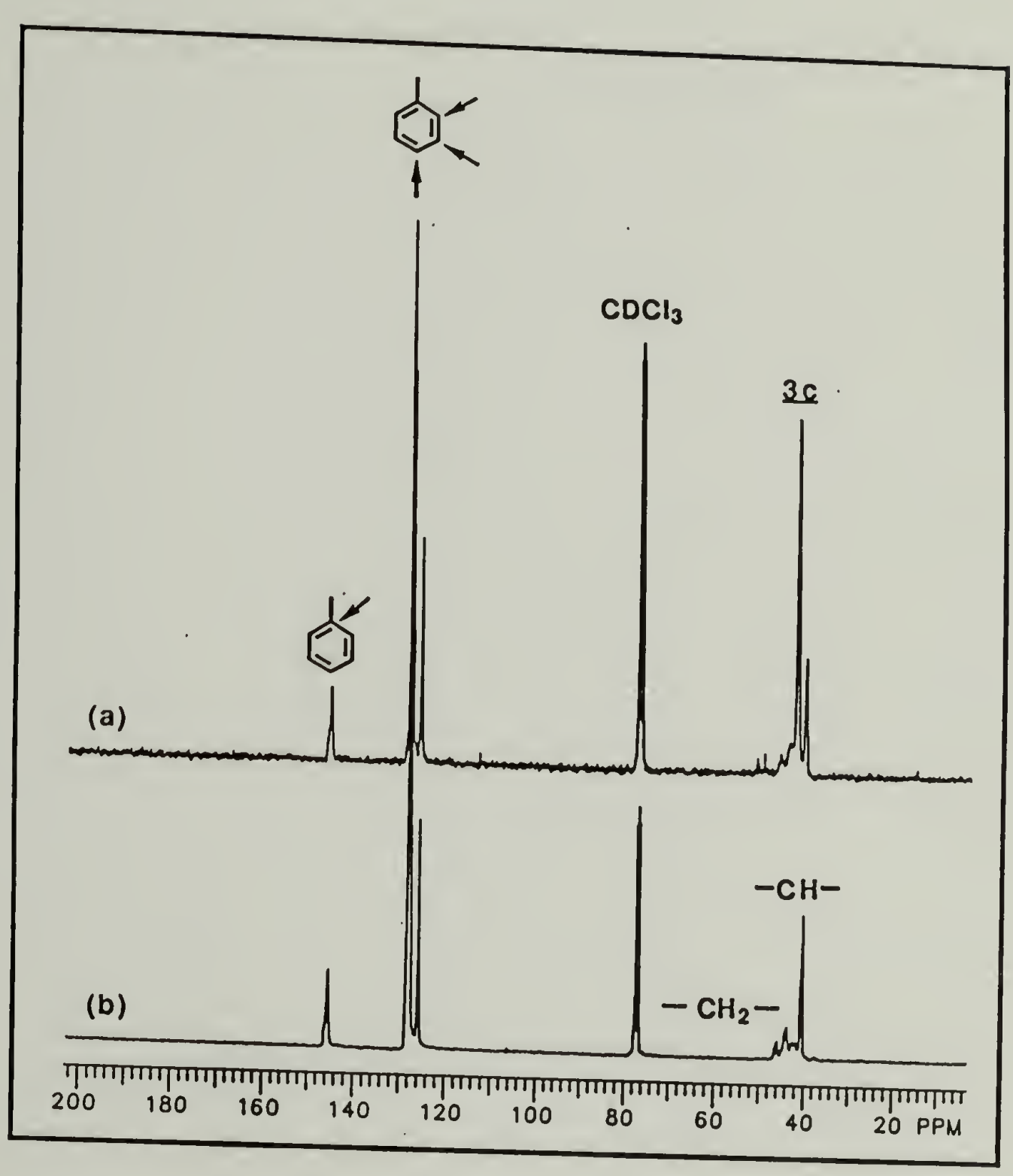

Figure 3.18. 75 MHz ^{13}C NMR spectra of (a) enriched and (b) natural-abundance polystyrene, derived from **1c**, in $CDCl_3$.

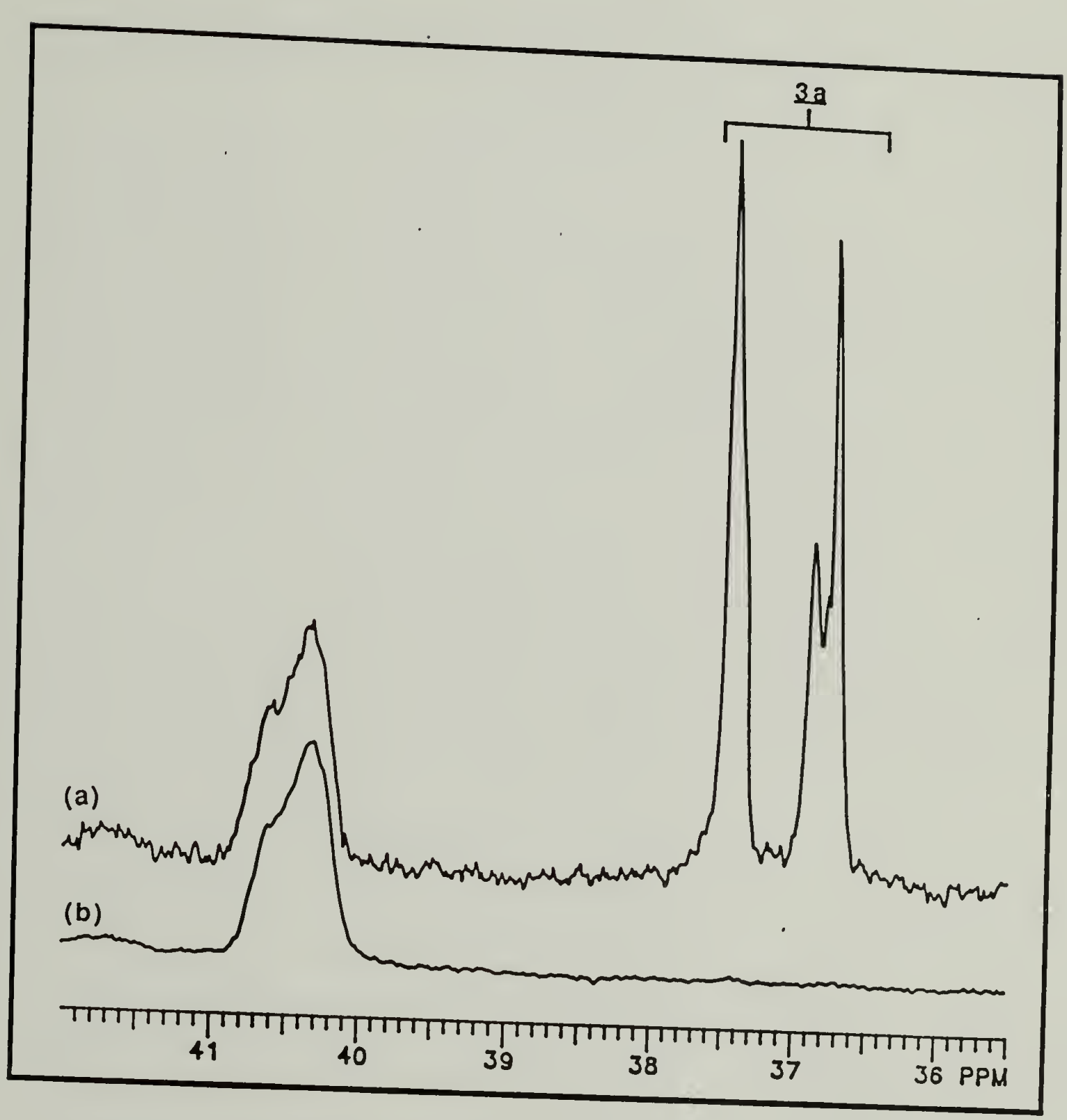

Figure 3.19. 75 MHz ^{13}C NMR spectra (expanded plots) of (a) enriched and (b) natural-abundance polystyrene, derived from **1a**, in $CDCl_3$.

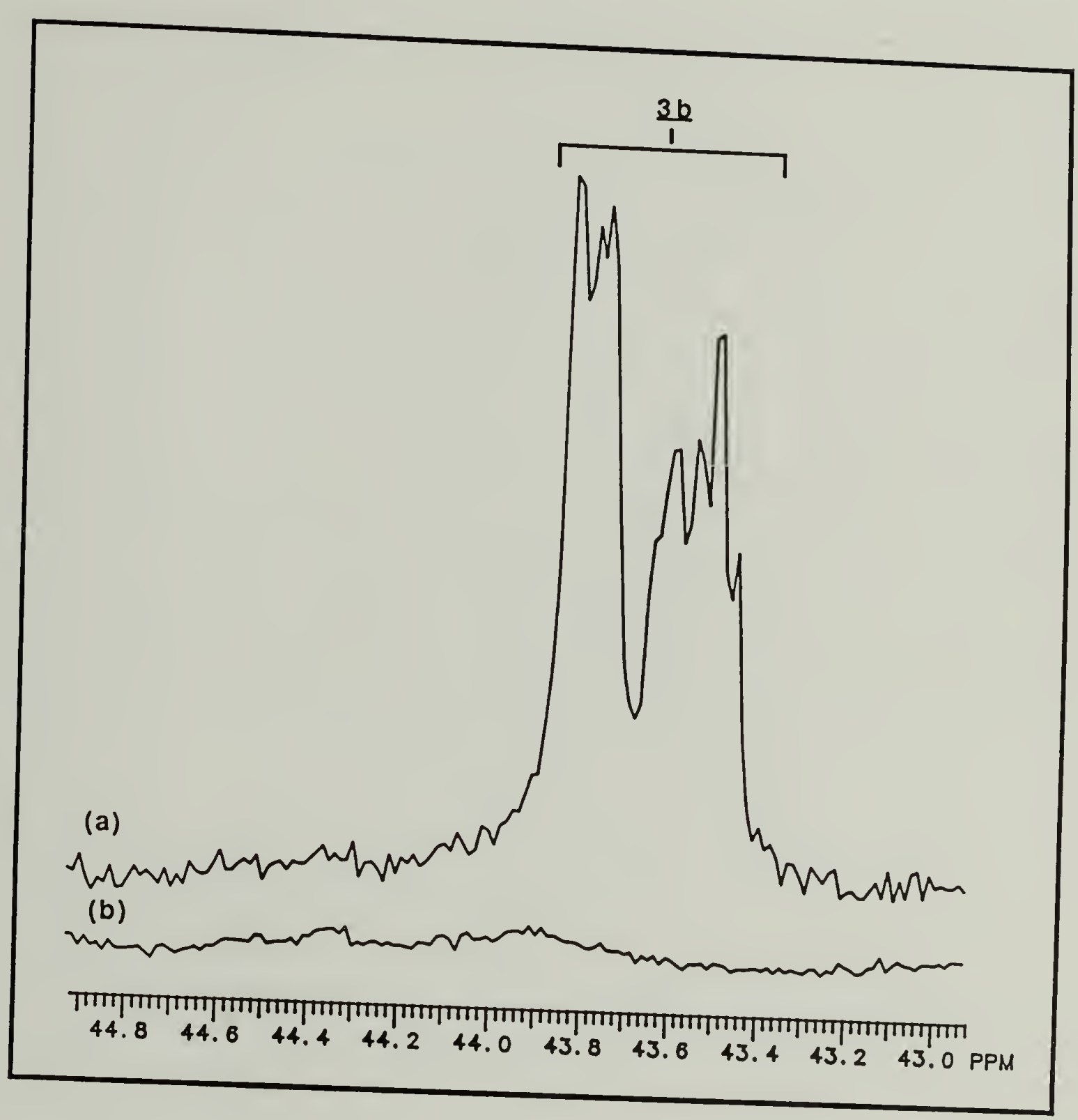

Figure 3.20. 75 MHz ^{13}C NMR spectra (expanded plots) of (a) enriched and (b) natural-abundance polystyrene, derived from **1b**, in deuterated diglyme at 140 °C.

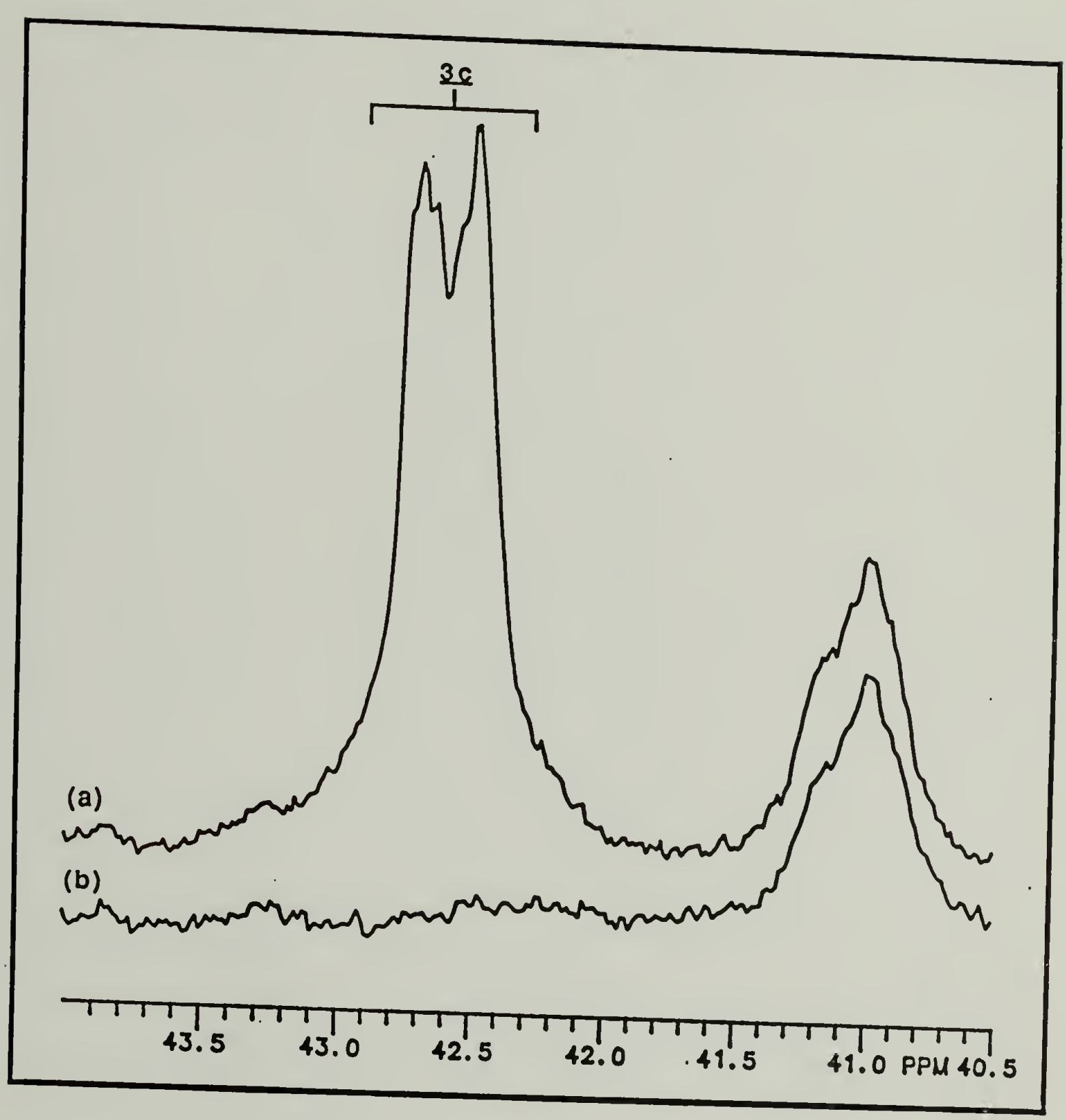

Figure 3.21. 75 MHz ^{13}C NMR spectra (expanded plots) of (a) enriched and (b) natural-abundance polystyrene, derived from **1c**, in deuterated bromobenzene at 136 °C.

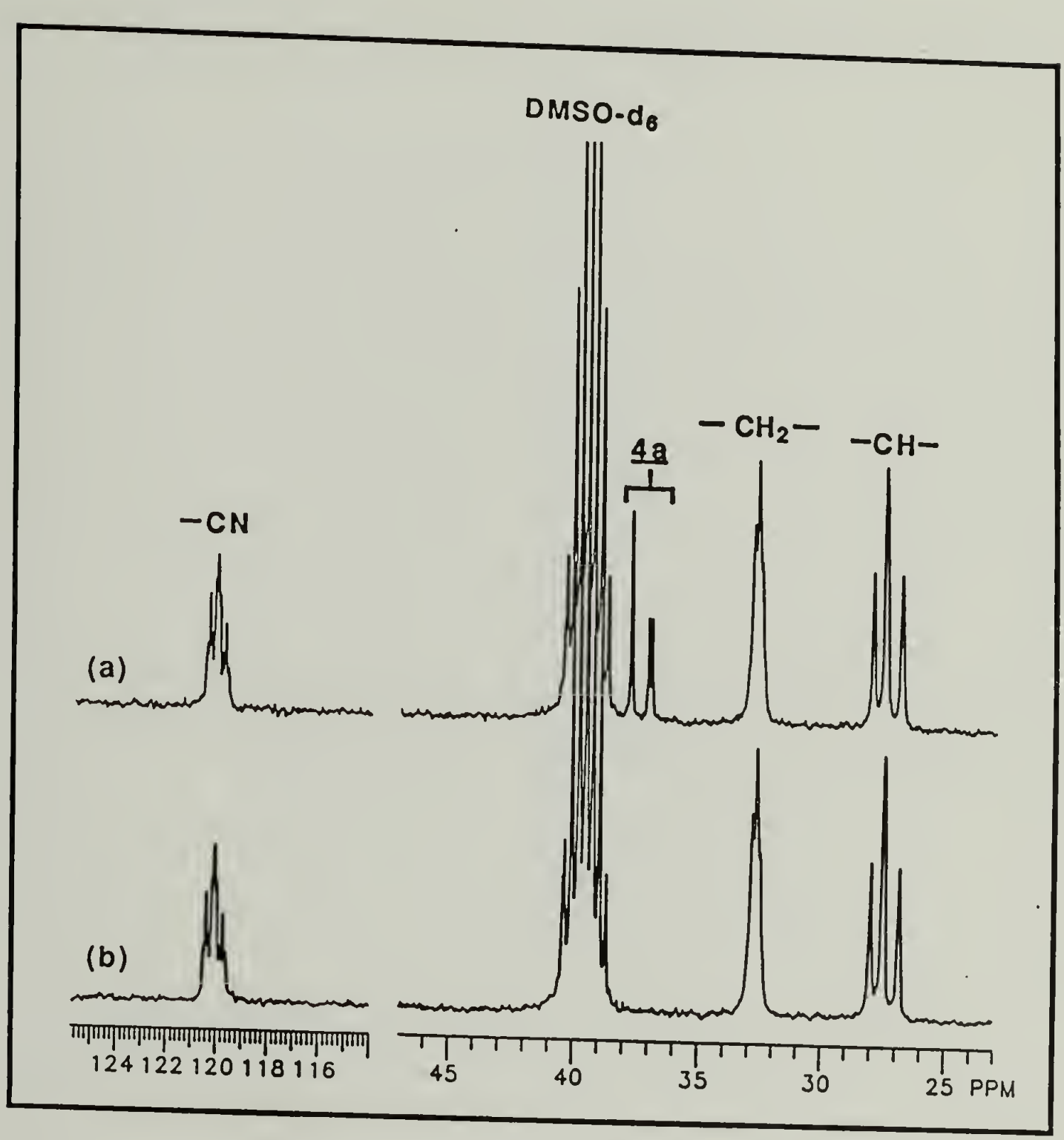

Figure 3.22. 75 MHz ^{13}C NMR spectra of (a) enriched and (b) natural-abundance poly(acrylonitrile) derived from **1a**, in DMSO-d_6. Spectral regions not shown contain no signals.

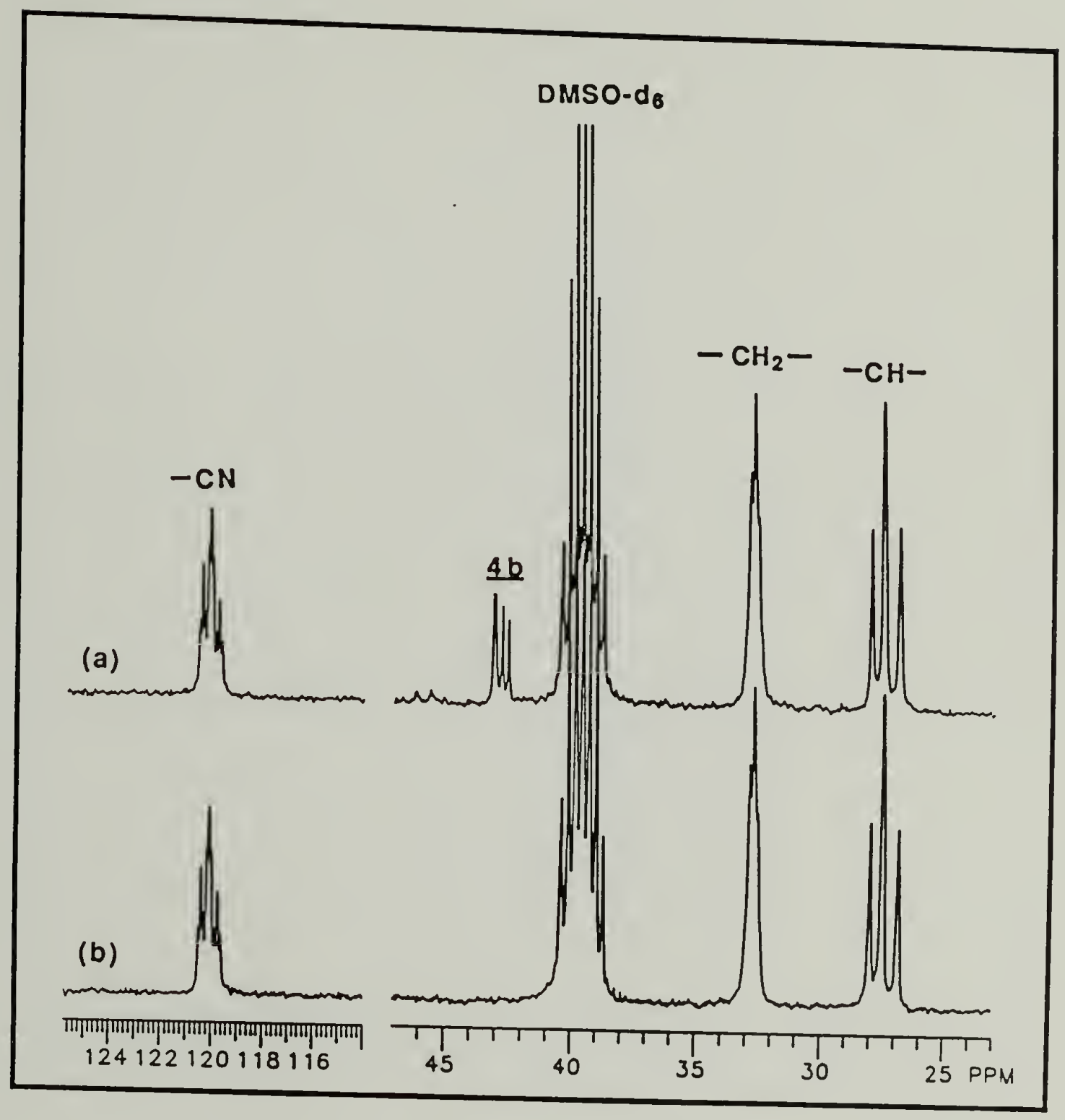

Figure 3.23. 75 MHz ^{13}C NMR spectra of (a) enriched and (b) natural-abundance poly(acrylonitrile), derived from **1b**, in DMSO-d_6. Spectral regions not shown contain no signals.

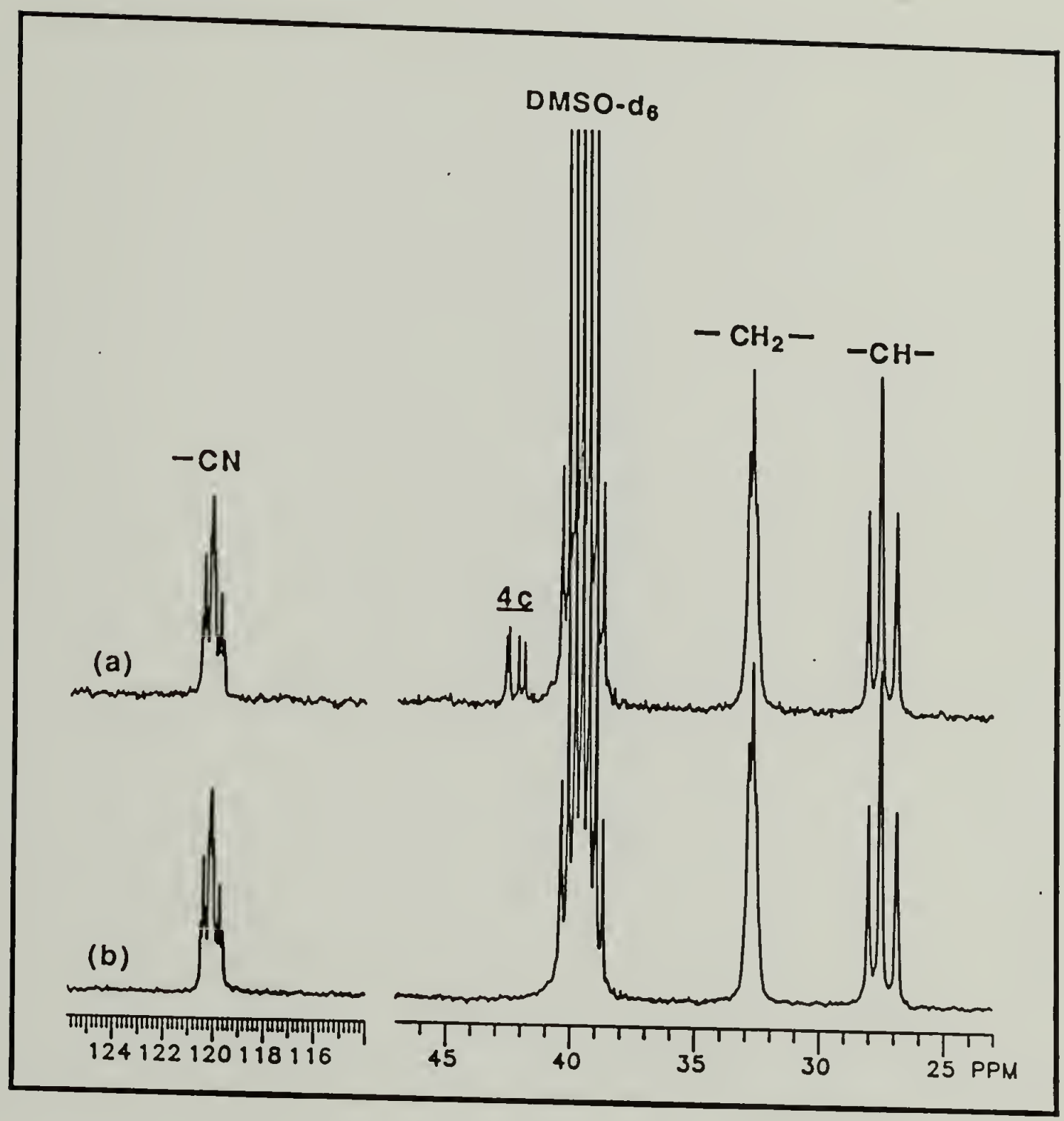

Figure 3.24. 75 MHz ^{13}C NMR spectra of (a) enriched and (b) natural-abundance poly(acrylonitrile), derived from **1c**, in DMSO-d_6. Spectral regions not shown contain no signals.

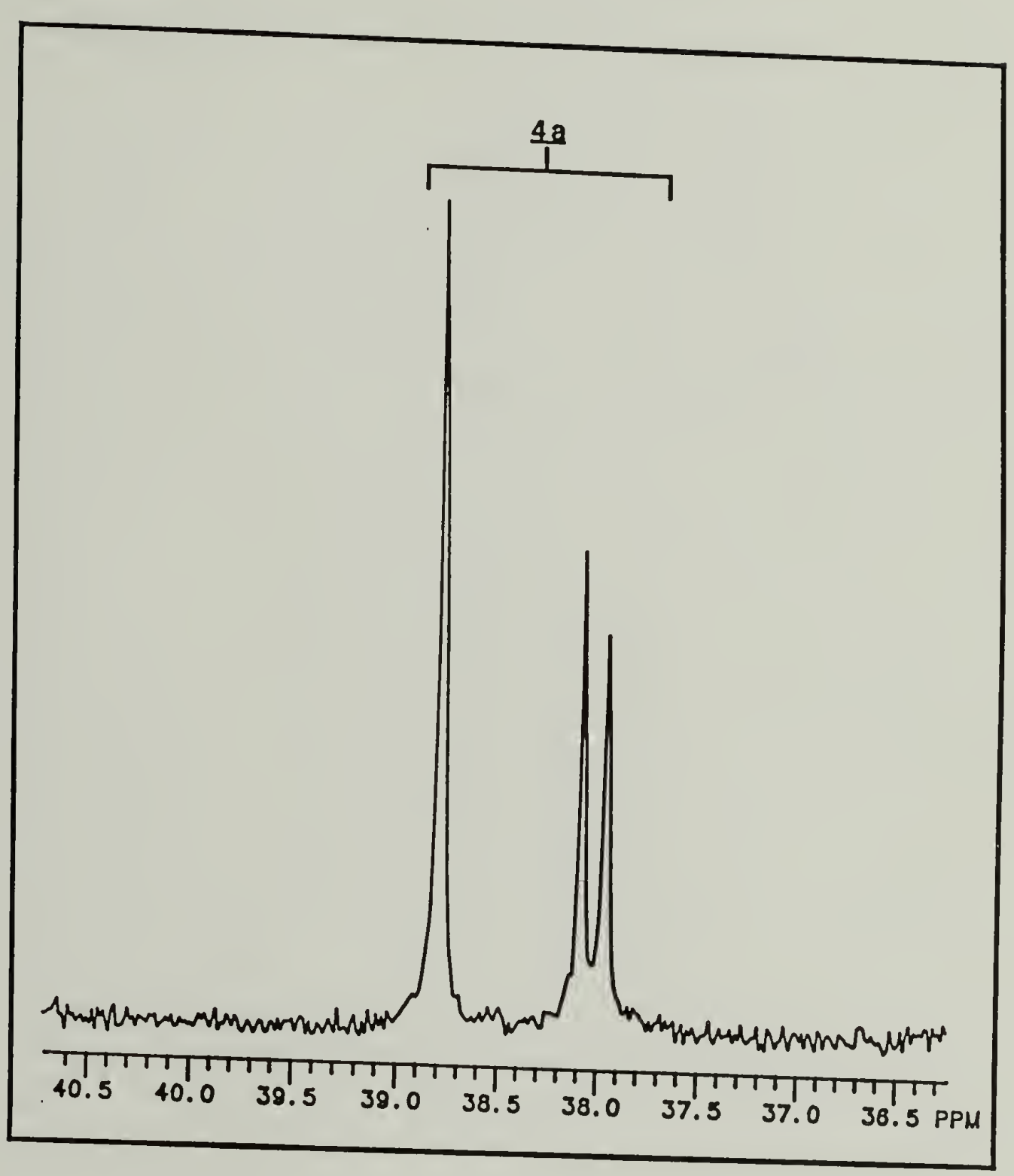

Figure 3.25. 75 MHz ^{13}C NMR spectrum (expanded plot) of enriched poly(acrylonitrile), derived from **1a**, in DMF-d_7.

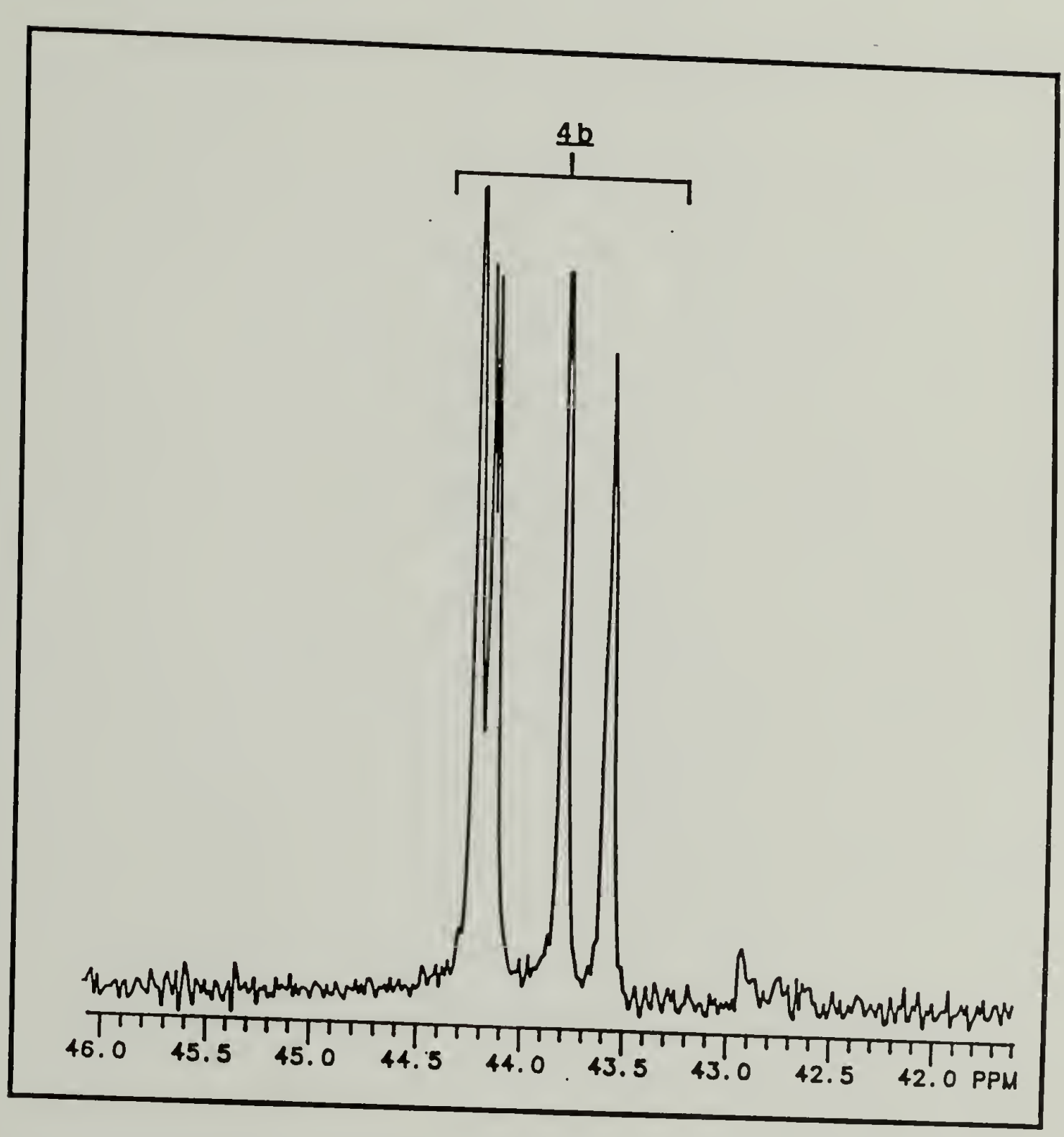

Figure 3.26. 75 MHz ^{13}C NMR spectrum (expanded plot) of enriched poly(acrylonitrile), derived from **1b**, in DMF-d_7.

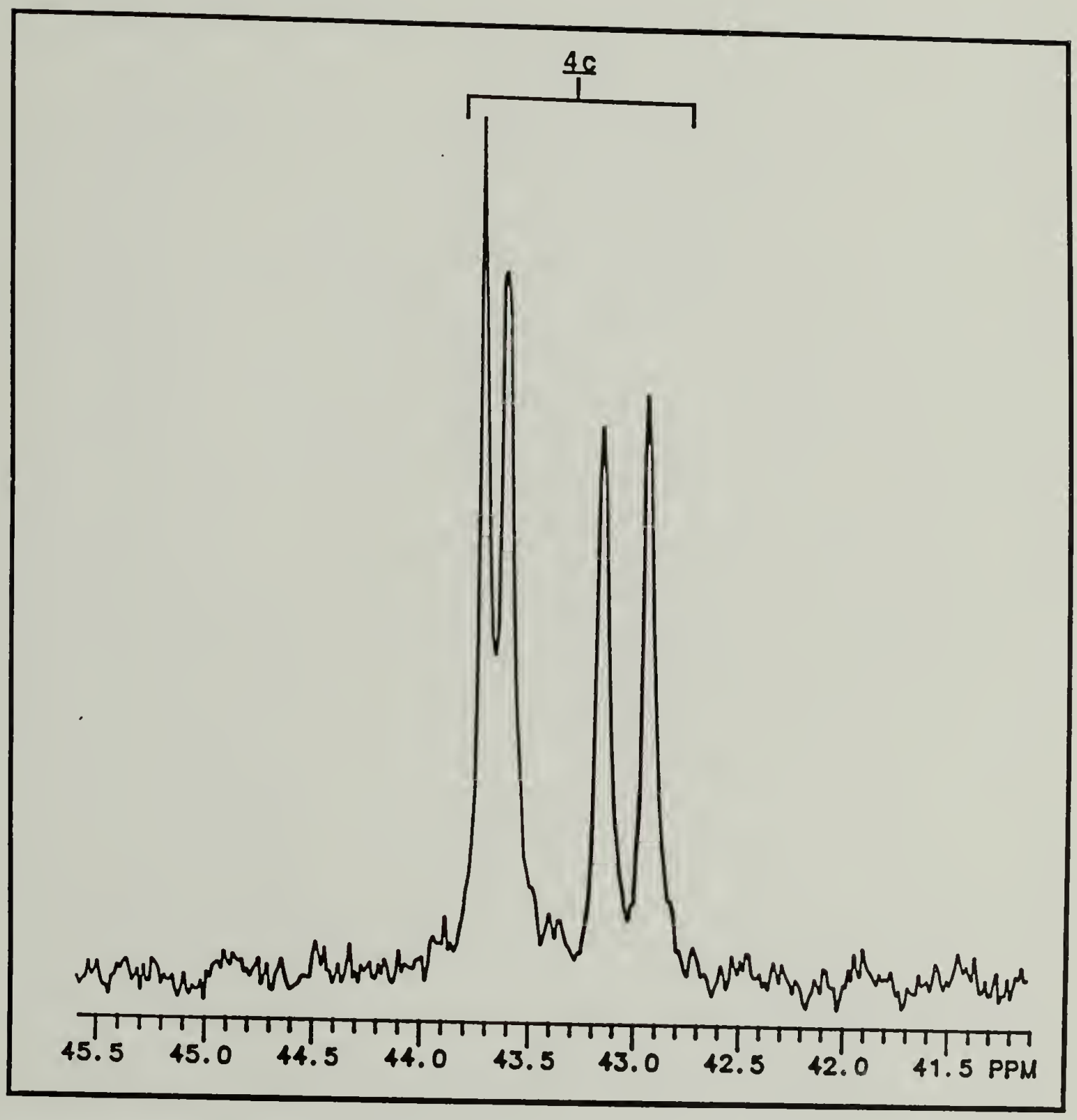

Figure 3.27. 75 MHz ^{13}C NMR spectrum (expanded plot) of enriched poly(acrylonitrile), derived from 1c, in DMF-d_7.

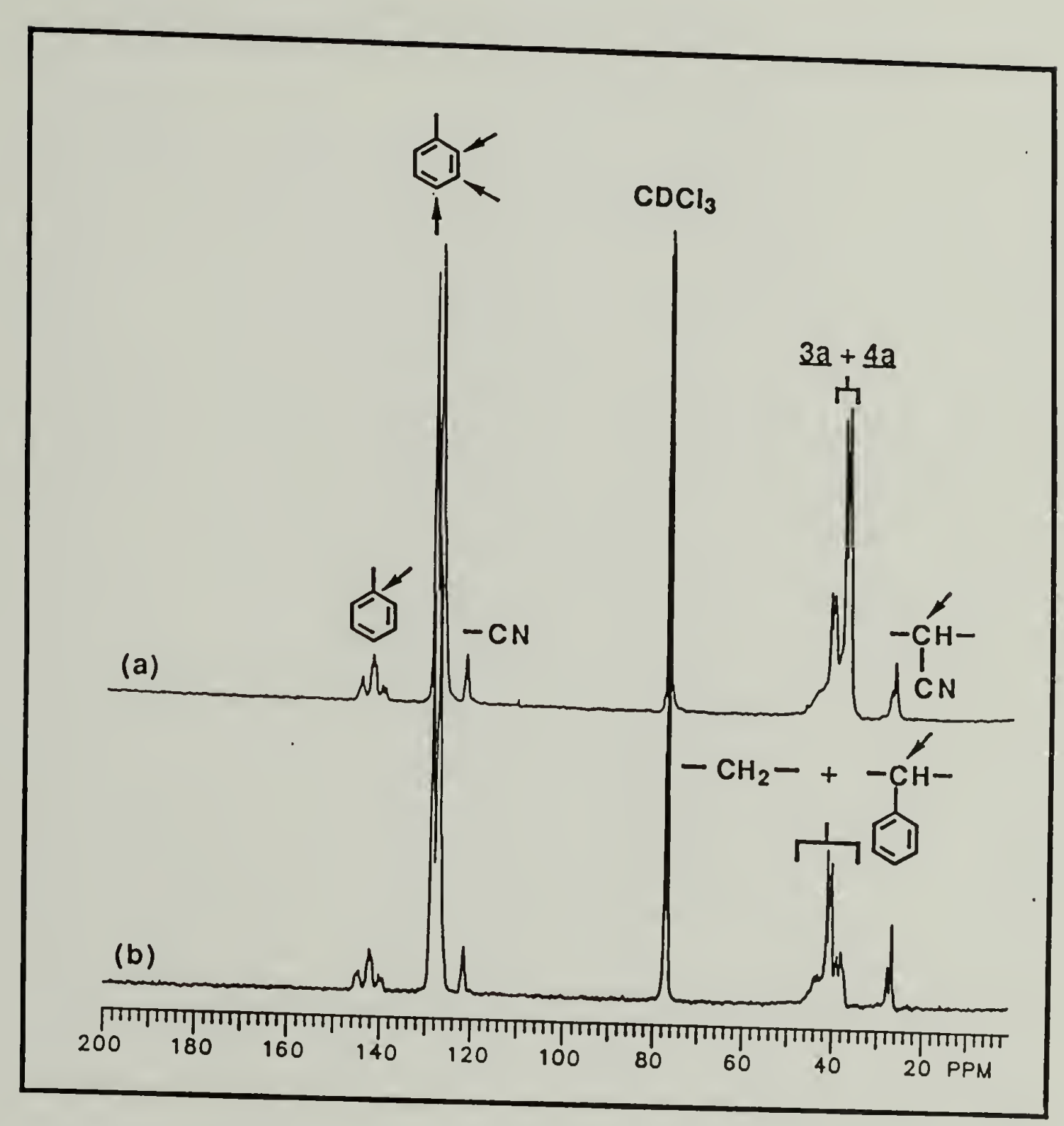

Figure 3.28. 75 MHz ^{13}C NMR spectra of (a) enriched and (b) natural-abundance SAN copolymers in $CDCl_3$ that were prepared from **1a** with a monomer feed ratio ([S]/[A]) of 3.06.

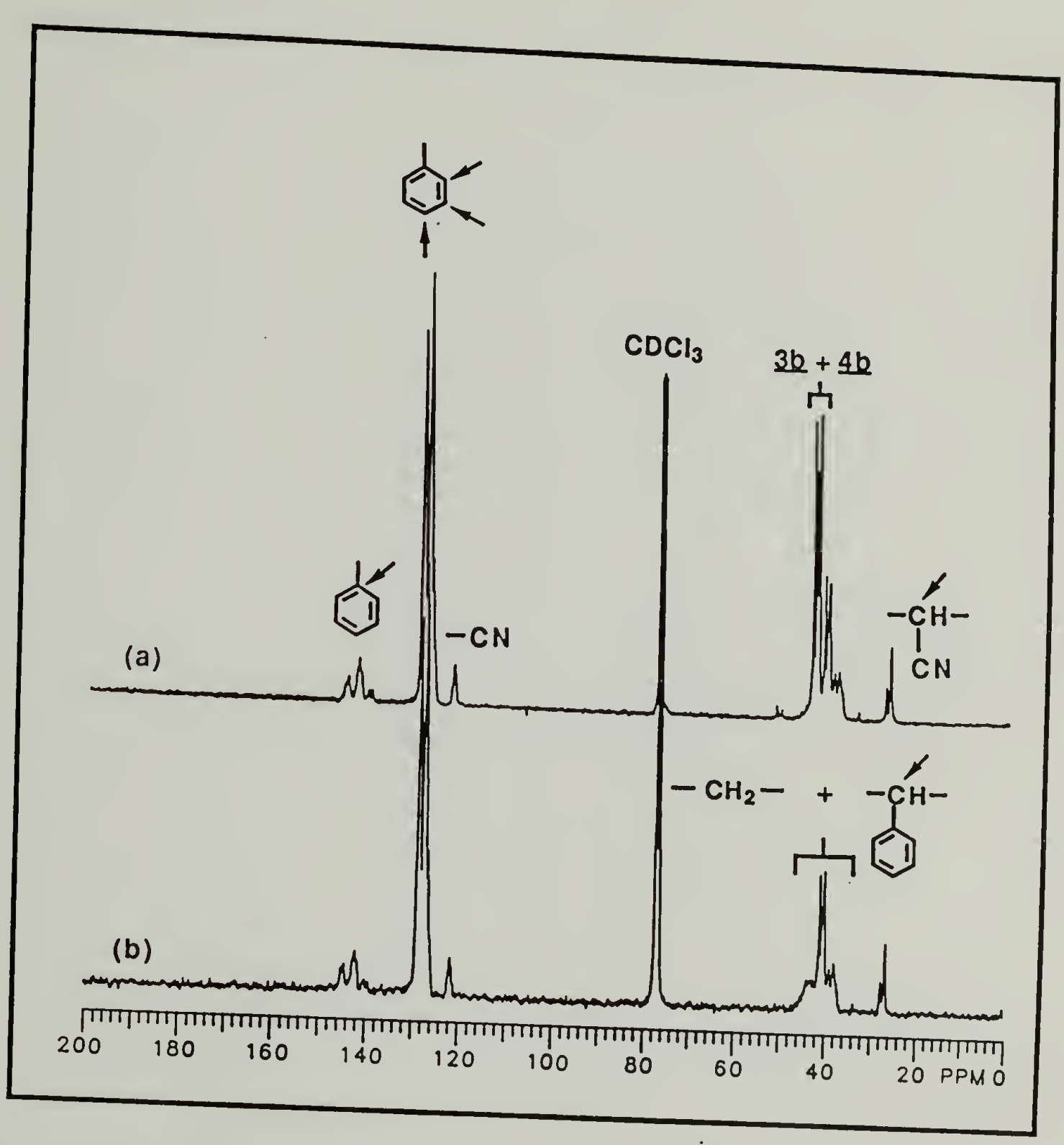

Figure 3.29. 75 MHz ^{13}C NMR spectra of (a) enriched and (b) natural-abundance SAN copolymers in $CDCl_3$ that were prepared from **1b** with a monomer feed ratio ([S]/[A]) of 4.00.

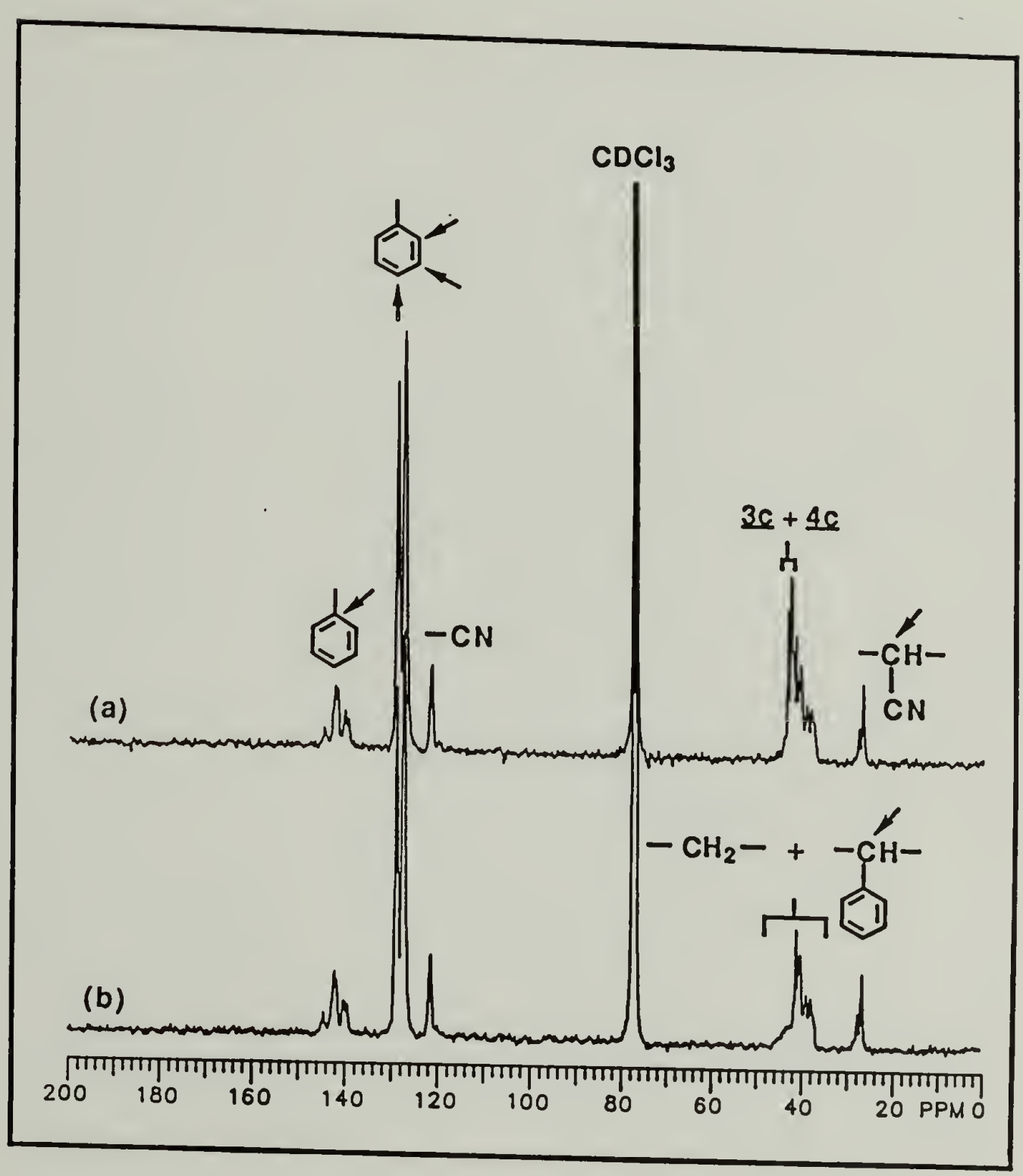

Figure 3.30. 75 MHz ^{13}C NMR spectra of (a) enriched and (b) natural-abundance SAN copolymers in $CDCl_3$ that were prepared from **1c** with a monomer feed ratio ([S]/[A]) of 1.87.

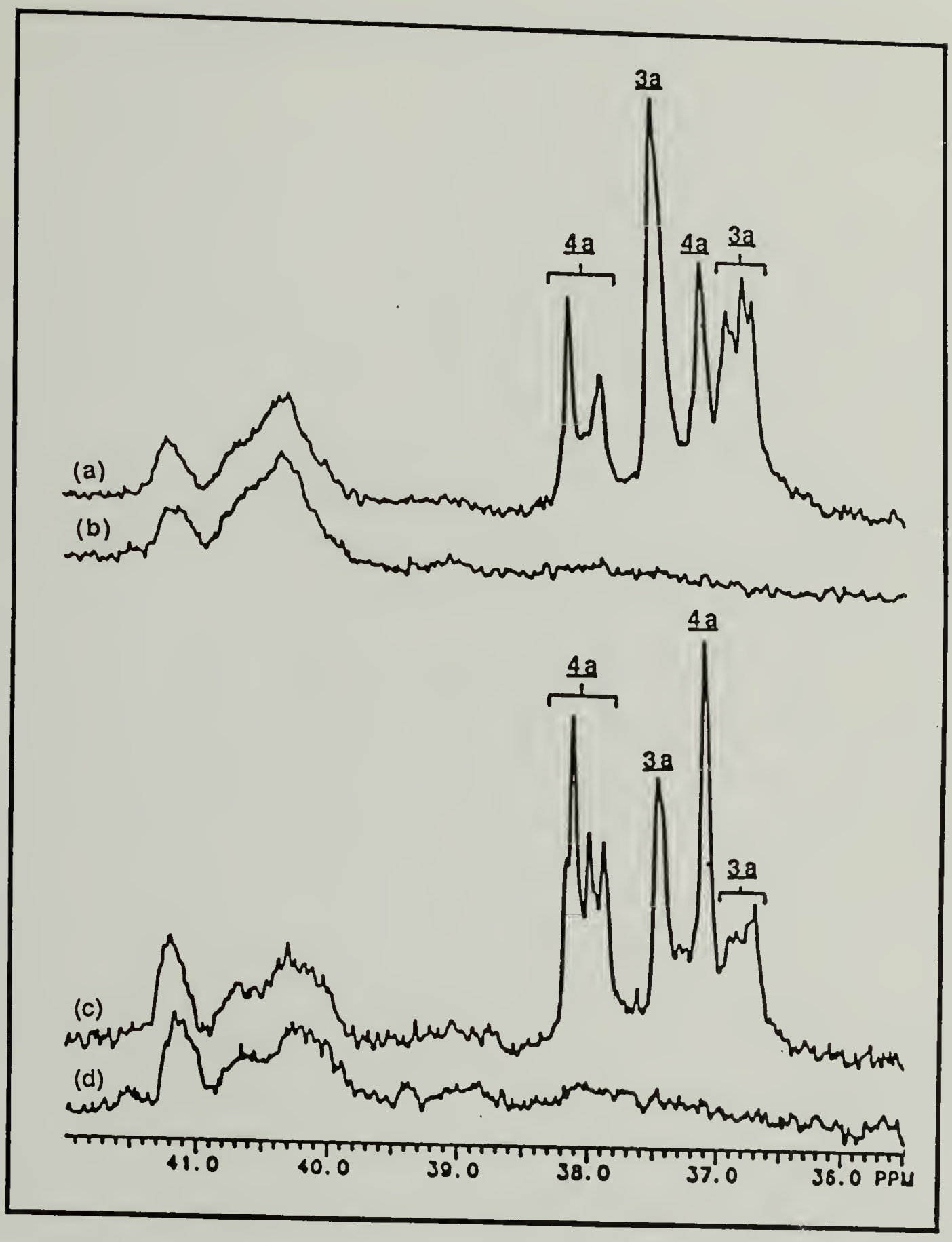

Figure 3.31. 75 MHz ^{13}C NMR spectra (expanded plots) of enriched (a and c) and natural-abundance (b and d) SAN copolymers in $CDCl_3$ that were prepared from 1a with monomer feed ratios ([S]/[A]) of 9.14 (top) and 3.06 (bottom).

Figure 3.32. 75 MHz ^{13}C NMR spectra (expanded plots) of enriched (a and c) and natural-abundance (b and d) SAN copolymers in deuterated diglyme at 140 °C that were prepared from **1b** with monomer feed ratios ([S]/[A]) of 7.26 (top) and 3.40 (bottom).

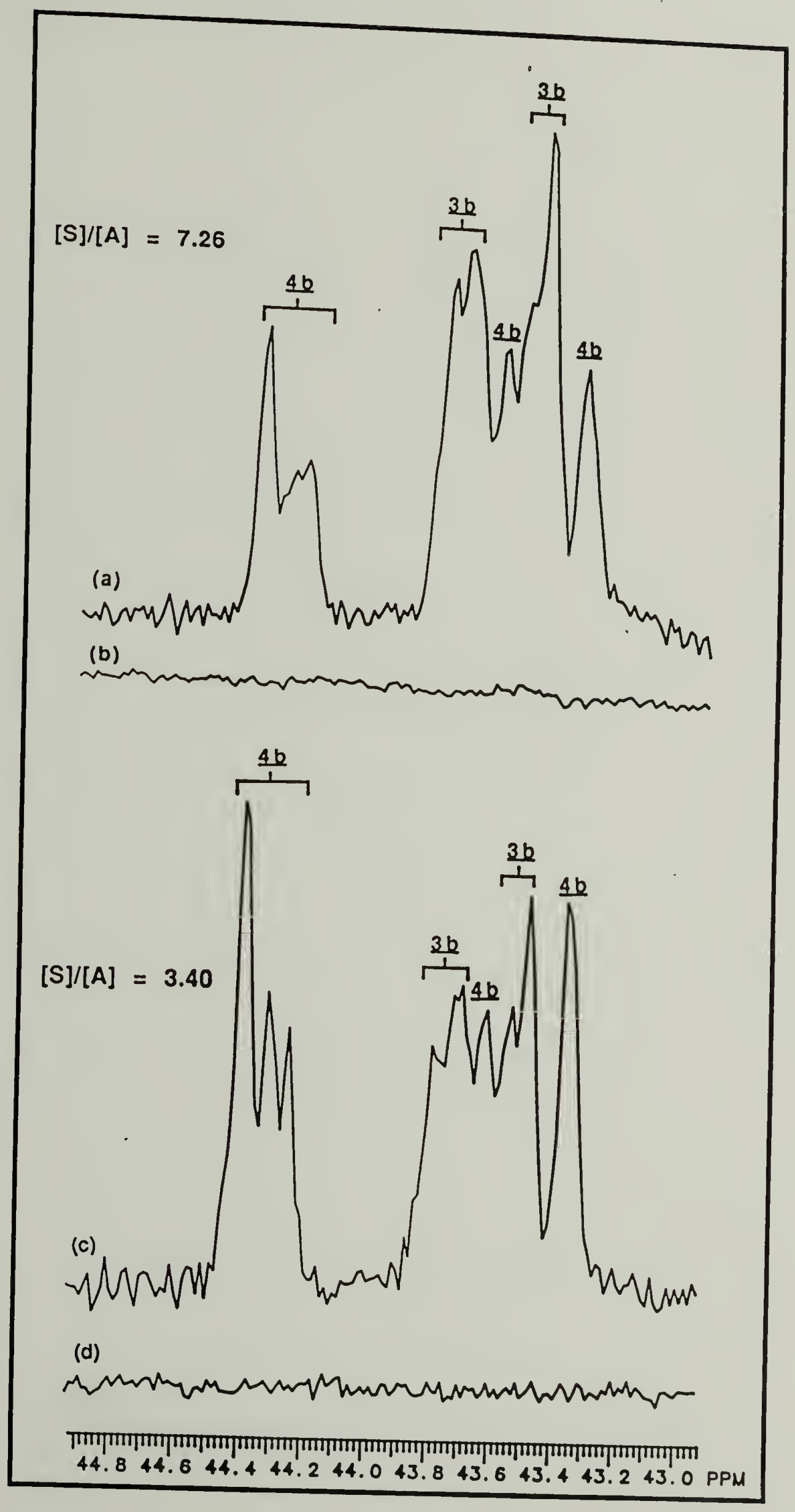
[S]/[A] = 7.26
3b
3b
3b
4b
4b
4b
(a)
(b)
4b
3b
3b
4b
4b
[S]/[A] = 3.40
(c)
(d)
44.8 44.6 44.4 44.2 44.0 43.8 43.6 43.4 43.2 43.0 PPM

Figure 3.33. 75 MHz ^{13}C NMR spectra (expanded plots) of enriched (a and c) and natural-abundance (b and d) SAN copolymers in deuterated bromobenzene at 136 °C that were prepared from **1c** with monomer feed ratios ([S]/[A]) of 2.75 (top) and 0.872 (bottom).

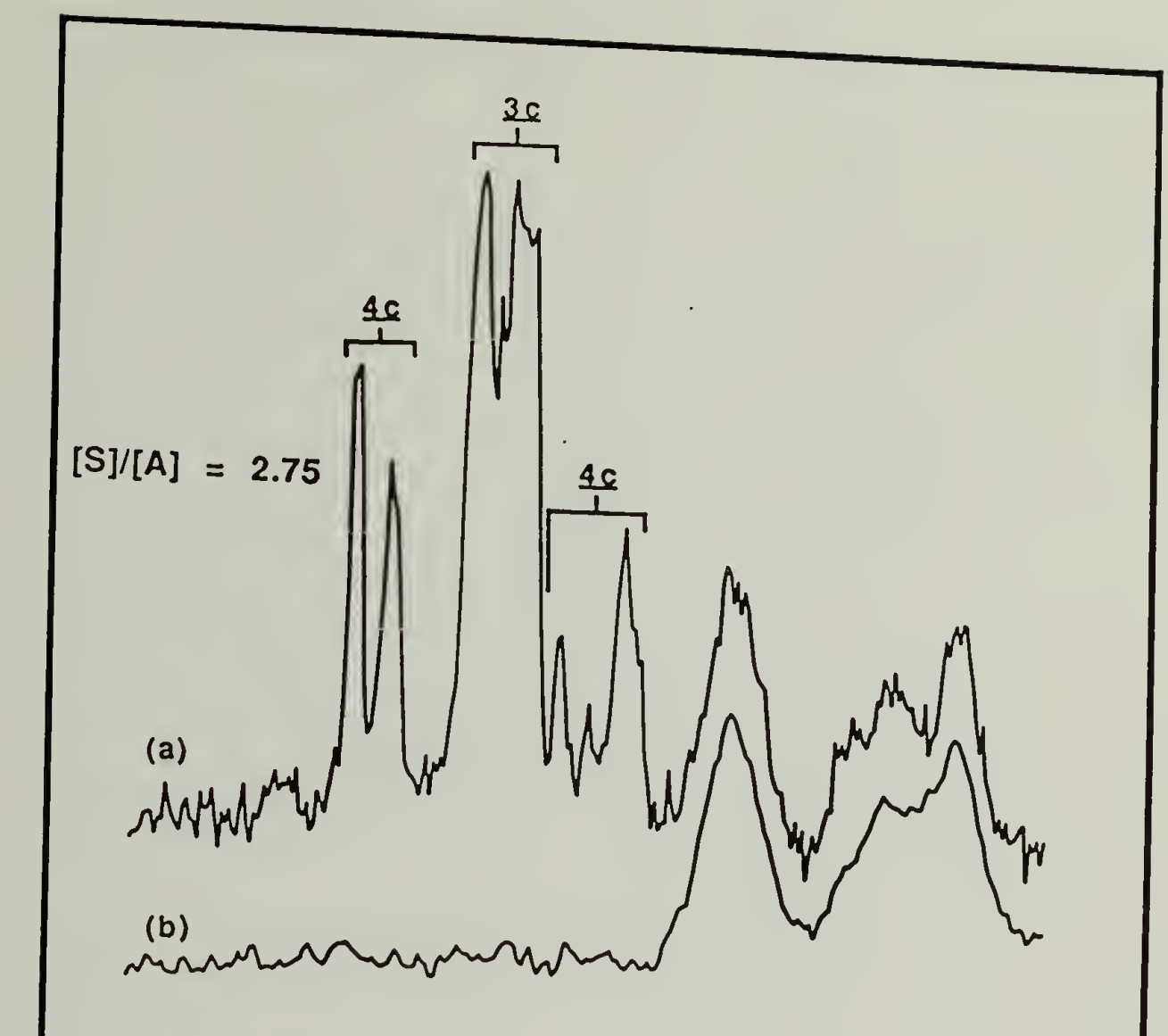
3C
4C
4C
[S]/[A] = 2.75
(a)
(b)
4C
4C
3C
[S]/[A] =0.872
(c)
(d)
43.5
43.0
42.5
42.0
41.5
41.0 PPM

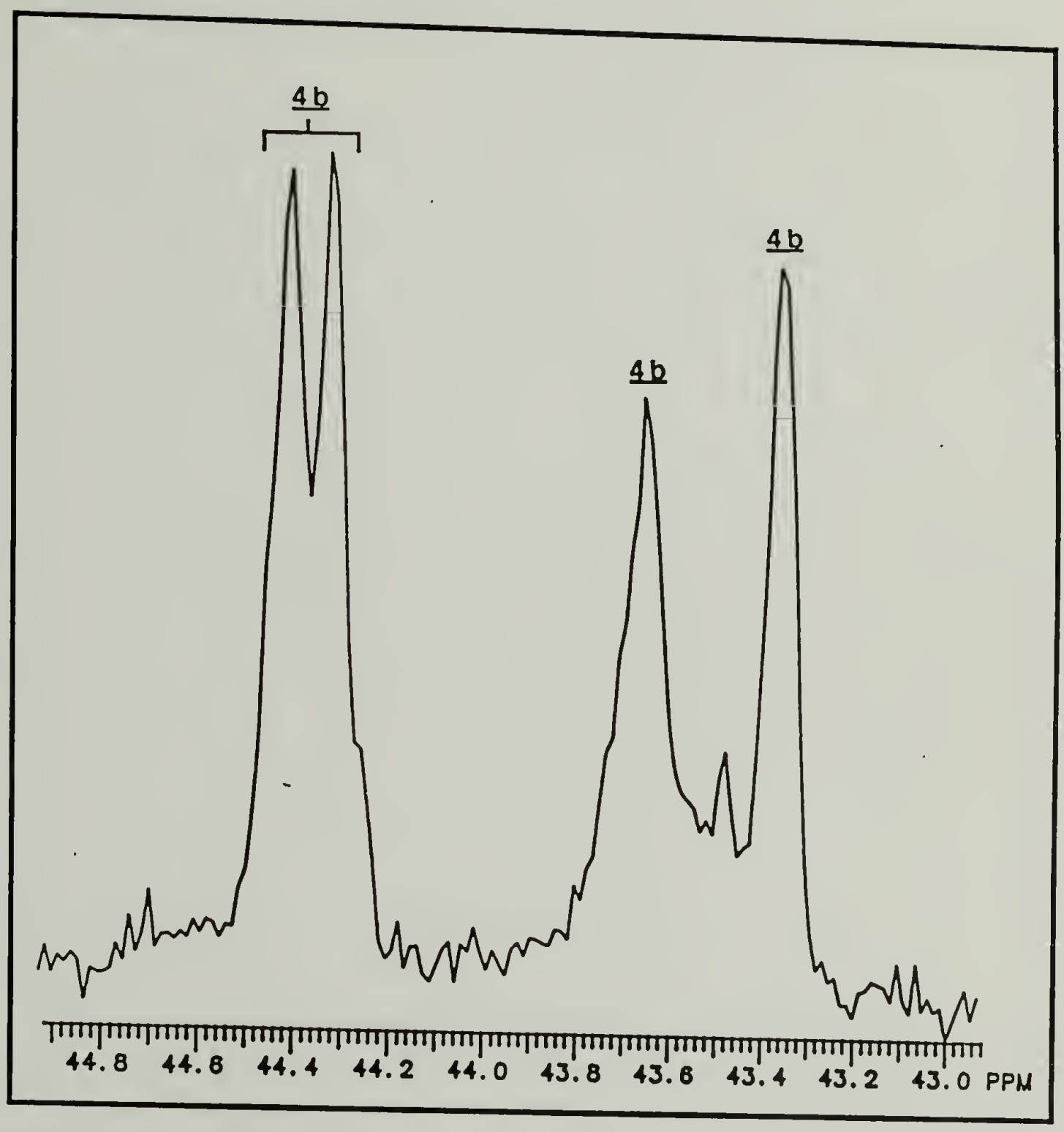

Figure 3.34. 75 MHz ^{13}C NMR spectrum (expanded plot) of an enriched SAN copolymer in deuterated diglyme at 140 °C that was prepared from **1b** with a monomer feed ratio ([S]/[A]) of 0.826.

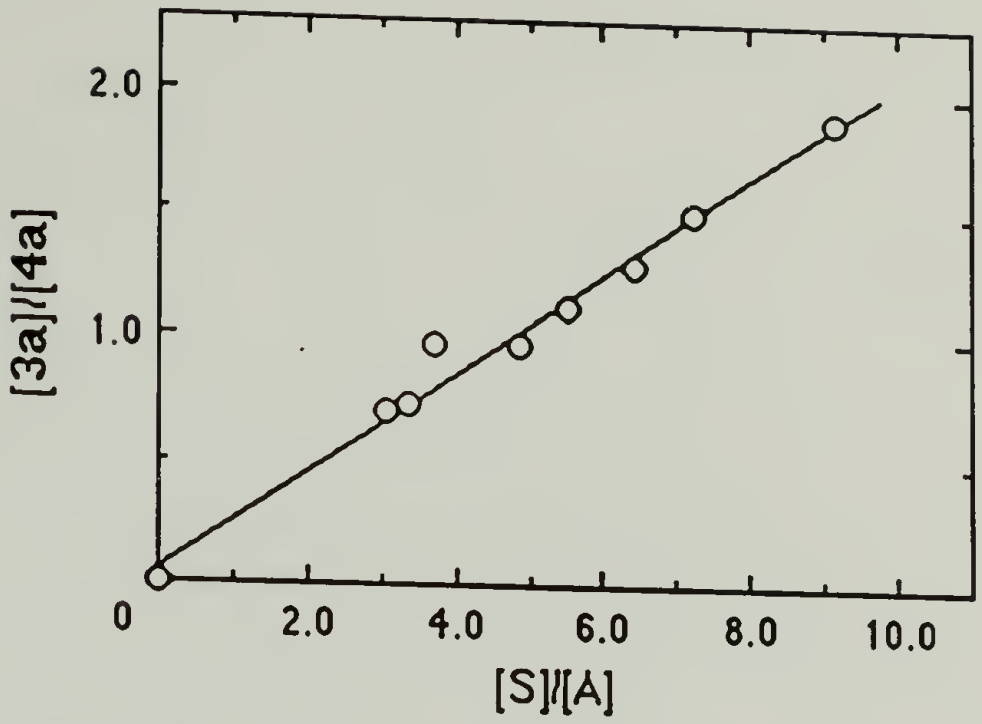

Figure 3.35. Plot of relative end-group concentration ([3a]/[4a]) vs. monomer feed ratio ([S]/[A]) for enriched SAN copolymers derived from 1a (copolymers 1-8 listed in Table 2.3).

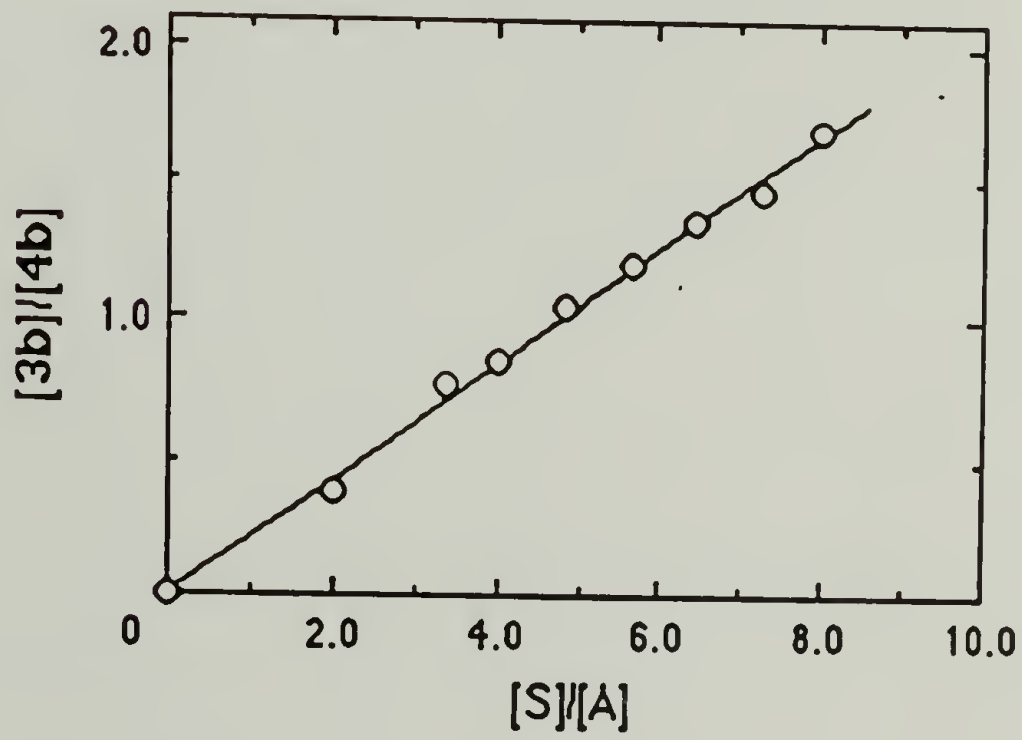

Figure 3.36. Plot of relative end-group concentration ([3b]/[4b]) vs. monomer feed ratio ([S]/[A]) for enriched SAN copolymers derived from 1b (copolymers 9-16 listed in Table 2.4).

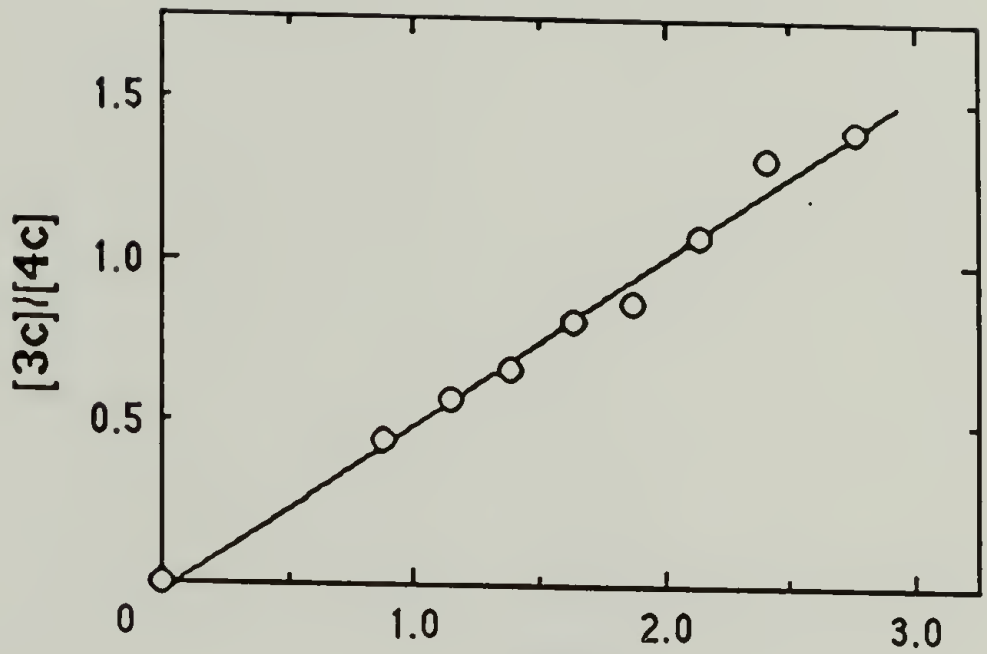

Figure 3.37. Plot of relative end-group concentration ([3c]/[4c]) vs. monomer feed ratio ([S]/[A]) for enriched SAN copolymers derived from 1c (copolymers 18-25 listed in Table 2.5).

(a) Hill et al :

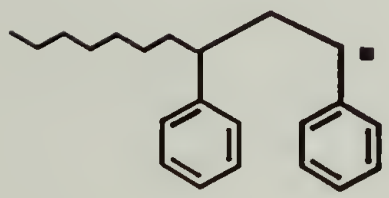

4.35

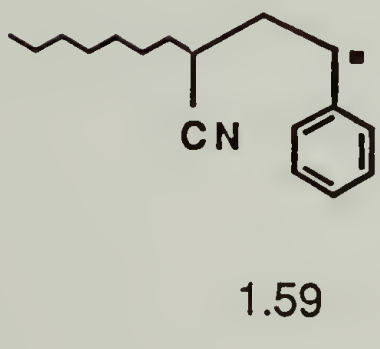

1.59

(b) This work :

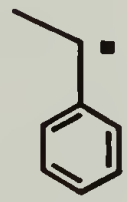

2a

5.0 ± 0.5

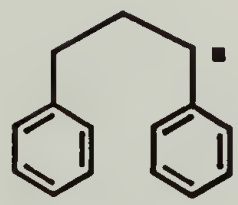

2b

4.8 ± 0.3

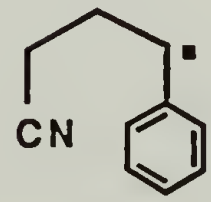

2c

1.9 ± 0.1

(c) Previous work :

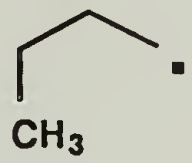

24.5 ± 1.1

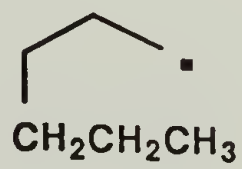

26.3 ± 2.4

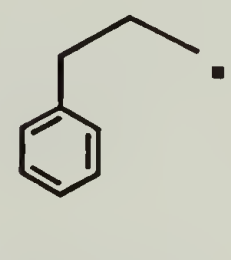

22.6 ± 2.0

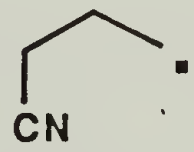

6.8 ± 0.6

Figure 3.38. Comparison of k_A/k_S values (a) calculated from the best-fit penultimate reactivity ratios in Hill and coworkers' analysis of SAN copolymerization (53), (b) determined in work presented in this dissertation, and (c) determined in previous work from this laboratory (57).

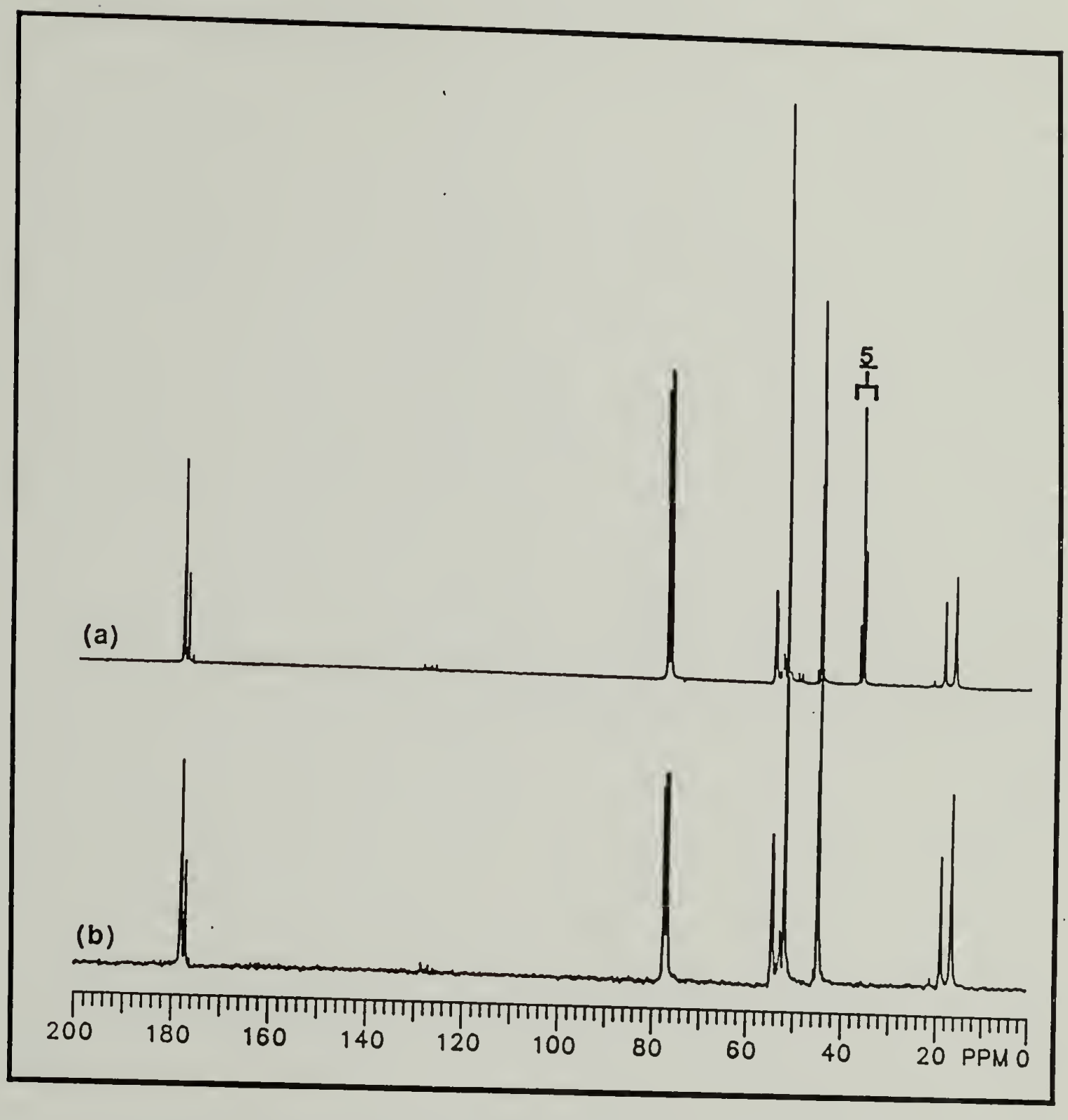

Figure 3.39. 75 MHz ^{13}C NMR spectra of (a) enriched and (b) natural-abundance poly(methyl methacrylate), derived from **1a**, in $CDCl_3$.

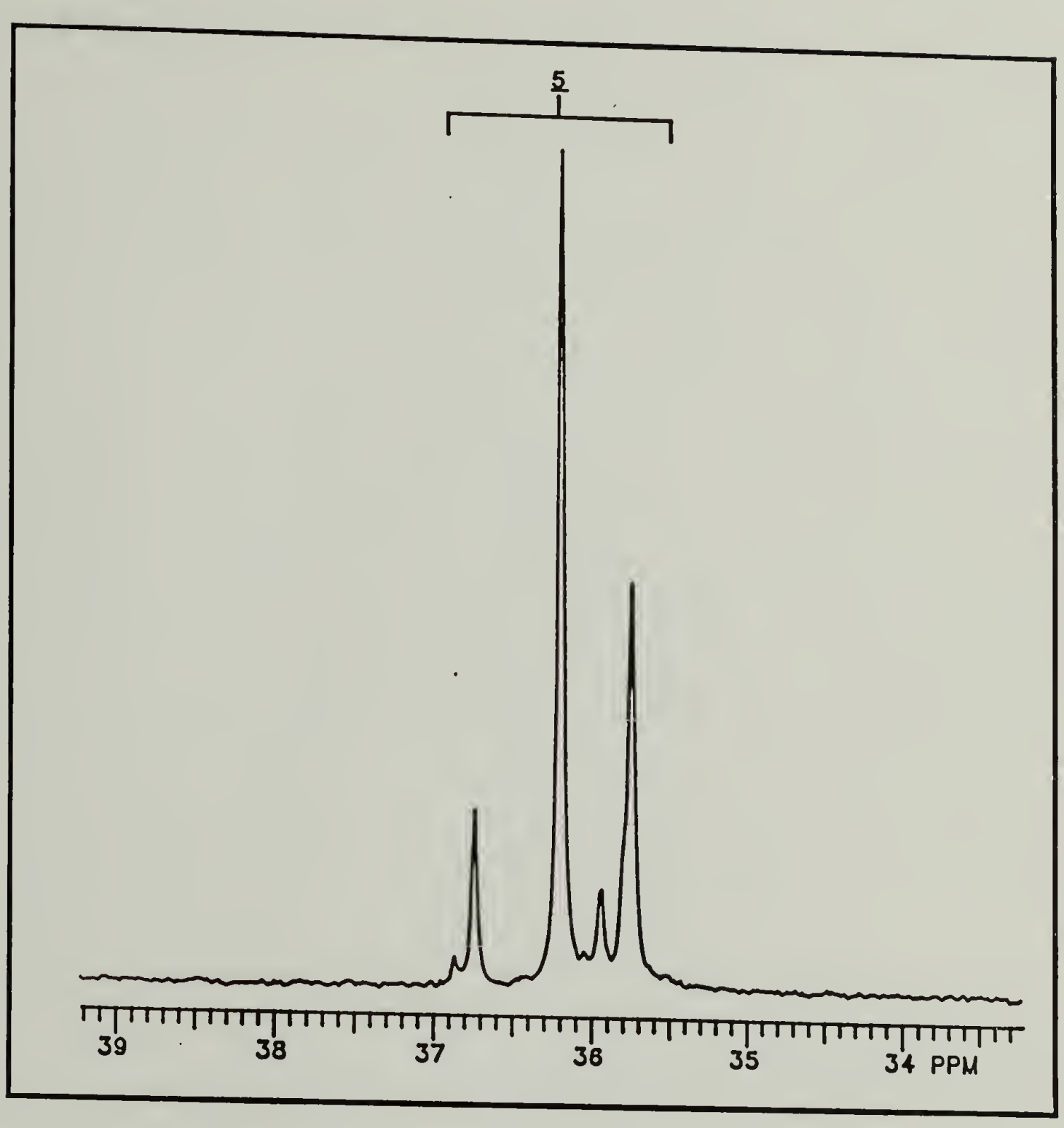

Figure 3.40. 75 MHz ^{13}C NMR spectrum (expanded plot) of enriched poly(methyl methacrylate), derived from **1a**, in $CDCl_3$.

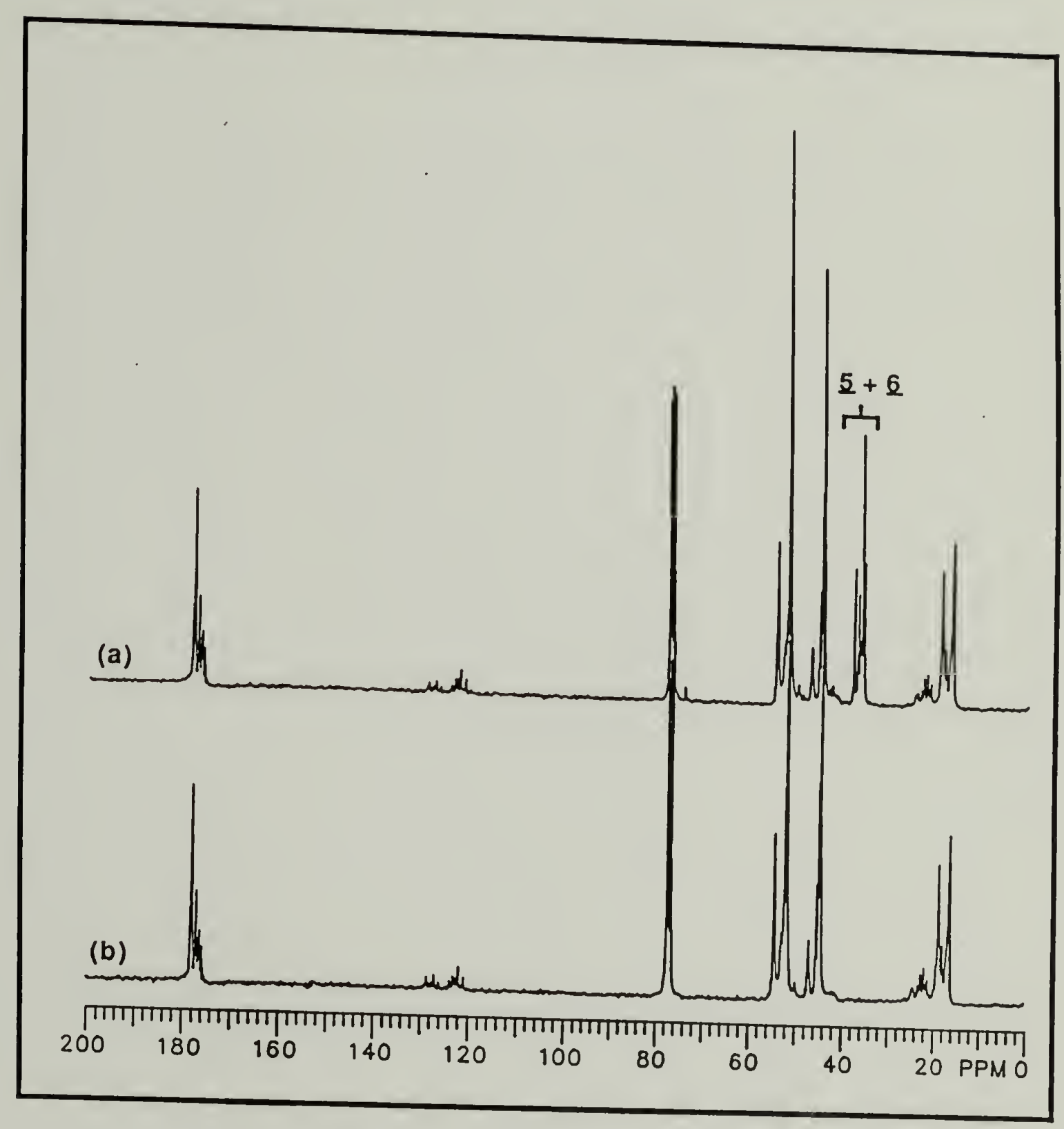

Figure 3.41. 75 MHz ^{13}C NMR spectra of (a) enriched and (b) natural-abundance AMMA copolymers in $CDCl_3$ that were prepared from **1a** with a monomer feed ratio ([MMA]/[A]) of 5.26.

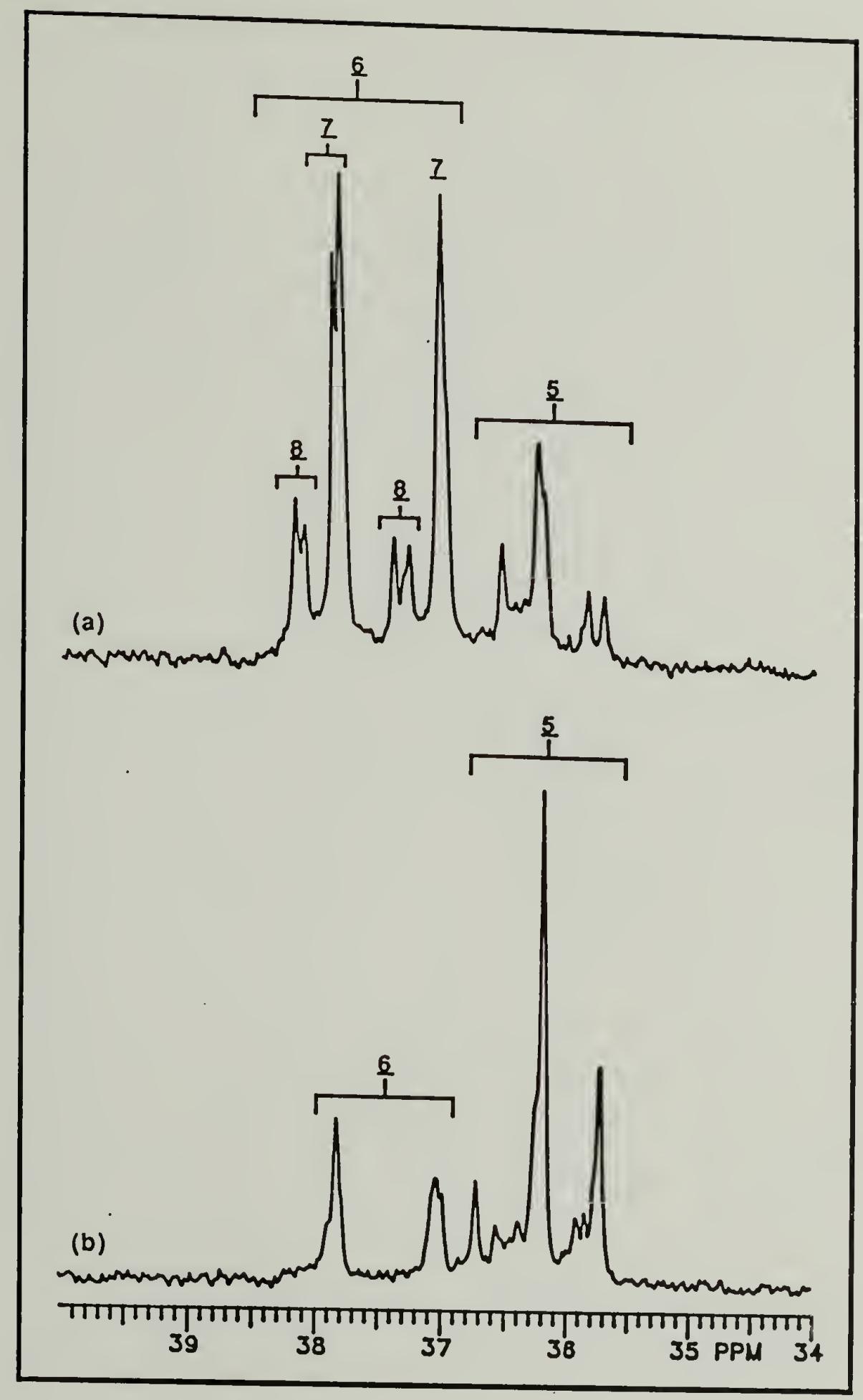

Figure 3.42. 75 MHz ^{13}C NMR spectra (expanded plots) of enriched AMMA copolymers in $CDCl_3$ that were prepared from **1a** with monomer feed ratios ([MMA]/[A]) of (a) 0.999 and (b) 6.62.

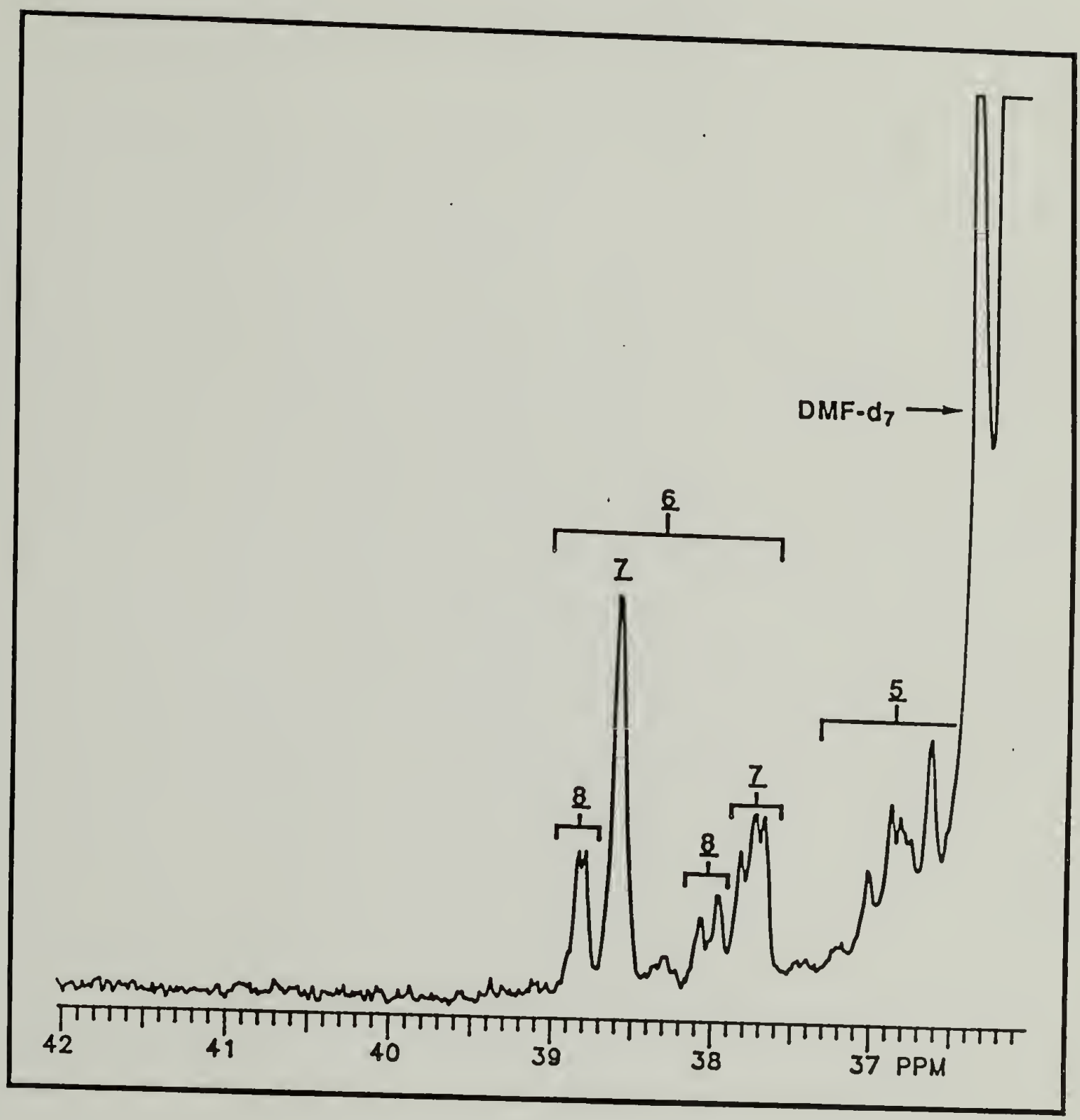

Figure 3.43. 75 MHz ^{13}C NMR spectrum (expanded plot) of an enriched AMMA copolymer in DMF-d7 that was prepared from **1a** with a monomer feed ratio ([MMA]/[A]) of 0.999.

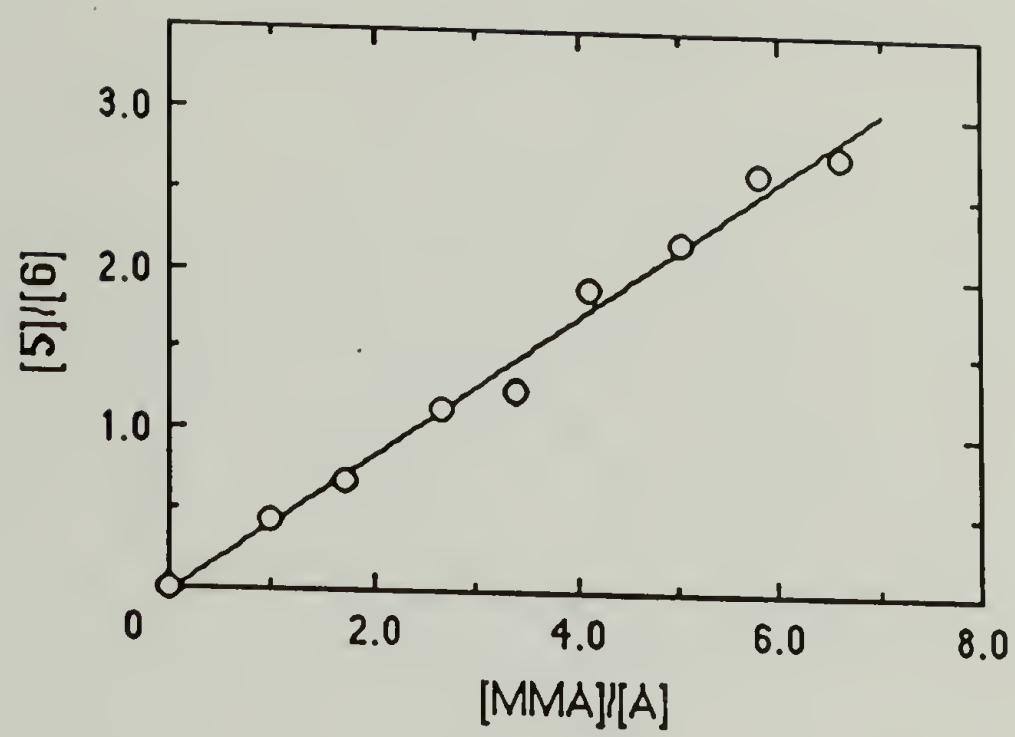

Figure 3.44. Plot of relative end-group concentration ([5]/[6]) vs. monomer feed ratio ([MMA]/[A]) for enriched AMMA copolymers derived from 1a (copolymers 28-35 listed in Table 2.6).

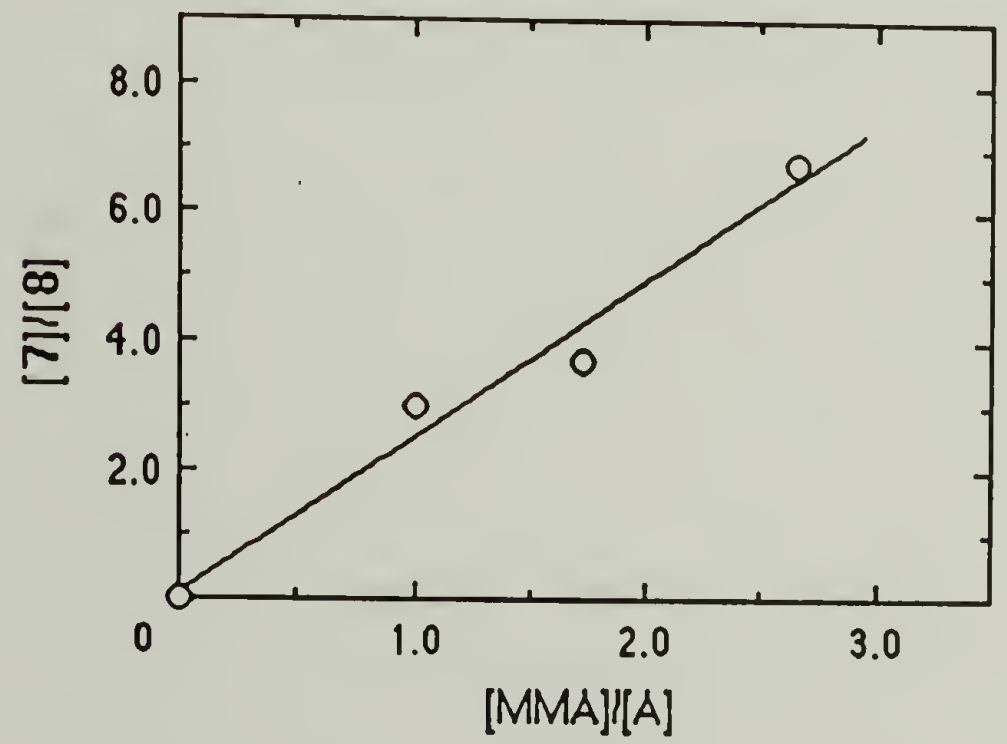

Figure 3.45. Plot of relative end-group concentration ([7]/[8]) vs. monomer feed ratio ([MMA]/[A]) for enriched AMMA copolymers derived from 1a (copolymers 33-35 listed in Table 2.6).

C. Conclusions

1,1'-Azobis(1-phenyl[1-^{13}C]ethane) (**1a**), 1,1'-azobis(1,3-[1-^{13}C]diphenylpropane) (**1b**), and 4,4'-azobis(4-phenyl[4-^{13}C]butyronitrile) (**1c**) serve as convenient sources of the corresponding radicals 1-phenylethyl (**2a**), 1-(1,3-diphenyl)propyl (**2b**), and 4-(4-phenyl)butyronitrile (**2c**). Analysis of end group concentrations in styrene(S)-acrylonitrile(A) copolymers prepared with **1a**, **1b**, or **1c** as initiator allows accurate determination of the relative rates of addition of these monomers to **2a**, **2b**, or **2c**, as the case may be. The following results are obtained: $k_S/k_A = 0.20 \pm 0.02$ for **2a**, 0.21 ± 0.01 for **2b**, and 0.52 ± 0.03 for **2c**. The 2.5-fold increase in k_S/k_A observed for **2c** as compared to **2a** or **2b** indicates that a cyano group in a position gamma to an α-phenylalkyl radical can bring about an appreciable decrease in the relative rate of acrylonitrile addition. This pattern of behavior is similar to what has been previously observed for primary alkyl radicals (57) of analogous structure. These results are also consistent with the penultimate model treatment of the styrene-acrylonitrile copolymerization by Hill, O'Donnell and O'Sullivan (53), and offer clear evidence for the existence of a penultimate unit effect for that system.

In the same way, analysis of end group concentrations in acrylonitrile (A)-methyl methacrylate (MMA) copolymers prepared with **1a** as initiator allows accurate determination of the relative rates of addition of these monomers to **2a**, and $k_{MMA}/k_A = 0.44 \pm 0.03$ is obtained. This value is in reasonable agreement with the product of k_S/k_A for 2a and the reciprocal of the terminal model reactivity ratio r_1 for the styrene-methyl methacrylate (S = 1, MMA = 2) copolymerization, using $r_1 = 0.51$ as measured by Fukuda (13). This suggests that 2a and a styryl terminated S-MMA macroradical have similar selectivities with regard to addition of styrene, acrylonitrile, and methyl methacrylate. The ^{13}C NMR method of analysis employed is sufficiently sensitive in this case to allow determination from the same data of k_{MMA}/k_A for the 2-(4-phenyl)pentanenitrile radical, which is produced upon the addition of acrylonitrile to the primary radical **2a**. A value of 2.4 ± 0.4 is obtained.

5-Phenyl-1-pentylmercuric bromide and 5-cyano-1-pentylmercuric bromide can serve as sources of the 5-phenyl-1-pentyl and 5-cyano-1-pentyl radicals, respectively, upon reduction with $NaBH_4$. Analysis of the relative concentrations of simple adducts formed in this reaction when carried out in binary solutions of alkenes allows determination of rate constant ratios for addition of the alkenes to the radicals; results obtained are summarized in Table 3.1 (p. 80). For

each of the competition reactions investigated, the selectivities of these radicals are identical to each other. Most notably, there is no change in k_S/k_A for a simple alkyl radical upon replacement of an ε-phenyl substituent with cyano, this being in contrast to behavior that has been previously observed for simple alkyls bearing γ-phenyl and γ-cyano substituents (57).

APPENDIX A

IR and NMR Spectra of Azo Compounds and Precursors Thereof

^{1}H NMR SPECTRUM: [1-^{13}C]acetyl chloride

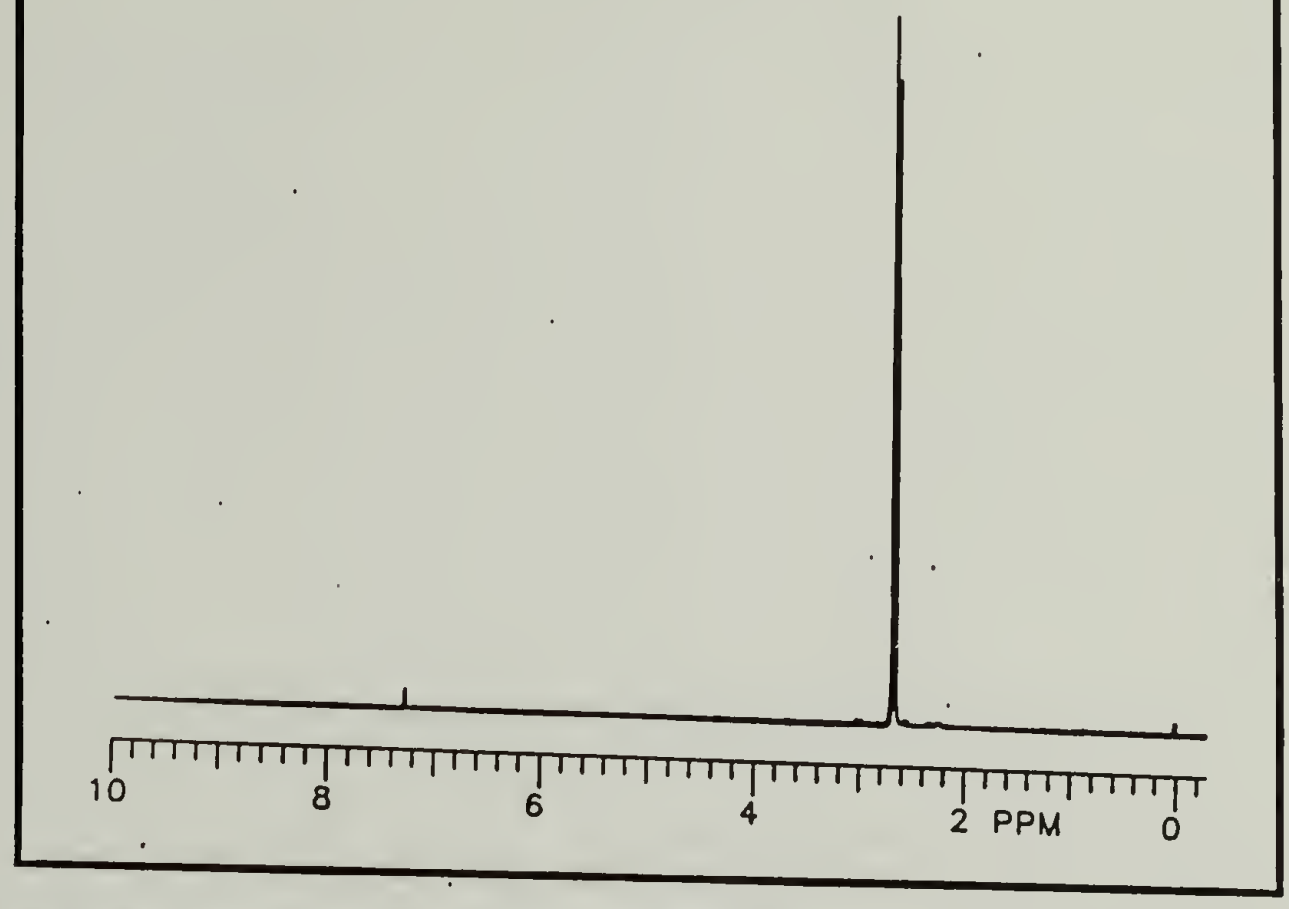

INFRARED SPECTRUM: [1-^{13}C]acetyl chloride

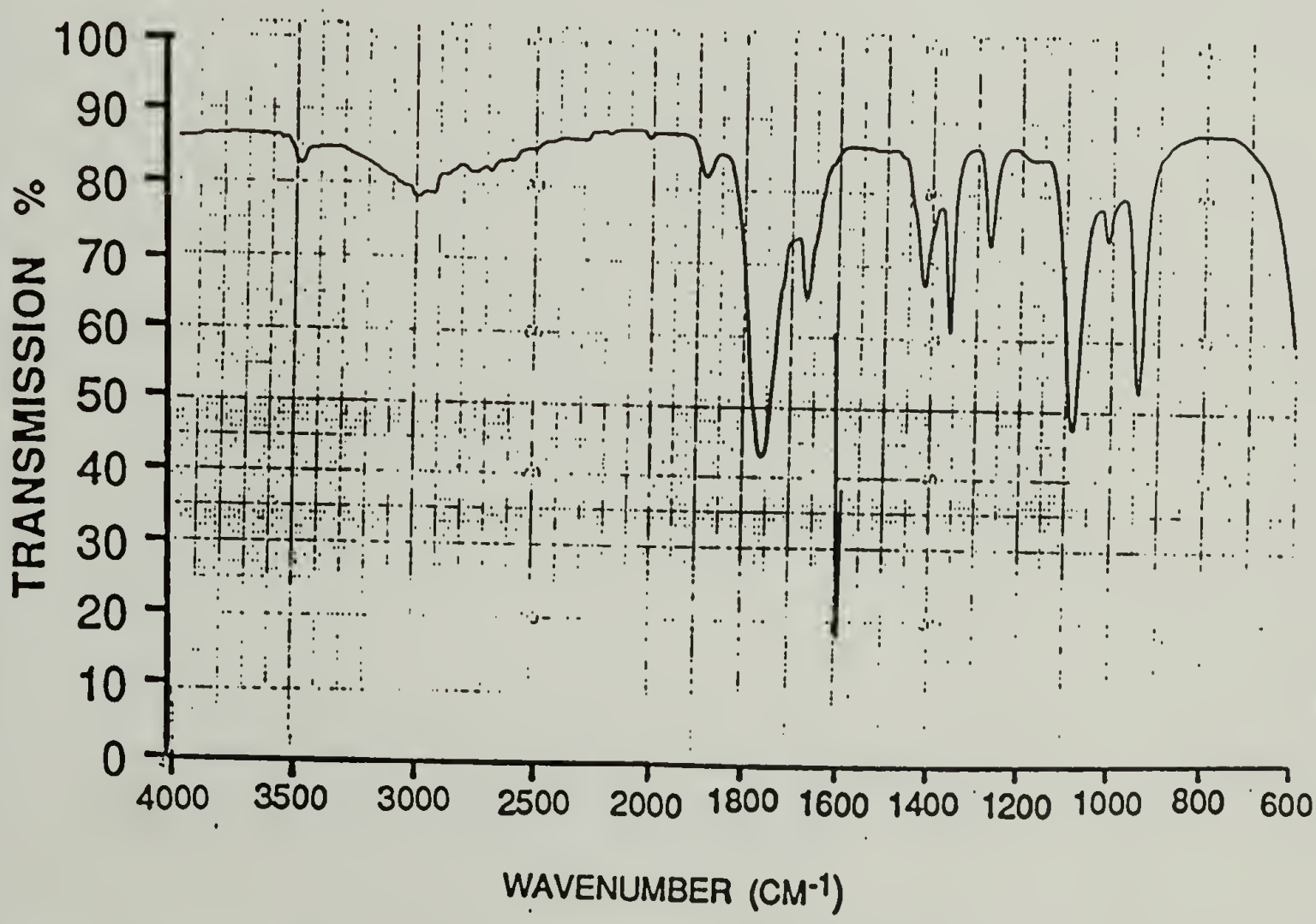

^{1}H NMR SPECTRUM: [1-^{13}C]acetophenone

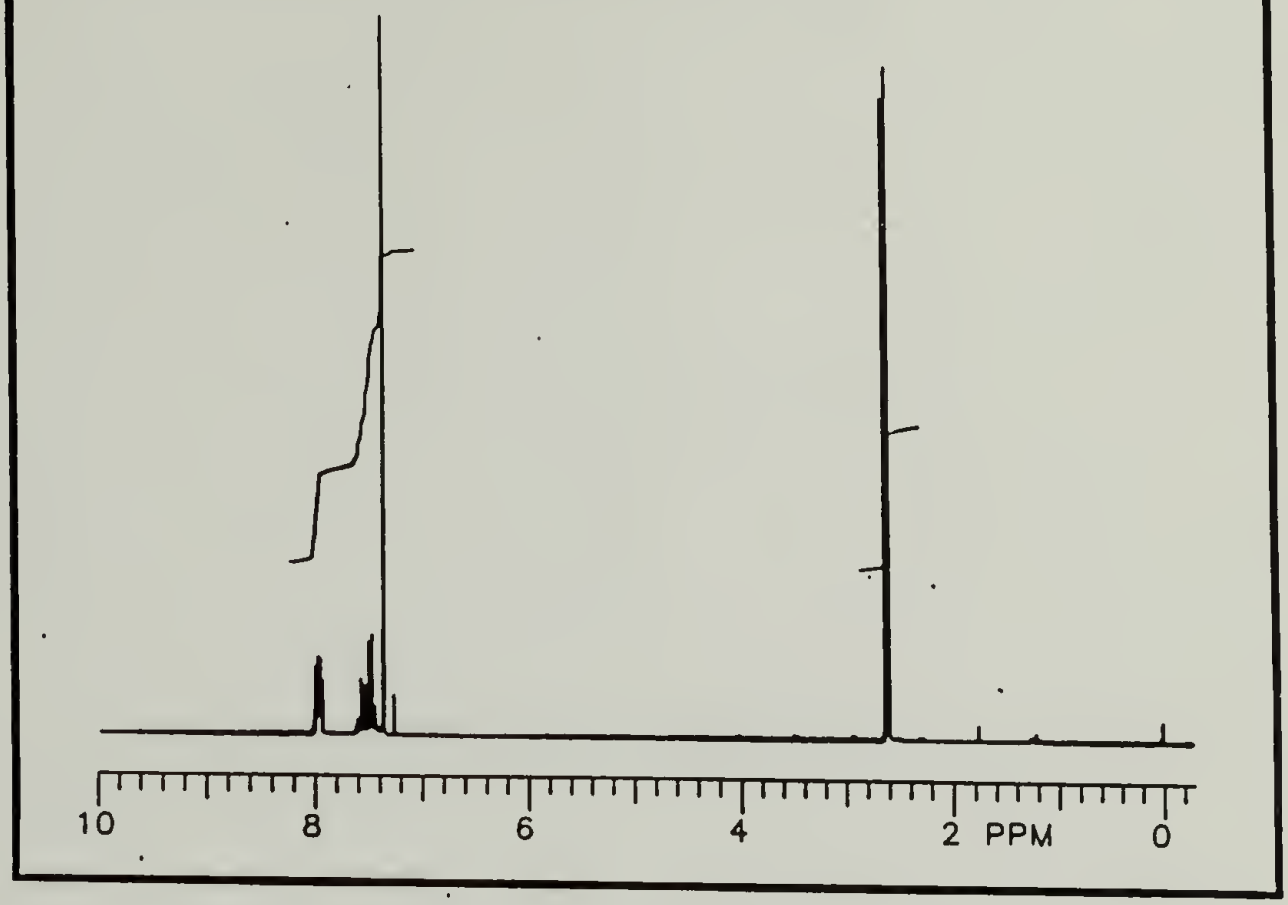

INFRARED SPECTRUM: [1-^{13}C]acetophenone

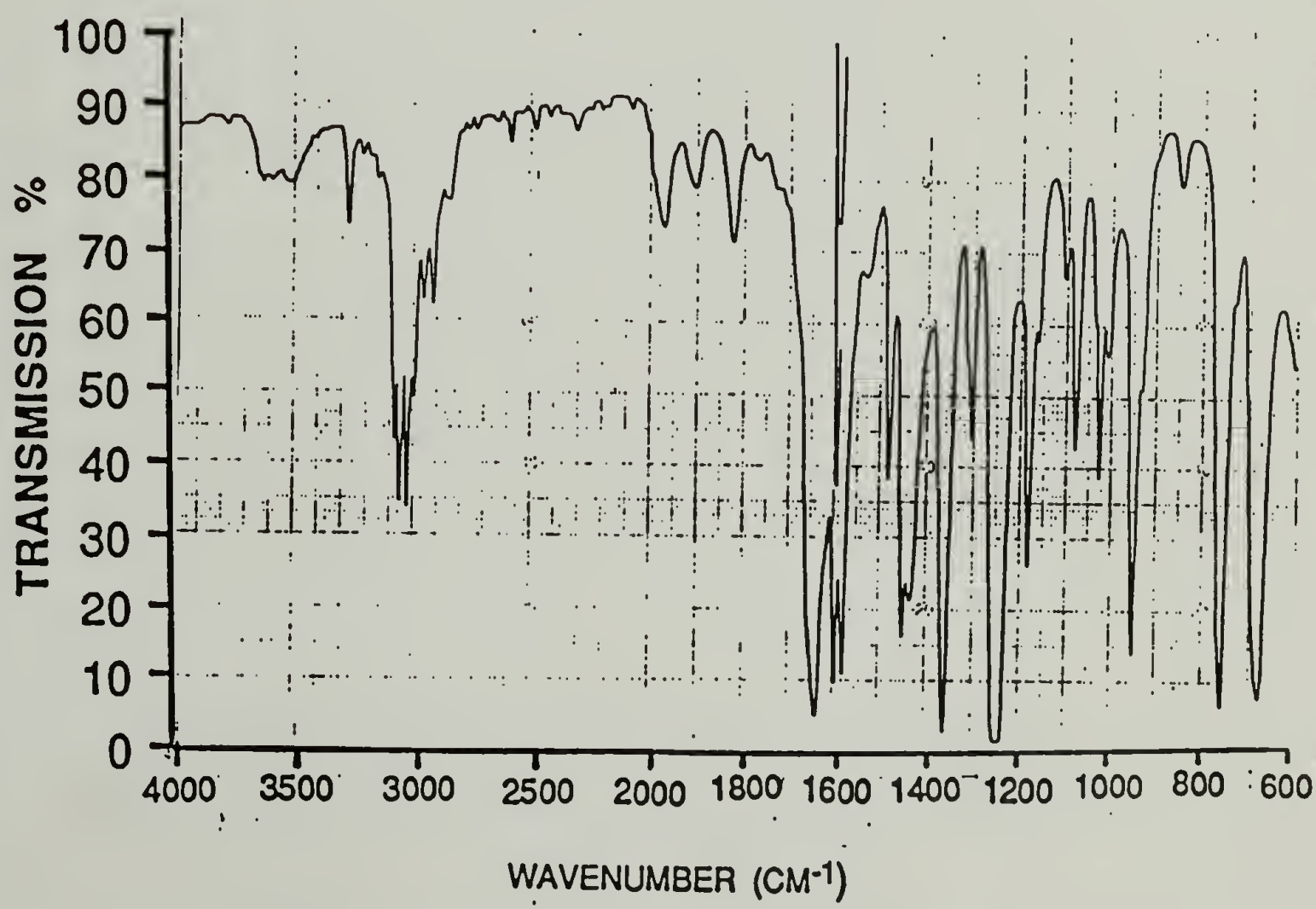

^{1}H NMR SPECTRUM: [1-^{13}C]acetophenone azine

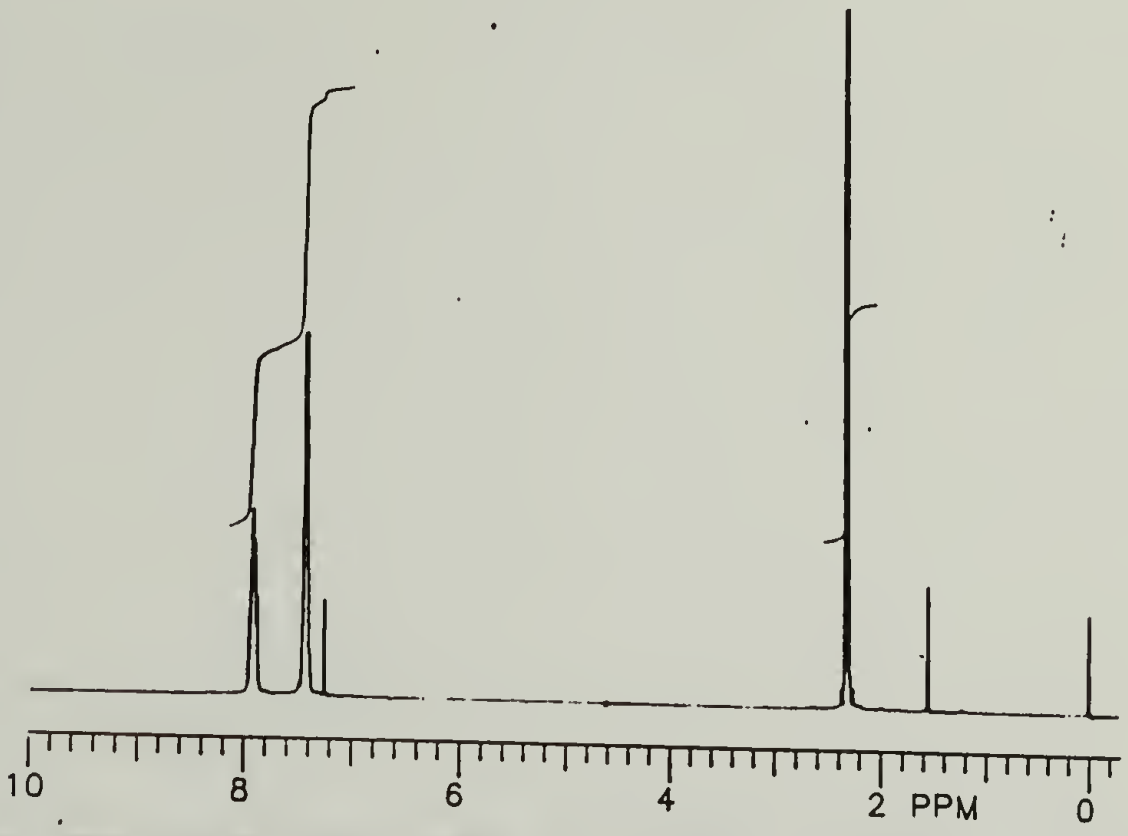

INFRARED SPECTRUM: [1-^{13}C]acetophenone azine

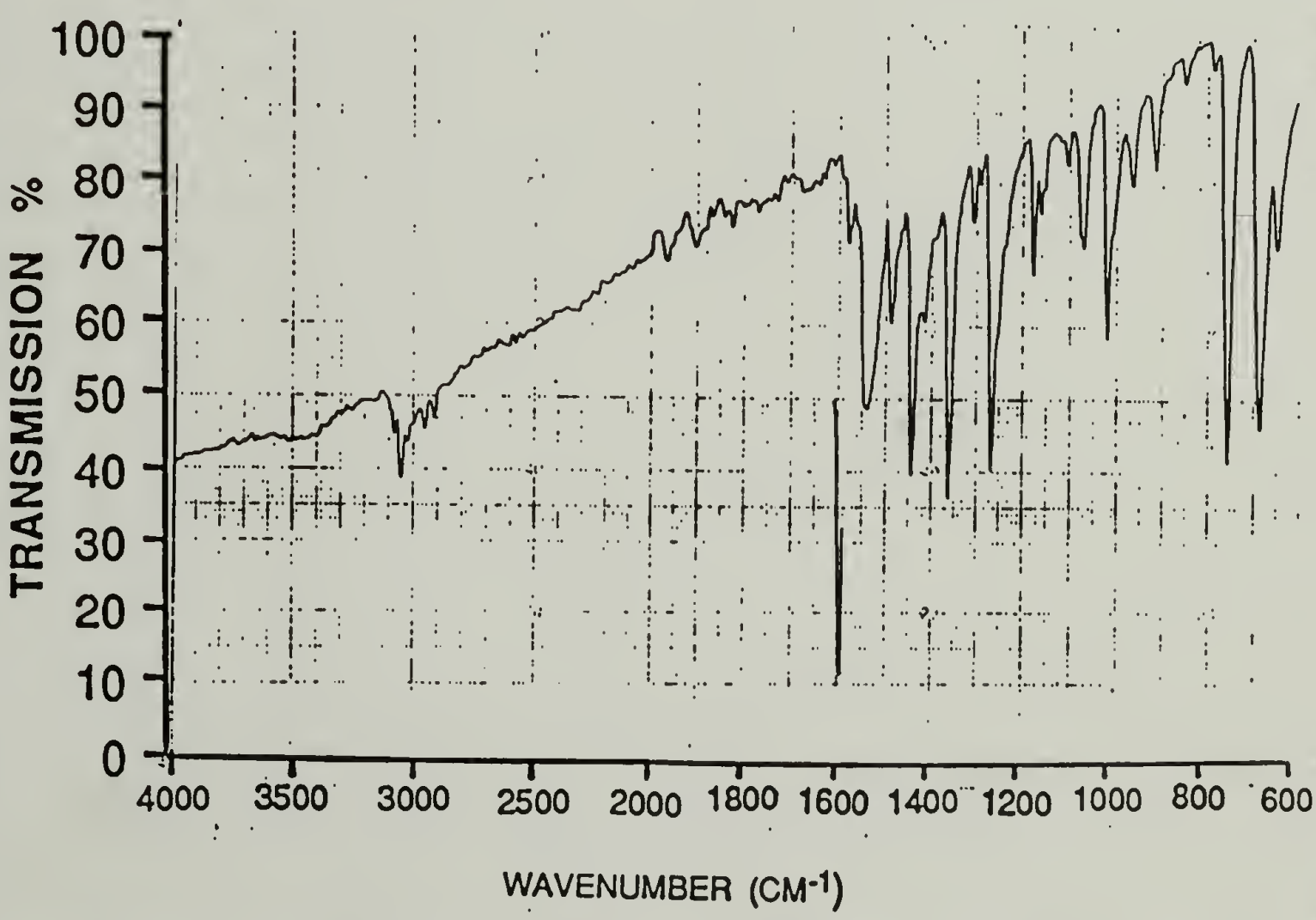

^{1}H NMR SPECTRUM: acetophenone azine

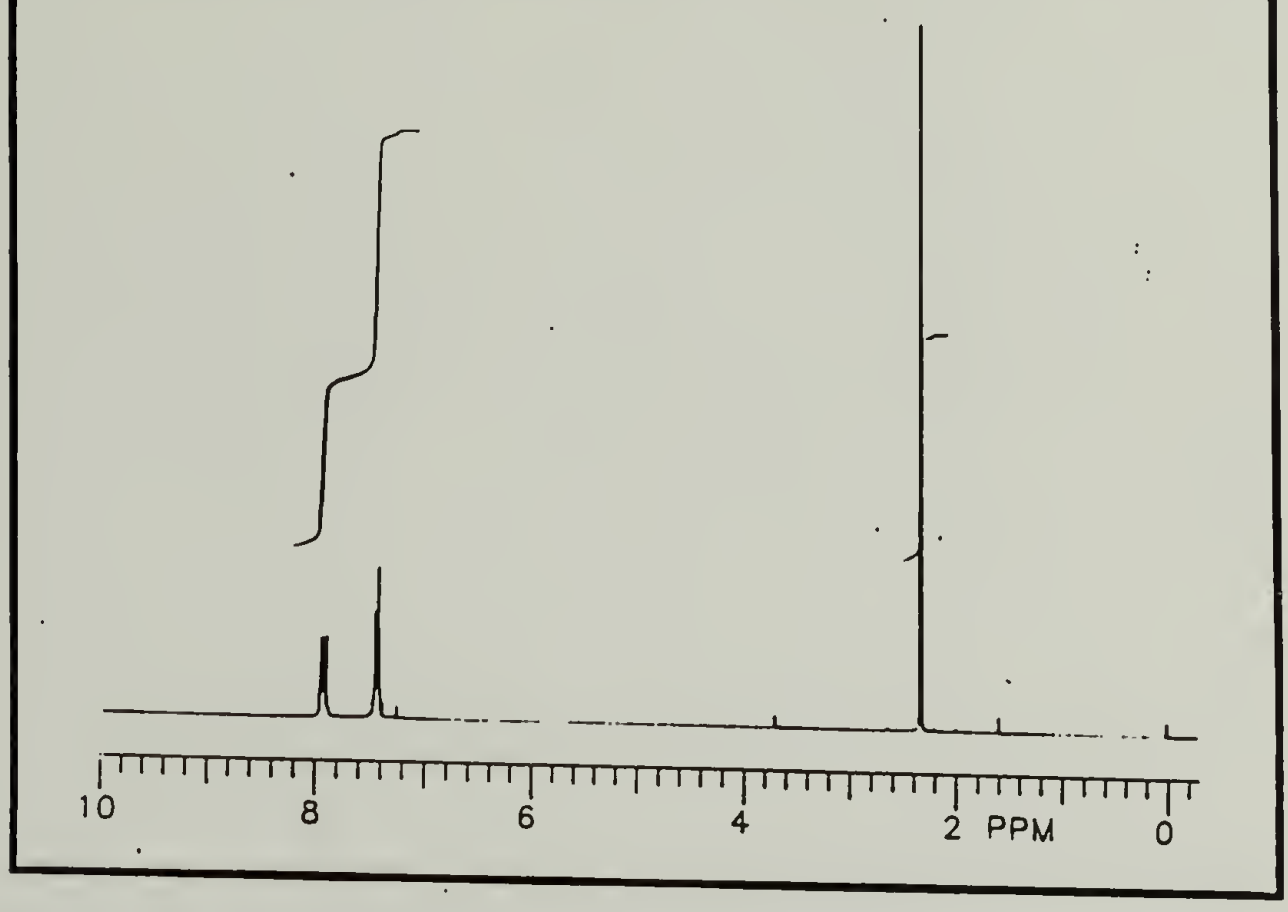

INFRARED SPECTRUM: acetophenone azine

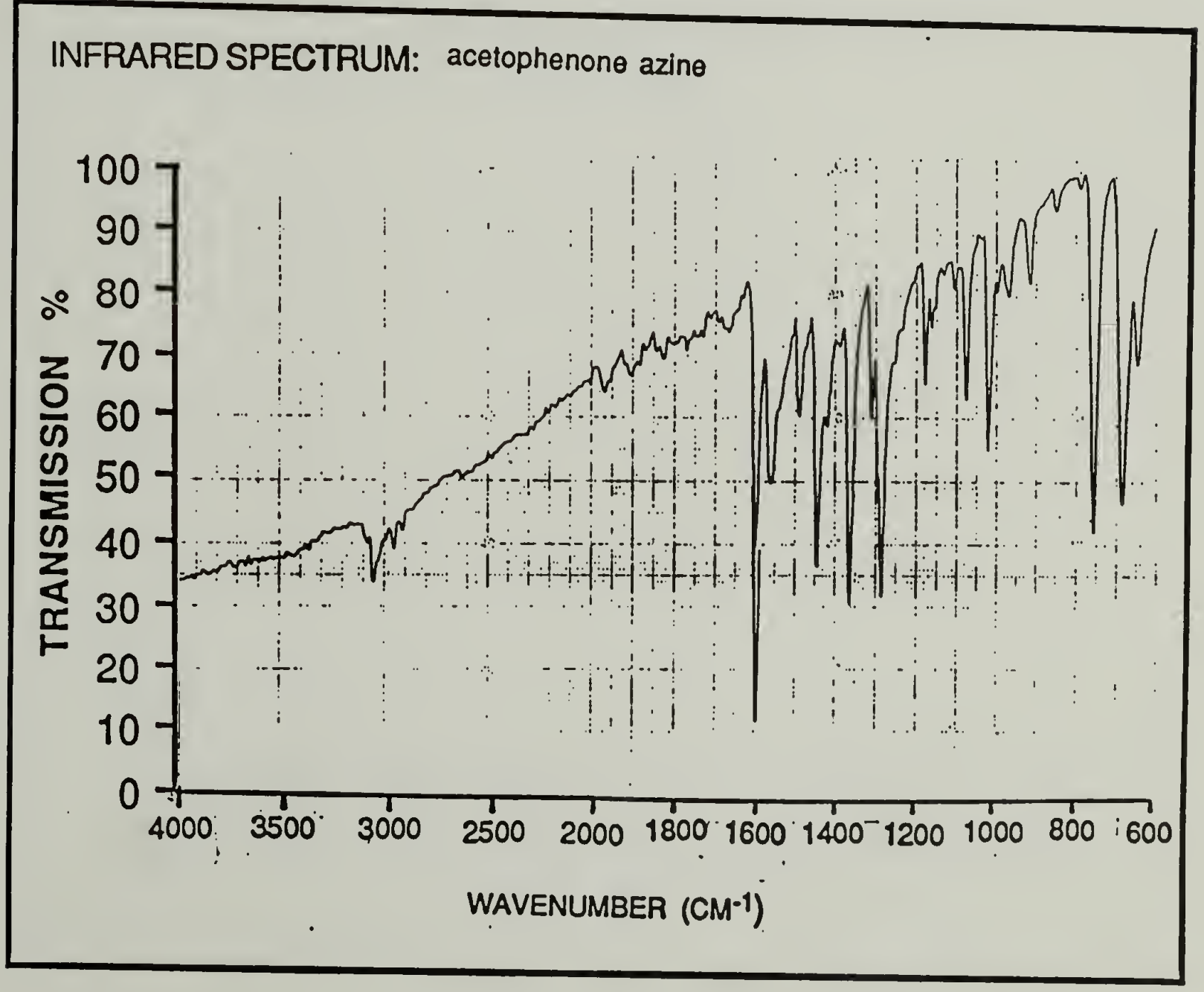

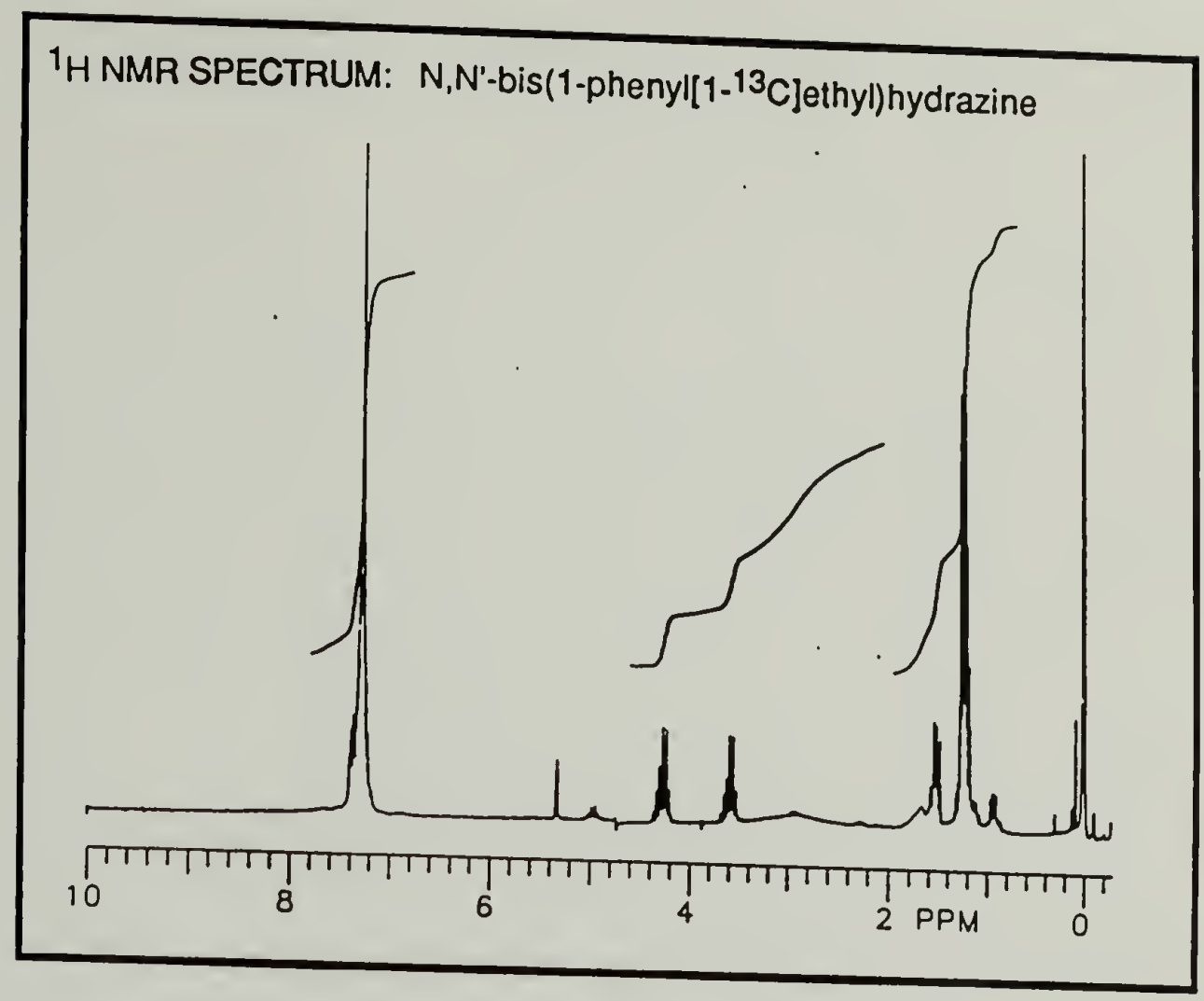
^{1}H NMR SPECTRUM: N,N'-bis(1-phenyl[1-^{13}C]ethyl)hydrazine
10
8
6
4
2 PPM
0

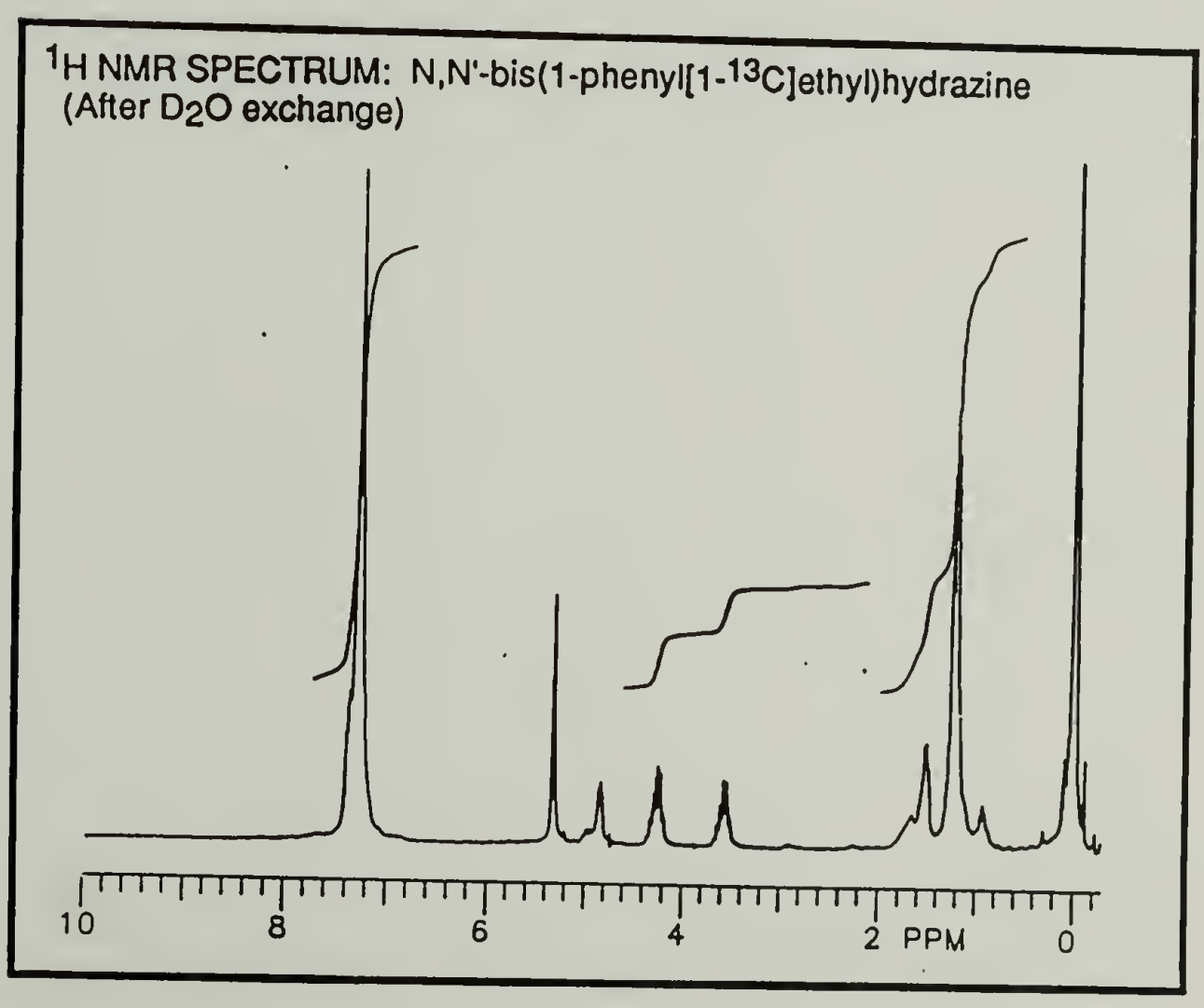
^{1}H NMR SPECTRUM: N,N'-bis(1-phenyl[1-^{13}C]ethyl)hydrazine
(After D_2O exchange)
10
8
6
4
2 PPM
0

INFRARED SPECTRUM: N,N'-bis(1-phenyl[1-^{13}C]ethyl)hydrazine

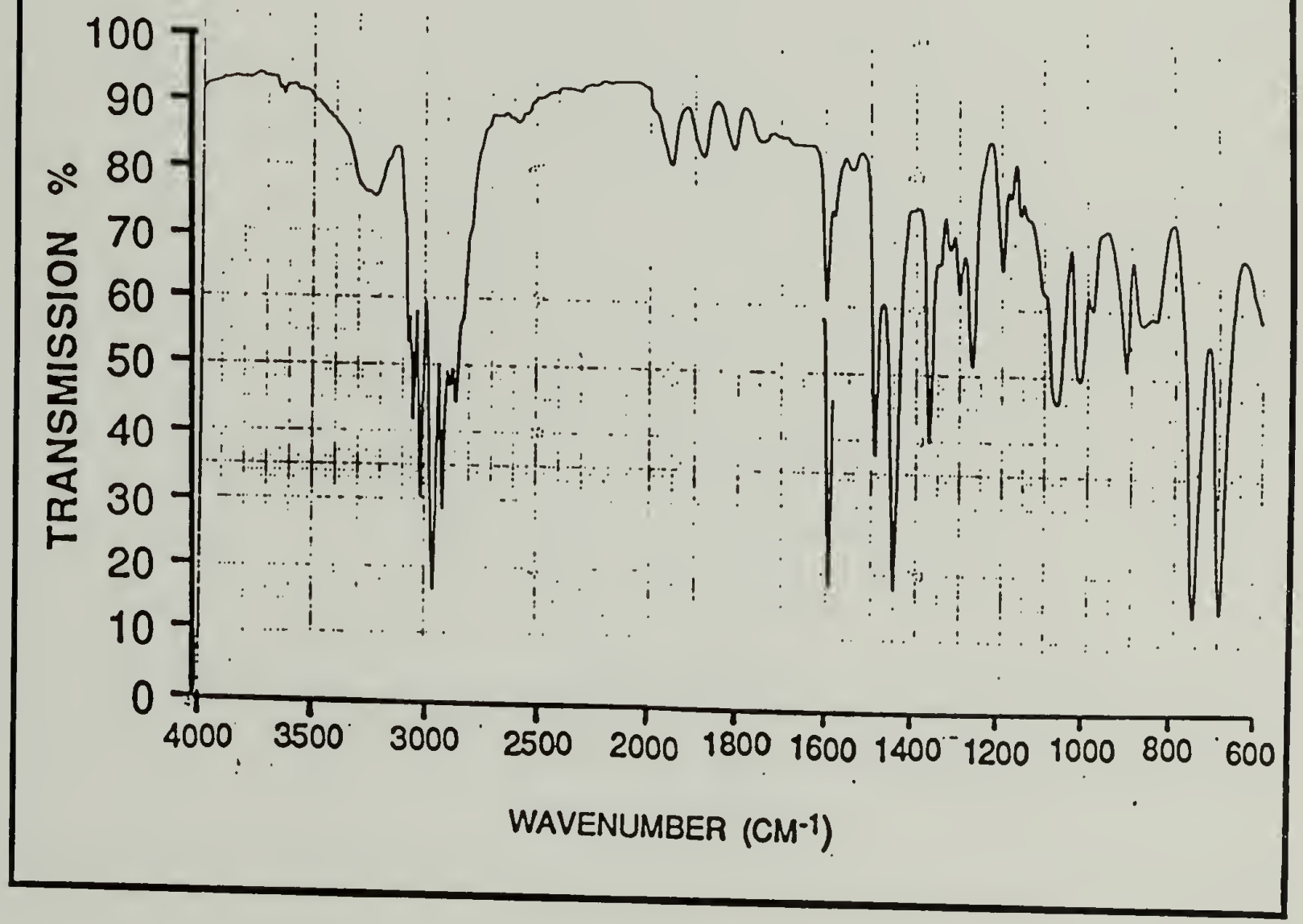

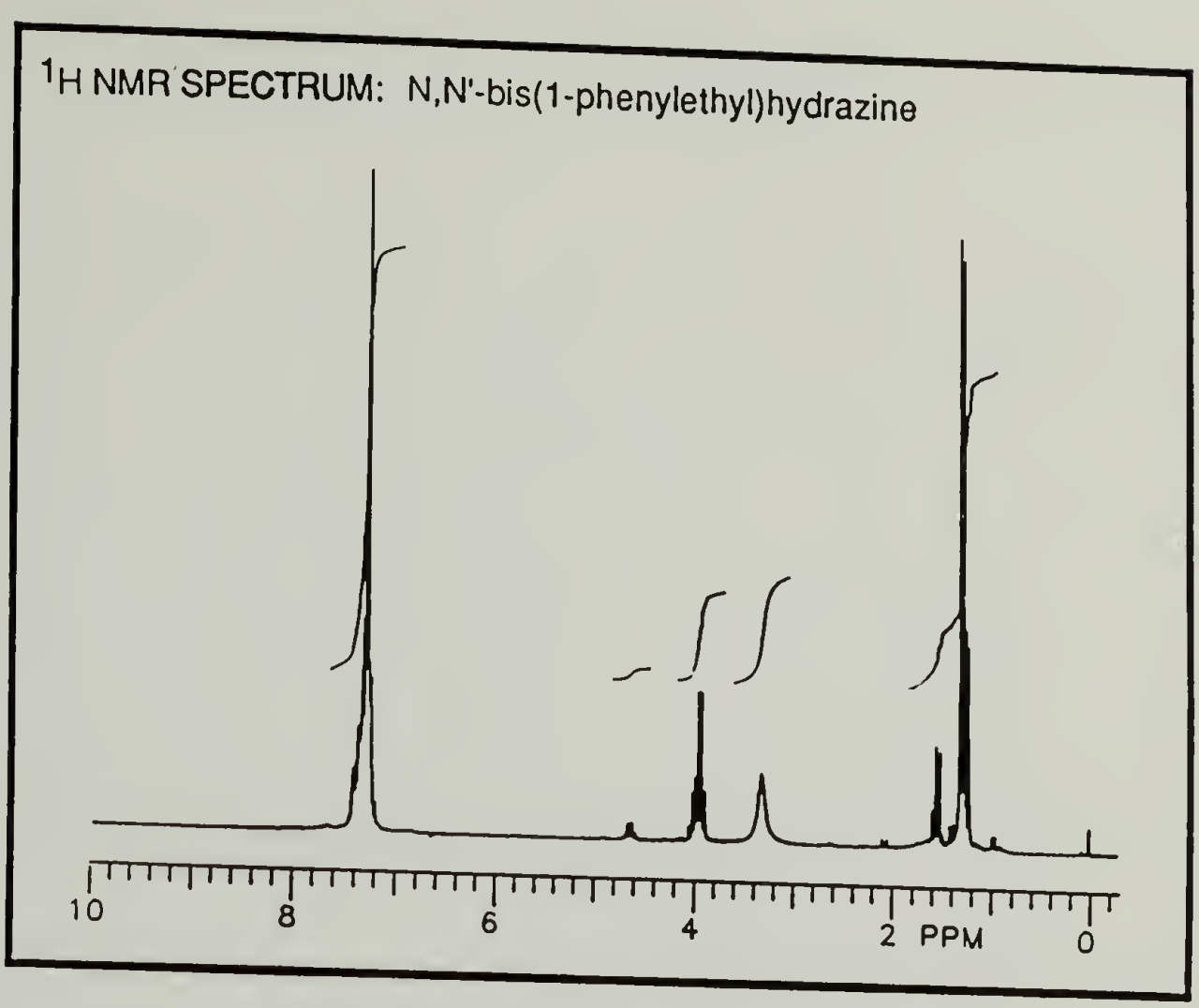
^{1}H NMR SPECTRUM: N,N'-bis(1-phenylethyl)hydrazine
10
8
6
4
2 PPM
0

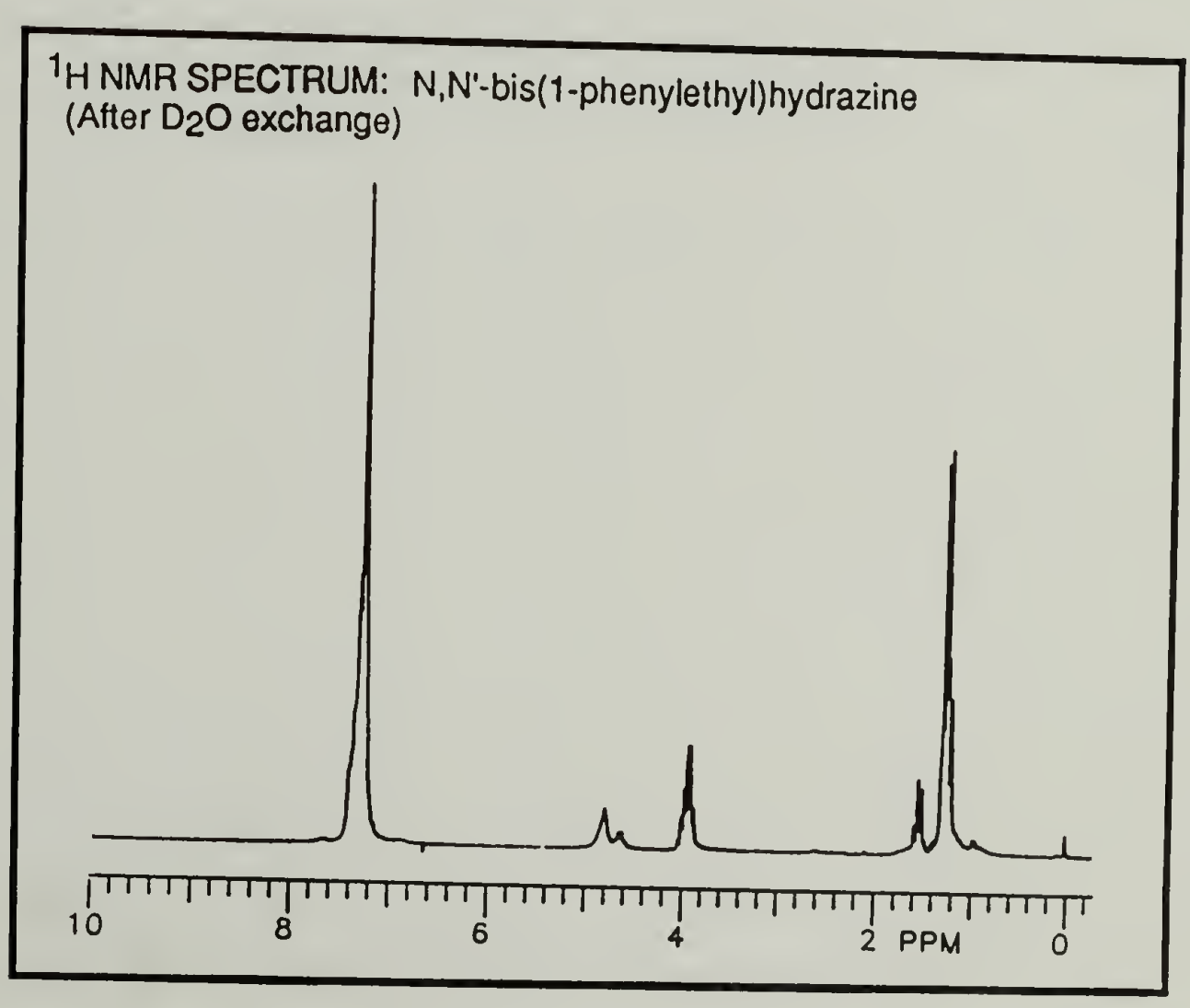
^{1}H NMR SPECTRUM: N,N'-bis(1-phenylethyl)hydrazine
(After D_2O exchange)
10
8
6
4
2 PPM
0

INFRARED SPECTRUM: N,N'-bis(1-phenylethyl)hydrazine

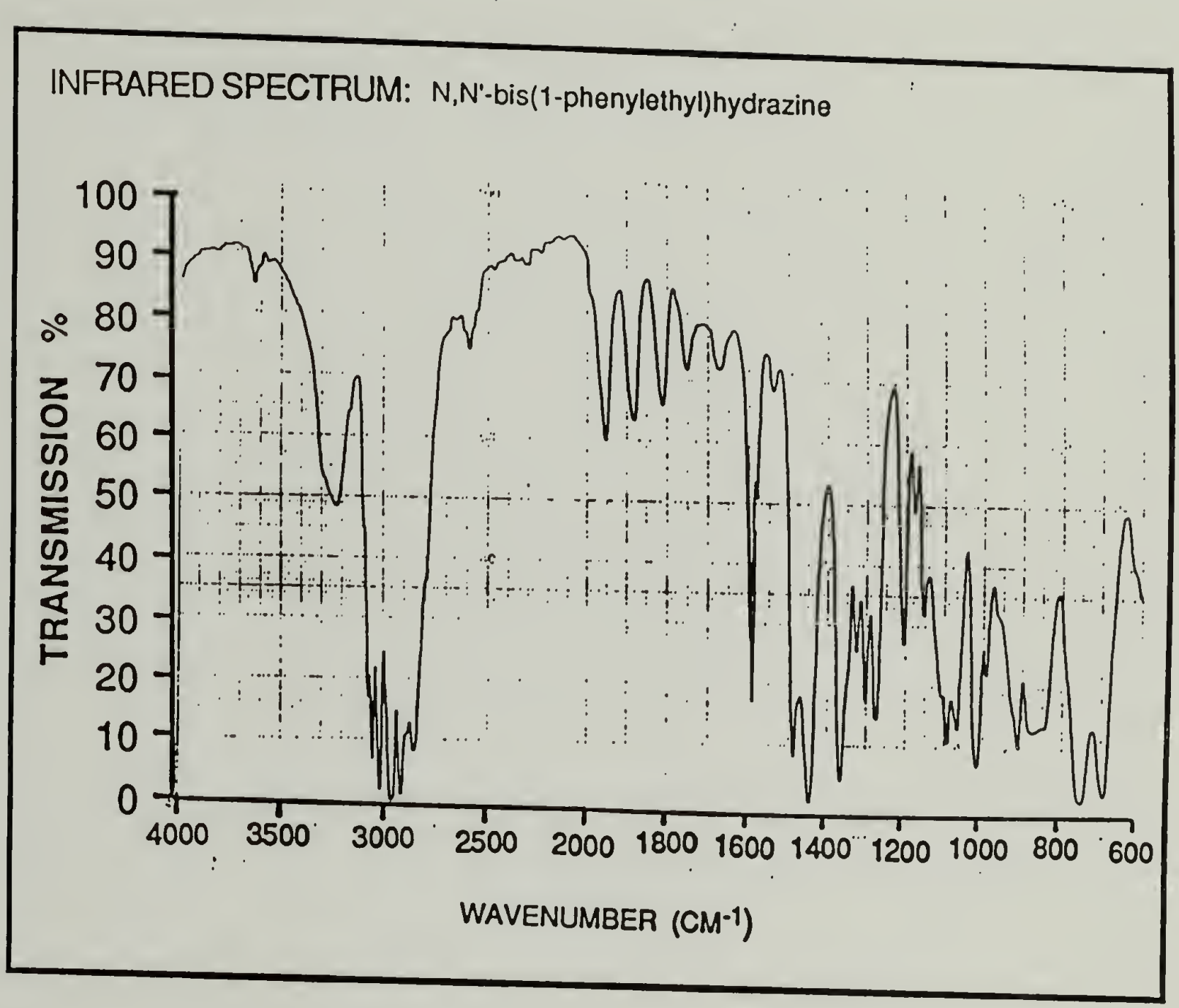

^{1}H NMR SPECTRUM: 1,1'-azobis(1-phenyl[1-^{13}C]ethane) (1a)

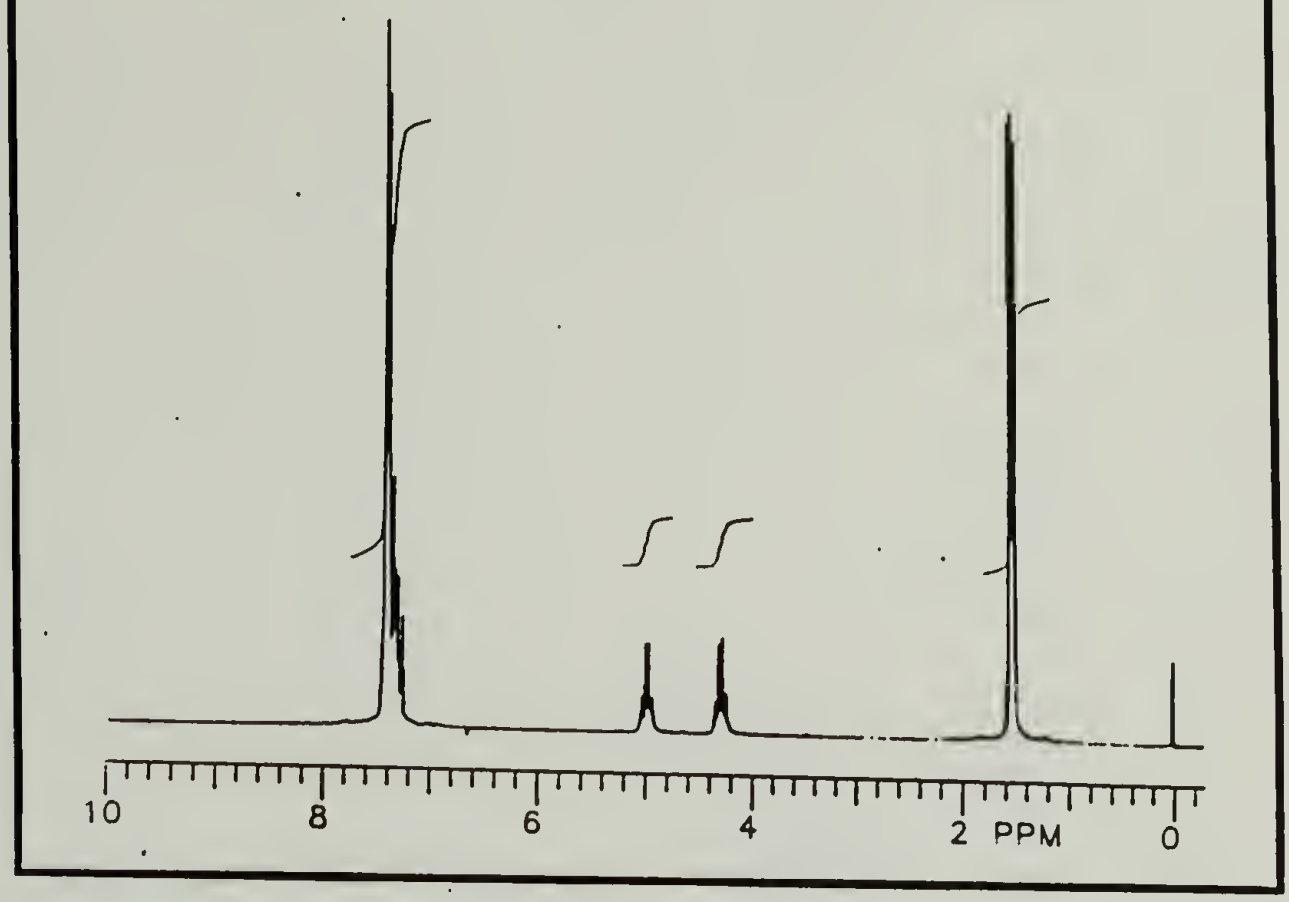

INFRARED SPECTRUM: 1,1'-azobis(1-phenyl[1-^{13}C]ethane) (1a)

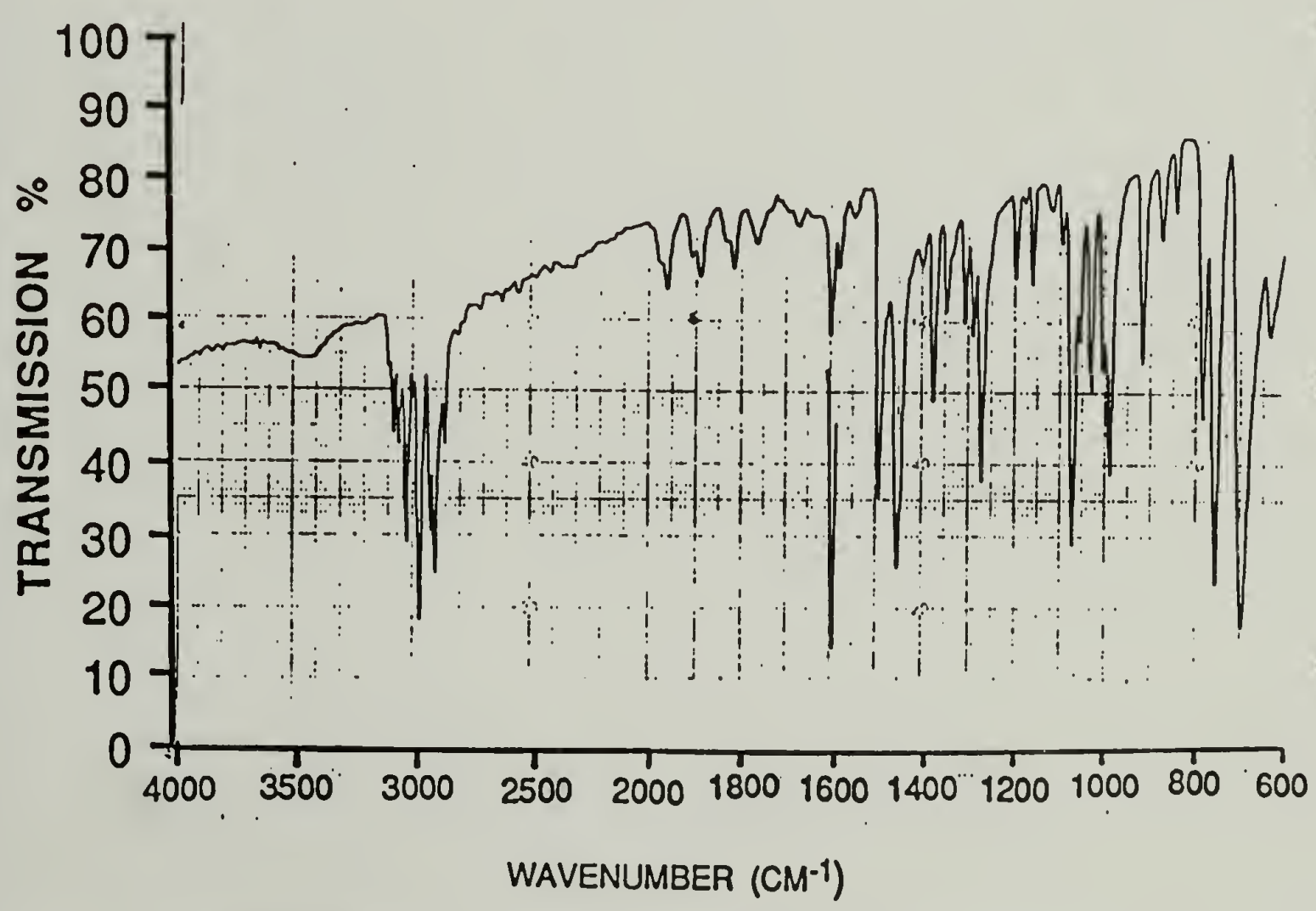

^{13}C NMR SPECTRUM: 1,1'-azobis(1-phenyl[1-^{13}C]ethane) (1a)

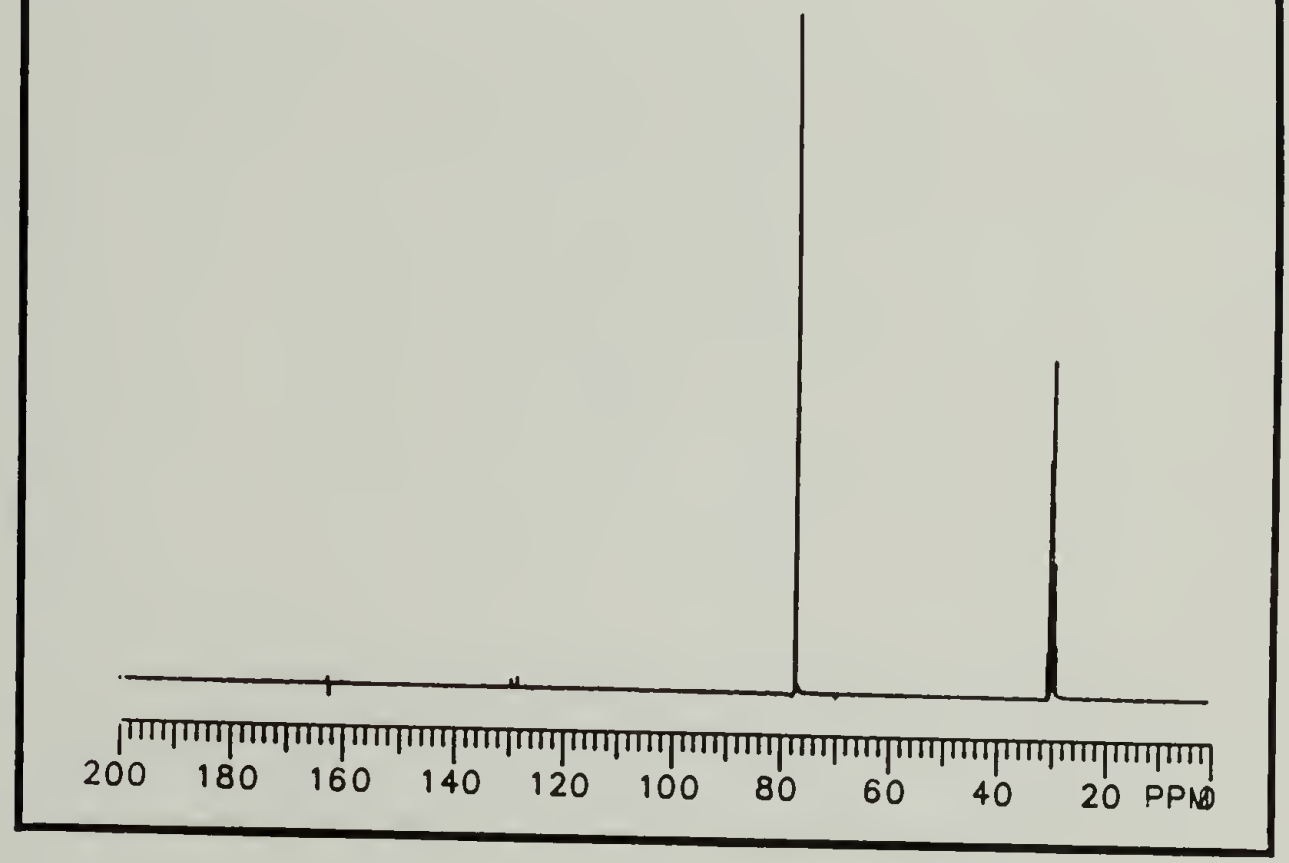

^{1}H NMR SPECTRUM: 1,1'-azobis(1-phenylethane)

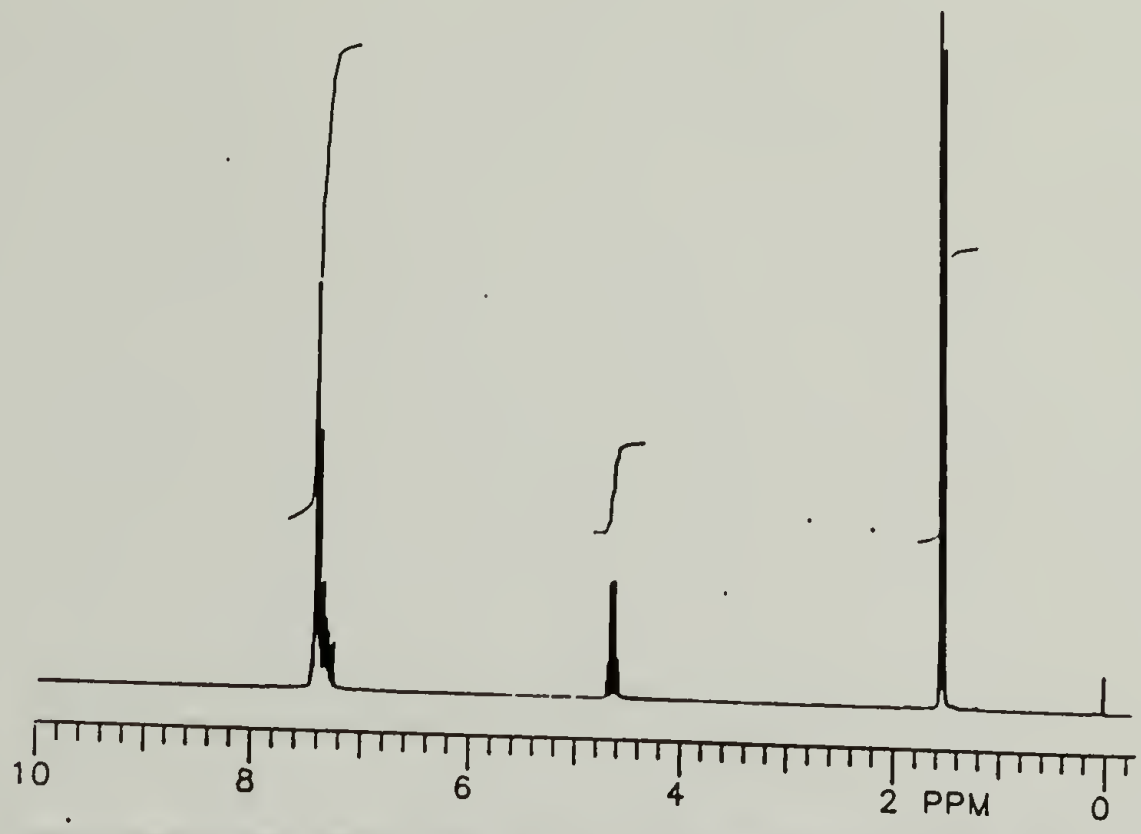

INFRARED SPECTRUM: 1,1'-azobis(1-phenylethane)

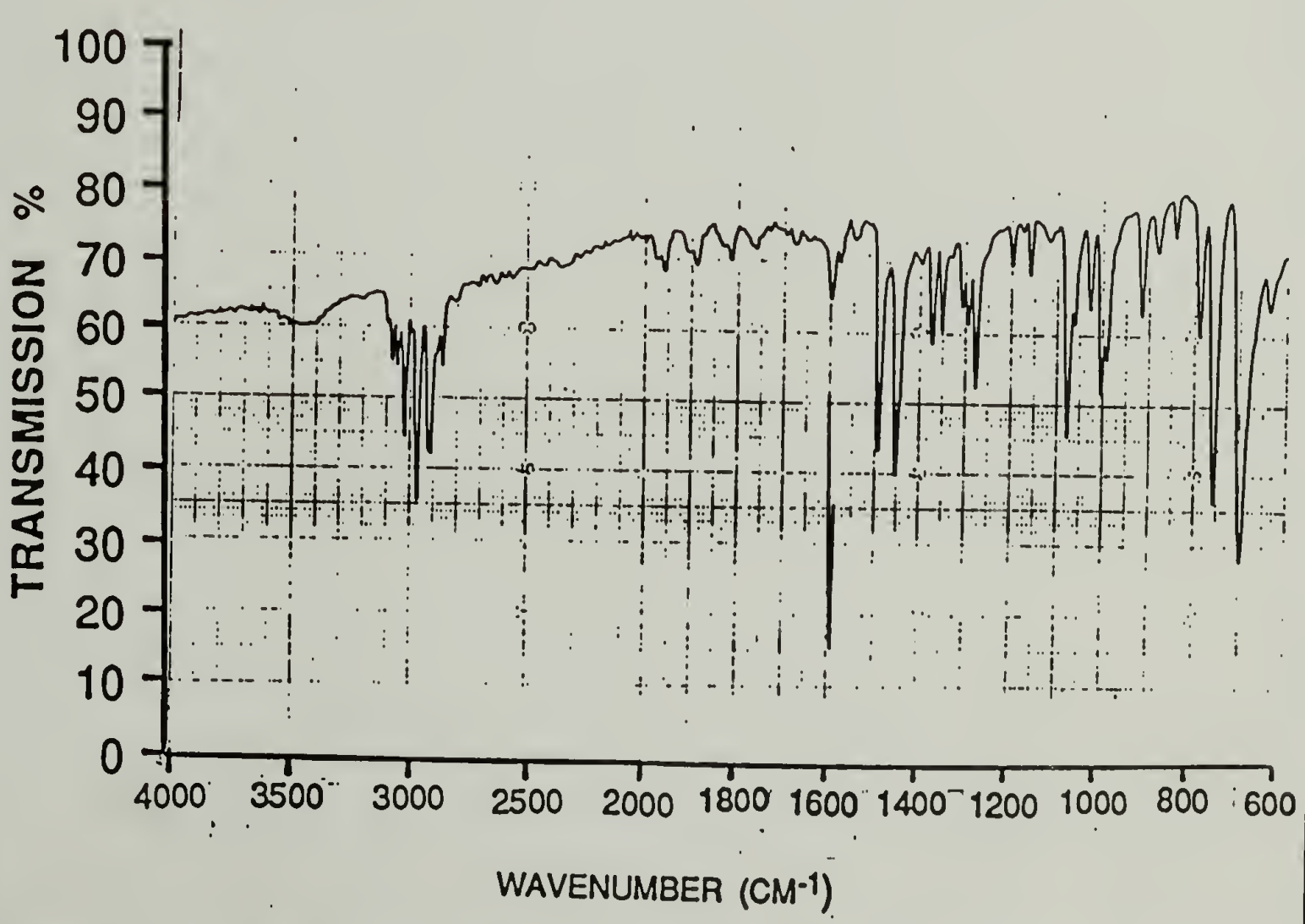

^{13}C NMR SPECTRUM: 1,1'-azobis(1-phenylethane)

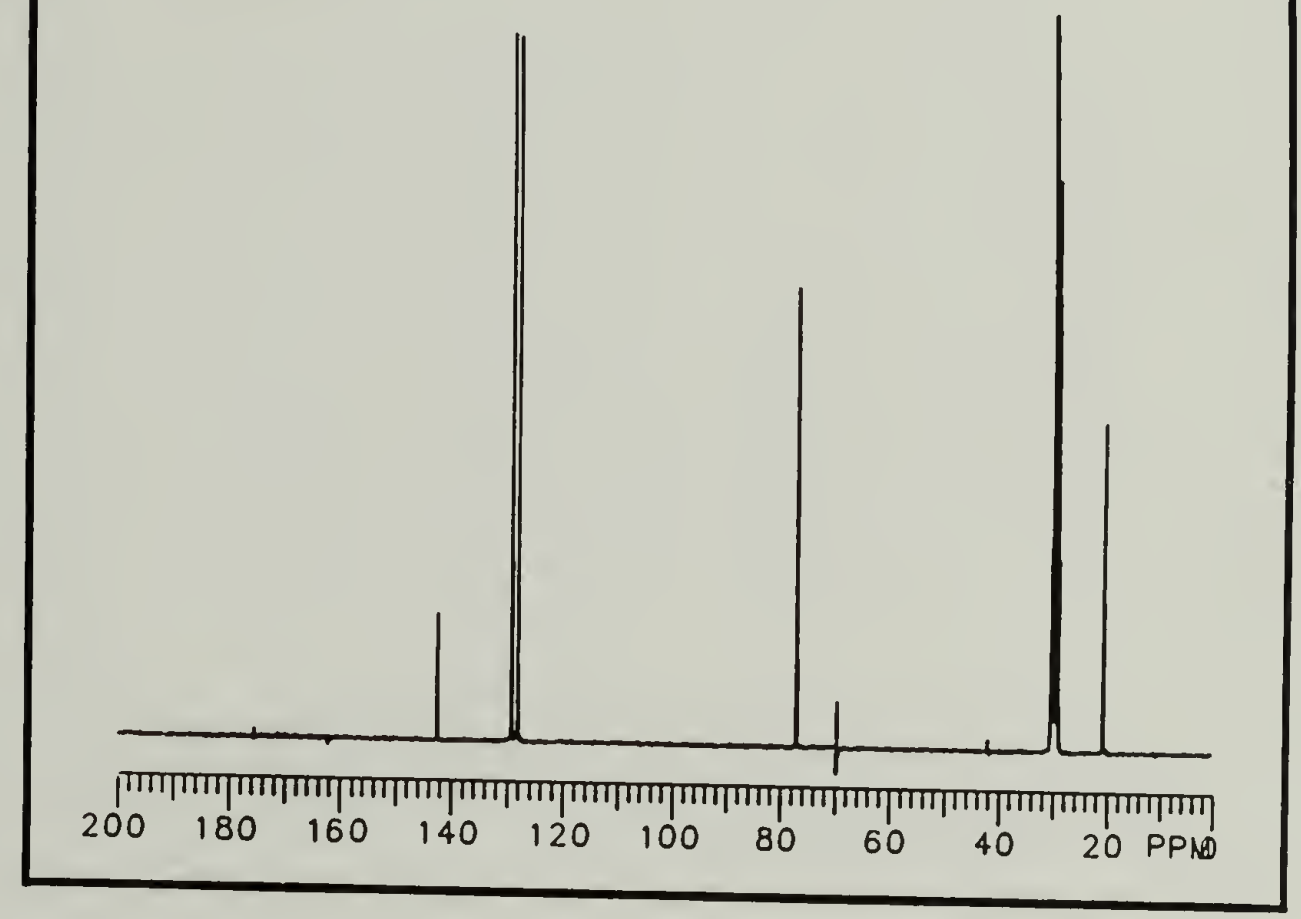

^{1}H NMR SPECTRUM: [1-^{13}C]benzoic acid

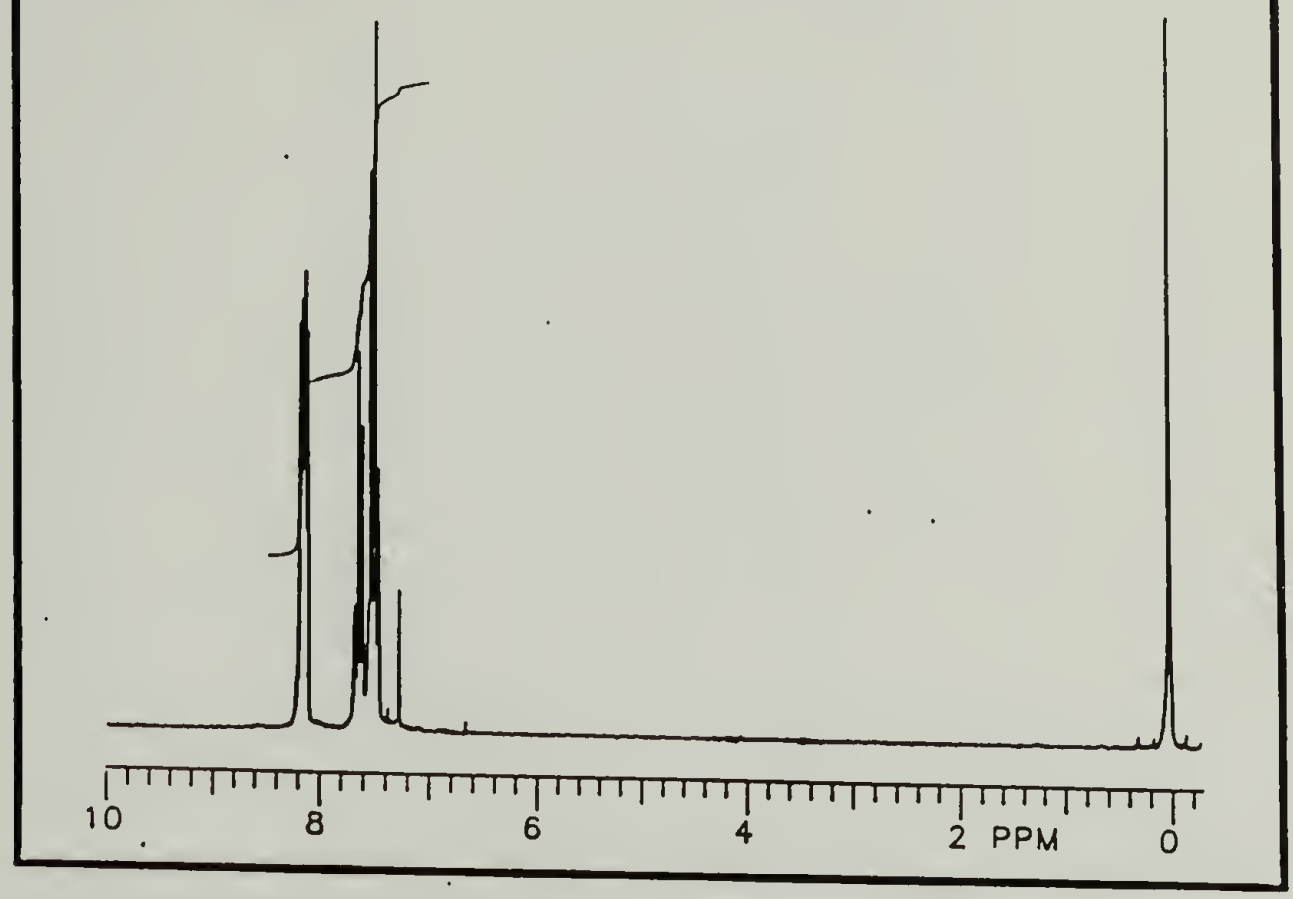

INFRARED SPECTRUM: [1-^{13}C]benzoic acid

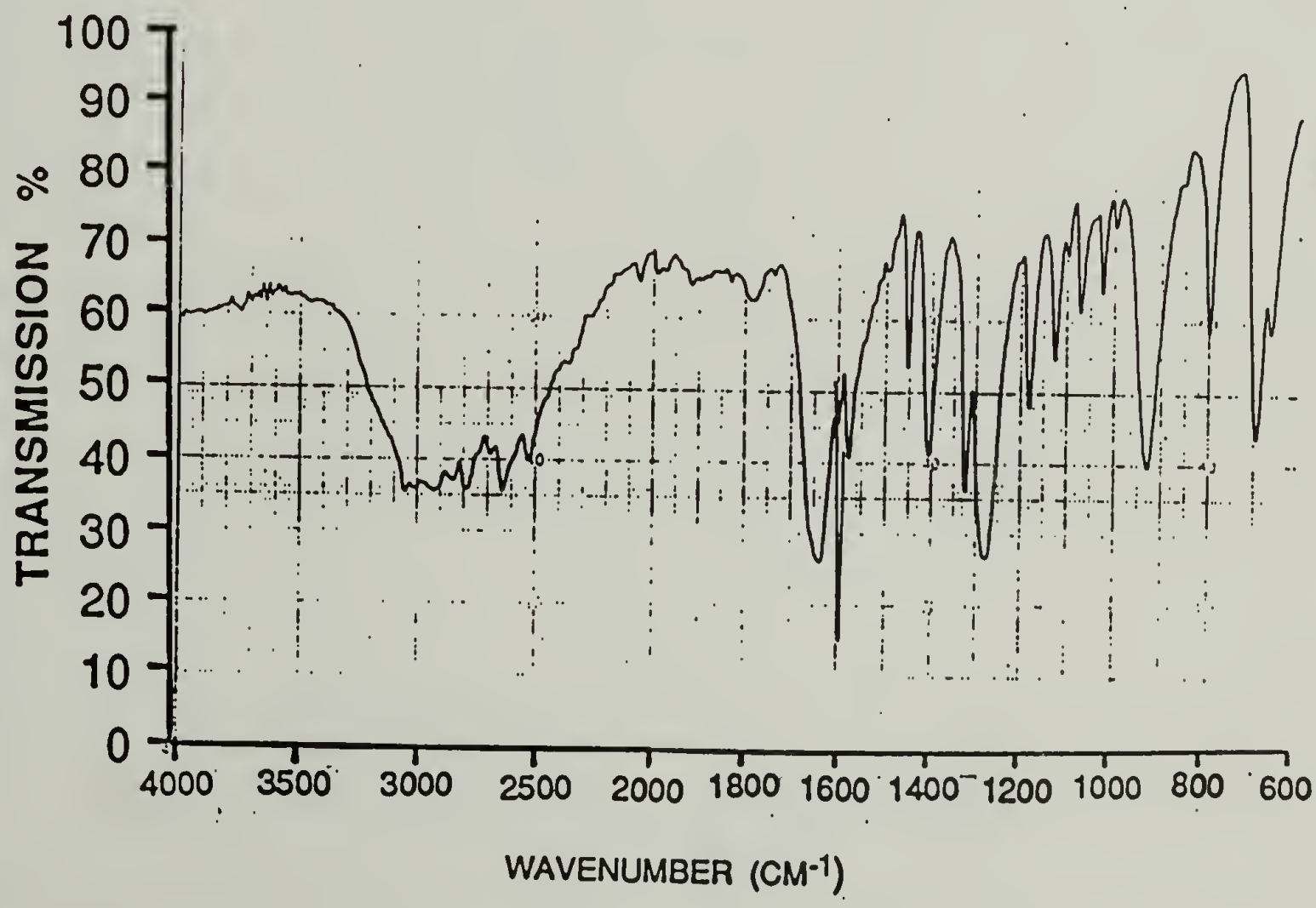

^{1}H NMR SPECTRUM: [1-^{13}C]benzoyl chloride

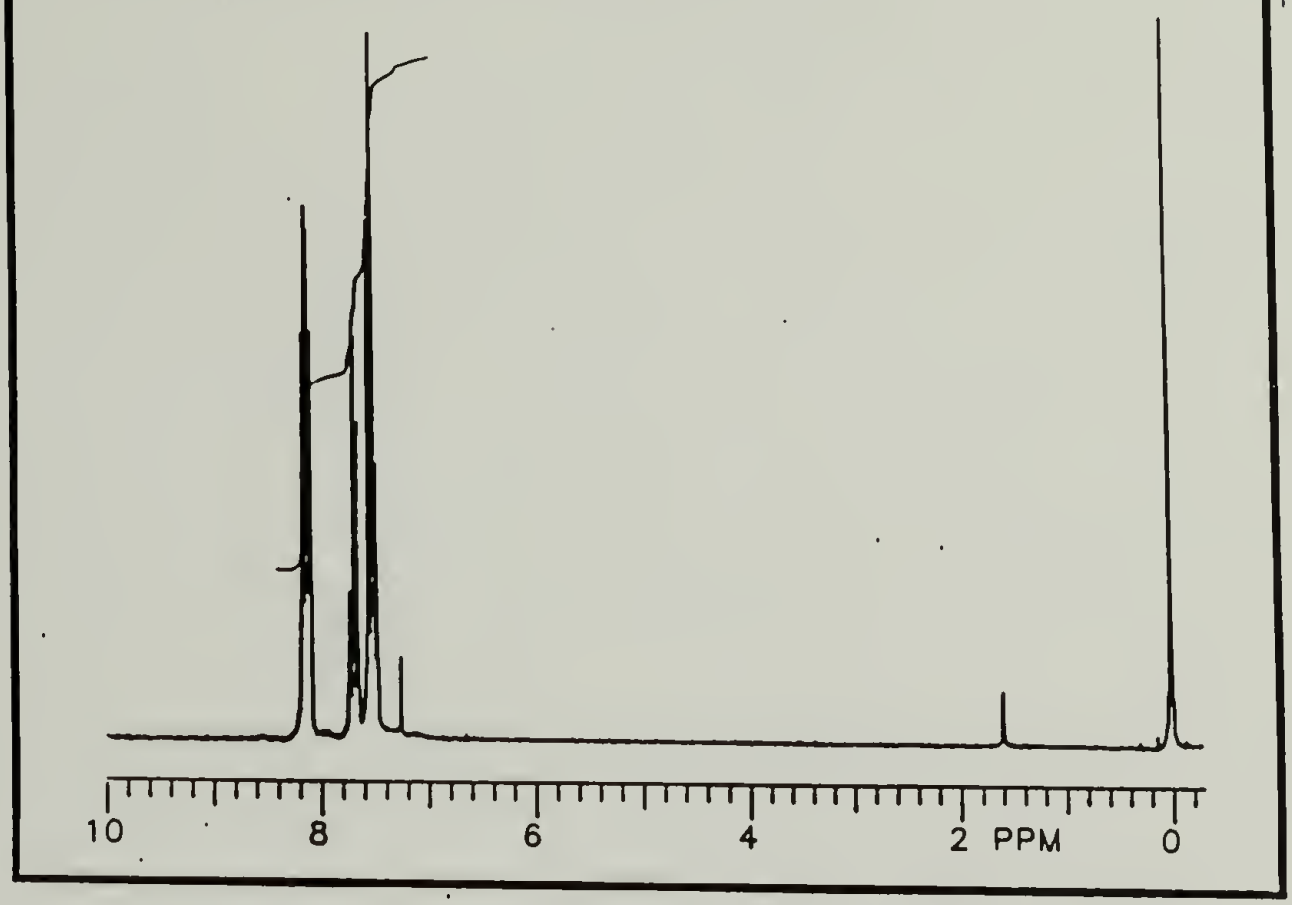

INFRARED SPECTRUM: [1-^{13}C]benzoyl chloride

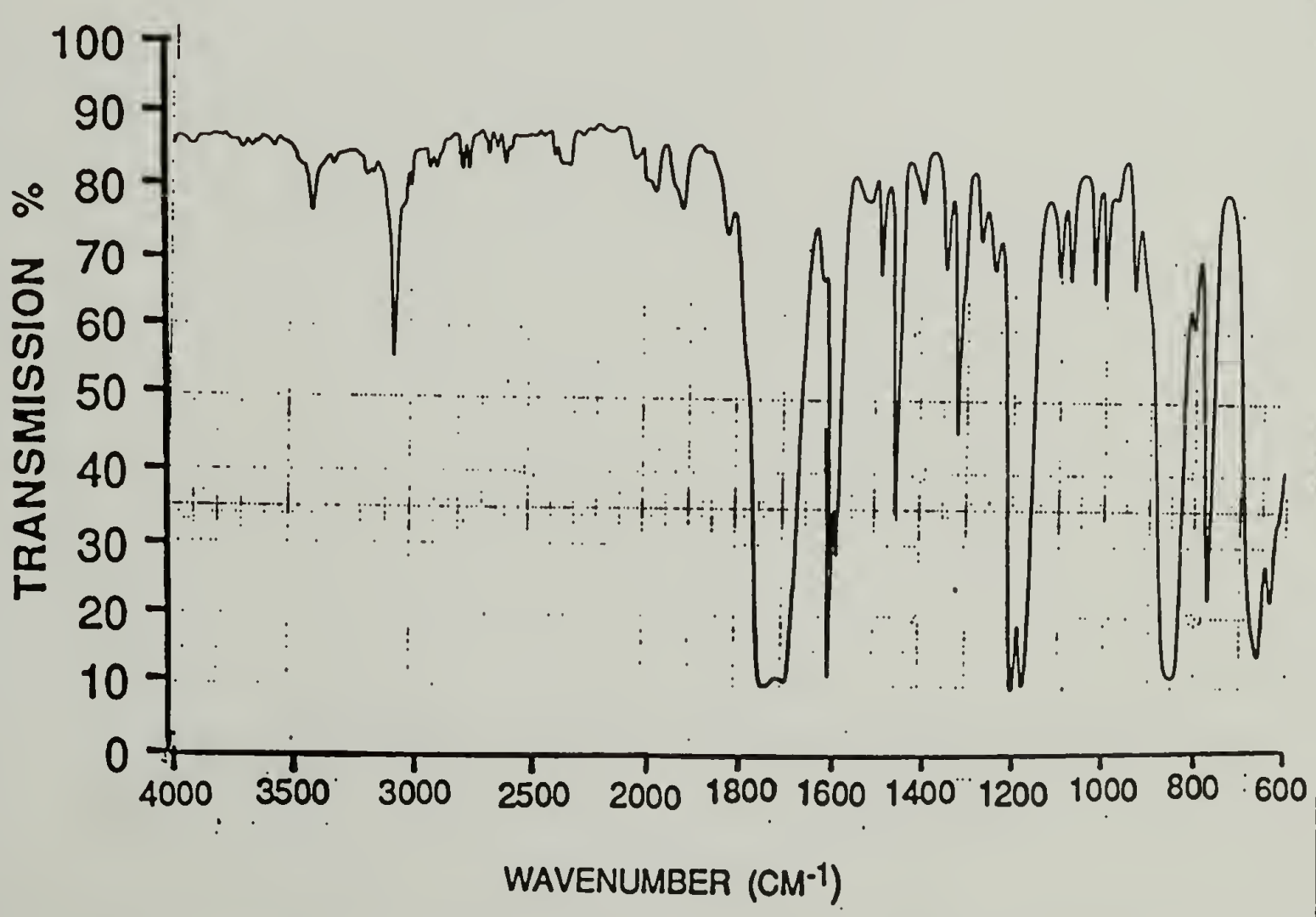

^{1}H NMR SPECTRUM: 1,3-diphenyl-1-[1-^{13}C]propanone

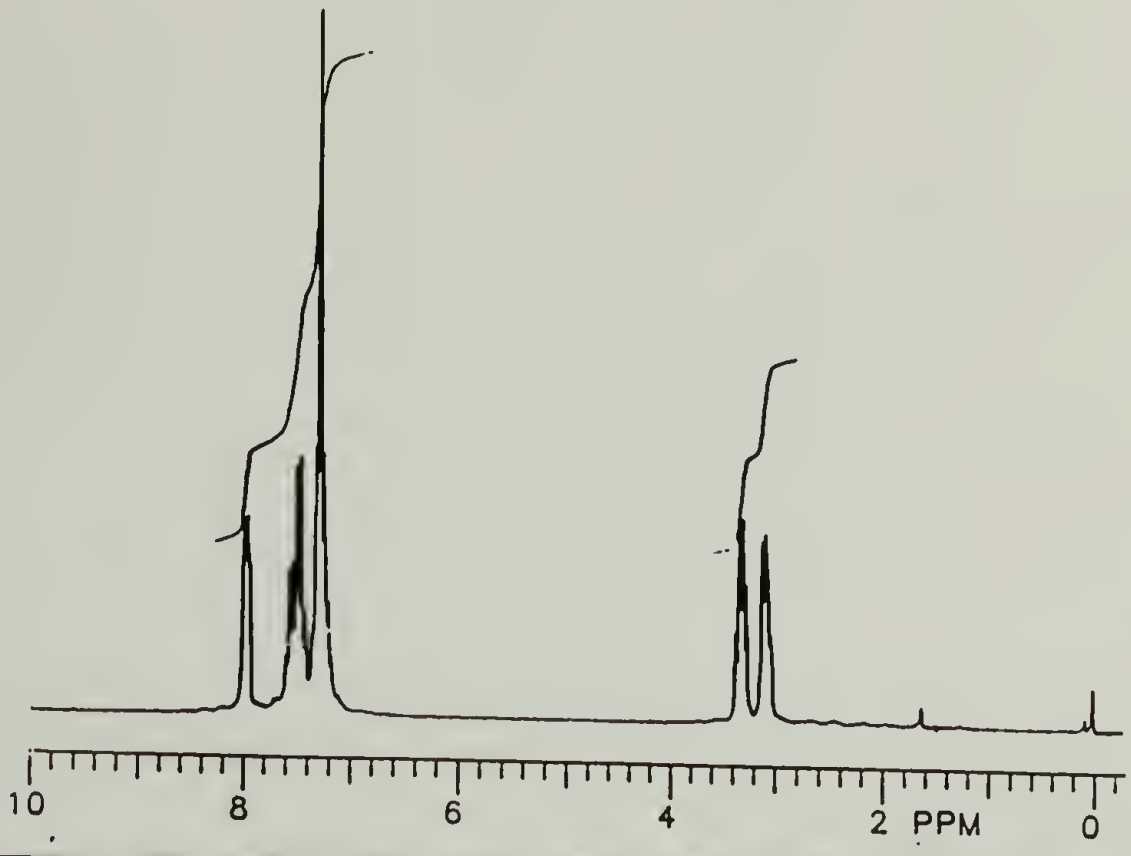

INFRARED SPECTRUM: 1,3-diphenyl-1-[1-^{13}C]propanone

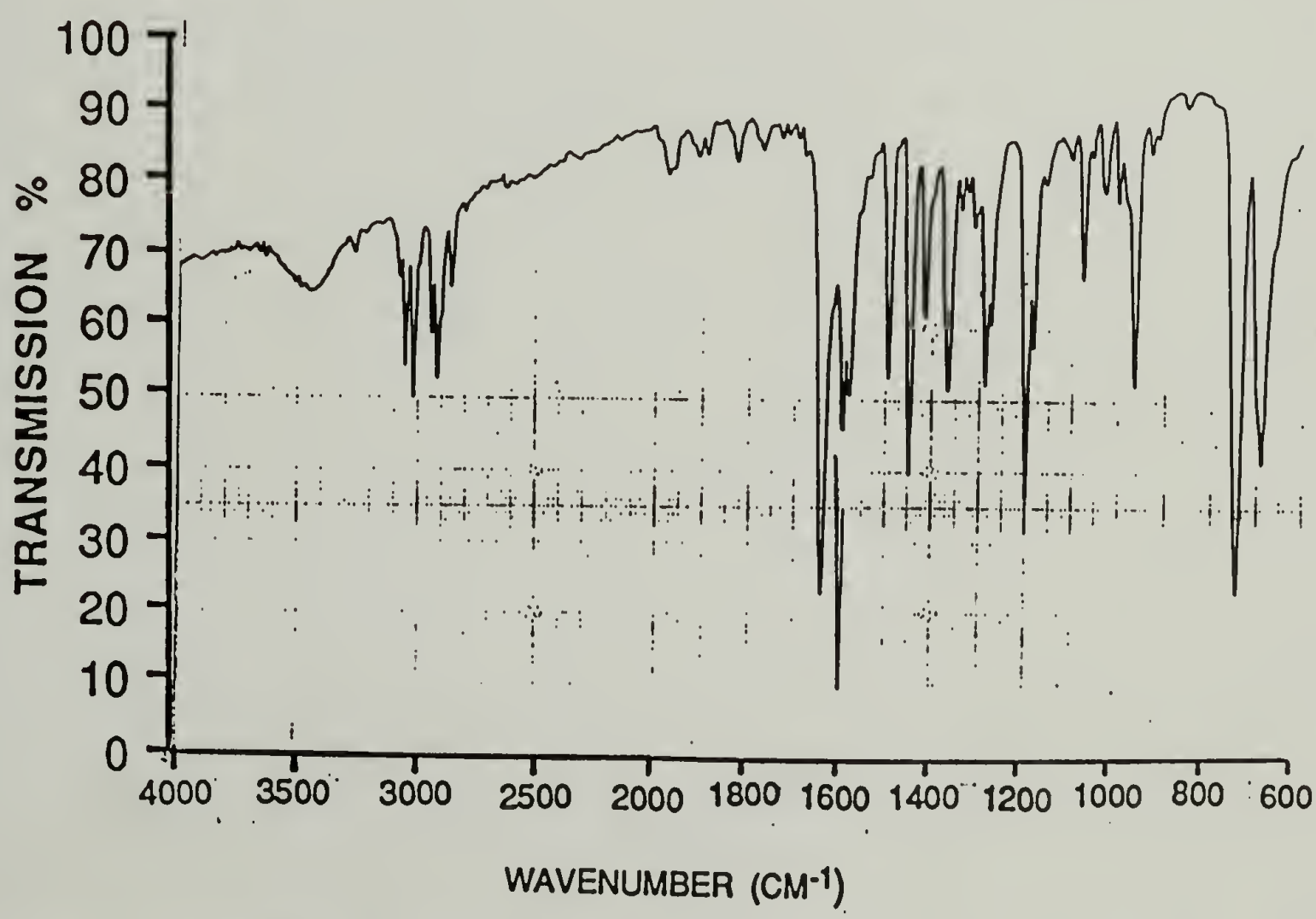

^{1}H NMR SPECTRUM: 1,3-diphenyl-1-propanone

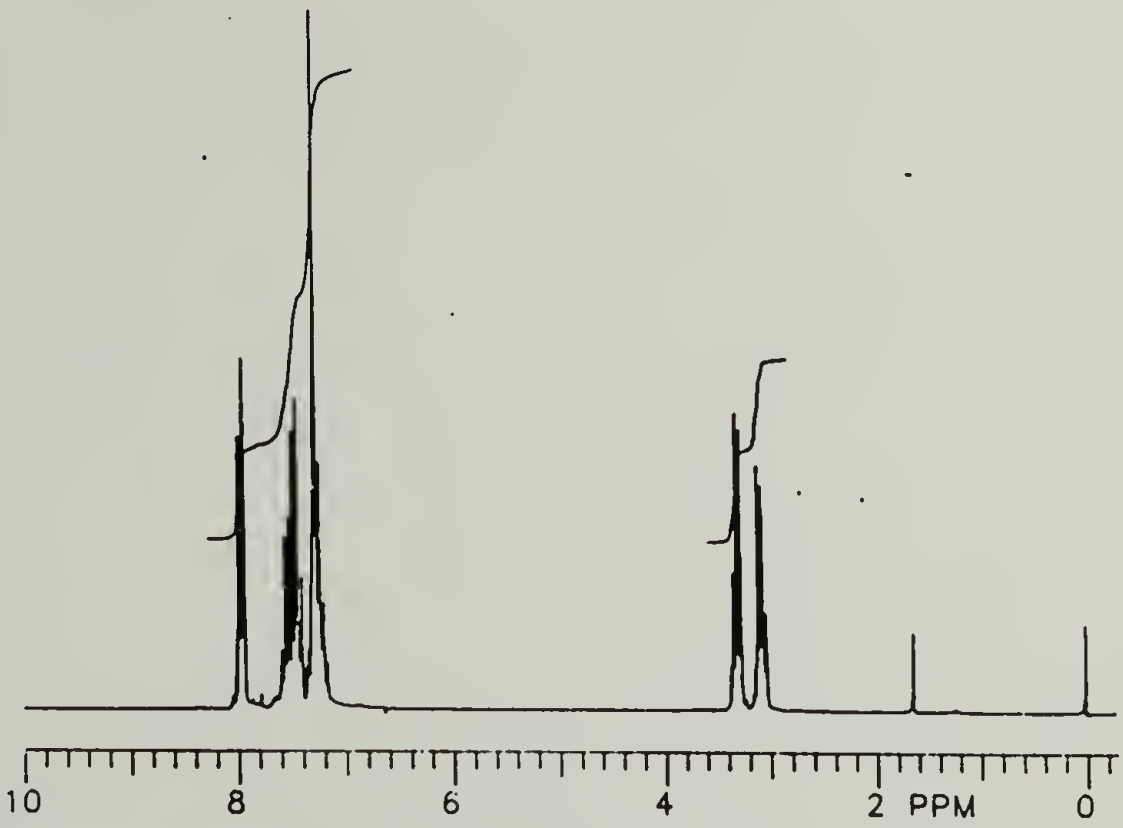

INFRARED SPECTRUM: 1,3-diphenyl-1-propanone

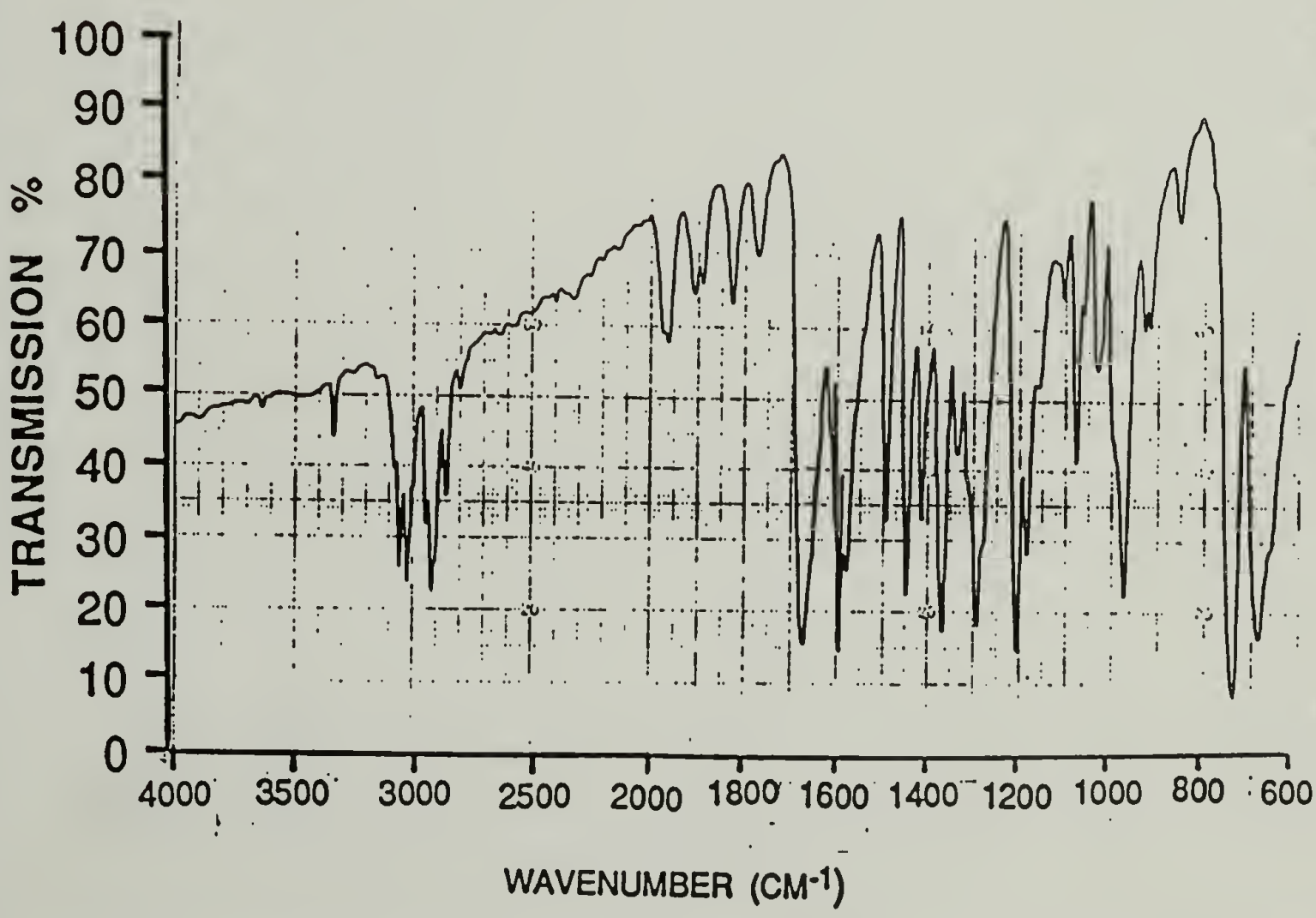

^{1}H NMR SPECTRUM: 1,3-diphenyl-1-[1-^{13}C]propanone azine

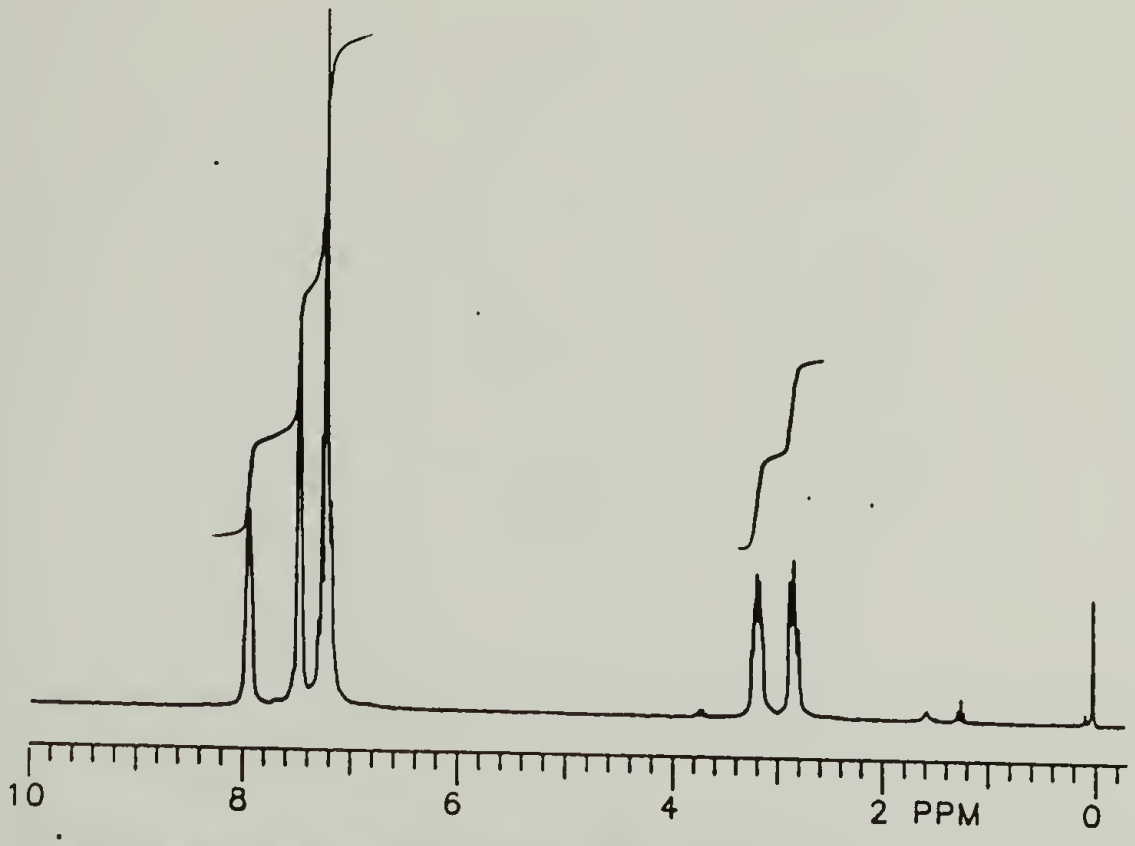

INFRARED SPECTRUM: 1,3-diphenyl-1-[1-^{13}C]propanone azine

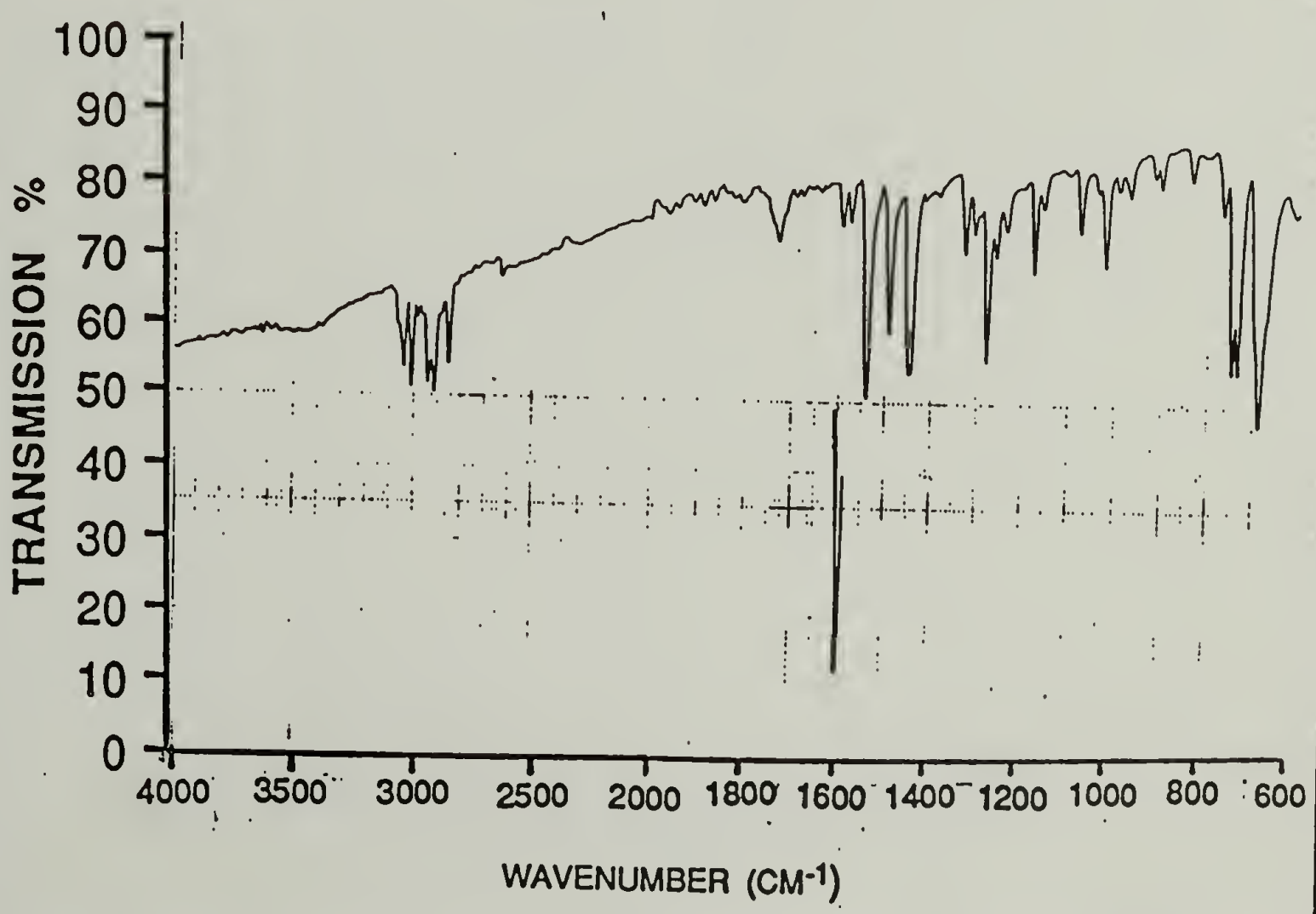

^{1}H NMR SPECTRUM: 1,3-diphenyl-1-propanone azine

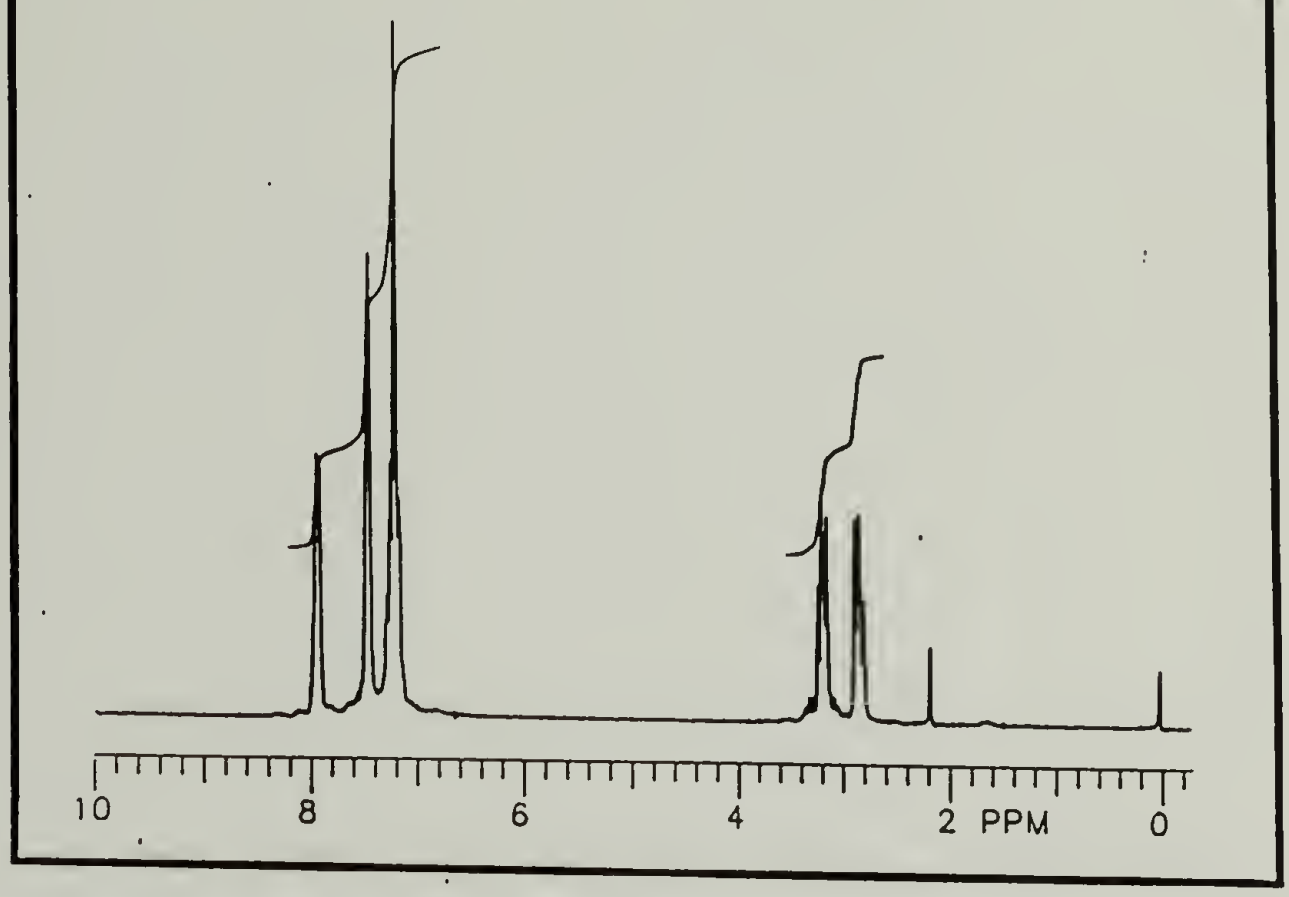

INFRARED SPECTRUM: 1,3-diphenyl-1-propanone azine

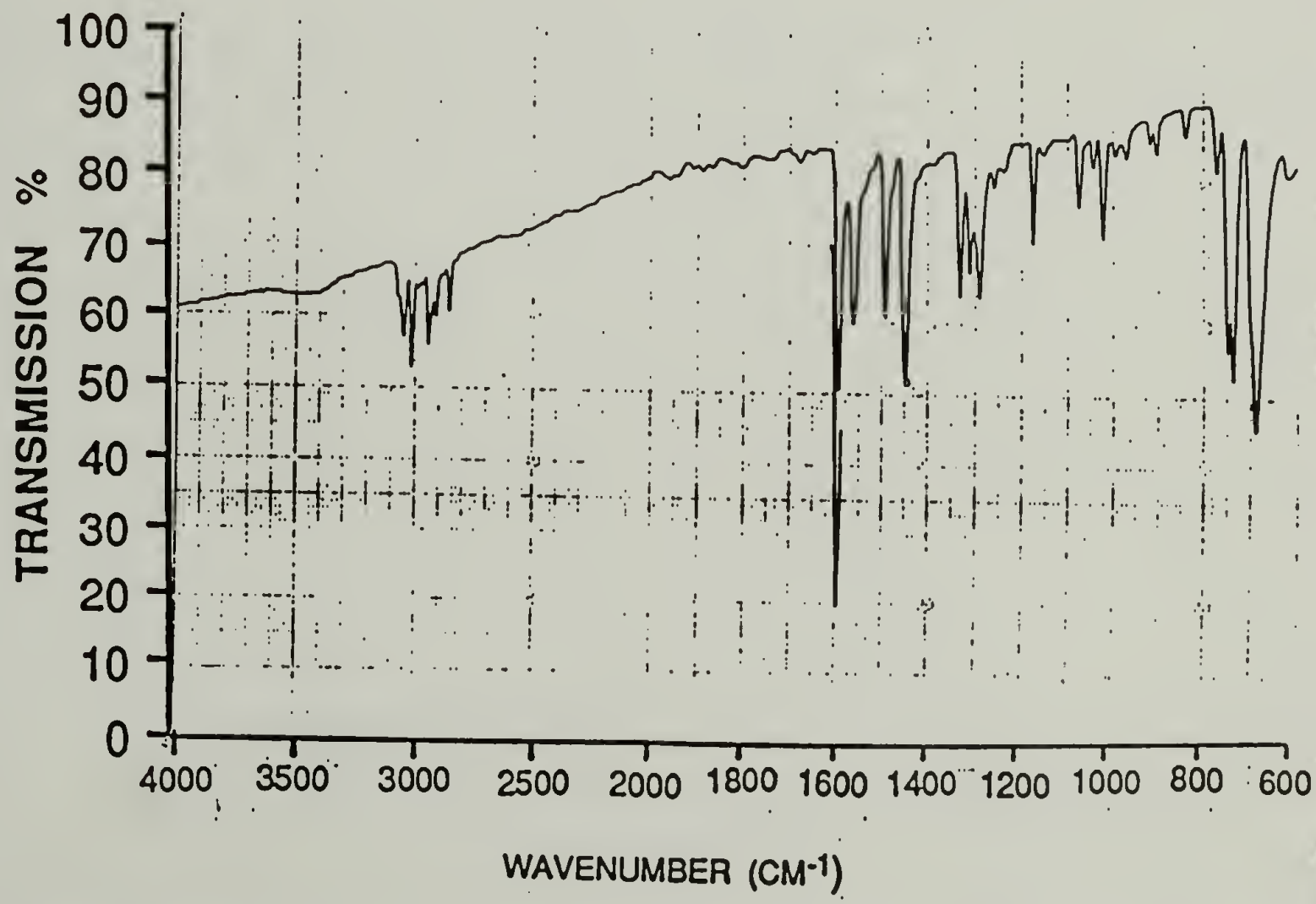

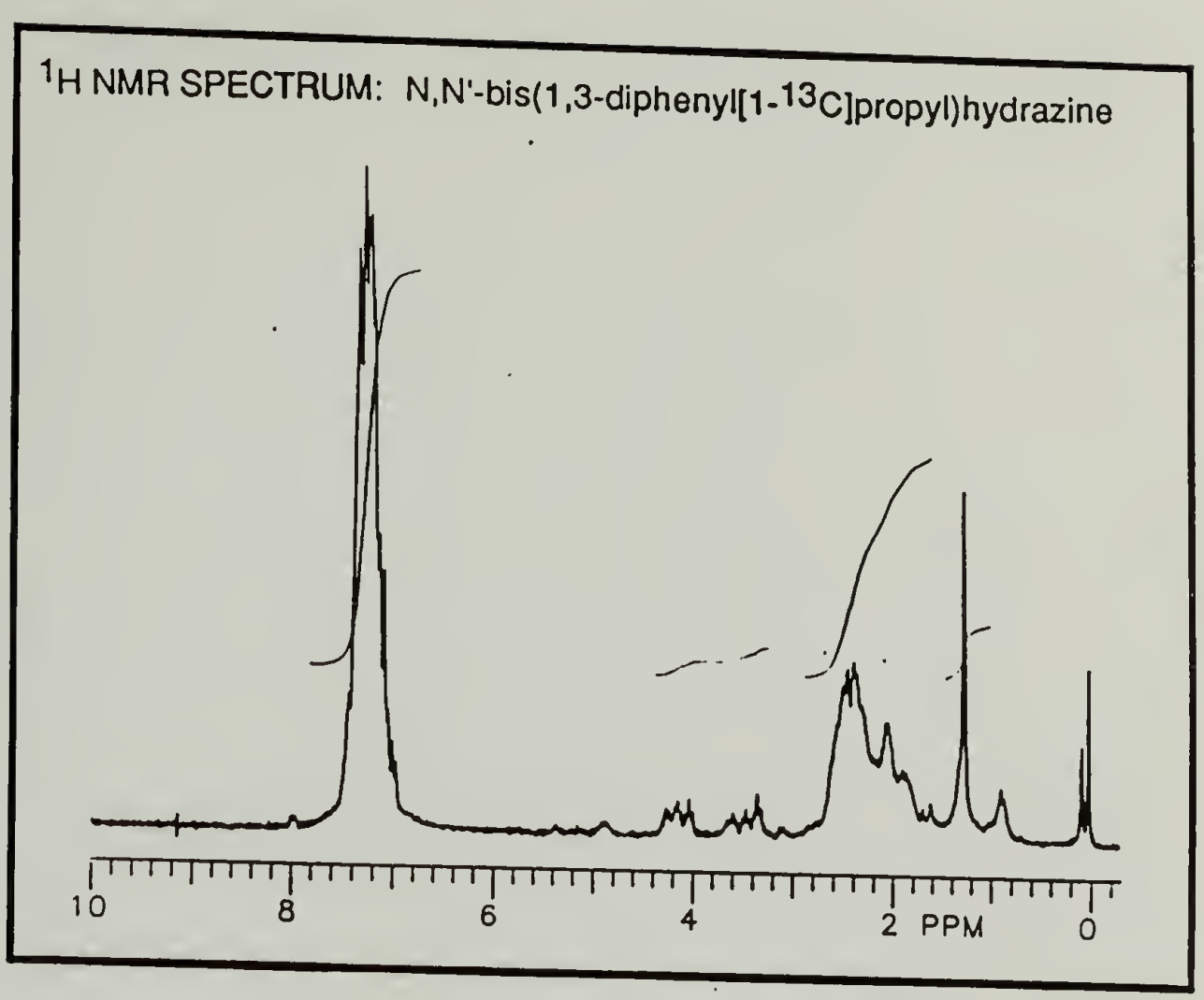
^{1}H NMR SPECTRUM: N,N'-bis(1,3-diphenyl[1-^{13}C]propyl)hydrazine
10
8
6
4
2 PPM
0

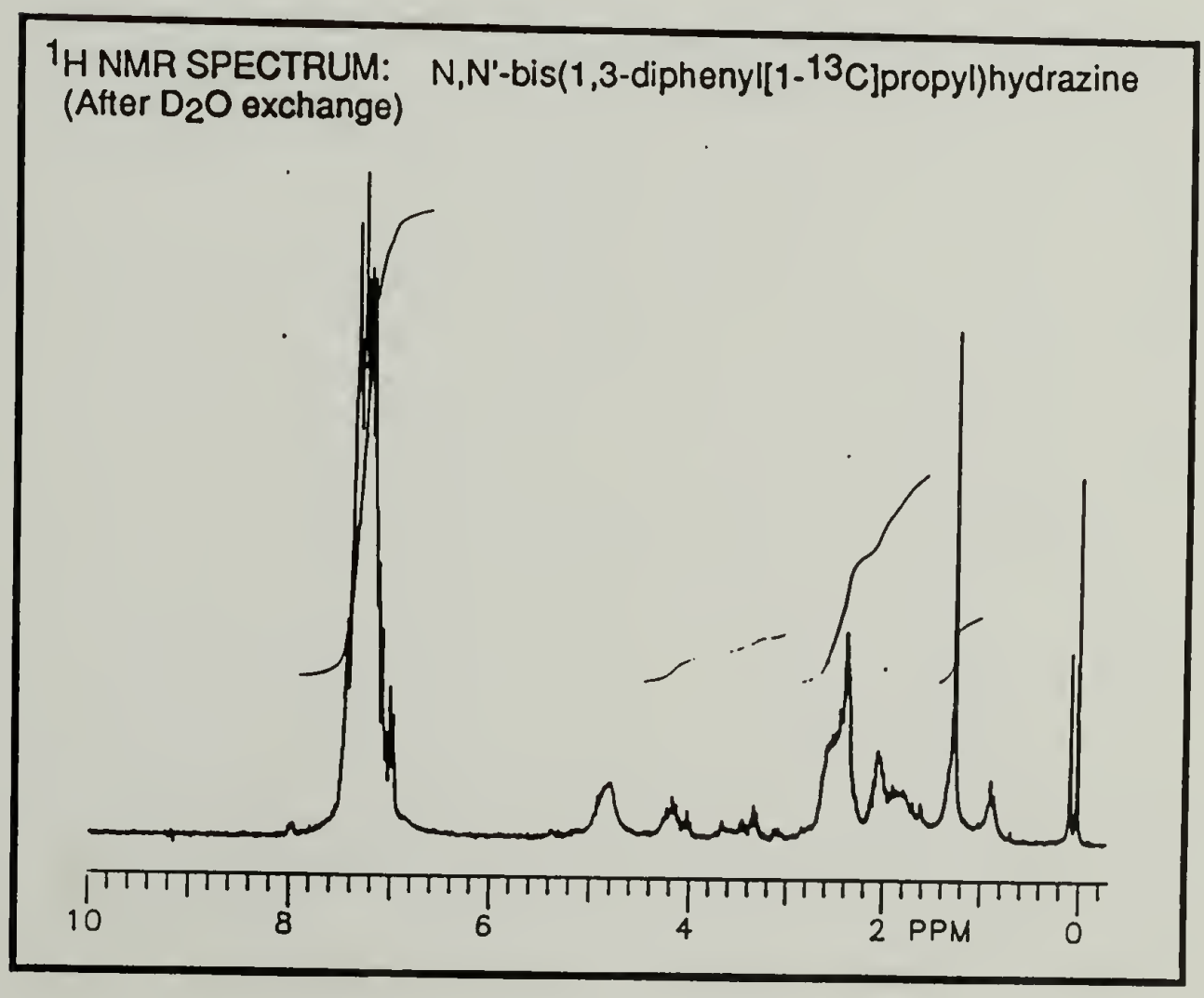
^{1}H NMR SPECTRUM: N,N'-bis(1,3-diphenyl[1-^{13}C]propyl)hydrazine
(After D_2O exchange)
10
8
6
4
2 PPM
0

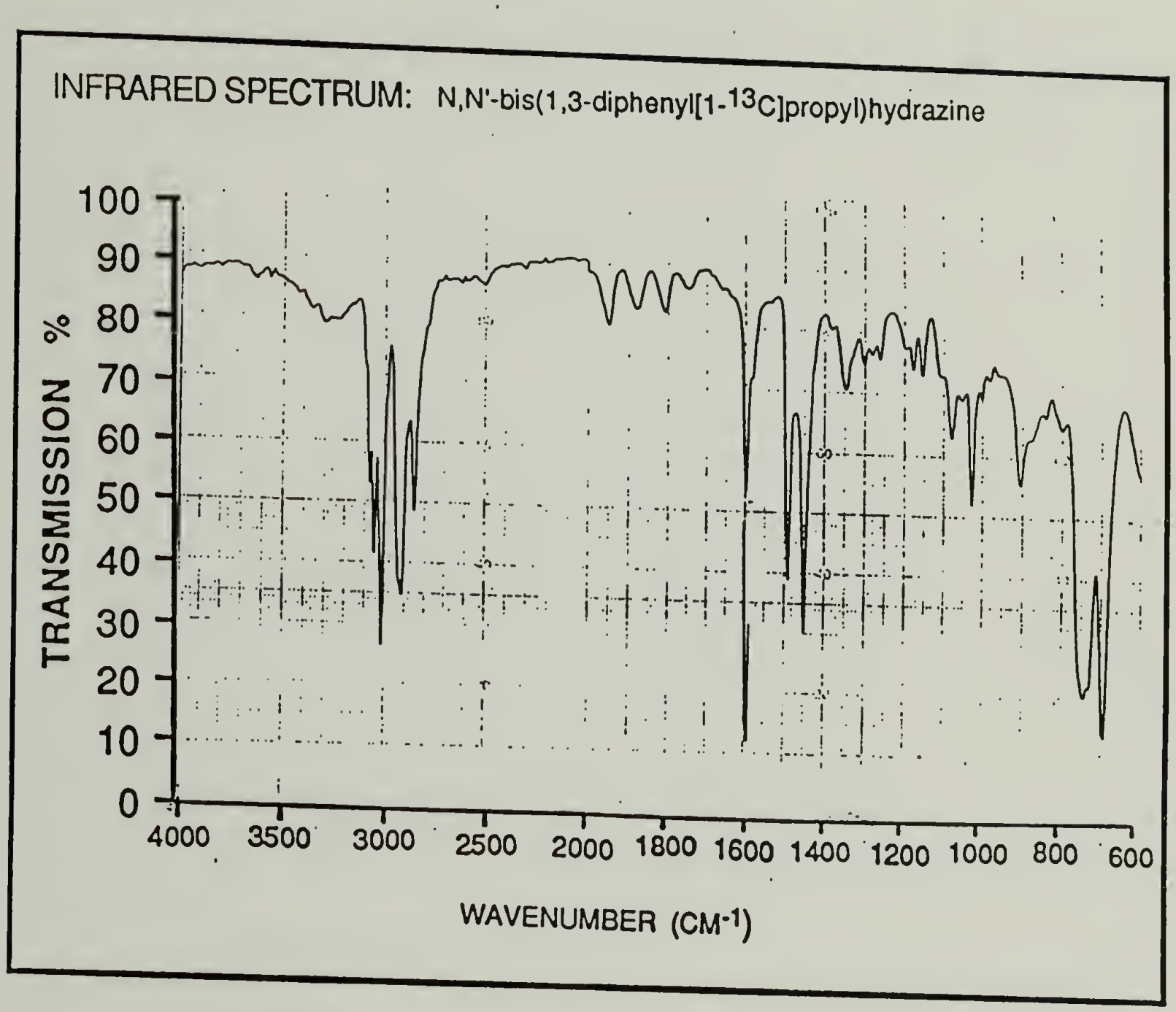
INFRARED SPECTRUM: N,N'-bis(1,3-diphenyl[1-13C]propyl)hydrazine
TRANSMISSION %
100
90
80
70
60
50
40
30
20
10
0
4000
3500
3000
2500
2000
1800
1600
1400
1200
1000
800
600
WAVENUMBER (CM-1)

^{1}H NMR SPECTRUM: N,N'-bis(1,3-diphenylpropyl)hydrazine

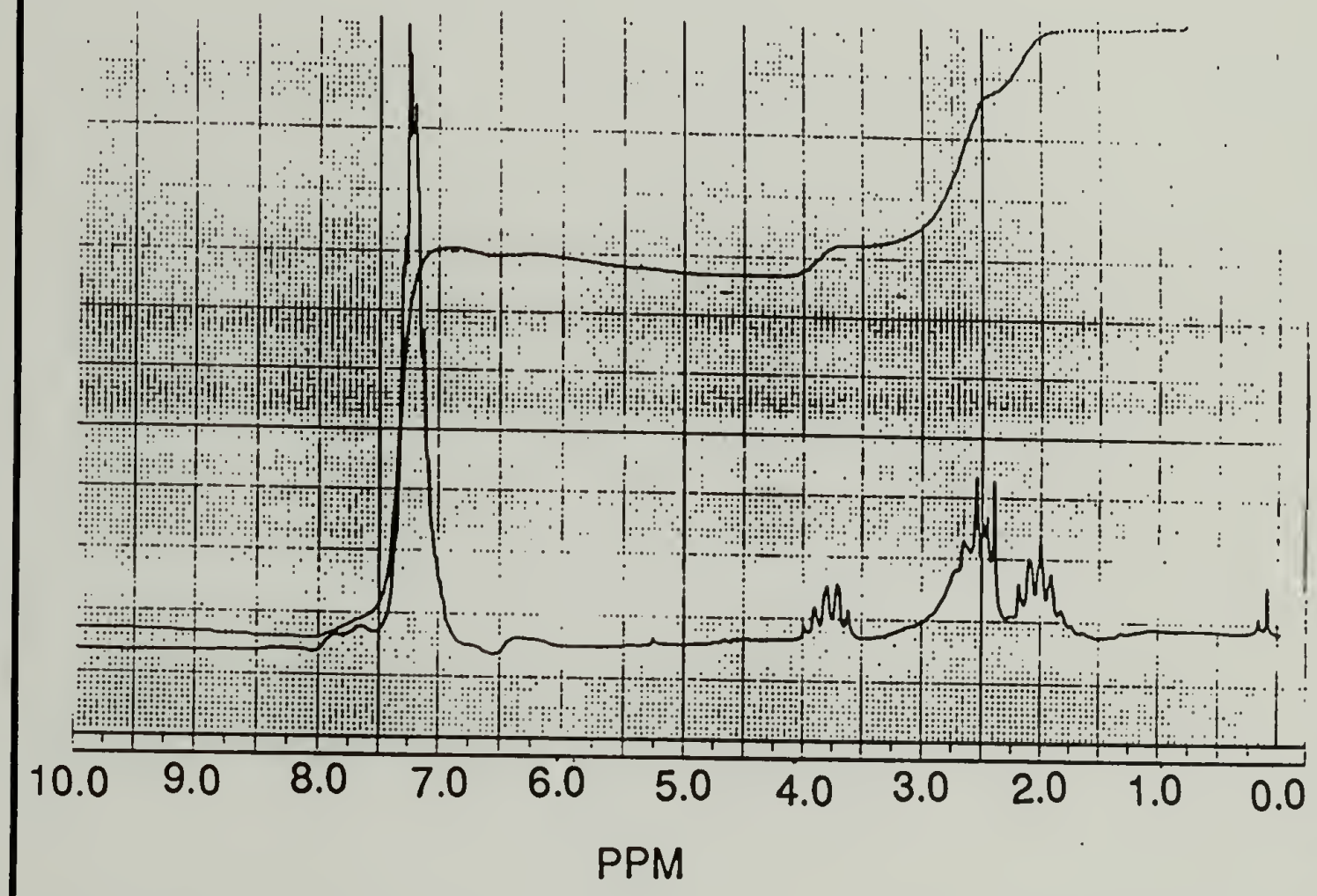

^{1}H NMR SPECTRUM: N,N'-bis(1,3-diphenylpropyl)hydrazine
(After D_2O exchange)

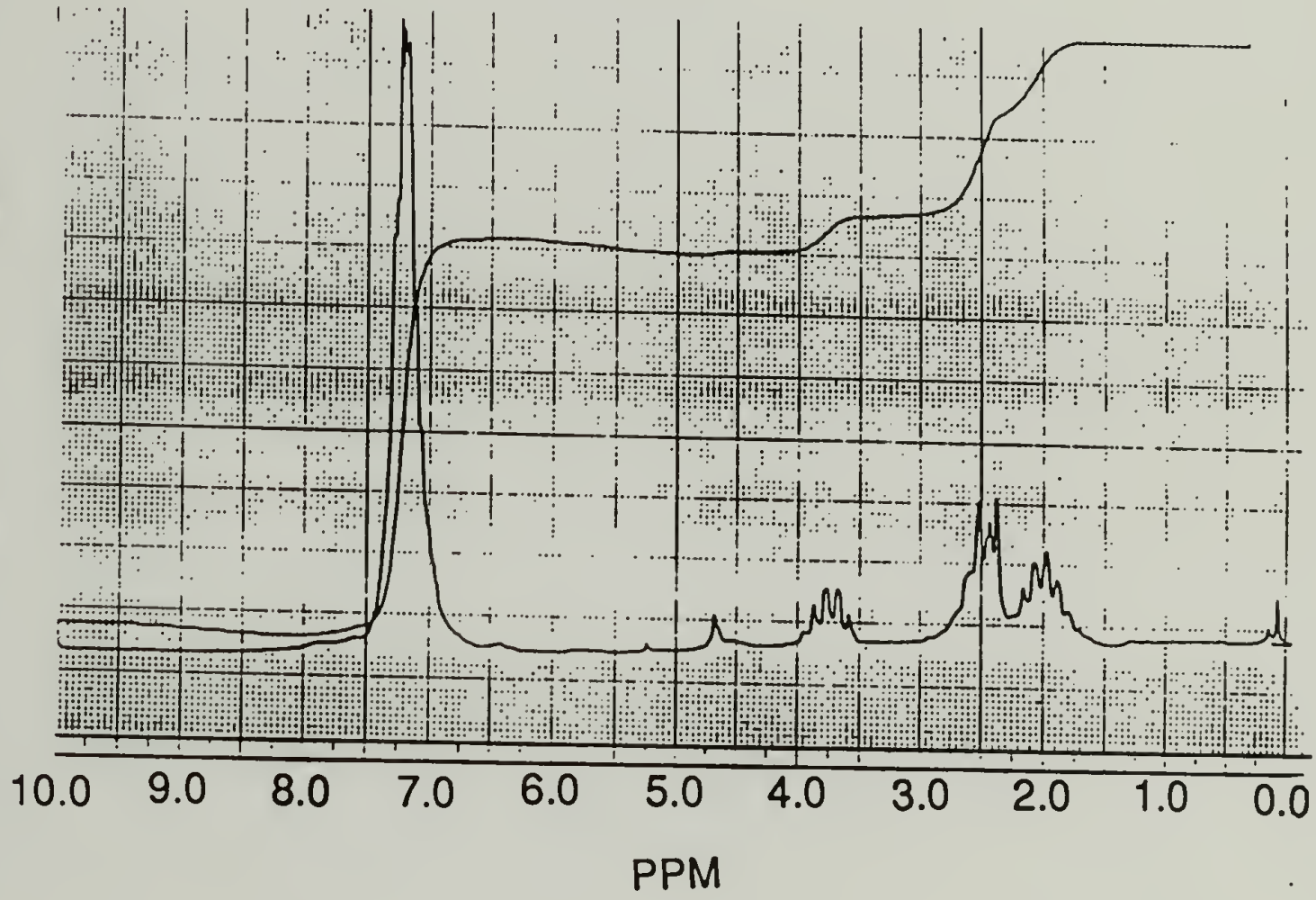

INFRARED SPECTRUM: N,N'-bis(1,3-diphenylpropyl)hydrazine

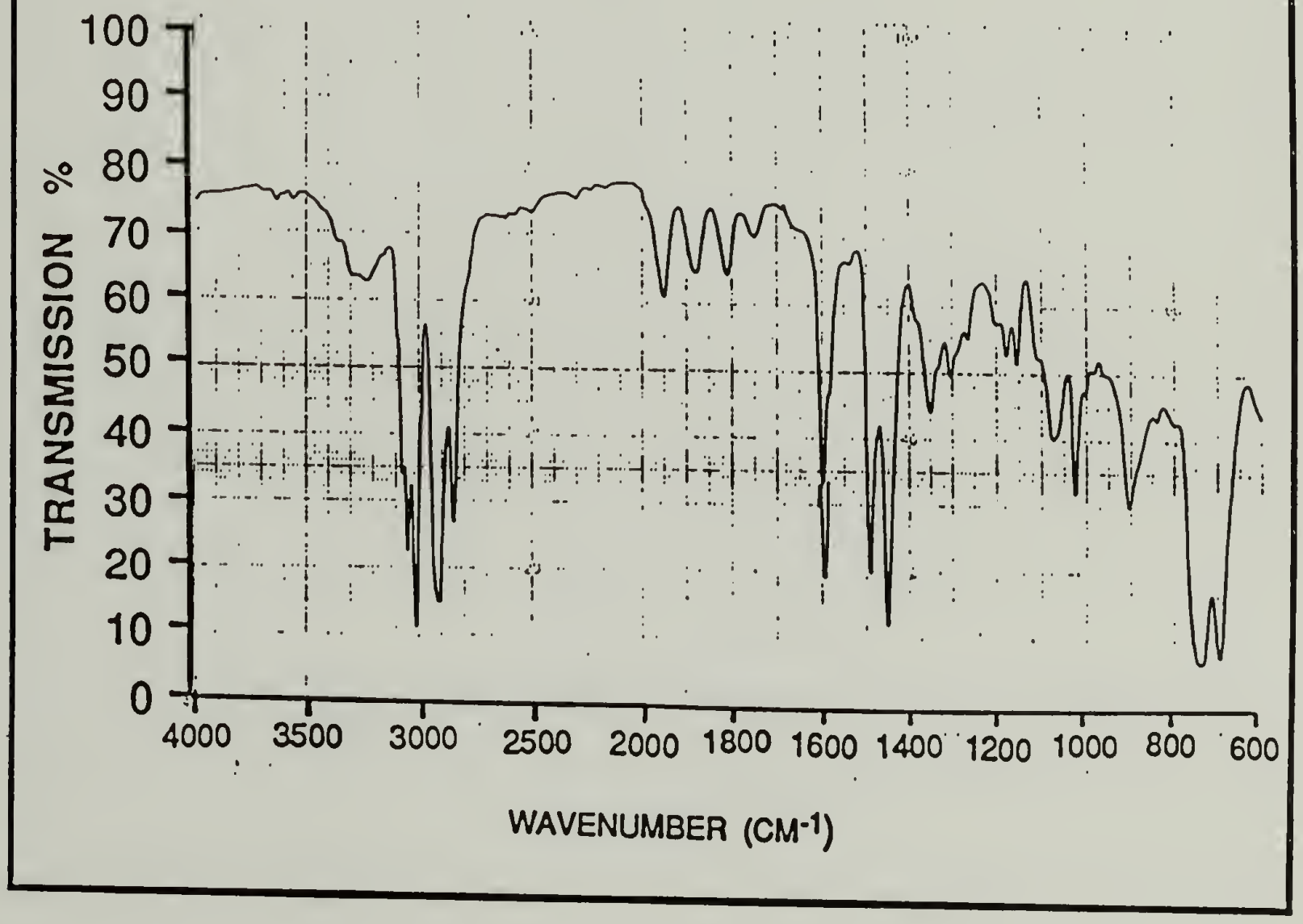

^{1}H NMR SPECTRUM: 1, 1'-azobis(1,3-[1-^{13}C]diphenylpropane) (1b)

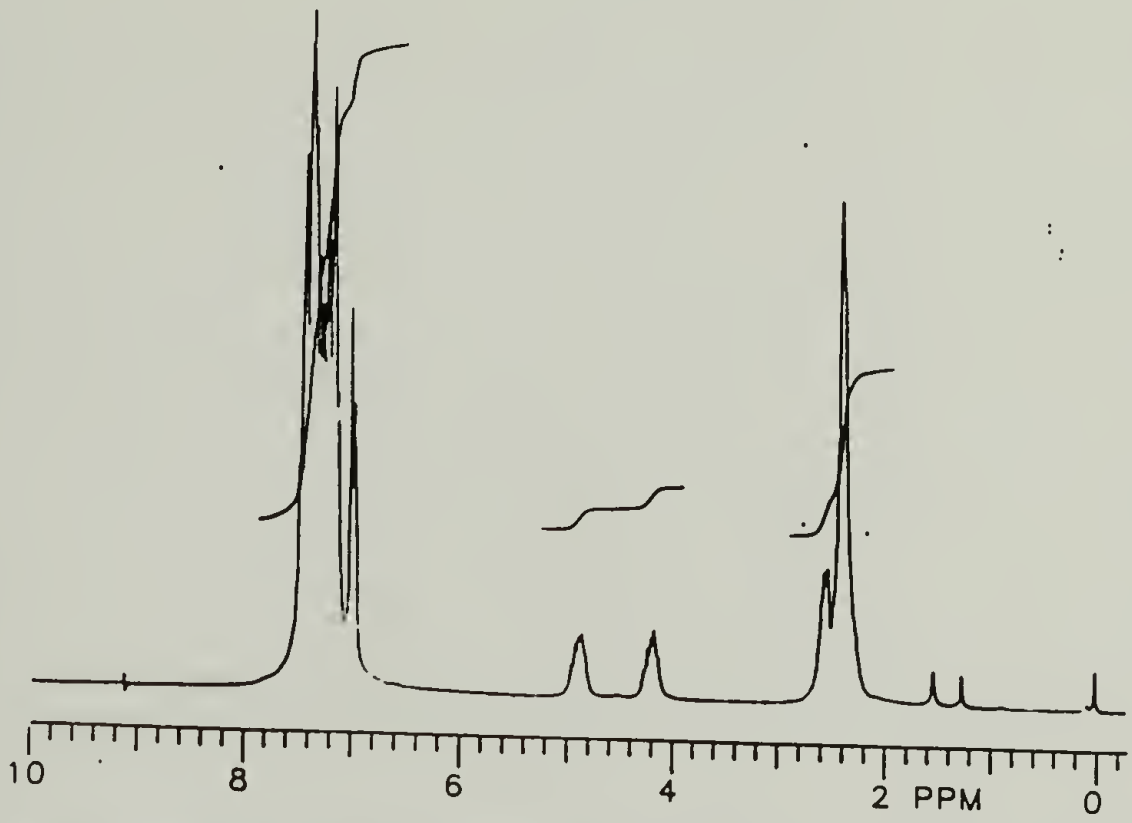

INFRARED SPECTRUM: 1, 1'-azobis(1,3-[1-^{13}C]diphenylpropane) (1b)

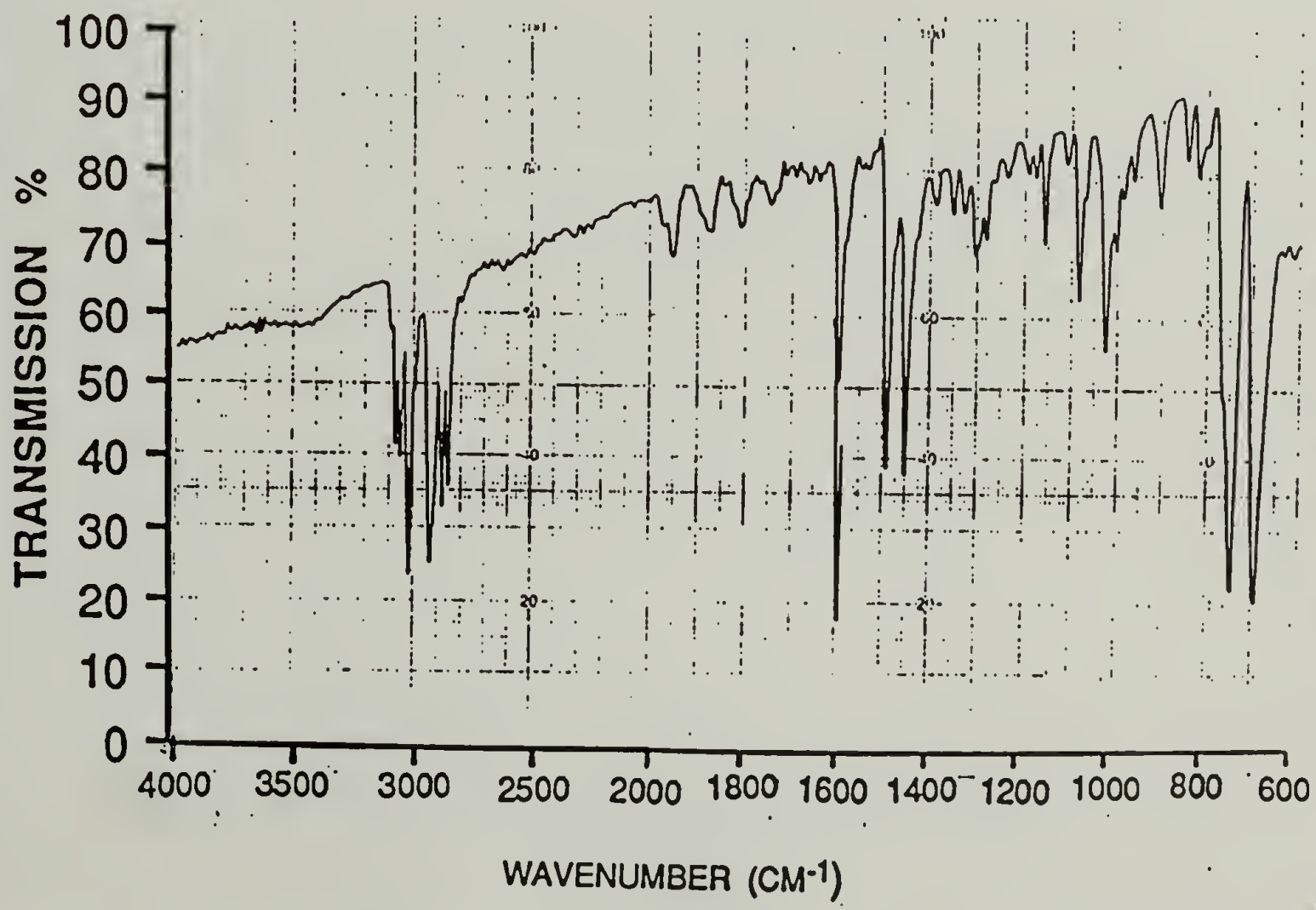

^{13}C NMR SPECTRUM: 1, 1'-azobis(1,3-[1-^{13}C]diphenylpropane) (**1b**)

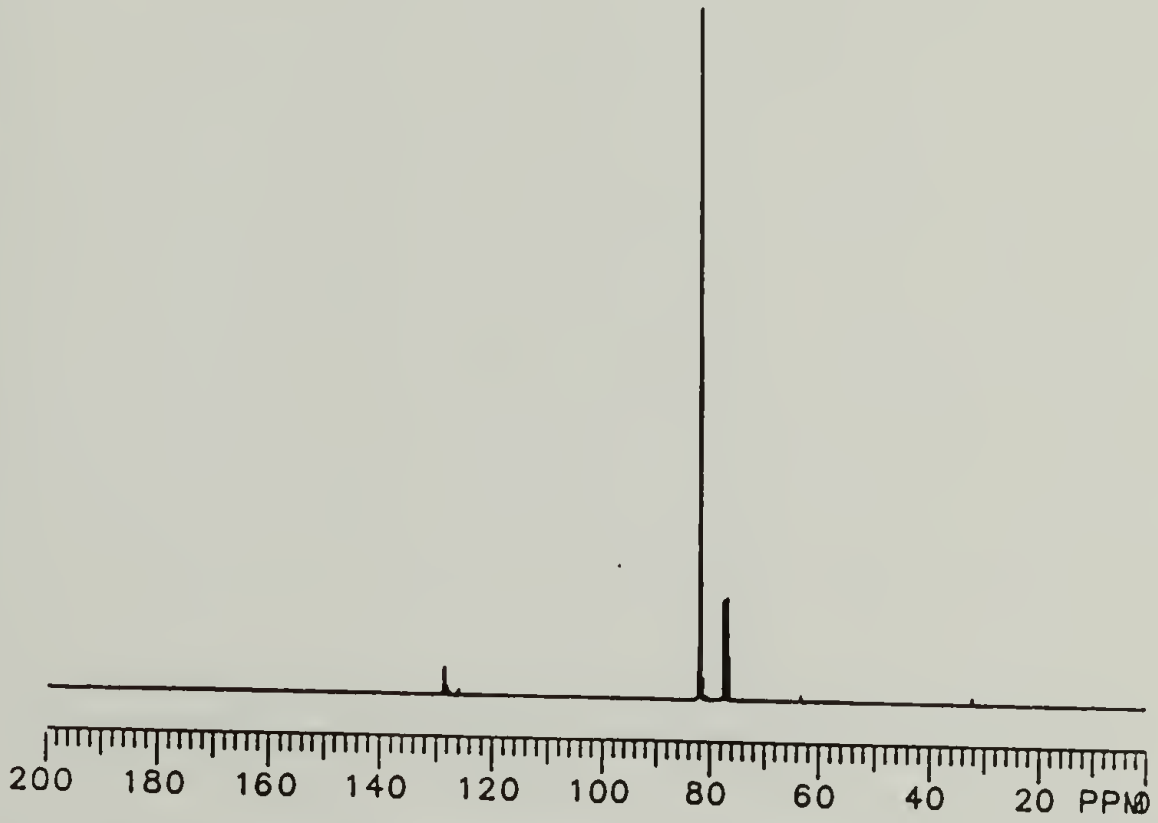

^{1}H NMR SPECTRUM: 1,1'-azobis(1,3-diphenylpropane)

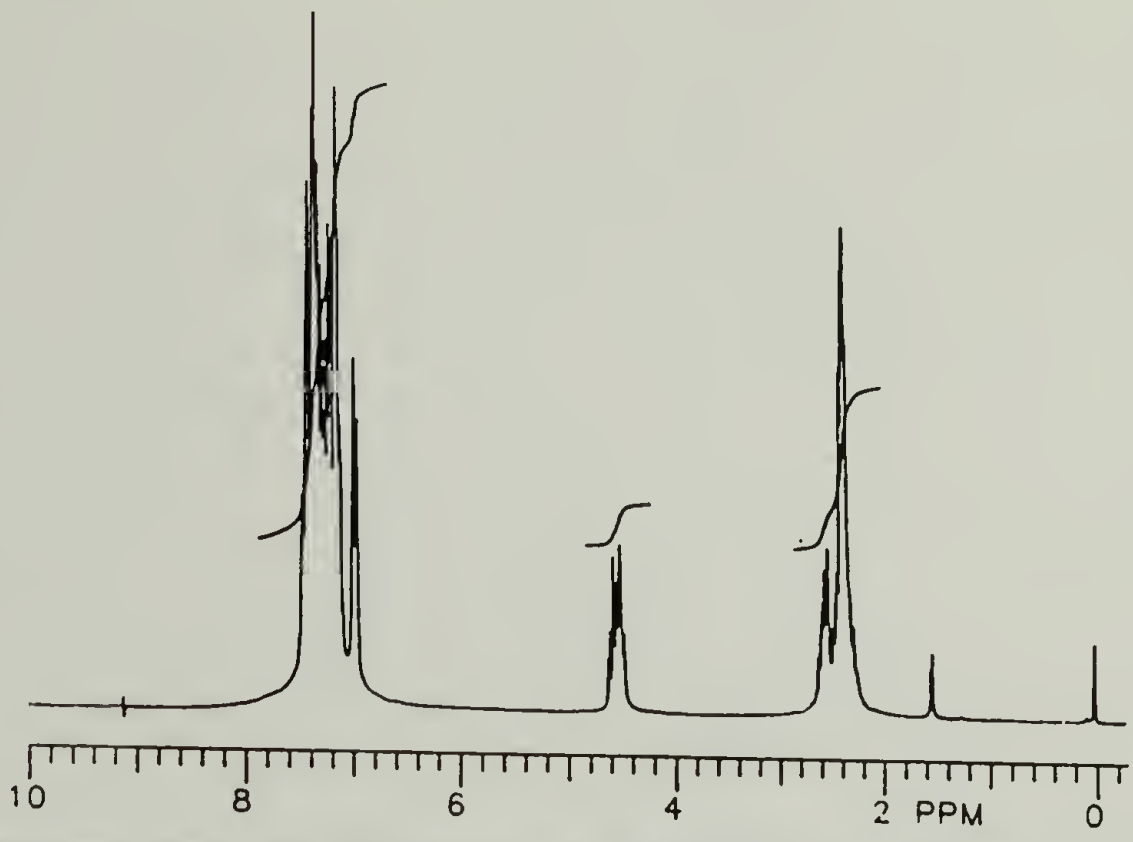

INFRARED SPECTRUM: 1,1'-azobis(1,3-diphenylpropane)

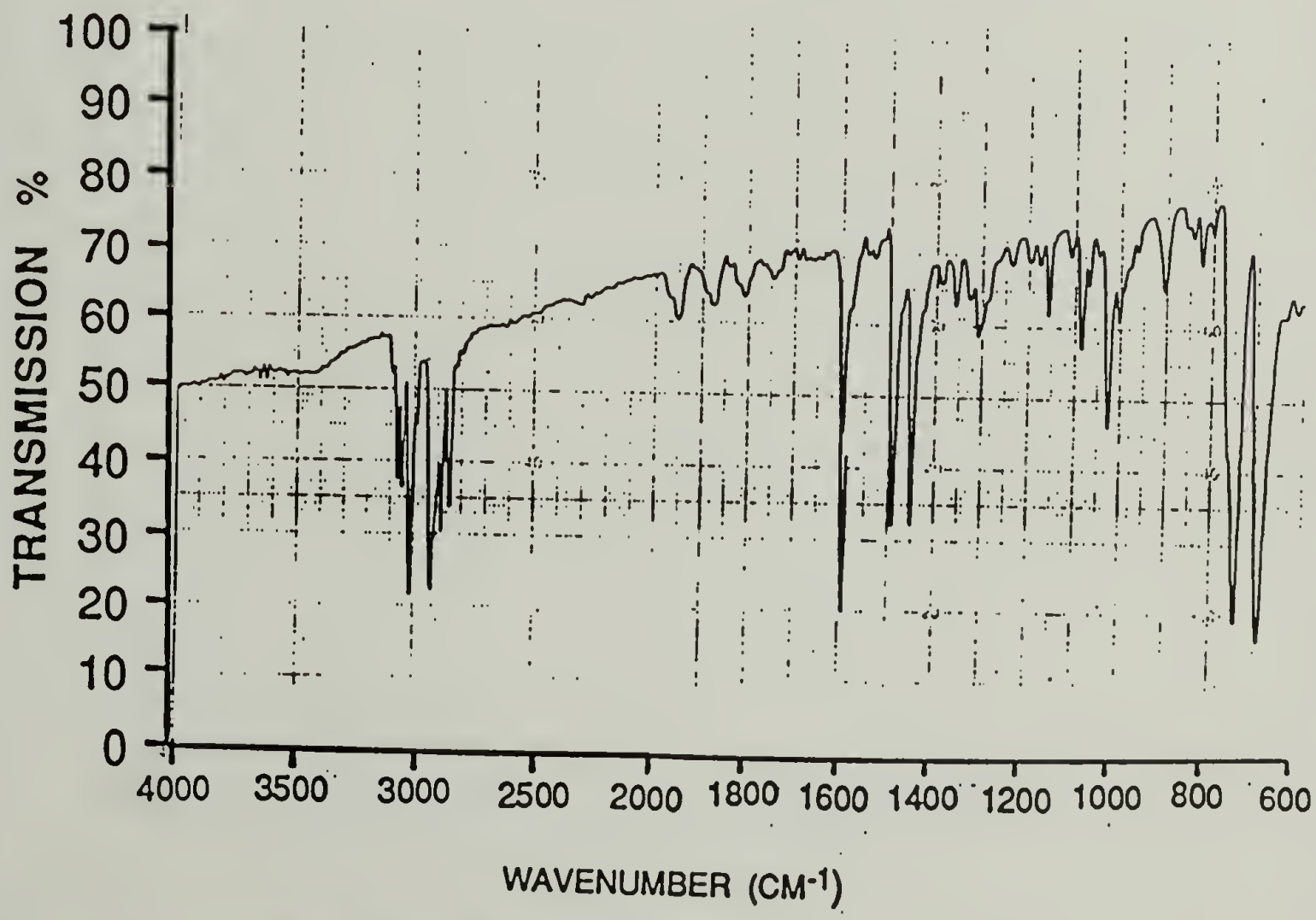

^{13}C NMR SPECTRUM: 1,1'-azobis(1,3-diphenylpropane)

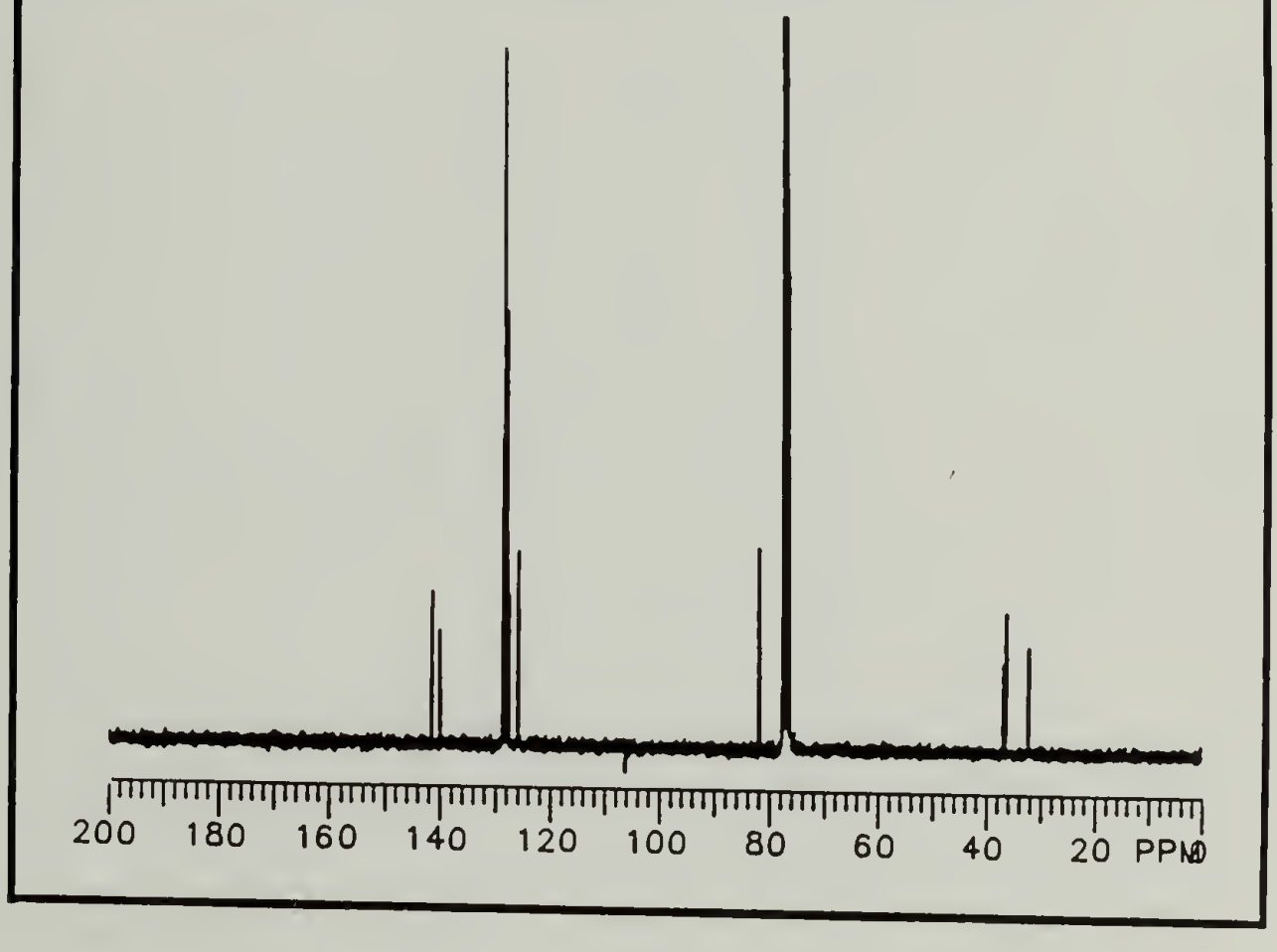

^{1}H NMR SPECTRUM: ethyl 3-phenyl-3-keto[3-^{13}C]propionate

INFRARED SPECTRUM: ethyl 3-phenyl-3-keto[3-^{13}C]propionate

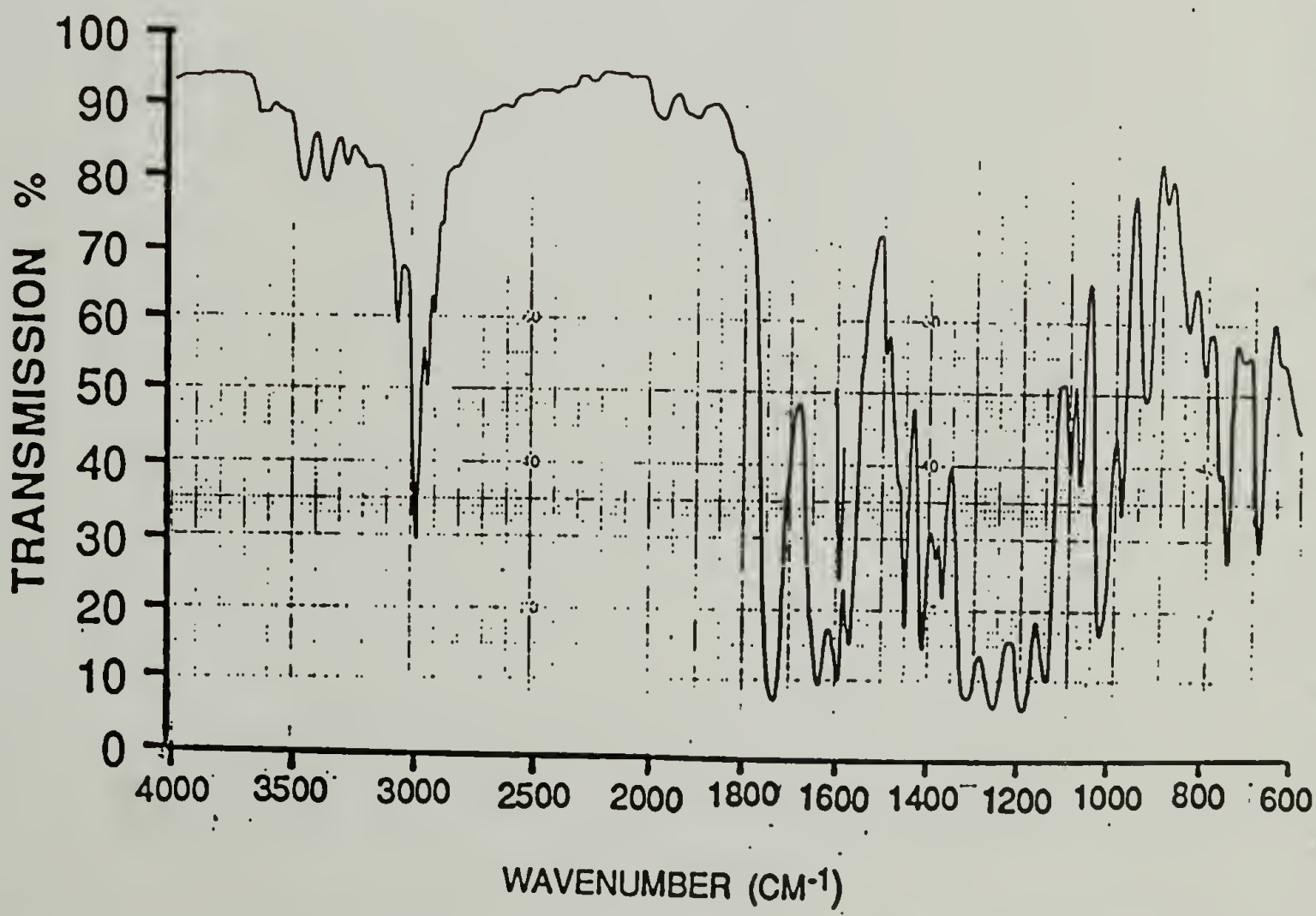

^{1}H NMR SPECTRUM: ethyl 3-phenyl-3-methoxylimino[3-^{13}C]propionate

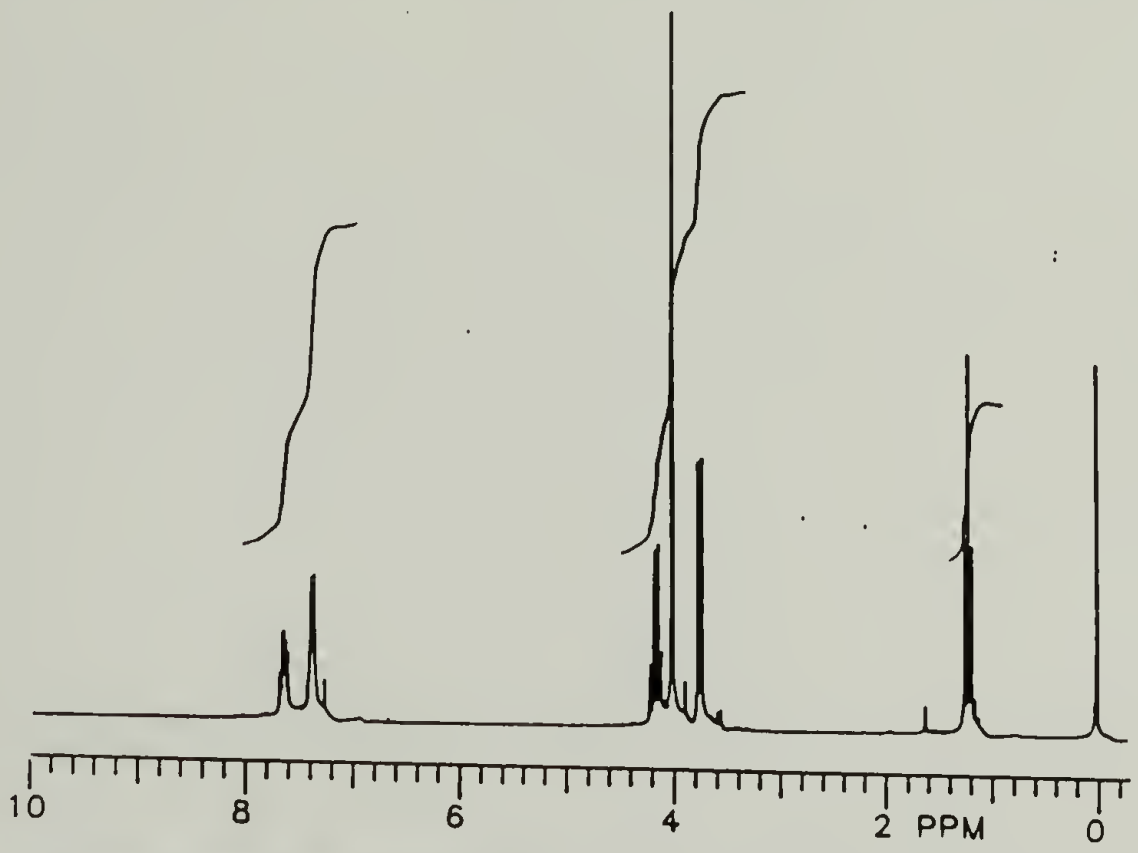

INFRARED SPECTRUM: ethyl 3-phenyl-3-methoxylimino[3-^{13}C]propionate

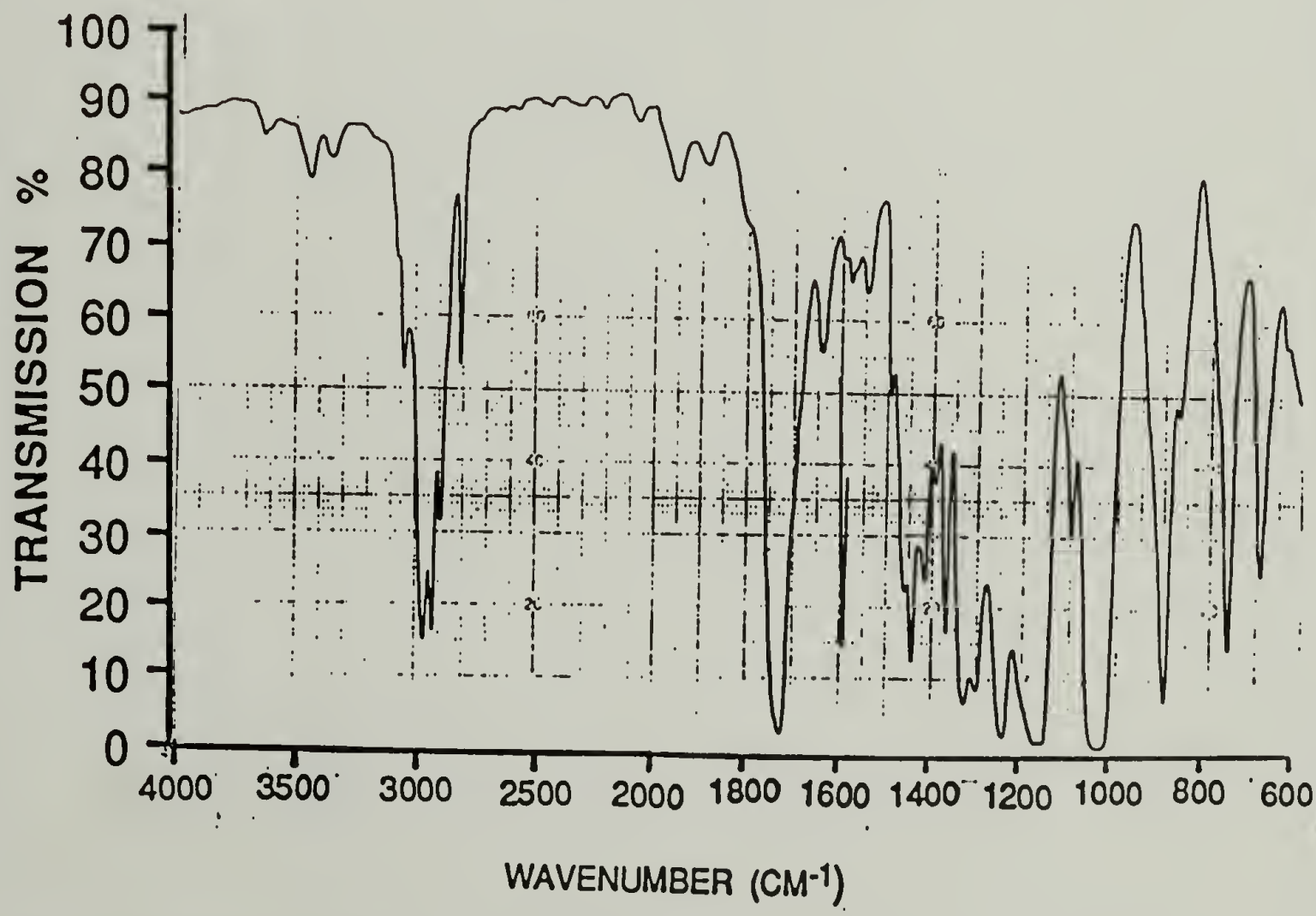

^{1}H NMR SPECTRUM: ethyl 3-phenyl-3-methoxyliminopropionate

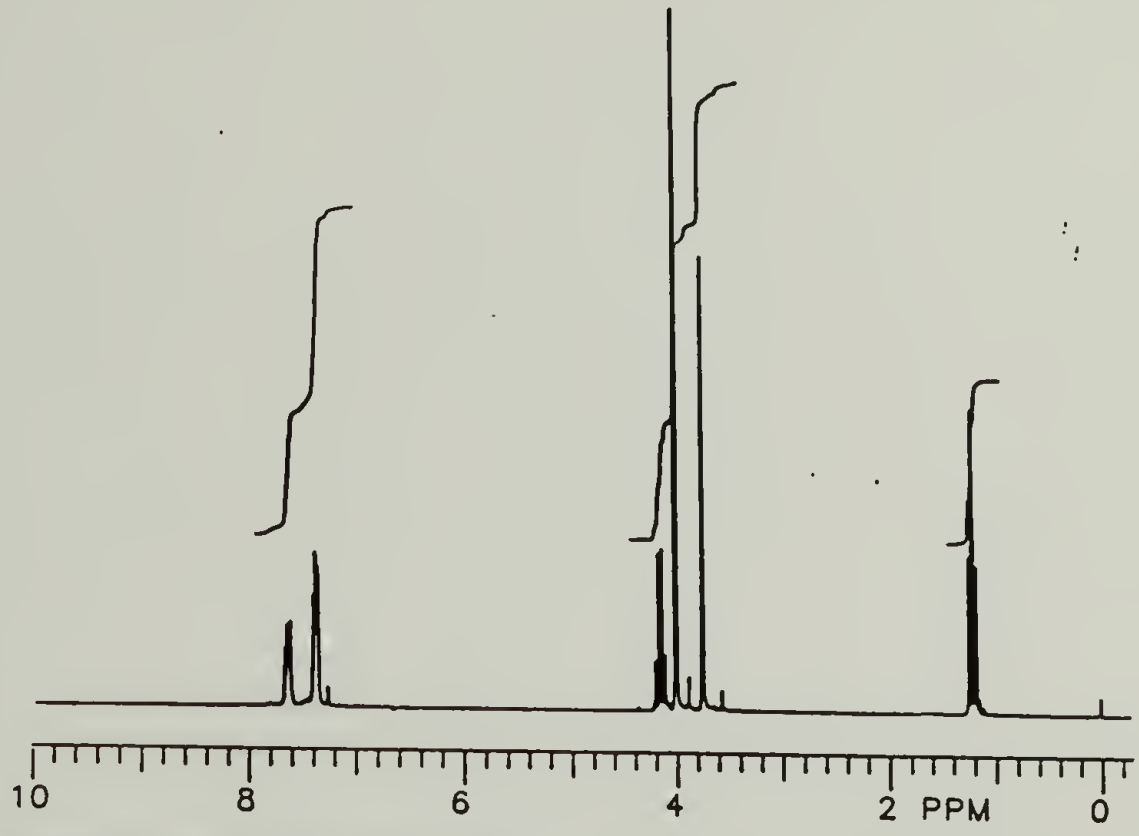

INFRARED SPECTRUM: ethyl 3-phenyl-3-methoxyliminopropionate

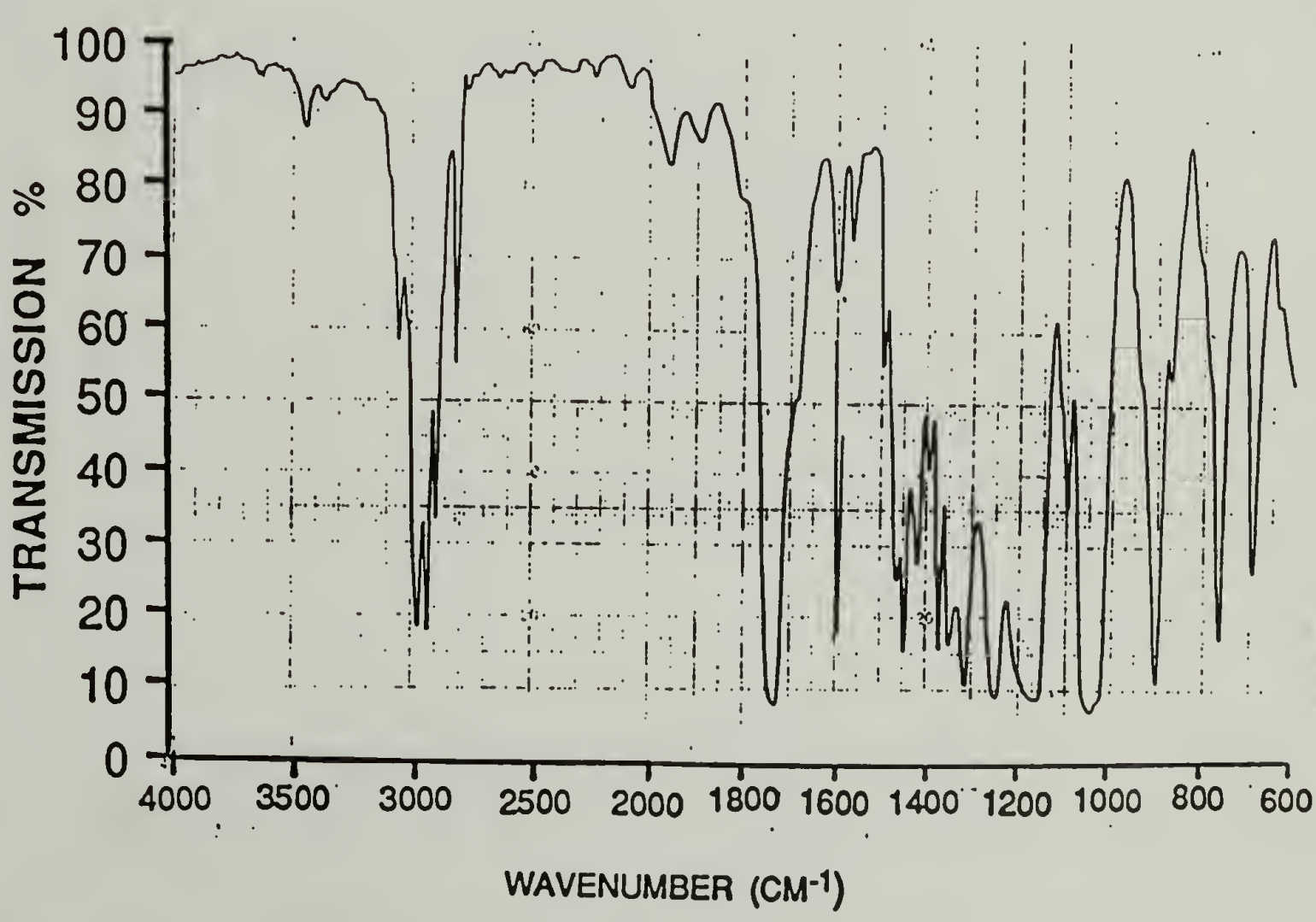

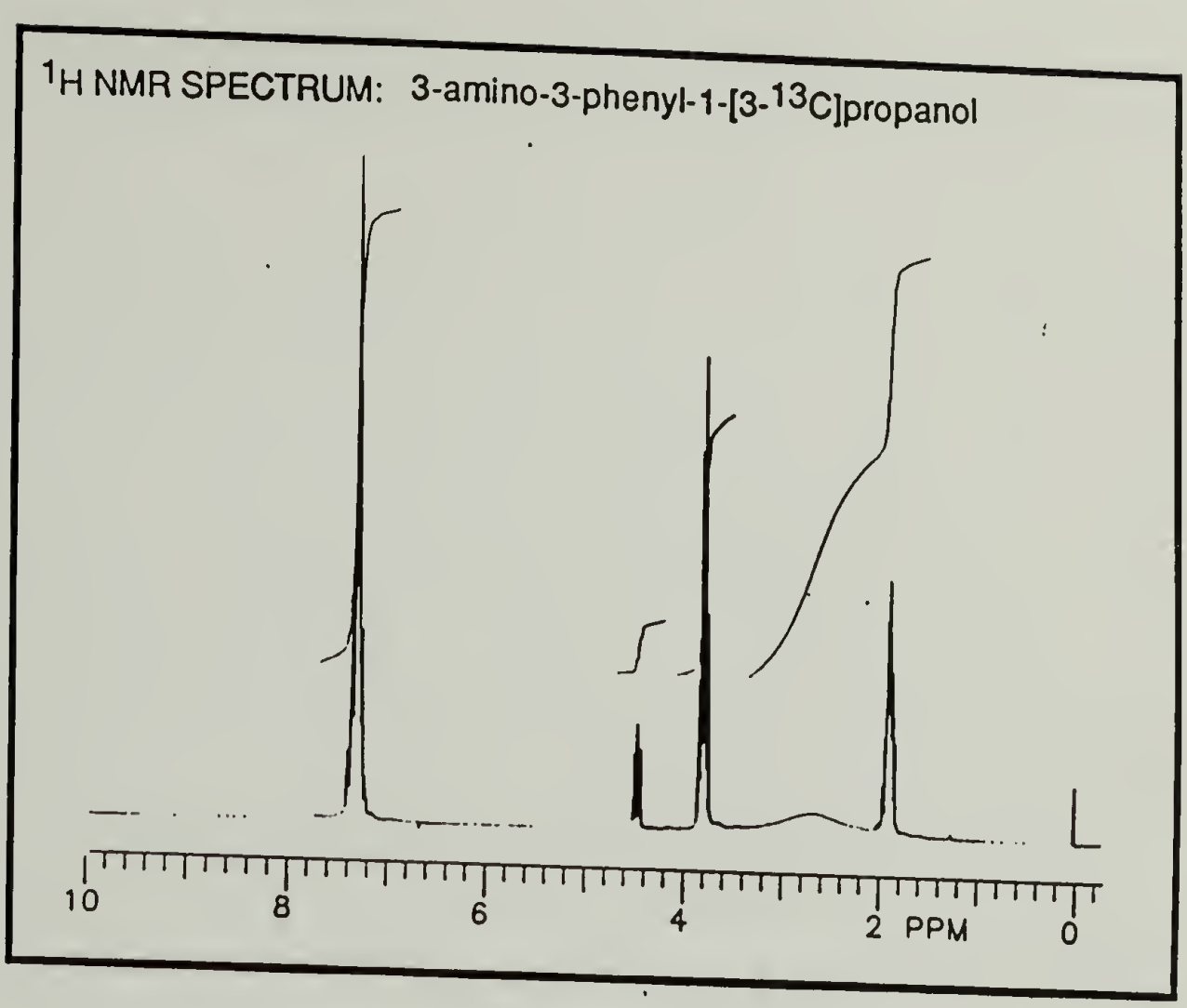
^{1}H NMR SPECTRUM: 3-amino-3-phenyl-1-[3-^{13}C]propanol
10
8
6
4
2 PPM
0

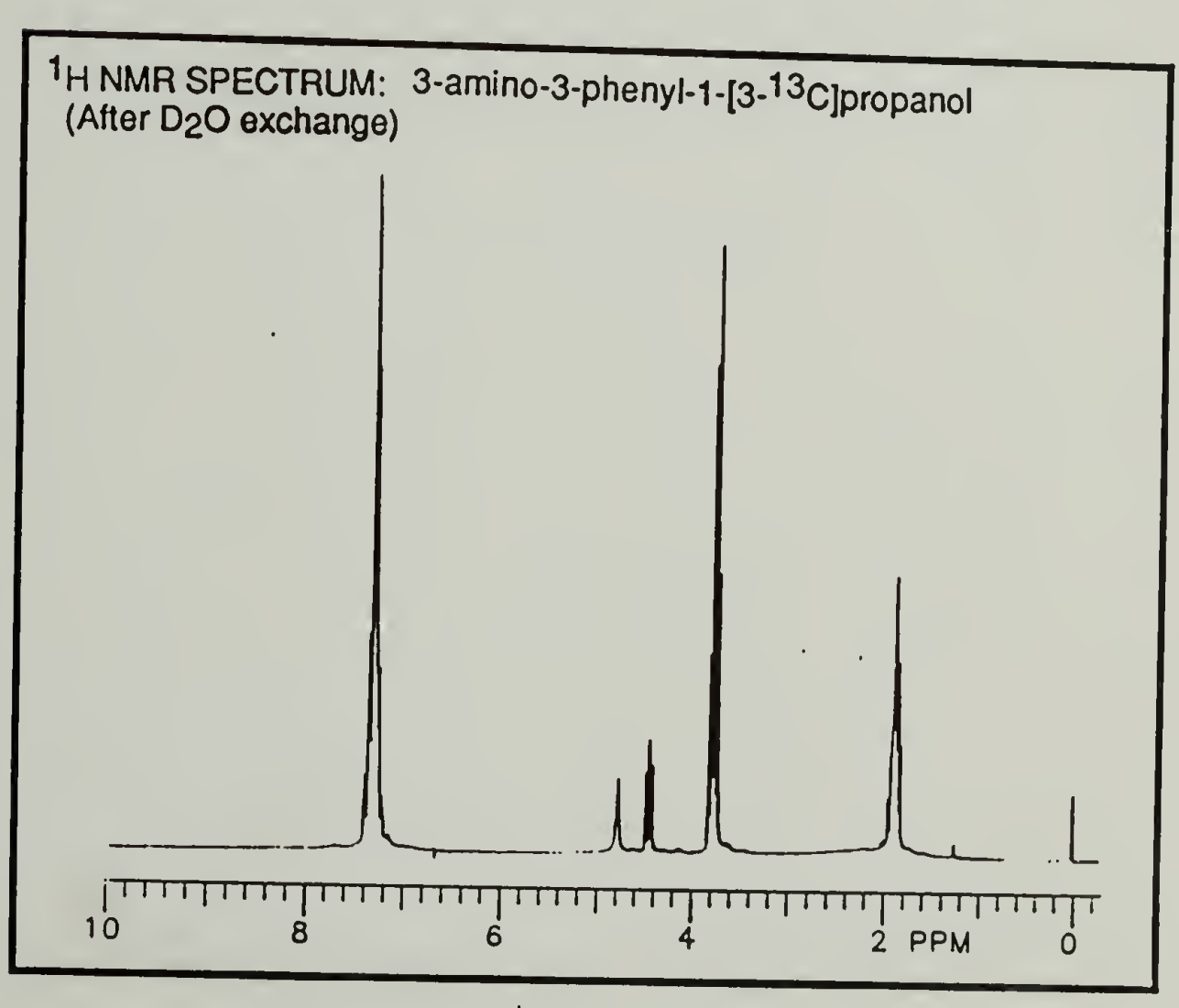
^{1}H NMR SPECTRUM: 3-amino-3-phenyl-1-[3-^{13}C]propanol
(After D_2O exchange)
10
8
6
4
2 PPM
0

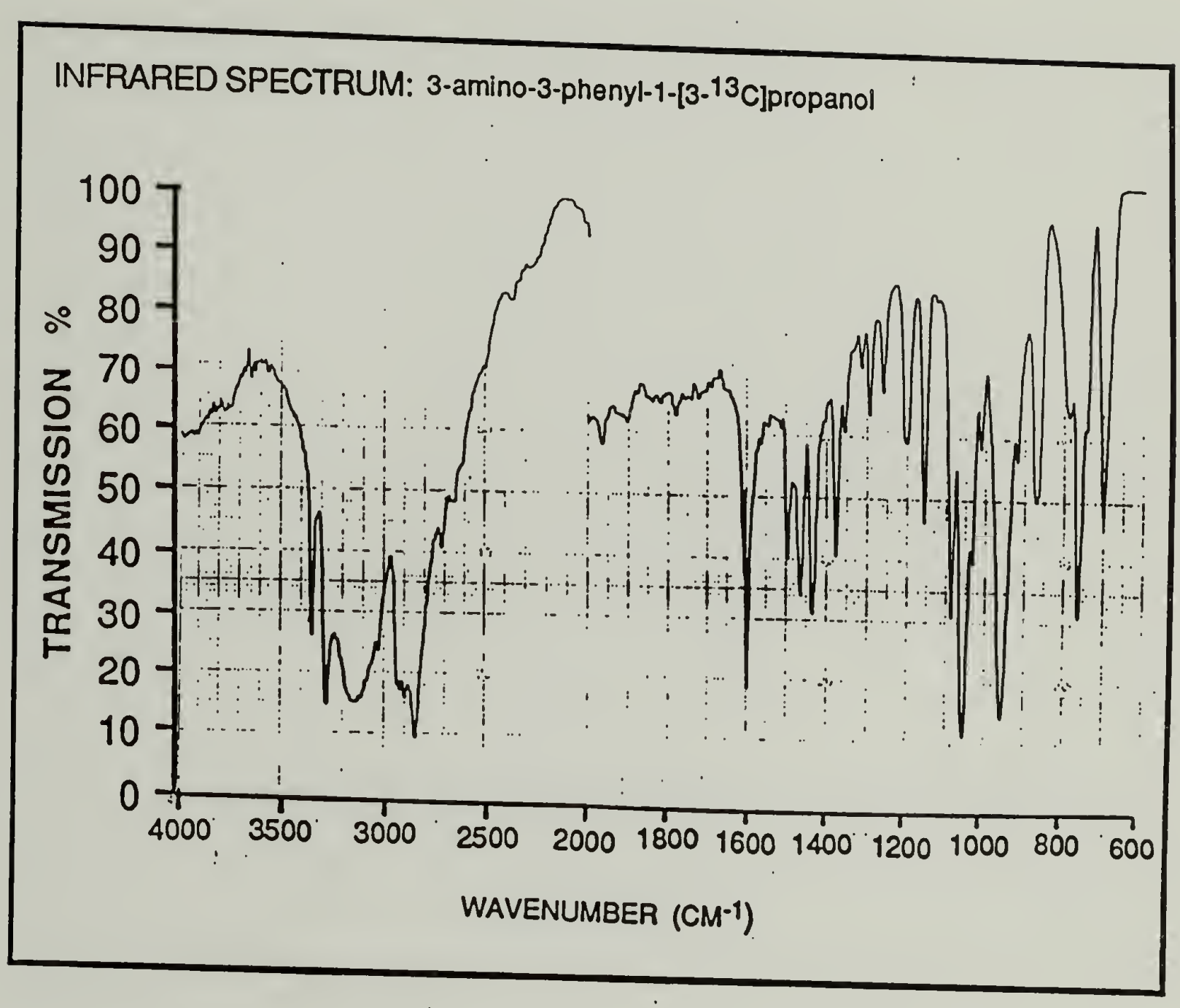
INFRARED SPECTRUM: 3-amino-3-phenyl-1-[3-13C]propanol
TRANSMISSION %
100
90
80
70
60
50
40
30
20
10
0
4000
3500
3000
2500
2000
1800
1600
1400
1200
1000
800
600
WAVENUMBER (CM-1)

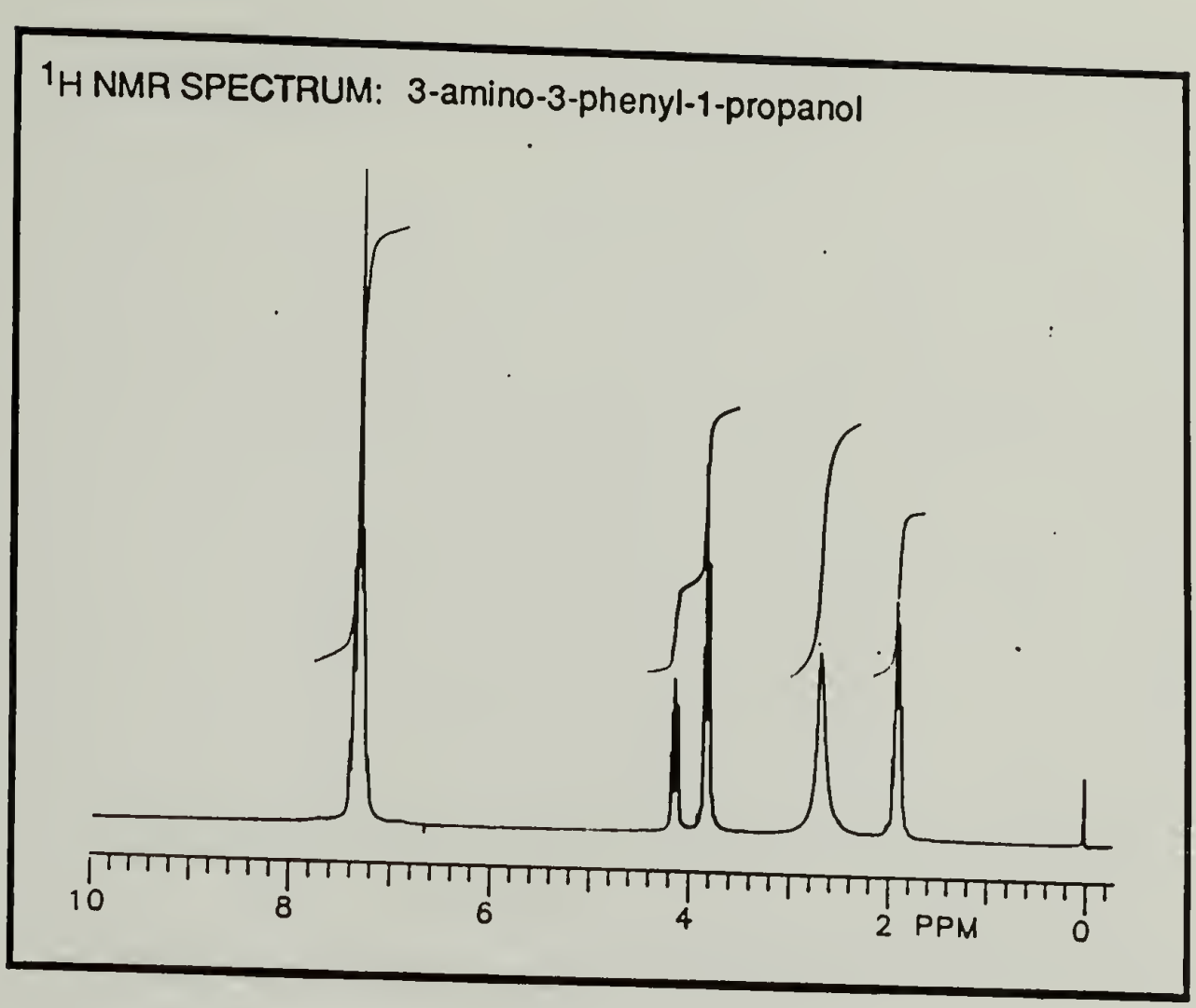
^{1}H NMR SPECTRUM: 3-amino-3-phenyl-1-propanol
10
8
6
4
2 PPM
0

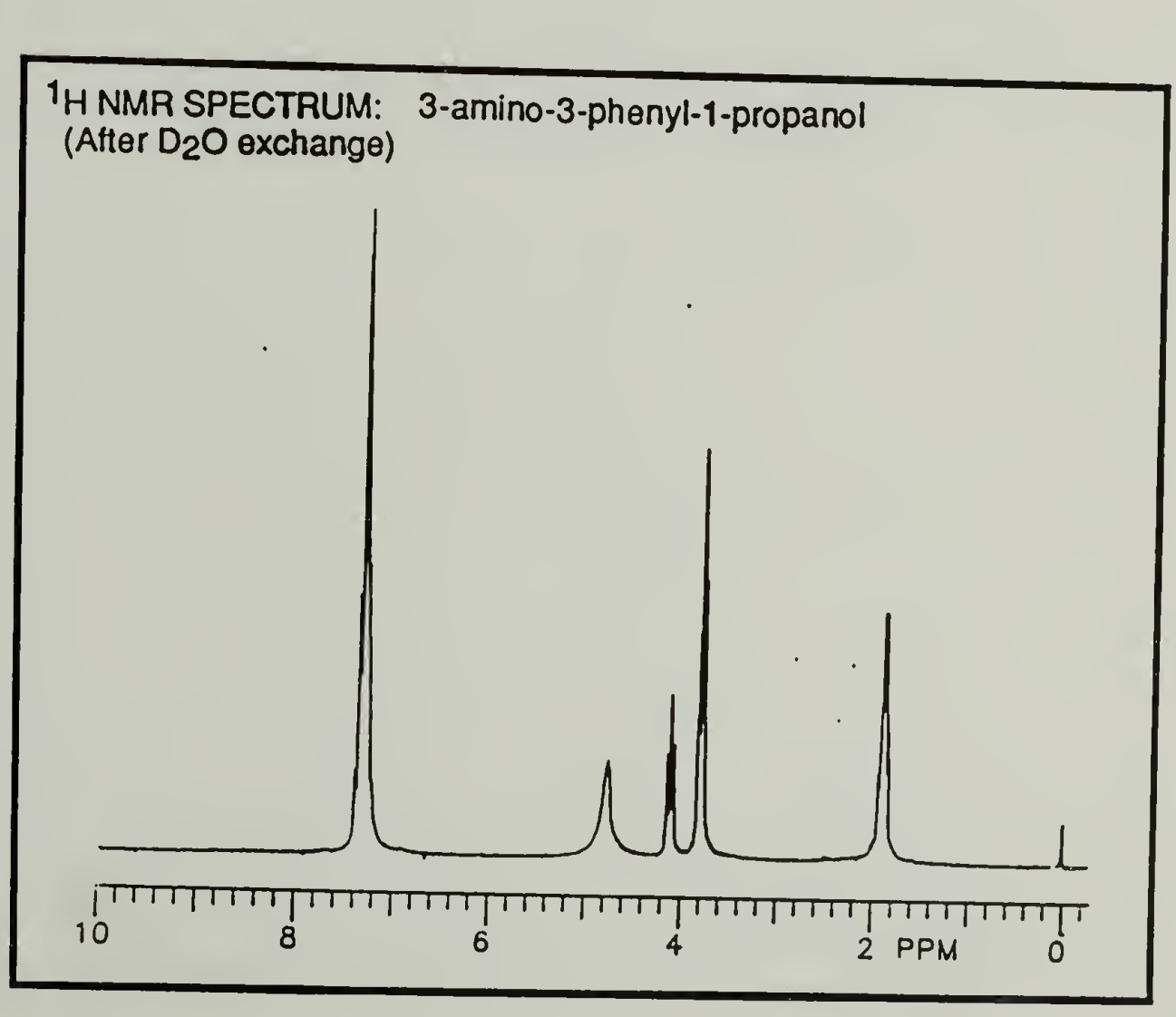
^{1}H NMR SPECTRUM: 3-amino-3-phenyl-1-propanol
(After D_2O exchange)
10
8
6
4
2 PPM
0

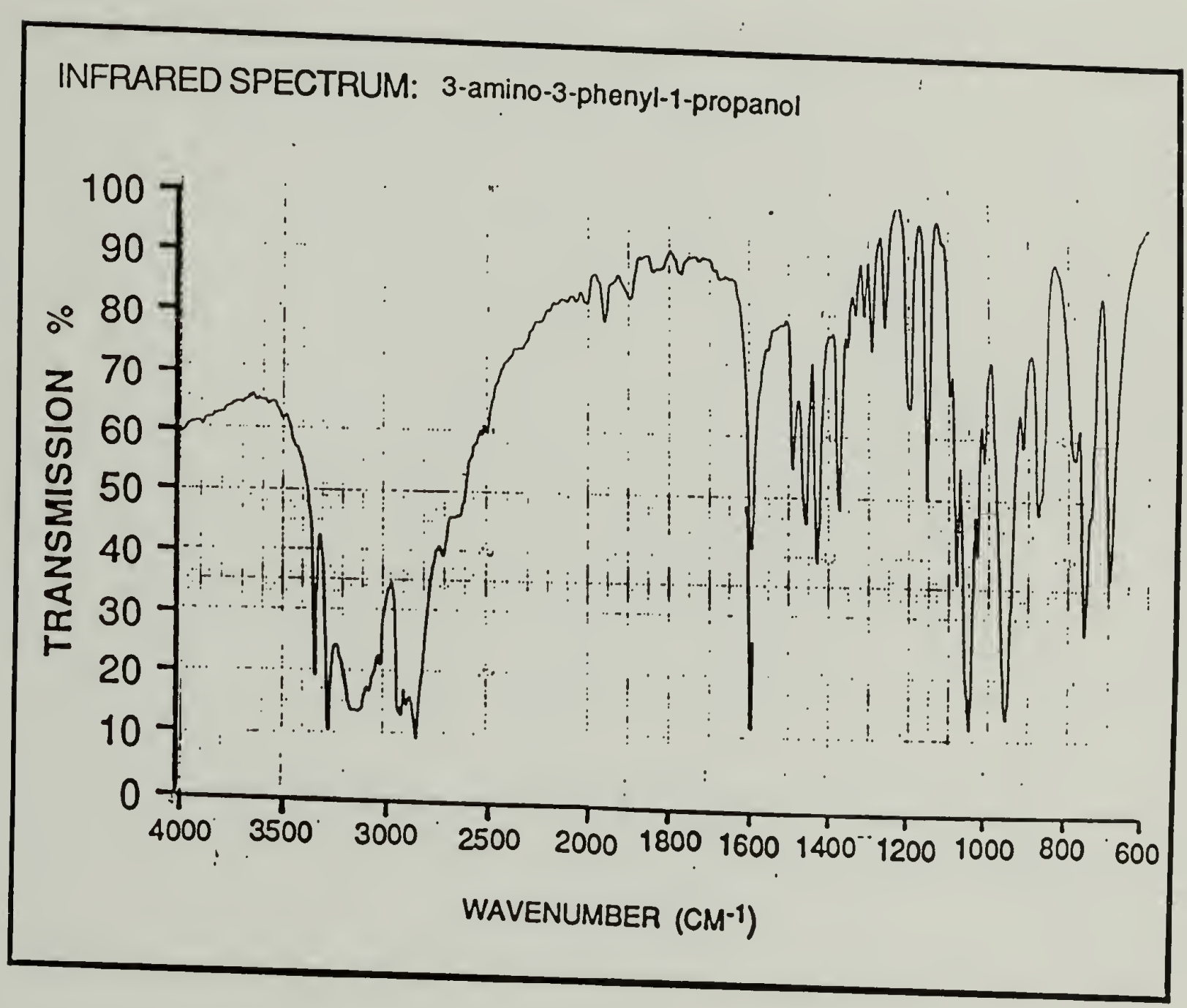
INFRARED SPECTRUM: 3-amino-3-phenyl-1-propanol
TRANSMISSION %
100
90
80
70
60
50
40
30
20
10
0
4000
3500
3000
2500
2000
1800
1600
1400
1200
1000
800
600
WAVENUMBER (CM-1)

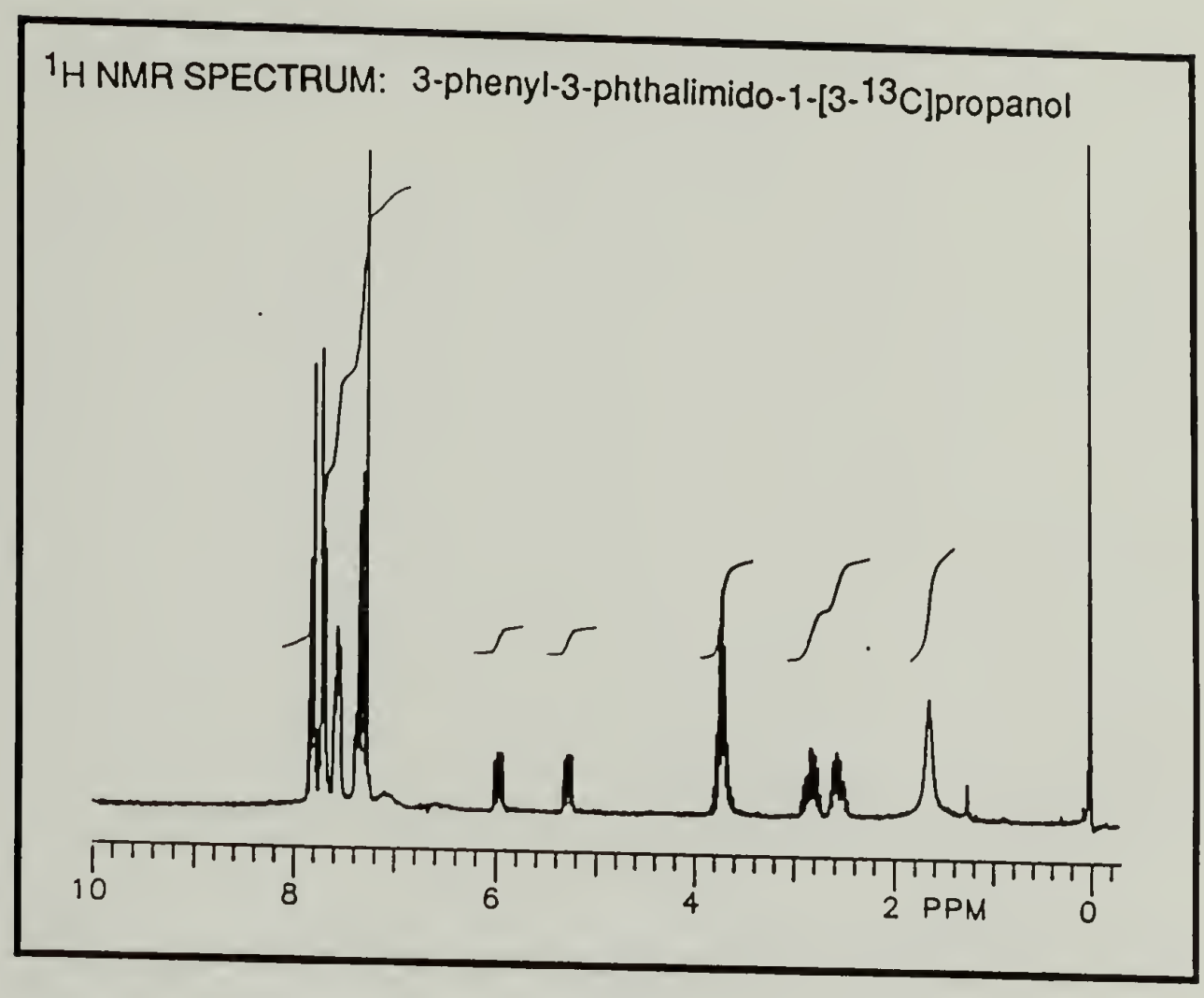
^{1}H NMR SPECTRUM: 3-phenyl-3-phthalimido-1-[3-^{13}C]propanol
10
8
6
4
2 PPM
0

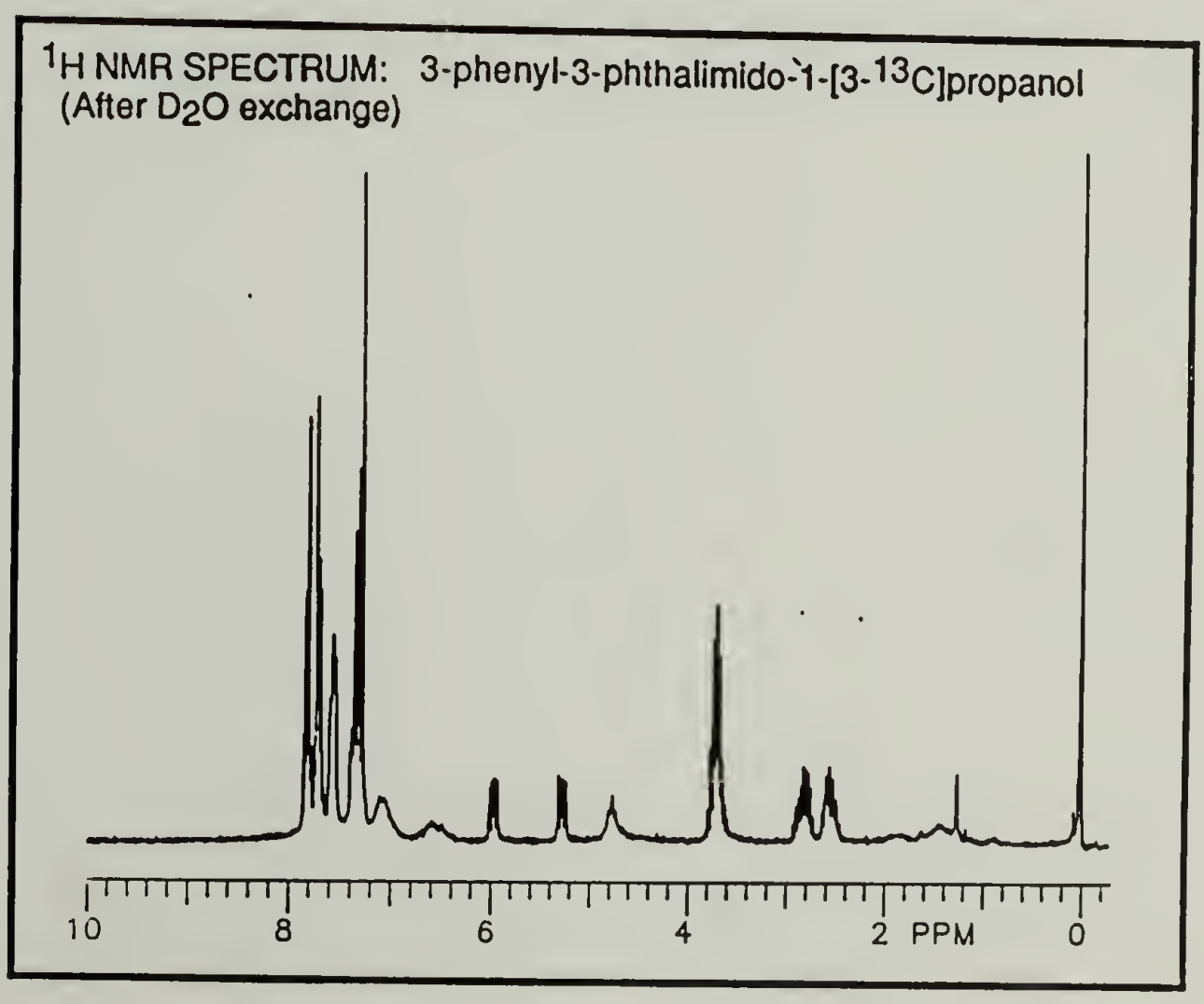
^{1}H NMR SPECTRUM: 3-phenyl-3-phthalimido-1-[3-^{13}C]propanol
(After D_2O exchange)
10
8
6
4
2 PPM
0

INFRARED SPECTRUM: 3-phenyl-3-phthalimido-1-[3-^{13}C]propanol

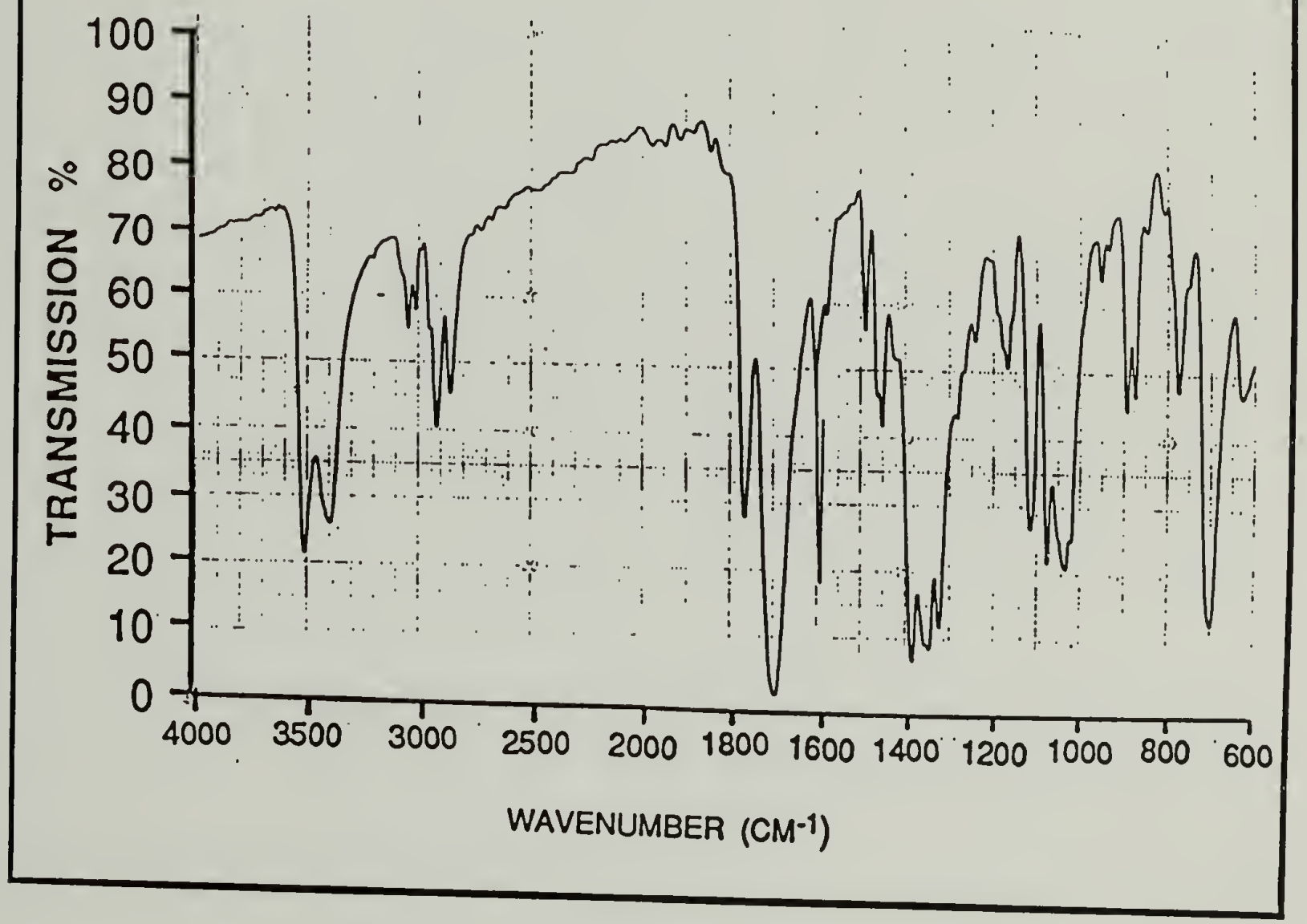

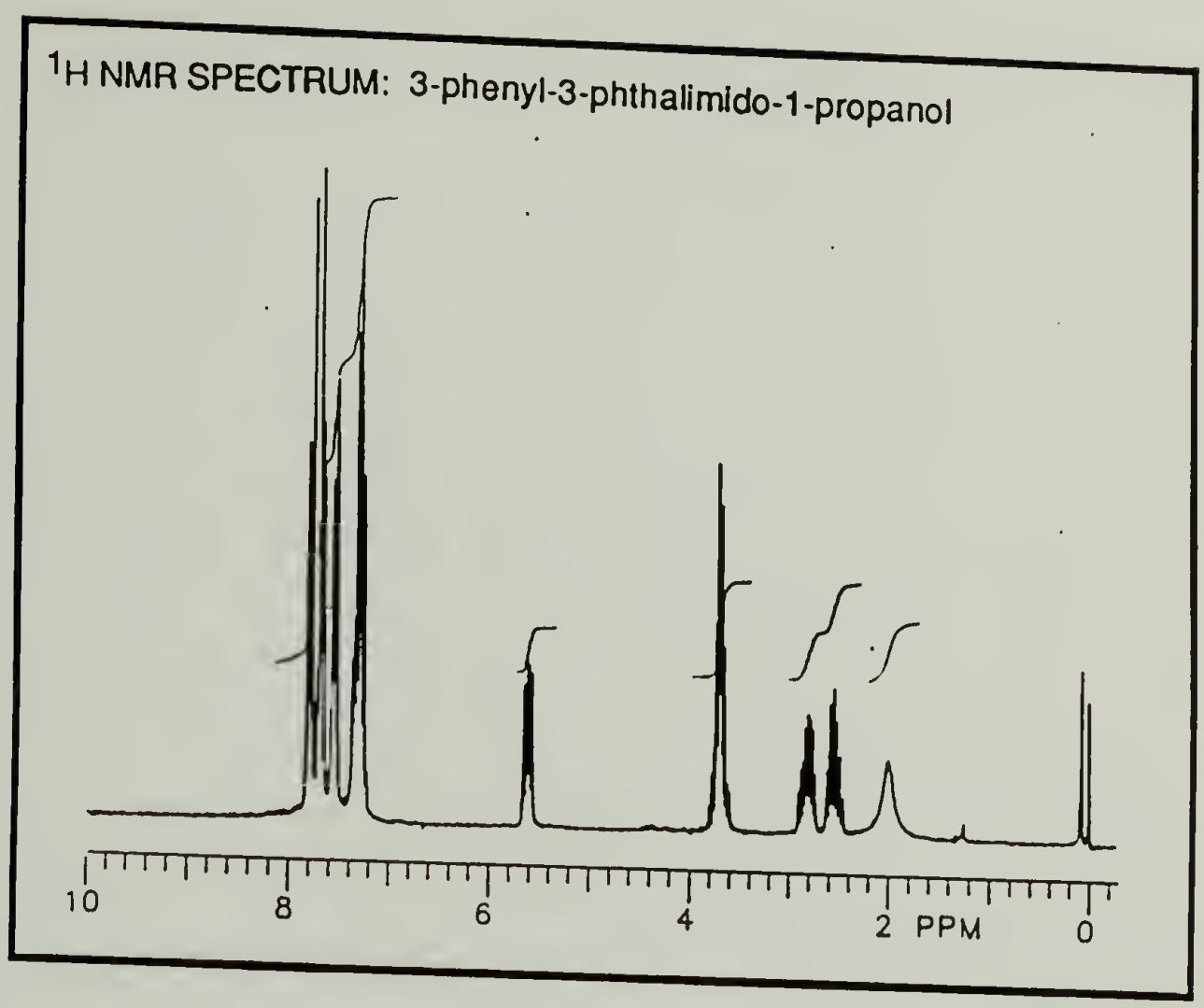
^{1}H NMR SPECTRUM: 3-phenyl-3-phthalimido-1-propanol
10
8
6
4
2 PPM
0

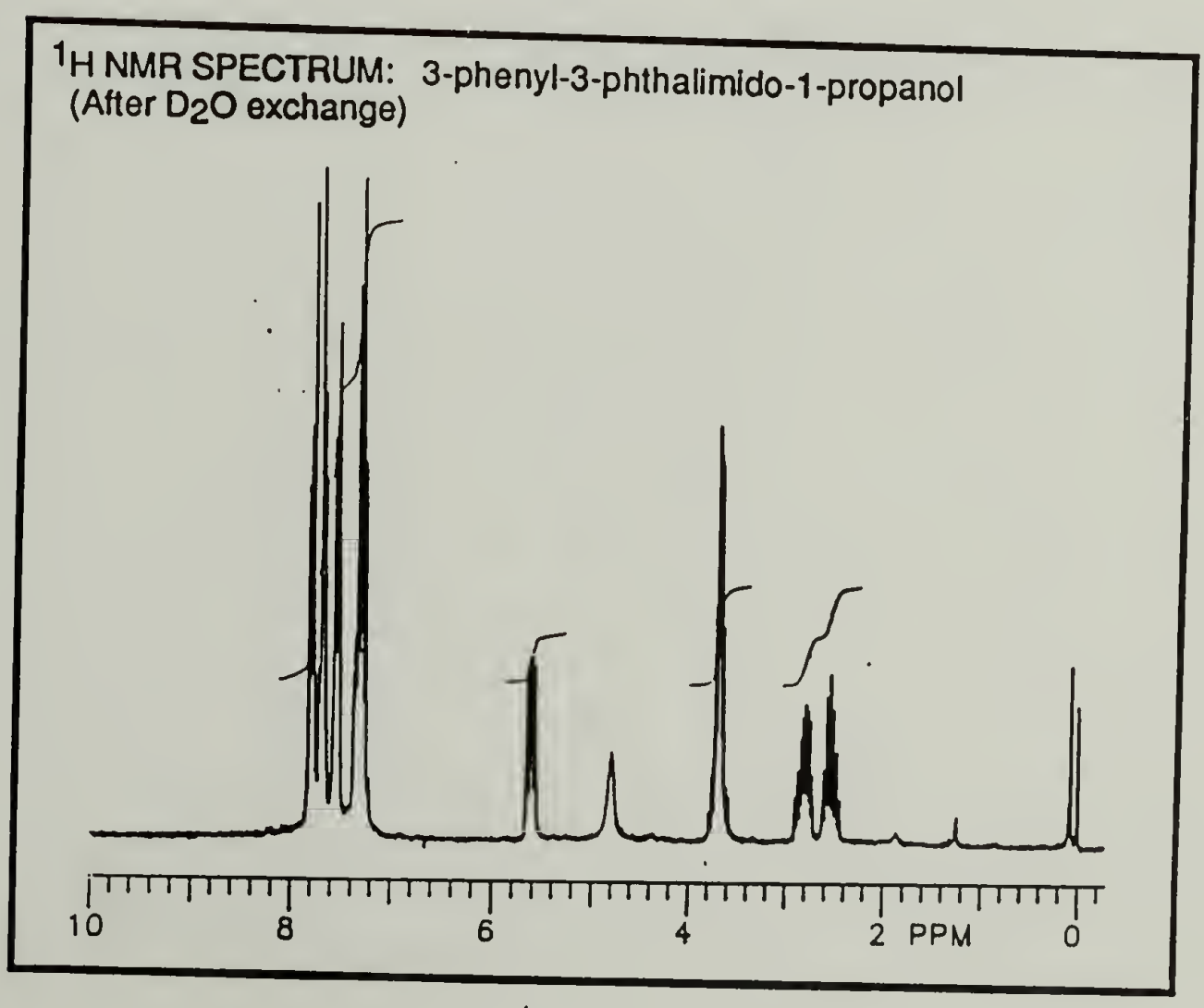
^{1}H NMR SPECTRUM: 3-phenyl-3-phthalimido-1-propanol
(After D_2O exchange)
10
8
6
4
2 PPM
0

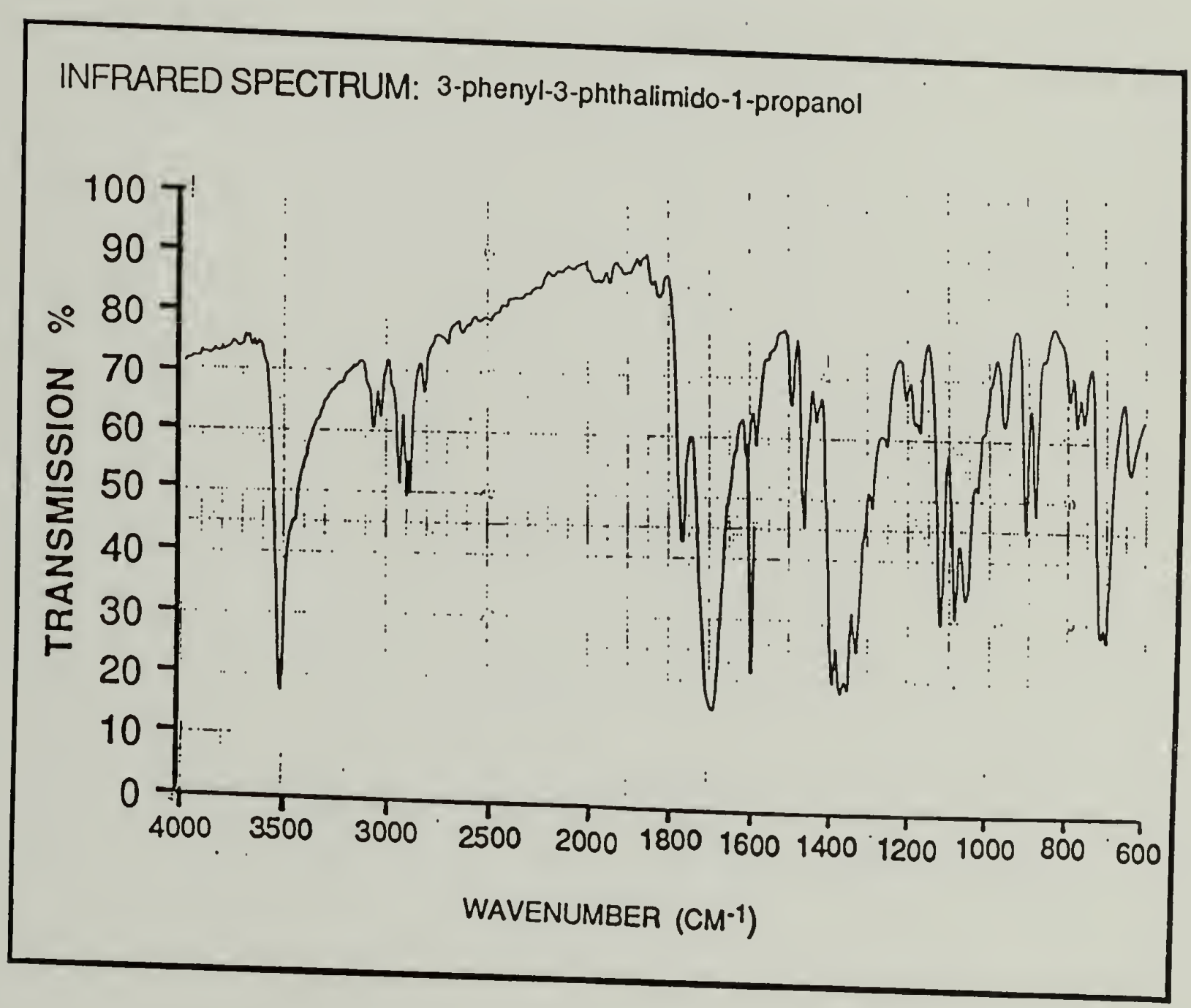
INFRARED SPECTRUM: 3-phenyl-3-phthalimido-1-propanol
TRANSMISSION %
100
90
80
70
60
50
40
30
20
10
0
4000
3500
3000
2500
2000
1800
1600
1400
1200
1000
800
600
WAVENUMBER (CM-1)

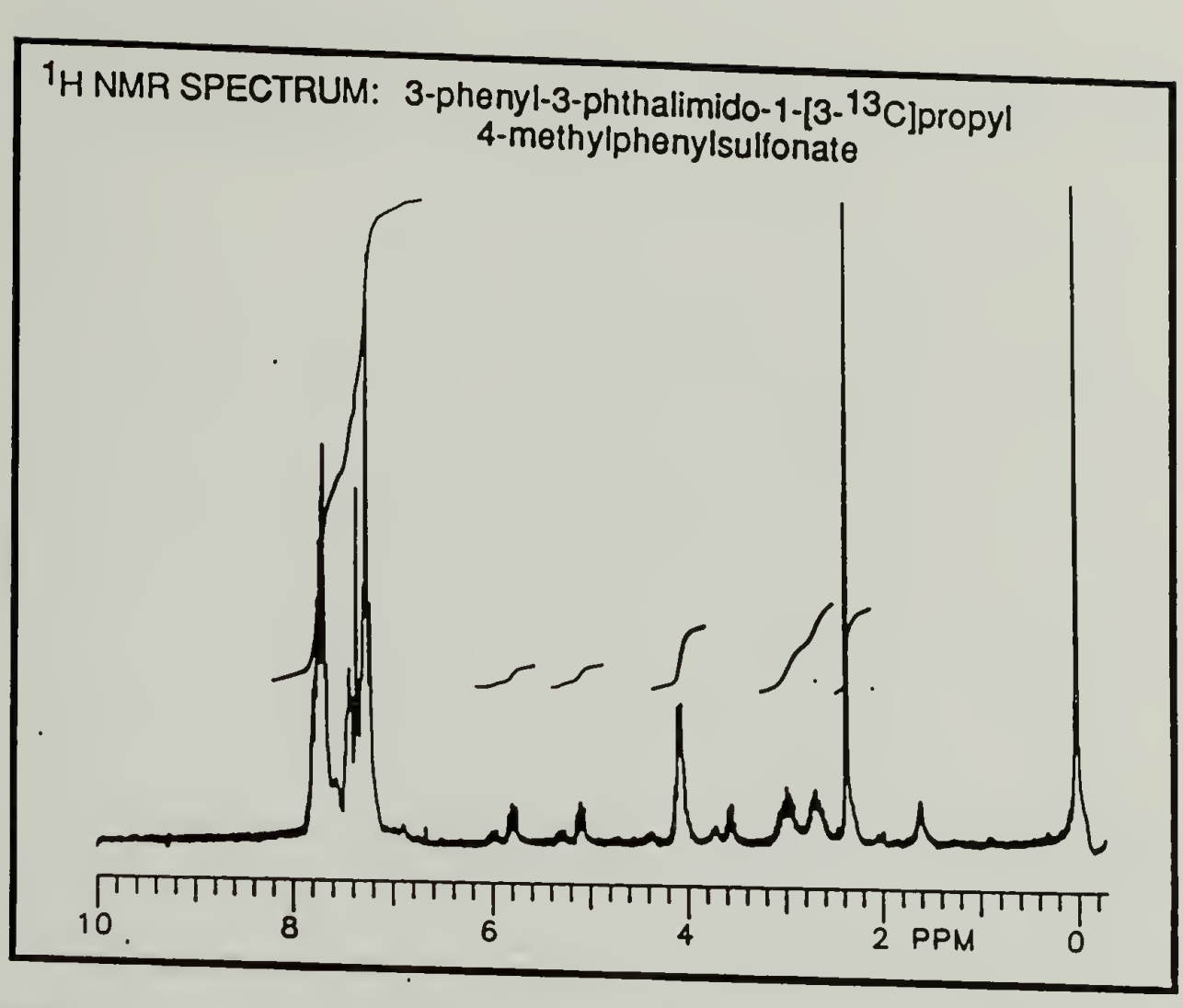
^{1}H NMR SPECTRUM: 3-phenyl-3-phthalimido-1-[3-^{13}C]propyl 4-methylphenylsulfonate
10
8
6
4
2 PPM
0

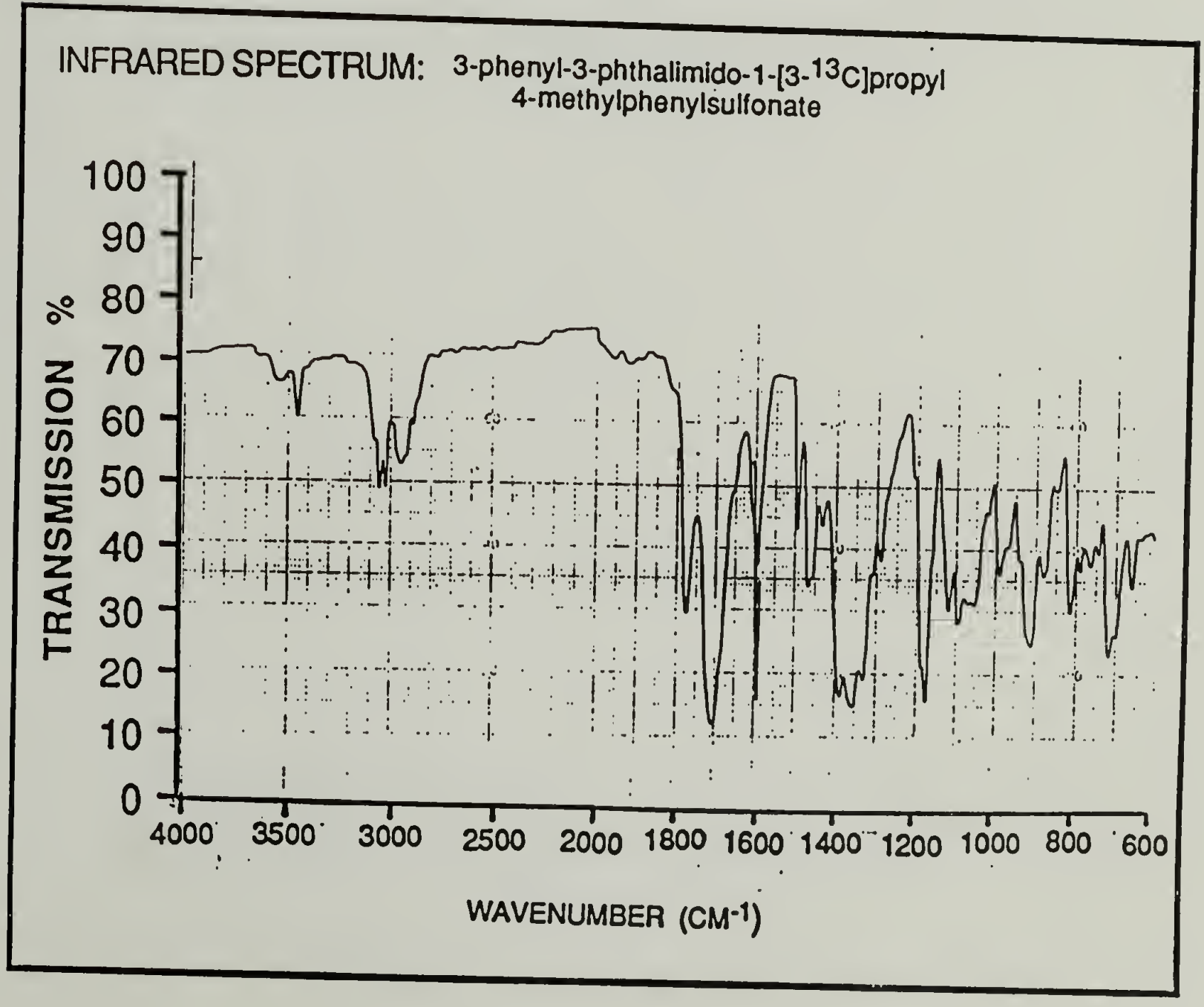
INFRARED SPECTRUM: 3-phenyl-3-phthalimido-1-[3-^{13}C]propyl 4-methylphenylsulfonate
TRANSMISSION %
100
90
80
70
60
50
40
30
20
10
0
4000
3500
3000
2500
2000
1800
1600
1400
1200
1000
800
600
WAVENUMBER (CM^{-1})

^{1}H NMR SPECTRUM: 3-phenyl-3-phthalimido-1-propyl 4-methylphenylsulfonate

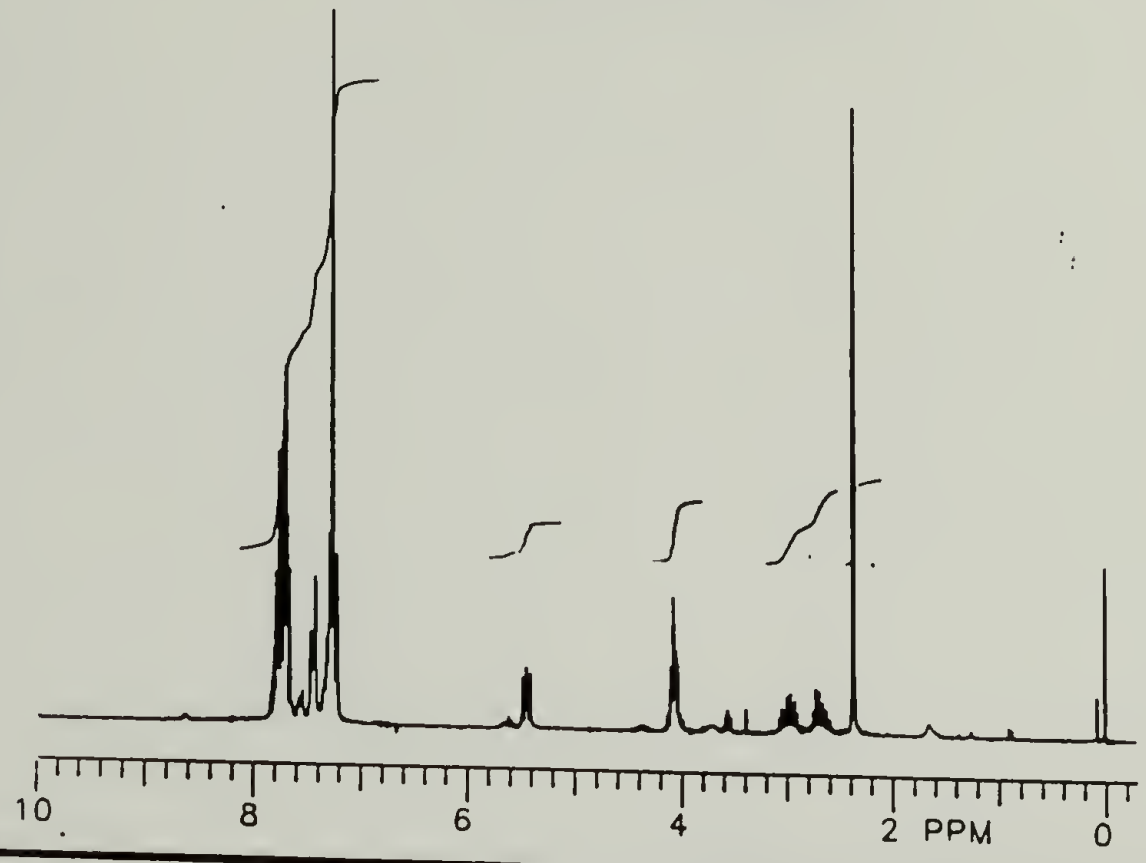

INFRARED SPECTRUM: 3-phenyl-3-phthalimido-1-propyl 4-methylphenylsulfonate

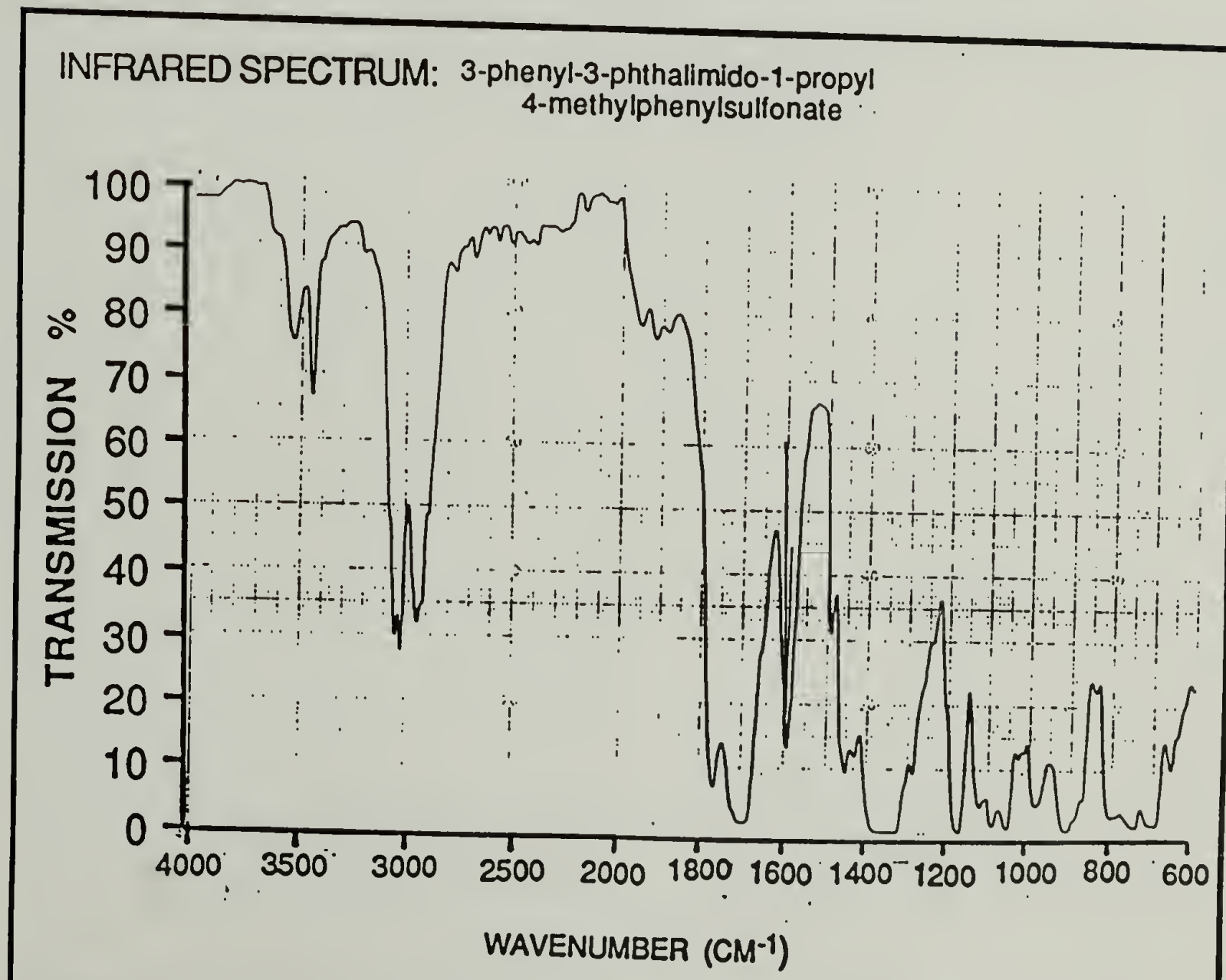

^{1}H NMR SPECTRUM: 4-phenyl-4-phthalimido[4-^{13}C]butyronitrile

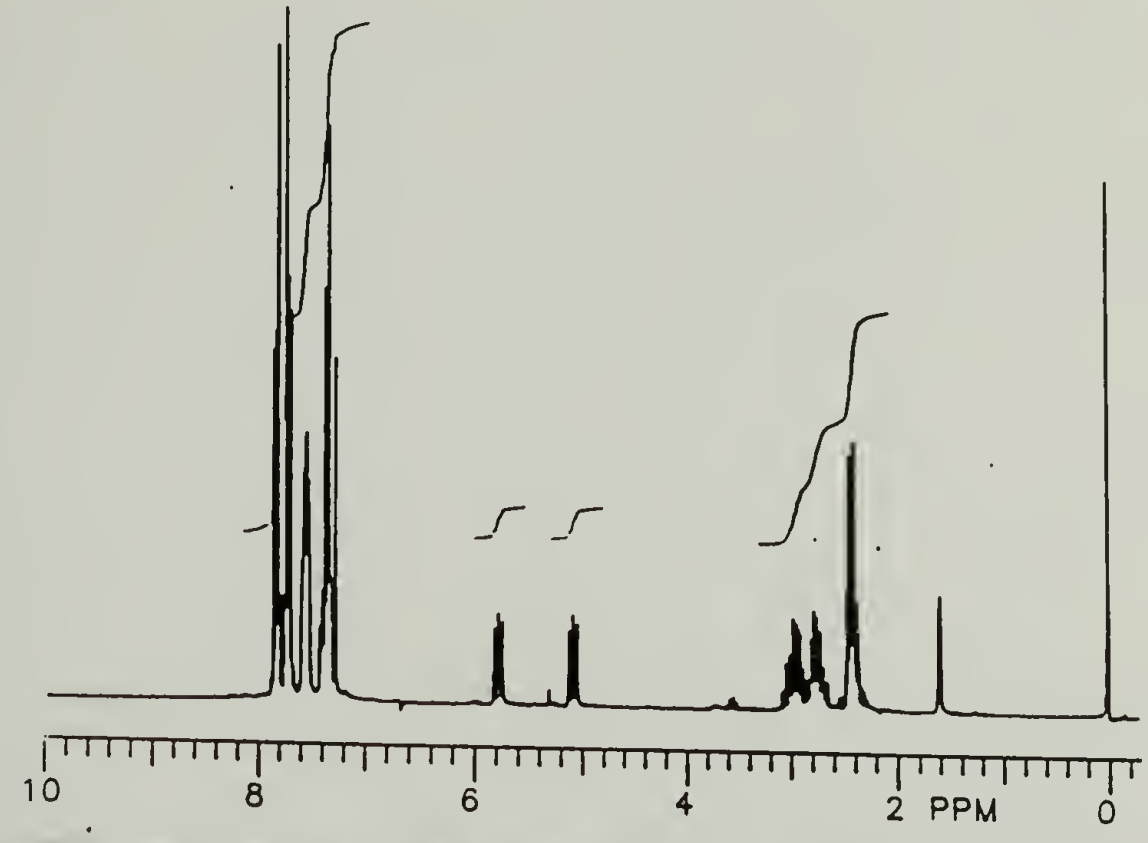

INFRARED SPECTRUM: 4-phenyl-4-phthalimido[4-^{13}C]butyronitrile

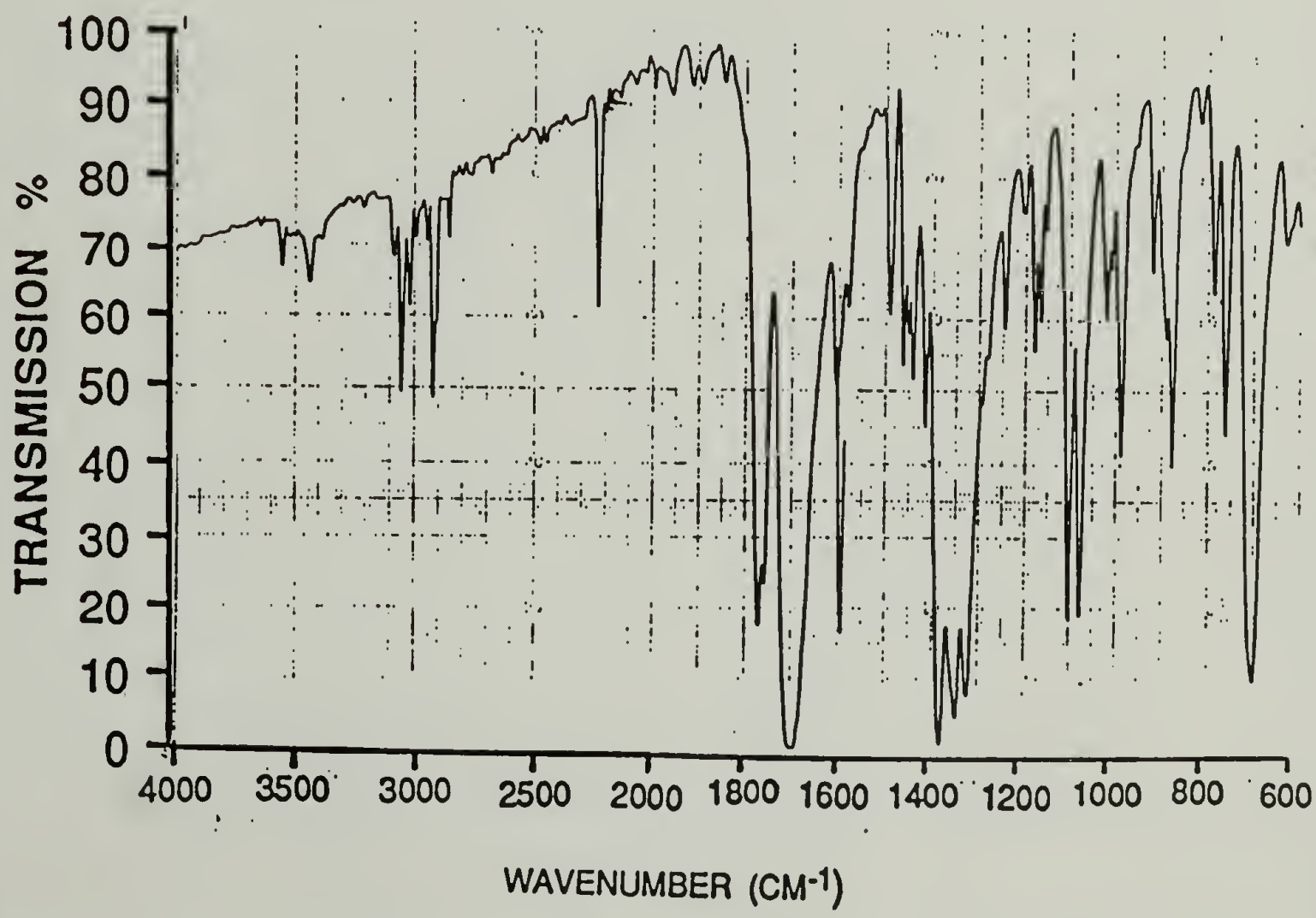

^{1}H NMR SPECTRUM: 4-phenyl-4-phthalimidobutyronitrile

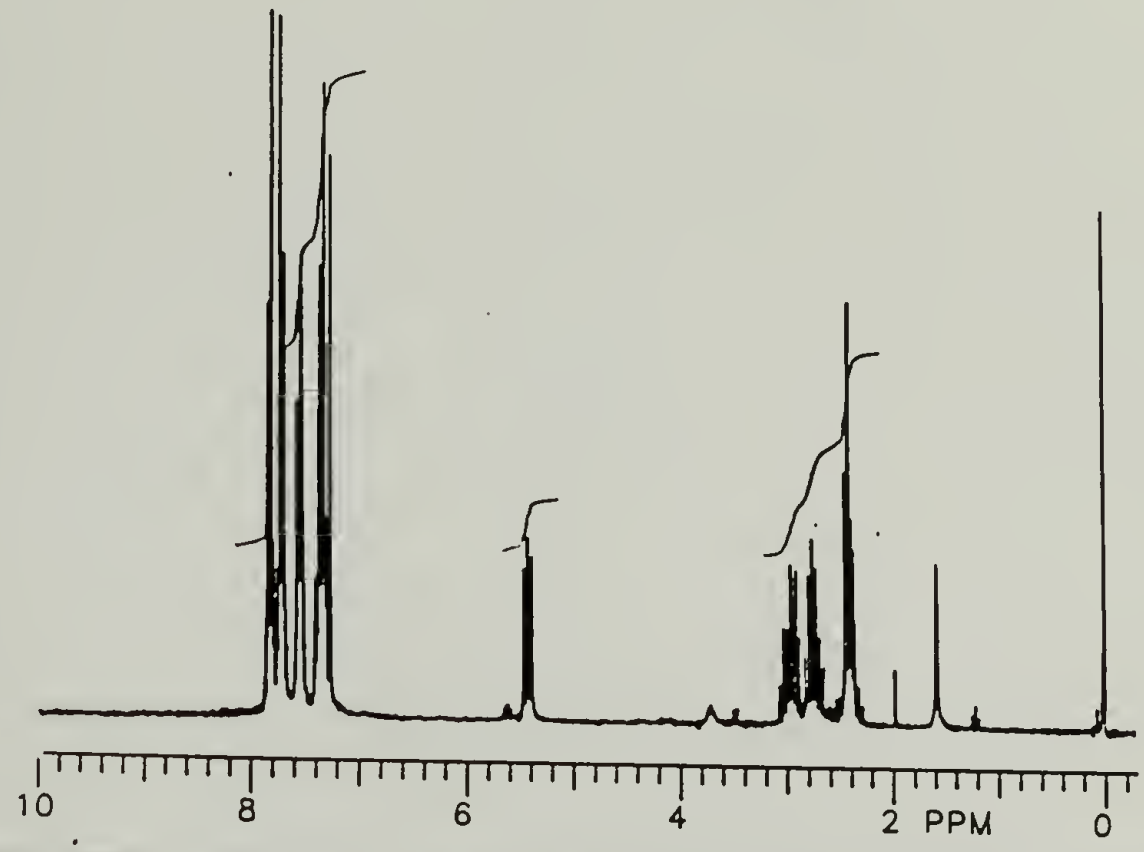

INFRARED SPECTRUM: 4-phenyl-4-phthalimidobutyronitrile

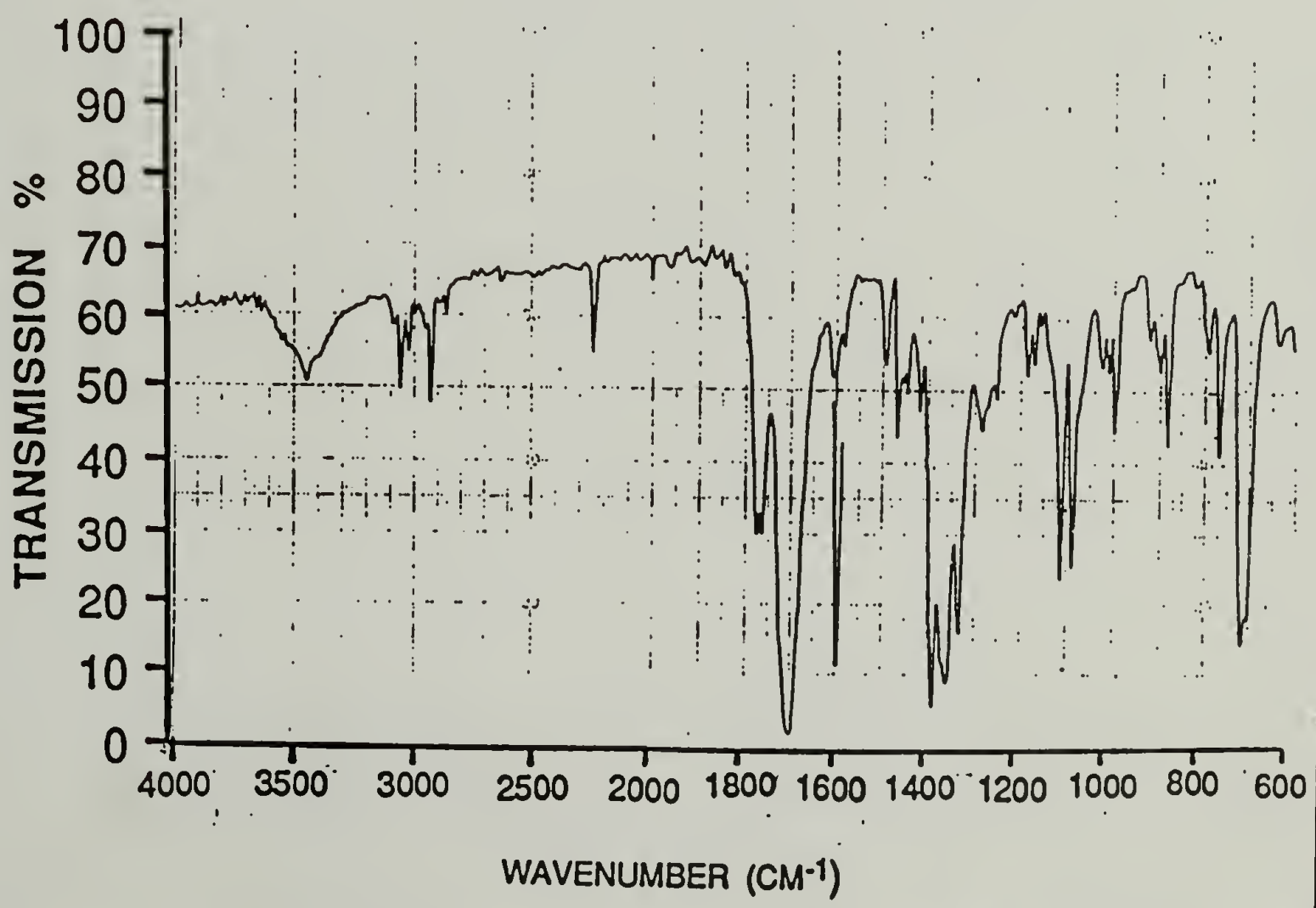

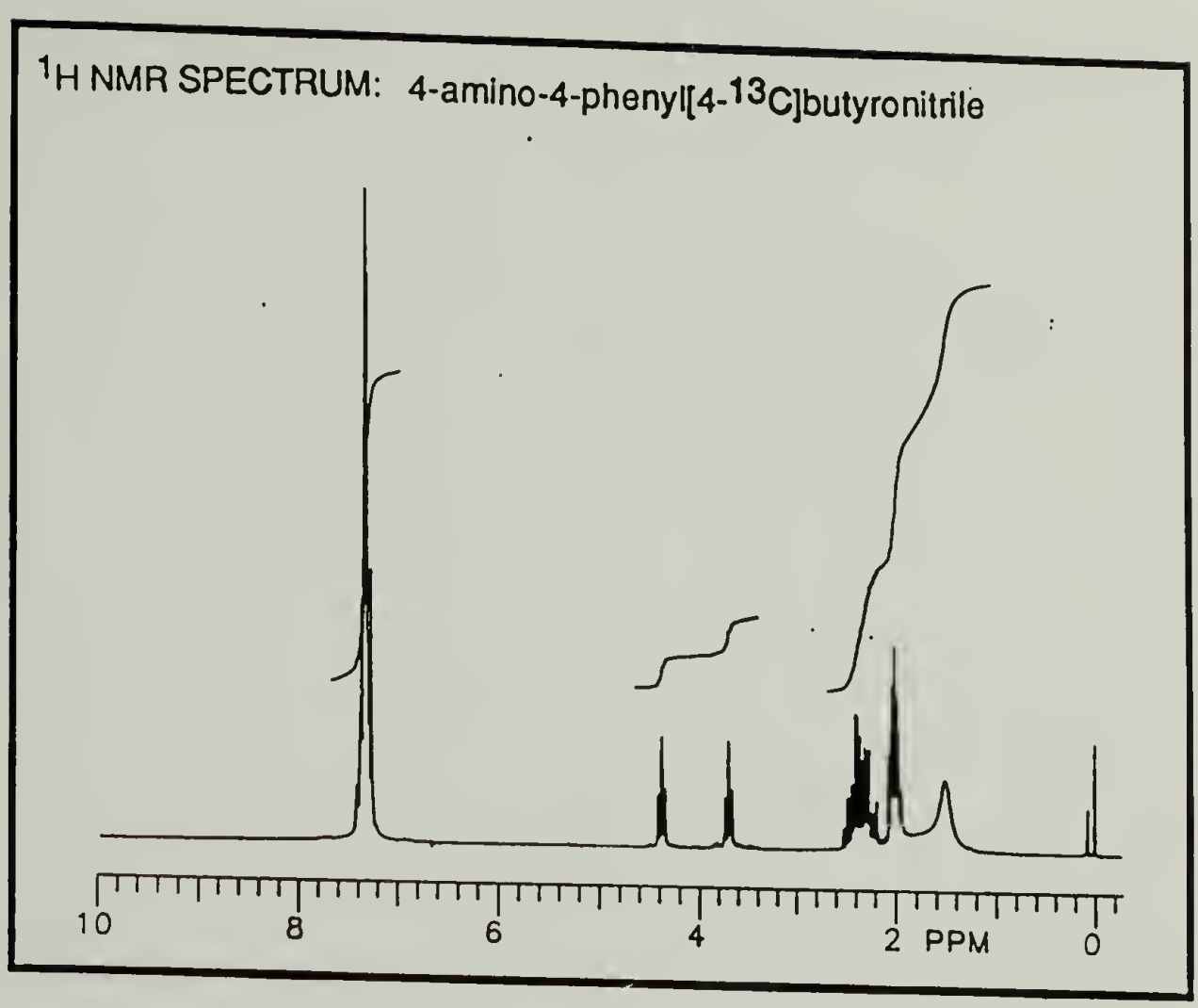
^{1}H NMR SPECTRUM: 4-amino-4-phenyl[4-^{13}C]butyronitrile
10
8
6
4
2 PPM
0

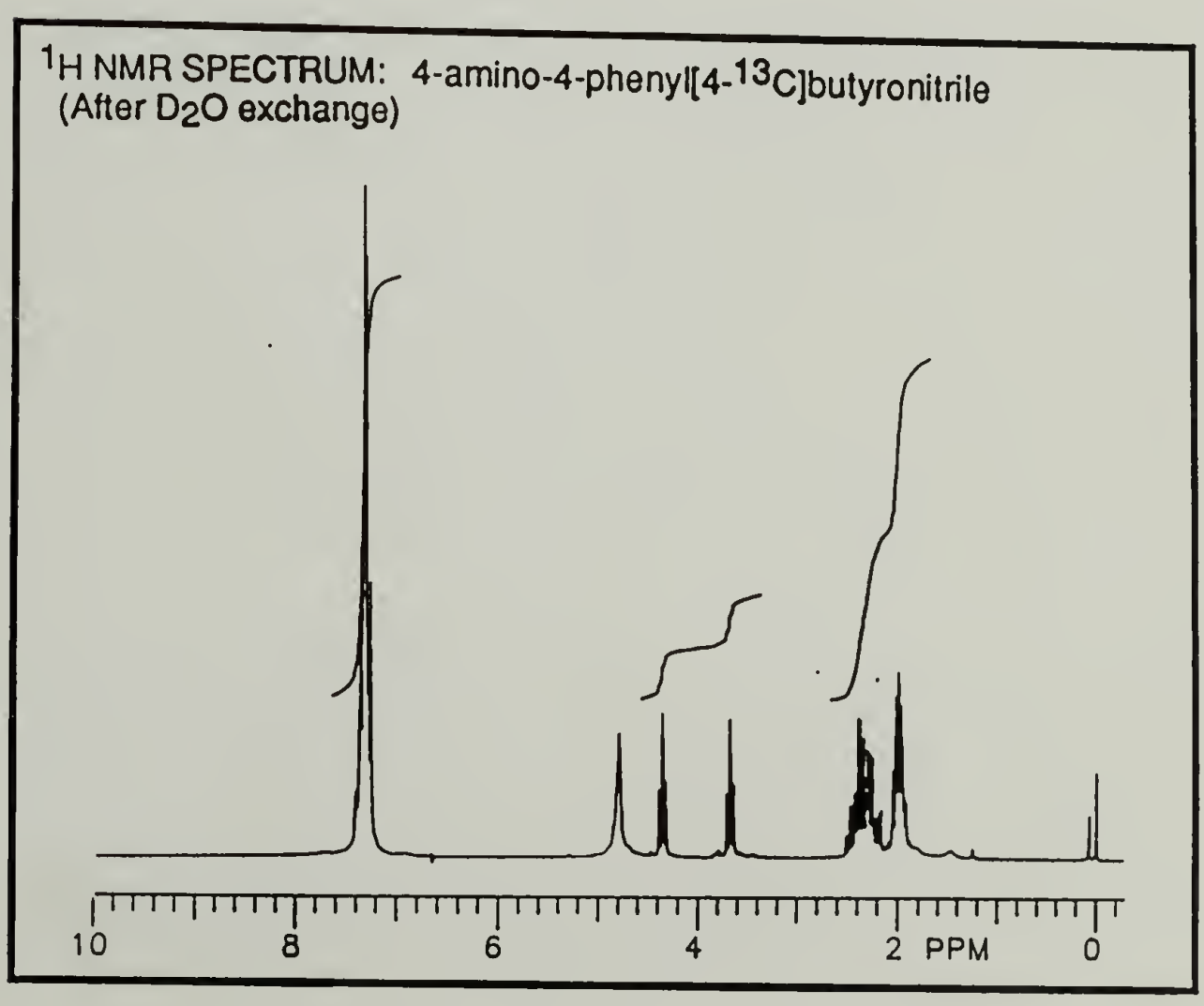
^{1}H NMR SPECTRUM: 4-amino-4-phenyl[4-^{13}C]butyronitrile
(After D_2O exchange)
10
8
6
4
2 PPM
0

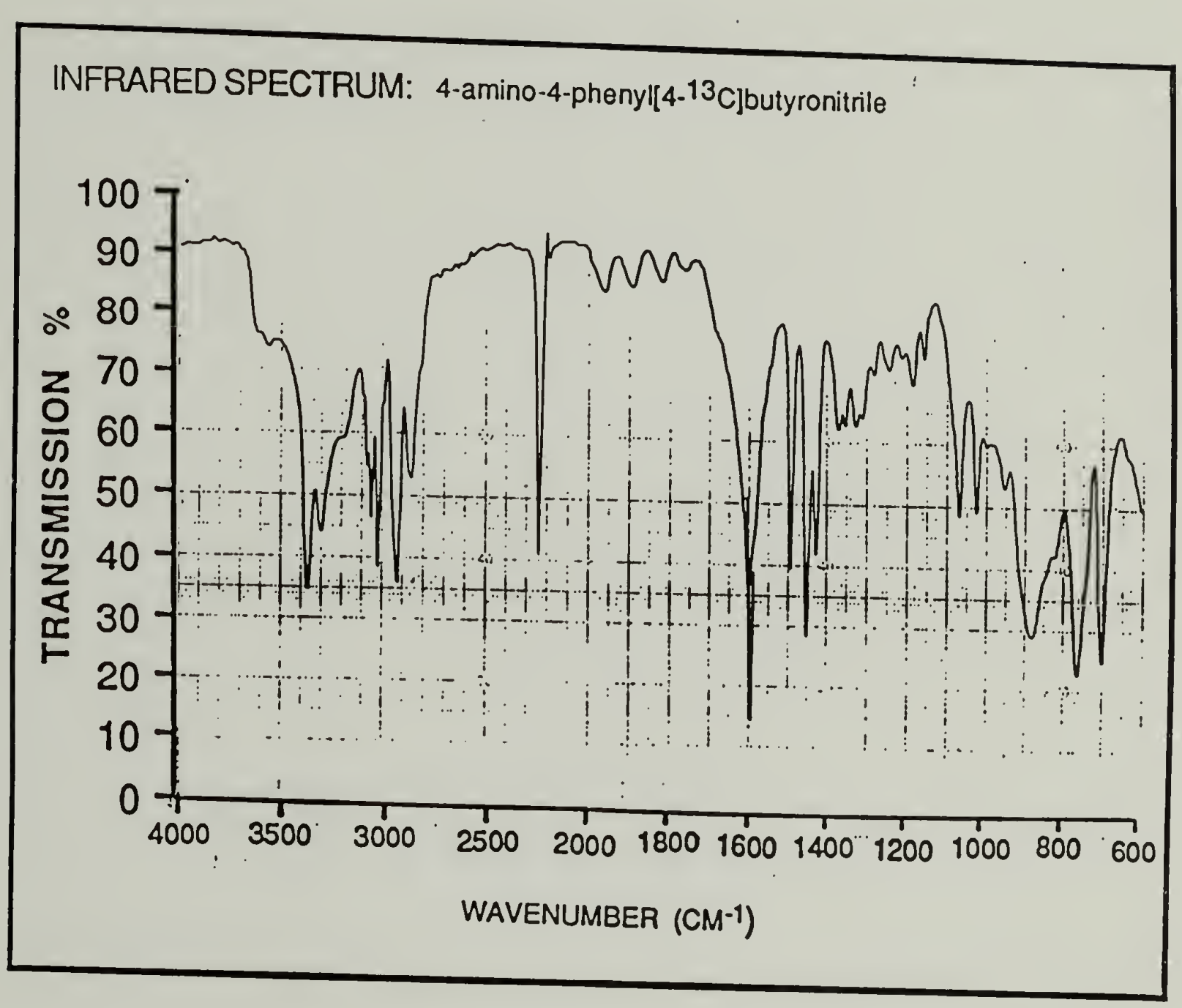
INFRARED SPECTRUM: 4-amino-4-phenyl[4-13C]butyronitrile
TRANSMISSION %
100
90
80
70
60
50
40
30
20
10
0
4000
3500
3000
2500
2000
1800
1600
1400
1200
1000
800
600
WAVENUMBER (CM-1)

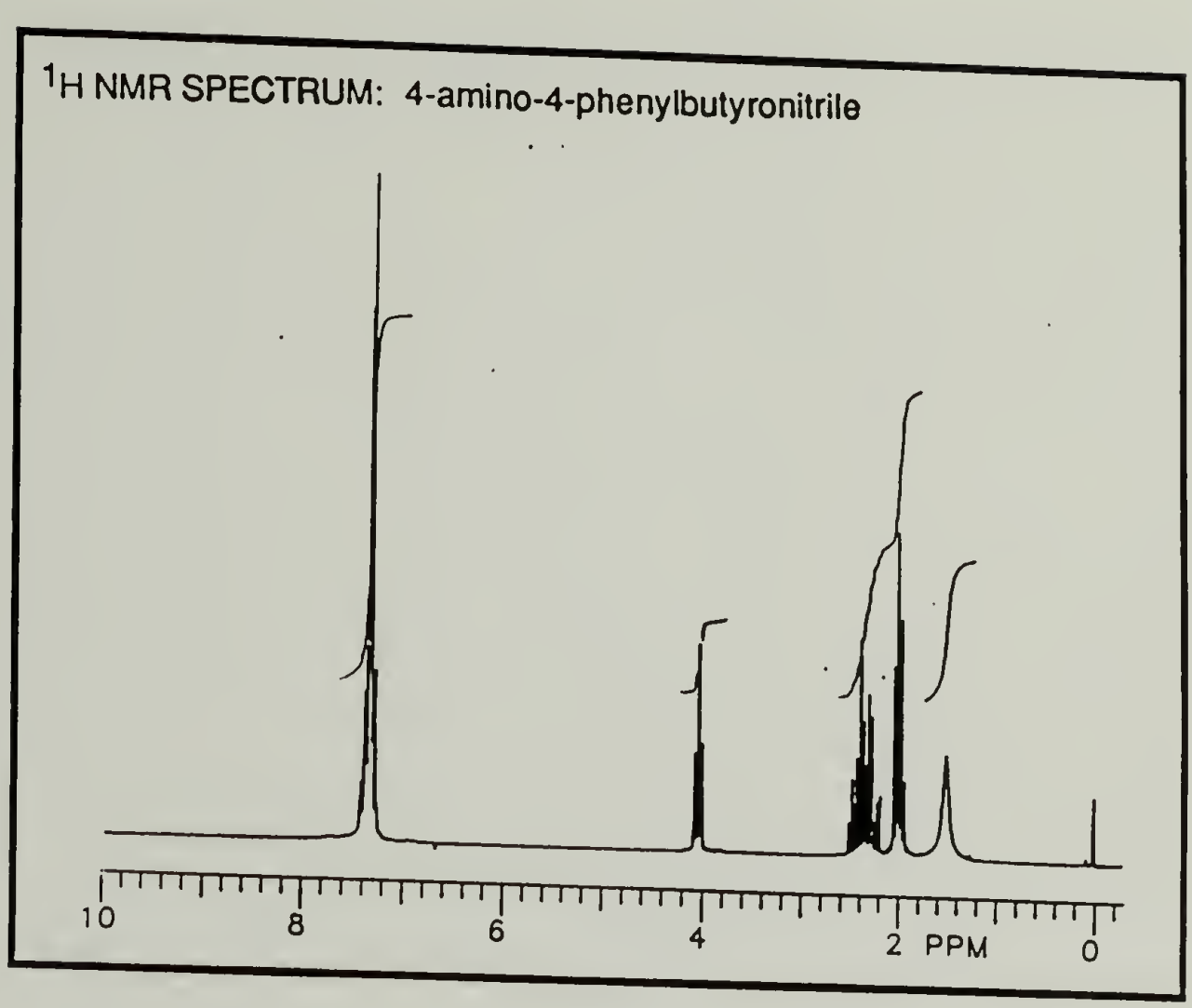
^{1}H NMR SPECTRUM: 4-amino-4-phenylbutyronitrile
10
8
6
4
2 PPM
0

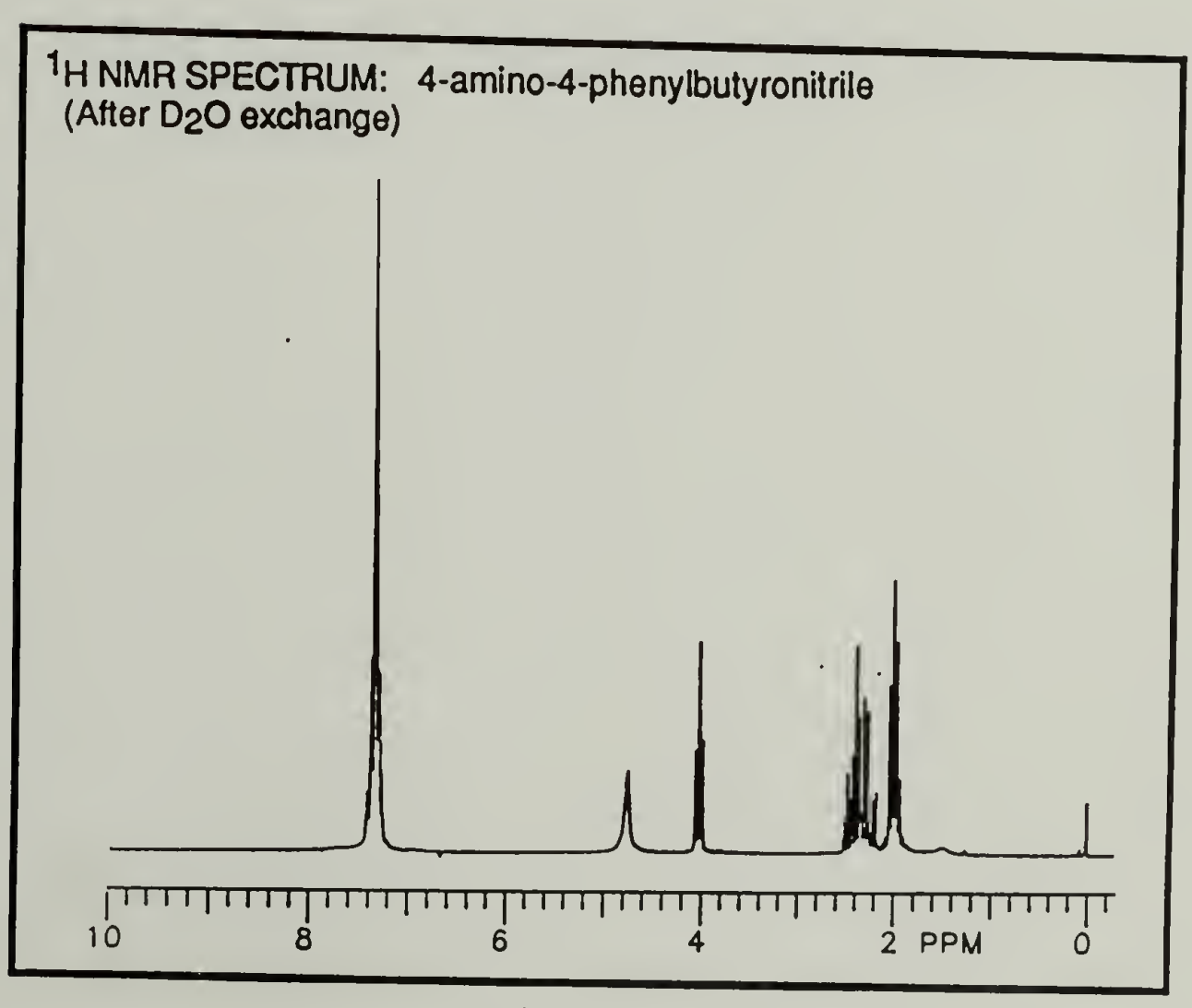
^{1}H NMR SPECTRUM: 4-amino-4-phenylbutyronitrile
(After D_2O exchange)
10
8
6
4
2 PPM
0

INFRARED SPECTRUM: 4-amino-4-phenylbutyronitrile

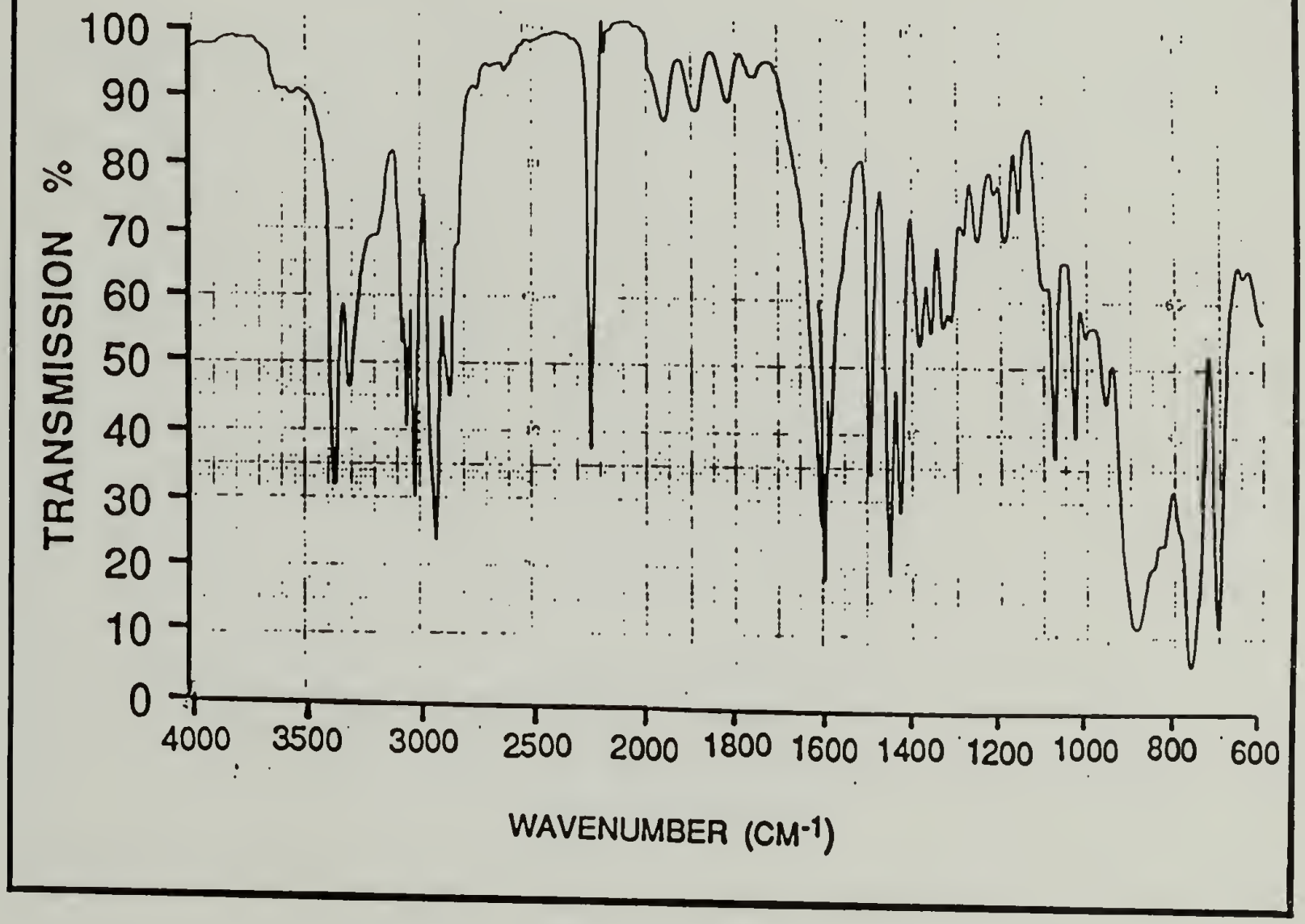

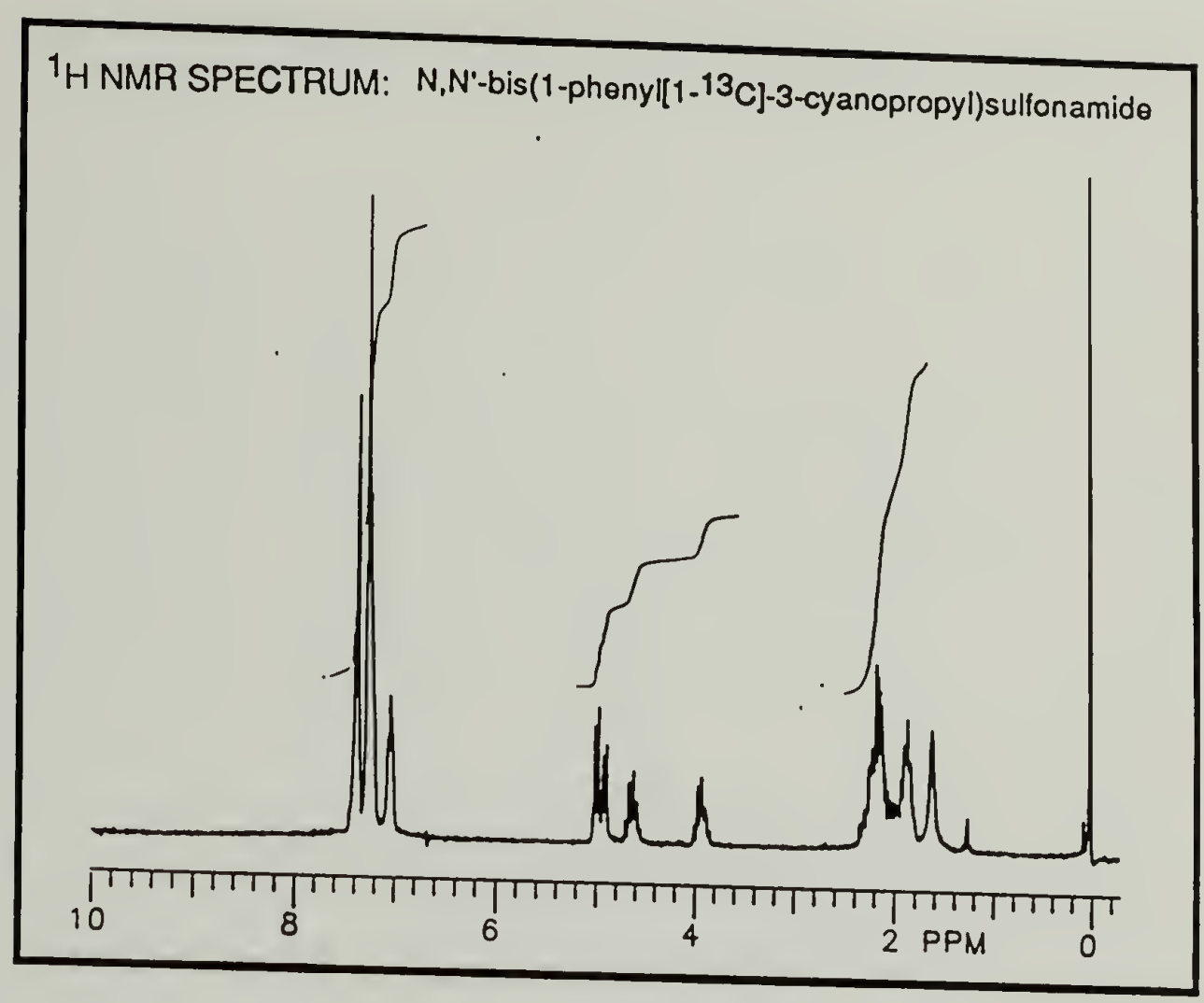
^{1}H NMR SPECTRUM: N,N'-bis(1-phenyl[1-^{13}C]-3-cyanopropyl)sulfonamide
10
8
6
4
2 PPM
0

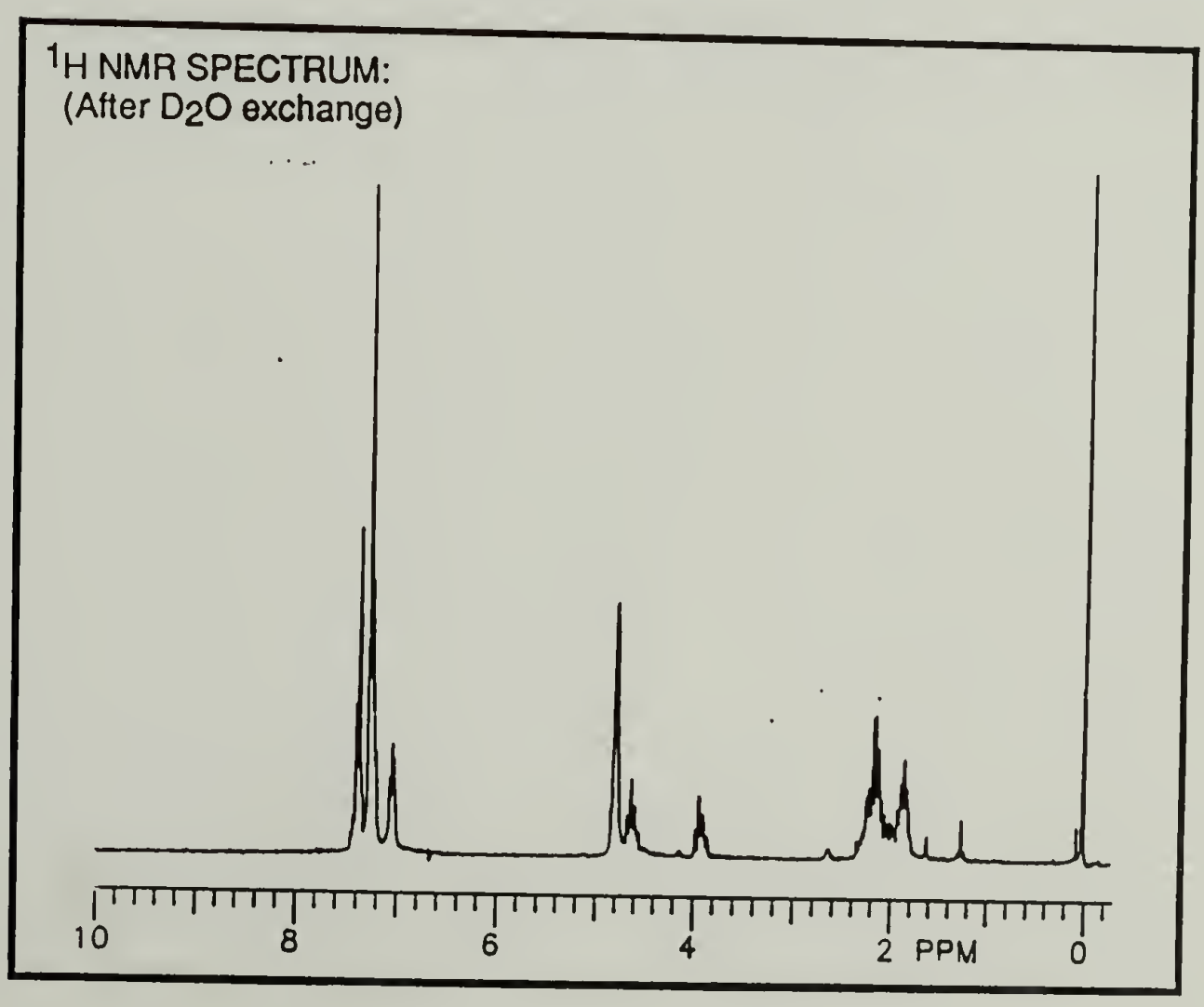
^{1}H NMR SPECTRUM:
(After D_2O exchange)
10
8
6
4
2 PPM
0

INFRARED SPECTRUM: N,N'-bis(1-phenyl[1-^{13}C]-3-cyanopropyl)sulfonamide

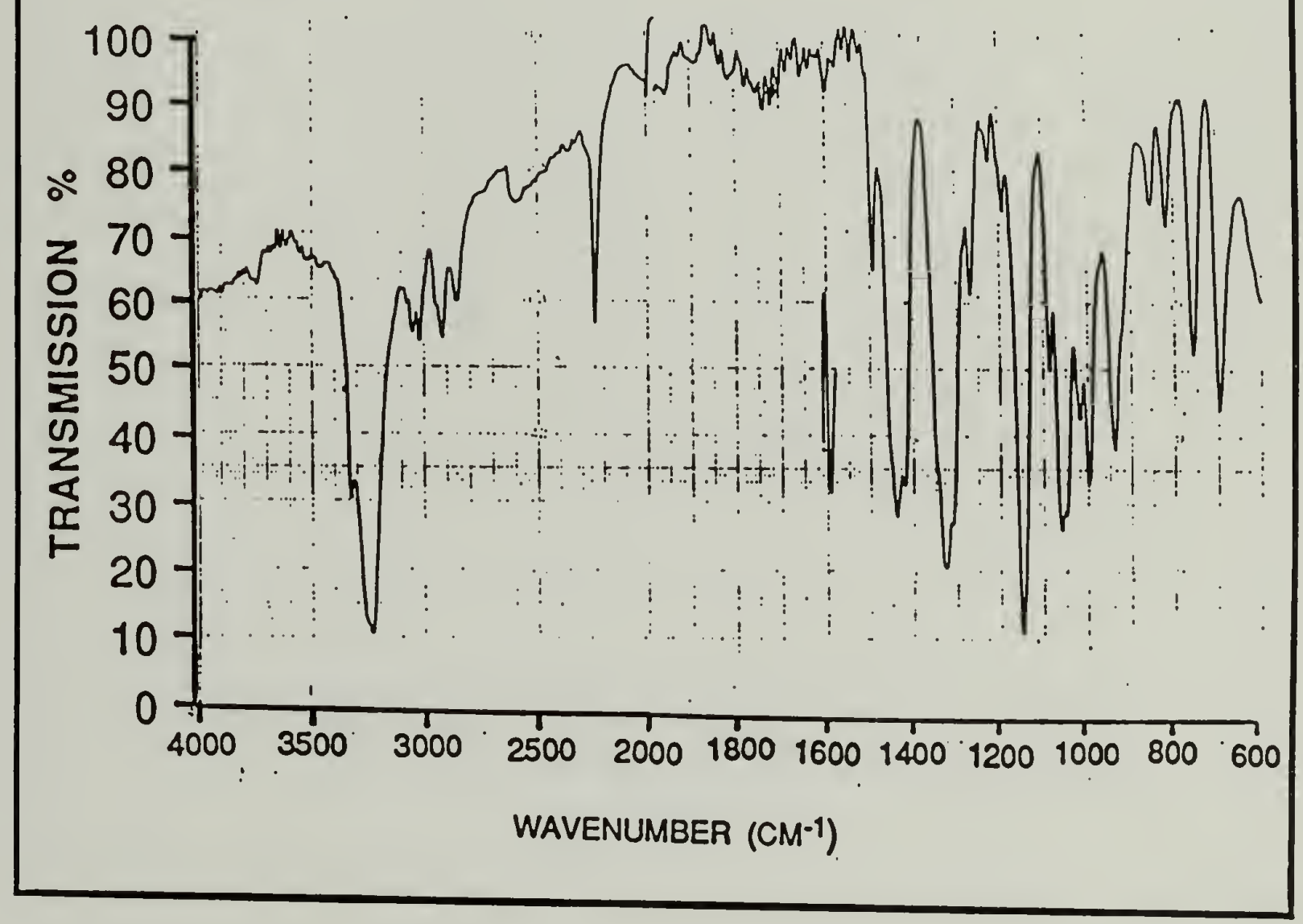

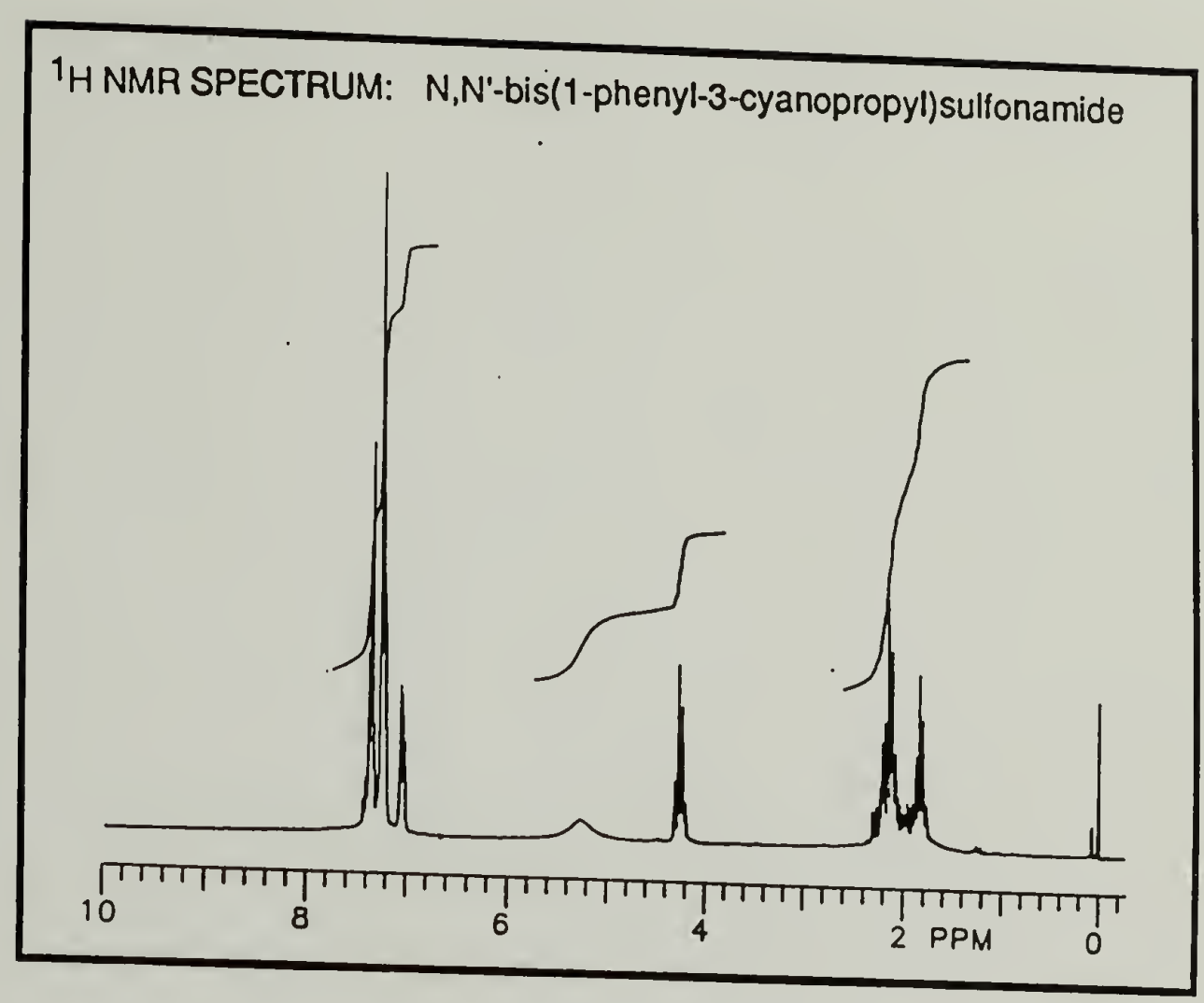
^{1}H NMR SPECTRUM: N,N'-bis(1-phenyl-3-cyanopropyl)sulfonamide
10
8
6
4
2 PPM
0

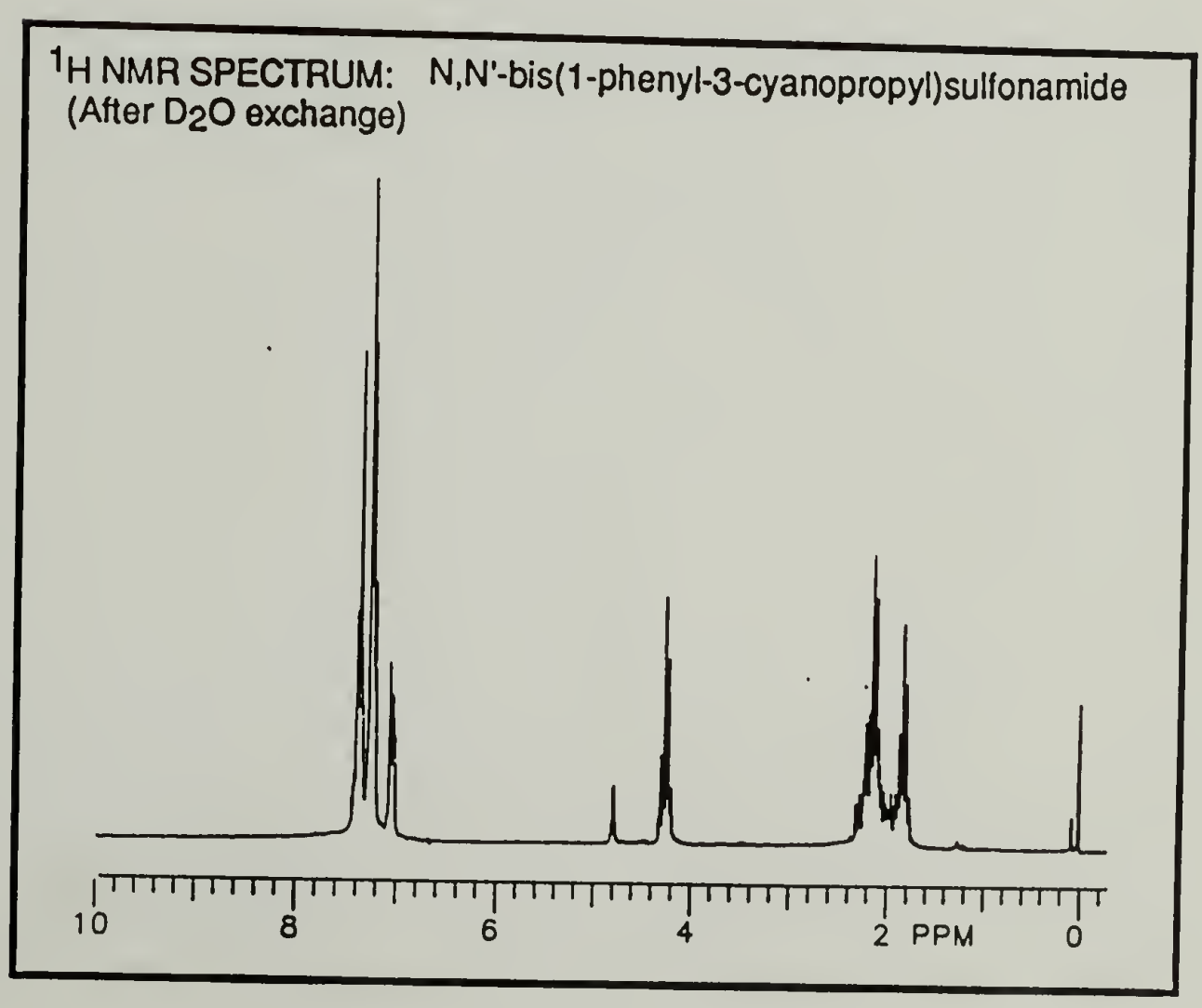
^{1}H NMR SPECTRUM: N,N'-bis(1-phenyl-3-cyanopropyl)sulfonamide
(After D_2O exchange)
10
8
6
4
2 PPM
0

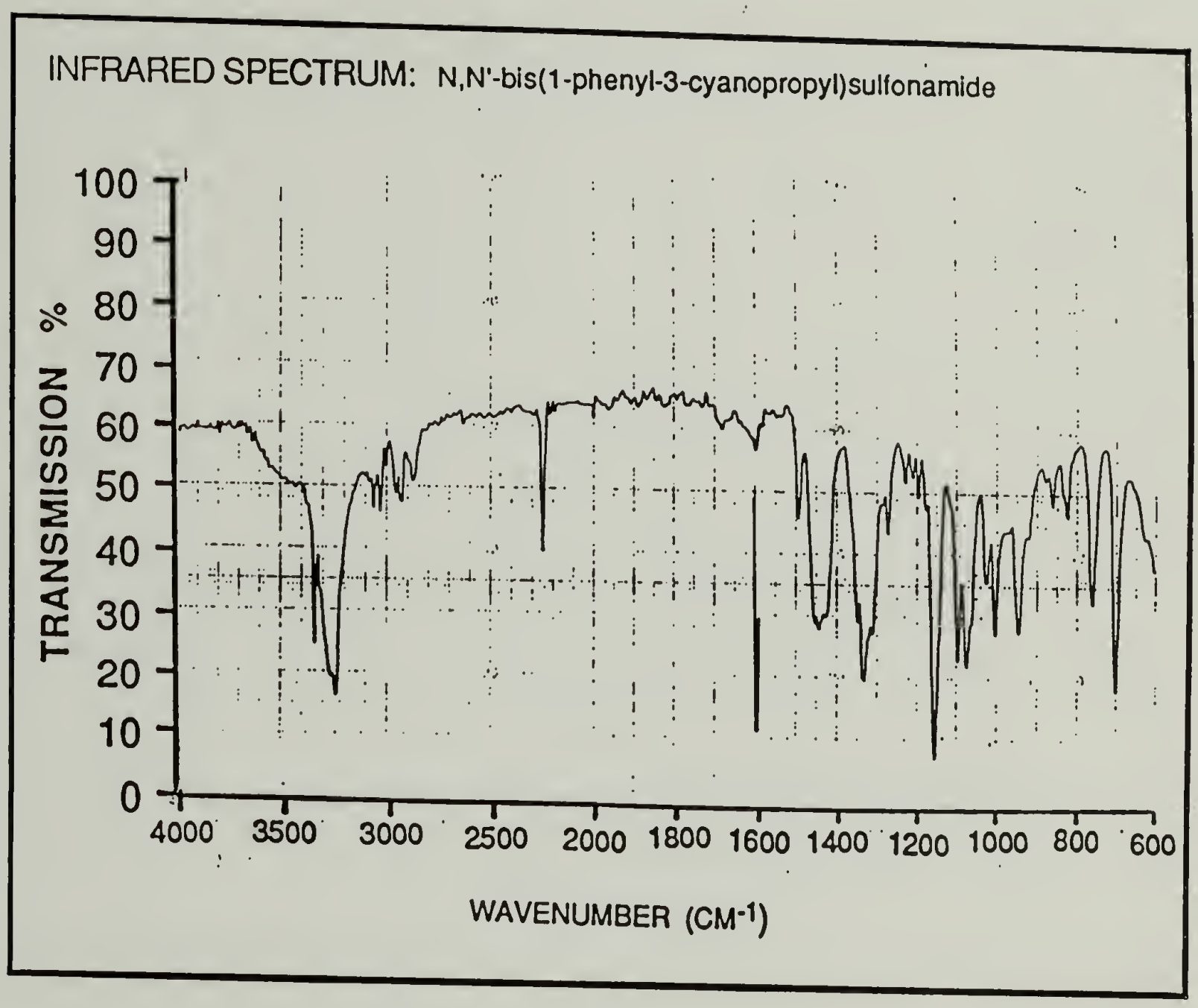
INFRARED SPECTRUM: N,N'-bis(1-phenyl-3-cyanopropyl)sulfonamide
TRANSMISSION %
100
90
80
70
60
50
40
30
20
10
0
4000
3500
3000
2500
2000
1800
1600
1400
1200
1000
800
600
WAVENUMBER (CM-1)

^{1}H NMR SPECTRUM: 4,4'-azobis(4-phenyl[4-^{13}C]butyronitrile) (1c)

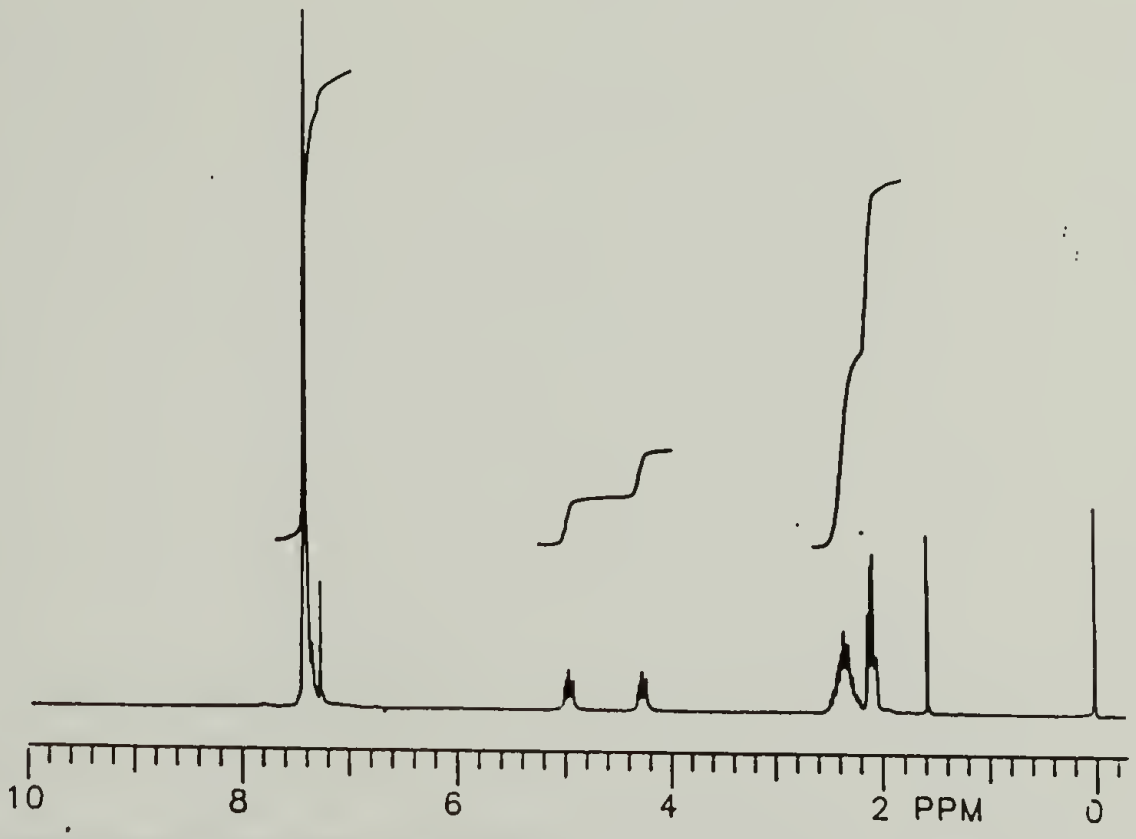

INFRARED SPECTRUM: 4,4'-azobis(4-phenyl[4-^{13}C]butyronitrile) (1c)

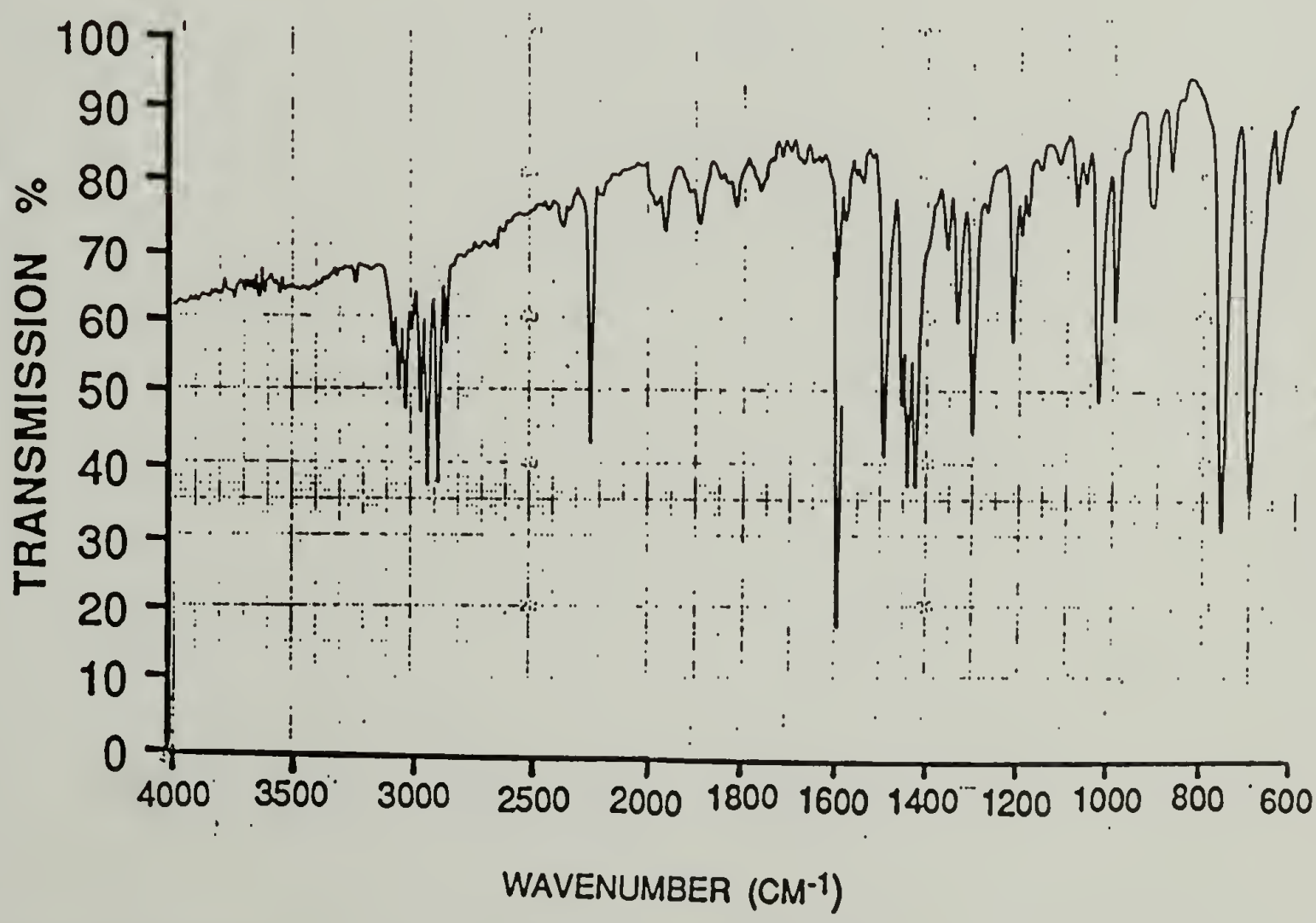

^{13}C NMR SPECTRUM: 4,4'-azobis(4-phenyl[4-^{13}C]butyronitrile) (1c)

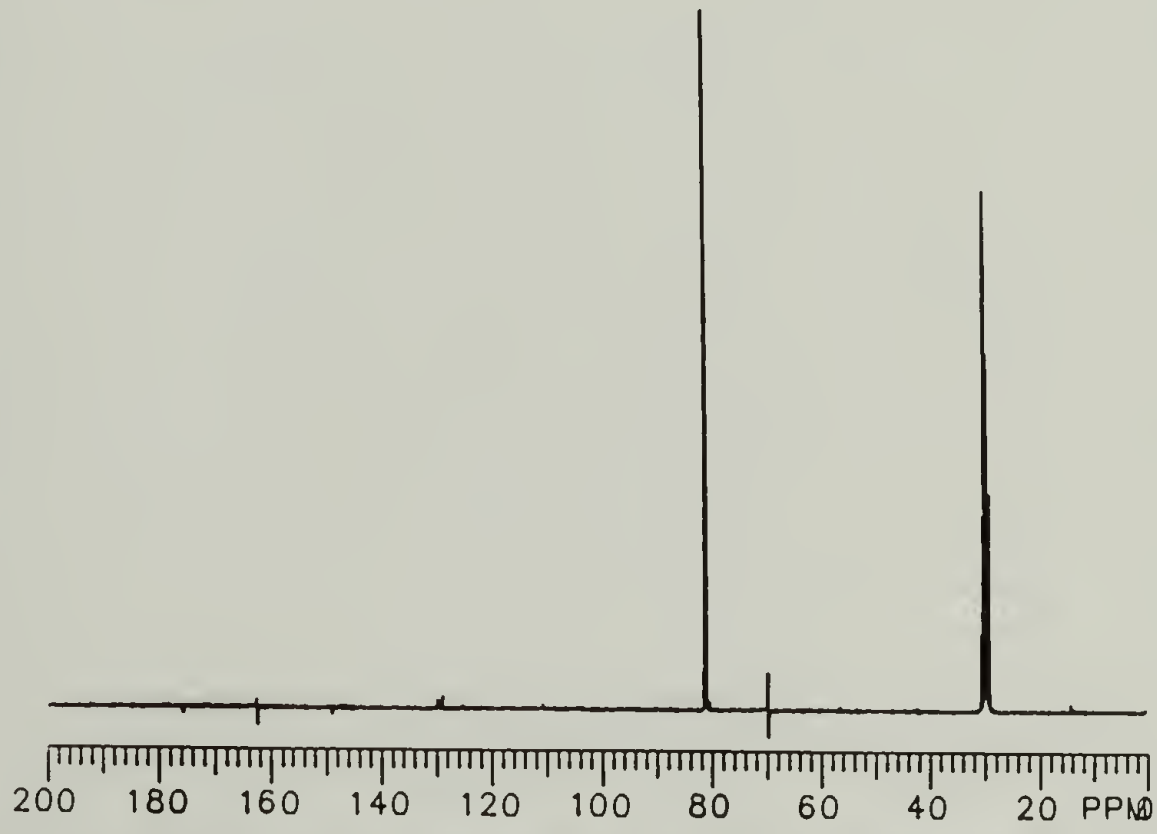

^{1}H NMR SPECTRUM: 4,4'-azobis(4-phenylbutyronitrile)

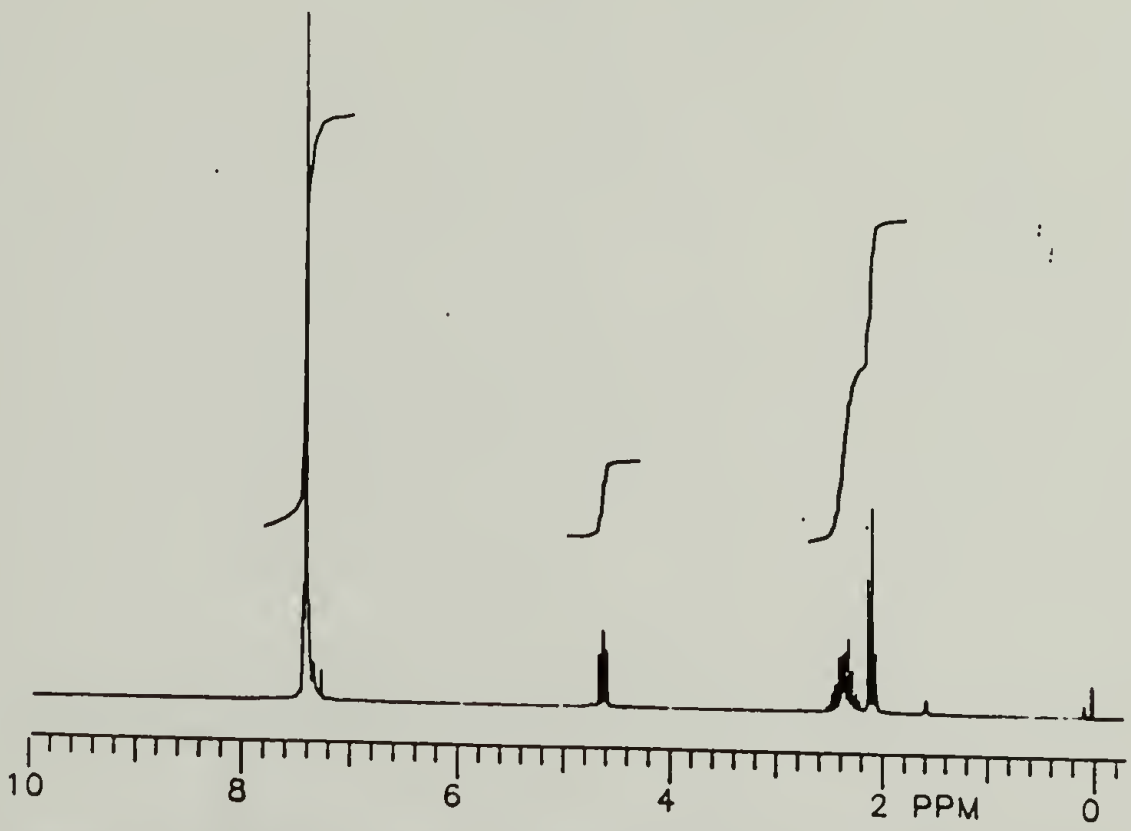

INFRARED SPECTRUM: 4,4'-azobis(4-phenylbutyronitrile)

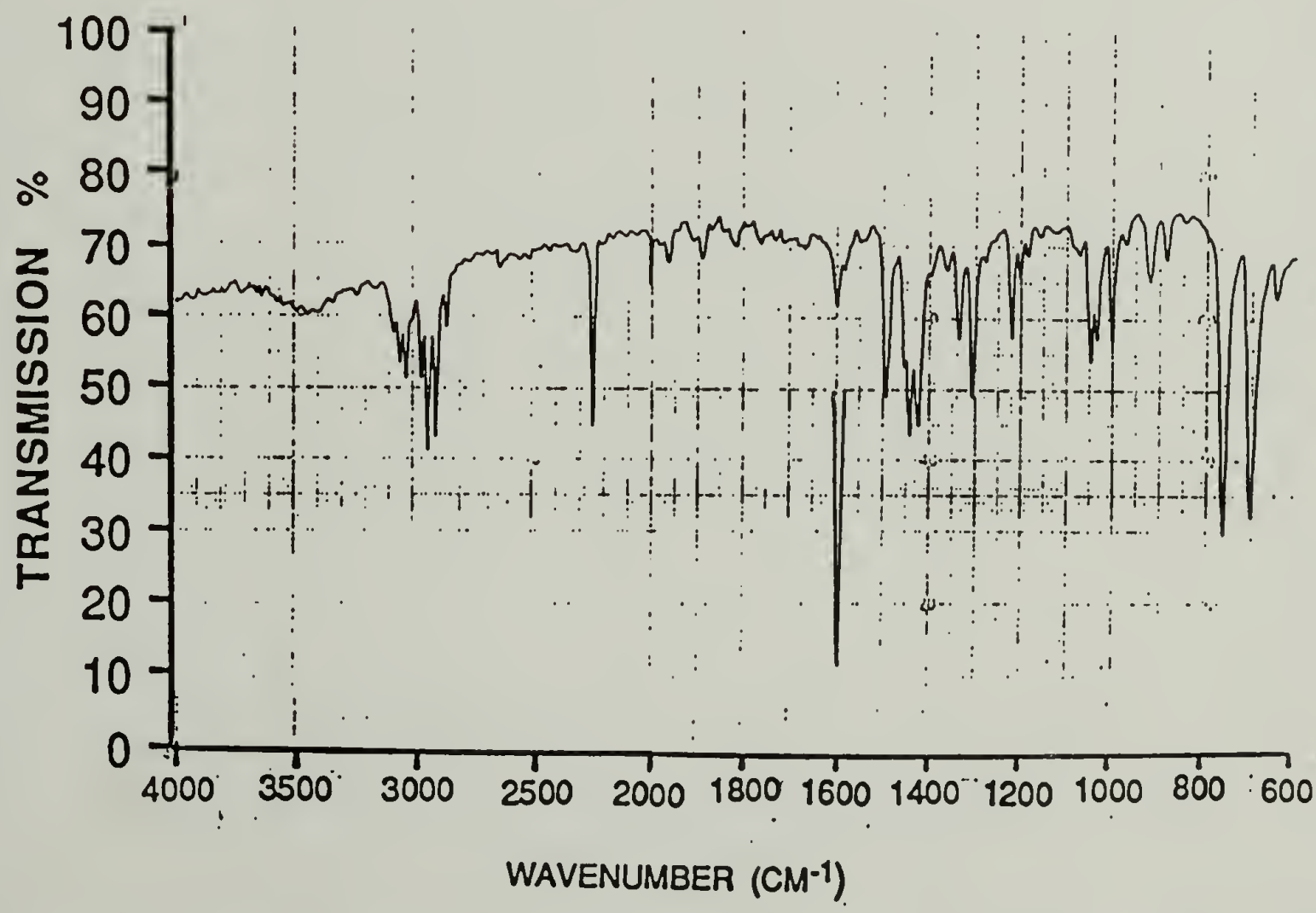

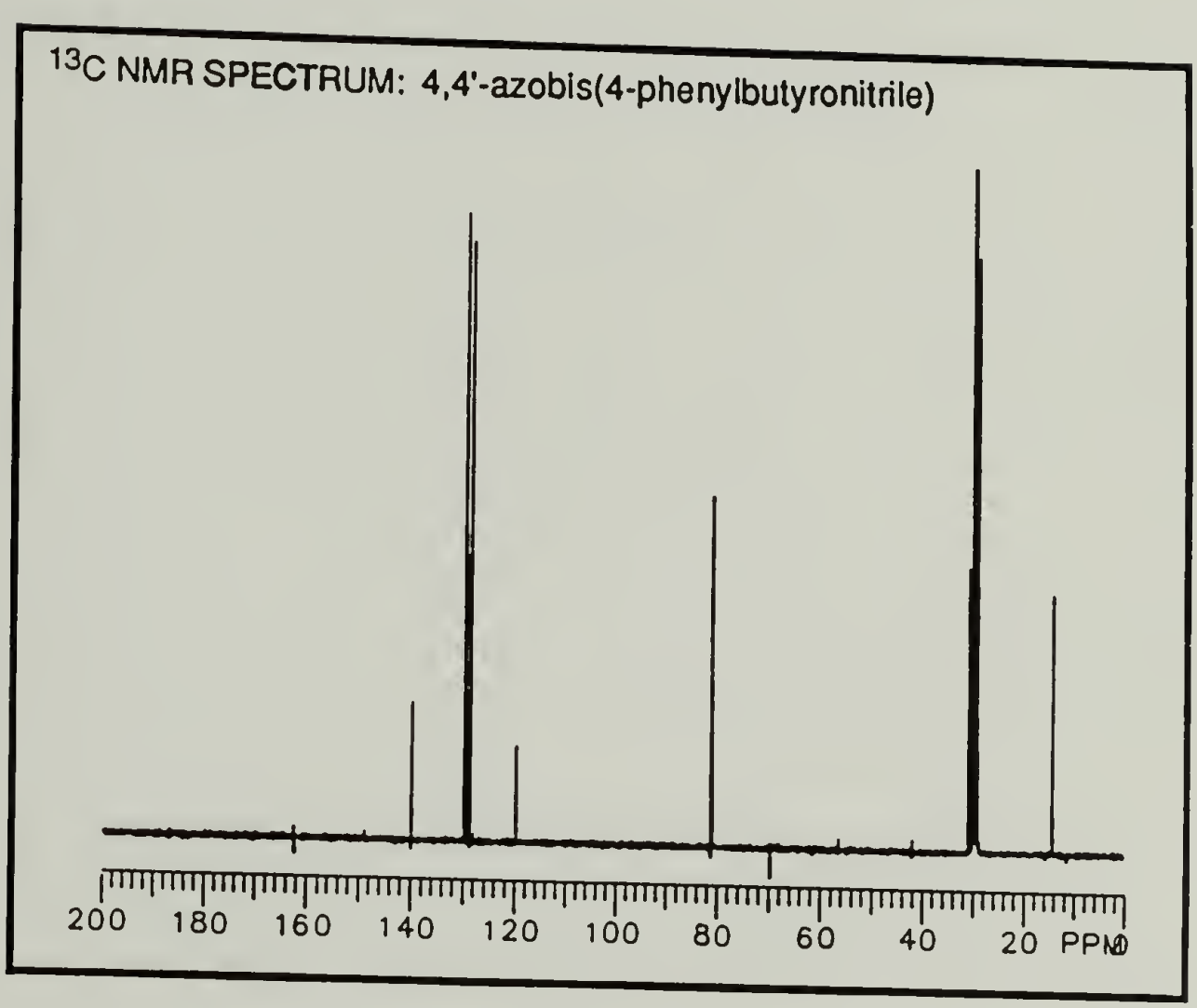
^{13}C NMR SPECTRUM: 4,4'-azobis(4-phenylbutyronitrile)
200
180
160
140
120
100
80
60
40
20
PPM

APPENDIX B

Polymerization Data for Natural-Abundance SAN Copolymers

Table B-1. Polymerization Data for SAN Copolymers Derived from Natural-Abundance **1a**.[a]

copolymer[b]	styrene, mmol	acrylonitrile, mmol	styrene / acrylonitrile ([S]/[A])	polymer, mg	convn, %
1N	7.700	2.484	3.10	98	10.5
2N	7.883	2.280	3.46	98	10.4
3N	8.029	2.158	3.72	94	9.9
4N	8.412	1.743	4.83	92	9.5
5N	8.397	1.511	5.56	88	9.2
6N	8.371	1.317	6.36	85	9.0
7N	8.574	1.189	7.21	94	9.8
8N	8.609	0.9159	9.40	84	8.9

[a] Conditions: 14.5 mg of natural-abundance **1a**; 2.62 g of benzene; 33 °C; 3 h irradiation with 350 nm light.
[b] The number given in this column is the number of the enriched copolymer prepared with the same or nearly the same monomer feed ratio ([S]/[A]).

Table B-2. Polymerization Data for SAN Copolymers Derived from Natural-Abundance **1b**.[a]

copolymer[b]	styrene, mmol	acrylonitrile, mmol	styrene / acrylonitrile ([S]/[A])	polymer, mg	convn, %	time[c], min
9N	15.84	7.900	2.00	186	9.0	157
10N	17.35	5.079	3.42	220	10.6	215
11N	17.63	4.159	4.24	157	7.6	180
12N	17.93	3.734	4.80	158	7.6	180
13N	18.20	3.183	5.72	159	7.7	197
14N	18.41	2.863	6.43	155	7.5	197
15N	18.55	2.533	7.32	171	8.3	215
16N	18.67	2.277	8.20	170	8.2	215

[a] Conditions: 80 mg of natural-abundance **1b**; 5.0 g of benzene; 33 °C.
[b] The number given in this column is the number of the enriched copolymer prepared with the same or nearly the same monomer feed ratio ([S]/[A]).
[c] This is the time of irradiation with 350 nm light.

Table B-3. Polymerization Data for SAN Copolymers Derived from Natural-Abundance **1c**.[a]

copolymer[b]	styrene, mmol	acrylonitrile, mmol	styrene / acrylonitrile ([S]/[A])	polymer, mg	convn, %	time[c], min
18N	7.880	2.867	2.75	88	9.0	217
19N	7.798	3.232	2.41	99	10.1	217
20N	7.572	3.566	2.12	95	9.7	207
21N	7.387	3.965	1.86	99	10.1	207
22N	7.062	4.412	1.60	98	10.1	202
23N	6.762	4.957	1.36	93	9.6	180
24N[d]	6.406	5.712	1.12	97	10.0	165
25N	5.877	6.772	0.868	105	10.8	160

[a] Conditions: 25 mg of natural-abundance **1c**; 2.62 g of benzene; 33 °C.
[b] The number given in this column is the number of the enriched copolymer prepared with the same or nearly the same monomer feed ratio ([S]/[A]).
[c] This is the time of irradiation with 350 nm light.
[d] Spectra of copolymer 24N were used to assign the baselines in the spectra of copolymer 26 used for NOE measurements.

APPENDIX C

Mass Spectra for Mercury Method Experiments

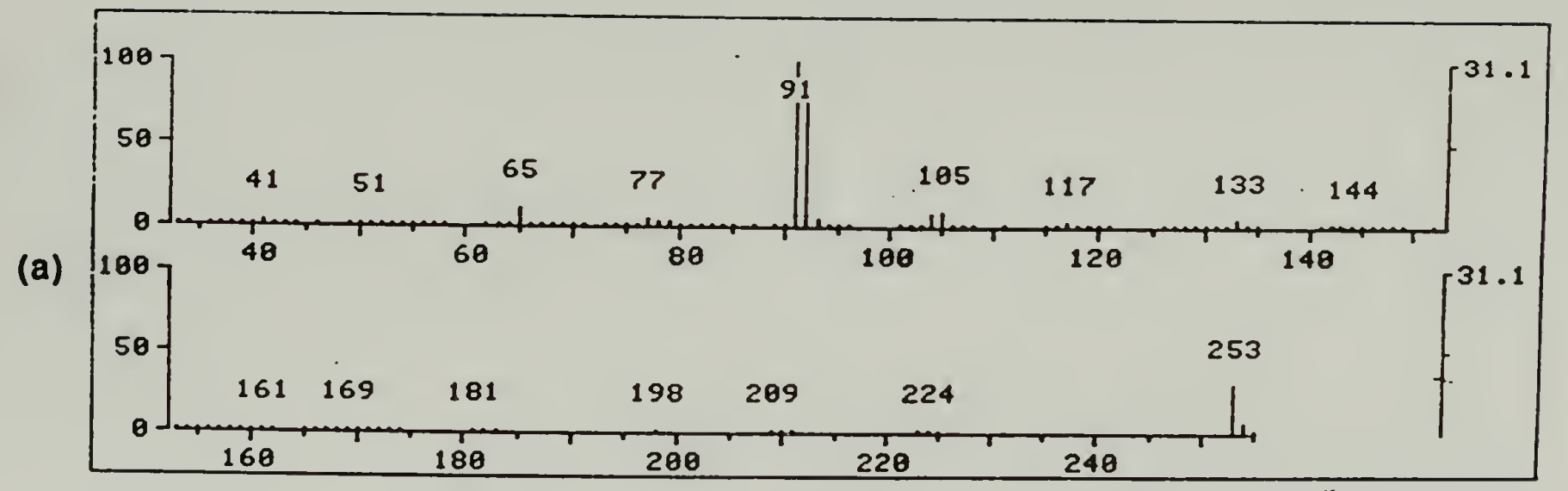

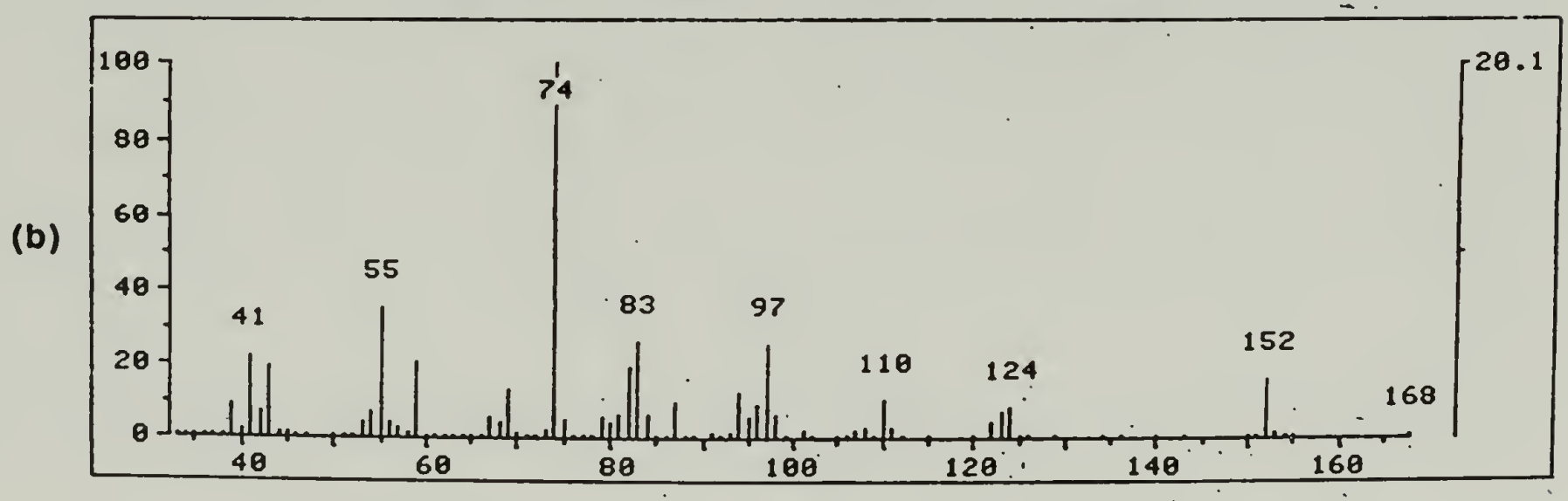

Figure C-1. Mass spectra of authentic samples of (a) 1,7-diphenylheptane, and (b) methyl 8-cyanooctanoate.

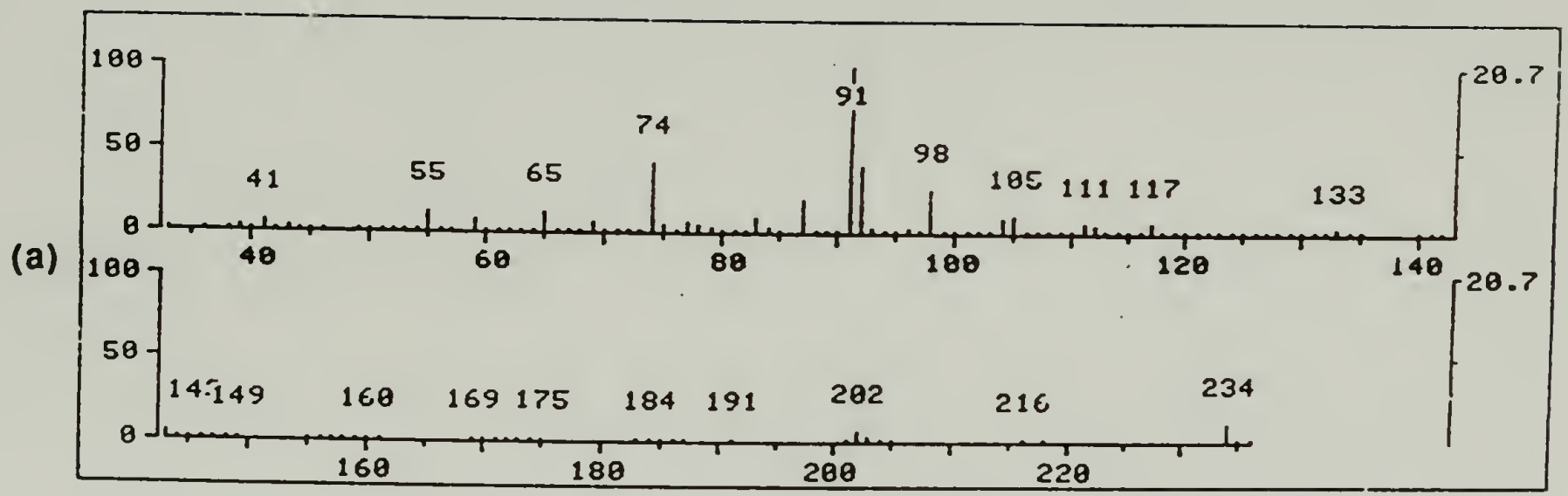

Figure C-2. Mass spectra of authentic samples of (a) methyl 8-phenyloctanoate, and (b) nonanedinitrile.

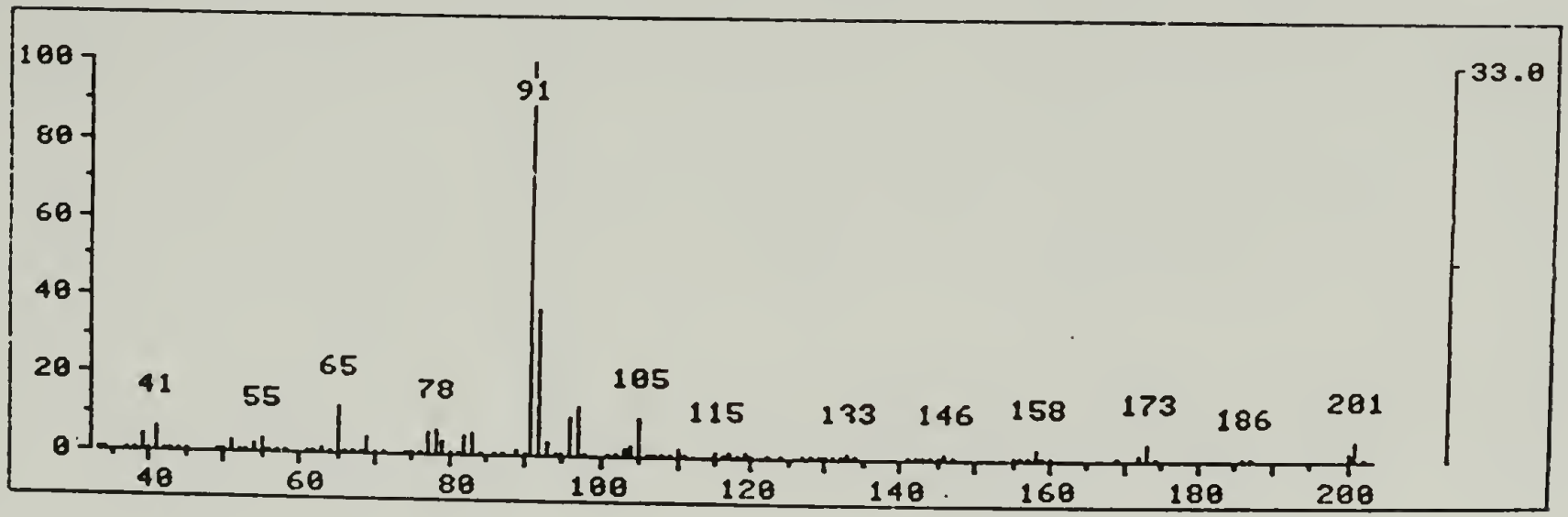

Figure C-3. Mass spectrum of an authentic sample of 8-phenyloctanenitrile.

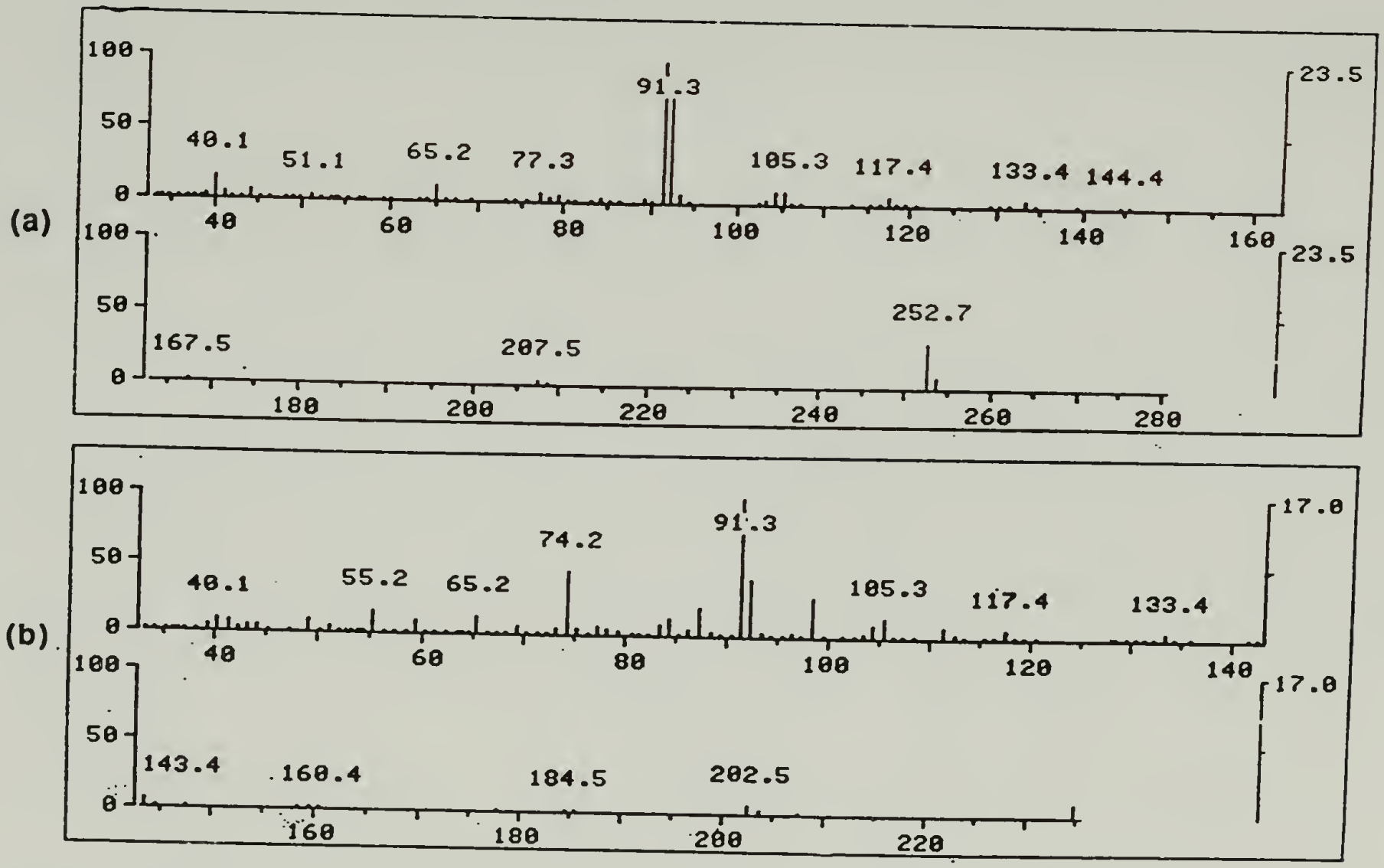

Figure C-4. Mass spectra of (a) 1,7-diphenylheptane, and (b) methyl 8-phenyloctanoate from a 5-phenyl-1-pentylmercuric bromide/styrene/methyl acrylate reaction mixture.

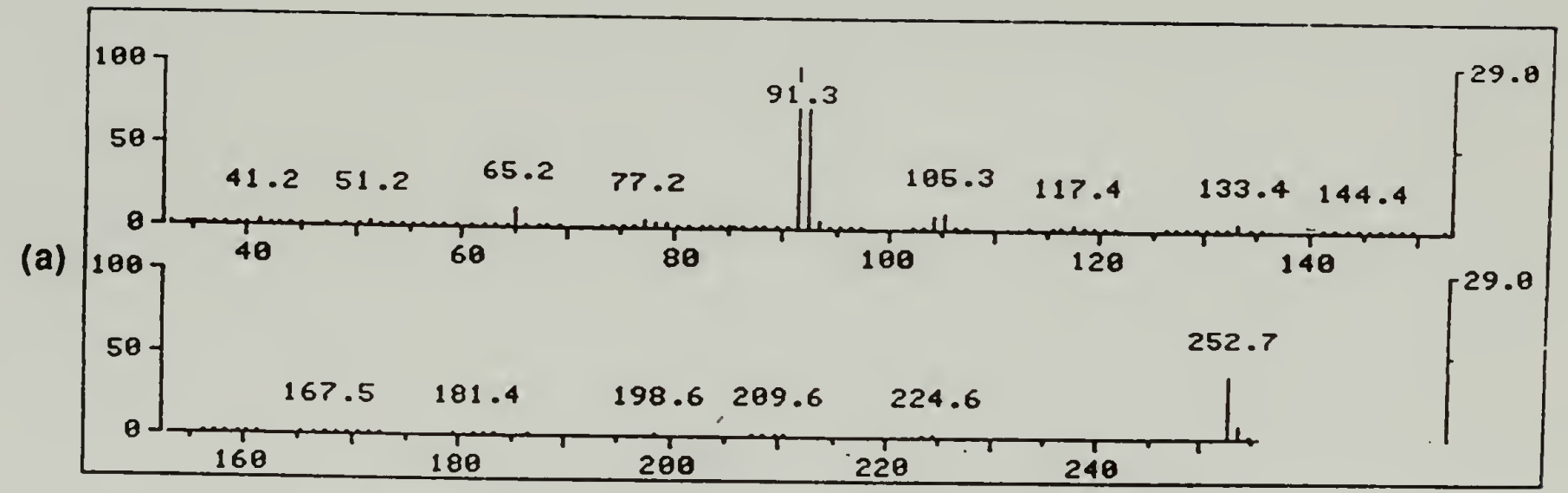

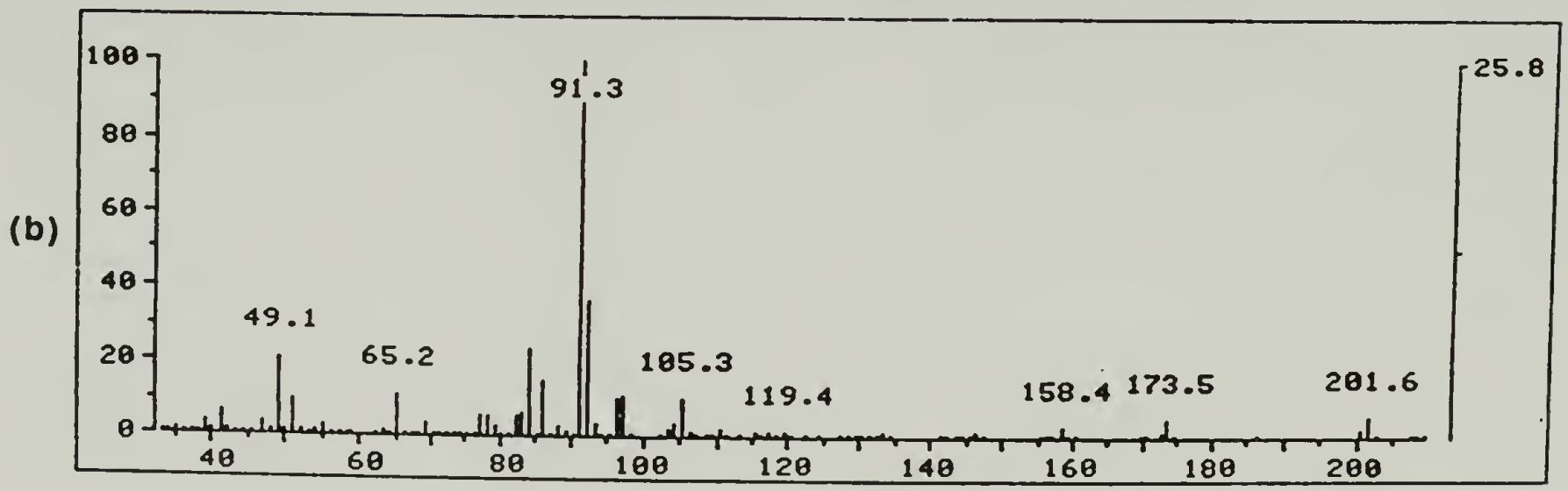

Figure C-5. Mass spectra of (a) 1,7-diphenylheptane, and (b) 8-phenyloctanenitrile from a 5-phenyl-1-pentylmercuric bromide/styrene/acrylonitrile reaction mixture.

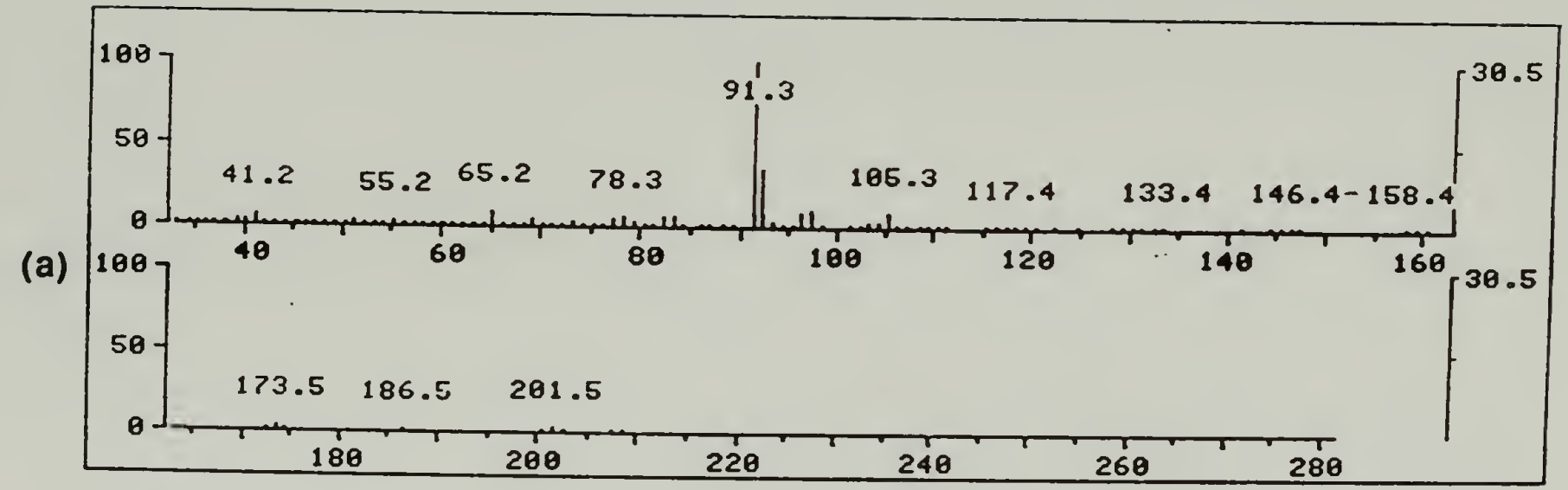

Figure C-6. Mass spectra of (a) 8-phenyloctanenitrile, and (b) nonanedinitrile from a 5-cyano-1-pentylmercuric bromide/styrene/acrylonitrile reaction mixture.

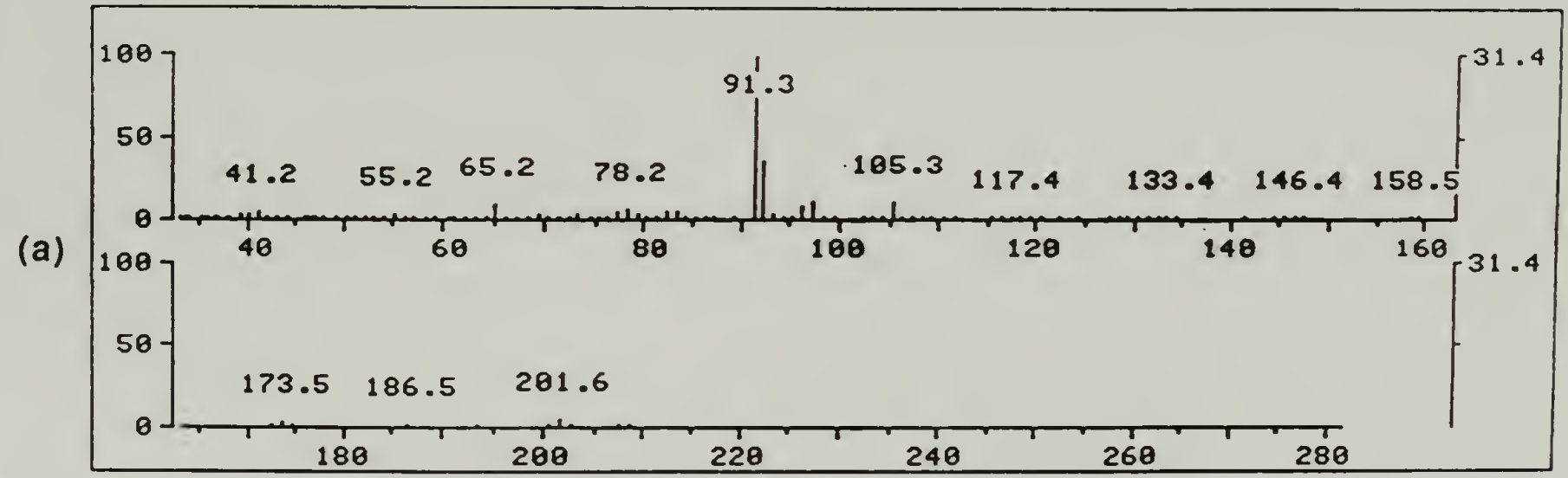

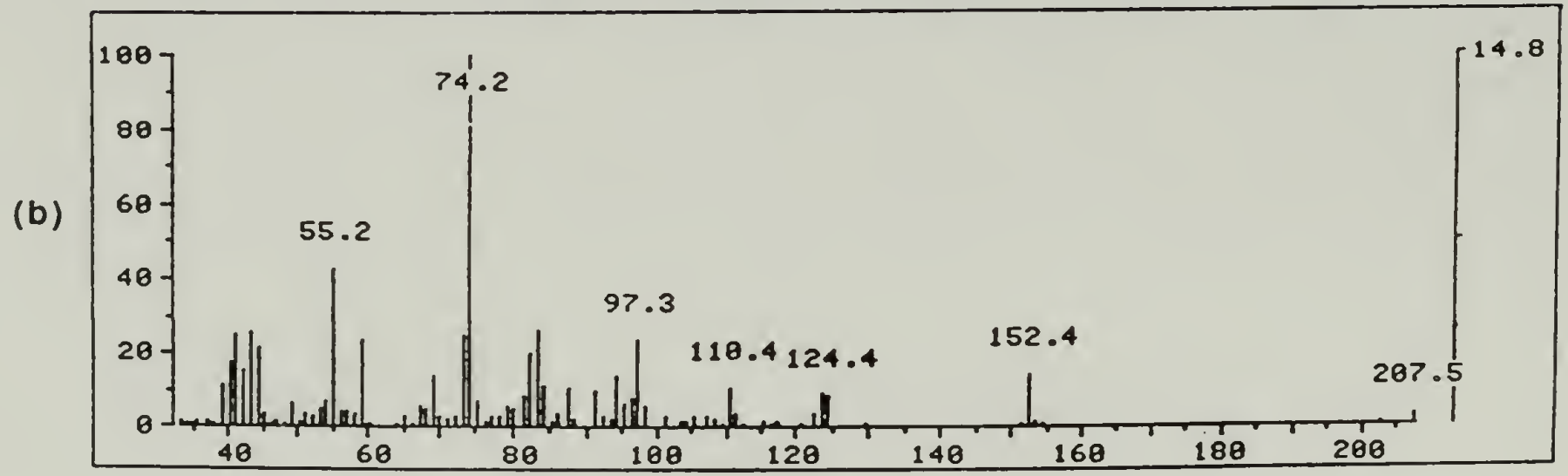

Figure C-7. Mass spectra of (a) 8-phenyloctanenitrile, and (b) methyl 8-cyanooctanoate from a 5-cyano-1-pentylmercuric bromide/styrene/methyl acrylate reaction mixture.

APPENDIX D

Miscellaneous ^{13}C NMR Spectra

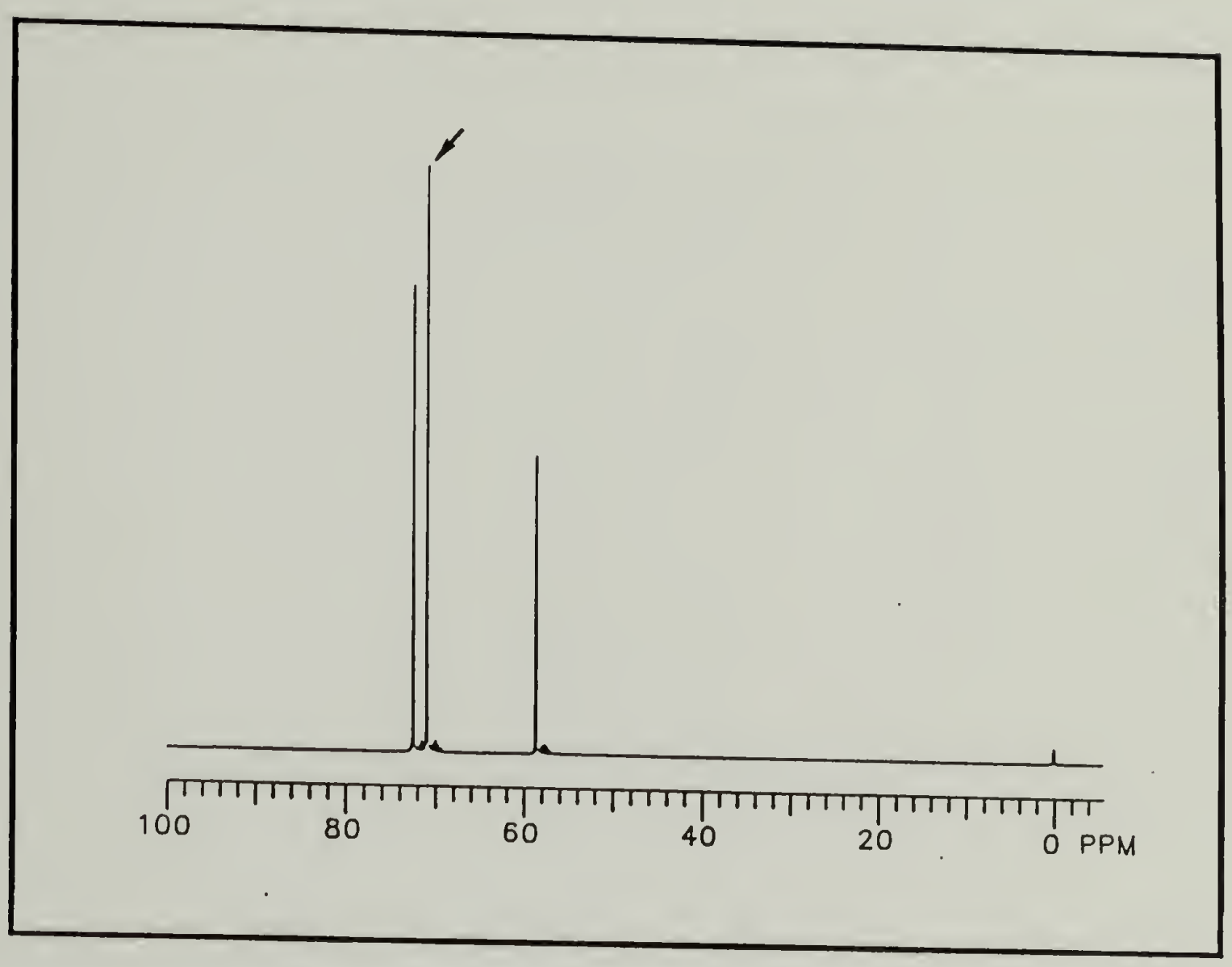

Figure D-1. 75 MHz ^{13}C NMR spectrum of a 3:2 mixture of diglyme and diglyme-d_{14} at 140 °C; the arrow indicates the reference signal.

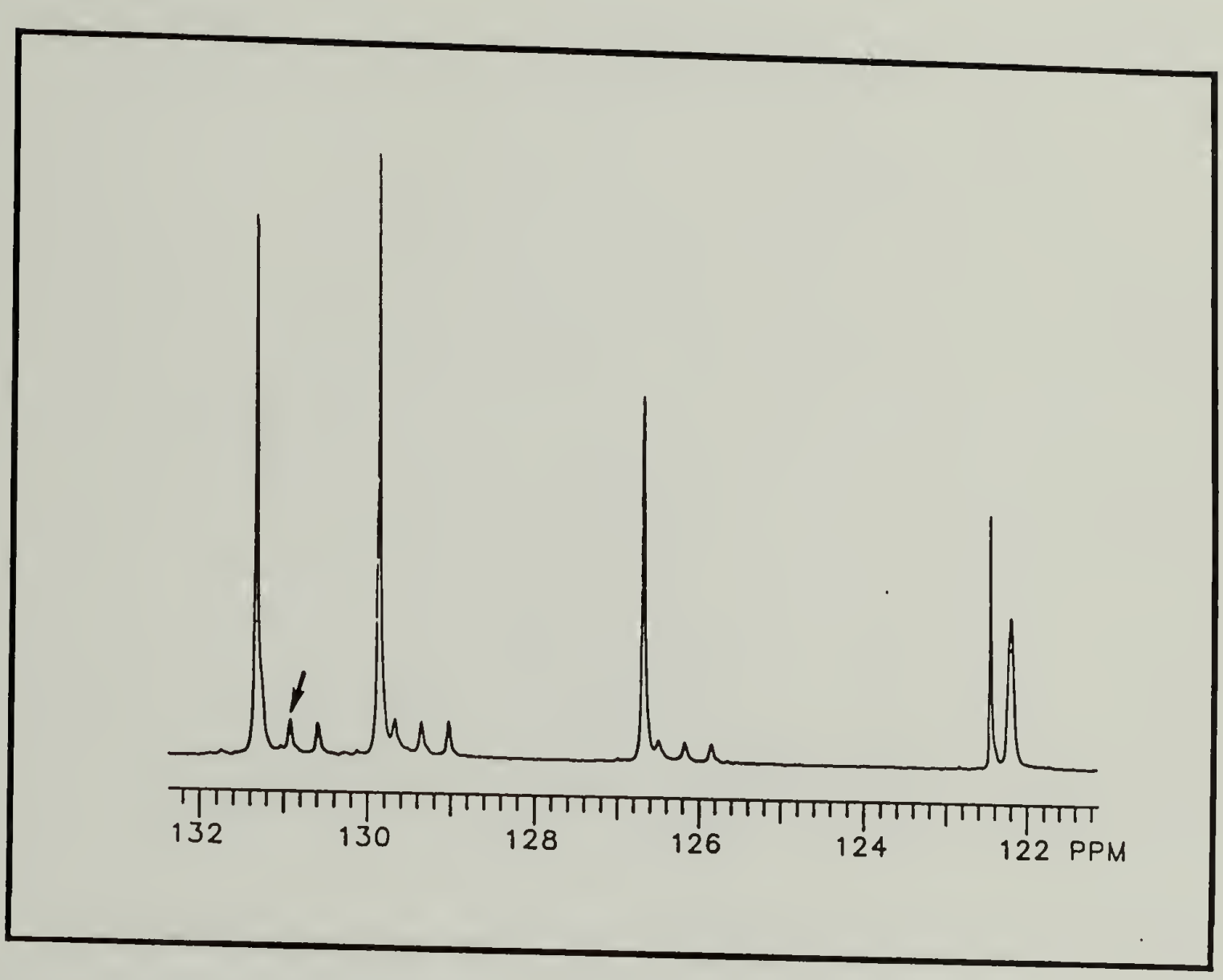

Figure D-2. 75 MHz ^{13}C NMR spectrum of a 3:2 mixture of bromobenzene and bromobenzene-d_5 at 136 °C; the arrow indicates the reference signal.

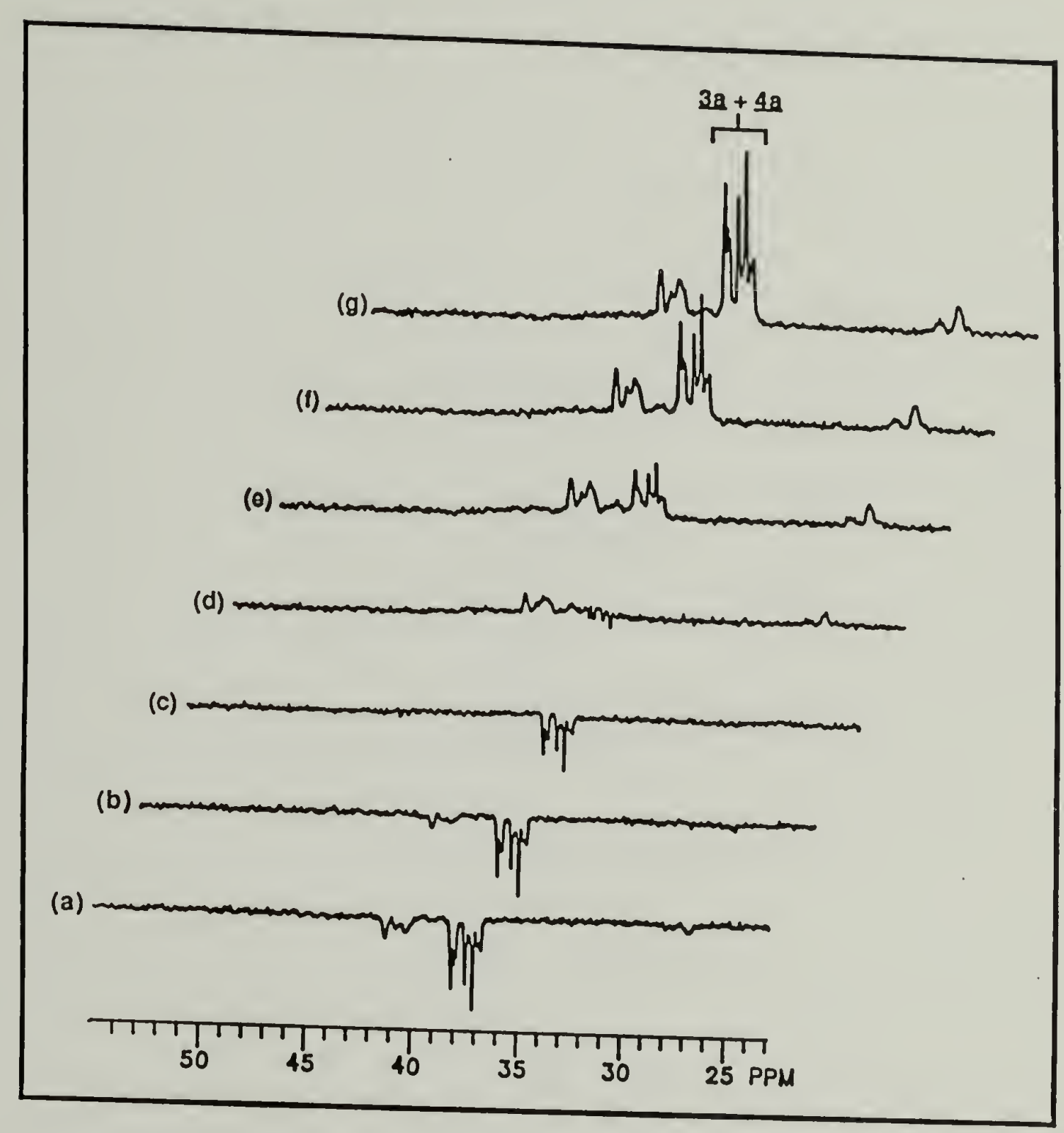

Figure D-3. 75 MHz ^{13}C NMR spectra from inversion-recovery experiment to determine T_1 values for endgroups 3a and 4a. Copolymer 1 in $CDCl_3$ was used and relaxation delay times of (a) 0.029 s, (b) 0.058 s, (c) 0.115 s, (d) 0.23 s, (e) 0.46 s, (f) 0.92 s, and (g) 1.84 s were employed.

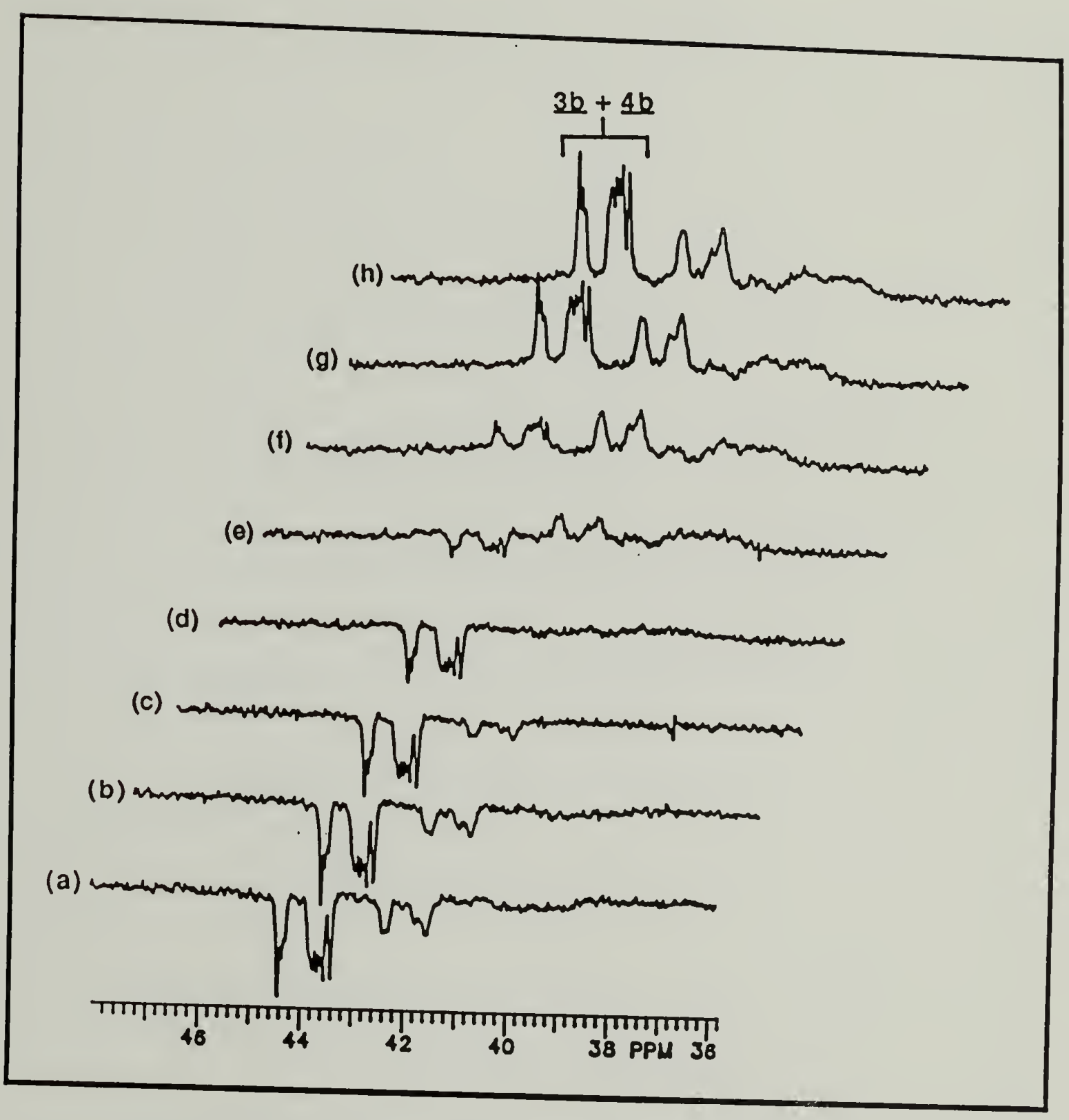

Figure D-4. 75 MHz ^{13}C NMR spectra from inversion-recovery experiment to determine T_1 values for endgroups 3b and 4b. Copolymer 10 in deuterated diglyme at 140 °C was used and relaxation delay times of (a) 0.038 s, (b) 0.075 s, (c) 0.150 s, (d) 0.30 s, (e) 0.60 s, (f) 1.20 s, (g) 2.40 s, and (h) 4.80 s were employed.

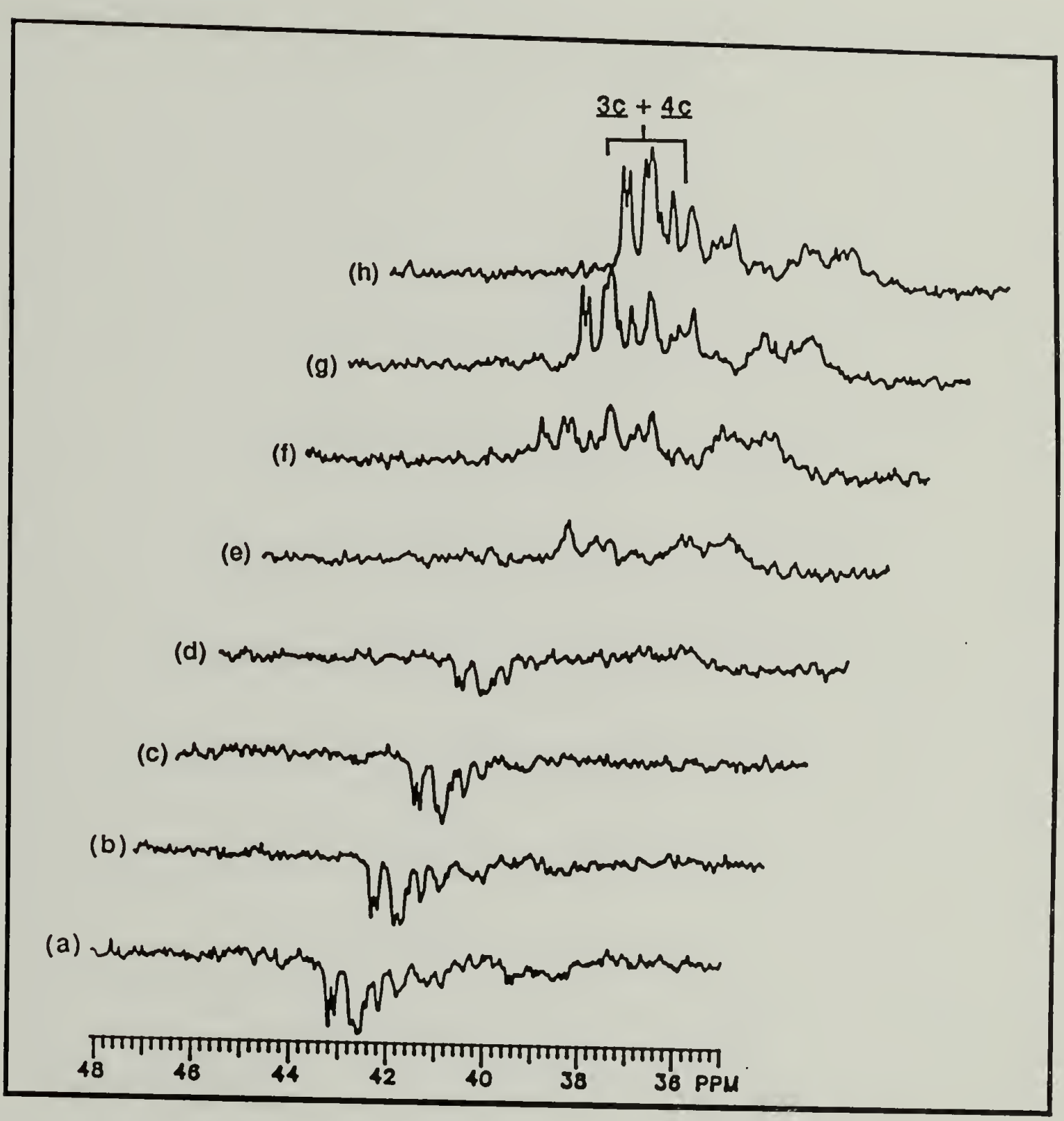

Figure D-5. 75 MHz ^{13}C NMR spectra from inversion-recovery experiment to determine T_1 values for endgroups 3c and 4c. Copolymer 22 in deuterated bromobenzene at 136 °C was used and relaxation delay times of (a) 0.038 s, (b) 0.075 s, (c) 0.150 s, (d) 0.30 s, (e) 0.60 s, (f) 1.20 s, (g) 2.40 s, and (h) 4.80 s were employed.

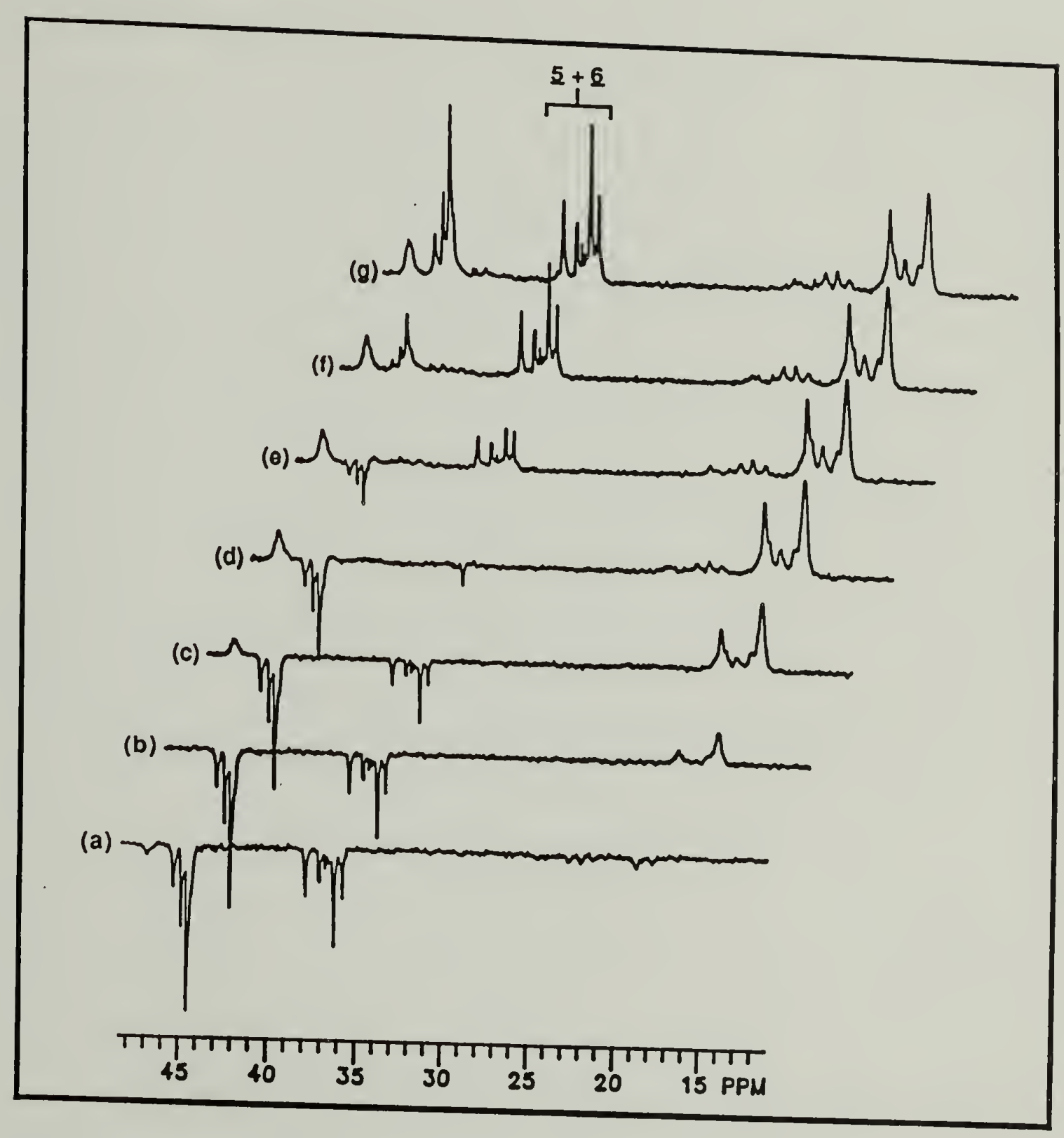

Figure D-6. 75 MHz ^{13}C NMR spectra from inversion-recovery experiment to determine T_1 values for endgroups 5 and 6. Copolymer 36 in $CDCl_3$ was used and relaxation delay times of (a) 0.029 s, (b) 0.058 s, (c) 0.115 s, (d) 0.23 s, (e) 0.46 s, (f) 0.92 s, and (g) 1.84 s were employed.

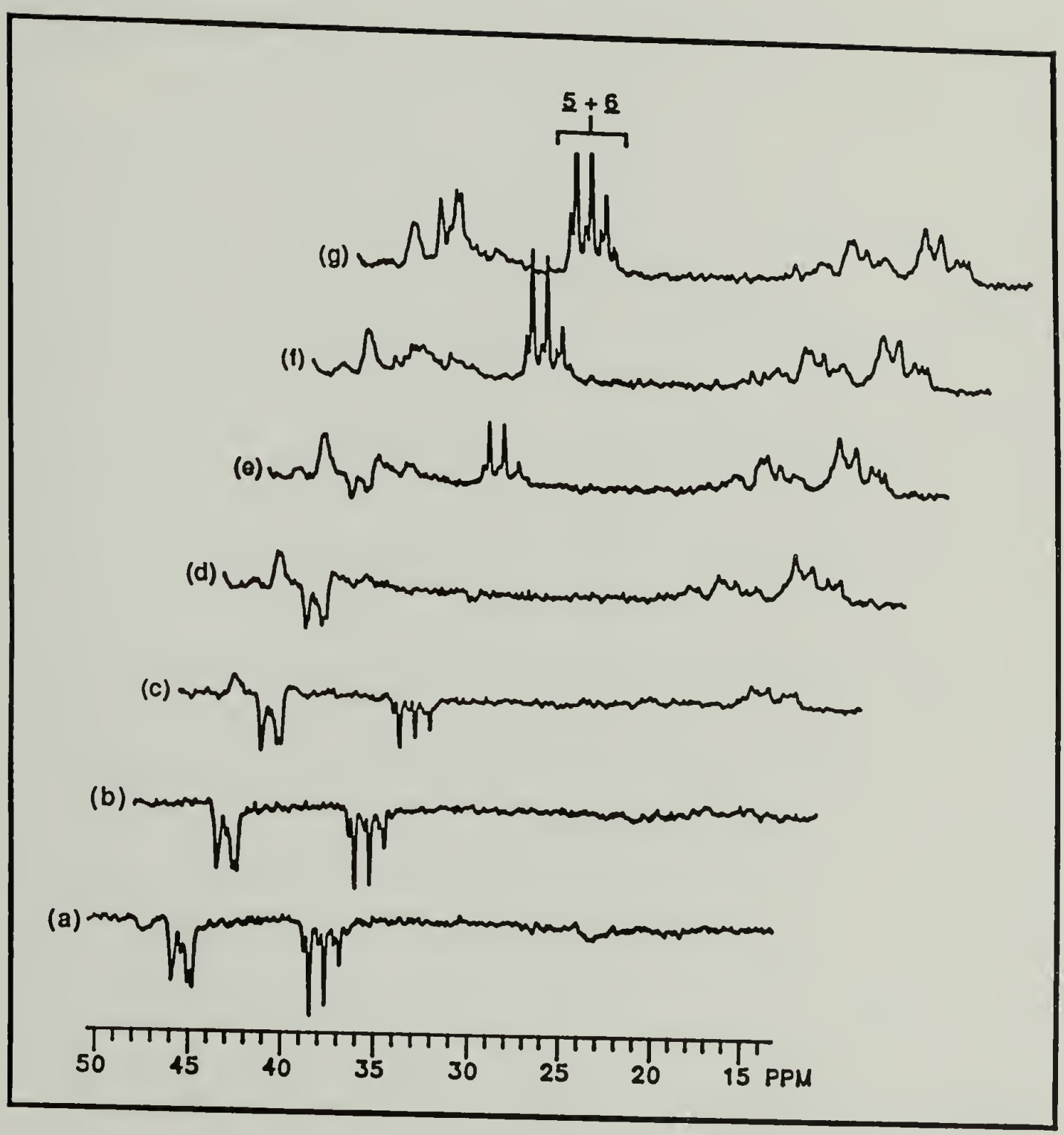

Figure D-7. 75 MHz ^{13}C NMR spectra from inversion-recovery experiment to determine T_1 values for endgroups 7 and 8. Copolymer 35 in $CDCl_3$ was used and relaxation delay times of (a) 0.029 s, (b) 0.058 s, (c) 0.115 s, (d) 0.23 s, (e) 0.46 s, (f) 0.92 s, and (g) 1.84 s were employed.

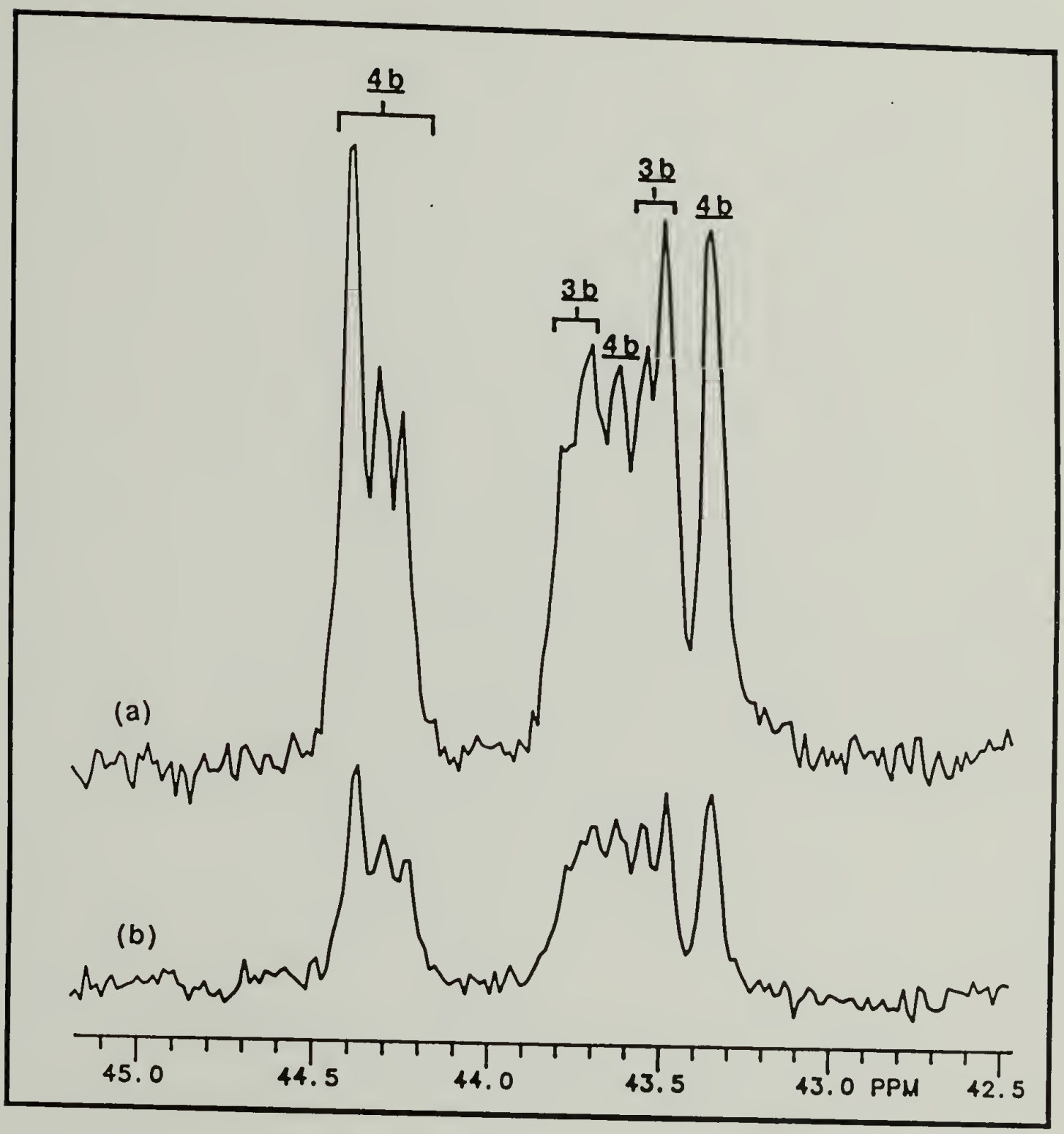

Figure D-8. 75 MHz ^{13}C NMR spectra of copolymer 10 in deuterated diglyme at 140 °C (a) with the NOE and (b) with suppression of the NOE.

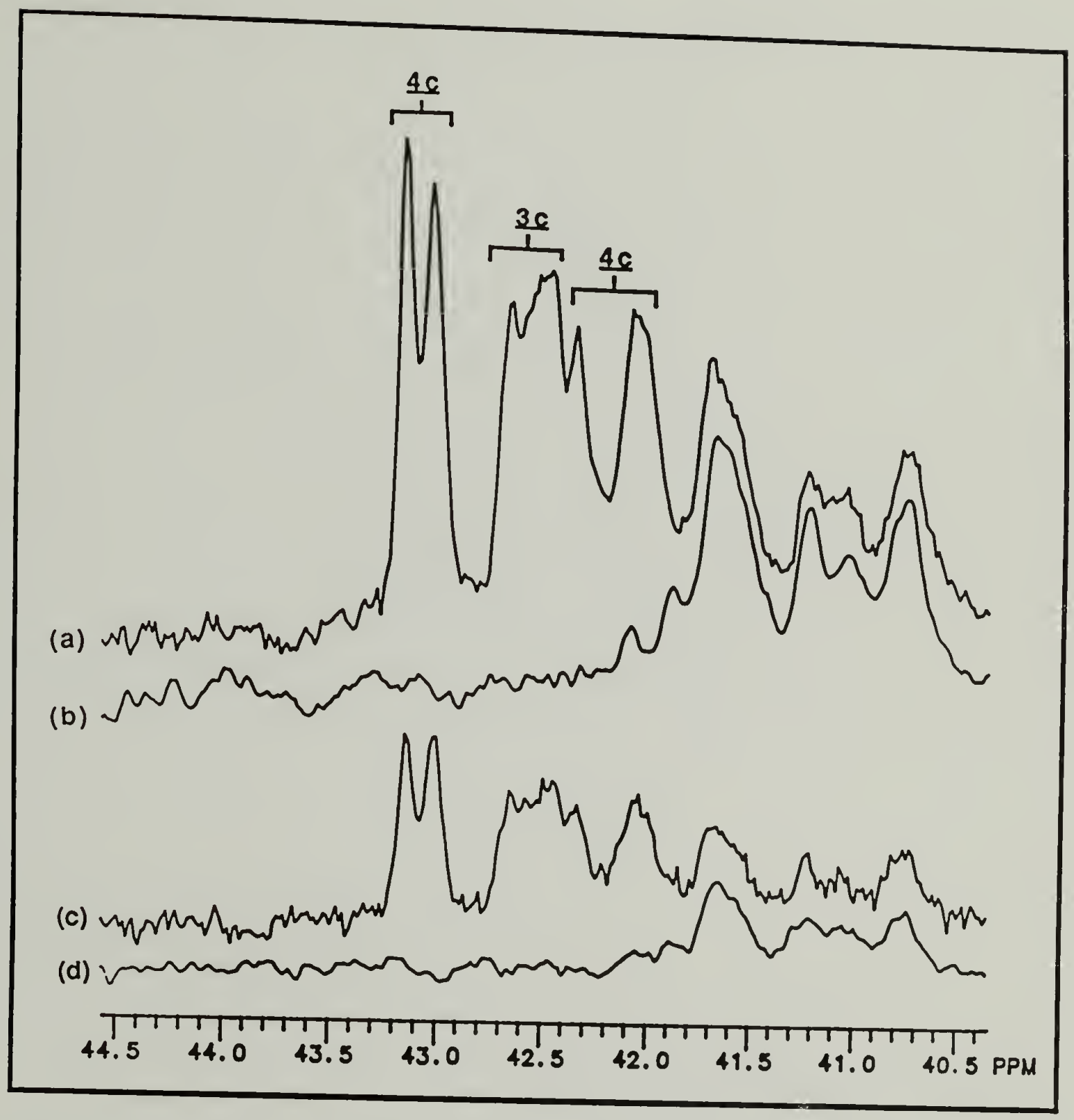

Figure D-9. 75 MHz ^{13}C NMR spectra of copolymer 26 (a and c) and of copolymer 24N (b and d) in deuterated bromobenzene at 136 °C with the NOE (a and b) and with suppression of the NOE (c and d).

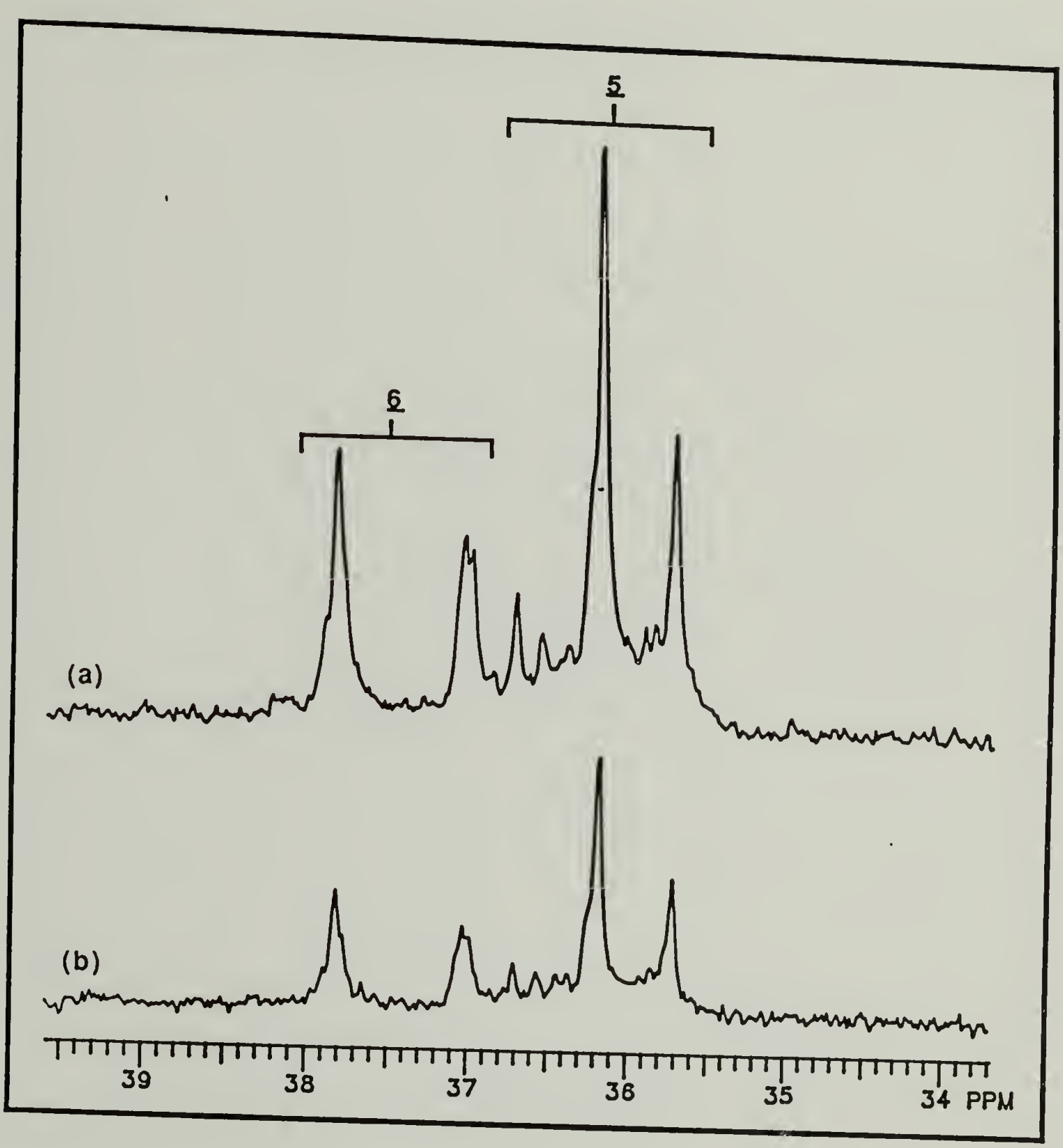

Figure D-10. 75 MHz ^{13}C NMR spectra of copolymer 36 in $CDCl_3$ (a) with the NOE and (b) with suppression of the NOE.

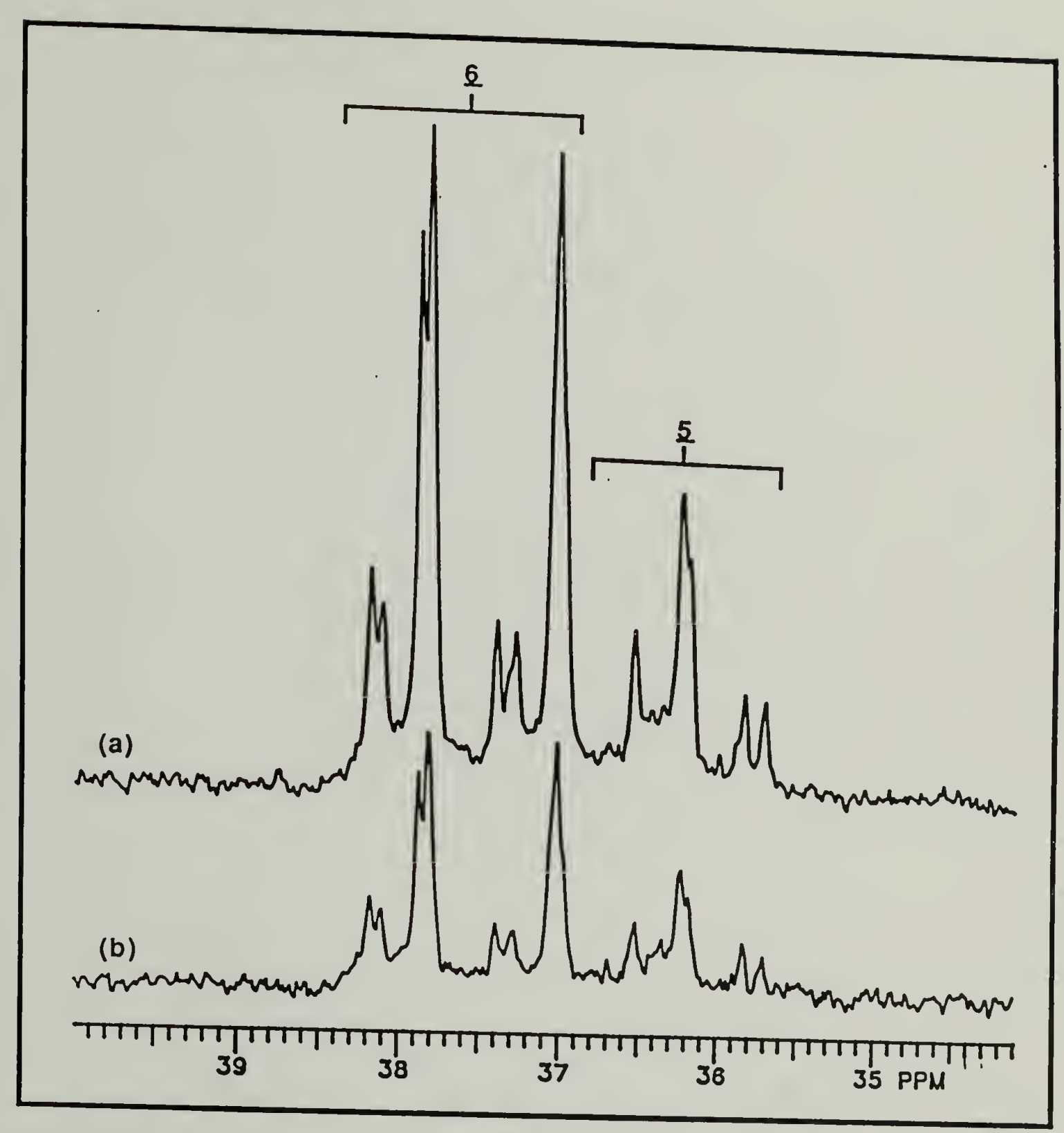

Figure D-11. 75 MHz ^{13}C NMR spectra of copolymer 35 in $CDCl_3$ (a) with the NOE and (b) with suppression of the NOE.

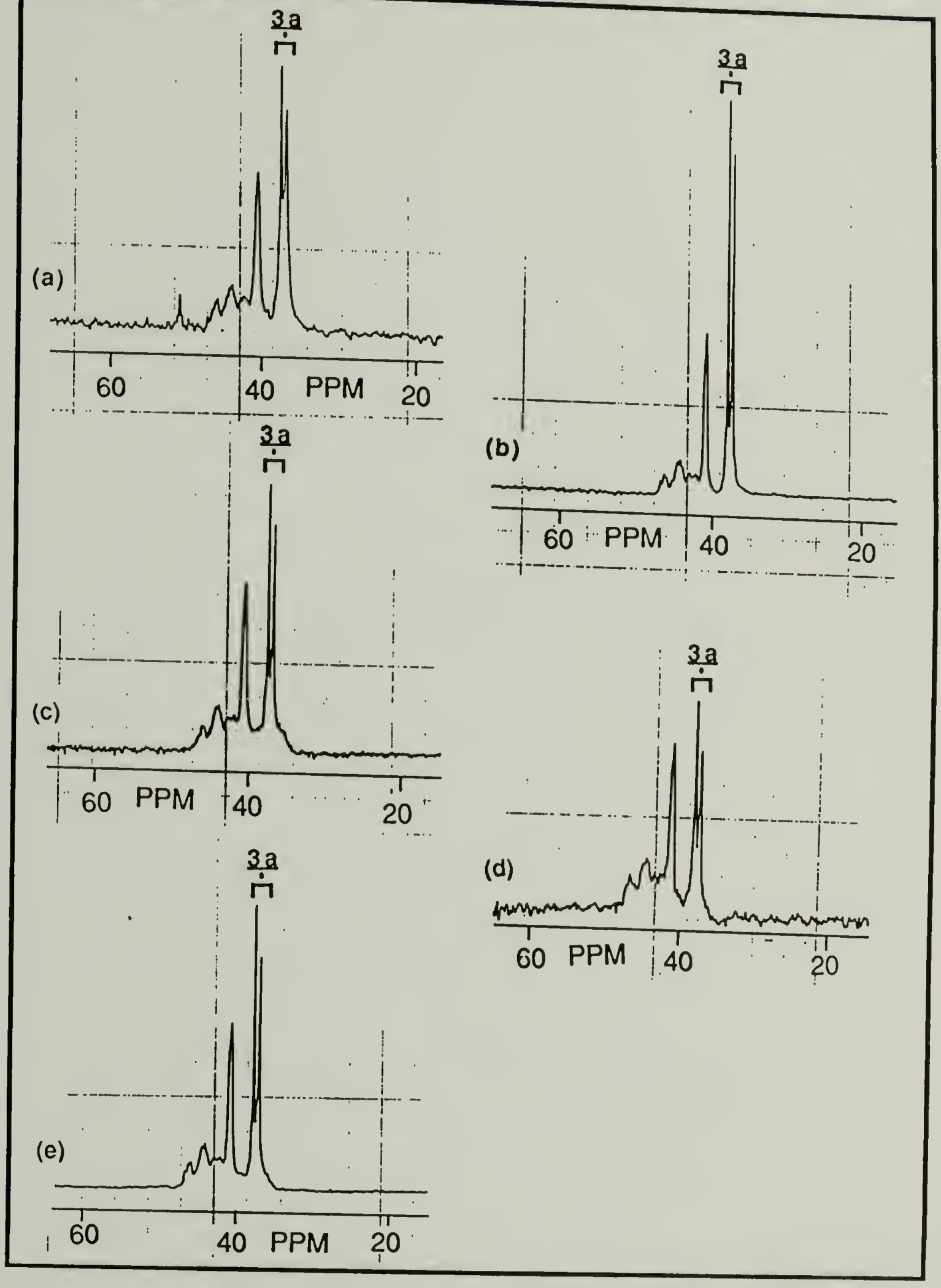

Figure D-12. 50 MHz ^{13}C NMR spectra of polystyrenes in $CDCl_3$ that were prepared from 1a at polymerization temperatures of (a) 0 °C, (b) 25-40 °C, (c) 35 °C, (d) 42 °C, and (e) 52 °C.

Figure D-13. 75 MHz ^{13}C NMR spectra of polyacrylonitriles in DMF-d_7 that were prepared from **1a** at polymerization temperatures of (a) 10 °C, (b) 33 °C, and (c) 60 °C.

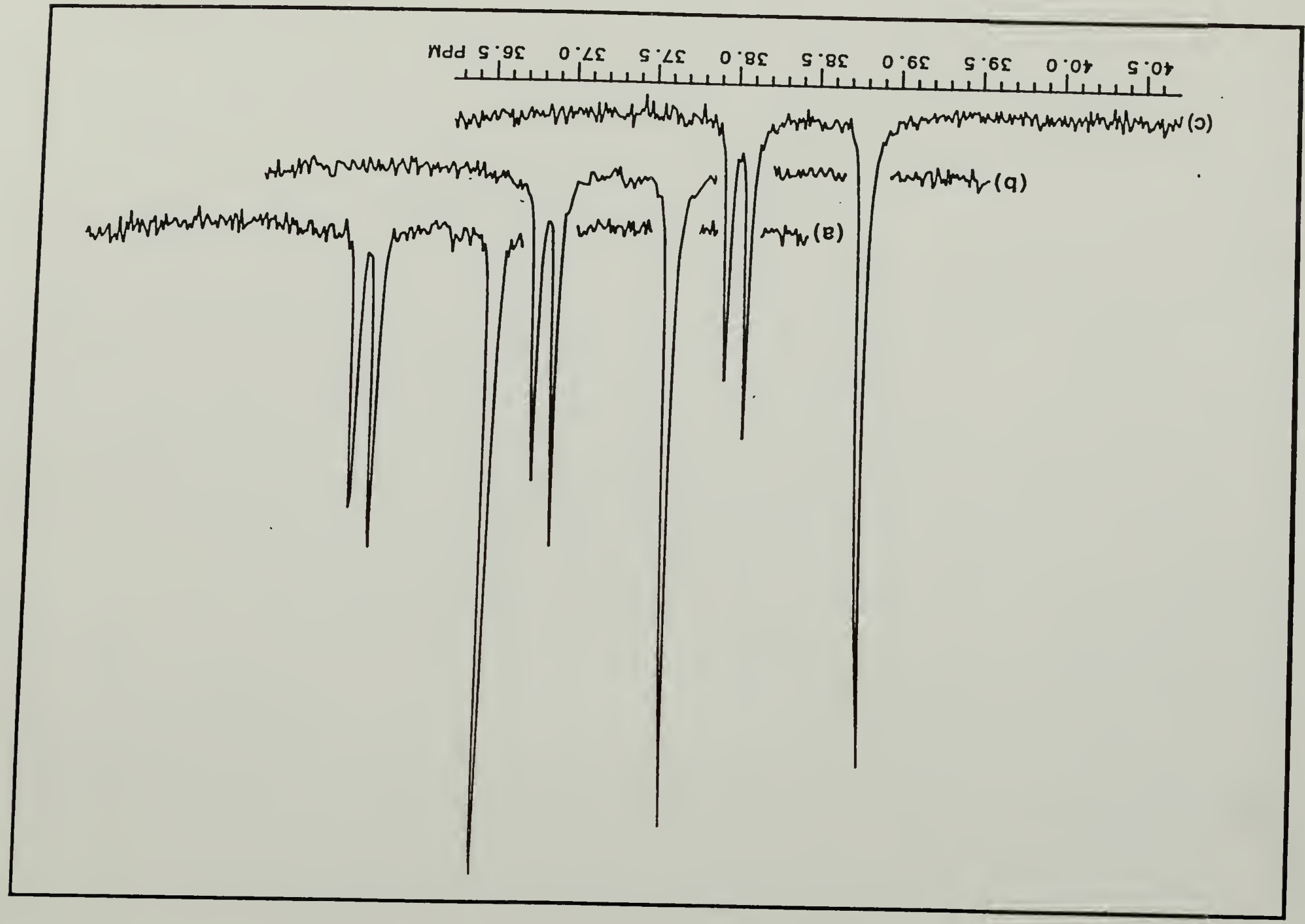
40.5 40.0 39.5 39.0 38.5 38.0 37.5 37.0 36.5 PPM
(c)
(b)
(a)

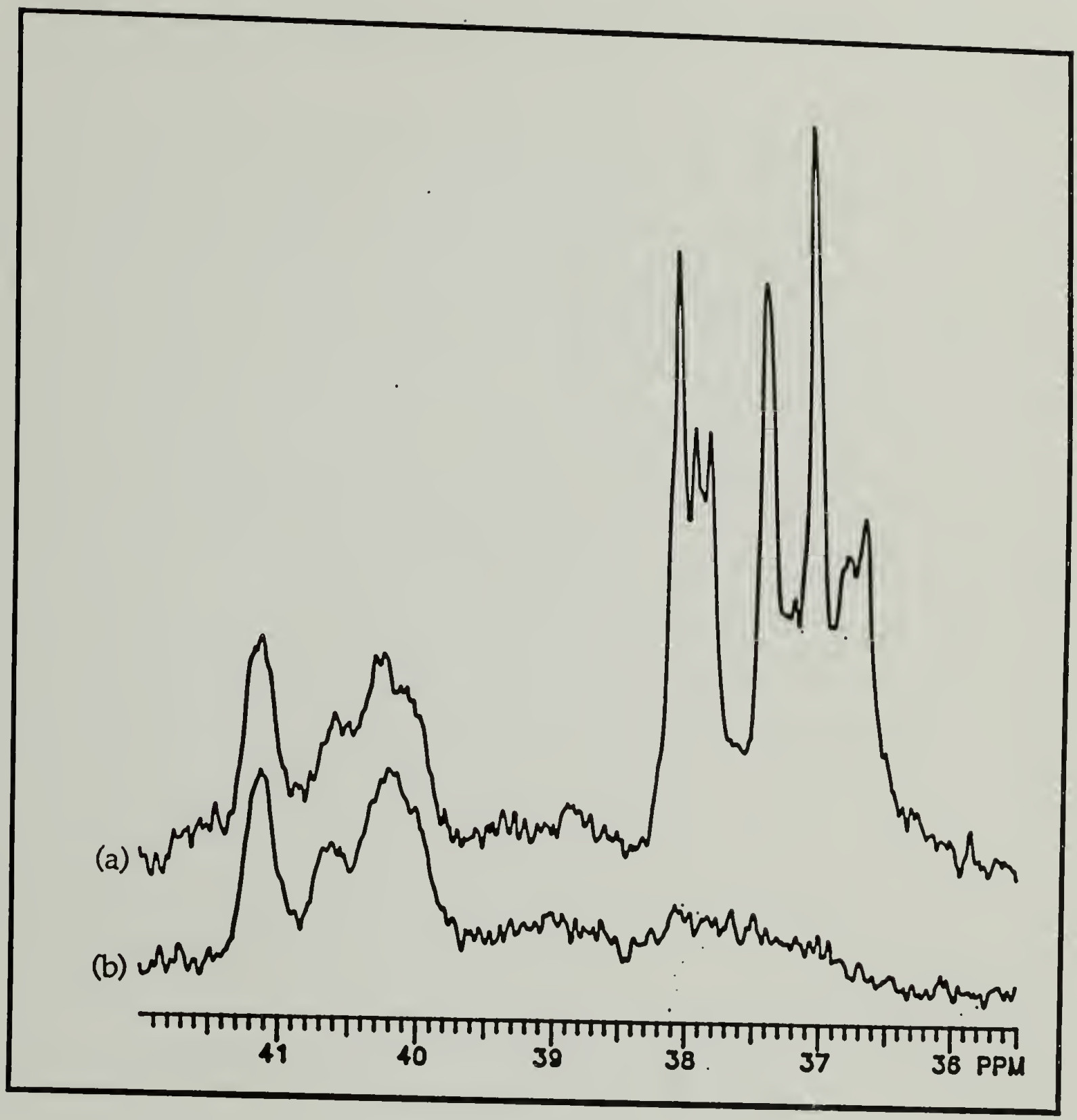

Figure D-14. 75 MHz ^{13}C NMR spectra (expanded plots) of (a) enriched and (b) natural-abundance SAN copolymers in $CDCl_3$ that were prepared from 1a with a monomer feed ratio ([S]/[A]) of 3.35.

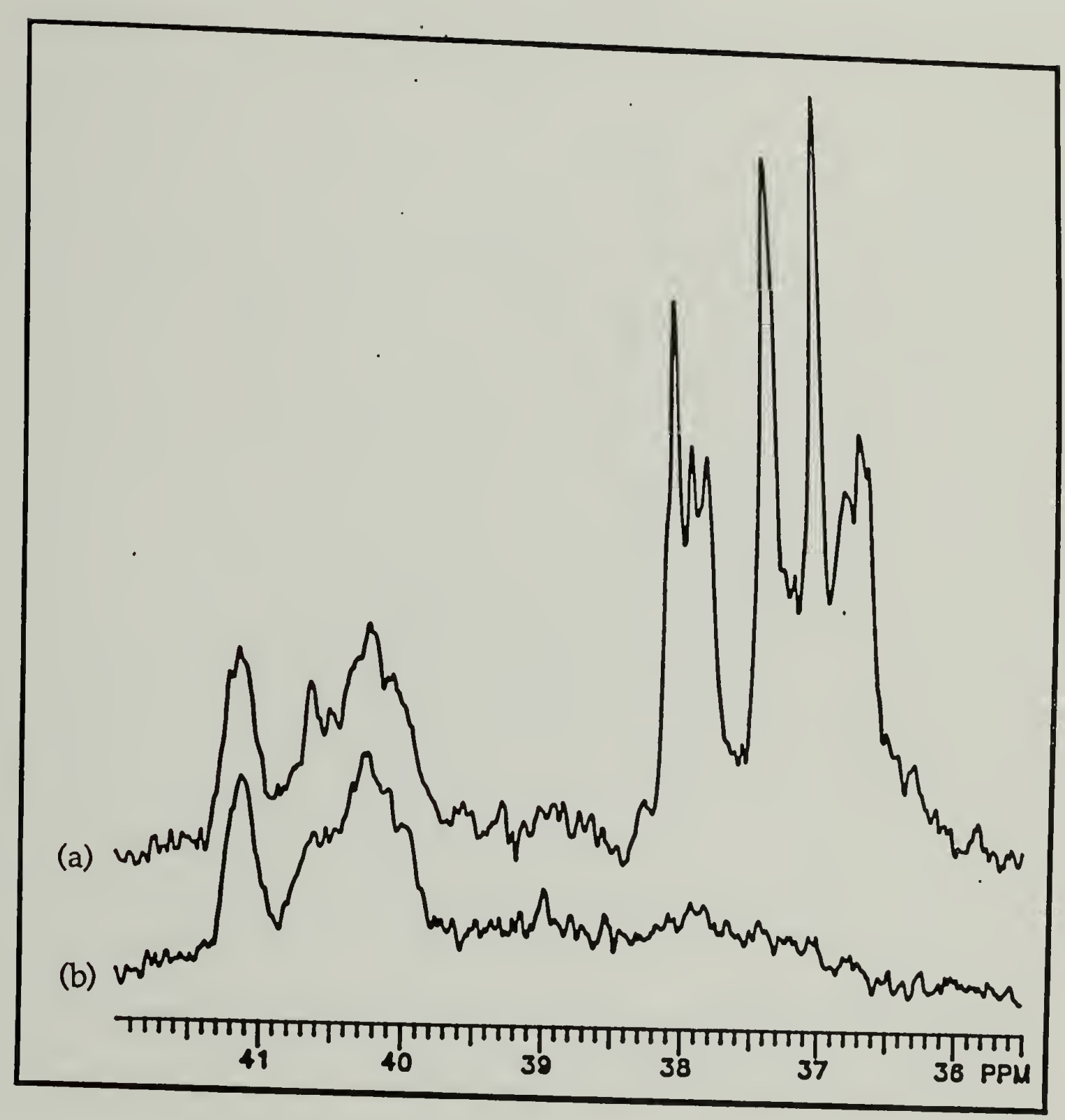

Figure D-15. 75 MHz ^{13}C NMR spectra (expanded plots) of (a) enriched and (b) natural-abundance SAN copolymers in $CDCl_3$ that were prepared from 1a with a monomer feed ratio ([S]/[A]) of 3.70.

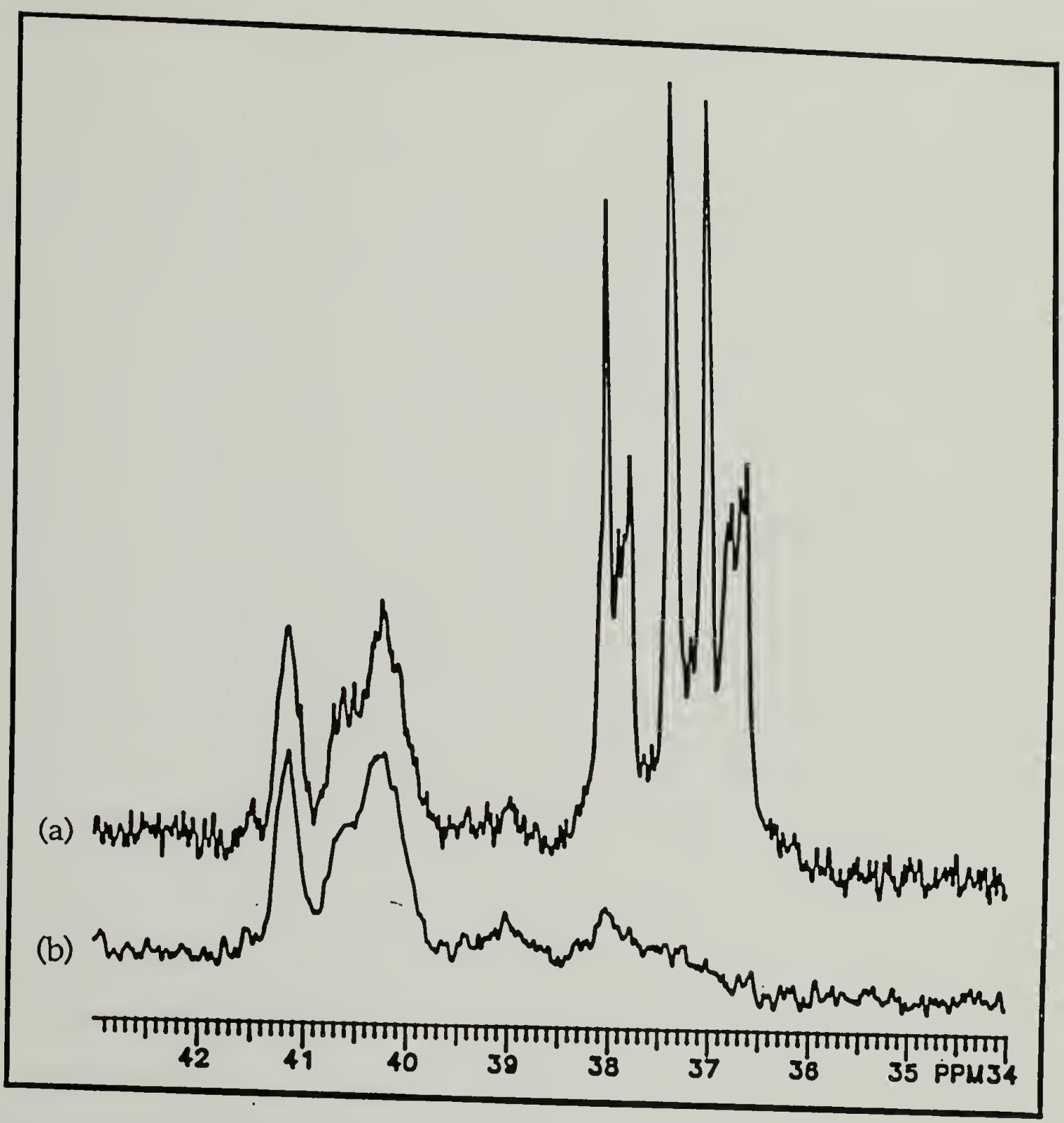

Figure D-16. 75 MHz ^{13}C NMR spectra (expanded plots) of (a) enriched and (b) natural-abundance SAN copolymers in $CDCl_3$ that were prepared from 1a with a monomer feed ratio ([S]/[A]) of 4.86.

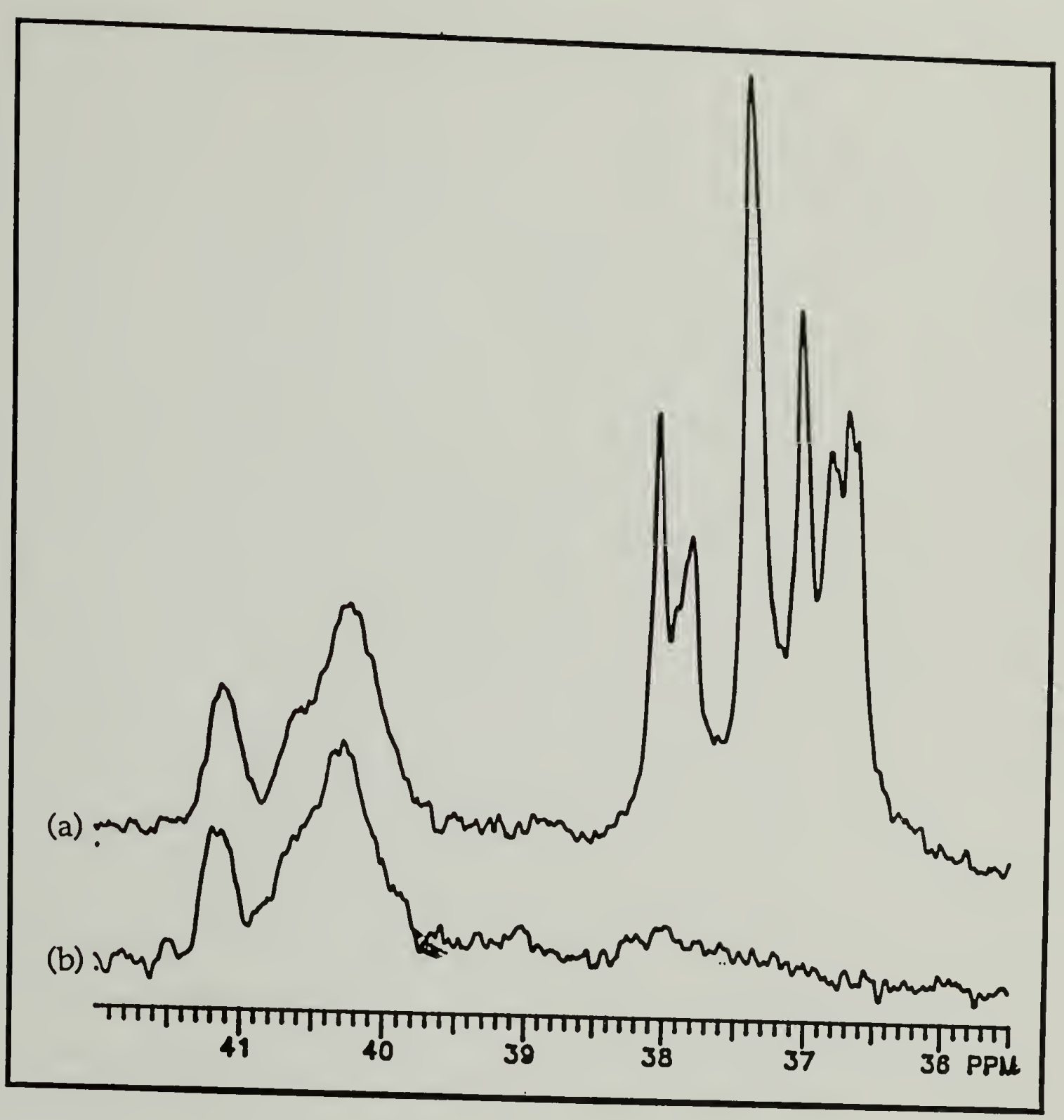

Figure D-17. 75 MHz ^{13}C NMR spectra (expanded plots) of (a) enriched and (b) natural-abundance SAN copolymers in $CDCl_3$ that were prepared from 1a with a monomer feed ratio ([S]/[A]) of 5.54.

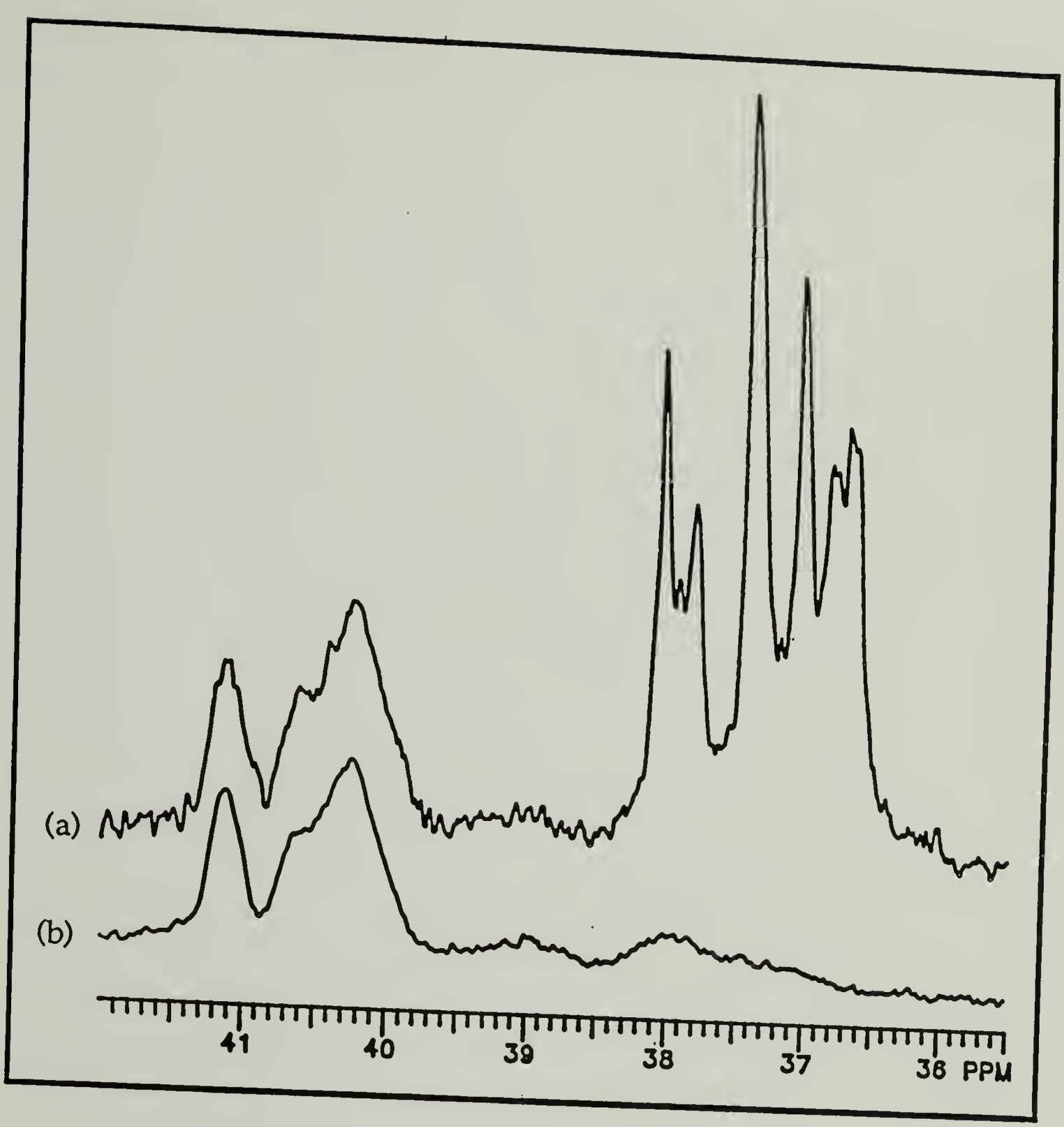

Figure D-18. 75 MHz ^{13}C NMR spectra (expanded plots) of (a) enriched and (b) natural-abundance SAN copolymers in $CDCl_3$ that were prepared from 1a with a monomer feed ratio ([S]/[A]) of 6.41.

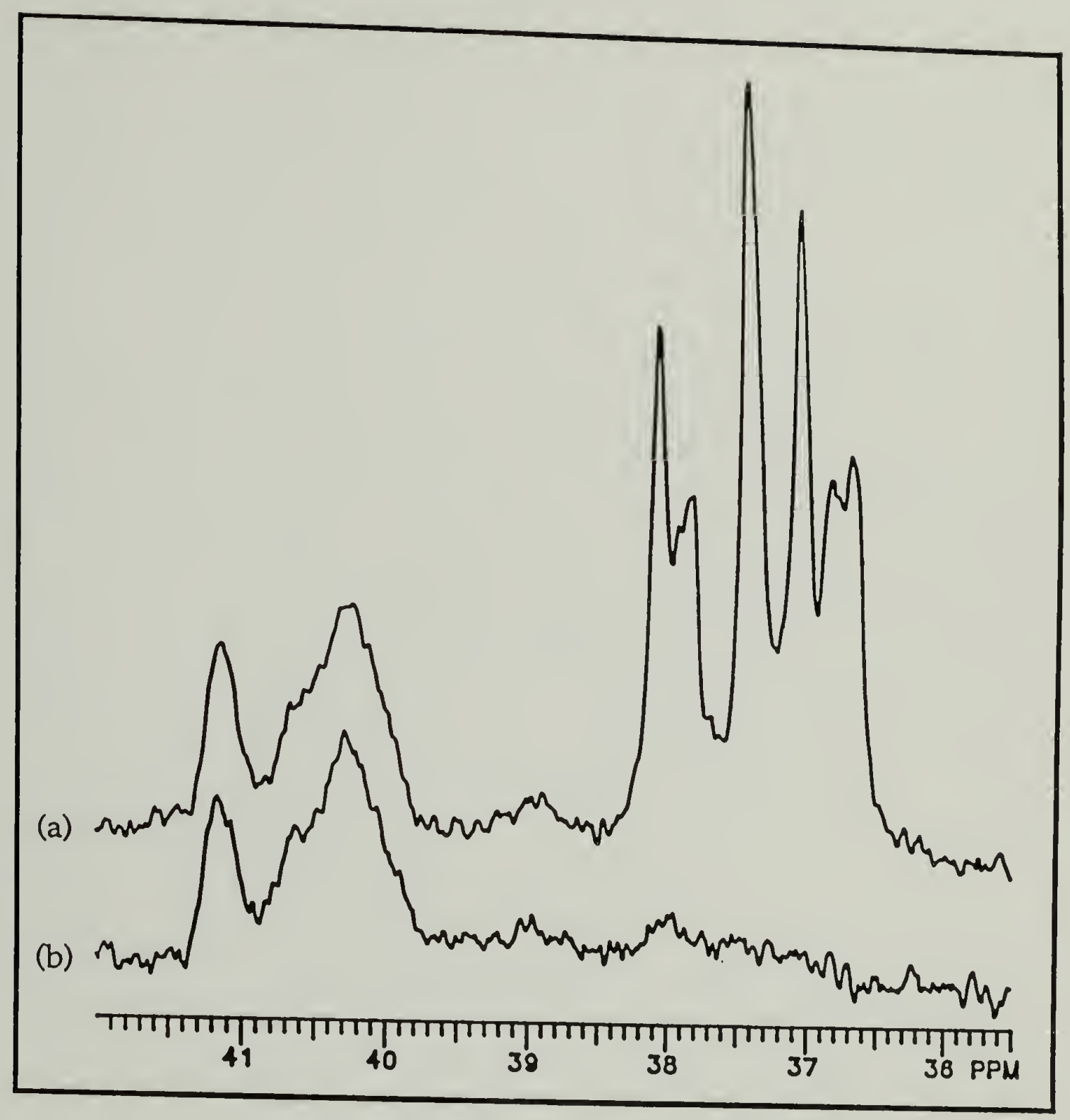

Figure D-19. 75 MHz ^{13}C NMR spectra (expanded plots) of (a) enriched and (b) natural-abundance SAN copolymers in $CDCl_3$ that were prepared from 1a with a monomer feed ratio ([S]/[A]) of 7.23.

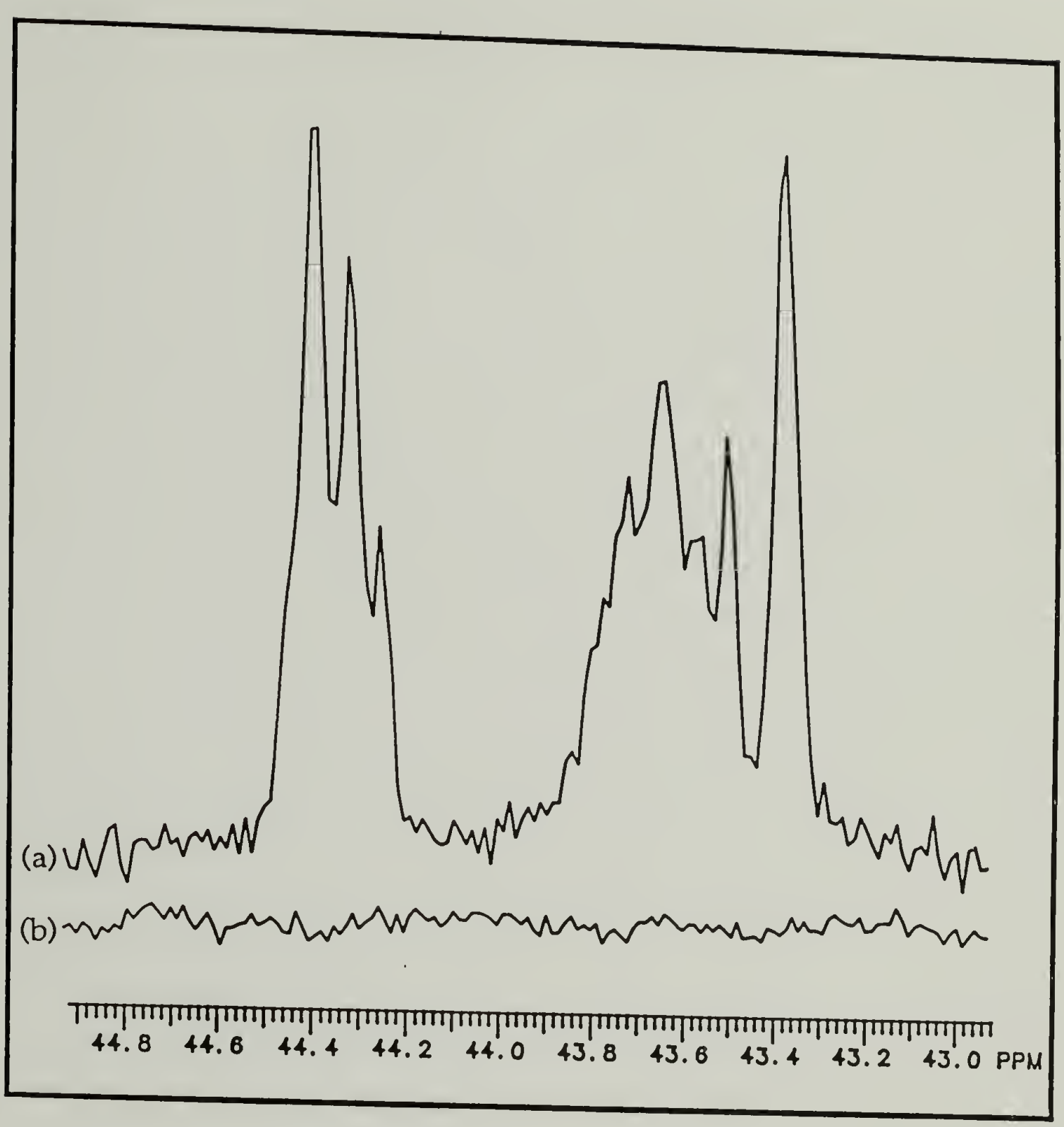

Figure D-20. 75 MHz ^{13}C NMR spectra (expanded plots) of (a) enriched and (b) natural-abundance SAN copolymers in deuterated diglyme at 140 °C that were prepared from **1b** with a monomer feed ratio ([S]/[A]) of 2.02.

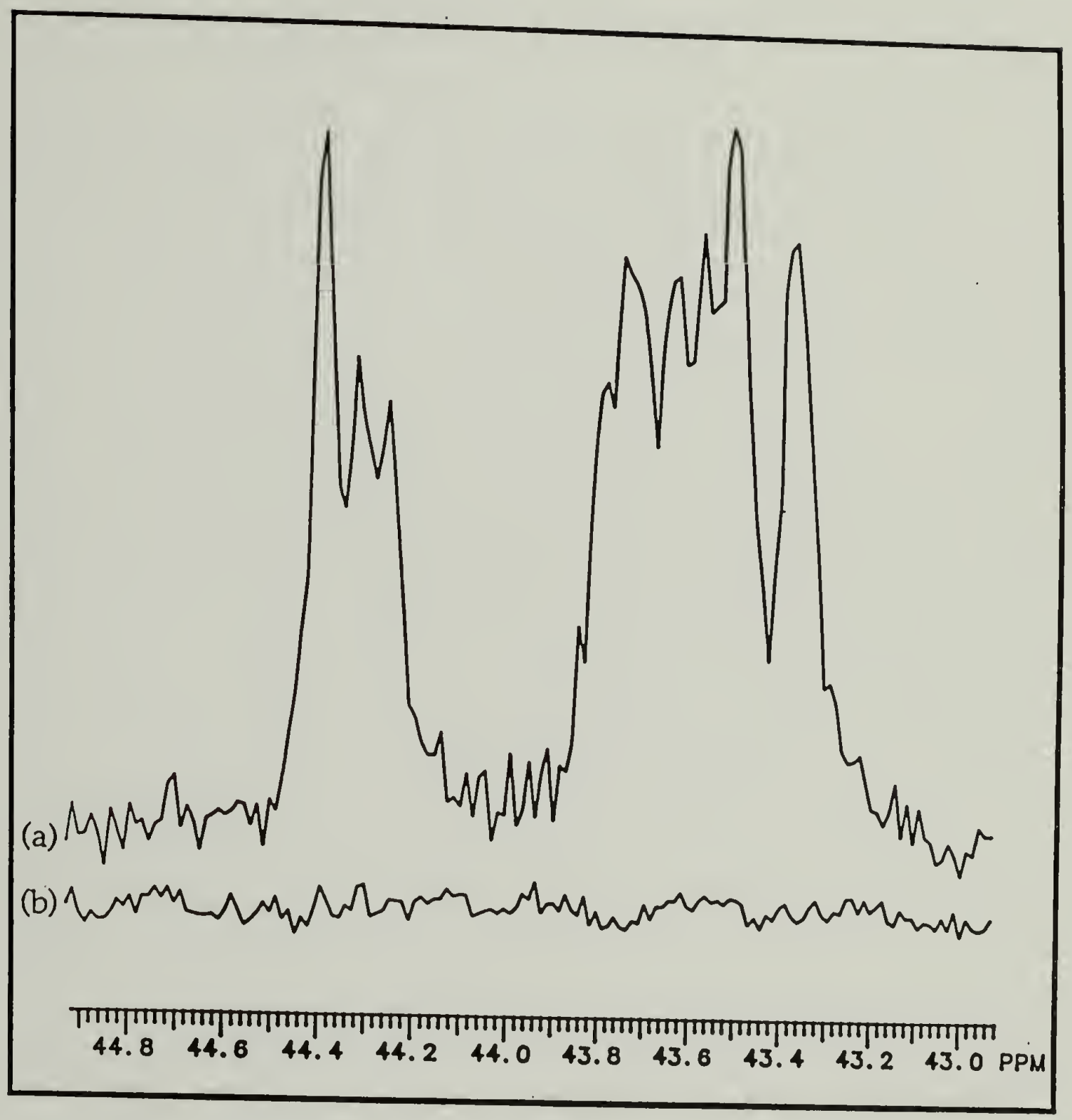

Figure D-21. 75 MHz ^{13}C NMR spectra (expanded plots) of (a) enriched and (b) natural-abundance SAN copolymers in deuterated diglyme at 140 °C that were prepared from **1b** with a monomer feed ratio ([S]/[A]) of 4.00.

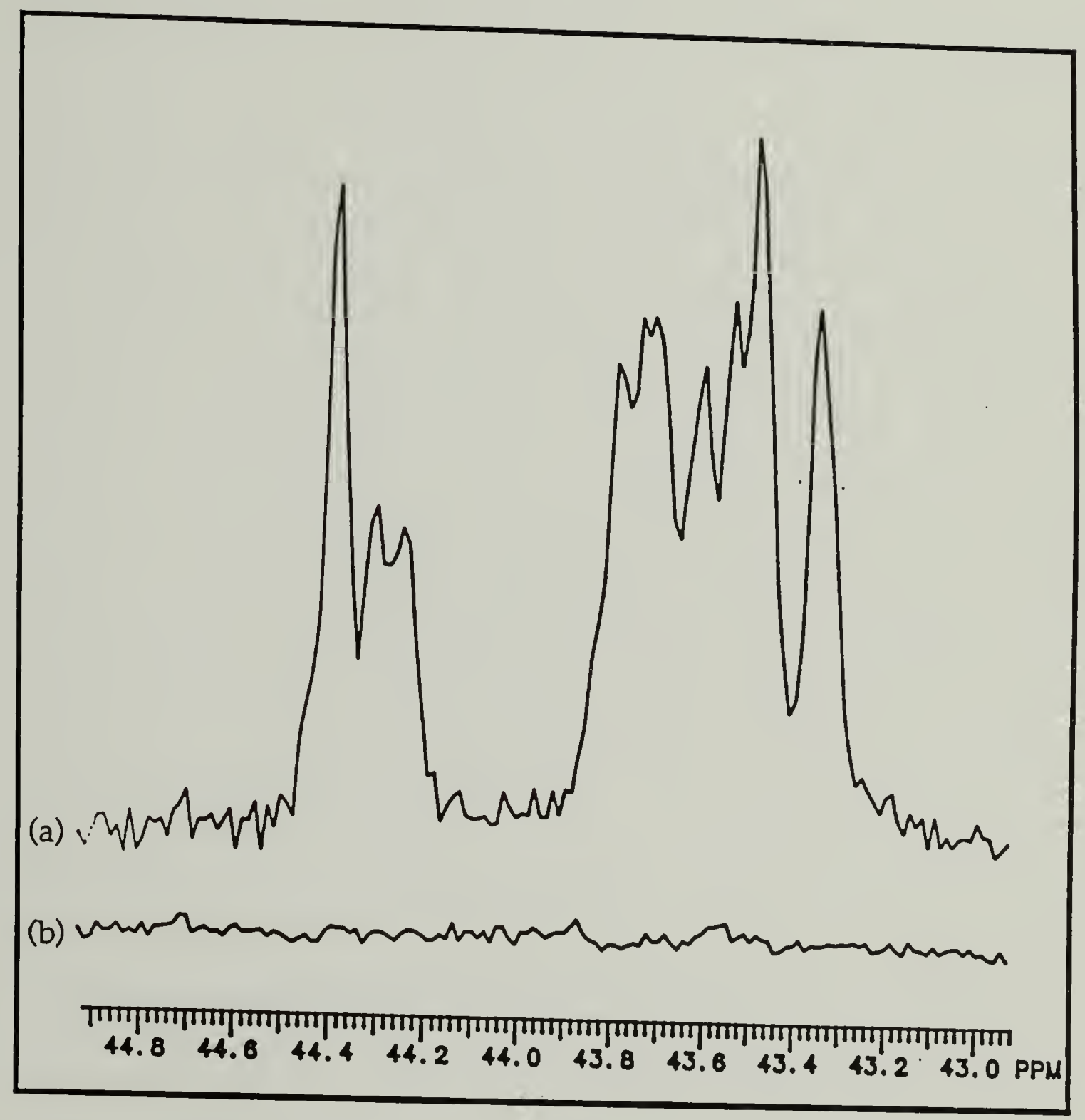

Figure D-22. 75 MHz ^{13}C NMR spectra (expanded plots) of (a) enriched and (b) natural-abundance SAN copolymers in deuterated diglyme at 140 °C that were prepared from 1b with a monomer feed ratio ([S]/[A]) of 4.84.

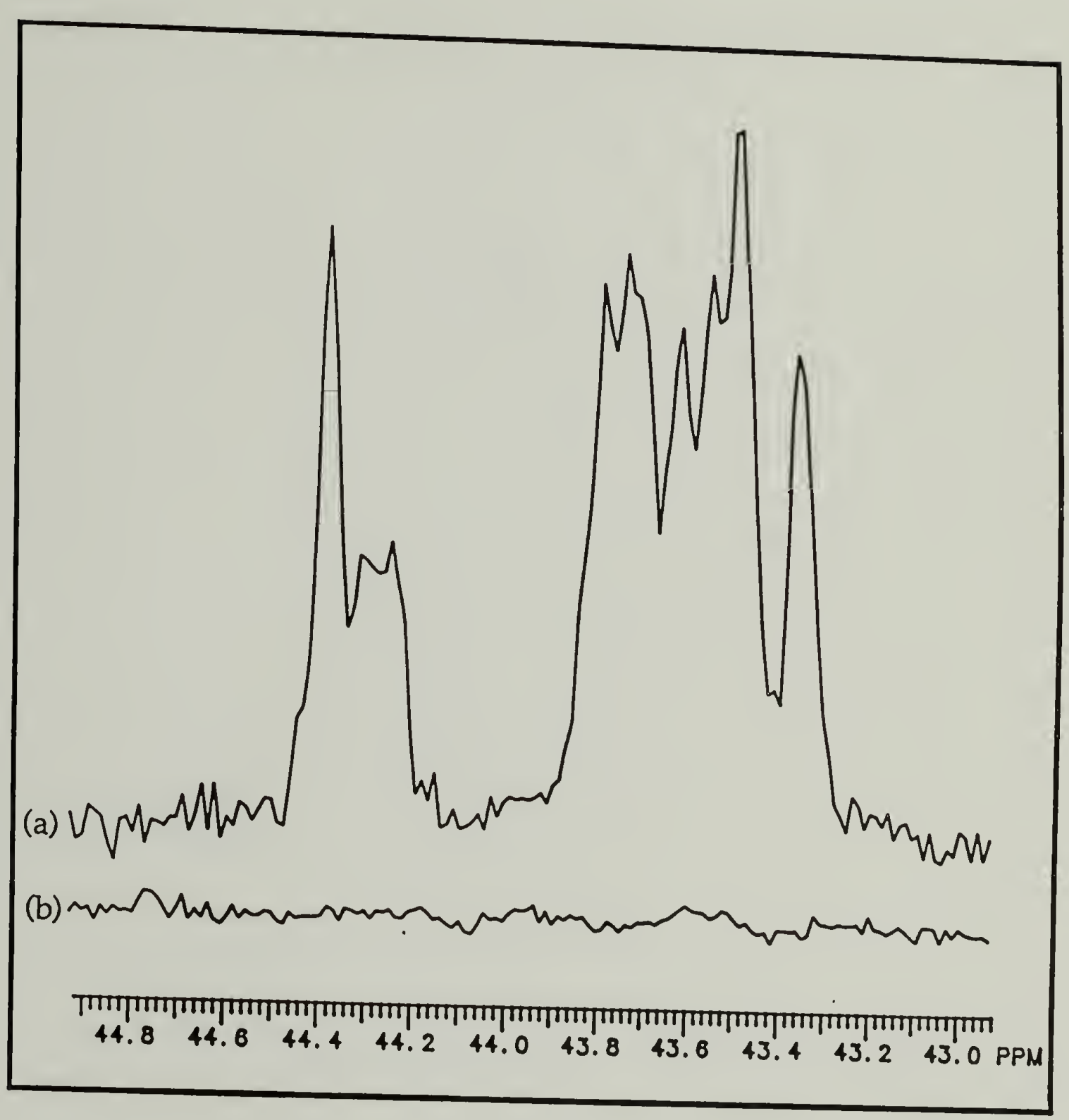

Figure D-23. 75 MHz ^{13}C NMR spectra (expanded plots) of (a) enriched and (b) natural-abundance SAN copolymers in deuterated diglyme at 140 °C that were prepared from **1b** with a monomer feed ratio ([S]/[A]) of 5.67.

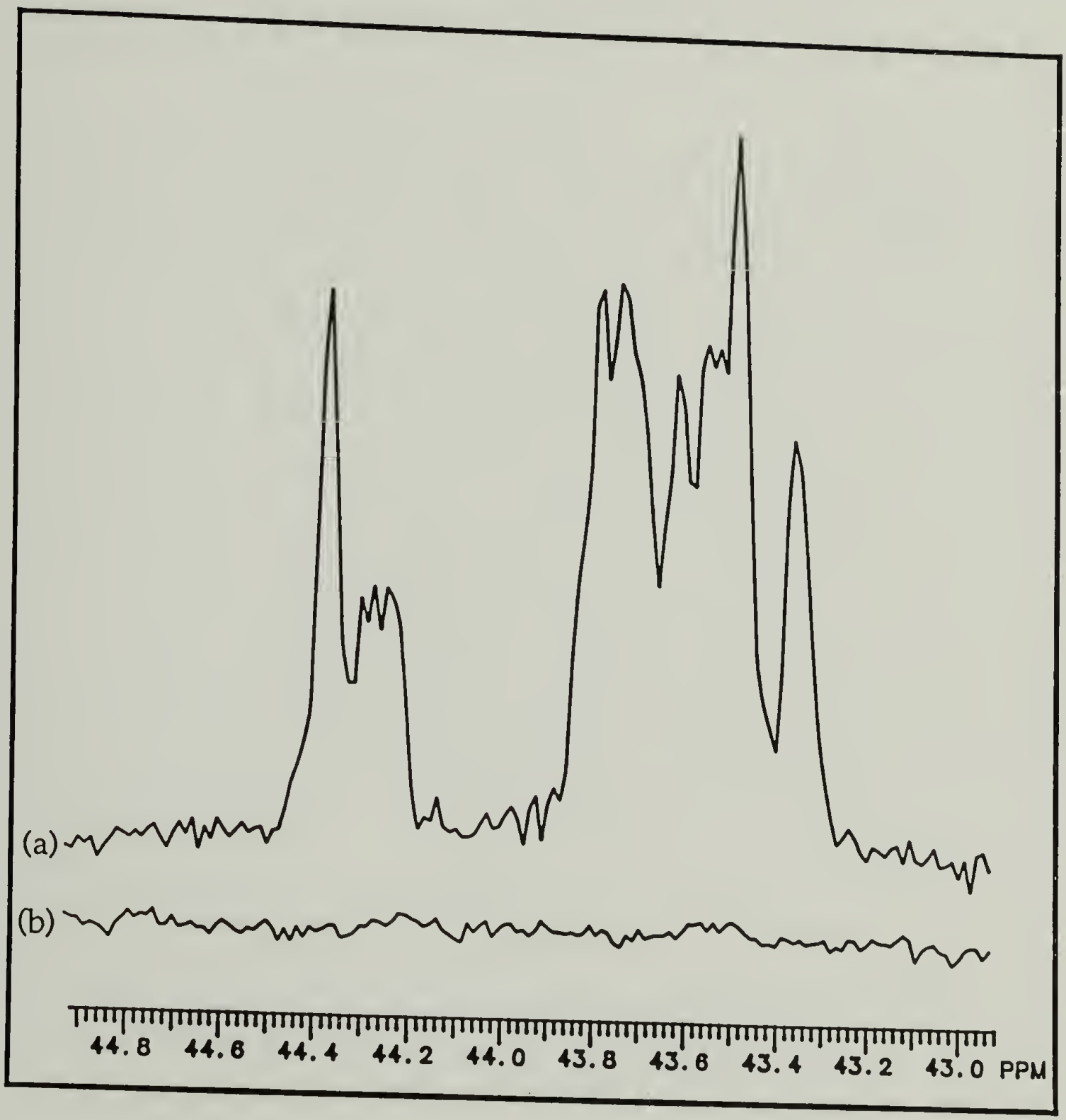

Figure D-24. 75 MHz ^{13}C NMR spectra (expanded plots) of (a) enriched and (b) natural-abundance SAN copolymers in deuterated diglyme at 140 °C that were prepared from **1b** with a monomer feed ratio ([S]/[A]) of 6.43.

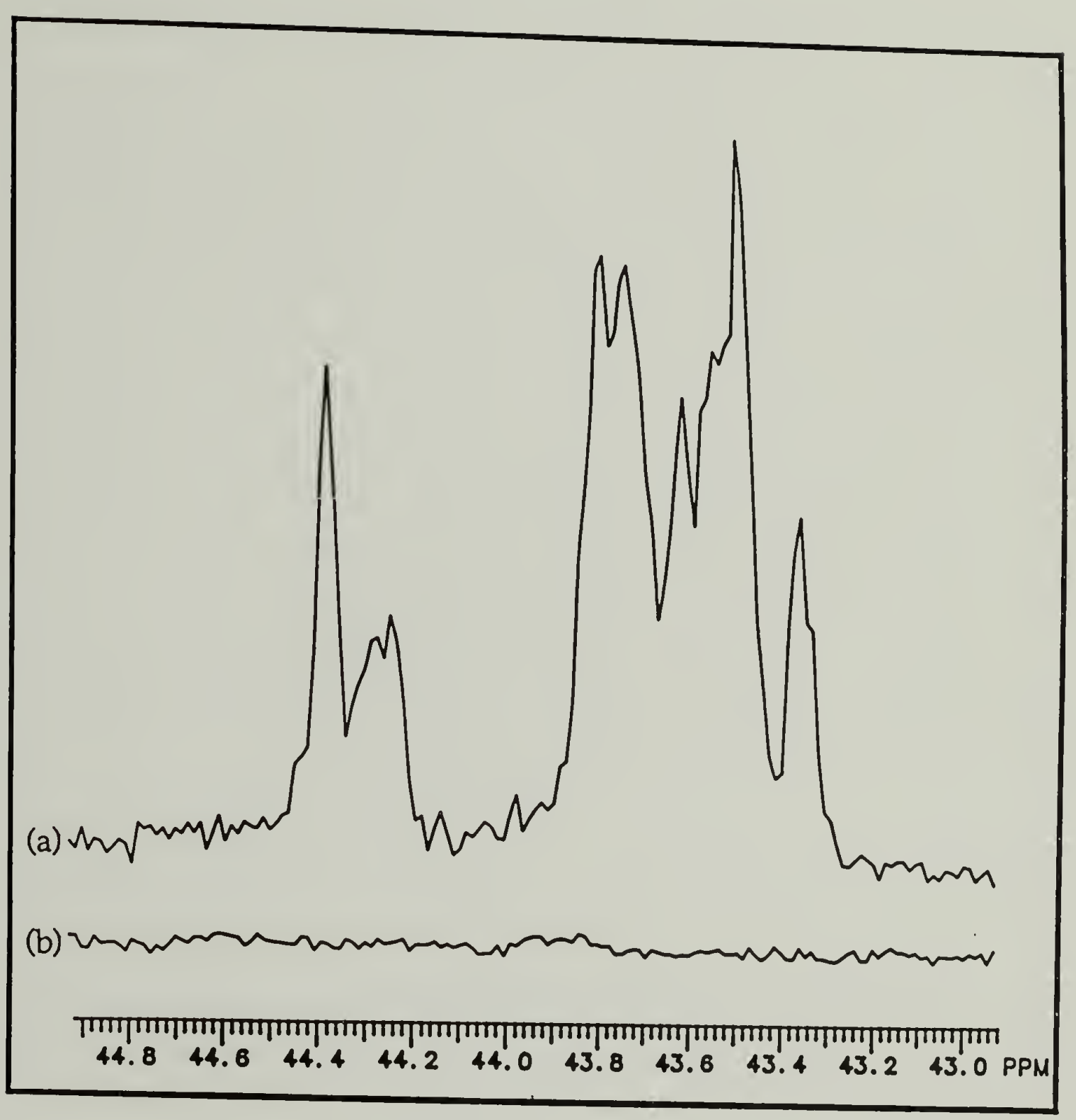

Figure D-25. 75 MHz ^{13}C NMR spectra (expanded plots) of (a) enriched and (b) natural-abundance SAN copolymers in deuterated diglyme at 140 °C that were prepared from **1b** with a monomer feed ratio ([S]/[A]) of 7.98.

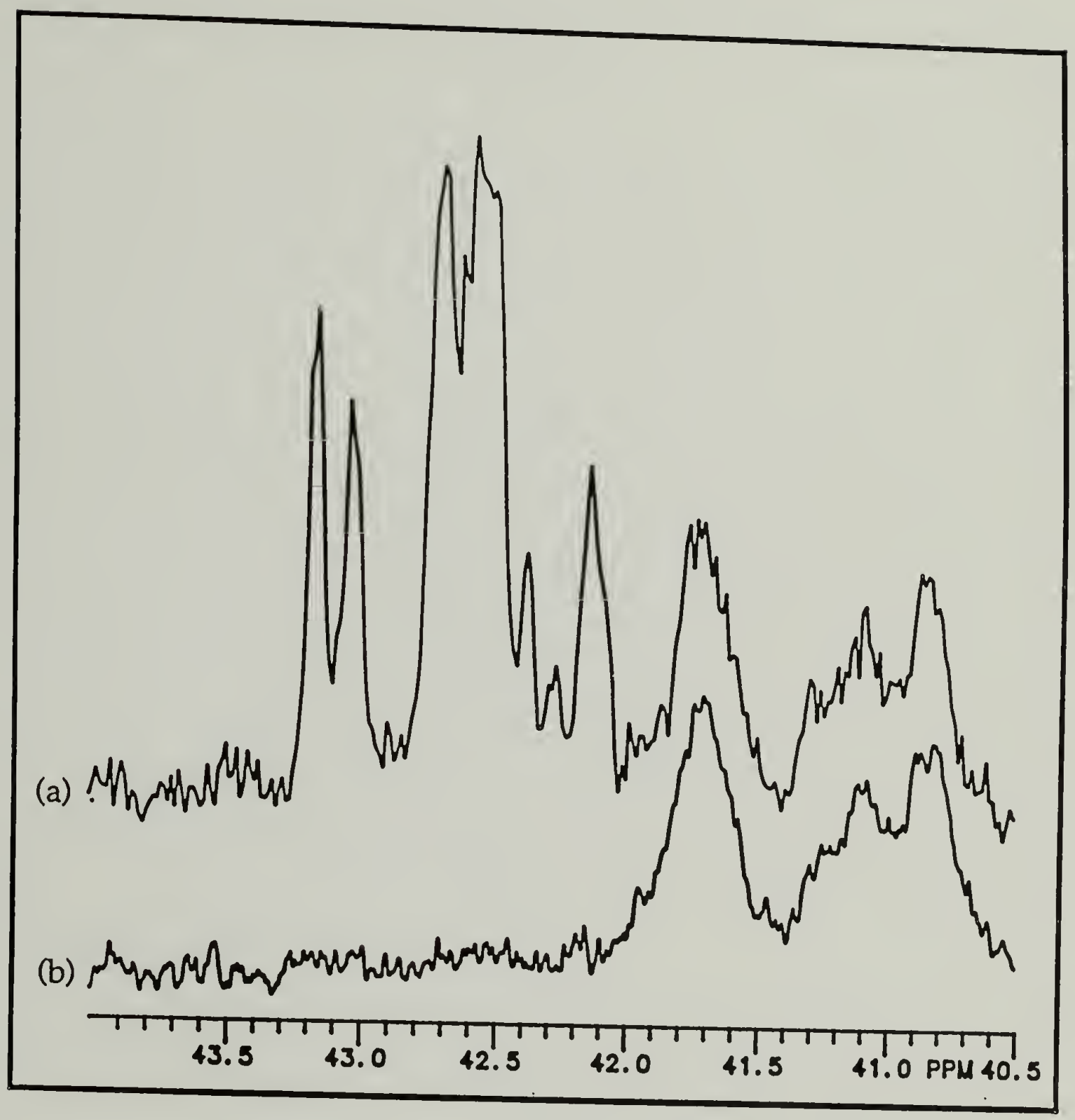

Figure D-26. 75 MHz ^{13}C NMR spectra (expanded plots) of (a) enriched and (b) natural-abundance SAN copolymers in deuterated bromobenzene at 136 °C that were prepared from **1c** with a monomer feed ratio ([S]/[A]) of 2.41.

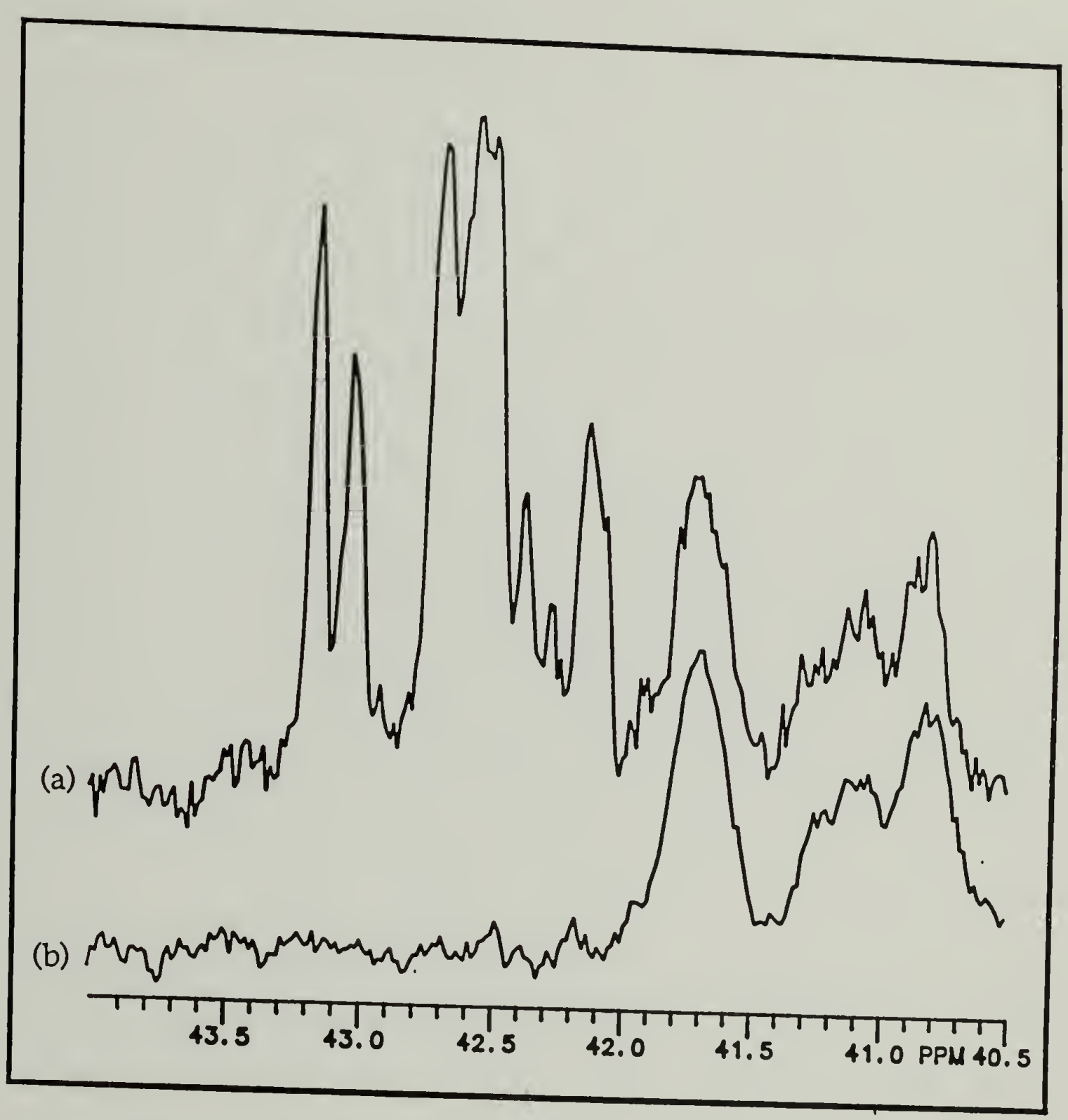

Figure D-27. 75 MHz ^{13}C NMR spectra (expanded plots) of (a) enriched and (b) natural-abundance SAN copolymers in deuterated bromobenzene at 136 °C that were prepared from **1c** with a monomer feed ratio ([S]/[A]) of 2.14.

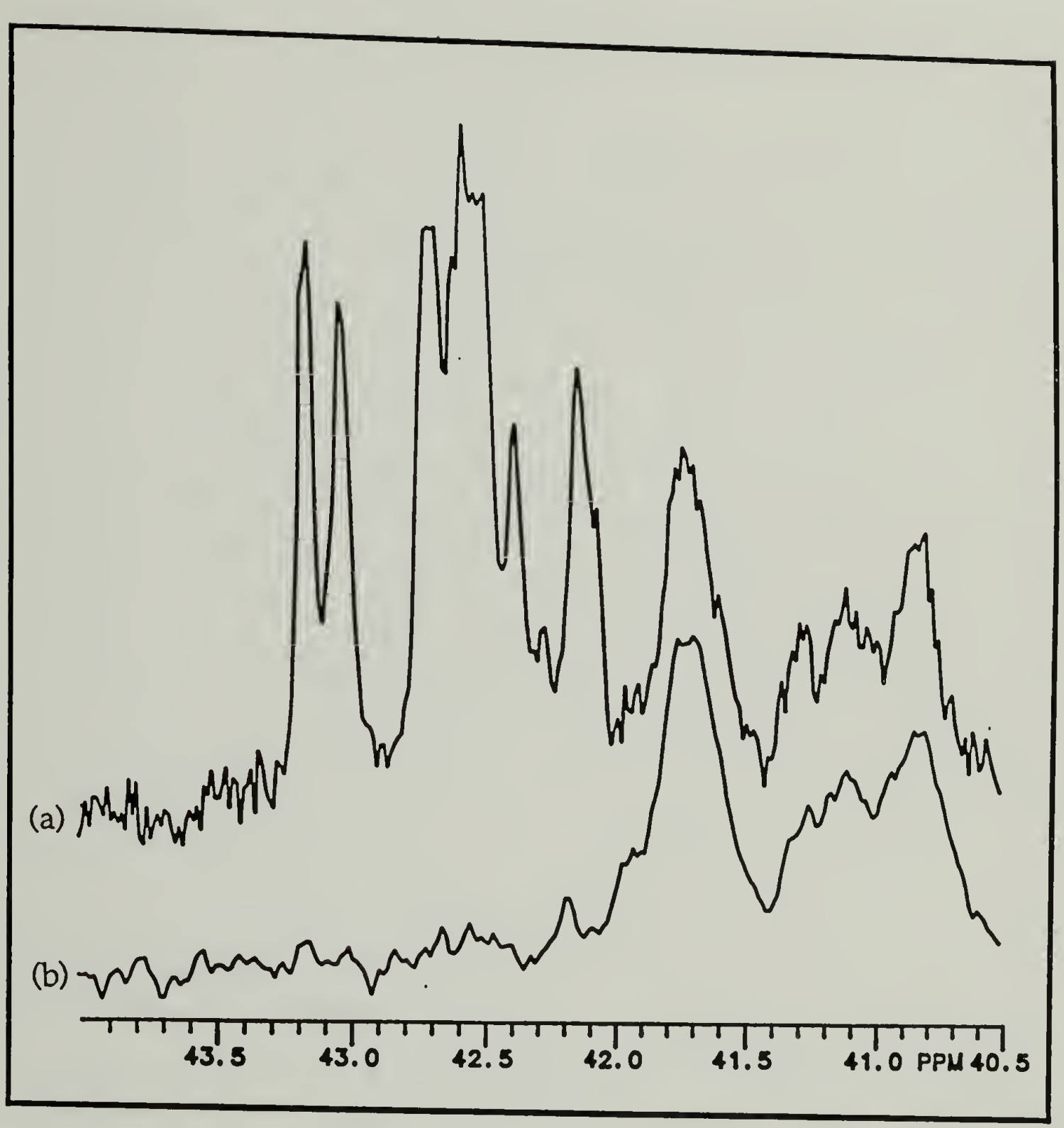

Figure D-28. 75 MHz ^{13}C NMR spectra (expanded plots) of (a) enriched and (b) natural-abundance SAN copolymers in deuterated bromobenzene at 136 °C that were prepared from 1c with a monomer feed ratio ([S]/[A]) of 1.87.

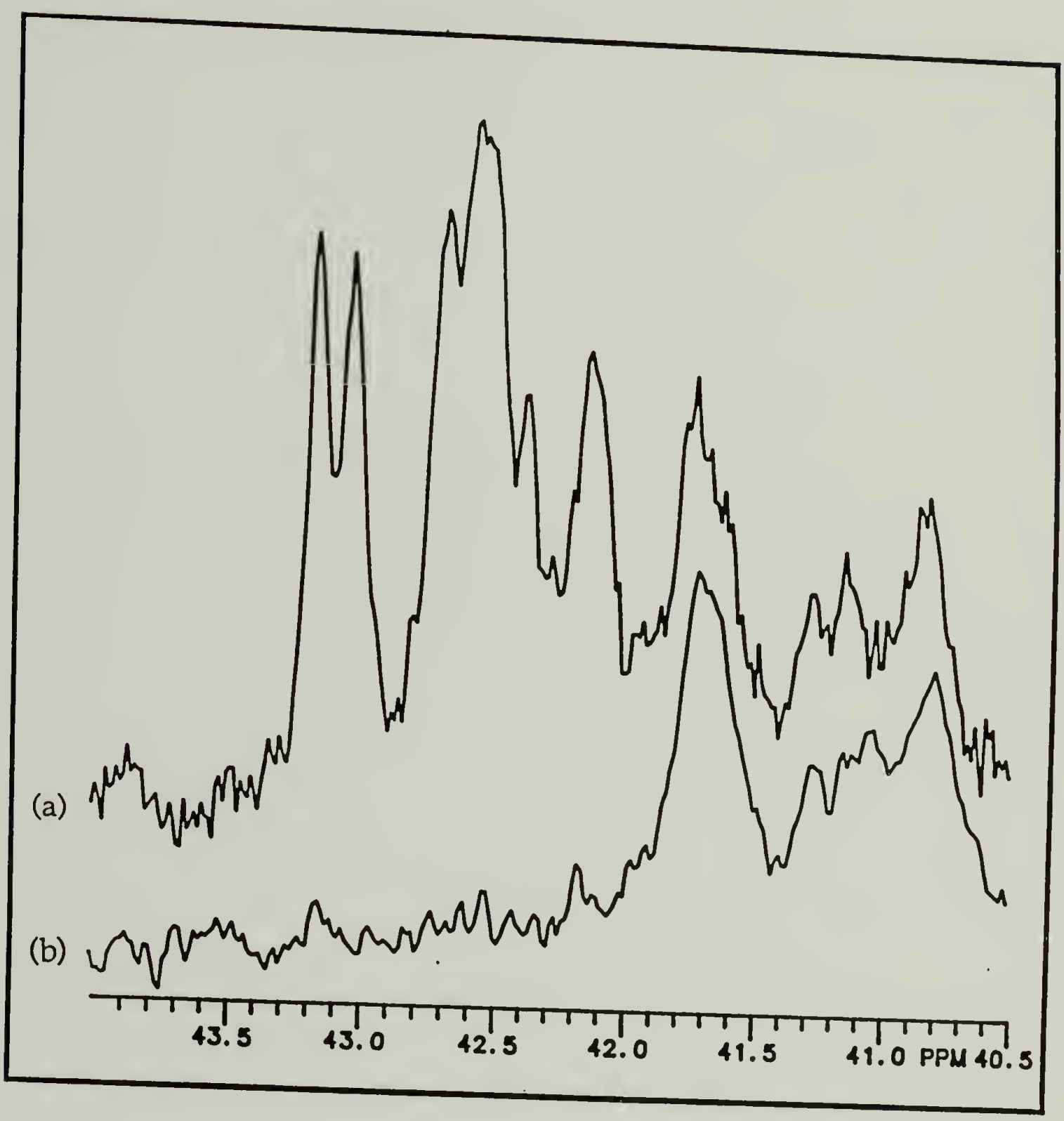

Figure D-29. 75 MHz ^{13}C NMR spectra (expanded plots) of (a) enriched and (b) natural-abundance SAN copolymers in deuterated bromobenzene at 136 °C that were prepared from **1c** with a monomer feed ratio ([S]/[A]) of 1.63.

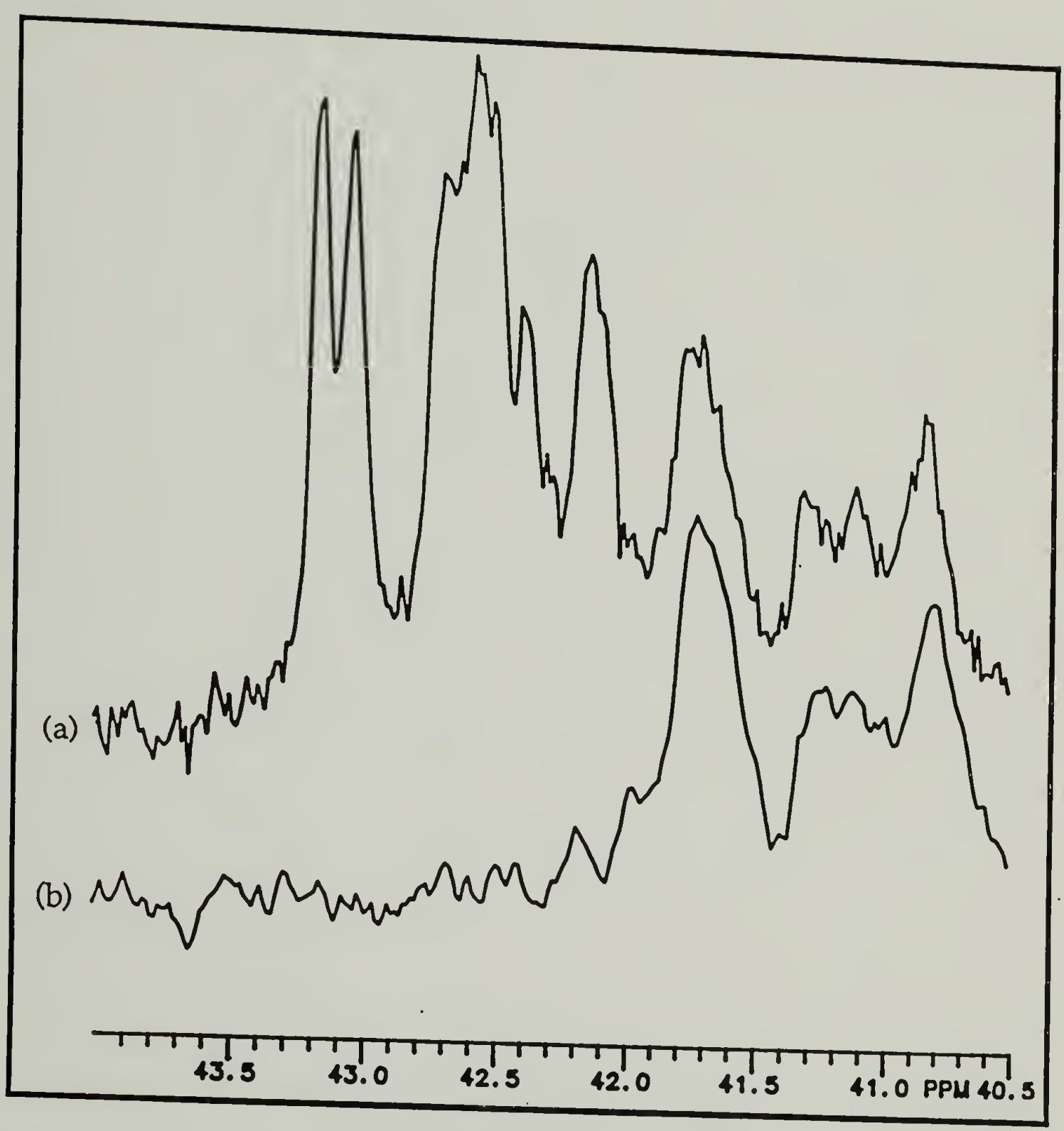

Figure D-30. 75 MHz ^{13}C NMR spectra (expanded plots) of (a) enriched and (b) natural-abundance SAN copolymers in deuterated bromobenzene at 136 °C that were prepared from **1c** with a monomer feed ratio ([S]/[A]) of 1.38.

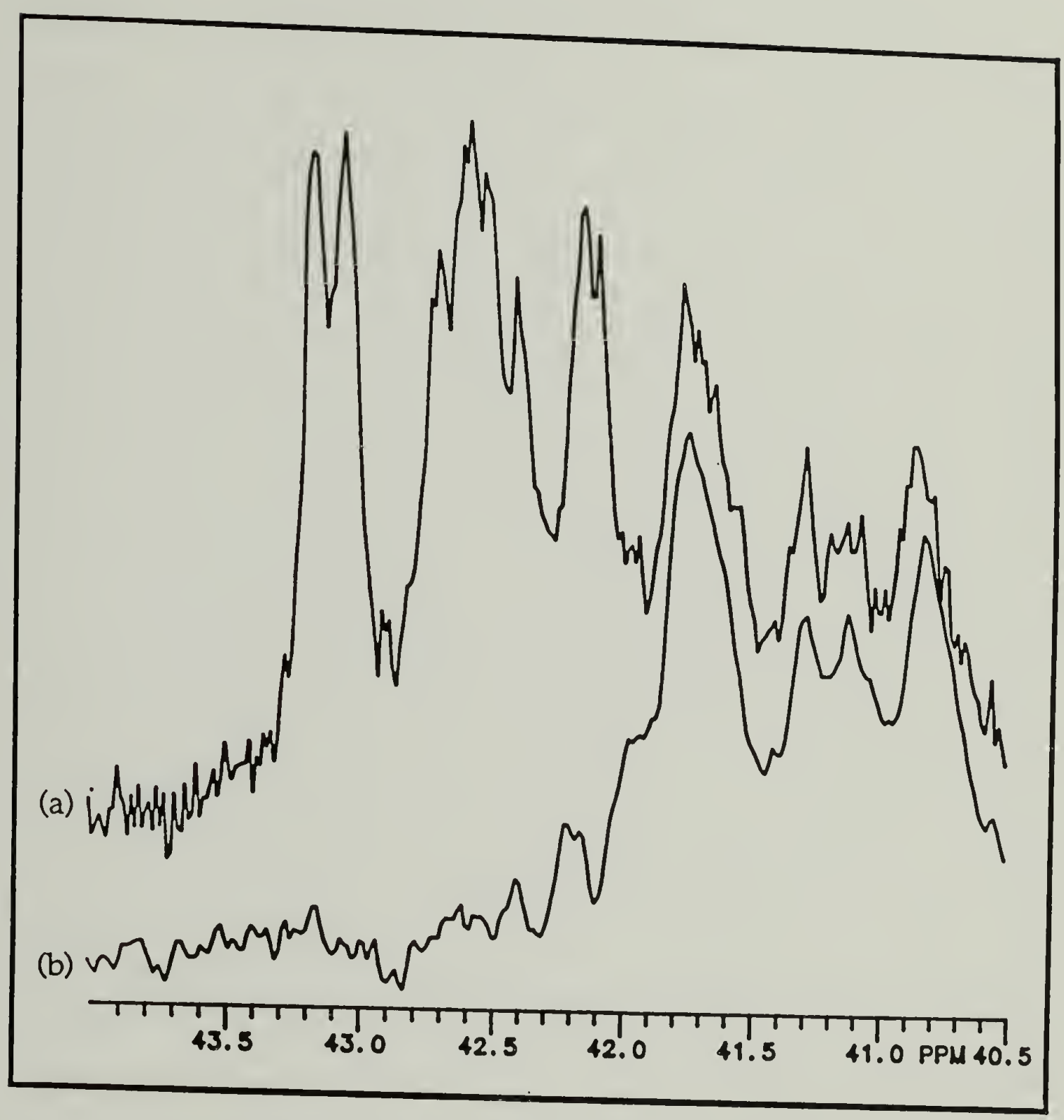

Figure D-31. 75 MHz ^{13}C NMR spectra (expanded plots) of (a) enriched and (b) natural-abundance SAN copolymers in deuterated bromobenzene at 136 °C that were prepared from **1c** with a monomer feed ratio ([S]/[A]) of 1.14.

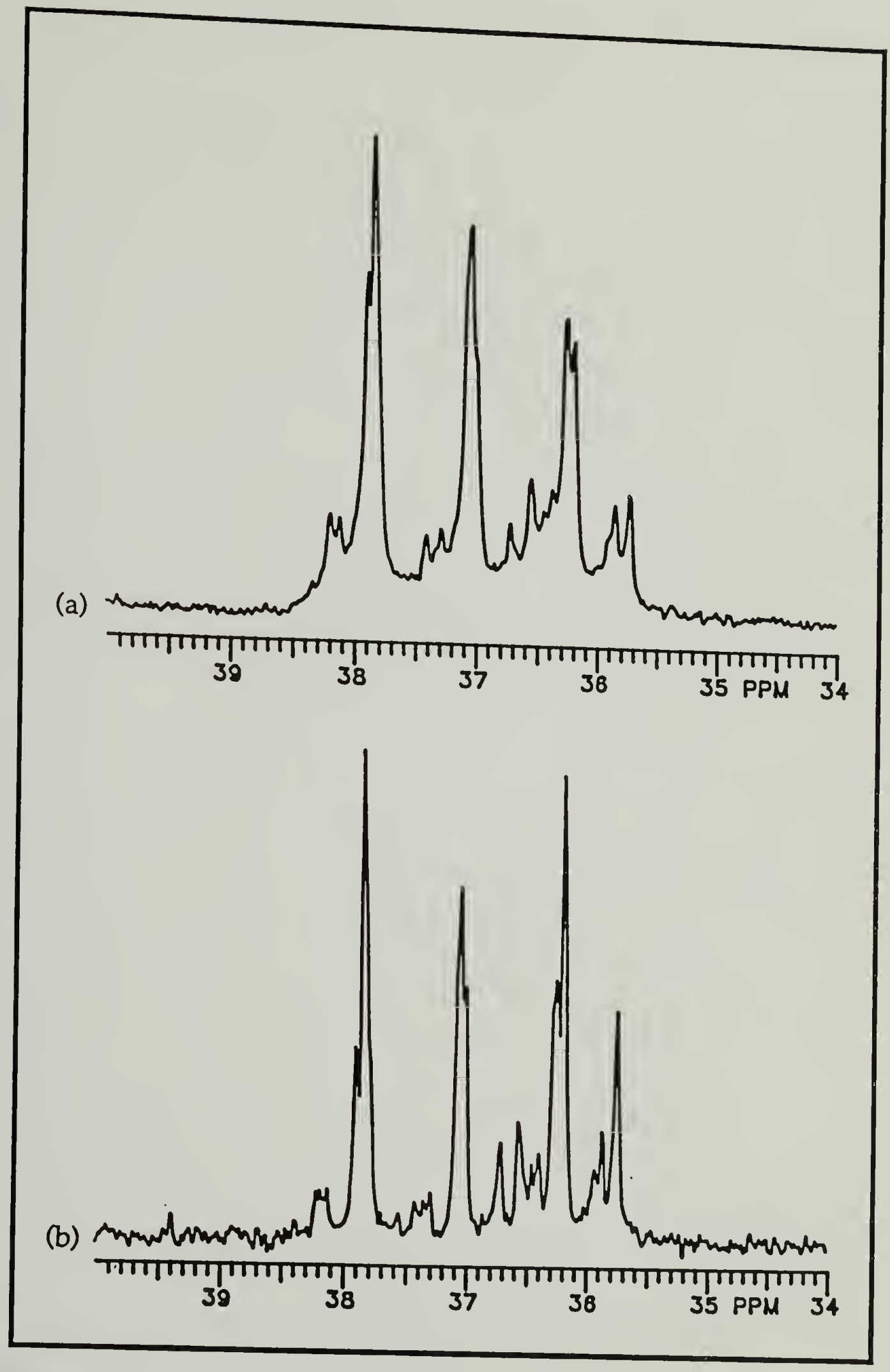

Figure D-32. 75 MHz ^{13}C NMR spectra (expanded plots) of enriched AMMA copolymers in $CDCl_3$ that were prepared from **1a** with monomer feed ratios ([MMA]/[A]) of (a) 1.72 and (b) 2.66.

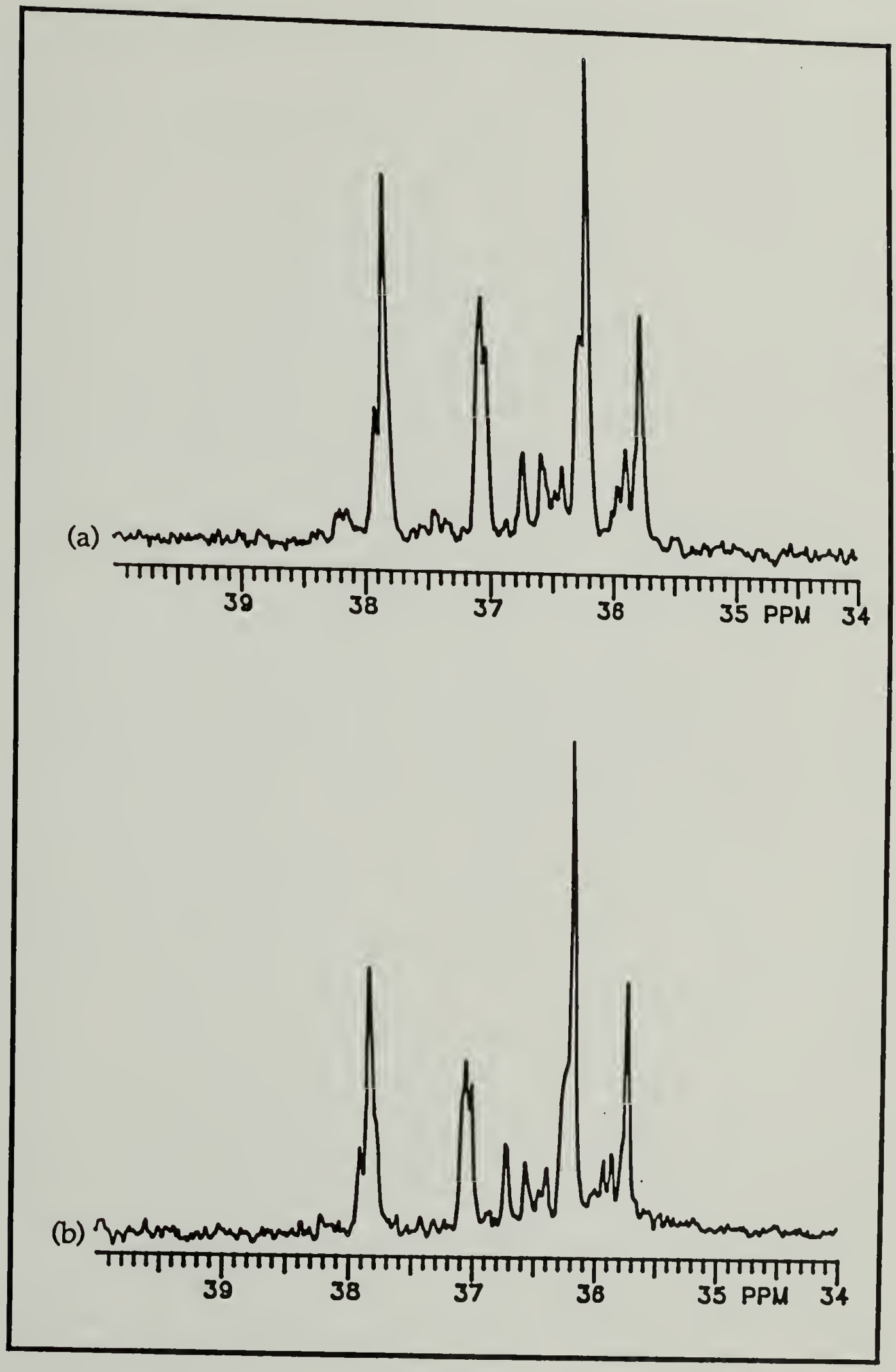

Figure D-33. 75 MHz ^{13}C NMR spectra (expanded plots) of enriched AMMA copolymers in $CDCl_3$ that were prepared from **1a** with monomer feed ratios ([MMA]/[A]) of (a) 3.42 and (b) 4.13.

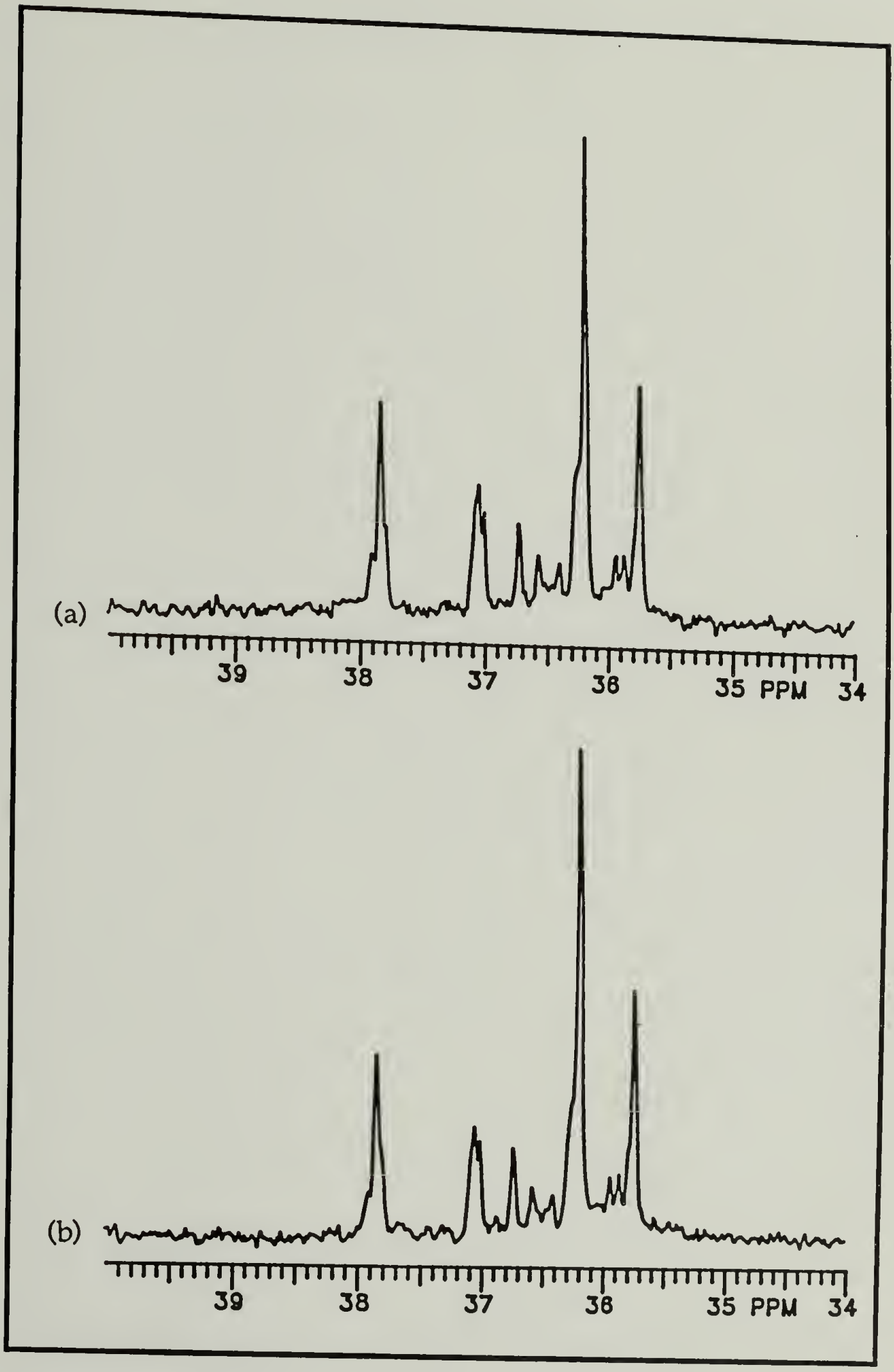

Figure D-34. 75 MHz ^{13}C NMR spectra (expanded plots) of enriched AMMA copolymers in $CDCl_3$ that were prepared from **1a** with monomer feed ratios ([MMA]/[A]) of (a) 5.03 and (b) 5.80.

REFERENCES

1. Lorand, J. P. In *Landolt-Bornstein, New Series*; Fischer, H., Ed.; Springer: New York, 1983; XIII, 135.

2. Tirrell, D. A., "Copolymerization", *Encyclopedia of Polymer Science and Engineering*, 2nd ed.; Wiley: New York, 1986; IV, 193.

3. Hill, D. J. T.; O'Donnell, J. H.; O,Sullivan, P. W. *Prog. Polym. Sci* 1982, *8*, 215.

4. Mayo, F. R.; Lewis, F.M. *J. Amer. Chem. Soc.* 1944, *66*, 1594.

5. Alfrey, T. Jr.; Goldfinger, G. *J. Chem. Phys.* 1944, *12*, 205.

6. Wall, F. T. *J. Amer. Chem. Soc.* 1944, *66*, 2050.

7. Tidwell, P. W.; Mortimer, G. A. *J. Polym. Sci. Part A* 1965, *3*, 369.

8. Tidwell, P. W.; Mortimer, G. A. *J. Macromol. Sci. Rev. Macromol. Chem.* 1970, *4*, 281.

9. McFarlane, R. C.; Reilly, P. M.; O'Driscoll, K. F. *J. Polym. Sci. Polym. Chem. Ed.* 1980, *18*, 251.

10. Leicht, R.; Fuhrmann, J. *J. Polym. Sci. Polym. Chem. Ed.* 1983, *21*, 2215.

11. Greenley, R. Z. *J. Macromol. Sci. Chem.* 1980, *14*, 445.

12. Merz, E.; Alfrey, T., Goldfinger, G. *J. Polym. Sci.* 1946, *1*, 75.

13. Fukuda, T.; Ma, Y. D.; Inagaki, H. *Macromolecules* 1985, *18*, 17.

14. Ham, G. E. *J. Polym. Sci.* 1954, *14*, 87.

15. Barb, W. G. *J. Polym. Sci.* 1953, *11*, 117.

16. Dodgson, K.; Ebdon, J. R. *Eur. Polym. J.* 1977, *13*, 791.

17. Borrows, E. T.; Haward, R. N.; Porges, J.; Street, J. *J. Appl. Chem.* 1955, *5*, 379.

18. Ma, Y. D.; Fukuda, T.; Inagaki, H. *Macromolecules* 1985, *18*, 26.

19. Hecht, J. K.; Ojha, N. D. *Macromolecules* **1969**, *2*, 94.

20. Van Der Meer, R.; Alberti, J. M.; German, A. L.; Linssen, H. N. *J. Polym. Sci. Polym. Chem. Ed.* **1979**, *17*, 3349.

21. Rounsefell, T.; Pittman, C. U. Jr. *J. Macromol. Sci. Chem.* **1979**, *A13*, 153.

22. Dainton, F. S.; Ivin, K.J. *Proc. R. Soc. Chem. London* **1952**, *212*, 96.

23. Dainton, F. S.; Ivin, K.J. *Proc. R. Soc. Chem. London* **1952**, *212*, 207.

24. Barb, W. G. *Proc. R. Soc. Chem. London* **1952**, *212*, 66.

25. Barb, W. G. *Proc. R. Soc. Chem. London* **1952**, *212*, 177.

26. Barb, W. G. *J. Polym. Sci.* **1953**, *10*, 49.

27. Walling, C. *J. Polym. Sci.* **1955**, *16*, 315.

28. Johnsen, V. U.; Kolbe, K. *Makromol. Chem.* **1968**, *116*, 173.

29. Lowry, G. G. *J. Polym. Sci.* **1960**, *42*, 463.

30. Howell, J. A.; Izu, M.; O'Driscoll, K. F. *J. Polym. Sci. Part A-1* **1970**, *8*, 699.

31. Bartlett, P. D.; Nozaki, K. *J. Amer. Chem. Soc.* **1946**, *68*, 1495.

32. Hyde, P.; Ledwith, A. In *Molecular Complexes*; Fister, R., Ed.; Paul Elek: London, 1974; II.

33. Cais, R. E.; Farmer, R. G.; Hill, D. J. T.; O'Donnell, J. H. *Macromolecules* **1979**, *12*, 835.

34. Farmer, R. G.; Hill, D. J. T.; O'Donnell, J. H. *J. Macromol. Sci. Chem.* **1980**, *14*, 51.

35. Hill, D. J. T.; O'Donnell, J. H.; O'Sullivan, P. W. *Prog. Polym. Sci.* **1982**, *8*, 215.

36. Olson, K. G.; Butler, G. B. *Macromolecules* **1984**, *17*, 2486.

37. Jones, S. A., Ph.D. Dissertation, Carnegie-Mellon University, 1986.

38. Jones, S. A.; Tirrell, D. A. *Macromolecules* **1986**, *19*, 2080.

39. Prementine, G. S., Ph.D. Dissertation, Carnegie-Mellon University, 1987.

40. Seiner, J. A.; Litt, M. *Macromolecules* **1971**, *4*, 308.

41. Litt, M. *Macromolecules* **1971**, *4*, 312.

42. Litt, M.; Seiner, J. A. *Macromolecules* **1971**, *4*, 314.

43. Litt, M.; Seiner, J. A. *Macromolecules* **1971**, *4*, 316.

44. Tsuchida, E.; Tomona, T. *Makromol. Chem.* **1971**, *141*, 265.

45. Tsuchida, E.; Tomona, T.; Sano, H. *Makromol. Chem.* **1972**, *151*, 245.

46. Tsuchida, E.; Toda, F.; Kosugi, M.; Torii, Y. *J. Polym. Sci. Part A-1* **1971**, *9*, 2423.

47. Deb, P. C.; Meyerhoff, G. *Eur. Polym. J.* **1984**, *20*, 713.

48. Deb, P. C. *J. Polym. Sci. Polym. Lett. Ed.* **1985**, *23*, 233.

49. Hill, D. J. T.; O'Donnell, J. H.; O'Sullivan, P. W. *Macromolecules* **1983**, *16*, 1295.

50. Pichot, C.; Zaganiaris, E.; Guyot, A. *J. Polym. Sci. Symposium No. 52* **1975**, 55.

51. Plochocka, K.; Harwood, H. J. *Polym. Prepr.* **1978**, *19*, 240.

52. Tudos, F.; Kelen, T.; Berezhnikh, T. F. *J. Polym. Sci. Symposium No. 50* **1975**, 109.

53. Hill, D. J. T.; O'Donnell, J. H.; O'Sullivan, P. W. *Macromolecules* **1982**, *15*, 960.

54. Giese, B.; Kretzschmar, G.; Meixner, J. *Chem. Ber.* **1980**, *113*, 2787.

55. Walling, C. *J. Amer. Chem. Soc.* **1949**, *71*, 1930.

56. Ito, K. *J. Polym. Sci. Polym. Chem. Ed.* **1978**, *16*, 2725.

57. Jones, S. A.; Prementine, G. S.; Tirrell, D. A. *J. Amer. Chem. Soc.* **1985**, *107*, 5275.

58. Prementine, G. S., Tirrell, D. A. *Macromolecules* **1987**, *20*, 3034.

59. Walling, C. *Free Radicals in Solution*; Wiley: New York, 1957.

60. Tedder, J. M.; Walton, J. C. *Acc. Chem. Res.* **1976**, *9*, 183.

61. Ruchardt, C. *Topics of Current Chemistry*; Boschke, E., Ed.; Springer-Verlag: New York, 1980; I.

62. Tedder, J. M. *Angew. Chem., Int. Ed. Eng.* **1982**, *21*, 401.

63. Giese, B. *Angew. Chem., Int. Ed. Eng.* **1983**, *22*, 753.

64. Munger, K.; Fischer, H. *Int. J. Chem. Kin.* **1985**, *17*, 809.

65. Young, L. J. In *Polymer Handbook*, 2nd ed.; Brandrup, J., Immergut, E. H., Eds.; Wiley: New York, 1975; p. II-105.

66. Kerr, J. A.; Parsonage, M. J. *Evaluated Kinetic Data on Gas-Phase Addition Reactions. Reactions of Atoms and Radicals with Alkenes, Alkynes, and Aromatic Compounds*; Butterworths: London, 1972.

67. Minisci, F.; Zammori, P.; Bernardi, R.; Cecere, M.; Galli. R. *Tetrahedron* **1970**, *26*, 4153.

68. Caronna, T.; Citterio, A.; Ghirardini, M.; Minisci, F. *Tetrahedron* **1977**, *33*, 793.

69. Citterio, A.; Arnoldi, A.; Minisci, F. *J. Org. Chem.* **1979**, *44*, 2674.

70. Giese, B.; Meixner, J. *Angew. Chem., Int. Ed. Eng.* **1977**, *16*, 178.

71. Giese, B.; Meixner, J. *Chem. Ber.* **1977**, *110*, 2588.

72. Giese, B.; Meixner, J. *Angew. Chem., Int. Ed. Eng.* **1979**, *18*, 154.

73. Baban, J. A.; Robers, B. D. *J. Chem. Soc. Perkin Trans. II* **1981**, 161.

74. Giese, B.; Feix, C. *Israel. J. Chem.* **1985**, *26*, 387.

75. Fleming, I. *Frontier Orbitals and Organic Chemical Reactions* ; Wiley: New York, 1976.

76. Giese, B.; Meixner, J. *Tetrahedron Lett.* **1977**, 2779.

77. Pasto, D. J.; Gontarz, J. A. *J. Amer. Chem. Soc.* **1969**, *91*, 719.

78. Gray, G. A.; Jackson, W. R. *J. Amer. Chem. Soc.* **1969**, *91*, 6205.

79. Whitesides, G. M.; San Filippo, J. Jr. *J. Amer. Chem. Soc.* **1970**, *92*, 6611.

80. Quirk, R. P. *J. Org. Chem.* **1972**, *37*, 3554.

81. Giese, B.; Kretzschmar, G. *Chem. Ber.* **1984**, *117*, 3160.

82. Quirk, R. P.; Lea, R. E. *J. Amer. Chem. Soc.* **1976**, *98*, 5973.

83. Russell, G. A.; Guo, D. *Tetrahedron Lett.* **1984**, 5239.

84. Hill, C. L.; Whitesides, G. M. *J. Amer. Chem. Soc.* **1974**, *96*, 870.

85. Bevington, J. C.; Ebdon, J. R.; Huckerby, T. N. *Eur. Polym. J.* **1985**, *21*, 685 and references therein.

86. Bevington, J. C.; Breuer, S. W.; Heseltine, E. N. J.; Huckerby, T. N.; Varma, S. C. *J. Polym. Sci. Polym. Chem. Ed.* **1987**, *25*, 1085.

87. Moad, G.; Solomon, D. H.; Johns, S. R.; Willing, R. I. *Macromolecules* **1984**, *17*, 1094.

88. Strauz, O. P.; Berkley, R. E.; Gunning, H. E. *Can. J. Chem.* **1969**, *47*, 3470.

89. Arin, M. L.; Steel, C. *J. Phys. Chem.* **1972**, *76*, 1685.

90. Drewer, R. J. In *The Chemistry of the Hydrazo, Azo, and Azoxy Groups* ; Patai, S., Ed.; Wiley: New York, 1975; 935.

91. Green, J. G.; Dubay, G. R.; Porter, N. A. *J. Amer. Chem. Soc.* **1977**, *99*, 1264 and references therein.

92. Symons, M. C. R. *Nature* **1967**, *213*, 1226.

93. Ayscough, P. B.; Brooks, B. R.; Evans, H. E. *J. Phys. Chem.* **1964**, *68*, 3889.

94. Leermakers, P. A.; Thomas, H. J.; Weiss, L. D.; James, F. C. *J. Amer. Chem. Soc.* 1966, *88*, 5075.

95. Diazomethane solutions were prepared - using purchased N-methyl-N-nitroso-p-toluenesulfonamide - according to: De Boer, Th. J.; Backer, H. J. In *Organic Syntheses Collective Volume IV* ; Rabjohn, N., Ed.; Wiley: New York, 1963; 250.

96. Dauben, W. G.; Reid, J. C.; Yankwich, P. E. *Anal. Chem.* **1947**, *19*, 828.

97. Gilman, H.; Zoellner, E. A.; Dickey, J. B. *J. Amer. Chem. Soc.* **1929**, *51*, 1576.

98. Straley, J. M.; Adams, A. C. In *Organic Syntheses Collective Volume IV* ; Rabjohn, N., Ed.; Wiley: New York, 1963; 415.

99. Secor, H. V.; Sanders, E. B. *J. Org. Chem.* **1978**, *43*, 2539.

100. *XL-Series NMR Spectrometer System Advanced Operation, Publication #87-146056, Revision B1084*; Varian Associates: 1984; p. 2-1.

101. Timberlake, J. W.; Stowell, J. C. In *The Chemistry of the Hydrazo, Azo, and Azoxy Groups*; Patai, S., Ed.; Wiley: New York, 1975; 69.

102. Schulze, W. A.; Lochte, H. L. *J. Amer. Chem. Soc.* **1926**, *48*, 1031.

103. Cohen, S. G.; Groszos, S. J.; Sparrow, D. B. *J. Amer. Chem. Soc.* **1950**, *72*, 3947.

104. Gibian, M. J.; Corley, R. C. *J. Amer. Chem. Soc.* **1972**, *94*, 4178.

105. Robertson, J. A. *Chem. Abstr.* **1952**, *45*, P1384g; U.S. Patent 2 520 339 (to Du Pont), Aug. 29, 1950.

106. Seltzer, S. *J. Amer. Chem. Soc.* **1961**, *83*, 2625.

107. Shelton, J. R.; Liang, C. K. *Synthesis* **1971**, 204.

108. Grizzle, P. L.; Miller, D. W.; Scheppele, S. E. *J. Org. Chem.* **1975**, *40*, 1902.

109. Daub, G. H.; Cannizzo, L. F. *J. Org. Chem.* **1982**, *47*, 5034.

110. Greene, F. D.; Berwick, M. A.; Stowell, J. C. *J. Amer. Chem. Soc.* **1970**, *92*, 867.

111. Silverstein, R. M.; Bassler, G. C.; Morrill, T. C. *Spectrometric Identification of Organic Compounds* ; Wiley: New York, 1981; p. 258.

112. Pichot, C.; Pham, Q. T. *Makromol. Chem.* **1979**, *180*, 2539.

113. Odian, G. *Principles of Polymerization* , 2nd ed.; Wiley: New York, 1981; p. 584.

114. Simionescu, C.; Asandei, N.; Liga, A. *Makromol. Chem.* **1967**, *110*, 278.

115. Joshi, R. M.; Kapur, S. L. *J. Sci. Ind. Res.* **1957**, *16B*, 379.

116. Lewis, F. M.; Mayo, F. R.; Hulse, W. F. *J. Amer. Chem. Soc.* **1945**, *67*, 1701.

117. Burkhart, R. D.; Zutty, N. L. *J. Polym. Sci.* **1962**, *57*, 783.

BIBLIOGRAPHY

Alfrey, T. Jr.; Goldfinger, G. *J. Chem. Phys.* **1944**, *12*, 205.

Arin, M. L.; Steel, C. *J. Phys. Chem.* **1972**, *76*, 1685.

Ayscough, P. B.; Brooks, B. R.; Evans, H. E. *J. Phys. Chem.* **1964**, *68*, 3889.

Baban, J. A.; Robers, B. D. *J. Chem. Soc. Perkin Trans. II* **1981**, 161.

Barb, W. G. *J. Polym. Sci.* **1953**, *10*, 49.

Barb, W. G. *J. Polym. Sci.* **1953**, *11*, 117.

Barb, W. G. *Proc. R. Soc. Chem. London* **1952**, *212*, 66.

Barb, W. G. *Proc. R. Soc. Chem. London* **1952**, *212*, 177.

Bartlett, P. D.; Nozaki, K. *J. Amer. Chem. Soc.* **1946**, *68*, 1495.

Bevington, J. C.; Breuer, S. W.; Heseltine, E. N. J.; Huckerby, T. N.; Varma, S. C. *J. Polym. Sci. Polym. Chem. Ed.* **1987**, *25*, 1085.

Bevington, J. C.; Ebdon, J. R.; Huckerby, T. N. *Eur. Polym. J.* **1985**, *21*, 685 and references therein.

Borrows, E. T.; Haward, R. N.; Porges, J.; Street, J. *J. Appl. Chem.* **1955**, *5*, 379.

Burkhart, R. D.; Zutty, N. L. *J. Polym. Sci.* **1962**, *57*, 783.

Cais, R. E.; Farmer, R. G.; Hill, D. J. T.; O'Donnell, J. H. *Macromolecules* **1979**, *12*, 835.

Caronna, T.; Citterio, A.; Ghirardini, M.; Minisci, F. *Tetrahedron* **1977**, *33*, 793.

Citterio, A.; Arnoldi, A.; Minisci, F. *J. Org. Chem.* **1979**, *44*, 2674.

Cohen, S. G.; Groszos, S. J.; Sparrow, D. B. *J. Amer. Chem. Soc.* **1950**, *72*, 3947.

Dainton, F. S.; Ivin, K.J. *Proc. R. Soc. Chem. London* **1952**, *212*, 96.

Dainton, F. S.; Ivin, K.J. *Proc. R. Soc. Chem. London* **1952**, *212*, 207.

Daub, G. H.; Cannizzo, L. F. *J. Org. Chem.* **1982**, *47*, 5034.

Dauben, W. G.; Reid, J. C.; Yankwich, P. E. *Anal. Chem.* **1947**, *19*, 828.

De Boer, Th. J.; Backer, H. J. In *Organic Syntheses Collective Volume IV* ; Rabjohn, N., Ed.; Wiley: New York, 1963; 250.

Deb, P. C. *J. Polym. Sci. Polym. Lett. Ed.* **1985**, *23*, 233.

Deb, P. C.; Meyerhoff, G. *Eur. Polym. J.* **1984**, *20*, 713.

Dodgson, K.; Ebdon, J. R. *Eur. Polym. J.* **1977**, *13*, 791.

Drewer, R. J. In *The Chemistry of the Hydrazo, Azo, and Azoxy Groups* ; Patai, S., Ed.; Wiley: New York, 1975; 935.

Farmer, R. G.; Hill, D. J. T.; O'Donnell, J. H. *J. Macromol. Sci. Chem.* **1980**, *14*, 51.

Fleming, I. *Frontier Orbitals and Organic Chemical Reactions* ; Wiley: New York, 1976.

Fukuda, T.; Ma, Y. D.; Inagaki, H. *Macromolecules* **1985**, *18*, 17.

Gibian, M. J.; Corley, R. C. *J. Amer. Chem. Soc.* **1972**, *94*, 4178.

Giese, B. *Angew. Chem., Int. Ed. Eng.* **1983**, *22*, 753.

Giese, B.; Feix, C. *Israel. J. Chem.* **1985**, *26*, 387.

Giese, B.; Kretzschmar, G. *Chem. Ber.* **1984**, *117*, 3160.

Giese, B.; Kretzschmar, G.; Meixner, J. *Chem. Ber.* **1980**, *113*, 2787.

Giese, B.; Meixner, J. *Angew. Chem., Int. Ed. Eng.* **1977**, *16*, 178.

Giese, B.; Meixner, J. *Angew. Chem., Int. Ed. Eng.* **1979**, *18*, 154.

Giese, B.; Meixner, J. *Chem. Ber.* **1977**, *110*, 2588.

Giese, B.; Meixner, J. *Tetrahedron Lett.* **1977**, 2779.

Gilman, H.; Zoellner, E. A.; Dickey, J. B. *J. Amer. Chem. Soc.* **1929**, *51*, 1576.

Gray, G. A.; Jackson, W. R. *J. Amer. Chem. Soc.* **1969**, *91*, 6205.

Green, J. G.; Dubay, G. R.; Porter, N. A. *J. Amer. Chem. Soc.* **1977**, *99*, 1264 and references therein.

Greene, F. D.; Berwick, M. A.; Stowell, J. C. *J. Amer. Chem. Soc.* **1970**, *92*, 867.

Greenley, R. Z. *J. Macromol. Sci. Chem.* **1980**, *14*, 445.

Grizzle, P. L.; Miller, D. W.; Scheppele, S. E. *J. Org. Chem.* **1975**, *40*, 1902.

Ham, G. E. *J. Polym. Sci.* **1954**, *14*, 87

Hecht, J. K.; Ojha, N. D. *Macromolecules* **1969**, *2*, 94.

Hill, C. L.; Whitesides, G. M. *J. Amer. Chem. Soc.* **1974**, *96*, 870.

Hill, D. J. T.; O'Donnell, J. H.; O'Sullivan, P. W. *Macromolecules* **1982**, *15*, 960.

Hill, D. J. T.; O'Donnell, J. H.; O'Sullivan, P. W. *Macromolecules* **1983**, *16*, 1295.

Hill, D. J. T.; O'Donnell, J. H.; O'Sullivan, P. W. *Prog. Polym. Sci.* **1982**, *8*, 215.

Hill, D. J. T.; O'Donnell, J. H.; O,Sullivan, P. W. *Prog. Polym. Sci* **1982**, *8*, 215.

Howell, J. A.; Izu, M.; O'Driscoll, K. F. *J. Polym. Sci. Part A-1* **1970**, *8*, 699.

Hyde, P.; Ledwith, A. In *Molecular Complexes*; Fister, R., Ed.; Paul Elek: London, 1974; II.

Ito, K. *J. Polym. Sci. Polym. Chem. Ed.* **1978**, *16*, 2725.

Johnsen, V. U.; Kolbe, K. *Makromol. Chem.* **1968**, *116*, 173.

Jones, S. A., Ph.D. Dissertation, Carnegie-Mellon University, 1986.

Jones, S. A.; Prementine, G. S.; Tirrell, D. A. *J. Amer. Chem. Soc.* **1985**, *107*, 5275.

Jones, S. A.; Tirrell, D. A. *Macromolecules* **1986**, *19*, 2080.

Joshi, R. M.; Kapur, S. L. *J. Sci. Ind. Res.* **1957**, *16B*, 379.

Kerr, J. A.; Parsonage, M. J. *Evaluated Kinetic Data on Gas-Phase Addition Reactions. Reactions of Atoms and Radicals with Alkenes, Alkynes, and Aromatic Compounds;* Butterworths: London, 1972.

Leermakers, P. A.; Thomas, H. J.; Weiss, L. D.; James, F. C. *J. Amer. Chem. Soc.* 1966, *88*, 5075.

Leicht, R.; Fuhrmann, J. *J. Polym. Sci. Polym. Chem. Ed.* **1983**, *21*, 2215.

Lewis, F. M.; Mayo, F. R.; Hulse, W. F. *J. Amer. Chem. Soc.* **1945**, *67*, 1701.

Litt, M. *Macromolecules* **1971**, *4*, 312.

Litt, M.; Seiner, J. A. *Macromolecules* **1971**, *4*, 314.

Litt, M.; Seiner, J. A. *Macromolecules* **1971**, *4*, 316.

Lorand, J. P. In *Landolt-Bornstein, New Series;* Fischer, H., Ed.; Springer: New York, 1983; XIII, 135.

Lowry, G. G. *J. Polym. Sci.* **1960**, *42*, 463.

Ma, Y. D.; Fukuda, T.; Inagaki, H. *Macromolecules* **1985**, *18*, 26.

Mayo, F. R.; Lewis, F.M. *J. Amer. Chem. Soc.* **1944**, *66*, 1594.

McFarlane, R. C.; Reilly, P. M.; O'Driscoll, K. F. *J. Polym. Sci. Polym. Chem. Ed.* 1980, *18*, 251.

Merz, E.; Alfrey, T., Goldfinger, G. *J. Polym. Sci.* **1946**, *1*, 75.

Minisci, F.; Zammori, P.; Bernardi, R.; Cecere, M.; Galli. R. *Tetrahedron* **1970**, *26*, 4153.

Moad, G.; Solomon, D. H.; Johns, S. R.; Willing, R. I. *Macromolecules* 1984, *17*, 1094.

Munger, K.; Fischer, H. *Int. J. Chem. Kin.* **1985**, *17*, 809.

Odian, G. *Principles of Polymerization* , 2nd ed.; Wiley: New York, 1981; p. 584.

Olson, K. G.; Butler, G. B. *Macromolecules* **1984**, *17*, 2486.

Pasto, D. J.; Gontarz, J. A. *J. Amer. Chem. Soc.* **1969**, *91*, 719.

Pichot, C.; Pham, Q. T. *Makromol. Chem.* **1979**, *180*, 2539.

Pichot, C.; Zaganiaris, E.; Guyot, A. *J. Polym. Sci. Symposium No. 52* **1975**, 55.

Plochocka, K.; Harwood, H. J. *Polym. Prepr.* **1978**, *19*, 240.

Prementine, G. S., Ph.D. Dissertation, Carnegie-Mellon University, 1987.

Prementine, G. S., Tirrell, D. A. *Macromolecules* **1987**, *20*, 3034.

Quirk, R. P. *J. Org. Chem.* **1972**, *37*, 3554.

Quirk, R. P.; Lea, R. E. *J. Amer. Chem. Soc.* **1976**, *98*, 5973.

Robertson, J. A. *Chem. Abstr.* **1952**, *45*, P1384g; U.S. Patent 2 520 339 (to Du Pont), Aug. 29, 1950.

Rounsefell, T.; Pittman, C. U. Jr. *J. Macromol. Sci. Chem.* **1979**, *A13*, 153.

Ruchardt, C. *Topics of Current Chemistry*; Boschke, E., Ed.; Springer-Verlag: New York, 1980; I.

Russell, G. A.; Guo, D. *Tetrahedron Lett.* **1984**, 5239.

Schulze, W. A.; Lochte, H. L. *J. Amer. Chem. Soc.* **1926**, *48*, 1031.

Secor, H. V.; Sanders, E. B. *J. Org. Chem.* **1978**, *43*, 2539.

Seiner, J. A.; Litt, M. *Macromolecules* **1971**, *4*, 308.

Seltzer, S. *J. Amer. Chem. Soc.* **1961**, *83*, 2625.

Shelton, J. R.; Liang, C. K. *Synthesis* **1971**, 204.

Silverstein, R. M.; Bassler, G. C.; Morrill, T. C. *Spectrometric Identification of Organic Compounds* ; Wiley: New York, 1981; p. 258.

Simionescu, C.; Asandei, N.; Liga, A. *Makromol. Chem.* **1967**, *110*, 278.

Straley, J. M.; Adams, A. C. In *Organic Syntheses Collective Volume IV* ; Rabjohn, N., Ed.; Wiley: New York, 1963; 415.

Strauz, O. P.; Berkley, R. E.; Gunning, H. E. *Can. J. Chem.* **1969**, *47*, 3470.

Symons, M. C. R. *Nature* **1967**, *213*, 1226.

Tedder, J. M. *Angew. Chem., Int. Ed. Eng.* **1982**, *21*, 401.

Tedder, J. M.; Walton, J. C. *Acc. Chem. Res.* **1976**, *9*, 183.

Tidwell, P. W.; Mortimer, G. A. *J. Macromol. Sci. Rev. Macromol. Chem.* **1970**, *4*, 281.

Tidwell, P. W.; Mortimer, G. A. *J. Polym. Sci. Part A* **1965**, *3*, 369.

Timberlake, J. W.; Stowell, J. C. In *The Chemistry of the Hydrazo, Azo, and Azoxy Groups*; Patai, S., Ed.; Wiley: New York, 1975; 69.

Tirrell, D. A., "Copolymerization", *Encyclopedia of Polymer Science and Engineering*, 2nd ed.; Wiley: New York, 1986; IV, 193.

Tsuchida, E.; Toda, F.; Kosugi, M.; Torii, Y. *J. Polym. Sci. Part A-1* **1971**, *9*, 2423.

Tsuchida, E.; Tomona, T. *Makromol. Chem.* **1971**, *141*, 265.

Tsuchida, E.; Tomona, T.; Sano, H. *Makromol. Chem.* **1972**, *151*, 245.

Tudos, F.; Kelen, T.; Berezhnikh, T. F. *J. Polym. Sci. Symposium No. 50* **1975**, 109.

Van Der Meer, R.; Alberti, J. M.; German, A. L.; Linssen, H. N. *J. Polym. Sci. Polym. Chem. Ed.* **1979**, *17*, 3349.

Varian Associates *XL-Series NMR Spectrometer System Advanced Operation, Publication #87-146056, Revision B1084*; Varian Associates: 1984; p. 2-1.

Wall, F. T. *J. Amer. Chem. Soc.* **1944**, *66*, 2050.

Walling, C. *Free Radicals in Solution*; Wiley: New York, 1957.

Walling, C. *J. Amer. Chem. Soc.* **1949**, *71*, 1930.

Walling, C. *J. Polym. Sci.* **1955**, *16*, 315.

Whitesides, G. M.; San Filippo, J. Jr. *J. Amer. Chem. Soc.* **1970**, *92*, 6611.

Young, L. J. In *Polymer Handbook*, 2nd ed.; Brandrup, J., Immergut, E. H., Eds.; Wiley: New York, 1975; p. II-105.